ISSN 2636-8498

# Environmental Research & Technology

Year 2024
Volume 7
Number 3

YTU PRESS

www.ert.yildiz.edu.tr

ISSN 2636-8498

# Environmental Research & Technology

Volume 7 Number 3 Year 2024



## Abstracting and Indexing

The following is a list of the Abstracting and Indexing databases that cover

**TUBITAK TR Index, Scopus, EBSCO, ROAD, SJIFactor, EurAsianScientific Journal Index (ESJI), Research Bib(Academic Resource Index), ScientificIndexing Services, ASOS Index, MIAR, IndexCopernicus, Open Ukranian Citation Index (OUCI), Scilit, Ideal Online, Google Scholar, Directory of Research Journals Indexing.**


## Publisher (Owner)

**Yıldız Technical University**

**Address:** Yıldız Technical University, Davutpaşa Kampusu, 34210 Esenler, İstanbul, Türkiye.

**Phone:** +90 212 383 20 18; **E-mail:** mbilgili@yildiz.edu.tr, ahmetd@yildiz.edu.tr

## Corporate Contributor (Publishing House)

**Kare Publishing - Kare Yayıncılık**

**Address:** Göztepe Mah., Fahrettin Kerim Gökay Cad., No: 200, Da: 2, Göztepe, Kadıköy, İstanbul, Türkiye

**Phone:** +90 216 550 61 11; **Web:** www.karepb.com; **E-mail:** kare@karepb.com

ISSN 2636-8498

# Environmental Research & Technology

Volume 7 Number 3 Year 2024

ISSN 2636-8498

# Environmental Research & Technology

Volume 7 Number 3 Year 2024

ISSN 2636-8498

# Environmental Research & Technology

Volume 7 Number 3 Year 2024

## CONTENTS

### Research Articles

ISSN 2636-8498

# Environmental Research & Technology

Volume 7 Number 3 Year 2024

## CONTENTS

*Environ Res Tec, Vol. 7, Issue. 3, pp. 291–302, September 2024*

**Environmental Research and Technology**
https://ert.yildiz.edu.tr - https://dergipark.org.tr/tr/pub/ert
DOI: https://10.35208/ert.1419914

**Research Article**

# What is the role of environmental stress on public health? Asymmetric evidence on carbon emissions, ecological footprint, and load capacity factor

**Ersin YAVUZ[*,1], Emre KILIC[2], Fatih AKCAY[1]**

[1]*Department of Public Finance, Pamukkale University, Denizli, Türkiye*
[2]*Department of Capital Markets and Portfolio Management, İstanbul Nişantaşı University, İstanbul, Türkiye*

## ARTICLE INFO

*Article history*
Received: 15 January 2024
Revised: 11 February 2024
Accepted: 18 March 2024

**Key words:**
Asymmetry; Health expenditures; Load capacity factor; Quantile co-integration

## ABSTRACT

The aim of this paper is to analyze the effects of carbon emission, ecological footprint, which takes into account the demand side of the environment, and load capacity factor, which takes into account both the supply and demand sides of the environment, on health expenditures with conventional and quantile methods. According to the conventional co-integration approach, there is no relationship between the environment and health expenditures. The other side, the findings obtained from the quantile co-integration method, which can give robust results in the presence of tailed distributions and possible endogeneity problems and consider the asymmetric structure in the data set, show the existence of a long-term relationship between the variables. According to the coefficient estimates, while carbon emission and ecological footprint increase health expenditures, the load capacity factor decreases.

**Cite this article as:** Ersin Yavuz, Emre Kılıç, Fatih Akcay. What is the role of environmental stress on public health? Asymmetric evidence on carbon emissions, ecological footprint, and load capacity factor. Environ Res Tec 2024;7(3)291–302.

## INTRODUCTION

Although a clean environment is indispensable for human health and well-being, environmental problems increase the pressure on human health day by day. For example, air pollution, one of the main environmental problems, has reached unsustainable levels. Today, almost all of the global population (99%) is breathing highly polluted air exceeding the limits in the World Health Organization (WHO) guideline clearly reveals the extent of the danger [1]. When all environmental issues are taken into account, more striking statistics are reached. For example, one in four deaths (13.7 million) in 2016 was caused by environmental risks. In addition, evidence has been presented that environmental degradation causes many health problems such as heart diseases, chronic respiratory diseases, cancer, stroke, infectious diseases, and allergenic diseases [2, 3]. According to WHO, which is a projection for the future, in the 2030–2050 period, in addition to the deaths directly caused by environmental pollution, 250 thousand additional deaths may occur due to reasons such as malnutrition, diarrhea, and heat stress due to climate change [4].

Environmental factors are one of the main determinants of human health after genetic susceptibility. These controllable factors can lead to various health consequences directly or indirectly (Decrease in the supply of food products due to deforestation and desertification, widespread malnutrition, damage to biodiversity, emergence of zoonotic diseases such as COVID-19, dramatic increases in the number of

***Corresponding author.**
*E-mail address: ersiny@pau.edu.tr

disasters caused by environmental degradation, etc.) [5–7]. Governments have great duties in combating health problems caused by environmental problems. For this purpose, governments apply many fiscal policy instruments such as environmental taxes, environmental protection expenditures, and green budget. However, it may not be sufficient in terms of targets to deal with environmental problems only by governments. Because, in the historical process, environmental challenges such as water and air pollution at the local level spread to regional dimensions in the following periods. However, numerous environmental disasters in recent years reveal that environmental pollution has become global [8]. Therefore, there is a need for international cooperation as well as national-scale policies.

International developments in the relationship between environmental problems and health are discussed at many international conferences and summits held by the United Nations (UN), dating back nearly half a century. For example, at the 1972-Stockholm Conference, participants emphasized that clean air, water, shelter, and health needs are indispensable needs and rights for human beings [9]. At the 1992-Rio Conference, "Protection and Promotion of Human Health" was discussed as a separate section and suggestions were presented [10]. The 2000-New York Millennium Summit document emphasized goals such as combating diseases, fighting malaria, ensuring environmental sustainability, etc. [11]. Policies for promoting global public health were discussed at the Millennium Development Goals Summit held in the same city in 2010 [12]. At the 2015-Paris UN Climate Change Conference (Conference of the Parties-21), the right to health, especially environmental problems, was discussed, and countries made commitments for the steps to be taken [13, 14]. Finally, in 2022, at the Stockholm+50 and Sharm El-Sheikh COP27, important decisions were taken for environmental damage to human and planetary health, and the results of the policies produced so far were evaluated [15, 16]. In addition, one of the 17 Sustainable Development Goals (SDGs) determined by the UN has been established as "Ensure healthy lives and promote well-being for all at all ages". According to SDG-3.9, it is targeted to minimize the number of deaths and diseases caused by air, soil, water pollution, and hazardous chemicals by 2030 [17].

Similar to international regulations, some documents in Türkiye include the environment-health relationship. Firstly, according to Article 56 of the 1982 Constitution, "Everyone has the right to live in a healthy and balanced environment. It is the duty of the State and citizens to improve the natural environment, to protect the environmental health, and to prevent environmental pollution." This regulation points to the responsibility of both governments and citizens to tackle environmental problems. Secondly, the effects of declining environmental quality on health are mentioned in many documents by the Ministry of Health, which provides the highest level of service in this field. For example, according to the "National Program and Action Plan for Reducing the Negative Effects of Climate Change on Health" prepared by the Türkiye Public Health Institution, which is part of the Ministry, the number of injuries, illnesses, and deaths caused by weather events such as droughts, heat waves, storms, floods, and fires may increase due to environmental problems that also cover climate change [18]. In the SWOT (Strengths, Weaknesses, Opportunities, and Threats) analysis included in the 2019–2023 Strategic Plan, which is a different document prepared by the Ministry, "increasing environmental pollution and global warming" are reported among external threats. In the same document, PESTLE (Political, Economic, Social, Technology, Legal, and Environmental) analysis states that environmental pollution threatens to increase chronic diseases [19].

Analyzing environmental problems caused by human activities and discussing solutions is essential [20]. Because environmental degradation, which has become both a local and global problem, has consequences for human health, such as many diseases, injuries, and deaths, and also puts pressure on an upward trend in health expenditures (HE). WHO estimates that by 2030, the direct cost of environmental degradation to human health will be between $2 and $4 billion [4]. In this context, researchers prefer the HE indicator, which provides information about the entire health system, in the environment-health literature [21–24]. Empirical studies on the environment-health link shed light on the planning of the upcoming process. Because the analysis of the economic cost of health problems caused by environmental stress is critical in terms of providing concrete information for the environmental policies that governments will design [25].

This paper examines the effects of environmental indicators on HE in Türkiye. The study aims to contribute to the literature in two ways. First, there are two environmental pollution indicators (carbon emission ($CO_2$) and ecological footprint (EF)) and one environmental quality indicator (load capacity factor (LCF)) representing the environment in the study. In the environmental literature, the more comprehensive EF has become popular in recent years [26–29], while researchers often prefer $CO_2$ [30]. However, the study on LCF, which measures environmental pollution and environmental supply together, is limited [31–34]. To the best of our knowledge, this study is the first attempt for Türkiye to analyze the effects of EF and LCF indicators on HE. Therefore, the study confirms the empirical consistency of the results by comparing the findings of three different environmental indicators as well as presenting evidence to politicians in terms of new environmental indicators. Secondly, the study offers a methodically different perspective to the environmental-health literature with the Quantile Co-integration Regression (QCR) method proposed by Xiao [35] as well as the conventional method. The quantile co-integration method has many advantages over conventional co-integration methods. Conventional approaches have strict assumptions such as a normal distribution and no endogeneity. However, the QCR test may give resistant results in the presence of a non-normal distribution and possible end-of-endogeny. This method also provides a theoretical basis for examining positive and negative shocks by distinguishing between them.

The rest of the paper is organized as follows: The first section examines, in detail, the literature on environmental indicators and HE. The second section presents information about the dataset, descriptive statistics, and empirical methods in the analysis. The third section discusses the findings regarding conventional and quantile methods. The final section assesses the impact of environmental indicators on HE and provides policy recommendations.

**Literature Review**

The effects of air pollution on health have been the subject of intense research in the past, and there have been studies linking air pollution and changes in health in the short term and studies that track those exposed to pollution over time [36]. In one of the first studies to empirically address the relationship between environment and HE, Jerrett et al. [37] estimated a two-stage regression model using the 1991–1992 cross-sectional data for 49 counties in the Canadian province of Ontario. After controlling for other variables that may affect HE, it was concluded that HE is also high in counties where total toxic pollution output is high and lower in counties with higher environmental protection expenditures. A large part of the literature on the relationship between environmental pollution/quality and health expenditures in the following periods analyzes the effects of economic, financial, social, institutional, technological, and energy variables on environmental degradation by considering pollution indicators (such as $CO_2$, EF) and on environmental quality by considering the pollution indicators as the environmental quality variable [38–43]. The findings of these studies differ according to the countries, time period, and especially the method applied.

$CO_2$ emissions, one of the most important indicators of environmental pollution, negatively affect environmental quality and health, resulting in higher healthcare expenses for both individuals and the public [44]. Therefore, the demand for health services may increase health expenditures. Environmental degradation, on the one hand, may lead to an increase in the share of the environmental protection budget and a decrease in the share that can be allocated to health services. At this point, the results of the health-pollution relationship may change in the short and long term [45]. The analyses generally use one of the environmental pollution indicators such as $CO_2$ emissions and EF. When it comes to sustainability, $CO_2$ and EF, which reveal the demand side of the environment, are not enough to explain environmental quality and sustainability [32, 46]. The LCF, which is calculated as dividing the EF by biocapacity, considering both the demand and supply sides of the environment, as proposed by Siche et al. [47], is used in recent studies in terms of environmental quality and sustainability [33, 48–54].

Although there is a large body of literature on the nexus between $CO_2$ emissions and HE, there are very few studies on the relationship between HE and EF [22, 24, 31, 55–57]. Yang and Usman [22] analyzes the period 1995–2018 for the 10 countries with the highest HE and finds evidence of a bidirectional causality between the two variables, with EF increasing HE. There are also studies considering $CO_2$ emissions and EF variables together. For example, Alimi and Ajide [58] examine the nexus among $CO_2$ emissions, EF, and HE in SSA countries between 1996 and 2016. $CO_2$ emissions and EF increase the cost of HE, but the impact of $CO_2$ emissions is greater. Similarly, there are few papers in the literature that analyze the relationship between HE and LCF. Shang et al. [23] examine the link between HE, renewable energy, income, and LCF for ASEAN countries. The long-term effect of renewable energy and HE on the LCF is significant and positive, while income affects the LCF negatively. Adebayo and Samour [59] examine the nexus between fiscal policy and LCF for the BRICS countries between 1990 and 2018 in terms of using the public variable, even without health expenditures. There is a strong link between tax revenues, public expenditures variables, and the LCF. Panel causality findings show a one-way causality from public expenditures and tax revenues to the LCF.

There are two papers in the literature examining the relationship between HE and the environment for Türkiye. According to Demir et al. [60] examines the period from 1975 to 2018 using the NARDL method. According to the findings, positive shocks in $CO_2$ increase HE. Aydin and Bozatli [61] explore the same period with Fourier Shin and Frequency Domain Causality approaches. The findings indicate that the variables are cointegrated. In addition, the study suggests bidirectional causality between $CO_2$ and HE. Together with these papers, there are also panel studies covering Türkiye in the literature. From these studies, Chaabouni and Saidi [21], Benli [45] for developed countries, and Demir et al. [60] provide evidence that $CO_2$ promotes HE. However, Benli [45] for developing countries also provides findings supporting negative effects. Also, Erdogan et al. [62] observed unidirectional causality from $CO_2$ to HE, while Khan et al. [63] detects bidirectional causality between $CO_2$ and HE. In summary, the limited number of investigations of the environment-HE connection for Türkiye in the literature and only through $CO_2$ indicates that new evidence is needed in this area. This study aims to contribute to the gap in the literature by analyzing the effects of $CO_2$, with a special emphasis on EF and LCF, on HE.

Another striking point in the literature is the use of conventional approaches in most of the studies. Conventional methods are based on some solid assumptions and consider the relationship between variables as a whole. However, the nexus between variables may change over time. The quantile methods can be useful with their features, such as examining relationships that may change over time, giving resistant results against non-normal distributions, and taking into account the possible internality problem. In the literature examining the environment-health link, the use of quantile methods has become widespread in recent years. When the studies using the quantile method are examined, it is seen that some analyze $CO_2$ emissions [40, 64–66]; and some analyze LCF [48, 54, 67, 68]. Therefore, this study differs significantly from the literature by analyzing the nexus between $CO_2$ emissions, EF, LCF, and health expenditures for Türkiye with quantile methods.

**Table 1.** Definition of variables

| Variables | Abbreviation | Definition | Data source |
|---|---|---|---|
| Dependent variable | | | |
| Health expenditures | HE | Share of health expenditures in GDP (%) | OECD [70] |
| Independent variable | | | |
| Environmental pollution indicators | $CO_2$ | Carbon emission (tonne) | OWID [71] |
| | EF | Ecological footprint (global hectare) | GFN [72] |
| Environmental quality indicator | LCF | Load capacity factor (biocapacity/ecological footprint) | |

**Table 2.** Descriptive statistics

| | | | | | | | Test of normality | |
|---|---|---|---|---|---|---|---|---|
| Variables | Mean | Max. | Min. | SD | S | K | JB | Prob. |
| HE (%) | 3.43 | 5.49 | 1.49 | 1.27 | 0.14 | 1.42 | 4.73 | 0.090[c] |
| $CO_2$ (million tonne) | 218.48 | 430.22 | 65.42 | 114.90 | 0.35 | 1.86 | 3.43 | 0.180 |
| EF (million gha) | 164.08 | 286.20 | 81.35 | 60.64 | 0.35 | 1.90 | 3.11 | 0.210 |
| LCF (%) | 0.70 | 1.07 | 0.38 | 0.21 | 0.14 | 1.68 | 3.31 | 0.190 |

HE: Health expenditures; EF: Ecological footprint; LCF: Load capacity factor. JB refers to Jarque and Bera [73] normality test. S skewness, K kurtosis, and SD standard deviation. a, b, and c denote the significance level at 1%, 5%, and 10%, respectively. The statistics in the table are calculated with raw data. Descriptive statistics for HE are taken into account for the period 1975–2018.

## DATA, MODEL, AND METHODOLOGY

In this section, the data set used in the study, the formulation of the established models, and the econometric methodology related to the methods used in the empirical analysis are explained.

### Data Set

Three different models are established in the study, and the share of health expenditures in GDP is used as the dependent variable in all models. On the other hand, the explanatory variables $CO_2$, EF, and LCF are included in the models to represent the environment. Explanatory variables in the first two models, namely $CO_2$ (Model 1) and EF (Model 2), reflect environmental pollution, while the explanatory variable LCF in the third model reflects environmental quality. $CO_2$ is one of the most frequently used pollution indicators in the literature, providing information on environmental degradation. EF, another pollution indicator, has attracted attention in recent years. EF, including carbon footprint, consists of six components (carbon, forest products, agriculture, pasture, fisheries, and residential areas) and provides more information about environmental pollution when compared to $CO_2$ [69]. The LCF variable in Model 3, developed by Siche et al. [47], differs from the other two variables because it is an environmental quality indicator. The LCF value obtained by dividing the biocapacity, which reflects the supply side of the environment, by the EF, which reflects the demand side of the environment, indicates environmental sustainability if it is 1 and above. Values below 1 indicate that there is an ecological deficit, that is, environmental degradation is more dominant [46]. Therefore, analyses focused only on environmental pollution may present incomplete or misleading findings because they neglect the environmental supply. From this point of view, this study investigates more holistic evidence about the environment by comparing the findings on environmental pollution variables with the findings in the LCF model.

Due to data availability, the sampling periods taken into account in the models differ. In this framework, while the 1975–2020 period is considered in the model established for the $CO_2$ variable, the 1975–2018 period is examined in the models established for the ecological footprint and LCF variables. Annual data is used as the data frequency. Due to the scale differences in the variables, the data are used in logarithmic form. The definition and source information of the data are shown in detail in Table 1. Analyses were carried out with the GAUSS-21 program.[1]

Table 2 lists descriptive statistics for the variables. The results of the Jarque and Bera [73] test show that health expenditures have a non-normal distribution, while other variables have a normal distribution. Positive skewness values in the series indicate the presence of a right-tailed distribution, and negative values indicate the presence of a left-tailed distribution. The presence of a platykurtic distribution is indicated by a kurtosis value less than 3, that is, an extremely negative kurtosis, and leptokurtic distribution, i.e. an extremely positive kurtosis, is indicated by a value greater than 3. In light of this information, it is seen that the skewness values for all variables are greater than zero. In this context, there is a right-tailed structure in

[1] The unit root tests were conducted with TSPDLIB developed by Nazlioglu [83].

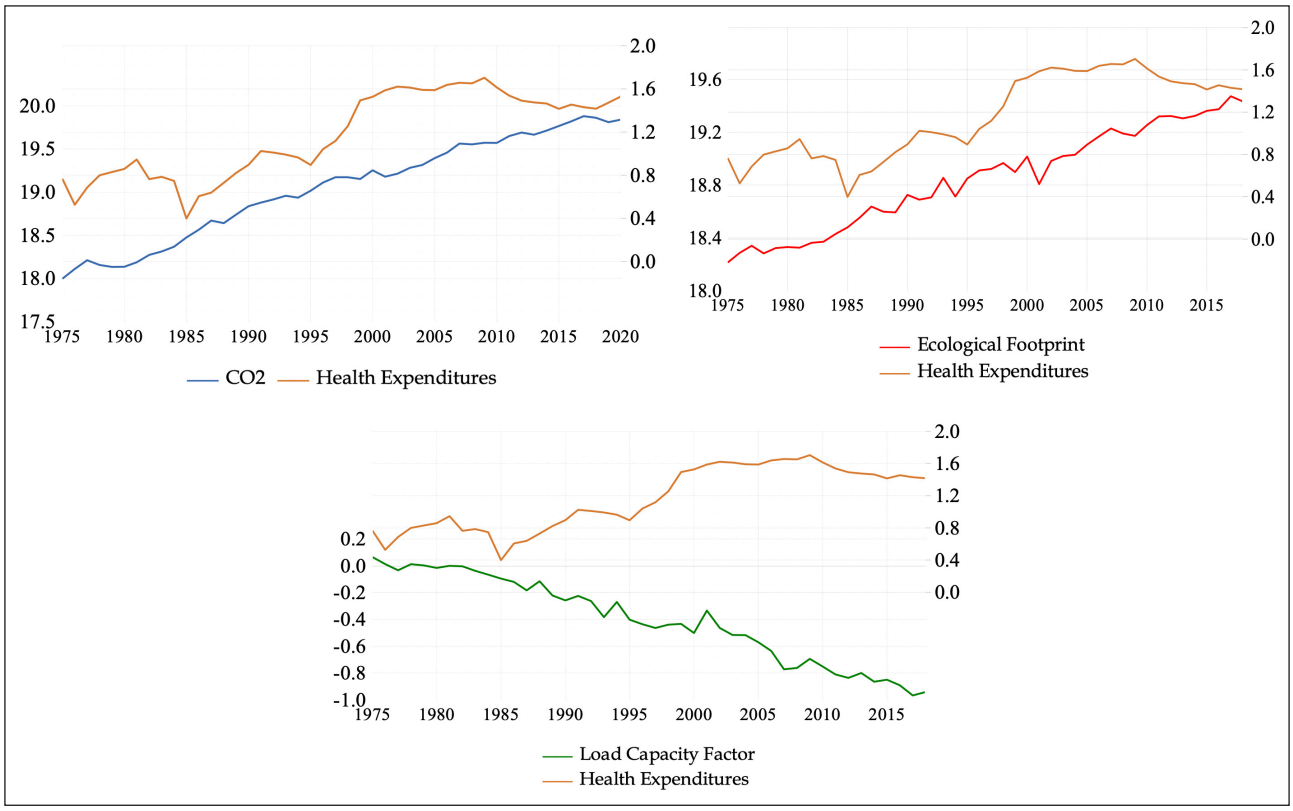


**Figure 1**. Time-based coherence of health expenditures and environmental indicators.

the distribution of variables. Kurtosis values are less than 3 for all variables. These statistics show the existence of a platykurtic distribution, which expresses negative extreme kurtosis in the variables.

When the development of statistics regarding the variables in Table 2 is examined, it is seen that HE has an average 3.4% share of GDP. HE, which was below the level of 3% until the second half of the 1990s, increased to levels of 4–5%, especially in the post-2000 period. In the same period, the EF increased by more than 250%, from 81 million to 286 million global hectares. On the other hand, the increase in biocapacity was limited to approximately 25%. Therefore, Türkiye has been experiencing a growing ecological deficit since the 1980s. This resulted in a dramatic decrease in the LCF. The LCF value, which permanently decreased below 1 in the post-1980 period, has decreased below the level of 0.4 in recent years, revealing that the ecological balance is unsustainable. Finally, the $CO_2$ indicator increased from 65 million tonnes to 430 million tonnes in the related period, increasing by approximately 560%. This statistic reveals strikingly the extent of environmental degradation in Türkiye.

Figure 1 shows the change in HE and environmental indicators over time. Accordingly, it is seen that health expenditures and environmental indicators act in harmony with each other. Although the relationship seems to break from time to time, it is slowly getting back into balance. The ruptures occurring at various periods show that the long-term relationship may change in the process. This situation causes a possible co-integration to change over time. At this point, it is important to use methods that allow the regression coefficient to change over time, such as the quantile approach, in order to better explain the data set.

## Model

Increasing environmental pollution potentially causes increased HE, putting increasing pressure on government budgets [74]. Jerrett et al. [37] conducted a discussion on the link between environmental government policies and controlling costs in the health system. For this reason, it is important to examine the relationship between health expenditures and environmental pollution.

In this study, the relationship between HE and environmental pollution is examined in Türkiye. There are many variables that explain environmental pollution. In this context, three environmental indicators that are prominent and frequently used in explaining environmental pollution in the relevant literature are taken into consideration. The fact that EF includes $CO_2$ and LCF is a ratio of EF causes the problem of multicollinearity. For this reason, the relationship of each indicator with health expenditures is examined separately.

The specifications for the established models are as shown in Equations 1, 2, and 3:

Model 1: $lnHE_t=\alpha_1+\beta_1\ lnCO2_t+\varepsilon_{1t}$ (1)

Model 2: $lnHE_t=\alpha_2+\beta_2\ lnEF_t+\varepsilon_{2t}$ (2)

Model 3: $lnHE_t=\alpha_3+\beta_3\ lnLCF_t+\varepsilon_{3t}$ (3)

where $\alpha$ is the constant term, $\beta_1$, $\beta_2$ and $\beta_3$ are the regression parameters, *ln* is the operation of the logarithm, t is the time dimension, and $\varepsilon_t$ is the error term.

**Table 3.** Unit root and co-integration analysis results

| | ADF (1979) | | | | EG (1987) | | |
|---|---|---|---|---|---|---|---|
| | Level | | First diffence | | | | |
| Variables | Statistic | Prob. | Statistic | Prob. | Model | Statistic | Prob. |
| $lnHE_t$ | -1.051(0) | 0.726 | -6.977(0)[a] | 0.000 | $lnSH_t$&$lnCO2_t$ | -2.050(0) | 0.508 |
| $lnCO2_t$ | -1.581(0) | 0.484 | -6.273(0)[a] | 0.000 | $lnSH_t$&$lnEA_t$ | -2.085(0) | 0.491 |
| $lnEF_t$ | -0.024(2) | 0.951 | -7.384(1)[a] | 0.000 | $lnSH_t$&$lnYKF_t$ | -1.895(0) | 0.587 |
| $lnLCF_t$ | 0.727(2) | 0.991 | -7.347(1)[a] | 0.000 | | | |

HE: Health expenditures; EF: Ecological footprint; LCF: Load capacity factor. The maximum lag length is set to 2 due to the use of annual data. The t-statistics criteria was used to determine the appropriate number of lags. The values in brackets give the appropriate lag length.

**Methodology**

The link between HE and the environment ($CO_2$, EF, and LCF) can be analyzed with the co-integration approach. Co-integration tests differ in terms of their assumptions. Traditional co-integration tests (For example, Engle and Granger (EG) [75]) are based on the assumption of a Gaussian distribution. However, Koenker and Xiao [76] show that in the presence of heavy-tailed distributions, conventional tests have weak power properties. In addition, traditional methods assume that there is no endogeneity problem in the model. However, models established for examining the relationship between economic variables may face the problem of endogeneity. This situation may cause deviations in the estimates [77].

Xiao [35] developed the QCR test, which can examine the asymmetric structure in the data set in detail and is resistant to the endogeneity problem. QCR testing extends the traditional co-integration model to a more general class of models that allow β to change over time. This test allows the relationship between variables to be analyzed by dividing them into quantiles. Syed et al. [78] state that the relationship between economic variables changes in different quantiles. In this regard, it offers a theoretical framework to explore the impact of positive and negative shocks by dissecting the asymmetric structure in the dataset into quantiles. In this context, methods that yield results on the basis of quantiles are useful in order to examine the asymmetric structure in detail.

The initial model in the QCR test is given by Equation 4.

$$y_t=\alpha+\beta X_t+\varepsilon_t \quad (4)$$

The expanded version of Equation 4 by allowing $\beta$ to change over time is shown in Equation 5:

$$y_t=\alpha+\beta_t X_t+\varepsilon_t \quad (5)$$

where $\varepsilon_t$ shows the errors for each quantile is expressed with $F_\varepsilon(\cdot)$. In accordance with the methodology of Xiao [35], the $\tau$ th conditional quantile of $y_t$ is given by Equation 6.

$$Q_{i_t}(\tau|X_t) = \alpha(\tau) + \beta(\tau)X_t + \sum_{j=-K}^{K} \gamma_j(\tau)\cdot X_{t-j} + F_\varepsilon^{-1}(\tau) \quad (6)$$

where $\beta(\tau)$ is the co-integration coefficient, which is different for each quantile. $K$ denotes the leads of $\Delta X_t$, and $-K$ denotes the lags. To overcome the problem of endogeneity, leads and lags are included in the model. In order to determine the existence of the co-integration, the $\gamma_n$ statistics are calculated. The formulation for the $\gamma_n$ statistic is as shown in Equation 7:

$$\gamma_n = \frac{1}{\omega_\psi^* \sqrt{n}} \sum_{j=1}^{K} \psi_\tau(\varepsilon_{j\tau}) \quad (7)$$

where $\omega_\psi^*$ denotes the long-run variance of $\psi_\tau(\varepsilon_{j\tau})$. $\varepsilon_{j\tau}$ is the errors obtained from quantile co-integration regression. The $H_0$ (null) hypothesis reveals that there is co-integration between variables, and $H_A$ (alternative) hypothesis reveals that there is no co-integration between variables. If the $\gamma_n$ statistic is greater than the critical values of t-table, $H_0$ hypothesis is rejected, and it is decided that there is no co-integration.

## FINDINGS

In the empirical analysis, firstly, whether the series contains a unit root or not is examined with the Augmented Dickey and Fuller (ADF) [79] test. Table 3 shows that the series contain unit roots at levels but become stationary when the first difference is taken (I(1)). Co-integration analysis is used to examine the relationship between non-stationary series. At this point, firstly, the effects of environmental indicators on HE is examined with the traditional co-integration test in order to make a comparison.

According to the EG co-integration test results, the null hypothesis that there is no co-integration in all models cannot be rejected. In other words, there is no relationship between HE and environmental indicators in Türkiye.

Then, the co-integration relationship between the series is examined with the QCR test, which allows to observe the time-varying co-integration, examines the effects of positive and negative shocks in detail, and gives a resistant estimate in the case of a non-normal distribution and possible endogeneity problems. The results are listed in Table 4.

First, the existence of a co-integration between the variables is examined on a model basis. When the $\gamma_n$ statistics of the models in Table 4 are examined, the null hypothesis that there is a co-integration relationship for all models cannot be rejected. In other words, according to the results of the QCR test, contrary to the EG test, it

**Table 4.** Quantile co-integration analysis results

| | 0.1 | 0.2 | 0.3 | 0.4 | 0.5 | 0.6 | 0.7 | 0.8 | 0.9 |
|---|---|---|---|---|---|---|---|---|---|
| Independent variables | | | | | | | | | |
| $lnCO2_t$ | | | | | | | | | |
| $\hat{\beta}_{(\tau)}$ | 0.351[a] | 0.481[a] | 0.488[a] | 0.491[a] | 0.528[a] | 0.609[a] | 0.664[a] | 0.611[a] | 0.583[a] |
| SD | 0.132 | 0.101 | 0.098 | 0.102 | 0.098 | 0.110 | 0.105 | 0.095 | 0.090 |
| t-stat. | 2.658 | 4.744 | 4.961 | 4.817 | 5.390 | 5.554 | 6.349 | 6.407 | 6.488 |
| $lnEF_t$ | | | | | | | | | |
| $\hat{\beta}_{(\tau)}$ | 1.059[a] | 0.906[a] | 0.916[a] | 0.843[a] | 0.828[a] | 0.873[a] | 1.068[a] | 0.963[a] | 0.945[a] |
| SD | 0.162 | 0.159 | 0.180 | 0.175 | 0.174 | 0.166 | 0.152 | 0.130 | 0.132 |
| t-stat. | 6.556 | 5.714 | 5.094 | 4.817 | 4.757 | 5.271 | 7.047 | 7.433 | 7.141 |
| *lnLCFt* | | | | | | | | | |
| $\hat{\beta}_{(\tau)}$ | -1.157[a] | -0.947[a] | -0.999[a] | -0.971[a] | -1.054[a] | -1.116[a] | -1.172[a] | -1.273[a] | -1.275[a] |
| SD | 0.186 | 0.174 | 0.164 | 0.168 | 0.180 | 0.192 | 0.196 | 0.200 | 0.223 |
| t-stat. | -6.224 | -5.442 | -6.082 | -5.772 | -5.849 | -5.811 | -5.968 | -6.374 | -5.726 |
| | Test stat. ($\gamma_n$) | Prob. | %1 | %5 | %10 | | | | |
| Models | | | | | | | | | |
| $lnHE_t$&$lnCO2_t$ | 0.935 | 0.936 | 1.79 | 1.60 | 1.52 | | | | |
| $lnHE_t$&$lnEF_t$ | 0.986 | 0.939 | 1.93 | 1.66 | 1.60 | | | | |
| $lnHE_t$&$lnLCF_t$ | 1.248 | 0.386 | 1.89 | 1.60 | 1.51 | | | | |

HE: Health expenditures; EF: Ecological footprint; LCF: Load capacity factor. Where the $\gamma_n$ statistic is used to examine the existence of a co-integration, 0.1, …, 0.9 represent quantiles. SD represents a standard deviation. 1,645, 1,960, and 2,578 are t-table values expressing significance at 10%, 5%, and 1%, respectively. The probability values for the $\gamma_n$ statistics were generated with 1,000 replications.

is determined that health expenditures ($lnSH_t$) and environmental indicators move together in the long term in Türkiye.

After the determination of the co-integration relationship, long-term coefficient estimates are made in order to determine the size and direction of the relationship. One of the most important advantages of quantile approaches is that they allow us to analyze this relationship on a quantile basis. In this context, coefficient estimates for each quantile are listed in Table 4. First of all, when the signs of the coefficients are examined, it is seen that the increases in $CO_2$ and EF in all quantiles increase the HE, while the increase in the LCF decreases the HE (Fig. 2). These results are in line with expectations. As the threat to human health from environmental pollution increases day by day, it plays a triggering role in health services and, thus, in HE. On the other hand, the decreasing effect of the LCF, namely the increase in environmental quality, on HE as a result of positive effects on human health supports the findings of $CO_2$ and EF on HE. When the coefficient sizes are examined in general, while $CO_2$ increases HE by 0.35% in negative shocks, this effect doubles when the direction of the shock changes. The coefficients of extreme negative and positive shocks in the EF are greater compared to the middle quantiles. Finally, there is no significant difference in the coefficient sizes for positive and negative shocks for the LCF, and the effect of the LCF on HE is higher for extreme positive shocks.

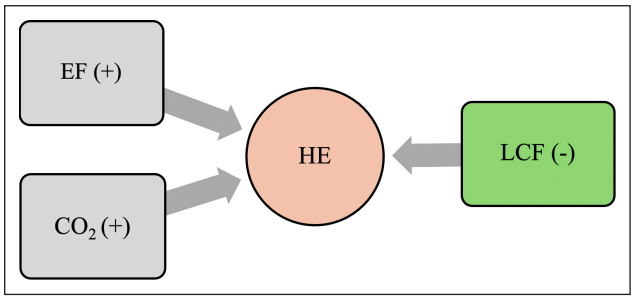


**Figure 2**. QCR test based coefficient signs of environmental indicators.

## RESULTS AND DISCUSSION

The response to the question of how the environment affects HE in Türkiye differs on the basis of empirical approaches. According to the analysis results, the conventional co-integration (EG) test results reveal that there is no long-term relationship in the models. However, the models are cointegrated according to the QCR quantile co-integration method, which can better explain the data structure and give resistant estimates in cases of a non-normal distribution and possible endogeneity problem. This result supports the studies of Aydin and Bozatli [61], who discovered the co-integration between different environmental indicators and HE. The coefficient estimates of the method on the basis of quantiles show that the $CO_2$ and EF variables affect HE positively. In the literature, Demir

et al. [60] studies reached similar findings. On the other hand, coefficient estimates provide evidence that the LCF variable negatively affects EH. When the findings of the three models are compared, the effects of environmental indicators on EH are consistent. The finding that environmental pollution increases HE and environmental quality decreases HE supports the expectations in the literature.

When the overall coefficient (0.5 quantile) results are examined, EF negatively affects HE 63.7% more than $CO_2$. Based on the average of the analysis period, the carbon footprint in EF represents 50.7% [69]. The fact that these two ratios are close to each other strengthens the reliability of the analysis's results. In addition, the coefficients for LCF, which provides the most comprehensive information about the environment among the models, are larger compared to other indicators. Considering biocapacity in the LCF model transforms the degrading effect of the environment on HE into a curative effect.

The study finally analyzes the quantile-based results for all models. Accordingly, the coefficients for $CO_2$ increase from negative shocks to positive shocks. This demonstrates the positive pressure of increases in $CO_2$ on HE. On the other hand, EF increases HE more in extremely large negative and positive shocks. Environmental pollution increases EH in positive shocks, which is in line with the expectations in the literature. However, the repulsive effect of negative shocks in EF on HE is a surprising finding. The reason for this result can be explained with the help of Figure 1. Accordingly, during the 2001 and 2008 economic crisis periods, human-induced EF declined due to the decrease in production and demand. However, in the same periods, instead of a decrease in HE, the course of increase continues. In times of crisis, the assumption that social stress is higher and the need for healthcare services increases may partly explain the increases in HE. Findings for LCF in the third model are similar to those for EF in terms of quantile-based coefficient change. In addition, LCF coefficient values are higher than those of $CO_2$ and EF. Therefore, the increase in environmental quality provides benefits beyond compensating for the increase in HE caused by environmental pollution. In positive shocks of LCF, the reducing effect of environmental quality on HE increases its severity.

## CONCLUSION

The paper explores the effect of environmental indicators on HE with conventional and quantile co-integration methods. For this purpose, three models are created in the study. In the first two models, $CO_2$ and EF variables represent environmental pollution. In the third model, LCF, which has become popular recently and measures environmental quality, is preferred. Incorporating environmental supply over biocapacity into the calculation as well as environmental pollution, LCF provides holistic evidence and new perspectives on the effects of the environment on HE. Analyzing three environmental models in the study allows for comparison of findings and evaluation of consistency.

Among the empirical findings, firstly, the EG test finds no relationship between environmental indicators and HE, while the QCR test discovers different levels of relationship in the models. The quantile approach offers evidence through three models that, on the one hand, environmental degradation ($CO_2$ and EF models) encourages HE and, on the other hand, environmental improvement (LCF model) minimizes the need for HE. In addition, it confirms the existence of an asymmetric structure by revealing that the coefficients of the models change in negative and positive shocks.

Findings from all models indicate that for sustainable HE, governments should both combat environmental degradation and develop policies to increase environmental supply, namely biocapacity. In this context, some policy recommendations that will improve environmental quality and reduce HE can be listed as follows: Firstly, the share of renewable energy sources should be increased by minimizing fossil fuel consumption. As of 2019, the share of renewable energy consumption in Türkiye is only 14.1% of the total [80]. An increase in this rate will also contribute to the reduction of $CO_2$, which is the most important cause of environmental pollution. Secondly, public transportation should be encouraged instead of personal transportation vehicles, whose number is increasing day by day, especially in metropolitan cities. While the number of motor land vehicles in Türkiye was approximately 786 thousand in 1975, it increased approximately 32 times and reached 26.4 million in 2022 [81]. During the same period, the population increased by only 111% [82]. Therefore, new policies based on a sustainable environment, especially taxation, are needed for motor vehicles emitting $CO_2$. Third, governments should strive to spread healthy lifestyles among the population. Individuals should be encouraged to walk and eat healthy instead of using vehicles when appropriate. The policies governments develop in response to these three recommendations, in accordance with WHO, can prevent 7 million premature deaths globally each year [3]. Fourthly, environmentally friendly production should be encouraged by taxes and subsidy instruments in sectors that directly concern human health, especially agriculture. On the other hand, the prohibition of sectors with more environmental damage or the implementation of deterrent policies will improve the environment and human health. Finally, legislative arrangements should be made to prevent biocapacity resources such as rivers, lakes, seas, forests, and grasslands, which are known as common goods in the fiscal literature, from being damaged or destroyed due to excessive consumption. Because only reducing pollution is not enough for a sustainable environment, environmental supply sources need to be developed.

For further studies, researchers may prefer new and inclusive environmental indicators such as LCF and up-to-date empirical methods that take into account the characteristics of the data structure.

## DATA AVAILABILITY STATEMENT

The author confirm that the data that supports the findings of this study are available within the article. Raw data that support the finding of this study are available from the corresponding author, upon reasonable request.

## CONFLICT OF INTEREST

The author declared no potential conflicts of interest with respect to the research, authorship, and/or publication of this article.

## USE OF AI FOR WRITING ASSISTANCE

Not declared.

## ETHICS

There are no ethical issues with the publication of this manuscript.

## REFERENCES


[1] World Health Organization, "Air pollution," https://www.who.int/health-topics/air-pollution#tab=tab_1 Accessed on Jan 17, 2023.

[2] EEA, "European Environment Agency, 2023. https://www.eea.europa.eu/themes/human/intro Accessed on Jan 10, 2023.

[3] World Health Organization, "Environmental health," https://www.who.int/health-topics/environmental-health#tab=tab_2 Accessed on Jan 17, 2023.

[4] World Health Organization, "Climate change," https://www.who.int/health-topics/climate-change#tab=tab_1, World Health Organization website. Accessed on Jan 17, 2023.

[5] I. L. Pepper, C. P. Gerba, and M. L. Brusseau, "The Extent of Global Pollution," I. L. Pepper, C. P. Gerba, and M. L. Brusseau, (Eds.), Environmental and pollution science. Academic Press, Elsevier Inc., pp. 3–12, 2006.

[6] UN, "United Nations," 2023, https://www.un.org/sustainabledevelopment/biodiversity/ Accessed on Jan 10, 2023.

[7] World Meteorological Organization. https://public.wmo.int/en/media/press-release/weather-related-disasters-increase-over-past-50-years-causing-more-damage-fewer Accessed on Jan 10, 2023.

[8] M. J. Ahern, and A. J. McMichael, "Global environmental changes and human health," R. E. Hester, and R. M. Harrison, (Eds.), Global environmental change-issues in environmental science and technology. The Royal Society of Chemistry, Cambridge, 2002. [CrossRef]

[9] United Nations, "Report of the United Nations conference on the human environment, "Stockholm, 5-16 June 1972, United Nations, New York, 1973.

[10] United Nations, "Report of the United Nations conference on environment and development," Rio de Janeiro, 3-14 June 1992, United Nations, New York, 1993.

[11] United Nations, "United Nations millennium declaration, resolution adopted by the general assembly," Fifty-Fifth Session Agenda Item 60 (b), General Assembly, United Nations, 2000.

[12] United Nations, "Keeping The Promise: United to Achieve The Millennium Development Goals," Resolution Adopted by The General Assembly on 22 September 2010, Fifty-Fifth Session Agenda Item 13 and 115, General Assembly, United Nations, 2010.

[13] United Nations, "Paris aggrement, https://unfccc.int/sites/default/files/english_paris_agreement.pdf, 2015.

[14] United Nations, "Climate change Paris-agreement," https://www.un.org/en/climatechange/paris-agreement. Accessed on Jan 22, 2023.

[15] United Nations, "Stockholm+50: a healthy planet for the prosperity of all – our responsibility, our opportunity," https://www.stockholm50.global/ Accessed on Jan 22, 2023.

[16] United Nations, "United Nations Framework Convention on Climate Change," https://unfccc.int/cop27, Accessed on Jan 22, 2023.

[17] UN, "UN Department of Economic and Social Affairs, Sustainable Development," https://sdgs.un-.org/goals/goal3 Accessed on Jan 10, 2023.

[18] Ministry of Health. National Program and Action Plan for Reducing the Negative Effects of Climate Change on Health, Turkiye Public Health Institution, Department of Environmental Health, Ministry Publication No: 998, 2015.

[19] Ministry of Health. 2019-2023 Strategic plan (Updated version-2022), Publication No: 1223, 2022.

[20] A. Çelekli, and Ö. E. Zariç, "From emissions to environmental impact: understanding the carbon footprint," International Journal of Environment and Geoinformatics, Vol. 10(4), pp. 146–156, 2023. [CrossRef]

[21] S. Chaabouni, and K. Saidi, "The dynamic links between carbon dioxide (CO2) emissions, health spending and GDP growth: A case study for 51 countries," Environmental Research, Vol. 158, pp. 137–144, 2017. [CrossRef]

[22] B. Yang, and M. Usman, "Do industrialization, economic growth and globalization processes influence the ecological footprint and healthcare expenditures? Fresh insights based on the STIRPAT model for countries with the highest healthcare expenditures," Sustainable Production and Consumption, Vol. 28, pp. 893–910, 2021. [CrossRef]

[23] Y. Shang, A. Razzaq, S. Chupradit, N. B. An, and Z. Abdul-Samad, "The role of renewable energy consumption and health expenditures in improving load capacity factor in ASEAN countries: Exploring new paradigm using advance panel models," Renewable Energy, Vol. 191, pp. 715–722, 2022. [CrossRef]

[24] B. N. Abbasi, Z. Luo, A. Sohail, L. Yang, L. Huimin, and C. Rongrong, "Global Shocks of Education, Health, and Environmental Footprint on Nation-

al Development in the Twenty-First Century: A Threshold Structural VAR Analysis," Journal of the Knowledge Economy, pp. 1–37, 2023. [CrossRef]
[25] OECD (2001). "OECD Environmental Outlook - Human Health and the Environment," OECD Publications, 2001.
[26] N. Kongbuamai, Q. Bui, H. M. A. U. Yousaf, and Y. Liu, "The impact of tourism and natural resources on the ecological footprint: a case study of ASEAN countries," Environmental Science and Pollution Research, Vol. 27, pp. 19251–19264, 2020. [CrossRef]
[27] A. E. Caglar, E. Yavuz, M. Mert, and E. Kilic, "The ecological footprint facing asymmetric natural resources challenges: evidence from the USA," Environmental Science and Pollution Research, Vol. 29, pp. 10521–10534, 2022. [CrossRef]
[28] Z. Wang, H. Chen, and Y. P. Teng, "Role of greener energies, high tech-industries and financial expansion for ecological footprints: Implications from sustainable development perspective," Renewable Energy, Vol. 202, pp. 1424–1435, 2023. [CrossRef]
[29] E. Yavuz, E. Ergen, T. Avci, F. Akcay, and E. Kilic, "Do the effects of aggregate and disaggregate energy consumption on different environmental quality indicators change in the transition to sustainable development? Evidence from wavelet coherence analysis," Environmental Science and Pollution Research, pp. 1–21, 2023. [CrossRef]
[30] M. Shahbaz, and A. Sinha, "Environmental Kuznets curve for CO2 emissions: a literature survey," Journal of Economic Studies, Vol. 46(1), pp. 106–168, 2019. [CrossRef]
[31] U. K. Pata, M. Aydin, and I. Haouas, "Are natural resources abundance and human development a solution for environmental pressure? Evidence from top ten countries with the largest ecological footprint," Resources Policy, Vol. 70, Article 101923, 2021. [CrossRef]
[32] U. K. Pata, and C. Isik, "Determinants of the load capacity factor in China: a novel dynamic ARDL approach for ecological footprint accounting. Resources Policy, Vol. 74, Article 102313, 2021. [CrossRef]
[33] D. Xu, S. Salem, A. A. Awosusi, G. Abdurakhmanova, M. Altuntaş, D. Oluwajana, D. Kirikkaleli, and O. Ojekemi, "Load capacity factor and financial globalization in Brazil: the role of renewable energy and urbanization," Frontiers in Environmental Science, Vol. 9, Article 823185, 2022. [CrossRef]
[34] E. Yavuz, E. Kilic, and A. E. Caglar, "A new hypothesis for the unemployment-environment dilemma: is the environmental Phillips curve valid in the framework of load capacity factor in Turkiye?," Environment, Development and Sustainability, pp. 1–18, 2023. [CrossRef]
[35] Z. Xiao, "Quantile cointegrating regression," Journal of Econometrics, Vol. 150(2), pp. 248–260, 2009.
[36] B. Brunekreef, and S. T. Holgate, "Air pollution and health," The Lancet, Vol. 360(9341), pp. 1233–1242, 2002. [CrossRef]
[37] M. Jerrett, J. Eyles, C. Dufournaud, and S. Birch, "Environmental influences on healthcare expenditures: an exploratory analysis from Ontario, Canada," Journal of Epidemiology & Community Health, Vol. 57(5), pp. 334–338, 2003. [CrossRef]
[38] P. K. Narayan, and S. Narayan, "Does environmental quality influence health expenditures? Empirical evidence from a panel of selected OECD countries," Ecological Economics, Vol. 65(2), pp. 367–374, 2008. [CrossRef]
[39] H. Abdullah, M. Azam, and S. K. Zakariya, "The impact of environmental quality on public health expenditure in Malaysia," Asia Pacific Institute of Advanced Research, Vol. 2(2), pp. 365–379, 2016.
[40] N. Apergis, R. Gupta, and C. K. M. Lau, and Z. Mukherjee, "US state-level carbon dioxide emissions: does it affect health care expenditure?," Renewable and Sustainable Energy Reviews, Vol. 91, pp. 521–530, 2018. [CrossRef]
[41] O. Y. Alimi, K. B. Ajide, and W. A. Isola, "Environmental quality and health expenditure in ECOWAS," Environment, Development and Sustainability, Vol. 22, pp. 5105–5127, 2020. [CrossRef]
[42] S. Nasreen, "Association between health expenditures, economic growth and environmental pollution: Long-run and causality analysis from Asian economies," The International Journal of Health Planning and Management, Vol. 36(3), pp. 925–944, 2021. [CrossRef]
[43] Z. Xing, and X. Liu, "Health expenditures, environmental quality, and economic development: State-of-the-art review and findings in the context of COP26," Frontiers in Public Health, Vol. 10, Article 954080, 2022. [CrossRef]
[44] J. Bu, and K. Ali, "Environmental degradation in terms of health expenditure, education and economic growth. Evidence of novel approach," Frontiers in Environmental Science, Vol. 10, Article 1046213, 2022. [CrossRef]
[45] M. Benli, "Carbon emission as a determinant of health expenditures," Social Sciences Research Journal, Vol. 11(2), pp. 250–257, 2022.
[46] U. K. Pata, and A. Samour, "Do renewable and nuclear energy enhance environmental quality in France? A new EKC approach with the load capacity factor," Progress in Nuclear Energy, Vol. 149, Article 104249, 2022. [CrossRef]
[47] R. Siche, L. Pereira, F. Agostinho, and E. Ortega, "Convergence of ecological footprint and emergy analysis as a sustainability indicator of countries: Peru as case study," Communications in Nonlinear Science and Numerical Simulation, Vol. 15(10), pp. 3182–3192, 2010. [CrossRef]
[48] Z. Fareed, S. Salem, T. S. Adebayo, U. K. Pata, and F. Shahzad, "Role of export diversification and renewable energy on the load capacity factor in Indonesia: a Fourier quantile causality approach," Frontiers in Environmental Science, Vol. 9, Article 770152, 2021. [CrossRef]

[49] X. Liu, V. O. Olanrewaju, E. B. Agyekum, M. F. El-Naggar, M. M. Alrashed, and S. Kamel, "Determinants of load capacity factor in an emerging economy: The role of green energy consumption and technological innovation," Frontiers in Environmental Science, Vol. 10, Article 2071, 2022. [CrossRef]

[50] U. K. Pata, M. T. Kartal, T. S. Adebayo, and S. Ullah, "Enhancing environmental quality in the United States by linking biomass energy consumption and load capacity factor," Geoscience Frontiers, Vol. 14(3), Article 101531, 2023. [CrossRef]

[51] A. E. Caglar, and E. Yavuz, "The role of environmental protection expenditures and renewable energy consumption in the context of ecological challenges: Insights from the European Union with the novel panel econometric approach," Journal of Environmental Management, Vol. 331, Article 117317, 2023. [CrossRef]

[52] W. X., Zhao, A. Samour, K. Yi, and M. A. S. Al-Faryan, "Do technological innovation, natural resources and stock market development promote environmental sustainability? Novel evidence based on the load capacity factor," Resources Policy, Vol. 82, Article 103397, 2023. [CrossRef]

[53] U. Khan, A. M. Khan, M. S. Khan, P. Ahmed, A. Haque, and R. A. Parvin, "Are the impacts of renewable energy use on load capacity factors homogeneous for developed and developing nations? Evidence from the G7 and E7 nations," Environmental Science and Pollution Research, Vol. 30(9), pp. 24629–24640, 2023. [CrossRef]

[54] B. Guloglu, A. E. Caglar, and U. K. Pata, "Analyzing the determinants of the load capacity factor in OECD countries: Evidence from advanced quantile panel data methods," Gondwana Research, Vol. 118, pp. 92–104, 2023. [CrossRef]

[55] M. Gündüz, "Healthcare expenditure and carbon footprint in the USA: evidence from hidden co-integration approach," The European Journal of Health Economics, Vol. 21(5), pp. 801–811, 2020. [CrossRef]

[56] D. Qaiser Gillani, S. A. S. Gillani, M. Z. Naeem, C. Spulbar, E. Coker-Farrell, A. Ejaz, and R. Birau, "The nexus between sustainable economic development and government health expenditure in Asian countries based on ecological footprint consumption," Sustainability, Vol. 13(12), Article 6824, 2021. [CrossRef]

[57] R. Triki, B. Kahouli, K. Tissaoui, and H. Tlili, "Assessing the link between environmental quality, green finance, health expenditure, renewable energy, and technology innovation," Sustainability, Vol. 15(5), Article 4286, 2023. [CrossRef]

[58] O. Y. Alimi, and K. B. Ajide, "The role of institutions in environment–health outcomes Nexus: empirical evidence from sub-Saharan Africa," Economic Change and Restructuring, Vol. 54(4), pp. 1205–1252, 2021. [CrossRef]

[59] T. S. Adebayo, and A. Samour, "Renewable energy, fiscal policy and load capacity factor in BRICS countries: novel findings from panel nonlinear ARDL model," Environment, Development and Sustainability, pp. 1–25, 2023. [CrossRef]

[60] S. Demir, H. Demir, C. Karaduman, and M. Cetin, "Environmental quality and health expenditures efficiency in Turkiye: The role of natural resources," Environmental Science and Pollution Research, Vol. 30(6), pp. 15170–15185, 2023. [CrossRef]

[61] M. Aydin, and O. Bozatli, "The impacts of the refugee population, renewable energy consumption, carbon emissions, and economic growth on health expenditure in Turkey: new evidence from Fourier-based analyses," Environmental Science and Pollution Research, Vol. 30(14), pp. 41286–41298, 2023. [CrossRef]

[62] S. Erdogan, M. Kirca, and A. Gedikli, "Is there a relationship between CO2 emissions and health expenditures? Evidence from BRICS-T countries," Business and Economics Research Journal, Vol. 11(2), pp. 293–305, 2020. [CrossRef]

[63] A. Khan, J. Hussain, S. Bano, and Y. Chenggang, "The repercussions of foreign direct investment, renewable energy and health expenditure on environmental decay? An econometric analysis of B&RI countries," Journal of Environmental Planning and Management, Vol. 63(11), pp. 1965–1986, 2020. [CrossRef]

[64] M. A. Rehman, Z. Fareed, S. Salem, A. Kanwal, and U. K. Pata, "Do diversified export, agriculture, and cleaner energy consumption induce atmospheric pollution in Asia? Application of method of moments quantile regression," Frontiers in Environmental Science, Vol. 9, Article 781097, 2021. [CrossRef]

[65] L. Du, H. Jiang, T. S. Adebayo, A. A. Awosusi, and A. Razzaq, "Asymmetric effects of high-tech industry and renewable energy on consumption-based carbon emissions in MINT countries," Renewable Energy, Vol. 196, pp. 1269-–280, 2022. [CrossRef]

[66] T. S. Adebayo, U. K. Pata, and S. S. Akadiri, "A comparison of CO2 emissions, load capacity factor, and ecological footprint for Thailand's environmental sustainability," Environment, Development and Sustainability, Vol. 26, pp. 2203–2223, 2022. [CrossRef]

[67] M. T. Kartal, A. Samour, T. S. Adebayo, and S. K. Depren, "Do nuclear energy and renewable energy surge environmental quality in the United States? New insights from novel bootstrap Fourier Granger causality in quantiles approach," Progress in Nuclear Energy, Vol. 155, Article 104509, 2023. [CrossRef]

[68] E. Akhayere, M. T. Kartal, T. S. Adebayo, and D. Kavaz, "Role of energy consumption and trade openness towards environmental sustainability in Turkey," Environmental Science and Pollution Research, Vol. 30(8), pp. 21156–21168, 2023. [CrossRef]

[69] Global Footprint Network, "Data," https://data.footprintnetwork.org/?_ga=2.104275776.1558657453.1678090741-992159244.1678090741#/aboutthe Accessed on Jan 23, 2023.

[70] OECD, "Organisation for Economic Co-operation and Development," https://data.oecd.org/healthres/health-spending.htm Accessed on Jan 05, 2023.
[71] "Our World In Data," https://ourworldindata.org/co2-emissions Accessed on Jan 05, 2023.
[72] "Global Footprint Network," https://www.footprintnetwork.org/ Accessed on Jan 05, 2023.
[73] C. M. Jarque, and A. K. Bera, "A Test for Normality of Observations and Regression Residuals," International Statistical Review, pp. 163–172, 1987. [CrossRef]
[74] D. W. Pearce, and R. K. Turner, "Economics of Natural Resources and The Environment, Johns Hopkins University Press.
[75] R. F. Engle, and C. W. Granger, "Co-integration and error correction: representation, estimation, and testing," Econometrica: Journal of the Econometric Society, pp. 251–276, 1987. [CrossRef]
[76] R. Koenker, and Z. Xiao, "Unit root quantile autoregression inference," Journal of The American Statistical Association, Vol. 99(467), pp. 775–787, 2004. [CrossRef]
[77] S. Portnoy, "Asymptotic behavior of regression quantiles in non-stationary, dependent cases," Journal of Multivariate Analysis, Vol. 38(1), pp. 100–113, 1991. [CrossRef]
[78] Q. R. Syed, W. S. Malik, and B. H. Chang, "Volatility spillover effect of federal reserve's balance sheet on the financial and goods markets of Indo-Pak region," Annals of Financial Economics, Vol. 14(03), Article 1950015, 2019. [CrossRef]
[79] D. A. Dickey, and W. A. Fuller, "Distribution of the estimators for autoregressive time series with a unit root," Journal of the American Statistical Association, Vol. 74(366a), pp. 427–431, 1979. [CrossRef]
[80] "World Bank" https://databank.worldbank.org/source/world-development-indicators Accessed on Jan 25, 2023.
[81] "Turkish Statistical Institute," https://data.tuik.gov.tr/Search/Search?text=motorlu%20kara Accessed on Jan 24.
[82] "Turkish Statistical Institute," https://data.tuik.gov.tr/Kategori/GetKategori?p=Nufus-ve-Demografi-109, website. [Online]. Accessed on Jan 24.
[83] S. Nazlioglu, TSPDLIB: GAUSS Time Series and Panel Data Methods (Version 2.1). Source Code, 2021. https://github.com/aptech/tspdlib Accessed on Jul 17, 2024.

*Environ Res Tec, Vol. 7, Issue. 3, pp. 303–312, September 2024*

**Environmental Research and Technology**
https://ert.yildiz.edu.tr - https://dergipark.org.tr/tr/pub/ert
DOI: https://10.35208/ert.1391806

Environmental Research & Technology

**Research Article**

# Organophosphate, carbamate and synthetic pyrethroid pesticide residues in muscle tissues of fish from Loktak Lake, a Ramsar Site in Manipur, India

**Maisnam SAPANA DEVI[*1], Thingbaijam Binoy SINGH[2], Abhik GUPTA[3]**

*[1]Thambal Marik College, Oinam, Manipur, India*
*[2]Manipur University, Canchipur, Imphal, India*
*[3]Assam University, Silchar, Assam, India*

## ARTICLE INFO

*Article history*
Received: 22 December 2023
Revised: 19 February 2024
Accepted: 20 March 2024

**Key words:**
Fish; High-performance liquid chromatography; Loktak Lake; Maximum residue limit; Pesticide residues

## ABSTRACT

The muscle tissues of *Channa punctatus* and *Anabas testudineus* collected from the Loktak Lake (a Ramsar site) and its three major feeder rivers in Manipur, Northeastern India, were analyzed using high-performance liquid chromatography for the presence of residues of organophosphorus, carbamate, and synthetic pyrethroid pesticides. Pesticide residues of all the three typeswere detected in the fish tissues. Pesticide residues in *Channa punctatus* ranged from 0.002–0.043 μg $g^{-1}$, and from 0.008–0.027 μg $g^{-1}$ in *Anabas testudineus* from Loktak Lake in pre-monsoon and post-monsoon seasons. Pesticide residues were detected only in *Anabas testudineus* (0.002–0.078 μg $g^{-1}$) in Nambul River, while these were detected only in *Channa puctatus* (0.001–0.032 μg $g^{-1}$) in Moirang River. In Nambol River, pesticide concentrations ranged from 0.002–0.026 μg $g^{-1}$ in *Channa punctatus*, and from 0.004–0.005 μg $g^{-1}$ in *Anabas testudineus*. Among the five pesticides detected, concentrations of dichlorvos residues detected in the present study (0.027 and 0.032 μg $g^{-1}$ wet weight) exceeded the *Codex Alimentarius* maximum residue limit (MRL) of 0.01 mg $kg^{-1}$ for animal tissues. The rest of the compounds were within the MRL. None of the pesticide residues was detected in the two fish species collected from the control or reference site. The present study indicates that pesticide contamination is emerging as a threat to the water quality and aquatic biodiversity of Loktak Lake, which calls for more detailed studies on the extent and magnitude of these threats.

**Cite this article as:** Sapana Devi M, Singh TB, Gupta A. Organophosphate, carbamate and synthetic pyrethroid pesticide residues in muscle tissues of fish from Loktak Lake, a Ramsar Site in Manipur, India. Environ Res Tec 2024;7(3)303–312.

## INTRODUCTION

Pesticides, besides killing the target pests, also kill or adversely affect the non-target organisms, contaminate the environment, and pose threats to aquatic ecosystems and human health [1]. Organophosphates, carbamates and synthetic pyrethroids are among the commonly used pesticides known to affect human health and the environment [2]. It is well established that organophosphate pesticides are the long lasting inhibitors of cholinesterases and a number of organophosphates are prohibited in many countries from being sold in the market due to their toxicity at low doses [3]. The carbamates are known to impair acetylcholinesterase (AChE) activity in a way similar to the mode of action of organophosphate pesticides. They are also known to cause reproductive failure through endocrine disruption and infertility [4]. Synthetic pyrethroids which are fast replacing organophosphates are also extremely toxic to fish because

***Corresponding author.**
*E-mail address: sapana.devi@gmail.com

of their neurotoxic effects [5, 6]. Therefore, the detection of the residues of these pesticides in different environmental compartments becomes an issue of global concern.

Pesticides applied in agricultural fields can reach aquatic ecosystems via surface runoff and leave harmful residues in the ecosystems that can adversely affect aquatic biota, particularly fish. The pesticide residues in aquatic ecosystems are often transferred to humans through the food chain via phytoplankton, zooplankton and fish [7]. Several studies have shown that continuous intake of pesticide residues through food, even in lowdoses, can cause adverse effects on the environment as well as on plants, fish, wildlife, and other non-target organisms [8]. These effects could comprise endocrine disruption, neurological damages, and birth defects [9–11].

Several organophosphate, carbamate and synthetic pyrethroid pesticides are being increasingly usedfor controlling agricultural pests in Manipur - a state in the northeastern region of India - during the past several decades. Many studies have suggested that indiscriminate application of pesticides in agricultural activities such as in paddy fields and other cultivated areas near aquatic ecosystems have increased the probability of the entry of pesticide residues into the lakes where the rivers finally drain [12–14]. In this regard, Loktak Lake in Manipur, which is a "wetland of international importance" (Ramsar Site) and the largest freshwater Lake in northeast India, is highly vulnerable to contamination by pesticide residues through its three major feeder rivers: the Nambul, the Moirang and the Nambol [15]. These rivers receive agricultural and domestic wastes from inhabited areas to ultimately drain into the Loktak Lake, a Ramsar site in Manipur, India. The heavy influx of such wastes threatens the biodiversity of the lake, especially aquatic macrophytes and indigenous freshwater fishes. The situation has been made more precarious by the construction of the Ithai barrage, which has obstructed the outlet of the lake. This has affected the normal movement of water in the lake, thereby raising the possibility of accumulation of pesticide residues in water, sediment and biota, particularly fish, in the Lake. It is also pertinent to mention here that different species of fish which were once abundantly available in the Lake such as (state fish of Manipur) etc. are now becoming threatened [16]. It is possible that reproductive failure due to continuous exposure to low concentrations of pesticide residues accumulated in the Lake over a period of time could be one of the reasons for the decimation of fish fauna in the Lake.

Among aquatic organisms, fish is considered a useful component for monitoring environmental contaminants and an important source of animal protein to humans. Contamination of fish by pesticide residues, therefore, has proven to be a serious risk to its consumers including humans [17]. The two fish species, *Channa punctatus* and *Anabas testudineus* selected in this study are abundantly available in Loktak Lake, and also comprise favorite food items of the local people. While *Channa punctatus* is a carnivore, *Anabas testudineus* is an omnivore [18, 19].

Several analytical methods have been used for determination of pesticide residues in foodstuffs including fisheries products [17, 20]. Among these methods, high-performance liquid chromatography (HPLC) is regarded as a useful tool in the laboratory because of its highly precise quantitative results, very low detection limits and an exceptional degree of selectivity for qualitative identifications of target analytes [21]. Moreover, HPLC with a diode-array detector (DAD) is considered as an advanced method which has the capability of collecting chromatographic data and UV spectra simultaneously [22].

In the last few years, several studies have been conducted worldwide to analyze the presence of pesticide residues in freshwater ecosystems [20, 23–33]. On the other hand, investigations on detection of pesticide residues in freshwater ecosystems in India are relatively rare and more so in the freshwater lakes and wetlands of North-east India [34]. In this context, this study investigates the presence of pesticide residues in two fish species *Channa punctatus* and *Anabas testudineus* representing two different trophic levels, and collected from the Loktak Lake and its three major feeder rivers. Six pesticides including three organophosphates (dichlorvos, malathion and monocrotophos), one carbamate (carbofuran), and two synthetic pyrethroids (deltamethrinand cypermethrin), which are commonly used in the study area, were selected for analysis and possible detection in fish muscle. This is probably the first study that aims to ascertain the status of pesticide residues in fish of Loktak Lake. The findings are expected to throw light on the status of pesticide contamination of Loktak Lake and serve as an 'early warning report' of the threats posed by pesticides to this important ecosystem along with potential health risks to the people of Manipur who are consumers of its fish.

## MATERIALS AND METHODS

### Study Sites

Loktak Lake (24°33′N 93°47′E) of Manipur, North East India and its three major feeder rivers, viz., the Nambul River (northern feeder), the Nambol River (western feeder), and the Moirang River (south western feeder), were selected for the present study. Loktak Lake, about 45 km from Imphal, the capital of Manipur, is a "wetland of international importance" (Ramsar Site) since 1990 and is well-known for being the only natural habitat of the endangered brow-antlered deer (Ruc*ervus eldii eldii*) (Fig. 1). It is also the largest freshwater lake in the northeastern region of India. The central part of the lake was selected for the study because most of the central areas of the lake are covered by a large number of 'phumdis' (heterogeneous mass of floating vegetation) due to the construction of the Ithai Barrage across the natural outlet of the lake. Hence, the possibility of the concentration of pesticide residues was high in this part of the lake. Study sites selected in the three tributaries were near their point of entry into the lake after traversing extensively cultivated and inhabited areas. A fish pond, which was about 5.7 km away from paddy fields or other cultivated areas and 35 km away from the study sites of Loktak Lake, was selected as the control or reference site.

**Procurement of Fish, Selection of Sampling Season and Experimental Design**

Specimens of *Channa punctatus* and *Anabas testudineus* were collected from the five sampling sites in three seasons, viz., pre-monsoon (April–June), monsoon (July–September) and post-monsoon (October–December). Different types of nets, especially conventional gill nets were used to capture the fish with the help of local fishermen. The net was hauled at short intervals and trapped fish, if any, were immediately transferred to polythene bags containing water of the given site and saturated with extra oxygen. Since both the fish species are air-breathing, this practice of sampling exerted minimum stress. Fish samples comprising of six individuals of similar size (length and weight 24±1 g and 15±1 cm, respectively, for *Channa punctatus*; 22±1 g and 11±1 cm, respectively, for *Anabas testudineus*) belonging to both species were collected from each study site in the three seasons. The fish were brought to the laboratory and immediately sacrificed by injecting a high dose of Tricaine Methanesulfonate (MS-222) after taking their morphometric measurements. Each fish was dissected and muscles from the mid dorsal side were collected. The analysis of pesticide residues in the sampled fish muscles tissues was conducted by using high-performance liquid chromatography (HPLC) with diode-array detector (DAD).

**High-Performance Liquid Chromatography Analysis of Pesticide Residues**

***Procurement of Pesticide Standards and Reagents***

Altogether six (6) pesticide standards belonging to three major pesticide groups were purchased from the Sigma-Aldrich Laborchemikalien GmbH D – 30918 Seelze, Quality Management SA-LC. These comprised three organophosphates (malathion, monocrotophos, dichlorvos), one carbamate (carbofuran), and two synthetic pyrethroid (deltamethrin and cypermethrin) pesticides. The purity of all these pesticide standards was over 99% except for Cypermethrin (94.3%). Besides, HPLC grade water, acetone and acetonitrile were also purchased from Merck.

***Equipments***

The equipments used in various analytical procedures were: Shimadzu AUW 220D analytical balance, micropipette 200 µL and 1000 µL (Oxford, Ireland), rotary evaporator (Buchi, model 011, Switzerland), centrifuge (Remi Instrument Ltd.), and HPLC Agilent 1260 Infinity - DAD detector (Germany).

***Procedure for Extraction of Pesticide Residues from Fish Muscle Tissues***

The pesticide residue extraction procedure was performed by following a slight modification of the standard protocol of Sun et al. [17]. Six replicates of the two fish species *Channa punctatus* and *Anabas testudineus* collected from each study site were dissected and 2 g of muscle tissues for each fish species (either *Channa punctatus* or *Anabas testudineus*) in a pool were homogenized in a mortar and pestle with 5 ml of HPLC grade acetone. The resultant extracts were centrifuged at 4000 rpm for 10 minutesto remove all the cell debris and unwanted materials [35]. Two ml of the extracts were then evaporated to dryness under reduced pressure in a rotary evaporator at 40 °C. Finally, the dry extract was dissolved in 2 ml of HPLC grade acetonitrile and the resulting extracts were then centrifuged at 4000 rpm for 10 minutes and the supernatant was used for HPLC analysis. The sample preparation or sample extraction was repeated thrice to have three replicates of each sample from a study site of a particular season.

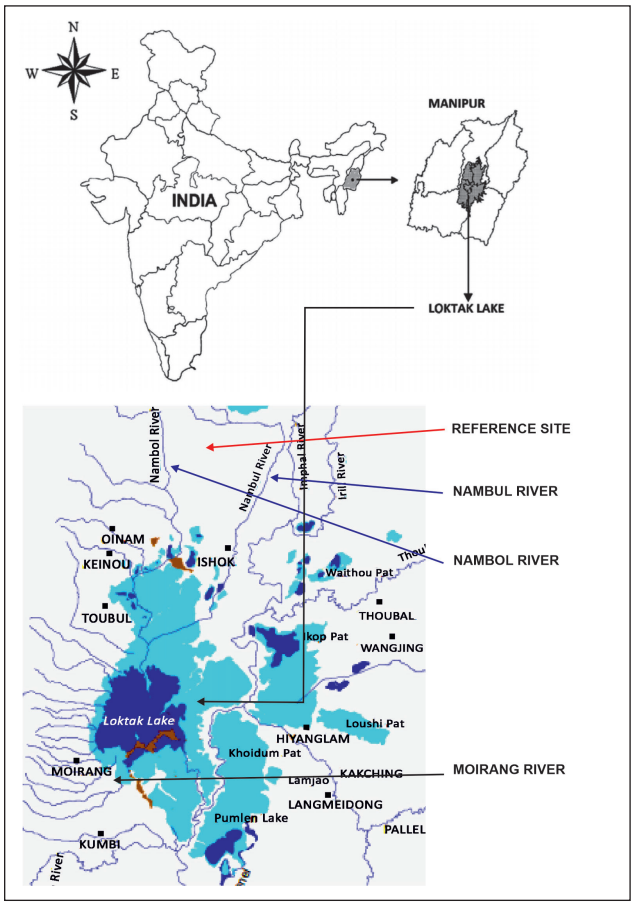


**Figure 1**. Map of Loktak Lake showing its feeder rivers of Nambul, Nambol and Moirang along with reference or control site.

***HPLC Conditions and Analysis***

The standards and samples were analyzed for pesticide residues by using HPLC Agilent 1260 Infinity having DAD detector. Standard calibration curves of each pesticide were drawn with three concentrations i.e. 1 ppm, 50 ppm and 100 ppm for each standard pesticide (dichlorvos, malathion, monocrotophos, carbofuran, deltamethrin and cypermethrin) respectively. Identification of pesticides was executed by comparing sample retention times with those obtained for the standards, while quantification of different pesticides was done by comparing the areas of sample peaks with those of their respective standards. All the glassware was washed with detergent,

**Table 1.** Concentrations of organophosphorus, carbamate and synthetic pyrethroid pesticides (μg $g^{-1}$ wet weight) in muscles of two fish species from Loktak Lake and its three major feeder rivers along with a reference site in three seasons

| Concentration in muscle tissue (μg g-1 wet weight) | | | | | | |
|---|---|---|---|---|---|---|
| **Fish species** | **Season** | **Loktak lake** | **Moirang river** | **Nambol river** | **Nambul river** | **Ref. site** |
| *Channa punctatus* | Pre-monsoon | Mt: 0.002±1E-04** | Mt: 0.001±5.77E-05** | ND | ND | ND |
| | Monsoon | Dv: 0.027±0.0006 | Dv: 0.032±0.0006 | ND | ND | ND |
| | | Cf: 0.043±0.0006 | | Mt: 0.002±5.77E-05** | | |
| | Post-monsoon | Mt: 0.027±0.0006** | ND | Cf: 0.026±0.0006 | ND | ND |
| *Anabas testudineus* | Pre-monsoon | Dm: 0.009±5.77E-05* | ND | Cm: 0.004±0.0001* | Mt: 0.019±0.0004** | ND |
| | | | | | Cm: 0.002±5.77E-05* | |
| | Monsoon | ND | ND | ND | ND | ND |
| | Post-monsoon | Mt: 0.008±5.77E-05** | ND | ND | Mt: 0.078±0.0004** | ND |
| | | | | Mt: 0.004±5.77E-05** | | |
| | | | | Cf: 0.005±5.77E-05 | | |

The values represent mean±SD {significance level: p≤0.05(*), p≤0.01(**)}. Ref: Reference; Cf: Carbofuran; Cm: Cypermethrin; Dv: Dichlorvos; Dm: Deltamethrin; Mt: Malathion; ND: Not detected.

rinsed with HPLC grade water and heated at 180 °C for 2 h before use. We tested different wavelengths between 202 and 290 nm for the optimum identification of pesticides in different samples. The wavelengths of 202 nm for deltamethrin, cypermethrin and malathion; 220 nm for dichlorvos; and 272 nm for carbofuran and monocrotophos were observed to be the optimum. Based on their respective wavelengths detected, pesticides were grouped as group 1, group 2 and group 3 employing standard HPLC conditions. Group 1 compriseddeltamethrin, cypermethrin and malathion, group 2 dichlorvos, and group 3 carbofuran and monocrotophos. The column and injection volume for all the three groups were Column (SB-C18), 250 × 4.6 mm, 5.0 μm and 20 μL, respectively. The flow rate was 1 ml $min^{-1}$ for group 1, and 1.4 ml $min^{-1}$ for both group 2 and 3. Mobile phase ratio for group 1 was acetonitrile/water (10% acetonitrile for 5 minutes, gradually increased to 100% acetonitrile within 15 minutes and then maintainedat 100% acetonitrile for 5 minutes) with a run time of 20 minutes; for both group 2 and 3, it was acetonitrile/water (40:60) with a run time of 10 minutes each. Sample analysis of three replicates of a particular fish (*C. punctatus* or *A. testudineus*) sample from a study site in a particular season was done consecutively following above conditions of HPLC.

### Data Analysis

The data were first checked for normality with the Shapiro-Wilk test. Since the data were not normally distributed, these were normalized by log transformation. Statistical significance of differences in concentration of pesticide residues among the sampling sites and fish species were determined by One-Way Analysis of Variance (ANOVA) using SPSS 20 software. The results were denoted significant at p ≤0.05, and highly significant at p ≤0.01.

## RESULTS AND DISCUSSION

### Standard Calibration Curves and Chromatogram

Calibration graph of the standard solution concentrations of each pesticide are shown in Appendices 1–6. The cal- culations were made following the equation y = mx + b, where m is the regression co-efficient, y is the area, x is the amount and b is the residual standard deviation. The retention times of the standard pesticides were found to be 2.13, 13.55, 0.74, 2.74, 16.28 and 16.14 minutes for dichlorvos, malathion, monocrotophos, carbofuran, deltamethrin and cypermethrin, respectively. Moreover, the standard calibration curves of peak area against concen tration as well as chromatograms of dichlorvos, malathion, monocrotophos, carbofuran, deltamethrin and cyper methrin are shown in Appendices 1–6.

### Pesticide Residue Analysis in Fish Muscle Tissue

The occurrence of the residues of the six pesticides in the muscle tissues of *Channa punctatus* and *Anabas testudineus* are presented in Table 1. Of the three organophosphate pesticides analyzed in the present study, dichlorvos residues were detected only in *Channa punctatus* collected from Loktak Lake (0.027±0.0006 μg $g^{-1}$) and Moirang River (0.032±0.0006 μg $g^{-1}$) during monsoon season. Malathion residue was detected in both *Channa punctatus* and *Anabas testudineus* collected from Loktak Lake (0.002±1E-04**μg $g^{-1}$; 0.027±0.0006**μg $g^{-1}$, 0.008±5.77E-05**μg $g^{-1}$), and Nambol River (0.002±5.77E-05**μg $g^{-1}$; 0.004±5.77E-05**μg $g^{-1}$) during pre-monsoon and post-monsoon seasons (p≤0.01), however, in Moirang River malathion residue was found only in *Channa punctatus* (0.001±5.77E-05**μg $g^{-1}$) in pre-monsoon; Nambul River only in *Anabas testudineus* collected during pre-monsoon (0.019±0.0004**μg $g^{-1}$) and post-monsoon (0.078±0.0004**μg $g^{-1}$) seasons respectively (Table 1). Monocrotophos residue was not detected

in fish collected from any study site in the three seasons. Residues of none of the organophosphorus pesticides were detected in the samples of the two fish species collected from the control or reference site (Table 1).

Dichlorvos residues detected in the present study (0.027 and 0.032 μg $g^{-1}$ wet weight) were above the MRL of 0.01 mg $kg^{-1}$ in animal tissue and products such as edible mammalian offal, eggs, mammalian fats, meat, milk, and fat, meat and offal of poultry, as laid down in the *Codex Alimentarius* [36]. An earlier study revealed that the strongest inhibition of brain AChE was found in association with high dichlorvos residues [37]. This indicates that the bioaccumulation of dichlorvos residues in fish tissues in the study area even in small quantities may alter or inhibit brain AChE- enzyme activities in fish which in turn could similarly affect its consumers including larger carnivorous fish, fish-eating mammals like otters, and humans, through the food chain. Brodeur et al. [26] also detected dichlorvos in tissues of one-sided livebearer fish (*Jenynsia multidentata*) which further revealed an inhibition in the activity of ChE in association with reduced body condition. The *Codex* limit for malathion in animal products is not available, although its concentrations were found to be higher on two occasions in *Anabas testudineus* than the MRL prescribed for some plant products such as sweet corn and tomato juice (0.02 and 0.01 mg $kg^{-1}$, respectively) [36]. Among all the pesticides, malathion residues were detected more frequently and in more study sites and seasons ($p \leq 0.01$)in both the fish species (Table 1), reflecting the fact that it is one of the most commonly applied pesticide in the study area. Amaraneni and Pillala [38] reported the detection of malathion residue in tissues of fish *Channa striata* and *Catla catla* collected from Kolleru Lake in India where the value was found to be 2.5 μg $g^{-1}$ wet weight, which was considerably higher than the highest concentration of malathion residue detected in the present study, i.e. 0.078 μg $g^{-1}$ wet weight in *Anabas testudineus* collected from the Nambul River during post-monsoon season (Table 1). Maurano et al. [39] detected malathion residues in the muscle tissues of two fish species *Carassius carassius* and *Mugil cephalus* collected from Sele River in SouthItaly where the concentrations were found to be 480 pg $g^{-1}$ and 582 pg $g^{-1}$ wet weight, respectively, which were comparatively much less than the lowest concentration of malathion residue detected in the present study i.e. 0.001 μg $g^{-1}$ wet weight in *Channa punctatus* collected from the Moirang River during pre-monsoon season (Table 1). Possible reasons for not detecting monocrotophos residues in the present study include its rapid hydrolysis and conjugation in fish tissues [40].

Carbofuran is a broad spectrum carbamate pesticide used world-wide to control insects, mites and nematodes, which has been widely detected in surface, ground and rain waters and is extremely toxic to aquatic organisms including fish [20, 41]. In our study, carbofuran was detected in *Channa punctatus* collected from Loktak Lake (0.043±0.0006 μg $g^{-1}$) and Nambol River (0.026±0.0006 μg $g^{-1}$) and in *Anabas testudineus* collected from Nambol River (0.005±5.77E-05 μg $g^{-1}$) during post-monsoon (Table 1). The value of 0.043 μg $g^{-1}$ recorded in *Channa punctatus* in Loktak Lake in post-monsoon was close to its *Codex* MRL of 0.05 μg $g^{-1}$ in animal products such as cattle, goat, sheep, pig and horse fat, and offal of cattle, goat, horse, sheep and pig [36]. Thus, carbofuran posed a health risk to the consumers of this fish in this area. Jabeen et al. [20] detected carbofuran residues in muscle tissues of fish *Labeo rohita* and *Channa marulius* collected from the Indus River around Mianwali where the concentrations ranged from 0.0425–0.066 μg $g^{-1}$ and 0.613–0.946 μg $g^{-1}$, respectively. Carbofuran concentrations in *Labeo rohita* were comparable to its levels in *Chana punctatus* in our study. Vryzas et al. [42] also mentioned about the detection of carbofuran at the highest concentration on a regular basis in the three trophic levels: algae, aquatic invertebrates and fish in drainage canals of two transboundary rivers of northeastern Greece, where its extreme concentrations were observed just after the occurrence of high rainfall during pesticide application, thus posing a threat to aquatic organisms and subsequently to the fish-consumers. Mahboob et al. [43] also recorded concentrations of carbofuran residue in the muscle tissues of fish, *Catla catla* at 1.23 and 8.53 μg $g^{-1}$ lipid-normalized weight. However, carbofuran is known to undergo rapid degradation and elimination from fish tissues [40].

In the last two decades, synthetic pyrethroids have been replacing organochlorines and organophosphates in India for controlling pests to increase agricultural productivity [7]. Deltamethrin and cypermethrin are commonly used synthetic pyrethroids in agriculture for controlling pests. Being type 2 (α-cyano) synthetic pyrethroids, these two pyrethroids are more potently neurotoxic than the non-cyano type 1 [6]. In the present study, deltamethrin residues were only recorded in the muscle tissue of *Anabas testudineus* collected from Loktak Lake during the pre-monsoon season ($p \leq 0.05$) at a concentration of 0.009±5.77E-05*μg $g^{-1}$ (Table 1) which was below the maximum residual limit (MRL) of 0.02 mg $kg^{-1}$ in poultry offal [36]. Notwithstanding this, it may be noted that deltamethrin could disrupt enzyme activities and reduce glycogen and protein levels in fish *Anabas testudineus* at a concentration (0.0007 mg $l^{-1}$) one order of magnitudelower than that recorded in the present study (0.009 μg $g^{-1}$) [44]. On the other hand, cypermethrin residues were detected in the muscle tissues of *Channa punctatus* and *Anabas testudineus* collected from Nambol and Nambul Rivers ($p \leq 0.05$) during post- and pre-monsoon seasons (Table 1) at concentrations of0.004±0.0001* μg $g^{-1}$ and 0.002±5.77E-05* μg $g^{-1}$, respectively, while the WHO-FAO MRL is0.05 mg $kg^{-1}$ in edible mammalian offal, and 0.01 mg $kg^{-1}$ in eggs. Deltamethrin and cypermethrin residues were not detected in the two fish species collected from the control or reference site (Table 1). Saqib et al. [45] reported the detection of deltamethrin residue in 7 samples of muscles, liver and fat tissue of the three species of *Labeo* found in two Lakes in Pakistan. Jabeen et al. [20] reported the presence of deltamethrin residues in muscles of fish *Cyprinus carpio* and *Channa marulius* with concentrations

ranging from 0.051–0.839 μg $g^{-1}$, and cypermethrin residues in fish *Channa marulius* (0.141–0.174 μg $g^{-1}$). These values are much higher than those detected in the present study. Mahboob et al. [43] reported that the concentration of deltamethrin in the muscle tissues of *Catla catla* in river Ravi was higher than the permissible limits for fish set by international agencies and it posed a potential risk to the aquatic organisms and ultimately to human health. Meanwhile, high concentrations of cypermethrin residues were also detected by Vryzas et al. [42] in three trophic levels including fish where its peak concentrations were observed just after high rainfall during pesticide application.In the present study, the detection of cypermethrin and deltamethrin residues in the muscle tissues of the two fish species *Channa punctatus* and *Anabas testudineus* ($p \leq 0.05$) at concentrations far below their maximum residual limits indicates that these two pesticides are yet to become a serious threat to the Loktak ecosystem.

## CONCLUSION

The present study revealed that most of the pesticide residues were detected in Loktak Lake in the post-monsoon season. This may be due to the continuous inflow of pesticide-contaminated agricultural runoff to the Lake via its feeder streams and rivers, and this inflow increased during the monsoon, leading to the detection of higher pesticide values in fish tissue during post-monsoon. Among the feeder rivers, more pesticide residues were detected in Nambol River than in the other two, because this river passes through a larger stretch of agricultural areas compared to Nambul and Moirang Rivers. Among the five pesticide residuesdetected, only dichlorvos exceeded the maximum residue limit (MRL) prescribed by the *Codex Alimentarius* for animal tissues, suggesting possible health risks to its consumers including predatory fish, migratory as well as resident waterfowl, and humans. The rest of the compounds were within the MRL laid down for eggs and animal tissues revealing low risk to the consumers of these fish. Nevertheless, pesticides even at sub-lethal levels are known to cause adverse effects on fish, besides posing human health risks on long-term exposure,especially because the inhabitants of the study area are regular consumers of fish and dried fish products. Hence, the concerned authorities and regulatory agencies both at the state and central (federal) levels in cooperation with local non-government organizations should make efforts to create awareness through print and electronic media so that people may realize the hazardous effects of pesticide residues to humans due to bioaccumulation and bio-magnification through the food chain. Moreover, the concerned authorities may promote organic farming and implement integrated pest management measures in the catchment area of the lake and introduce a continuous monitoring program in order to provide pesticide-free environment in the Loktak Lake, which is a "wetland of international importance" (Ramsar Site) and therefore, deserves all possible measures for improvement of its water quality and protection of its biodiversity.

## ACKNOWLEDGEMENTS

Maisnam Sapana Devi (MSD) is grateful to the Department of Biotechnology and Indian Institute of Sciences, Bangalore, Govt. ofIndia, for the award of DBT-Research Associateship Post-doctoral fellowship program. The authorsare thankful to the Department of Life Sciences and Department of Biotechnology, Manipur University, India and to the Indian Council of Agricultural Research (ICAR), North East Hill Region, Manipur Centre, Lamphel, Imphal, India for providing the required laboratory facilities during the research work. MSD is also thankful to Dr. Aribam Satishchandra Sharma and Dr. Bhaben Chowardhara for assisting her in carrying out the statistical analysis. The award of DBT-Research Associateship Post-doctoral fellowship program funded by Department of Biotechnology and Indian Institute of Sciences, Bangalore, Govt. of India.

## DATA AVAILABILITY STATEMENT

The author confirm that the data that supports the findings of this study are available within the article. Raw data that support the finding of this study are available from the corresponding author, upon reasonable request.

## CONFLICT OF INTEREST

The author declared no potential conflicts of interest with respect to the research, authorship, and/or publication of this article.

## USE OF AI FOR WRITING ASSISTANCE

Not declared.

## ETHICS

There are no ethical issues with the publication of this manuscript.

## REFERENCES

[1] S. S. Anigol, S. B. Neglur, and M. David, "Blood glucose and glycogen levels as indicators of stress in the freshwater fish, Cirrihinus mrigal under Cyphenothrin intoxication," Toxicology International, Vol. 30(1), pp. 51–62, 2023. [CrossRef]

[2] D. B. Barr, and B. Buckley, "Reproductive and Developmental Toxicology," 2nd ed., R. C. Gupta, (Ed.), Academic Press, 2011.

[3] S. M. Barlow, F. M. Sullivan, and R. K. Miller, "Drugs during pregnancy and lactation," 3rd. ed., C. Schaefer, P. Peters, and R. K Miller (Eds.), Academic Press, 2015.

[4] R. C. Gupta, I. R. M. Mukherjee, R. B. Doss, J. K. Malik, and D. Milatovic, "Reproductive and Developmental Toxicology," 2nd ed., R. C. Gupta, Ed.), Academic Press, 2017.

[5] E. L. Amweg, D. P. Weston, J. You, and M. J. Lydy, "Pyrethroid insecticides and sediment toxicity in urban creeks from California and Tennessee," Environmental Science & Technology, Vol. 40, pp. 1700–1706, 2006. [CrossRef]

[6] A. Kaviraj, and A. Gupta, "Biomarkers of type II synthetic pyrethroid pesticides in freshwater fish," Biomarkers of Environmental Pollutants, Vol. 2014, Article 928063, 2014. [CrossRef]

[7] B. K. Das, and S. C. Mukherjee,"Toxicity of cypermethrin in Labeo rohita fingerlings: biochemical, enzymatic and haematological consequences," Comparative Biochemistry and Physiology C: Toxicology & Pharmacology, Vol. 134, pp. 109–121, 2003. [CrossRef]

[8] C. A. Damalas, and I. G. Eleftherohorinos, "Pesticide exposure, safety issues and risk assessment indicators," International Journal of Environmental Research and Public Health, Vol.8, pp. 1402–1419, 2011. [CrossRef]

[9] A. C. Gore, "Organochlorine pesticides directly regulate gonadotropin-releasing hormone gene expression and biosynthesis in the GT1-7 hypothalamic cell line," Molecular and Cellular Endocrinology, Vol. 192, pp. 157–170, 2002. [CrossRef]

[10] L. G. Costa, G. Giordano, M. Guizzetti, and A. Vitalone, "Neurotoxicity of pesticides: a brief review," Frontiers in Bioscience, Vol. 13, pp, 1240–1249, 2008. [CrossRef]

[11] L. Fenster, B. Eskenazi, M. Anderson, and A. Vitalone, "Association of in utero organochlorine pesticide exposure and fetal growth and length of gestation in an agricultural population," Environmental Health Perspectives, Vol. 114, pp. 597–602, 2006. [CrossRef]

[12] R. J. Gilliom, and D. G. Clifton, "Organochlorine pesticide residues in bed sediments of the San Joaquin river, California," Journal of the American Water Resources Association, Vol. 26, pp. 11–24, 1990. [CrossRef]

[13] S. M. Gitahi, D. M. Harper, M. Muchiri, M. P. Tole, and R. N. Ng'ang'a, "Organochlorine and organophosphorus pesticide concentrations in water, sediment, and selected organisms in Lake Naivasha (Kenya)," Hydrobiologia, Vol. 488, pp. 123–128, 2002. [CrossRef]

[14] E. Y. A. Pazou, M. Boko, C. A. M.Van Gestel, H. Ahissou, P. Lalèyè, S. Akpona, B. van Hattum, K. Swart, and N. M. van Straalen, "Organochlorine and organophosphorous pesticide residues in the Ouémé River catchment in the Republic of Bénin," Environment International, Vol. 32, pp. 616–623, 2006. [CrossRef]

[15] S. Gupta, "Loktak lake in Manipur, North east India: major issues in conservation and management of a Ramsar site," Bionano Frontier, pp. 6–10, 2012.

[16] S. Samom, "Polluted river in Manipur devastates fish and humans," News Blaze, Sunday, May 4, 2008.

[17] F. Sun, S. S. Wong, G. C. Li, and S. N. Chen, "A preliminary assessment of consumer's exposure to pesticide residues in fisheries products," Chemosphere, Vol. 62, pp. 674–680, 2006. [CrossRef]

[18] A. Khan, and K. Ghosh,"Characterization and identification of gut-associated phytase-producing bacteria in some freshwater fish cultured in ponds," ActaIchthyologica et Piscatoria, Vol. 42, pp. 37–45, 2012. [CrossRef]

[19] B. C.Biswas, and A. K. Panigrahi, "Diversity of exotic fishes and their ecological importance in southwestern part of Bangladesh," International Journal of Innovative Research in Science Engineering and Technology, Vol. 1, pp. 129–131, 2014.

[20] F. Jabeen, A. S. Chaudhry, S. Manzoor, and T. Shaheen, "Examining pyrethroids, carbamates and neonicotenoids in fish, water and sediments from the Indus River for potential health risks," Environmental Monitoring and Assessment, Vol. 187(2), Article 29, 2015. [CrossRef]

[21] S. J. Lehotay, K. Mastovska, A. R. Lightfield, R. A. Gates, "Multi-analyst, multi-matrix performance of the QuEChERS approach for pesticide residues in foods and feeds using HPLC/MS/MS analysis with different calibration techniques," Journal of AOAC International, Vol. 93, pp. 355–367, 2010. [CrossRef]

[22] Y. Cho, N. Matsuoka, and A. Kamiya, "Determination of organophosphorous pesticides in biological samples of acute poisoning by HPLC with diode-array detector," Chemical and Pharmaceutical Bulletin, Vol. 45, pp. 737–740, 1997. [CrossRef]

[23] T. A. Anderson, C. J. Salice, R. A. Erickson, S. T. McMurry, S. B. Cox, and L. M. Smith, "Effects of landuse and precipitation on pesticides and water quality in playa lakes of the southern high plains," Chemosphere, Vol. 92(1), pp. 84–90, 2013. [CrossRef]

[24] E. M. Veljanoska-Sarafiloska, M. Jordanoskiand, and T. Stafilov, "Presence of DDT metabolites in water, sediment, and fish muscle tissue from Lake Prespa, Republic of Macedonia," Journal of Environmental Science and Health- Part B Pesticides, Food Contaminants, and Agricultural Wastes, Vol. 48, pp. 548–558, 2013. [CrossRef]

[25] M. Pirsaheb, H. Hossini, F. Asadi, and H. Janjnai," A systematic review on organochlorine and organophosphate pesticides content in water resources," Toxin Reviews, Vol. 36, pp. 210–221, 2016.

[26] J. C. Brodeur, M. Sanchez, L. Castro, D. E. Rojas, D. Cristos, M. J. Damonte, M. Belén Poliserpi, M. F. D'Andrea, and A. E. Andriulo, "Accumulation of current-use pesticides, cholinesterase inhibition and reduced body condition in juvenile one-sided livebearer fish (Jenynsia multidentata) from the agricultural Pampa region of Argentina," Chemosphere, Vol. 185, pp. 36–46, 2017. [CrossRef]

[27] M. Houbraken, V. Habimana, D. Senaeve, E. López-Dávila, and P. Spanoghe "Multi-residue determination and ecological risk assessment of pesticides in the lakes of Rwanda,"Science of the Total Environment, Vol. 576, pp. 888–894, 2017. [CrossRef]

[28] P. Kaczyński, B Łozowicka, M. Perkowski, and J. Rusilowska, "Multiclass pesticide residue analysis in fish muscle and liver on one-step extraction – cleanup strategy coupled with liquid chromatography tandem mass spectrometry," Ecotoxicology and Environmental Safety, Vol. 138, pp. 179–189, 2017. [CrossRef]

[29] W. Tang, D. Wang, J. Wang, Z. Wu, L. Li, M. Huang, S. Xu, and D. Yan "Pyrethroid pesticide residues in the global environment: an overview," Chemosphere, Vol. 191, pp. 990–1007, 2018. [CrossRef]

[30] A. Deknock, N. D. Troyer, M. Houbraken, L. Dominguez-Granda, I. Nolivos, W. Van Echelpoel, M. A. Eurie Forio, P. Spanoghe, P. Goethals, "Distribution of agricultural pesticides in the freshwater environment of the Guayas river basin (Ecuador)," Science of the Total Environment, Vol. 646, pp. 996–1008, 2019. [CrossRef]

[31] M. Kapsi, C. Tsoutsi, A. Paschalidou, and T. Albanis, "Environmental monitoring and risk assessment of pesticide residues in surface waters of the Louros River (N.W. Greece)," Science of the Total Environment, Vol. 650, pp. 2188–2198, 2019. [CrossRef]

[32] A. M. Taiwo, "A review of environmental and health effects of organochlorine pesticide residues in Africa," Chemosphere, Vol. 220, pp. 1126–1140, 2019. [CrossRef]

[33] C. Olisah, O. O. Okoh, and A. I. Okoh, "Occurrence of organochlorine pesticide residues in biological and environmental matrices in Africa: a two decade review," Heliyon, Vol. 6, Article e03518, 2020. [CrossRef]

[34] R. Mondal, A. Mukherjee, S. Biswas, and R. K. Kole, "GC-MS/MS determination and ecological risk assessment of pesticides in aquatic system: a case study in Hooghly River basin in West Bengal, India," Chemosphere, Vol. 206, pp. 217–230, 2018. [CrossRef]

[35] S. Wang, B. Xiang, and Q, Tang, "Trace determination of dichlorvos in environmental samples by room temperature ionic liquid-based dispersive liquid-phase microextraction combined with HPLC," Journal of Chromatographic Science, pp. 1–7, 2012. [CrossRef]

[36] WHO-FAO. Codex Alimentarius: International Food Standards. World Health Organization and Food and Agriculture Organization of the United Nations. 2016. Available: http://www.fao.org/fao-who-codexalimentarius/standards/pestres/pesticides/en/ Accessed on Apr 19, 2024.

[37] T. E. Horsberg, T. Høy, and I. Nafstad, "Organophosphate poisoning of Atlantic salmon in connection with treatment against salmon lice," Acta Veterinaria Scandinavica, Vol. 30, pp. 385–390, 1989. [CrossRef]

[38] S. R. Amaraneni, and R. R. Pillala,"Concentrations of pesticide residues in tissues of fish from Kolleru Lake in India," Environmental Toxicology, Vol. 16, pp. 550–556, 2001. [CrossRef]

[39] F. Maurano, M. Guida, G. Melluso, and G. Sansone, "Accumulation of pesticide residues in fishes and sediments in the river Sele (South Italy)," Journal of Preventive Medicine and Hygiene, Vol. 38, pp. 3–4, 1997.

[40] A. W. Abu-Qare, and M. B. Abou-Donia, "Simultaneous determination of malathion, permethrin, DEET (N N-diethyl-m-toluamide), and their metabolites in rat plasma and urine using high performance liquid chromatography," Journal of Pharmaceutical and Biomedical Analysis, Vol. 26, pp. 291–299, 2001. [CrossRef]

[41] C. Ensibi, D. Hernández-Moreno, M. P. Míguez Santiyán, M. N. Daly Yahya, F. S. Rodríguez, and M. Pérez-López,"Effects of carbofuran and deltamethrin on acetylcholinesterase activity in brain and muscles of common carp," Environmental Toxicology, Vol. 29, pp. 386–393, 2012. [CrossRef]

[42] Z.Vryzas, C.Alexoudis, G.Vassiliou, K. Galanis, and E. Papadopoulou-Mourkidou, "Determination and aquatic risk assessment of pesticide residues in riparian drainage canals in Northeastern Greece," Ecotoxicology and Environmental Safety, Vol. 74, pp. 174–181, 2011. [CrossRef]

[43] S. Mahboob, F. Niazi, K. Al Ghanim, S. Sultana, F. Al-Misned, and Z. Ahmed, "Health risks associated with pesticide residues in water, sediments and the muscle tissues of Catlacatla at Head Balloki on the River Ravi," Environmental and Monitoring Assessment, Vol. 187, Article 81, 2015. [CrossRef]

[44] M. Sapana Devi, and A. Gupta, "Sublethal toxicity of commercial formulations of deltamethrin and permethrin on selected biochemical constituents and enzyme activities in liver and muscle tissues of Anabas testudineus," Pesticide Biochemistry and Physiology, Vol. 115, pp. 48–52, 2014. [CrossRef]

[45] T. A. Saqib, S. N. Naqvi, P. A. Siddiqui, and M. A. Azmi, "Detection of pesticide residues in muscles, liver and fat of 3 species of Labeo found in Kalri and Haleji Lakes," Journal of Environmental Biology, Vol. 26, pp. 433–438, 2005.

## APPENDICES

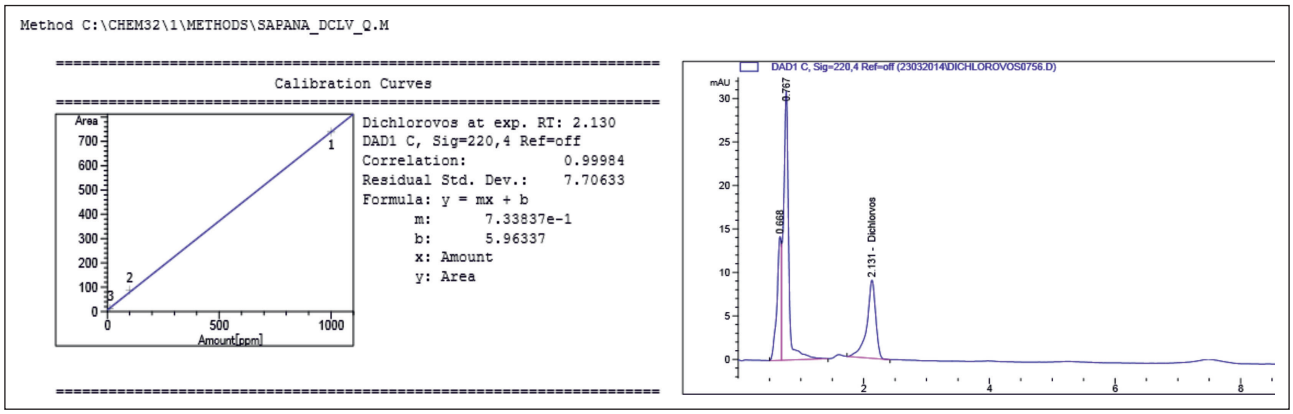


**Appendix 1**. Standard calibration curves and chromatogram of dichlorvos.

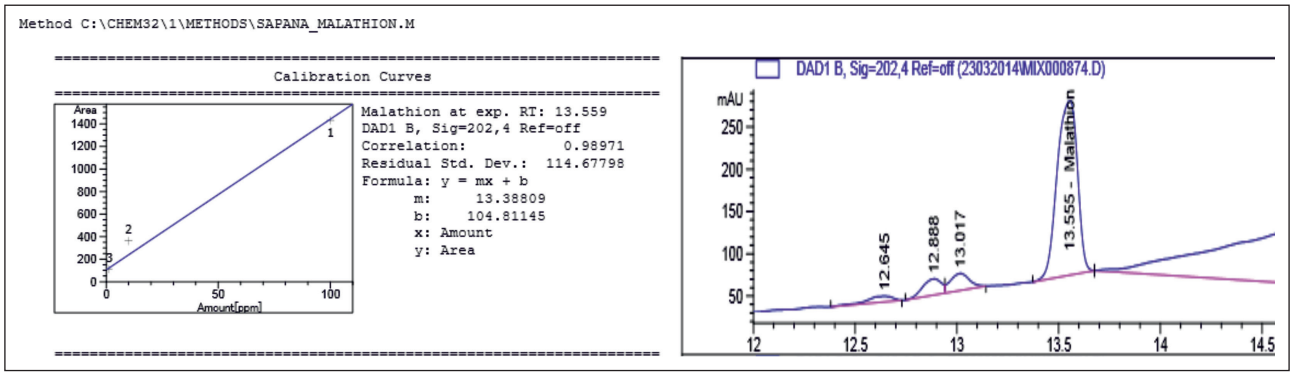


**Appendix 2**. Standard calibration curves and chromatogram of malathion.

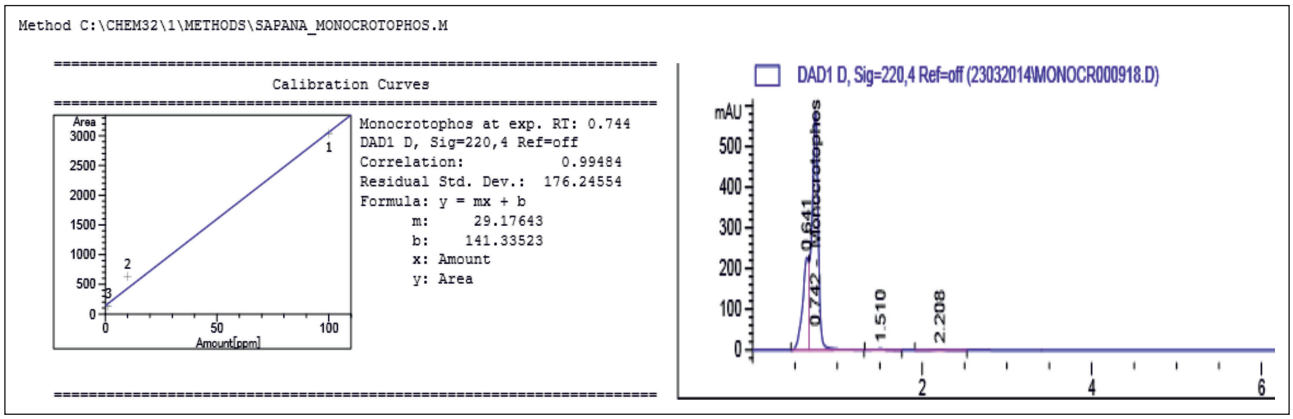


**Appendix 3**. Standard calibration curves and chromatogram of monocrotophos.

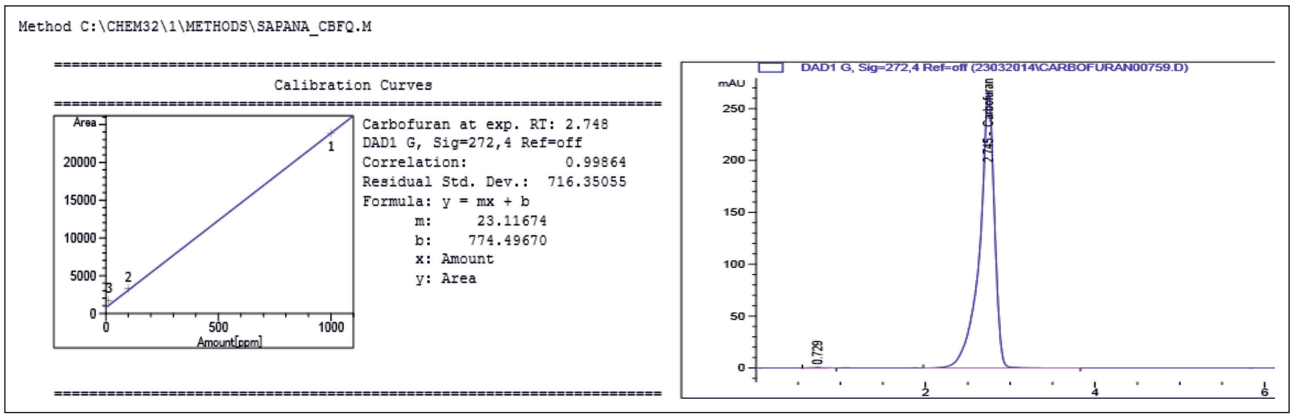


**Appendix 4**. Standard calibration curves and chromatogram of carbofuran.

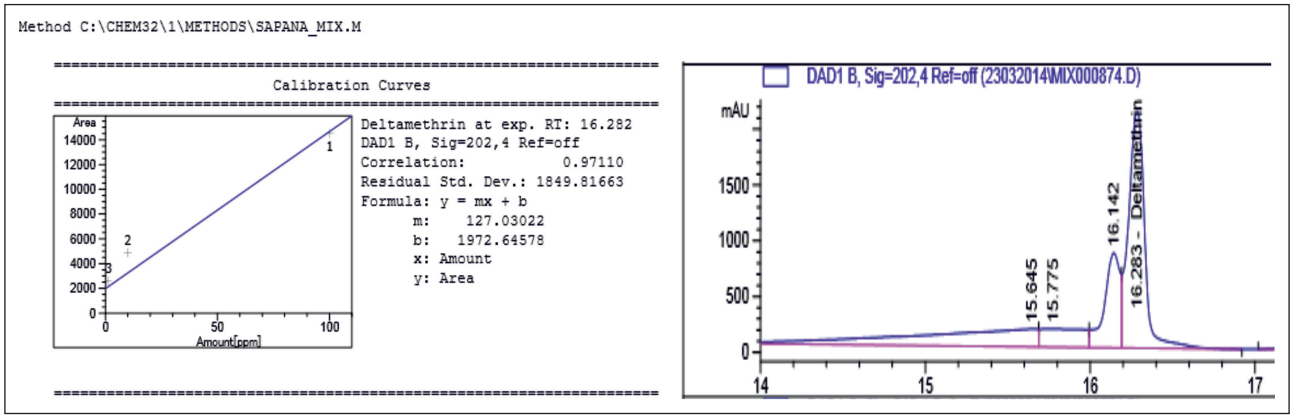


**Appendix 5**. Standard calibration curves and chromatogram of deltamethrin.

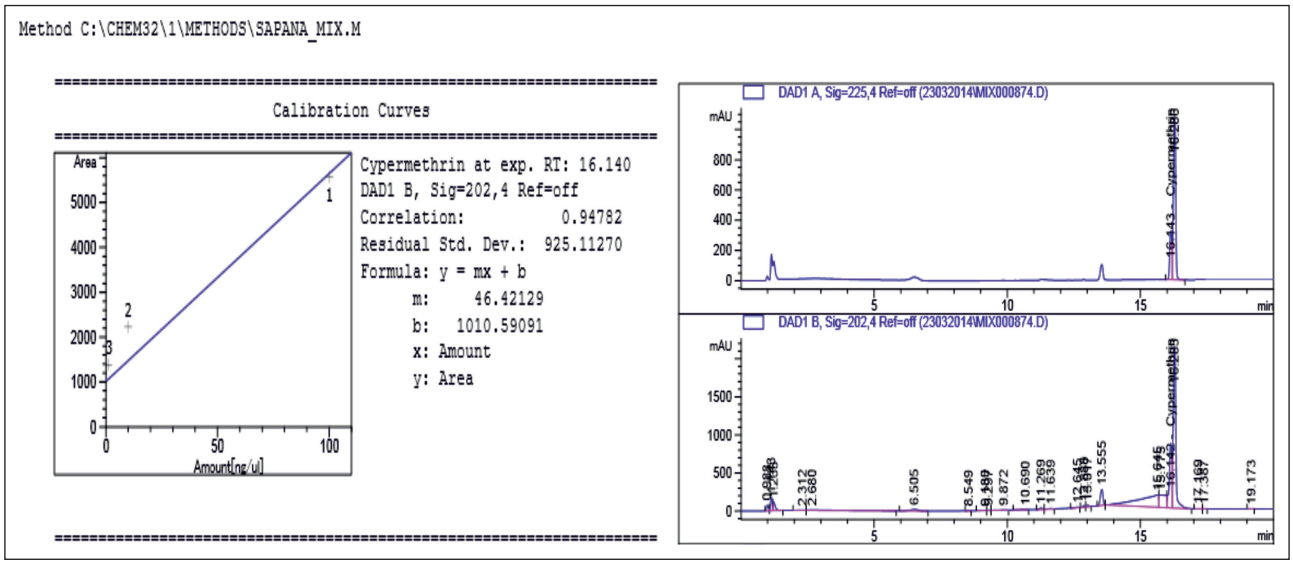


**Appendix 6**. Standard calibration curves and chromatogram of cypermethrin.

*Environ Res Tec, Vol. 7, Issue. 3, pp. 313–334, September 2024*

**Environmental Research and Technology**
https://ert.yildiz.edu.tr - https://dergipark.org.tr/tr/pub/ert
DOI: https://10.35208/ert.1405067

Environmental Research & Technology

**Research Article**

# The treatment of acid mine drainage (AMD) using a combination of selective precipitation and bio-sorption techniques: A hybrid and step-wise approach for AMD valorization and environmental pollution control

**Beauclair NGUEGANG, Abayneh Ataro AMBUSHE***

*Department of Chemical Sciences, University of Johannesburg, Faculty of Science, Johannesburg, South Africa*

## ARTICLE INFO

*Article history*
Received: 15 December 2023
Revised: 29 February 2024
Accepted: 01 April 2024

**Key words:**
Acid mine drainage;
Banana Peels; Bio-sorption;
Environmental pollution control;
Magnesium oxide (MgO);
Selective precipitation

## ABSTRACT

In this study, selective precipitation using magnesium oxide (MgO) and bio-sorption with banana peels (BPs) were explored for the treatment and valorization of acid mine drainage (AMD). The treatment chain comprised two distinct stages of which selective precipitation of chemical species using MgO (step1) and polishing of pre-treated AMD using BPs (step 2). In stage 1, 2.0 L of AMD from coal mine was used for selective precipitation and recovery of chemical species using MgO. The results revealed that chemical species of concern were precipitated and recovered at different pH gradients with Fe(III) precipitated at pH ≤4, Al at pH ≥4–5, Fe(II), Mn and Zn at pH ≥8 while Ca and $SO_4^{2-}$ were precipitated throughout the pH range. In stage 2, the pre-treated AMD water was polished using BPs. The results revealed an overall increase of pH from 1.7 to 10, and substantial removal of chemical species in the following removal efficiency: Al, Cu and Zn (100% each), ≥Fe and Mn (99.99% each), ≥Ni (99.93%), and ≥$SO_4^{2-}$ (90%). The chemical treatment step removed pollutants partially, whereas the bio-sorption step acted as a polishing stage by removing residual pollutants.

**Cite this article as:** Nguegang B, Ambushe AA. The treatment of acid mine drainage (AMD) using a combination of selective precipitation and bio-sorption techniques: A hybrid and step-wise approach for AMD valorization and environmental pollution control. Environ Res Tec 2024;7(3)313–334.

## INTRODUCTION

Acid mine drainage (AMD) is mine acidic by-product, containing elevated concentrations of metals and sulphate ions ($SO_4^{2-}$) and generated by active and abandoned mines, mostly coal and gold mines [1, 2]. Specifically, AMD is formed following the oxidation of sulphide bearing materials such as pyrite ($FeS_2$), arsenopyrite (FeAsS) and marcasite in contact with water [3]. Pyrite ($FeS_2$) is at the forefront of AMD formation process while the contribution of other sulphide bearing materials is negligible. As such, the AMD formation process can be summarized as illustrated in equation (1), (2) and (3).

$$2FeS_2+2H_2O+7O_2 \rightarrow 2Fe^{2+}+4SO_4^{2-}+4H^+ \quad (1)$$

The oxidation of $FeS_2$ in the presence of water and oxygen leads to the formation of $SO_4^{2-}$, ferrous ion [Fe(II)], and hydrogen ion ($H^+$) equation (1). Once formed, Fe(II) is continuously oxidized to form ferric ion [Fe(III)] as illustrated in equation (2).

$$4Fe^{2+}+O_2+4H^+ \rightarrow 4Fe^{3+}+2H_2O \quad (2)$$

The Fe(III) produced after equation (2) can later oxidize $FeS_2$ to generate more Fe(II) and more $H^+$ as shown in equation (3).

$$FeS_2+8H_2O+14Fe^{3+} \rightarrow 15Fe^{2+}+2SO_4^{2-}+16H^+ \quad (3)$$

***Corresponding author.**
*E-mail address: aambushe@uj.ac.za

The above-described chemical reactions occur spontaneously or can be merely mediated or stimulated by microorganisms (sulphate and iron oxidizing bacteria) with the net effect to produce more $H^+$ thereby increasing the acidity of the final product water [4]. Once formed, AMD becomes a matter of great environmental and human health concern and specifically in countries with intensive mining industry due to the presence of toxic chemical species that include metalloids such as arsenic (As), radionuclide such as uranium (U) and potentially toxic elements (PTEs) [5]. To be more precise, AMD is characterised by low pH (≤4.5), high concentration of major metals (Al, Fe, and Mn), very high concentration of $SO_4^{2-}$, low concentration of Cu, Ni, Zn and Pb and trace content of alkali earth metals such as Ca and Mg [6, 7]. This acidic water has the ability to cause undesirable eco-toxicological effects on different environmental compartments and severe human health effects, which include skin irritation, kidney damage, and neurological diseases amongst others [5, 8]. Due to its higher content of valuable natural resources, its eco-toxicological and human health effects, mining house, government, non-governmental organization (NGO) and scientific communities are constantly exploring long-term and sustainable solution for the management, treatment, and valorisation of AMD. In addition, regulatory body required AMD to be treated and all pollutants reduced to acceptable level prior to its release into different environmental compartments; thus, implying an emergency action to be taken to effectively manage this unpleasant mine wastewater.

In line with that, preventive techniques such as drainage channels and limestone backfill around the mine site to hinder the AMD formation have been explored [9–11]. In addition to AMD formation prevention, various treatment technologies have been developed and are currently applied for the treatment of already generated AMD. They include active methods such as neutralization [12, 13], passive methods such as constructed wetland [2, 14–16], limestone bed [17–20], phytoremediation [21–23], hybrid and integrated technologies [24–26]. However, literature reports indicated some drawbacks associated with the above-mentioned treatment technologies; thus, limiting their application for effective treatment and valorisation of AMD. For instance, active technologies release highly polluted toxic sludge containing metals and other chemical species, which can be recovered using specific techniques. Passive methods are ineffective to treat highly acidic AMD water while hybrid and integrated technologies are fragile and require high capital cost [27]. Based on that, studies are been oriented on the treatment and valorisation of acid mine water and it is mostly accomplished by increasing the pH to desired level, collect and valorise sludge by recovering valuable minerals using various techniques including precipitation (neutralization) [1, 28], adsorption [29], ion-exchange [30], membrane technology [31], desalination [32] and bio-sorption [33].

However, valuable minerals recovery from AMD is complex at industrial level due to various drawbacks associated with each technique. For instance, membrane technology has the problem of membrane fouling, brine generation and high capital cost. Adsorption and ion-exchange are ineffective to treat very acidic AMD water and are easily saturated. Desalination is not sustainable due to high capital and operational cost and the production of salt with impurities. Among those techniques, precipitation appears to be the most promising technology due to its ability to handle gigantic volume of AMD with very little dosage of alkaline chemicals, and the possibility to adjust it in stepwise fashion or selective precipitation to precipitate and recover chemical species at different pH gradients [1, 34]. On the other hand, bio-sorption is a physicochemical process that utilises the mechanism of absorption, adsorption, ion exchange and surface complexation to remove pollutants from aqueous solution [35, 36]. Furthermore, bio-sorption using agricultural by-products is cost effective, does not generate sludge and bio-adsorbent are readily available. Amongst the agricultural by-products, banana peels (BPs) is most suitable to remove chemical species (metals and sulphate) since its biomass contain functional group like carboxyl, hydroxyl and amine, which play a vital role for binding and remove pollutants from aqueous solution [37, 38].

As such, there is dire need to come up with innovative technologies that will exhibit the viability and feasibility of integrating fractional or sequential precipitation and bio-sorption for the treatment and valorisation of AMD and agricultural by-products in a circular economy approach (CEA) concept. Various techniques including electro reactions [39] and bio-electrochemical system [40] have been applied to recover valuable minerals from AMD while alkaline materials such as $Ca(OH)_2$ and $Na_2S$ [41], hydrated lime, soda ash and caustic soda [34], $Na_2SO_4$ [42], and $MgCO_3$ [1] have also been used to precipitate and recover valuables minerals from AMD. From literature, magnesium oxide (MgO) has high neutralisation capacity with optimum pH achievable of 9.5 and it has been successfully investigated for the active treatment of real AMD water [43–45], while BPs is effective bio-sorbent for chemical species removal in acid mine water, however, with limited efficiency in very acidic mine water [46, 47]. Owing to their disadvantages, which include the incapacity of MgO to increase the pH of AMD water above 9.5, and poor efficiency of BPs for concentrated acidic mine water, this complementary approach is being proposed to eliminate the drawbacks of each system to ensure the effective treatment and valorisation of AMD in order to control environmental pollution associated with both mining and agricultural activities. To the best of authors knowledge, the integration of fractional or sequential precipitation with MgO and bio-sorption using BPs has not been investigated for the treatment and valorization of AMD. Therefore, this is the first study in design and execution to explore the use of selective precipitation with MgO and bio-sorption with BPs for the treatment and valorization of real AMD. The proposed technique is cost effective, efficient, environmentally friendly and will open the route to introduce 4R (Recovery, reuse, recycle and repurpose) technology to valorize agricultural by-products, turn mining influenced water or AMD into beneficial products thereby controlling environmental pollution and reduce human health risks associated with exposure to contaminated waste.

## MATERIALS AND METHODS

**Reagents Acquisition and Standards Solution Preparation**
Analytical grade and commercially produced MgO (99.99%) was purchased from Merck, South Africa while multi-element standard solution was purchased from Sigma-Aldrich, st Louis, Mo, USA). The calibration standard solutions were prepared using 100 mg/L multi-element (Sigma-Aldrich, st Louis, Mo, USA) for metals analysis while a sulphate standard solution (HACH, USA) of 1000 mg/L was used to prepare the calibration standards for $SO_4^{2-}$ analysis. Ultrapure deionized water from a MilliQ Direct 8 water purifier system (Millipore S.A.S Molshein, France) with resistivity of 18.1 MΩ/cm at 25 °C was used for the preparation of all standard solutions.

**Raw AMD Collection and Bio-sorbents (BPs) Acquisition**
Raw AMD used in this study was collected from the discharge point of a coal mine in Limpopo province, South Africa. Acid mine water was collected using 5 L polyethylene container to prevent further oxidation and precipitation of metals. To obtain BPs which were used as bio-sorbent, ripe banana was purchased from a recognized franchised grocery store (Food Lover's Market), Johannesburg, South Africa. Once in the university laboratory, BPs were separated from banana, cut into small pieces, and cleaned using ultra-pure water to remove dirt, dried using an oven dryer and grinded to obtain a particle size of less than 100 µm.

**Treatment and Valorization of Real AMD Water**
This section is divided in 2 parts of which step 1 consists of selective precipitation and recovery of chemical species from real AMD, while step 2 focuses on the use of bio-sorbent (BPs) to polish the product water by bio-sorption technique.

**Selective Precipitation and Chemical Species Recovery Approach**
To assess the effects of MgO on chemical species precipitation, an initial quantity of MgO and AMD were mixed in the ratio of 1:2000 (1 g/2000 mL or w/v ratio) and stirred at 800 rpm. The pH of the solution was gradually raised in stepwise fashion by cautiously increasing the MgO dosage and stirred at 800 rpm using an overhead stirrer to reach the desired pH (pH 4, pH 6, pH 8 and pH 9.5). At each desired pH, the solution was allowed to stand for 3 h followed by the decantation of supernatant water and the recovery of sludge following the method of Masindi et al. [1]. The supernatant water siphoned at each pH level was used for the next step of the precipitation process to reach the next desired pH, however with the increasing of MgO dosage, if after stirring for 60 min, the desired pH gradients was not reached. The pH of the solution was monitored using a pH meter. The different pH intervals for chemical species precipitation were pH (1.7–4), pH (4–6), pH (6–8) and pH (8–9.5) and at pH (4, 6, 8 and 9.5), processed AMD water samples were collected for chemical species analysis while sludge materials were recovered for different characterization studies. The experiment was optimized using one-factor-a-time (OFAAT) approach whereby the effects of precipitator (MgO) was duly explored.

**Bio-sorption Technique Using Banana Peels**
Bio-sorption is a process of binding ions from aqueous solution in contact with functional group that are present on the surface of biomass [48]. To polish the product water using BPs, two parameters (contact time and bio-sorbent dosage) were investigated. To assess the effect of contact time, product water reclaimed at pH 9.5 was mixed with BPs at the ratio 1:100 mL (w/v or 1 g/100 mL). The mixture was stirred at 800 rpm and the effect of contact time was observed for 10, 30, 60, 90, 120, 150, 180, 210, 240 and 300 min. The mixture was then allowed to stand for 3 h followed by the recovery of supernatant water and filtration using 0.22 µm pore size nylon syringe filter membrane prior to analysis for chemical species concentration, while raw and AMD reacted BPs were characterized using different characterization techniques. To assess the effect of bio-sorbent dosage, an amount of 0.1, 0.25, 0.5, 0.75, 1, 1.25 and 1.5 g was added into separate beakers containing 100 mL of pre-treated AMD each. The mixture was stirred at 800 rpm at the optimum contact time of 300 min after which the solution was allowed to stand for 3 h followed by filtration using 0.22 µm pore size nylon syringe filter membrane and then analyzed for chemical species contents. The effect of pH was not evaluated since the quest was to mimic the system near real environmental conditions, and this comprise testing the system under ambient temperature and pH in order to understand the robustness of the system in a real environment where pH will not be evaluated or adjusted. Schematic representation of the hybrid and stepwise approach is shown in Figure 1.

**Samples Preparation and Analysis**
Raw AMD and treated water samples recovered at different pH levels during selective precipitation process and after bio-sorption technique were filtered using a 0.22 µm pore size nylon syringe filter membrane to remove particles and avoid absorption of metals [49], followed by the measurement of pH, EC and TDS. The water samples were then divided into two sub-samples of which sub-sample 1 was preserved by adding two drops of 65% nitric acid ($HNO_3$) to avoid ageing and immediate precipitation of metals and kept at 4 °C until analysis for metals concentration using inductively coupled plasma optical-emission spectrometry (ICP-OES), 5110 ICP-OES vertical dual view, (Agilent technologies, Australia). Sub-sample 2 was left non-acidified and analyzed for $SO_4^{2-}$ concentration using ion chromatography (IC) (850 professional IC Metrohm, Herisau, Switzerland). The two sub samples were analyzed following standard methods as stipulated by the American Public Health Association [50]. Sludge collected at different pH gradients were purified by drying at 125 °C for 24 H using dryer oven (Labotec Ltd, South Africa) while a grinder (Kambrook ASPIRE, South Africa) was used to mill the dried BPs to powder. After purification, 1 g of processed MgO was digested in a mixture of 6 mL of 37% hydrochloric acid (HCL) and 2 mL of 65% nitric acid ($HNO_3$) using microwave digestion system (Anto Paar Strasse, Austria) as described by Uddin et al. [51], while the rest of purified sludge was used for different

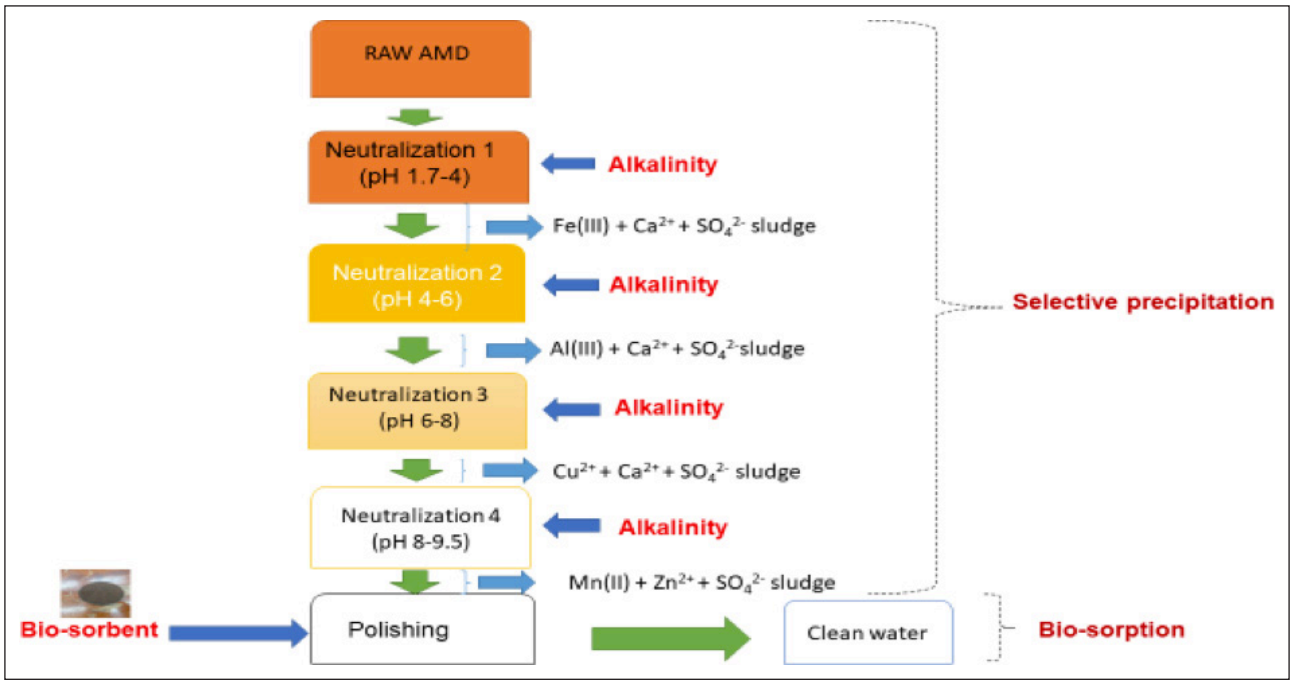


**Figure 1**. Schematic illustration of the hybrid system: selective precipitation and bio-sorption technique.

characterization studies. The digested samples were filtered using 0.22 µm pore size nylon syringe filter membrane followed by analysis for chemical species concentration.

### Characterization Studies

Characterization studies were performed using different analytical and state-of-art characterization techniques. To be precise, morphological structures of pure, processed MgO, pure and BPs after treatment were determined using high resolution scanning electron microscopy energy dispersive x-ray spectroscopy (HR-SEM-EDS) (TESCAN VEGA 3 LMH Brno-kohoutovice, Czech Republic) coupled to an EDS (Oxford Instruments, Buckinghamshire, UK). The crystallographic structure and mineralogical composition were ascertained using powder X-ray diffraction (p-XRD) (Philips PW 1710, Netherlands) while different functional group were determined by Fourier transform infrared (FTIR) spectroscopy (Shimadzu, Kyoto, Japan) in the wavelength range between 500 and 4500 $cm^{-1}$ and scanned at a resolution of 16 $cm^{-1}$. A PerkinElmer STA 6000 thermogravimetric analyser (TGA) (TA instruments, New Castle, USA) was used to determine the thermal stability of bio-sorbent and their fraction of components while a Malvern Zetasizer NANO-ZS ZEN3600 (Malvern panalytical, South Africa) was used to determine the particles in suspension on the surface of bio-sorbent.

### Regeneration of Banana Peels

A regeneration study was conducted for the BPs by mixing 0.5 g of bio-sorbent with a pre-treated AMD water collected at pH 9.5 with chemical species concentration as follows: Al (1.02 mg/L), Cu (0.01 mg/L), Fe (2.4 mg/L), Mn (1.03 mg/L), Ni (0.01 mg/L), Zn (0.09 mg/L) and $SO_4^{2-}$. The mixture was stirred at 800 rpm for a contact time of 300 min after which the bio-sorbent was recovered by filtration while the aqueous solution (pre-treated AMD) was analyzed for quantification of chemical species concentration. The same procedure was repeated 5 times to evaluate the reusability of bio-sorbent.

### Quality Control and Quality Assurance

A quality control (QC) and quality assurance (QA) process was implemented in this study to warrant the production of trustworthy results. The QC/QA process required all analysis to be conducted in triplicate and data reported as mean value and considered acceptable when the difference between triplicate samples was less than 5% while the limit of detection (LOD) and limit of quantification (LOQ) were determined using standard methods.

### Limit of Detection and Limit of Quantification

To determine the LOD and LOQ, calibration curves with the following concentration of each element: 0.1, 0.3, 0.7, 1, 1.3, 1.5, 2, 2.5, 3 and 3.5 were used. A reagent blanks were analyzed to calculate the LOD. A standard solution containing about 10 mg/L of each element was used to obtain the standard intensities signal and the LOD was then calculated following the methods as illustrated in Equation (4) [52].

$$LOD = \frac{3\times \sigma \times S}{I-\beta} \times V \quad (4)$$

Where:

σ is the standard deviation of the blank solution

S is the concentration of the standard (mg/L)

I is the signal intensity of the standard

β is the average intensity of the blank signal

V is the volume of the final volume of the sample (9 mL).

The LOQ was then determined taking into account the fact that LOQ is approximatively 3.333 times the LOD equation (5) [37].

$$LOQ = LOD \times 3.333 \quad (5)$$

**Table 1.** Raw AMD quality as compared to regulatory requirement

| Parameters | Unit | Raw AMD | DWS guideline for drinking water quality | WHO guideline for drinking water quality | DEA guideline for effluent discharge |
|---|---|---|---|---|---|
| pH | – | 1.7 | 5–9.8 | 6.5–8.5 | 6–12 |
| EC | µS/cm | 5000 | 150 | ≤400 | 0–700 |
| TDS | mg/L | 7380 | 1200 | ≤600 | 2400 |
| Al | mg/L | 160 | ≤0.3 | 0–0.1 | 20 |
| Cu | mg/L | 2.50 | ≤0.3 | 0–0.1 | 20 |
| Fe | mg/L | 6000 | ≤0.3 | 0–0.3 | 50 |
| Mn | mg/L | 40.7 | ≤0.1 | 0–0.08 | 20 |
| Ni | mg/L | 1.53 | ≤0.7 | 0–0.07 | 10 |
| Zn | mg/L | 8.00 | ≤0.5 | 0.0.1 | 20 |
| $SO_4^{2-}$ | mg/L | 12500 | ≤500 | ≤250 | 2400 |

AMD: Acid mine drainage; DWS: Department of Water and Sanitation; DEA: Department of Environmental Affairs.

**Mathematical Modelling and Removal Efficiency**

The efficiency of the hybrid approach (selective precipitation and bio-sorption) for the treatment and valorization of acid mine water was duly investigated. The removal efficiency (RE) was calculated for metals, EC, TDS and $SO_4^{2-}$ as demonstrated in equation (6) [14].

$$RE = \frac{Ci - Cf}{Ci} \quad (6)$$

Where $C_i$ and $C_f$ are the initial and final concentration of metals, respectively.

The pH increment was determined as illustrated in equation (7) [2].

$$I = pHf - pHi \quad (7)$$

Where pHf is the final pH of the product water, pHi is the initial pH of AMD, while I is the increment of pH after selective neutralization and bio-sorption.

The efficiency of selective precipitation using MgO and metals recovery was duly explored by determining the concentration of chemical species in sludge material and AMD water collected at each pH level followed by the calculation of the percentage of chemical species recovered at various stages of selective precipitation process as illustrated in equation (8) [53–57].

$$Recovery\ percentage\ (\%) = 100 \times \frac{Cp \times Mp}{C_{AMD} \times V_{AMD}} \quad (8)$$

$C_p$ is the concentration of the chemical species in the sludge material

$M_p$ is the mass of the sludge material

$C_{AMD}$ is the concentration of the chemical species in AMD water collected at each pH level

$V_{AMD}$ is the volume of AMD water at each pH gradients.

## RESULTS AND DISCUSSION

**Chemical Composition of Raw AMD**

The chemical properties of AMD sample was determined using standard methods for water and wastewater [50] and the results were compared to the South African regulatory bodies and World Health Organization (WHO) guidelines for drinking water and environmental discharge as presented in Table 1.

From Table 1, it follows that raw AMD collected was above national regulatory bodies, which include Department of Water and Sanitation (DWS) guidelines for drinking water, Department of Environmental Affairs (DEA) guidelines for effluent discharge and WHO water quality guidelines and therefore not suitable to be discharged untreated into different environmental compartments. The chemical composition revealed low pH, high EC and TDS, elevated concentration of major ions (Al, Fe, Mn and $SO_4^{2-}$) and low concentration of trace elements (Cu, Ni and Zn). The elevated concentrations of Al, Fe and Mn indicate that these metals can be potentially recovered from AMD, while the recovery of trace metals (Cu, Ni and Zn) will be challenging due to their low concentrations. The elevated concentrations of Fe and $SO_4^{2-}$ indicate that AMD used in this study was formed following the oxidation of $FeS_2$ as reported in previous study [7].

**Percentage of Chemical Species Recovered**

The percentage of chemical species recovered using selective precipitation under pH control was determined and the results are presented in Figure 2.

The Figure 2 depicted that Fe, Al, Mn, Zn and gypsum ($CaSO_4.2H_2O$) were the chemical species recovered throughout the pH range (1.7–9.5). At pH (1.7–4) interval, Fe(III) was the most recovered chemical species, followed by $CaSO_4.2H_2O$ and Al. The recovery of Fe(III) at this pH interval was expected since Fe(III) is mostly precipitated at pH (2.5–4) interval in the form of Fe-hydroxide and Fe-oxyhydrosulphates [1]. The small percentage of Al recovered at pH (1.7–4) interval may be credited to the presence of $SO_4^{2-}$ in AMD water. Typically, Al precipitates best at pH (4.5–7) [39]. However, the presence of $SO_4^{2-}$ slightly lowers the pH required for Al precipitation to less than 4 (pH ≤4)

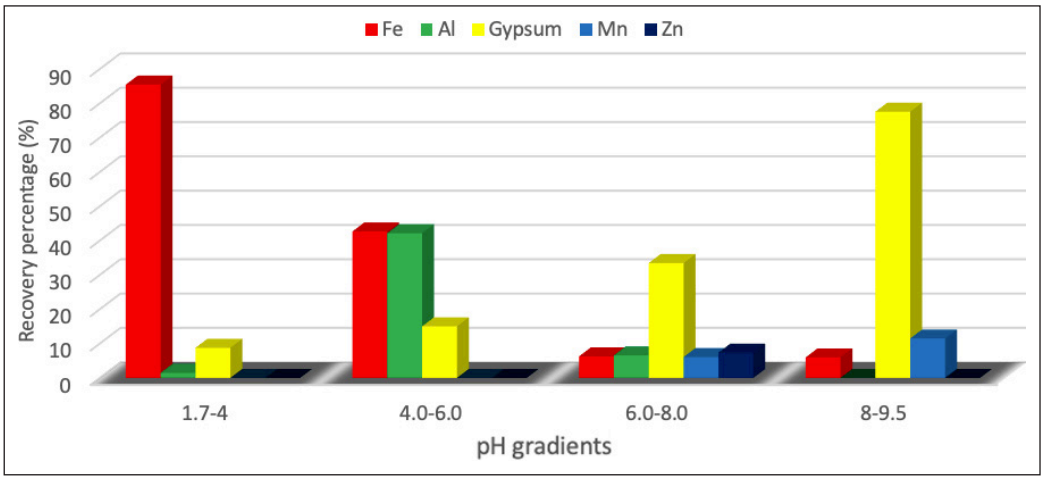


**Figure 2**. Recovery percentage of chemical species at four different pH intervals.

leading to the precipitation of minor quantity of Al at pH ≤4 and the formation of gibbsite [$Al(OH)_3$] or Al-hydroxide as reported by previous studies [40, 41]. The recovery of $CaSO_4.2H_2O$ at this pH interval and throughout the pH range may be attributed to the precipitation of $Ca^{2+}$ and $SO_4^{2-}$, which occurs at pH (2.5–11.5) interval [42, 43]. At pH (4–6) interval, Al and Fe were the most recovered chemical species and the quantity of Fe(III) recovered at this pH interval may be attributed to the continuous precipitation of $Fe^{3+}$ from initial pH of 1.7 to 7.5 as reported by Seo et al. [34]. The recovery of high percentage of Al at this pH interval was expected since Al ion is mostly precipitated at pH ≥4.5, while the continuous recovery of gypsum may be attributed to the continuous precipitation of $Ca^{2+}$ and $SO_4^{2-}$, which start at pH ≥2.5. At pH (6–8) interval, a minor percentage of Al and Fe was recovered and this may be attributed to the continuous precipitation of $Fe^{3+}$ and $Al^{3+}$ from pH 2.5 to pH of 7.5 and from pH ≥4, respectively [34]. The findings in Figure 2, further revealed that a minor percentage of Mn was recovered at pH (6–8) interval and this may be attributed to the precipitation of Mn(II), which occurs at pH >7 to form Mn(II) hydroxide [$Mn(OH)_2$] [58]. At pH (8–9.5) interval, $CaSO_4.2H_2O$ was the most recovered chemical species, while a moderate percentage of Mn in the form of $Mn(OH)_2$ was recovered at this pH interval. The recovery of $Mn(OH)_2$ may be attributed to the precipitation of $Mn^{2+}$ while the high percentage of $CaSO_4.2H_2O$ is attributed to the precipitation of $Ca^{2+}$ and $SO_4^{2-}$. Ideally, $Mn^{2+}$ and $Mn^{4+}$ are mostly precipitated at 8≥ pH ≤9.5 to form $MnO_2$ and this may justify the percentage of Mn recovered at pH (8–9.5) interval. The recovery of a minor percentage of Fe may be attributed to the presence of ferrous ions under compound form, which precipitates at pH ≥8 to form ferrous hydroxide [$Fe(OH)_2$] [59]. Overall, the chemical species recovered corroborated well with the EDS results.

**Effect of Selective Precipitation and Bio-sorption on Water Quality of AMD**

Raw AMD was treated using a combination of selective precipitation and bio-sorption techniques. Metals were gradually precipitated in raw AMD water using MgO, while BPs were used to polish the product water by removing residual metals and $SO_4^{2-}$ and the variation of the water quality is reported in Table 2.

As reported in Table 2, there was a significant increase of pH and reduction of chemical species concentrations with gradual or selective precipitation and bio-sorption techniques. Specifically, the selective precipitation and bio-sorption increased the pH from 1.7 to 10 corresponding to an increment of 8.3. The selective precipitation raised the pH from 1.7 to 9.5 which is the optimum pH level achievable using MgO while the bio-sorption by BPs bio-sorbent further raised the pH from 9.5 to 10. During the selective precipitation process using MgO, the mixture of MgO with AMD water stimulated the consumption of $H^+$ from AMD water leading to the reduction of acidity and increase in pH as result of hydroxyl group (-OH) by reaction with MgO [24, 60]. In fact, Once MgO is mixed with AMD, the reaction between MgO and $H_2SO_4$ leads to the production of $MgSO_4$ and water as illustrated in equation (9).

$$MgO+H_2SO_4 \rightarrow MgSO_4+H_2O \quad (9)$$

The continuous dissolution of MgO in acidic medium liberates magnesium ions ($Mg^{2+}$) and hydroxide ions ($OH^-$); thus, adding alkalinity in the solution and increasing of pH as shown in equation (10).

$$MgO+H^+ \rightarrow Mg^{2+}+OH^- \quad (10)$$

The bio-sorption step using BPs at 1:100 ratio (1 g:100 mL) (w/v) for a maximum contact time of 300 min allowed the binding of residual ions from aqueous solution via the adsorption mechanisms. In fact, BPs possesses various functional groups including hydroxyl group (-OH), carbonyl (C=O), amine group (-NH) and unsaturated C=C group, which serve for binding ions from aqueous solution [61, 62]. These functional groups have adsorbed and removed residual chemical species from pre-treated AMD leading to complete removal of Al, Cu and Zn, and significant removal of other chemical species (Fe, Mn, Ni and $SO_4^{2-}$). The removal of residual chemical species led to a slight increase of pH from 9.5 to 10. Overall, selective precipitation using MgO contributed to 94% of pH increment while

**Table 2.** Variation in AMD water quality as result of selective precipitation and bio-sorption

| Parameters | Raw AMD | Selective or fractional precipitation | | | | Bio-sorption |
|---|---|---|---|---|---|---|
| Volume (mL) | 2000 | 2000 | 1870 | 1800 | 1720 | 1640 |
| pH | 1.7 | 4 | 6 | 8 | 9.5 | 10 |
| MgO (g) | Nil | 1 | 1.4 | 1.9 | 2.3 | 2.3 + 1g BPs |
| Al (mg/L) | 160 | 141 | 2.30 | 1.79 | 1.02 | <0.001 |
| Cu (mg/L) | 2.50 | 2.50 | 1.05 | 0.700 | 0.010 | <0.002 |
| Fe (mg/L) | 6000 | 240 | 120 | 114 | 2.40 | 0.6 |
| Mn (mg/L) | 40.7 | 39.9 | 29.1 | 26.1 | 1.03 | 0.002 |
| Ni (mg/L) | 1.53 | 1.48 | 1.30 | 0.600 | 0.0100 | 0.001 |
| Zn (mg/L) | 8.00 | 7.72 | 3.21 | 2.30 | 0.0900 | <0.005 |
| $SO_4^{2-}$ (mg/L) | 12500 | 8400 | 6840 | 5400 | 3130 | 1250 |

AMD: Acid mine drainage.

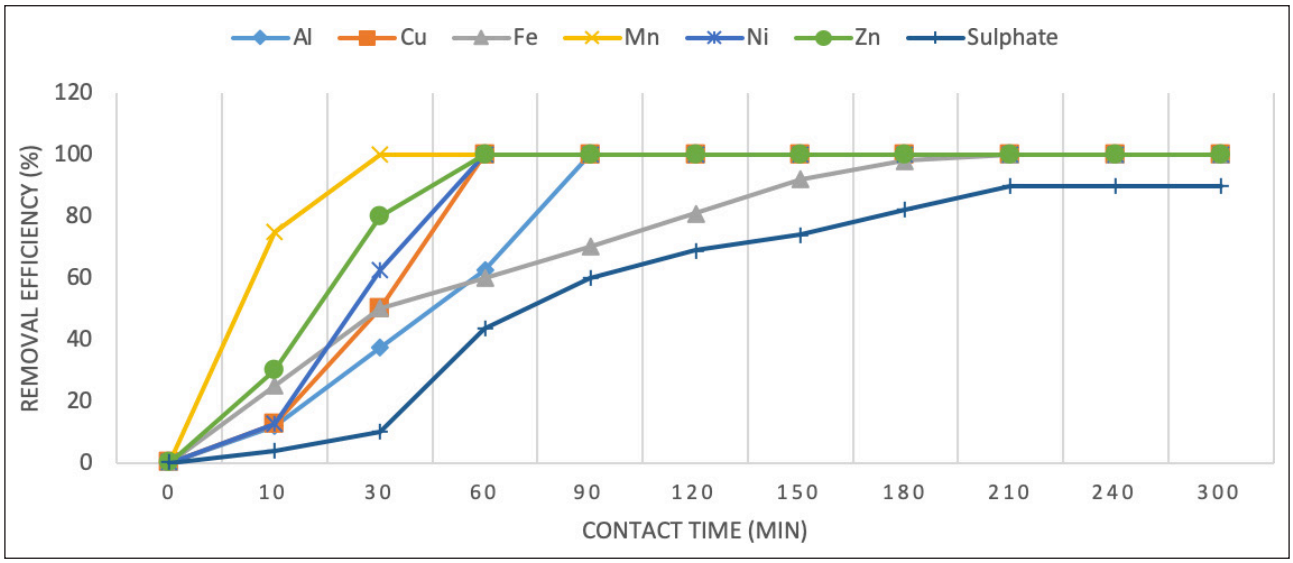


**Figure 3**. Effect of contact time on chemical species removal.

bio-sorption using BPs contributed to 6% of pH increment. The selective precipitation or step-wise precipitation process allows the pH to control the precipitation process and ensure the recovery of sludge rich in metals precipitated at different pH gradient as reported in the literature [1, 63]. The findings in Table 2 further revealed that pH 9.5 is the maximum pH level achievable using MgO for selective precipitation and neutralization. At the optimum pH level, chemical species were removed as follows: Fe (99.96%) > Cu (99.6%) > Al (99.36%) > Ni (99.34%) > Zn (99%) > Mn (97.47%) > $SO_4^{2-}$ (75%). The results were in line with previous studies [1, 28, 43], thereby confirming that selective precipitation using MgO is efficient to significantly attenuate and recover chemical species in AMD. The bio-sorption step using BPs further rose the AMD pH from 9.5 to 10 leading to more chemical species attenuation and at pH 10, the RE was very high (99.99%, 99.93%, 99.98% and 90%) for Fe, Ni, Mn and $SO_4^{2-}$, respectively while Al, Cu and Zn were below the LOD of 0.001, 0.002 and 0.005 mg/L, respectively. Overall, the combination of selective precipitation and bio-sorption techniques allowed to precipitate different metals at different pH and reclaim water that meet the DEA guidelines for effluent discharge; however, should be further treated to reclaim drinking water standard since Fe and $SO_4^{2-}$ concentrations were above maximum permissible levels (MPLs) as set by WHO and the DWS in the Republic of South Africa (RSA). This hybrid system can serve as the bottom line to implement CEA concept to control environmental pollution associated with mining activities and agricultural industry.

In order to polish the product water obtained after selective precipitation technique, two parameters (effect of contact time and effect of adsorbent dosage) were evaluated.

### Effect of contact time on the adsorption of chemical species by BPs

The effect of contact time in the bio-sorption step was assessed for chemical species of concern and the results are shown in Figure 3.

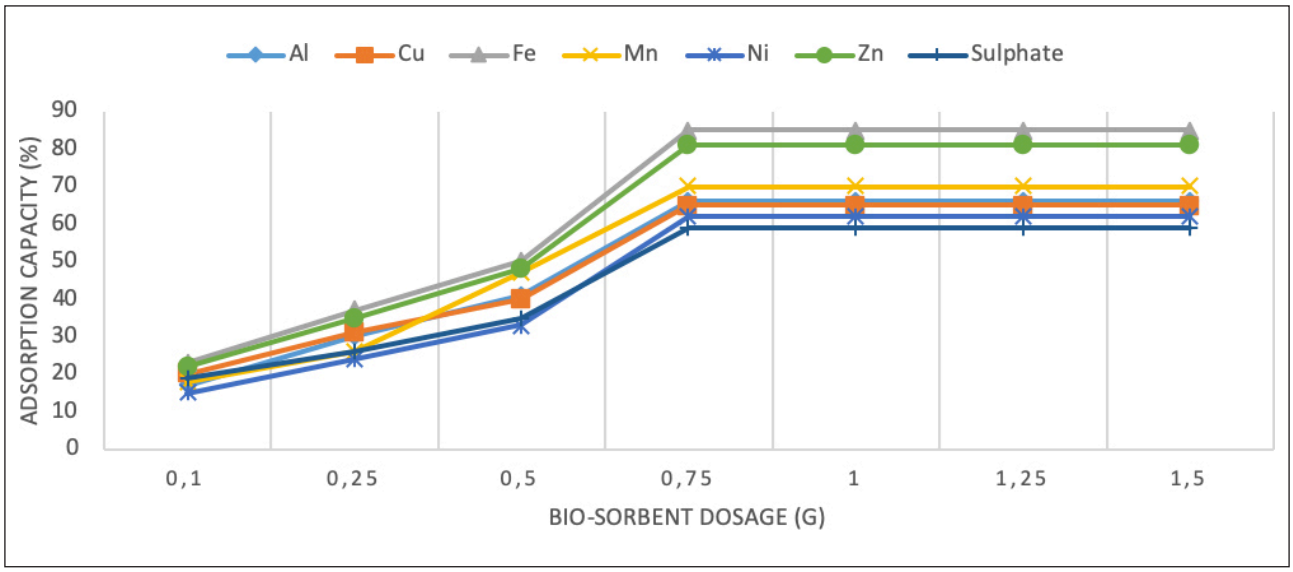


**Figure 4**. Effect of bio-sorbent (BPs) dosage on chemical species removal.

As shown in Figure 3, the contact time had a positive effect on chemical species adsorption since the RE of all chemical species increased as the contact time increased, however with different patterns. The significant increase in RE observed during the first 30 min may be attributed to the accessibility of active sites on the surface of bio-sorbent (BPs). However, the optimum contact differs for chemical species with 30 min being the optimum contact time for Mn, 60 min for Cu, Ni and Zn, 90 min for Al and 210 min for Fe and $SO_4^{2-}$. The difference in the optimum contact time may be attributed to the competition between chemical species to occupy available active sites on the surface of the bio-sorbent (BPs). According to Drew and Andrea [64], the competition process firstly involves cations competing with hydrogen ion ($H^+$) to bind to oxide or carboxyl site and on the other hand, involve anions and cations competing to bind amine group. The difference in the optimum contact time may also be credited to the initial content of chemical species in pre-treated AMD used in the bio-sorption step since chemical species (Al, Cu and Zn) with very low concentration were completely adsorbed, Mn and Ni were nearly complete adsorption, while Fe and $SO_4^{2-}$ were partially adsorbed. The complete adsorption of Al, Cu and Zn may be attributed to their very low concentrations after selective precipitation. However, the complete adsorption did not apply to Mn and Ni and this may be the result of competition process [64]. The partial adsorption of Fe and $SO_4^{2-}$ may be attributed to the threshold limit of contact time or saturation of active sites after which the prolonged contact does not have any effect in adsorption capacity of bio-sorbent (BPs) and this can be due to slow diffusion of solute into the interior of bio-sorbent [65, 66]. The partial adsorption of Fe and $SO_4^{2-}$ may also be credited to the saturation of active sites on the surface of bio-sorbent since after 210 min, the prolonged contact does not have any effect on the adsorption of Fe and $SO_4^{2-}$ thereby confirming the results obtained in previous studies [67, 68].

**Effect of BPs Dosage on the Removal of Chemical Species**

The bio-sorbent dosage was investigated for the pre-treated AMD water reclaimed at pH 9.5. The dosage of BPs was varied in the following order: 0.1, 0.25, 0.5, 0.75, 1, 1.25 and 1.5 g and the results are shown in Figure 4.

The Figure 4 clearly depicted that the increase of bio-sorbent dosage led to an increase of RE and this can be credited to the large number of active sites resulting from the increase of bio-sorbent dosage, which provide large surface areas to adsorb chemical species [69]. The increase of active sites is the result of number of oxygen bearing functional groups including alcohols, carboxylic acids and esters as revealed by FTIR spectroscopy analysis of BPs. The Figure 4 further indicates that all chemical species were gradually adsorbed, and the saturation was reached with 0.75 g of bio-sorbent dosage, however at different RE in the following order: Fe (85%) > Zn (81%) > Mn (70%) > Al (66%) > Cu (65%) > Ni (62%) > $SO_4^{2-}$ (59%). The variation in RE may be attributed to many factors, which include initial chemical species concentration, metals affinity to bio-sorbent, competing or co-existing ions and speed of agitation [70, 71]. The highest RE of Fe may be attributed to the facility of positively-charged metal to bind with an electron-rich hydroxyl group thereby confirming previous studies [72]. Overall, the effects of bio-sorbent dosage revealed two phases: phase 1 which is illustrated by a significant increase of RE from 0.1 g to 0.75 g and phase 2 which is illustrated by a constant RE from 0.75 g to 1.5 g and this can be credited to the availability of active sites during the phase 1 and the saturation of active sites during the phase 2 and the continuous addition of bio-sorbent does not have any effect on bio-sorbent capacity to adsorb chemical species. These results are in line with reports from previous studies [47]. This study proved that BPs have a great potential in chemical species removal and can be further investigated for polishing of pre-treated AMD.

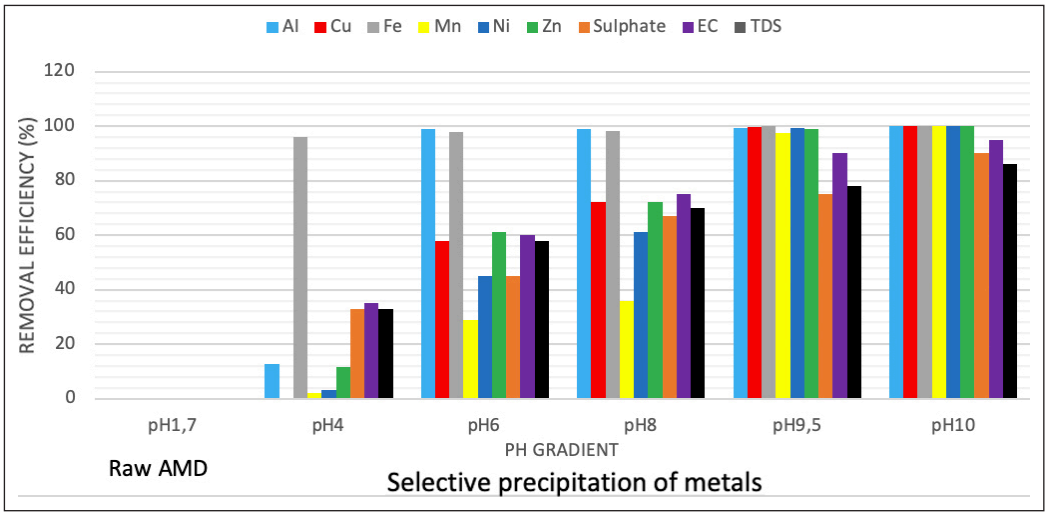


**Figure 5**. Variation in the percentage removal of chemical species as function of selective precipitation and bio-sorption.

**Removal Efficiency of the Hybrid System (Selective Precipitation and Bio-sorption) on AMD Quality Improvement**

The RE of the hybrid system (selective precipitation and bio-sorption) was gradually evaluated and the results are shown in Figure 5.

Figure 5 clearly portrayed that the RE increased gradually as results of selective precipitation and bio-sorption techniques. This allowed to raise the pH from 1.7 to 10, complete removal of Al, Cu and Zn and other chemical species as follows: Fe (99.99%) = Mn (99.99%) > Ni (99.93%) > EC (95%) > $SO_4^{2-}$ (90%) > TDS (86%) proving that metals can be recovered, and possible drinking water standard reclaimed using a combination of selective precipitation and bio-sorption techniques. In particular, the selective precipitation using MgO allowed to precipitate metals at different pH gradients, rose the pH from 1.7 to 9.5. The increase of pH may be credited to the dissolution of MgO in the presence of water to liberate $Mg^{2+}$ ion and hydroxide ion ($OH^-$), which react to form magnesium hydroxide [$Mg(OH)_2$] as illustrated in the following equation (11) and (12).

$$MgO+H_2O \rightarrow 2OH^- + Mg^{2+} \quad (11)$$

$$Mg^{2+}+2OH^- \rightarrow Mg(OH)_2 \quad (12)$$

The reactions add alkalinity in AMD thereby leading to pH increase, metals precipitation at different pH gradient and possible recovery. Selective precipitation reduced the concentration of chemical species with RE as follows: Cu (99.7%) > Fe (99.96%) > Al (99.36%) > Ni (99.34%) > Zn (99%) > Mn (97.47%) > $SO_4^{2-}$ (75%), while the bio-sorption technique further increased the pH from 9.5 to 10 and accounted for a minor fraction of chemical species removal with RE in the following order: $SO_4^{2-}$ (15%) > TDS (8%) > EC (5%) > Mn (2.53%) > Zn (1%) > Ni (0.66%) > Al (0.64%) > Cu (0.4%) > Fe (0.03%). The adsorption of chemical species using BPs led to more reduction of metals in aqueous solution and consequently reduction of $H^+$ resulting to slight pH increase from 9.5 to 10. However, Fe, Mn, Ni, EC, $SO_4^{2-}$ and TDS were not completely removed after treatment of mine water using selective precipitation and bio-sorption technique and the percentage of not removed were 0.01%, 0.01%, 0.07%, 5%, 10% and 14% for Fe, Mn, Ni, EC, $SO_4^{2-}$ and TDS, respectively. This combination of selective precipitation and bio-sorption techniques yielded the best result for AMD treatment and valorization. Overall, the chemical treatment step contributed close to 97% of overall pollutants removal, while the bio-sorption step contributed only to 3% of overall chemical species attenuation; thus, designating it as a polishing stage.

**Overall Water Quality**

Chemical properties of AMD before and after treatment using a combination of selective precipitation with MgO and bio-sorption using BPs were compared with guideline values for drinking water and effluent discharge as set by regulatory bodies and the results are presented in Table 3.

The parameters of concern were pH, TDS, EC and metals (Al, Cu, Fe, Mn, Ni, Zn) and sulphate ions. After the treatment using the hybrid technology, the pH of raw AMD rose from 1.7 to 10 leading to mostly complete removal of all metals of concerns except Fe and significant reduction of $SO_4^{2-}$, EC and TDS. The findings corroborated with previous studies as revealed in the literature for both chemical treatment and biological treatment. In fact, selective precipitation allowed to significantly reduce metals and $SO_4^{2-}$ concentration, which can further be recovered [1, 43], while the biological treatment using BPs served as polishing step to remove residual chemical pollutants [47, 73]. The values of all chemical parameters of concern were within the DEA guidelines standard for effluent discharge. However, drinking water standard as set by WHO and the DWS in the republic of South Africa could not be directly reclaimed using this hybrid technology due to the high concentration of $SO_4^{2-}$ (1250 mg/L) and Fe (0.6 mg/L) in final product water which are slightly above the MPLs of 500 mg/L and 0.1 mg/L for $SO_4^{2-}$ and Fe, respectively. Nevertheless, the finding of this study revealed that valuable minerals (Al, Fe, Mn, and gypsum) could be recovered from AMD using selective precipitation due to their high concentrations in raw

**Table 3.** Concentration of chemical species in AMD water before and after treatment compared to DEA, DWS and WHO

| Parameters of concern | Raw AMD | Treated AMD | Removal efficiency (%) | DWS guidelines for drinking water | WHO guidelines for drinking water | DEA guidelines for effluent discharge |
|---|---|---|---|---|---|---|
| pH | 1.7 | 10 | 8.3 (increment) | 5.5–9.7 | 6.5–8.5 | 6–12 |
| EC (µS/cm) | 5000 | 50 | 95 | 170 | <400 | 700 |
| TDS (mg/L) | 7380 | 1030 | 86 | 2400 | <600 | 1200 |
| Al (mg/L) | 160 | <0.001 | 100 | 0–0.3 | 0–0.1 | 20 |
| Cu (mg/L) | 2.50 | <0.002 | 100 | 0.1 | 0.1 | 20 |
| Fe (mg/L) | 6000 | 0.6 | 99.99 | 0–0.1 | 0–0.03 | 50 |
| Mn (mg/L) | 40.7 | 0.002 | 99.99 | 0–0.05 | 0–0.08 | 20 |
| Ni (mg/L) | 1.53 | 0.001 | 99.93 | 0–0.07 | 0–0.07 | 10 |
| Zn (mg/L) | 8.16 | <0.005 | 100 | 0–0.05 | 0–0.1 | 20 |
| $SO_4^{2-}$ (mg/L) | 12500 | 1250 | 90 | 0–500 | 0–250 | 2400 |

AMD: Acid mine drainage; DWS: Department of Water and Sanitation; WHO: World Health Organization; DEA: Department of Environmental Affairs.

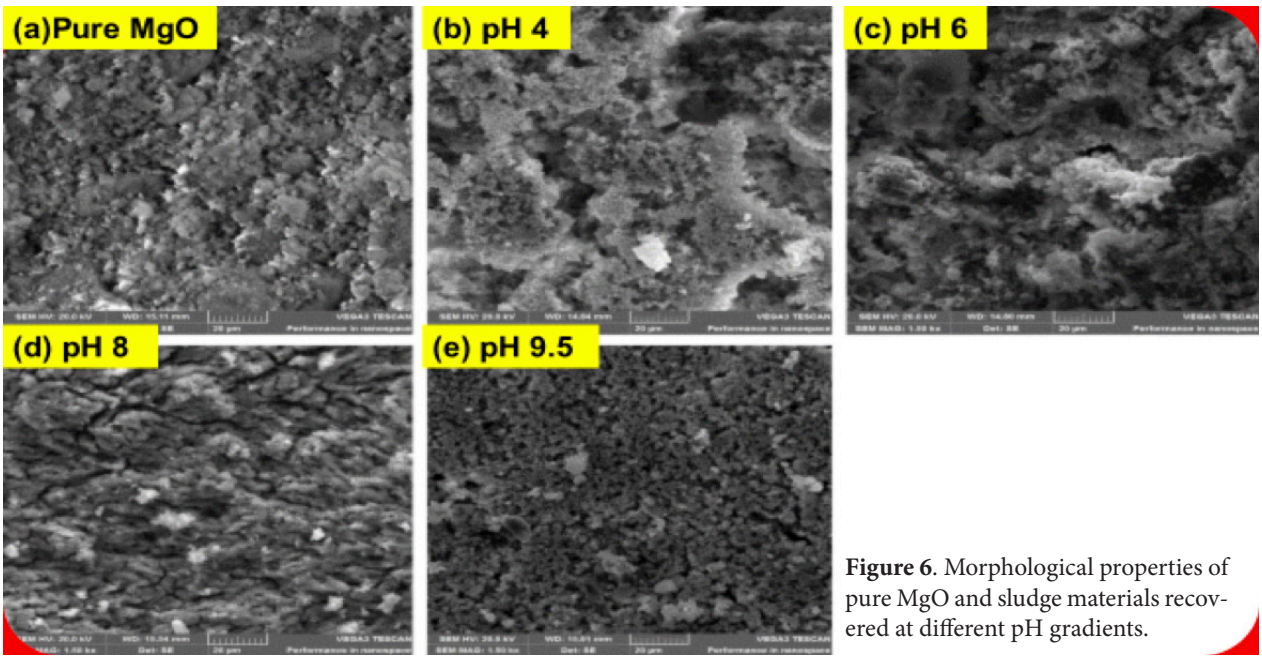


**Figure 6**. Morphological properties of pure MgO and sludge materials recovered at different pH gradients.

AMD water. However, Cu, Ni and Zn cannot be recovered due to the very low (trace) concentrations in raw AMD and as such, economically insignificant.

### Characterization of the Solid Samples

In this section, the results of mineralogical composition, chemical composition, elemental spectra, functional group of raw MgO and sludge materials recovered at each pH interval raw and AMD treated with BPs as well as the mass change in BPs samples are discussed.

### Morphological Properties of Raw MgO, Sludge and Banana Peels

#### *Morphology Property of MgO and Sludge*

Scanning electron microscopy analysis was performed to determine the morphological properties of pure MgO and sludge materials recovered at each pH interval and the results are shown in Figure 6a–e.

The SEM image of raw MgO (Fig. 6a) revealed flower-like and shaped particles of two different size on the surface indicating that the material is heterogeneous in nature and characterized by two different elements proving that this material is MgO as revealed by EDS results. The finding is in line with what have been reported in literature [74]. Figure 6b, which represents SEM image of sludge material collected at pH 4 showed sheet-like structure across the surface indicating that the material is heterogeneous. The sheet-like structure may be attributed to iron hydroxide [$Fe(OH)_3$] formed as results of Fe(III) precipitation. Similar results were obtained in previous studies [1, 43] proving that Fe(III) was effectively precipitated at pH ≤4 to form $Fe(OH)_3$ and Fe-oxyhydrosulphates. At pH 4 (Fig. 6c), the

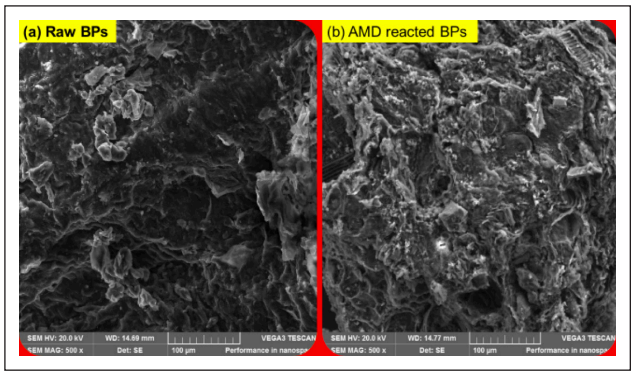


**Figure 7**. Morphological properties of raw and AMD treated with banana peels.

SEM images of sludge materials showed a sort of foliage like and unshaped structures assembled to give the whole materials an irregular structures and may indicate the presence of $Al(OH)_3$ in elevated concentration and minor concentration of $Fe(OH)_2$. This is a prove that Al were effectively precipitated from pH ≥4.5 [75]. The result corroborated with reports from previous studies [41]. At pH 8 (Fig. 6d), the SEM image of sludge materials showed an assemblage of cylindrical form clustered together to form a homogeneous structure across the whole surface. This is an indication of many chemical species precipitated including Cu which is precipitated at pH >6 [56, 57] and $Ca^{2+}$ and $SO_4^{2-}$ which are precipitated throughout the pH (2.5–9.5) range to form $CaSO_4.2H_2O$. At pH 9.5 (Fig. 6e), the SEM images of sludge materials collected showed a heterogeneous structure across the whole surface with large smooth surface, which may be attributed to the formation of $Mn(OH)_2$ followed the precipitation of Mn(II) and Mn(IV) suggesting that major chemical species susceptible to be recovered at pH (8–9.5) is Mn since it is precipitated at the pH 8–9.5 interval [76]. The presence of bright materials on the surface may represent silicon as confirmed by EDS results while the presence of round shapes may represent the formation of $Fe(OH)_2$ following the precipitation of Fe(II).

### *Morphological Properties of Banana Peels*

The SEM analysis of raw and AMD treated with BPs were performed, and the results are shown in Figure 7a, b.

The SEM micrograph of raw BPs and AMD treated with BPs showed different structure with raw BPs showing a smooth surface and various pores with fibers stacked together (Fig. 7a). This may be attributed to the presence of lignin, pectin and other bioactive compounds including phenolic, carotenoids, biogenic, amines and phytosterols [46]. After contact with AMD, the surface of BPs became less smooth with cave pores filled with a mass, which may represent residual chemical species adsorbed from AMD. The findings of this study confirmed what was reported in literature by other researchers when using BPs for metals removal in aqueous solution [77]. Overall, the SEM image of BPs results revealed that BPs contain organic compounds including cellulose that can absorb chemical species by allowing the ions of metals to be bonded by electron-rich functional group.

## EDS Results of Pure MgO, Sludge Materials and Banana Peels

### *EDS Results of Pure MgO and Sludge Recovered at Different pH Gradients*

The effect of selective precipitation process and pH control on metals recovery was gradually assessed using elemental distribution of minerals at each pH gradient and the results are shown in Figure 8a–e.

As shown in Figure 8a (pure MgO), EDS of raw MgO revealed that only two elements were present (Mg and O) with Mg as major element and O being a minor element. Magnesium is alkaline chemical with high chemical reactivity and contribute to increase the alkalinity when mixing with water [78, 79]. This makes MgO a suitable candidate for selective precipitation and metals recovery from AMD under pH control. At pH 4 (Fig. 8b), the EDS of sludge collected revealed that O, Mg and Fe as major components, moderate percentage of sulphur (S), minor percentages of Al, Ca and Mg, and $SO_4^{2-}$ and finally trace amounts of Si. The high percentage of O is attributed to the oxygen from MgO and from water molecule while the elevated percentage of Fe is attributed to the precipitation of Fe(III) from AMD leading to the formation of complexed iron hydroxides [$Fe(OH)_3$] and subsequently solid precipitates since Fe(III) is mostly precipitated in the pH ≤4 [80]. The moderate percentages of S and minor percentage of Al suggest that there is possibility of Fe-oxyhydrosulphates and aluminum hydroxide [$Al(OH)_3$] being formed at pH 3–4 as revealed by previous studies [80]. The minor percentage of Al obtained from sludge materials recovered at this pH ≤4 may also be attributed to the slight precipitation of Al due to the presence of $SO_4^{2-}$ thereby confirming the findings reported in previous studies where a minor proportion of Al is precipitated at pH ≤4 [54, 80].

At pH 6 (Fig. 8c), the recovered sludge material contains very high percentage of O, elevated percentage of Fe and Al. While the elevated percentage of Al is attributed to precipitation of $Al^{3+}$ mostly occurs at pH ≥4 [34, 75], the elevated percentage of Fe is the result of continuous precipitation of Fe(III). The presence of S and Ca as minor component in the sludge material collected at pH 6 indicates the continuous precipitation of Ca and $SO_4^{2-}$ and possible formation of $CaSO_4.2H_2O$ as reported in literature [1, 34, 53]. The EDS further revealed moderate percentage of Al and Fe, minor percentage of Ca, Mn, S, Si and Zn and trace amount of Cu, K and Y. At pH 9.5, the sludge material recovered revealed high percentage of Ca, Minor percentage of Mn, S and Fe and trace of Si, Cu and Na. The high percentage of Ca is attributed to the precipitation of Ca which reach the peak at pH 8.5 while the presence of minor narrow percentage of Fe may be credited to presence of Fe(II), which precipitate at pH ≥8 to form $Fe(OH)_2$ [59]. In addition, $Fe^{3+}$ is precipitated from initial pH to pH 7.5 [34] and this can explain the presence of Fe(III) in sludge material recovered at pH ≥4 thereby overlapping with Al at the precipitation pH interval since both Fe and Al are present in sludge materials recovered throughout the pH 4–8 interval. The presence

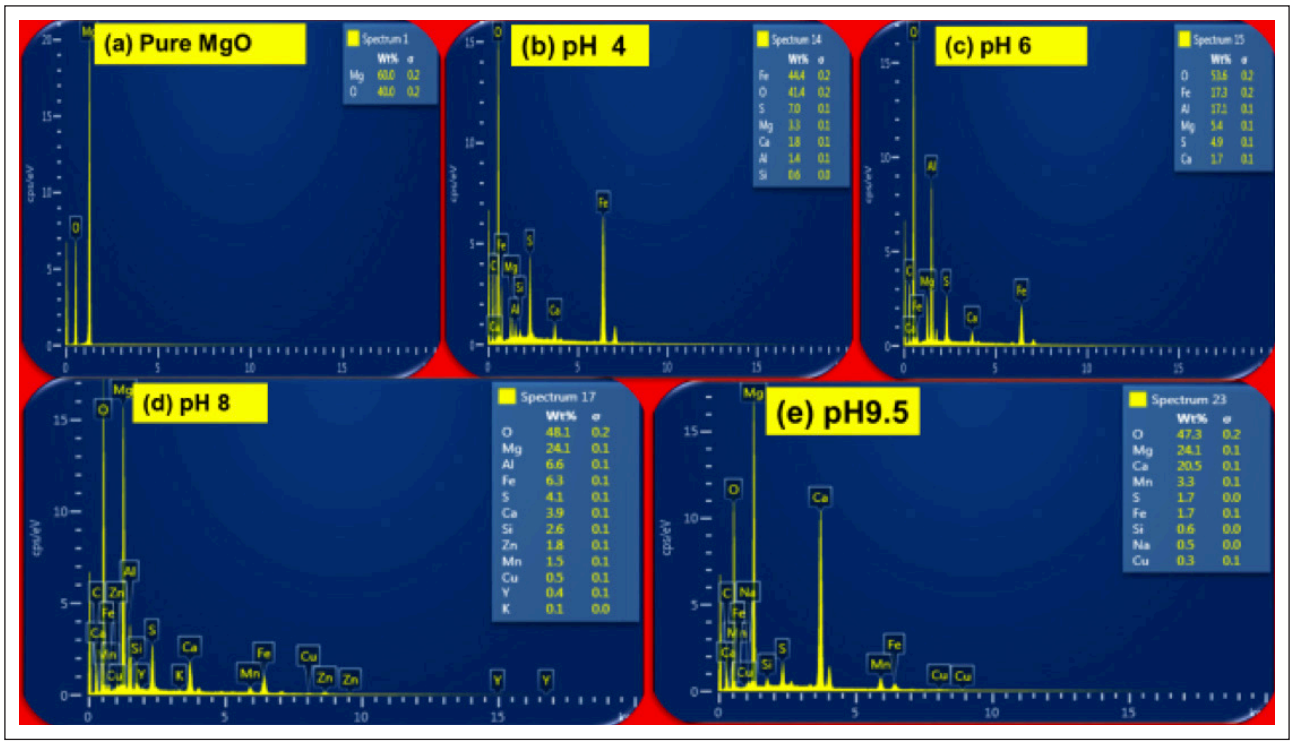


**Figure 8**. Energy dispersive X-ray spectroscopy results of pure MgO and sludge materials recovered at different pH gradients.

of Fe and Al in sludge materials recovered throughout the pH interval may also be attributed to the co-precipitation of Fe(III) and Al. In fact, Fe(II) precipitates at pH (8–9.5), while Al precipitates at pH ≥4.5 and this may justify the presence of Fe and Al in sludge materials recovered thereby confirming previous studies [80]. The presence of Al and S at pH 4–8 interval suggests the formation of Al-hydroxide and Al-oxyhydrosulphates, respectively thereby confirming the findings of studies conducted by previous researchers [80–82]. The presence of Mn indicates the precipitation of Mn(II) and Mn(IV) which occurs at pH ≥8 since EDS results of this study revealed the presence of Mn in sludge materials recovered at pH 8–9.5 interval. The results were in line with previous studies conducted by Masindi et al. [1] when they used cryptocrystalline magnesite for a selective precipitation of metals in AMD water. Due to its many oxidation states, Mn(II) and Mn(IV) precipitate at variable pH range (8≤ pH ≤10) and this justify the high percentage of Mn in sludge material recovered at pH (8–9.5) interval [83].

### *EDS Results of Raw and Treated with Banana Peels*

The product water reclaimed at pH 9.5 was further polished by means of bio-sorption techniques using BPs to remove residual chemical species and reclaim possible drinking water standard. The spectra of raw and AMD treated with BPs are shown in Figure 9a, b.

As illustrated in Figure 9a, the EDS of raw BPs revealed the presence of various elements along with O, K, Si and Ca as major components with percentage composition of 77.1%, 9.5%, 6.4% and 3.2%, respectively while P, Mg, S and Cl with percentage composition of 1%, 1%, 0.9% and 0.9%, respectively are trace components. The high levels of O, K, Si and

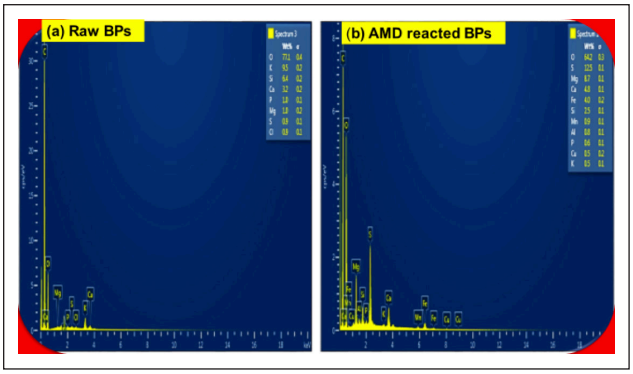


**Figure 9**. Energy dispersive X-ray spectroscopy of raw and AMD treated with banana peels.

Ca in raw BPs confirmed the heterogeneous structure of BPs bio-sorbent as reported in the literature [83–85]. This may be attributed to chemical composition and different functional groups present in BPs bio-sorbent. After contact with AMD water (Fig. 9b), the BPs revealed the presence of more elements of which O and Mg, were major components with a percentage of 45.7% each, Ca, S and Mn were minor elements with a percentage composition of 3.7%, 2% and 1.2%, respectively while Fe, Al Si, K and Cl were trace elements with a percentage composition of 0.5%, 0.4%, 0.4% 0.2% and 0.1%, respectively. The presence of S, Fe, Ca, Al and Mn, in AMD treated with BPs is attributed to its use as bio-sorbent to polish the AMD water previously treated using selective precipitation technique; thus, confirming that their removal from AMD. The EDS results proved that BPs adsorbed residual chemical species, thereby confirming the results obtained after analysis of final product water.

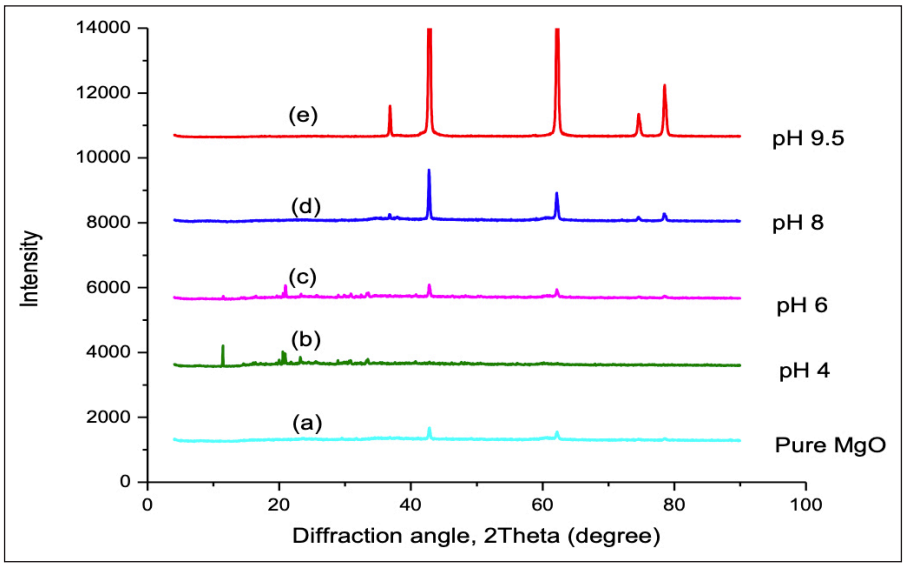


**Figure 10**. Powder X-ray diffraction results of pure MgO and sludge materials recovered at different pH interval: pH 4, pH 6, pH 8 and pH 9.

## Powder X-ray Diffraction Results of Pure MgO Sludge Materials And Bio-sorbent

### *Powder X-ray Diffraction of Pure MgO and Sludge Materials*

The sludge materials recovered at different pH levels were analyzed for chemical phase present and chemical composition information and the results are shown in Figure 10a–e.

From Figure 10, it follows that raw MgO is almost amorphous showing two peaks at 2θ = 43°and 2θ = 62° likely revealing the presence of polycrystalline cubic structure of MgO [86]. These peaks may correspond to periclase which is the only crystalline form of MgO as revealed by previous studies [86]. However, after using MgO for selective precipitation of metals in AMD water, the pH of AMD water rose from 1.7 to 4. The sludge material recovered at pH 4 interval showed a series of peaks at 2θ = 11°, 20°, 22°, 29° and 35°. These peaks may correspond to Fe-hydroxide formed at pH 3.5–4 thereby confirming SEM-EDS results, proving that Fe can be recovered from sludge materials recuperated at pH 4. Similar p-XRD results were obtained by previous researchers [1, 28, 43] where they used different chemical materials for metals recovery from AMD. At pH 6, the sludge materials recovered showed peaks at 2θ = 20°, 34°, 40° and 62°, which may indicate the presence of Al, calcite and gypsum. At pH 8 interval, p-XRD analysis revealed peaks at 2θ = 43°, 62°, 75° and 79°, which may indicate the presence of gypsum resulting from $SO_4^{2-}$ precipitation at pH ≥4.5 as revealed by previous studies [56]. At pH 9.5 interval, the sludge materials collected showed various peaks with peak at 2θ = 36°, which may indicate the presence of Mn. The peaks at 2θ = 43° and 62° indicate the presence of brucite, while the peaks at 2θ = 75° may correspond to copper(II) oxide (CuO) formed following the precipitation of Cu at pH >6 and the peak at 2θ = 79° may indicate the nickel oxide (NiO) following the precipitation of nickel at pH 8–9 interval [87]. The difference in intensity may be explained by the fact that as intensity increases, the diffraction process becomes narrower and more intense.

### *Powder X-ray Diffraction Results of BPs Bio-sorbent*

The product water reclaimed at pH 9.5 was polished using BPs and the p-XRD analysis results are shown in Figure 11a, b.

The p-XRD analysis of raw BPs (Fig. 11a) and AMD treated with BPs (Fig. 11b) revealed a typical cellulose structure at 2θ = 14° for raw BPs and 2θ = 20° for AMD treated with BPs [88, 89]. The series at 2θ = 30°, 34°, 37°, 40° and 52° in AMD treated with BPs is the evidence of the presence of chemical species notably Al, Cu, Fe, Mn and $SO_4^{2-}$ as revealed by EDS results thereby confirming what has been reported in literature [47]. Based on the p-XRD results, it can be concluded that BPs adsorbed residual chemical species from pre-treated AMD.

## Fourier Transform Infrared (FTIR) Spectra of Sludge and BPs

### *FTIR Spectra of Pure MgO and Sludge Materials*

The functional groups of pure MgO and sludge collected at different pH levels were analyzed and the results are shown in Figure 12a–e.

Figure 12 portrayed that raw MgO is characterized by the vibration at 500 $cm^{-1}$, which may be attributed to carbonate species chemisorbed on the surface of MgO as reported by previous researchers [90]. The FTIR spectra of pure MgO and all sludge materials recovered at different pH levels showed the doublets at 2000 and 2150 $cm^{-1}$, which may be attributed to the Mg-O stretching vibration [90], while the stretching vibration at 2600 $cm^{-1}$ in pure MgO may correspond to asymmetric stretching vibration of alkyl (C-H) functional group [90, 91]. The sludge materials recovered at pH 4, pH 6, pH 8 and pH 9.5, intervals showed peaks with stretching vibration at 1100 $cm^{-1}$, which may be attributed to carbonate esters functional group [$R_1O$-(C=O)-$OR_2$] from AMD water as confirmed by SEM-EDS analysis, while the vibration at 1670 $cm^{-1}$ may correspond to hydroxyl functional group (O-H) or carboxyl function-

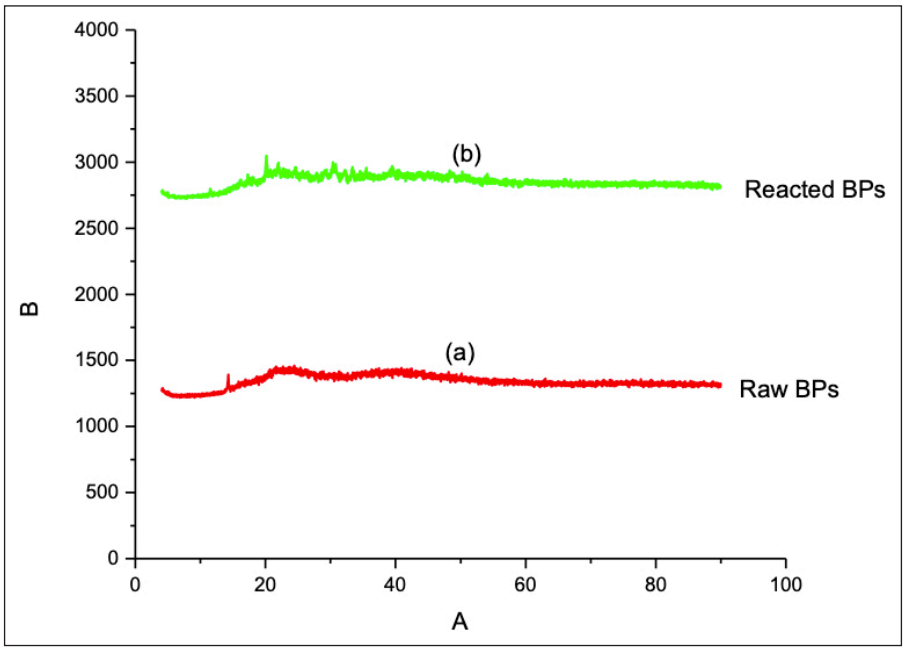


**Figure 11**. Powder X-ray diffraction results of raw and AMD treated with banana peels.

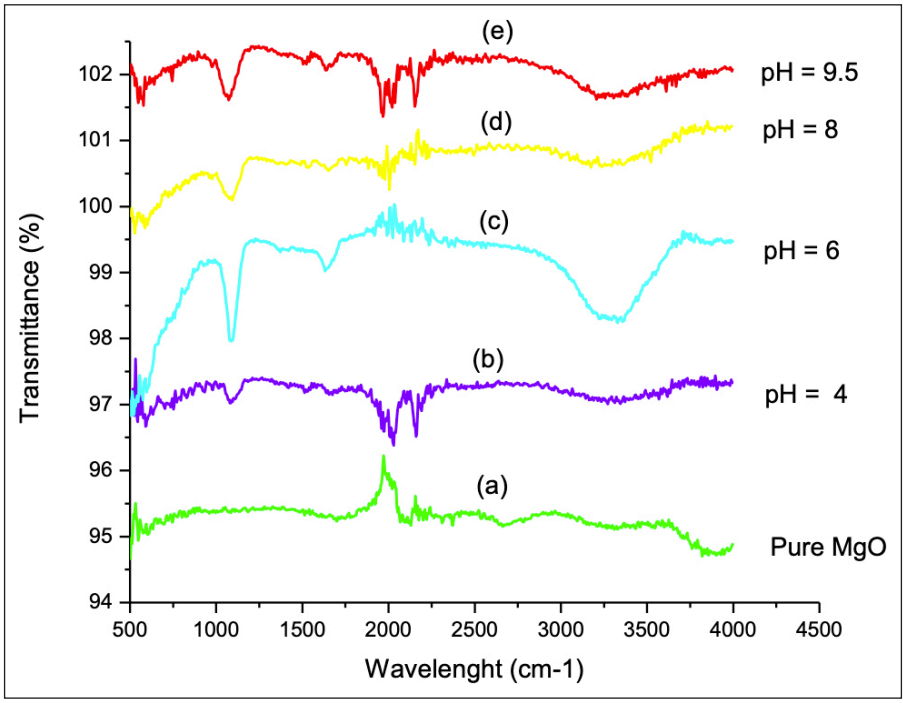


**Figure 12**. FTIR spectra of pure MgO and sludge materials recovered at different pH gradients.

al group (C=O) stretching vibration as revealed by previous studies [1]. In addition, the sludge recovered at pH 8 and at pH 9.5 interval showed the band at 600 $cm^{-1}$, which may correspond to Fe(II) and Fe(III) precipitated during the selective precipitation. The stretching vibration corresponding to band at 3250 $cm^{-1}$ observed in sludge materials collected at pH 6, pH 8 and pH 9.5 may correspond to Al-OH-Al functional group indicating the presence of aluminum hydroxide $Al(OH)_3$ confirming that Al could potentially be recovered from sludge materials collected at those pH gradients, which agree with SEM-EDS results. The peak at 1650 $cm^{-1}$ in sludge materials recovered at pH 9.5 may indicate the stretching vibration of Mn-OH-Mn functional group thereby confirming the presence of $Mn(OH)_2$. The findings corroborated with the results obtained in previous studies [1, 43], thereby confirming that many functional groups are formed during selective precipitation of metals in AMD water.

### *FTIR Spectra of BPs Bio-sorbent*

The product water collected at pH 9.5 was further polished by means of bio-sorption technique using BPs. Raw and

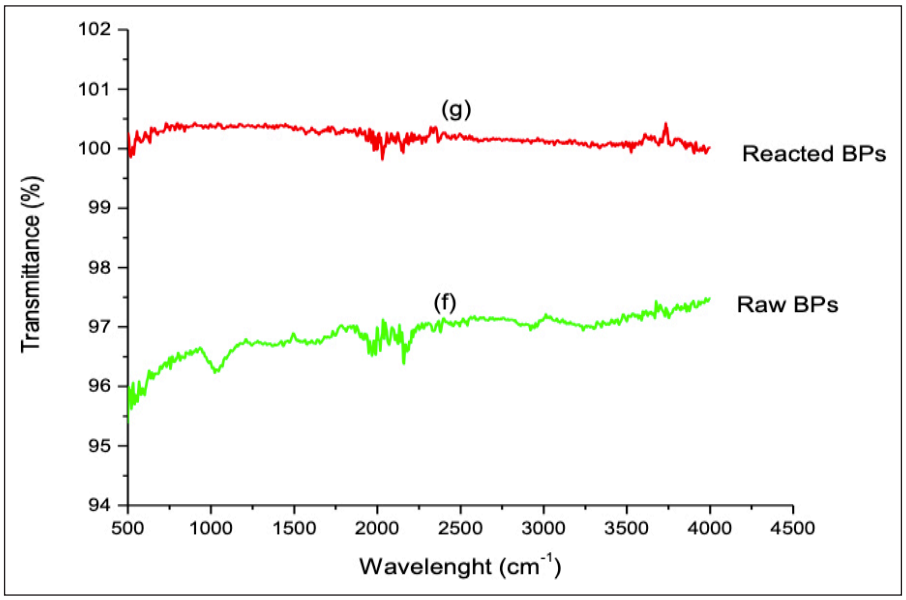


**Figure 13**. FTIR spectra of pure MgO and sludge materials recovered at different pH gradients.

AMD-treated with BPs were analyzed for functional group and the spectra as shown in Figure 13f, g.

The FTIR spectra revealed that BPs contain various functional groups that include hydroxyl, carboxyl and amine groups in its biomass, which facilitate the binding of metal ions from aqueous solution [35, 46]. Both spectra displayed several peaks, which may be attributed to the complex nature of BPs and its tendency to act as bio-sorbent. Bands appearing at 3750 $cm^{-1}$ for both spectra are indicative of hydroxyl group of polymeric compound, while bands with stretching vibration at 2000 $cm^{-1}$ may be attributed to carbonyl group (C=O) and carboxyl group (-COOH) thereby confirming the findings reported by Arifiyana and Devianti. [92]. The spectrum of raw BPs (Fig. 13f) displayed a peak at 1000 $cm^{-1}$ and 3000 $cm^{-1}$ indicating the presence of hydroxyl and carboxyl groups, respectively. Contrary to the spectrum of raw BPs, the spectrum of AMD treated with BPs (Fig. 13b) revealed significant reduction of intensity, which led to the complete disappearance of peaks at 1000 $cm^{-1}$ and 3000 $cm^{-1}$. The complete disappearance of these peaks in AMD reated with BPs may be attributed to the effective adsorption of pollutants onto the bio-sorbent surface. This finding corroborated with the results obtained by Rao et al. [93] and by Badessa et al. [94] when the used BPs based bio-sorbent for the removal of heavy metals from synthetic solutions and BPs powder for effective removal of chromium from wastewater, respectively.

**Thermogravimetric Analysis Results**

The thermal decomposition of BPs was studied using TGA analysis and the results revealed that raw and treated with BPs displayed the same patterns with two mass loss but at different temperature as shown in Figure 14a, b.

From Figure 14, it follows that the first mass loss happened between 3 and 14 and between 3 and 22 °C for raw and AMD treated with BPs, respectively. This may correspond to the loss of biomass as a result of moisture removal and some low molecular volatile compounds from the BPs biomass [95, 96]. The mild change in % of weight between raw and treated with BPs may be attributed to the presence of pollutants (chemical species) in AMD treated with BPs. In fact, following the contact of BPs with AMD water for an optimum contact time of 300 min, chemical species are adsorbed, and their degradation require high temperature, and this may explain the mild change in % between the raw and AMD treated with BPs. In the second mass loss (14 and 60 °C) for raw BPs (Fig. 14a) and between 23 and 85 °C for AMD treated with BPs (Fig. 14b), the 2 curves remain similar in nature but the slope of curve of raw BPs is steeper and this may indicate a faster conversion and mass loss with increasing temperature [96, 97]. The second mass loss in raw BPs may be attributed to the thermal degradation of cellulose, lignin and hemicellulose thereby confirming the finding reported by Kabenge et al. [98], when they studied the TGA analysis of pure BPs. The finding also revealed the continuous mass loss in AMD treated with BPs. Given that pollutants and specifically metals are difficult to decay, this may be indicating the presence of metals in AMD treated with BPs [95, 96]. Metals doping or impurities in the pre-treated AMD water were adsorbed by BPs and as result, require high temperature for their degradation.

**Zeta Potential of Bio-sorbent (BPs)**

The zeta potential measurements allow to determine the charge of adsorbent at a particular pH level and the point of zero charge (PZC), the point where the adsorbent has a zero charge [61]. In this study, the zeta potential of raw banana peels (BPs) and AMD treated with RBPs was evaluated in the pH range of 1 to 13 as illustrated in Figure 15.

Figure 15 depicted that the PZC were 2.6 and 2.9 for BPs and RBPs, respectively. It follows that both BPs and RBPs

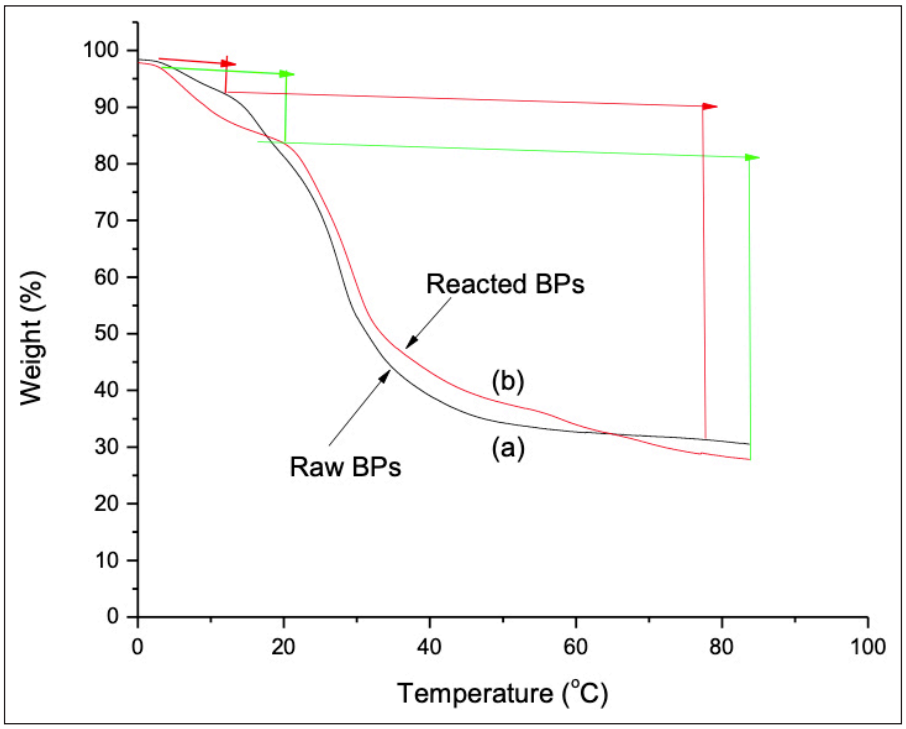


**Figure 14**. Thermogravimetric results of raw and AMD treated with banana peels.

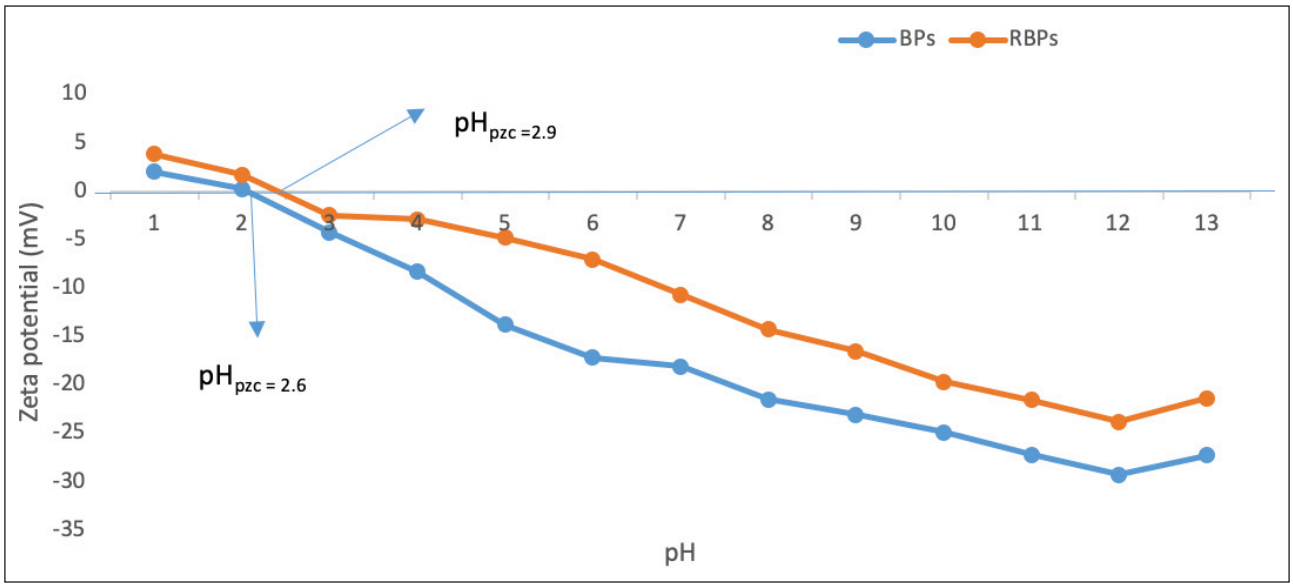


**Figure 15**. Zeta potentials of raw and AMD treated with banana peels.

assumed negative charge above the PZC. At pH below the PZC, the charge of the solid surface of bio-sorbent is positive and therefore accept protons since the basic group has the possibility to share electrons [99]. However, at pH above the PZC, the surface of the bio-sorbent (BPs) is negatively charged due to the deprotonation of acid groups leading to the interaction with cationic species. The zeta potential has a huge influence on the sorption of chemicals species since those with positive charges will be attracted by the sorbent materials bearing a negative charge while those with negative charges will be attracted by the sorbent materials bearing a positive charge [61, 100, 101]. The narrow difference between the PZC of BPs and RBPs suggest that after contact of BPs with AMD, the buffering capacity of the BPs increased as reported by previous studies [61].

**Limit of Detection and Limit of Quantification Results**

The LOD or minimum detectable concentration of analyte is the lower amount that can be detected using an analytical standard method while the LOQ is the concentration that can be determined in sample matrix precisely and accurately. The LOD and LOQ of metals (Al, Cu, Fe, Mn, Ni, Zn) and $SO_4^{2-}$ were obtained using ICP-OES and IC, respectively and the results are presented in Table 4.

**Table 4.** Limit of detection and limit of quantification of metals and sulphate ions

| Chemical species | Coefficient of determination ($R^2$) | LOD (mg/L) | LOQ (mg/L) |
|---|---|---|---|
| Al | 0.9993 | 0.001 | 0.003 |
| Cu | 0.9987 | 0.002 | 0.006 |
| Fe | 0.9997 | 0.03 | 0.099 |
| Mn | 0.9999 | 0.01 | 0.033 |
| Ni | 0.9989 | 0.05 | 0.166 |
| Zn | 0.9992 | 0.003 | 0.009 |
| $SO_4^{2-}$ | 0.9995 | 0.116 | 0.386 |

LOD: Limit of detection; LOQ: Limit of quantification.

The calibration curve was used to determine the linearity. The coefficient of determination ($R^2$) allowed to extrapolate and estimate statistical analysis of unknown concentration of chemicals species where data were considered accurate when $R^2$ was equal to or close to 1. Linear concentration ranged from 0.1 to 3.5 mg/L was used to test the linearity of calibration curves while the linearity of $SO_4^{2-}$ was tested in linear concentration ranged from 10 to 50 mg/L. The $R^2$ of all determined chemical species are 0.9993, 0.9987, 0.9997, 0.9999, 0.9989, 0.9992, 0.9995 and 1.0000 for Al, Cu, Fe, Mn, Ni, Zn and $SO_4^{2-}$, respectively. This merely means that unknown concentration of each chemical species of concern was extrapolated on the calibration curve with a prediction between 99.23 and 100% for Al, 99.77 and 100% for Cu, 99. 97 for Fe, 99.99 for Mn, 99.89 for Ni, 99.82 for Zn and 99.95 for $SO_4^{2-}$.

### Regeneration of BPs Results

In order to further ensuring environmental pollution control, a regeneration study was conducted since regeneration reduce the need of new adsorbent as well as the disposal of used adsorbent, thereby playing a vital role in environmental pollution control [102]. The reusability of BPs for the polishing of pre-treated AMD water was performed by investigating various adsorption-desorption cycles to assess the RE of bio-sorbent (BPs) in term of number of cycles that can be conducted to ensure complete regeneration and the results are shown in Figure 16.

Figure 16 depicted that the bio-sorbent RE decrease as well as the number of regeneration cycles increase, and this may be credited to the loss of bio-sorbent mass during filtration. Furthermore, the RE differs from one chemical species to another and this can be attributed to biochemical factors including sizes of chemical species, binding value constant with the BPs, extent of hydration and their tendency to attract electrons as revealed by previous studies [103, 104]. The results corroborated with previous findings proving that BPs can be an efficient bio-sorbent to be used in bio-sorption techniques for water treatment due to the possibility of regeneration of it without high impact on it bio-sorption capacity.

## CONCLUSION

The feasibility of selective precipitation of chemical species from AMD using MgO and the polishing of product water using BPs was evaluated. The pH of AMD water was gradually increased and metals were selectively precipitated and optimum condition of 2.3 g:2000 mL (w/v or 2.3:2000 ratio), was applied to reach the maximum pH of 9.5 achievable using MgO while the optimum condition for bio-sorption step was 1:500 mL or 1:500 ratio for a 300 min of equilibration as reported by Mahlangu et al. [47] were applied in this study. The chemical treatment using selective precipitation led to an increase of pH from 1.7 to 9.5, significant reduction of EC, TDS, $SO_4^{2-}$ and metals (Al, Cu, Fe, Mn, Ni and Zn). The analysis of sludge materials recovered at different pH gradients revealed that chemical species were selectively precipitated, thereby confirming that valuable chemical species including Al, Cu, Fe, Mn, Ni, Zn and $CaSO_4.2H_2O$ can be recovered using selective precipitation with Fe and $CaSO_4.2H_2O$ being the major chemical species as confirmed by their high percentage in EDS results. The polishing of product water using BPs further increased the pH from 9.5 to 10 leading to more removal of pollutants with an overall RE as follows: Al (100%), Cu (100%), Zn (100%) > Fe (99.99%), Mn (99.99%) > Ni (99.93%) > EC (95%) > $SO_4^{2-}$ (90%) > TDS (86%). The selective precipitation using MgO allowed to recover sludge

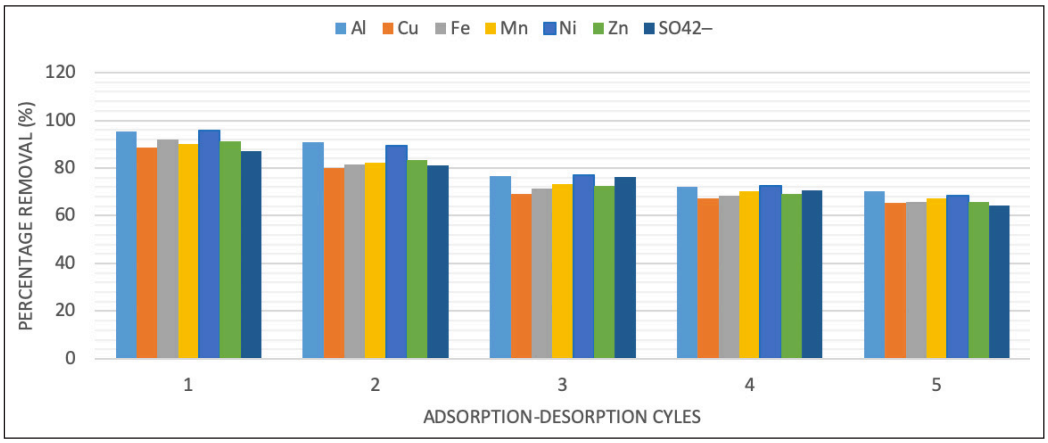


**Figure 16**. Adsorption-desorption cycles of chemicals species of concern.

rich in metals at different pH gradient and substantially contributed to overall removal of chemical species with RE in the following order: Fe (99.96%) > Cu (99.7%) > Al (99.36%) > Ni (99.34%) > Zn (99%) > Mn (97.47%) > EC (90%) > TDS (78%) > $SO_4^{2-}$ (75%), while the bio-sorption using BPs for 300 min accounted for a minor fraction of overall chemical species removal with RE as follows: $SO_4^{2-}$ (15%) > TDS (8%) > EC (5%) > Mn (2.53%) > Zn (1%) > Ni (0.66%) > Al (0.64%) > Cu (0.4%) > Fe (0.03%). This study revealed the efficiency of MgO in selective precipitation of metals from AMD; thereby, reducing pollutants concentration and the polishing potential of BPs. Overall, this study proved that AMD can be valorized through selective precipitation and recovery of metals using MgO and polish the product water using BPs to reclaim drinking water standards. This will go a long way to implement CEA in both mining and agricultural industries thereby controlling environmental pollution associated with the above mentioned industries. However, the technology presents some disadvantage such as the coloration of product water after polishing using BPs but calcinated BPs can be used to polish the pre-treated AMD water in order to avoid coloration of product water.

## ACKNOWLEDGEMENTS

The authors would like to acknowledge the Faculty of Science, University of Johannesburg for postdoctoral scholarship for NB. The project is supported by the Water Research Commission (WRC) of South Africa, Project Number C2022/2023-00933. We acknowledge the University of Johannesburg Research Centre for Synthesis and Catalysis and Spectrum for the facility.

## DATA AVAILABILITY STATEMENT

The author confirm that the data that supports the findings of this study are available within the article. Raw data that support the finding of this study are available from the corresponding author, upon reasonable request.

## CONFLICT OF INTEREST

The author declared no potential conflicts of interest with respect to the research, authorship, and/or publication of this article.

## USE OF AI FOR WRITING ASSISTANCE

Not declared.

## ETHICS

There are no ethical issues with the publication of this manuscript.

## REFERENCES

[1] V. Masindi, J. G. Ndiritu, and J. P. Maree, "Fractional and step-wise recovery of chemical species from acid mine drainage using calcined cryptocrystalline magnesite nano-sheets: An experimental and geochemical modelling approach," Journal of Environmental Chemical Engineering, Vol. 6(2), pp.1634–1650, 2018. [CrossRef]

[2] N. Beauclair, V. Masindi, T. A. M. Makudali, M. Tekere, and I. M. Ndoh, "Assessing the performance of horizontally flowing subsurface wetland equipped with Vetiveria zizanioides for the treatment of acid mine drainage," Advances in Environmental Technology, Vol. 8(2), pp. 103–127, 2022.

[3] V. Masindi, M. S. Osman, and R. "Shingwenyana, valorization of acid mine drainage (AMD): A simplified approach to reclaim drinking water and synthesize valuable minerals-Pilot study," Journal of Environmental Chemical Engineering, Vol. 7(3), Article 103082, 2019. [CrossRef]

[4] J. G. Skousen, P. F. Ziemkiewicz, and L. M. McDonald, "Acid mine drainage formation, control and treatment: Approaches and strategies," Extractive Industries and Society, Vol. 6(2), pp. 241–249, 2019. [CrossRef]

[5] K. Moeng, "Community perceptions on the health risks of acid mine drainage: the environmental justice struggles of communities near mining fields," Environmental Development Sustainaible, Vol. 21, pp. 2619–2640, 2019. [CrossRef]

[6] V. Akinwekomi, J. P. Maree, C. Zvinowanda, and V. Masindi, "Synthesis of magnetite from iron-rich mine water using sodium carbonate," Journal of Environmental Chemical Engineering, Vol. 5(3), pp. 2699–2707, 2017. [CrossRef]

[7] D. K. Nordstrom, D. W. Blowes, and C. J. Ptacek, "Hydrogeochemistry and microbiology of mine drainage: An update," Applied Geochemistry, Vol. 57, pp. 3–16, 2015. [CrossRef]

[8] A. Teresa, C. Francisco, A. Catarina, R. Loayza-Muro, S. Bruna, J. Diaz-Curiel…, and J.A. Grande, "Extremely acidic eukaryotic (Micro) organisms: Life in acid mine drainage polluted environments — mini-review," International Journal of Environmental Research and Public Health, Vol. 19(1), pp. 1–13, 2022. [CrossRef]

[9] M. A. Caraballo, T. S. Rötting, F. Macías, J. M. Nieto, and C. Ayora, "Field multi-step limestone and MgO passive system to treat acid mine drainage with high metal concentrations," Applied Geochemistry, Vol. 24(12), pp. 2301–11, 2009. [CrossRef]

[10] T. S. Rötting, M. A. Caraballo, J. A. Serrano, C. Ayora, and J. Carrera, "Field application of calcite Dispersed Alkaline Substrate (calcite-DAS) for passive treatment of acid mine drainage with high Al and metal concentrations," Applied Geochemistry, Vol. 23(6), pp. 1660–1674, 2008. [CrossRef]

[11] O. Y. Toraman and M. S. Delibalta, "Ultrasonic desulfurization of low rank Turkish coal using various chemical reagents," Journal of Multidisciplinary Engineering Sciences and Technology, Vol. 3(4), pp. 4621–4623, 2016.

[12] V. Masindi, M. W. Gitari, H. Tutu, and M. Debeer, "Efficiency of ball milled South African bentonite clay for remediation of acid mine drainage," Journal of Water Process Engineering, Vol. 8, pp. 227–240, 2015. [CrossRef]

[13] C. O. A. Turingan, K. S. Cordero, A. L. Santos, G. S. L. Tan, R. D. Alorro, and A. H. Orbecido. "Acid mine drainage treatment using a process train with laterite mine waste, concrete waste, and limestone as treatment media, Water, Vol. 14(7), pp. 1–21, 2022. [CrossRef]

[14] B. Nguegang, V. Masindi, T. A. M. Msagati, and M. Tekere. "The treatment of acid mine drainage using vertically flowing wetland: Insights into the fate of chemical species," Minerals, Vol. 11(5), pp. 1–24, 2021. [CrossRef]

[15] B. Nguegang, V. Masindi, T. A. M. Msagati, and T. Memory, "Passive remediation of acid mine drainage using phytoremediation: Role of substrate, plants, and external factors in inorganic contaminants removal," Wiley, 2023.

[16] L. Marchand, M. Mench, D. L. Jacob, and M. L. Otte, "Metal and metalloid removal in constructed wetlands, with emphasis on the importance of plants and standardized measurements: A review," Environmental Pollution, Vol. 158(12), pp. 3447–3461, 2010. [CrossRef]

[17] S. Alemdag, E. Akaryali, and M. A. Gücer, "Prediction of mine drainage generation potential and the prevention method of the groundwater pollution in the Gümüşköy (Kütahya) mineralization area, NW Turkey," Journal of Mountain Sciences, Vol. 17, pp. 2387–2404, 2020. [CrossRef]

[18] E. Akaryalı, M. A. Gücer, and S. Alemdağ, "Atık barajı rezervuarı ve cevher stok alanlarında asit maden drenajı (AMD) oluşumunun değerlendirilmesi: Gümüşhane örneği atık barajı rezervuarı ve cevher stok alanlarında asit maden drenajı (amd) oluşumunun değerlendirilmesi: Gümüşhane örneği," Journal of Natural Hazard and Environmentno, Vol. 4(2), pp. 192–209, 2018. [CrossRef]

[19] M. A. Gücer, S. Alemdağ, and E. Akaryali, "Assessment of acid mine drainage formation using geochemical and static tests in Mutki (Bitlis, SE Turkey) mineralization area," Turkish Journal of Earth Sciences Vol. 29, pp. 1189–1210, 2020. [CrossRef]

[20] G. H. Berghorn and G. R. Hunzeker, "Passive treatment alternatives for remediating abandoned- mine drainage," Remediation, Vol. 11(3), pp. 111–127, 2001. [CrossRef]

[21] J. D. Kiiskila, D. Sarkar, K. A. Feuerstein, and R. Datta, "A preliminary study to design a floating treatment wetland for remediating acid mine drainage-impacted water using vetiver grass (Chrysopogon zizanioides)," Environmental Sciences and Pollution Resarch, Vol. 24, pp. 27985–27993, 2017. [CrossRef]

[22] D. Kiiskila, D. Sarkar, S. Panja, S. V Sahi, and R. Datta, "Remediation of acid mine drainage-impacted water by vetiver grass (Chrysopogon zizanioides): A multi-scale long-term study," Ecological Engineering, Vol. 129, pp. 97–108, 2019. [CrossRef]

[23] B. G. Lottermoser and P. M. Ashley, "Trace element uptake by Eleocharis equisetina (spike rush) in an abandoned acid mine tailings pond, northeastern Australia: Implications for land and water reclamation in tropical regions," Environmental Pollution, Vol. 159(10), pp. 3028–3035, 2011. [CrossRef]

[24] B. Nguegang, V. Masindi, T. A. M. Msagati, and M. Tekere, "Effective treatment of acid mine drainage using a combination of MgO-nanoparticles and a series of constructed wetlands planted with Vetiveria zizanioides: A hybrid and stepwise approach," Journal of Environmental Management, Vol. 310, Article 114751, 2022. [CrossRef]

[25] B. Nguegang, V. Masindi, T. T.A.M. Msagati, M. Tekere, and A.A Ambushe, "Hybrid treatment of acid mine drainage using a combination of mgo-nps and a series of constructed wetland planted with vetiveria zizanioides," 35th International Conference on Chemical, Biological and Environmental Engineering (ICCBEE-22) Nov. 28–29, 2022 Johannesburg (South Africa), 2022.

[26] V. Masindi, M. S. Osman, and A. M, Abu-Mahfouz, "Integrated treatment of acid mine drainage using BOF slag, lime/soda ash and reverse osmosis (RO): Implication for the production of drinking water," Desalination, Vol. 424, pp. 45–52, 2017. [CrossRef]

[27] T. J. Hengen, M. K, Squillace, A. D. O'Sullivan, and J. J. Stone, "Life cycle assessment analysis of active and passive acid mine drainage treatment technologies," Resources Conservation and Recycling. Vol. 86, pp. 160–167, 2014. [CrossRef]

[28] E. MacIngova, and A. Luptakova, "Recovery of metals from acid mine drainage," Chemical Engineering Transactions, Vol. 28, pp. 109–114, 2012.

[29] A. N. Shabalala, S. O. Ekolu, S. Diop, and F. Solomon, "Pervious concrete reactive barrier for removal of heavy metals from acid mine drainage – Column study," Journal of Hazardous Materials, Vol. 323(Pt B), pp. 641–653, 2017. [CrossRef]

[30] A. Khan, (2014). "Ion exchange- A treatment option for acid mine drainage (Master's thesis)." Available from NTNU Open. 2002.

[31] O. Agboola, "The role of membrane technology in acid mine water treatment: A review," Korean Journal of Chemical Engineering, Vol. 36, pp. 1389–1400, 2019. [CrossRef]

[32] A. Munyengabe, C. Zvinowanda, J. Ramontja, and J.N. Zvimba, "Effective desalination of acid mine drainage using an advanced oxidation process: Sodium ferrate (VI) salt," Water (Switzerland), Vol. 13(19), Article 2619, 2021. [CrossRef]

[33] H. J. Choi, "Biosorption of heavy metals from acid mine drainage by modified sericite and microalgae hybrid system," Water Air Soil Pollution, Vol. 226(6), Article 185, 2015. [CrossRef]

[34] E. Y. Seo, Y. W. Cheong, G. J. Yim, K. W. Min, and J. N. Geroni, "Recovery of Fe, Al and Mn in acid coal mine drainage by sequential selective precipitation with control of pH," Catena, Vol. 148(Pt 1), pp.11–16, 2017. [CrossRef]

[35] E. Torres, "Biosorption: A review of the latest advances," Processes, Vol. 8(12), Article 1584, 2020. [CrossRef]

[36] M. Danouche, H. El Arroussi, W. Bahafid, and N. El Ghachtouli, "An overview of the biosorption mech-

anism for the bioremediation of synthetic dyes using yeast cells," Environmental Technology Reviews, Vol. 10(1), pp. 58–76, 2020. [CrossRef]

[37] R. J. Nathan, C. E. Martin, D. Barr, R. J. Rosengren, "Simultaneous removal of heavy metals from drinking water by banana, orange and potato peel beads: A study of biosorption kinetics," Applied Water and Sciences, Vol. 11(7), Article 116, 2021. [CrossRef]

[38] D. Ramutshatsha-Makhwedzha, R. Mbaya, and M. L. Mavhungu, "Application of activated carbon banana peel coated with Al2O3-Chitosan for the adsorptive removal of lead and cadmium from wastewater," Materials, Vol. 15(3), Article 869, 2022. [CrossRef]

[39] S. Park, and M. Lee, "Removal of copper and cadmium in acid mine drainage using Ca-alginate beads as biosorbent," Geosciences Journal, Vol. 21, pp. 373–383, 2017. [CrossRef]

[40] L. F. Leon-Fernandez, H. L. Medina-Díaz, O. G. Pérez, R. Romero, J. Villasenor, and F. J. Fernández-Morales, "Acid mine drainage treatment and sequential metal recovery by means of bioelectrochemical technology," Journal of Chemical Technology and Biotechnology, Vol. 96(6), pp.1543–1552, 2021. [CrossRef]

[41] T. Chen, B. Yan, C. Lei, and X. Xiao, "Pollution control and metal resource recovery for acid mine drainage," Hydrometallurgy, Vol. 147–148, pp.112–119, 2014. [CrossRef]

[42] C. Oh, Y. S. Han, J. H. Park, S. Bok, Y. Cheong, G. Yim, and S. Ji, "Field application of selective precipitation for recovering Cu and Zn in drainage discharged from an operating mine," Sciences of the Total Environment, Vol. 557–558, pp. 212–220, 2016. [CrossRef]

[43] A. Navarro, M. I. Martínez da Matta, "Application of magnesium oxide for metal removal in mine water treatment," Sustainability, Vol. 14(23), Article 15857, 2022. [CrossRef]

[44] A. Sulaiman, A. Othman, and Ibrahim I, "The use of magnesium oxide in acid mine drainage treatment," Materials Today: Proceeding, Vol. 5(10), pp. 21566–21573, 2018. [CrossRef]

[45] E. Mamakoa, V. Masindi, H. Neomagus, "Comparison of MgO and MgCO3 in the treatment of Acid Mine Drainage." 2020. http://eares.org/siteadmin/upload/5831EAP1120216.pdf. data/QCL Accessed on Apr 24, 2023.

[46] A. Ali, "Removal of Mn(II) from water using chemically modified banana peels as efficient adsorbent," Environmental Nanotechnology Monitoring and Management, Vol. 7, pp. 57–63, 2017. [CrossRef]

[47] J. M. Mahlangu, G. S. Simate, and M. Beer, "Adsorption of Mn2+ from the acid mine drainage using banana peel," International Journal of Water and Wastewater Treatment, Vol. 4(1), pp. 1–9, 2018. [CrossRef]

[48] P. Pourhakkak, A. Taghizadeh, M. Taghizadeh, M. Ghaedi, and S. Haghdoust, "Chapter 1- Fundamentals of Adsorption Technology," Vol. 33, pp. 1–70, 2021. [CrossRef]

[49] W. J. Shin, H. S. Shin, J. H. Hwang, and K. S. Lee, "Effects of filter-membrane materials on concentrations of trace elements in acidic solutions," Water (Switzerland), Vol. 12(12), Article 3497, 2020. [CrossRef]

[50] American Public Health Association (APHA), "American Water Works Association) Water Environment Federation, Stand. Methods Exam. Water Wastewater," American Public Health Associatio, 2002.

[51] A. B. M. Helal Uddin, R. S. Khalid, M. Alaama, A. M. Abdualkader, A. Kasmuri, S. A. Abbas, "Comparative study of three digestion methods for elemental analysis in traditional medicine products using atomic absorption spectrometry," Journal of Analytical Sciences and Technology, Vol. 1, Article 6, 2020.

[52] H. Hernández-Mendoza, M. Mejuto, A. I. Cardona, A. García-Álvarez, R. Millán, and A. Yllera, "Optimization and validation of a method for heavy metals quantification in soil samples by inductively coupled plasma sector field mass spectrometry (ICP-SFMS)," American Journal of Analytical Chemistry, Vol. 4, Article 10b, 2013. [CrossRef]

[53] H. B. Vaziri, Y. Shekarian, and M. Rezaee, "Selective precipitation of rare earth and critical elements from acid mine drainage - Part I: Kinetics and thermodynamics of staged precipitation process," Resources Conservation and Recycling, Vol.188, Article 106654, 2023. [CrossRef]

[54] C. Rodríguez, E. Leiva-Aravena, J. Serrano, and E. Leiva, "Occurrence and removal of copper and aluminum in a stream confluence affected by acid mine drainage," Water (Switzerland), Vol. 10(4), Article 516, 2018. [CrossRef]

[55] J. S. España, "Chapter 7- The behavior of iron and aluminum in acid mine drainage. Speciation, mineralogy, and environmental significance," Thermodynamics, Solubility and Environment Issues, pp.137–150, 2007. [CrossRef]

[56] M. Santander-Muñoz, P. Cardozo-Castillo, and L. Valderrama-Campusano, "Removal of sulfate ions by precipitation and flotation, Ingineering Investigation," Chemical, Food, and Environmental Engineering, Vol. 41, Article 3, 2021. [CrossRef]

[57] A. G. Reiss, G, Ittai, Y. O. Rosenberg, I. J. Reznik, A. Luttge, S. Emmanuel, and J. Ganor, "Gypsum precipitation under saline conditions: Thermodynamics, kinetics, morphology, and size distribution," Minerals. Vol. 11(2), Article 141, 2021. [CrossRef]

[58] R. M. Freitas, T. A. G. Perilli, and A. C. Q. Ladeira, "Oxidative precipitation of manganese from acid mine drainage by potassium permanganate," Journal of Chemistry, Vol. 2013, Article 287257, 2013. [CrossRef]

[59] M. Hove, R. P. Van Hille, and A. E. Lewis. "Mechanisms of formation of iron precipitates from ferrous

solutions at high and low pH," Chemical Engineering Sciences, Vol. 63(6), 1626–1635, 2008. [CrossRef]

[60] V, Masindi, M. W. Gitari, H. Tutu, M. De Beer, "Passive remediation of acid mine drainage using cryptocrystalline magnesite: A batch experimental and geochemical modelling approach," Water SA, Vol. 41(5), pp. 677–682, 2015. [CrossRef]

[61] F. O. Afolabi, P. Musonge, and B. F. Bakare, "Adsorption of copper and lead ions in a binary system onto orange peels: Optimization, equilibrium and kinetic study," Sustainability, Vol. 14(17), Article 10860, 2022. [CrossRef]

[62] H. Mohd, J. Roslan, S. Saallah, E. Munsu, N. Shaeera, and W. Pindi, "Banana peels as a bioactive ingredient and its potential application in the food industry," Journal of Function Foods, Vol. 92, Article 105054, 2021. [CrossRef]

[63] M. M. Miranda, J. M. Bielicki, S. Chun, and C. M. Cheng, "Recovering rare earth elements from coal mine drainage using industrial byproducts: Environmental and economic consequences," Environmental Engineering Sciences, Vol. 39(9), pp. 770–783, 2022. [CrossRef]

[64] D. F. Parsons, and A. Salis, "The impact of the competitive adsorption of ions at surface sites on surface free energies and surface forces," Journal of Chemistry and Physics, Vol. 142(13), Article 134707, 2015. [CrossRef]

[65] S. Indah, D. Helard, T. Edwin, and R. Pratiwi, "Utilization of pumice from Sungai Pasak, West Sumatera, Indonesia as low-cost adsorbent in removal of manganese from aqueous solution," AIP Conference Proceeding, Vol. 1823(1), pp.1823–1830, 2017. [CrossRef]

[66] A. Mohan, "Study of sugarcane bagasse and orange peel as adsorbent for treatment of industrial effluent contaminated with nickel," International Resources Journal of Engineering and Technology, Vol. 6, pp. 4725–4731, 2019.

[67] M. Negroiu, A. T. Anca, E. Matei, M. Râpă, C. I. Covaliu, A. M. Predescu…, and C. Predescu, "Novel adsorbent based on banana peel waste for removal of heavy metal ions from synthetic solutions," Materials, Vol. 14(14), pp. 3946–3958. [CrossRef]

[68] M. Abd-Elaziz, M. G. Taha, M. Gahly, and H. T. Hefnawy, "Removal of Fe3+ and Pb2+ ions from aqueous solutions by adsorption using banana peels," Zagazig Journal of Agricultural Resources, Vol. 49(4), pp. 853–864, 2022. [CrossRef]

[69] N. R. Molaudzi, and A. A Ambushe, "Sugarcane bagasse and orange peels as low-cost biosorbents for the removal of lead ions from contaminated," Water, Vol. 14(21), Article 3395, 2022. [CrossRef]

[70] G. Teng, X. Yuen, and X. Fen, "Adsorption of pollutants in wastewater via biosorbents, nanoparticles and magnetic biosorbents: A review," Environmental Resources, Vol. 212(Pt B), Article 113248, 2022. [CrossRef]

[71] M. Bilal, I. Ihsanullah, M. Younas, and M. H.Shah, "Recent advances in applications of low-cost adsorbents for the removal of heavy metals from water: A critical review," Separation and Purification Technology, Vol. 278, Article 119510, 2021. [CrossRef]

[72] K. Khairiah, E. Frida, K. Sebayang, P. Sinuhaji, and S. Humaidi, "Data on characterization, model and adsorption rate of banana peel activated carbon (Musa Acuminata) for adsorbents of various heavy metals (Mn, Pb, Zn, Fe), Data in Brief, Vol. 39, Article 107611, 2021. [CrossRef]

[73] R M. Mohamed, N. Hashim, A. Suhaila, N. Abdullah, A. Mohamed, M. A. A. Daud…, and S. Abdullah, "Adsorption of heavy metals on banana peel bioadsorbent," Journal of Physics, Vol. 1521, Article 012014, 2020. [CrossRef]

[74] Y. Zheng, X. Zhang, Z. Bai, and Z. Zhang, "Characterization of the surface properties of MgO using paper spray mass spectrometry," Rapid Commun Mass Spectrum, Vol. 30(S1), pp. 217–225, 2016. [CrossRef]

[75] X. Wei, R. C. Viadero, and K. M. Buzby, "Recovery of iron and aluminum from acid mine drainage by selective precipitation," Environmental Engineering Sciences, Vol. 22(6), 745–755, 2005. [CrossRef]

[76] Y. Li, Z. Xu, H. Ma, and A. S. Hursthouse, "Removal of manganese(II) from acid mine wastewater: A review of the challenges and opportunities with special emphasis on mn-oxidizing bacteria and microalgae," Water (Switzerland), Vol. 11(12), Article 2493. [CrossRef]

[77] R. M. Salim, A. Jalal, K. Chowdhury, and R. Rayathulhan, "Biosorption of Pb(II) and Cu(II) from aqueous solution using banana peel powder Biosorption of Pb and Cu from aqueous solution using banana peel powder," Desalination and Water Treatment, Vol. 57(1), pp. 303–314, 2016. [CrossRef]

[78] Y. Zhang, S. Liao, Y. Fan, J. Xu, and F. Wang, "Chemical reactivities of magnesium nanopowders," Journal of Nanoparticle Research, Vol. 3(1), pp. 23–26, 2001. [CrossRef]

[79] I. Shancita, N. G. Vaz, G. D. Fernandes, A. J. A. Aquino, D. Tunega, and M. L. Pantoya, "Regulating magnesium combustion using surface chemistry and heating rate," Combustion and Flame, Vol. 226, pp. 419–429, 2021. [CrossRef]

[80] R. Coetzee, C. Dorfling, and S. M. Bradshaw, "Characterization of precipitate formed during the removal of iron and precious metals from sulphate leach solutions," Journal of Southern African Institute of Minerals and Metallurgic, Vol. 117, pp. 771–778, 2017. [CrossRef]

[81] W. M. Gitari, L. F. Petrik, O. Etchebers, D. L. Key, E. Iwuoha, and C. Okujeni, "Passive neutralisation of acid mine drainage by fly ash and its derivatives: A column leaching study," Fuel, Vol. 87(8–9), pp. 1637–1650, 2008. [CrossRef]

[82] V. Masindi, 1A novel technology for neutralizing acidity and attenuating toxic chemical species from

acid mine drainage using cryptocrystalline magnesite tailings," Journal of Water Process Engineering, Vol. 10, pp. 67–77, 2016. [CrossRef]

[83] R. Khosravi, R. Fatahi, H. Siavoshi, and F. Molaei, "Recovery of manganese from zinc smelter slag," American Journal of Engineering Applied Sciences, Vol. 13(4), pp. 748–758, 2020. [CrossRef]

[84] D. Gopi, K. Kanimozhi, N. Bhuvaneshwari, J. Indira, and L. Kavitha, "Novel banana peel pectin mediated green route for the synthesis of hydroxyapatite nanoparticles and their spectral characterization," Spectrochimica Acta Part A Molecular and Biomolecular Spectroscopy, Vol. 118, pp. 589–597, 2014. [CrossRef]

[85] J. R. Memon, S. Q. Memon, M. I. Bhanger, G. Z. Memon, A. El-Turki, and G. C. Allen, "Character-ization of banana peel by scanning electron micros-copy and FT-IR spectroscopy and its use for cadmi-um removal. Colloids Surfaces B Biointerfaces," Vol. 66, pp. 260–265, 2008. [CrossRef]

[86] G. Balakrishnan, R. Velavan, B. K. Mujasam, and E.H. Raslan," Microstructure, optical and photocatalytic properties of MgO nanoparticles," Results in Physics, Vol. 16, Article 103013. 2020. [CrossRef]

[87] J. T. Richardson, R. Scates, and M. V. Twigg, "X-ray diffraction study of nickel oxide reduction by hydrogen," Applied Catalyst A General, Vol. 246, pp. 137–150, 2003. [CrossRef]

[88] H. Tibolla, F. M. Pelissari, J. T. Martins, A. A. Vicente, and F.C. Menegalli, "Cellulose nanofibers produced from banana peel by chemical and mechanical treatments: Characterization and cytotoxicity assessment," Food Hydrocoll, Vol. 75, pp.192–201, 2018. [CrossRef]

[89] S. Mishra, B. Prabhakar, P. S. Kharkar, and A. M. Pethe, "Banana peel waste: An emerging cellulosic material to extract nanocrystalline cellulose," ACS Omega,Vol. 8(1), pp.1140–1145, 2023. [CrossRef]

[90] N. K. Nga, N. T. Thuy Chau, and P. H. Viet, "Prepa-ration and characterization of a chitosan/MgO com-posite for the effective removal of reactive blue 19 dye from aqueous solution," Journal of Sciences and Advances Materials Devices, Vol. 5(1), pp. 65–72, 2020. [CrossRef]

[91] N. Sutradhar, S. Apurba, S. K. Pahari, P. Pal, C.H. Bajaj, I., Mukhopadhyay, and A. B. Panda, "Controlled synthesis of different morphologies of MgO and their use as solid base catalysts," Journal of Physics and Chemistry, Vol. 115(25), pp.12308–12316, 2011. [CrossRef]

[92] D. Arifiyana, and V. A. Devianti, "Biosorption of Fe(II) ions from aqueous solution using banana peels (Musa a cuminate)," Jurnal Kimia Dan Pendidikan Kimia, Vol. 6(2), pp. 206–215, 2021. [CrossRef]

[93] H. J. Rao, "Characterization studies on adsorption of lead and cadmium using activated carbon prepared from waste tyres," Natural Environmental Pollution Technology, Vol. 20, pp. 561–568, 2021. [CrossRef]

[94] T. S. Badessa, E. Wakuma, and A. M. Yimer, "Bio-sorption for effective removal of chromium(VI) from wastewater using Moringa stenopetala seed powder (MSSP) and banana peel powder (BPP)," BMC Chemistry, Vol. 14, Article 71, 2020. [CrossRef]

[95] R. C. Rivas-Cantu, K. D. Jones, and P. L. Mills, "A citrus waste-based biorefinery as a source of renewable energy: Technical advances and analysis of engineering challenges," Waste Management and Resources, Vol. 31(4), pp. 413–420, 2013. [CrossRef]

[96] J. R. Ayala, G. Montero, M. A. Coronado, C. Garcia, M. A. Curiel-Alvarez, J. A. Leon…, and D. G. Montes, "Characterization of orange peel waste and valorization to obtain reducing sugars," Molecules, Vol. 26(5), Article 1348, 2021. [CrossRef]

[97] J. I. Z. Montero, A. S. C. Monteiro, E. S. J. Gontijo, C. C. Bueno, M. A. De Moraes, and A. H. Rosa, "High efficiency removal of As(III) from waters using a new and friendly adsorbent based on sugarcane bagasse and corncob husk Fe-coated biocharsi," Ecotoxicology and Environmental Safety, Vol. 162, pp. 616–624, 2018. [CrossRef]

[98] I. Kabenge, G. Omulo, N. Banadda, J. Seay, A. Zziwa, and N. Kiggundu, "Characterization of banana peels wastes as potential slow pyrolysis feedstock," Journal of Sustainable Development, Vol. 11(2), pp.14–24, 2018. [CrossRef]

[99] F. O. Afolabi, P. Musonge, and B. F. Bakare, "Bio-sorption of a bi-solute system of copper and lead ions onto banana peels: characterization and optimization," Journal of Environmetal Health Sciences and Engineering, Vol. 19, pp. 613–624, 2021. [CrossRef]

[100] F. O. Afolabi, P. Musonge, and B. F. Bakare, "Bio-sorption of copper and lead ions in single and binary systems onto banana peels," Cogent Engineering, Vol. 8(1), Article 1886730, 2021. [CrossRef]

[101] A. Moubarik, and N. Grimi, "Valorization of olive stone and sugar cane bagasse by-products as biosorbents for the removal of cadmium from aqueous solution," Food Research International, Vol. 73, pp. 169–175, 2015. [CrossRef]

[102] M. A. Hossain, H. H. Ngo, W. S. Guo, and T. V. Nguyen, "Removal of copper from water by adsorption onto banana peel as bioadsorbent," International Journal of Geomate, Vol. 2, pp. 227–234, 2012. [CrossRef]

[103] G. Alaa El-Din, A. A. Amer, G. Malsh, and M. Hussein, "Study on the use of banana peels for oil spill removal," Alexandria Engineering Journal, Vol. 57(3), pp. 2061–2068, 2018. [CrossRef]

[104] R. M. Alghanmi, "ICP-OES determination of trace metal ions after preconcentration using silica gel modified with 1,2-dihydroxyanthraquinone," Journal of Chemistry, Vol. 9, Article 279628, 2012. [CrossRef]

*Environ Res Tec, Vol. 7, Issue. 3, pp. 335–346, September 2024*

**Environmental Research and Technology**
https://ert.yildiz.edu.tr - https://dergipark.org.tr/tr/pub/ert
DOI: https://10.35208/ert.1432036

Environmental Research & Technology

**Research Article**

# Radiation shielding and spectroscopic features of replacement materials: Reusing of agricultural and industrial wastes

**Zeynep AYGÜN*[,1], Murat AYGÜN[2]**

[1]*Vocational School of Technical Sciences, Bitlis Eren University, Bitlis, Türkiye*
[2]*Department of Physics, Bitlis Eren University, Faculty of Science and Arts, Bitlis, Türkiye*

## ARTICLE INFO

*Article history*
Received: 05 February 2024
Revised: 02 March 2024
Accepted: 18 March 2024

**Key words:**
Agricultural wastes; Industrial waste; Radiation shielding; Phy-X/PSD

## ABSTRACT

Environmental pollution increases due to the large amounts of waste production and raw material consumption depending on the increasing population. Agricultural and industrial wastes which are some of the sources of the pollution need to be reuse to reduce the negative impact on the environment and also contribute positive effect to the economy. In this context, industrial wastes such as clay types (red and green) and agricultural wastes such as egg shell, walnut shell and banana shell were used to prepare materials which can be used as replacement materials for construction industry. Radiation attenuation parameters (mass attenuation coefficients, effective atomic number, linear attenuation coefficients, mean free path, half-value layer, exposure and energy absorption build up factors, fast neutron removal cross-section) were acquired by Phy-X/PSD code. Spectroscopic techniques (XRD, EPR, SEM-EDS) were performed for the structural analysis. The existence of calcite main phase peaks (≈29.7) as well as $SiO_2$ (≈20° and 26°) and cellulose phases (≈16° and 34.7°) were observed by XRD. $Mn^{+2}$ sextet lines with five weak doublets attributed to the forbidden transition lines of $Mn^{+2}$ and a singlet with a g value of ≈2.00 and linewidth of ≈10 G were recorded by EPR. Among the samples, it was found that K1 (Red clay (20%)-eggshell waste (60%)-Bayburt stone waste (20%)), K3 (Red clay (60%)-eggshell waste (20%)-Bayburt stone waste (20%)), C3 (Red clay (60%)-eggshell waste (20%)-walnut shell waste (20%)) and Z3 (Green clay (60%)-egg shell waste (20%)-Bayburt stone waste (20%)) have the highest shielding potentials. All samples examined with good protection performances can be used as substitute materials instead of cement or aggregate for the aim of reusing the wastes and supporting the environmental and economic benefits.

**Cite this article as:** Aygün Z, Aygün M. Radiation shielding and spectroscopic features of replacement materials: Reusing of agricultural and industrial wastes. Environ Res Tec 2024;7(3)335–346.

## INTRODUCTION

Climate change and global warming are among the current main environmental problems, and carbon dioxide emissions appear to be the main reason of these problems. As a natural result of the widespread concreting trend in the construction sector, among many sectors, the high cement production contributes to carbon dioxide emissions. Replacement materials using instead of cement are the research subjects of investigations around the world recently. Among these materials, wastes have a significant place in the studies. Clay types, ceramics, marble etc. which are generally thrown away as waste and known as construction material wastes can be reused or recycled to be used again as building materials. Replacing waste with common building materials to some extent has yielded positive results in

***Corresponding author.**
*E-mail address: zeynepyarbasi@hotmail.com

terms of durability and mechanical properties [1, 2]. Beyond on the industrial wastes, food wastes such as egg shell waste, banana shell waste and walnut shell wastes which are mostly consumed in our homes or in the food industry can be also evaluated for replacement. With the increasing population, environmental pollution also increases due to large amounts of waste production and raw material consumption. The storage situation of both agricultural waste and industrial waste is becoming an important problem, reaching a level that endangers public health. Such wastes need to be transformed into useful materials in order to reduce the negative impact on the environment and at the same time contribute to the economy [3]. Eggshell, marble dust and clay types are widely used and recycled wastes in engineering applications. Clay with refractory properties such as melting point, mechanical strength and thermochemical properties, has been preferred as one of the main building materials [4, 5]. Eggshell and marble dust which have nearly the same chemical contents (higher calcite amount) can be used as replacement instead of cement or aggregates. Since they have good pozzolanic and refractory properties, eggshell with high calcium (Ca) content and clay with high silicon (Si) percentage can make the mixture optimum for building materials.

In the recent years, due to the increase in radiation applications such as agriculture, scientific research, technology, industry, medical imaging and radiotherapy, information on protective measures against the harms of radiation has become valuable and interesting. In order to reduce radiation exposure, it is meaningful to obtain information on how much a building material reduces the transmission of gamma radiation. For this reason, the content of the material is important. Materials such as sand, cement, brick and concrete are also used with their protective properties as building materials. The radiation shielding features (RSF) of these materials can be developed by adding different components. In order to increase the performance of materials, environmentally friendly and lower cost resources can be developed by supplementing with natural materials and waste types. By reusing of wastes, it is possible to reduce environmental and economic problems. There is a great interest in researches involving radiation attenuation parameters that provide considerable information about the radiation shielding potentials (RSP) of materials [6–18]. These parameters are; mass attenuation coefficient, linear attenuation coefficient, mean free path, half value layer, one-tenth value layer, total atomic and electronic cross sections, effective atomic number, fast neutron removal cross section and buildup factors. In the study, the radiation attenuation parameters of developed new materials with clays, eggshell waste, walnut shell waste, banana shell waste mixtures were examined by the Phy-X/PSD program [19]. Thus, it is expected to determine whether the mixtures to be made are more advantageous in terms of shielding or not, and it is aimed to contribute to the literature with their spectroscopic properties and detailed analyzes. For this purpose, spectroscopic methods such as X-ray diffraction (XRD), electron paramagnetic resonance (EPR), energy dispersive spectroscopy (EDS) and scanning electron microscopy (SEM) were also performed for structural properties. Recycling more waste products such as eggshell, walnut shell waste, banana shell and utilizing environmental friendly products such as clay as additives for building materials can promote green and safer environment.

**Table 1.** The ratios (wt %) of the ingredients of the sample groups

| Y group | Y1 | Y2 | Y3 |
|---|---|---|---|
| GC-ESW-WSW | 20-60-20 | 40-40-20 | 60-20-20 |
| Z group | Z1 | Z2 | Z3 |
| GC-ESW-BSW | 20-60-20 | 40-40-20 | 60-20-20 |
| K group | K1 | K2 | K3 |
| RC-ESW-BSW | 20-60-20 | 40-40-20 | 60-20-20 |
| C group | C1 | C2 | C3 |
| RC-ESW-WSW | 20-60-20 | 40-40-20 | 60-20-20 |

GC: Green clays; ESW: Eggshell waste; WSW: Walnut shell waste; BSW: Banana shell waste.

## MATERIALS AND METHODS

### Sample Preparation

Four sample groups consisting of red and green clays (RC, GC), eggshell waste (ESW), banana shell waste (BSW) and walnut shell waste (WSW) were produced in different ratios and are given in Table 1. The elemental powders used in the manufacture of the alloys were mixed using a V-blender. Then, the element mixture to be pelletized was added to the mold with a diameter of 13 mm and a pressure of 8 MPa was applied.

### Instrumentation

X-band JEOL JESFA300 EPR spectrometer with a 100 kHz and ≈9.2 GHz frequency was used for detecting room temperature EPR spectra of the alloys. 4 mm size samples were put in diamagnetic tubes for EPR measurements. XRD patterns were taken by BRUKER D8 ADVANCE X-ray diffractometer. X-ray diffractograms of the alloys were obtained with a scanning speed of 2.5°/min (40 kV and 40 mA) and radiation Cu-Kα (λ=1.54060 Å) in the range of 2Θ≈5°-90°. SEM images were recorded by ZEISS EVO LS10. EDS results were taken by JEOL JSM-6610 spectrometer.

### Calculation Process

A recently developed Phy-X/PSD code is performed by entering the composition of the material as mole fraction or weight fraction. Density (g/cm$^3$) of the material knowledge is also necessary for obtaining the shielding parameters. A wide energy ranges 1 keV-100 GeV, some radioactive sources or some characteristic K-shell energies can be selected for performing the code. Parameters can be chosen depending on the purpose of the studies. The good feature of the code for obtaining the results is to get them in MS excel file.

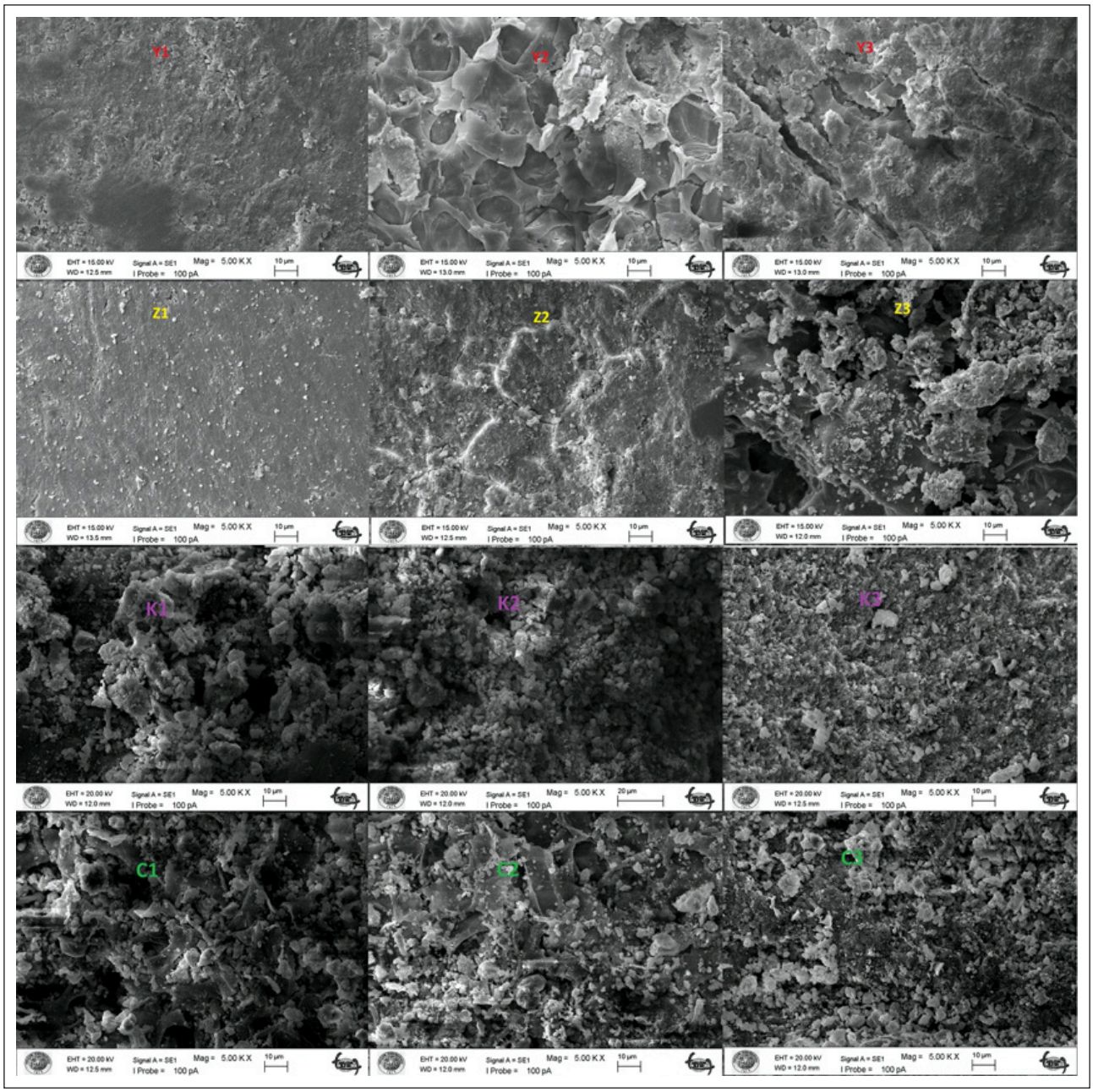


**Figure 1**. SEM images of the samples.

The mixture rule is used for the determination of density ($\rho_{mix}$) of the samples [20]:

$$\rho_{mix} = \frac{\sum_{i=1}^{n} c_i A_i}{\sum_{i=1}^{n} \frac{c_i A_i}{\rho_i}} \quad (1)$$

$A_i$, $c_i$ and $\rho_i$, and are atomic fraction, atomic weight of element $i_{th}$ and density, respectively.

The MAC can be determined based on the Beer–Lambert as:

$$I = I_0 e^{-\mu t} \quad (2)$$

$$\mu_m = \frac{\mu}{\rho} = ln(I_0/I)/\rho t = ln(I_0/I)/t_m \quad (3)$$

where $t_m$ (g/cm$^2$), t (cm), μ(cm$^{-1}$) and $\mu_m$(cm$^2$/g) are the sample mass thickness and thickness (the mass per unit area), LAC and MAC, respectively. MAC can be also acquired by Eq. 4 [21];

$$\mu/\rho = \sum_i w_i (\mu/\rho)_i \quad (4)$$

where $w_i$ and $(\mu/\rho)_i$ and are the weight fraction and the MAC of the $i_{th}$ constituent element, respectively.

MFP and HVL can be determined by the formulas,

$$MFP = \frac{1}{\mu} \quad (5)$$

$$HVL = \frac{In(2)}{\mu} \quad (6)$$

ACS ($\sigma_a$) and ECS ($\sigma_e$) can be calculated by the Eqs. 7, 8;

$$ACS = \sigma_a = \frac{N}{N_A}(\mu/\rho) \quad (7)$$

$$ECS = \sigma_e = \frac{\sigma_a}{Z_{eff}} \quad (8)$$

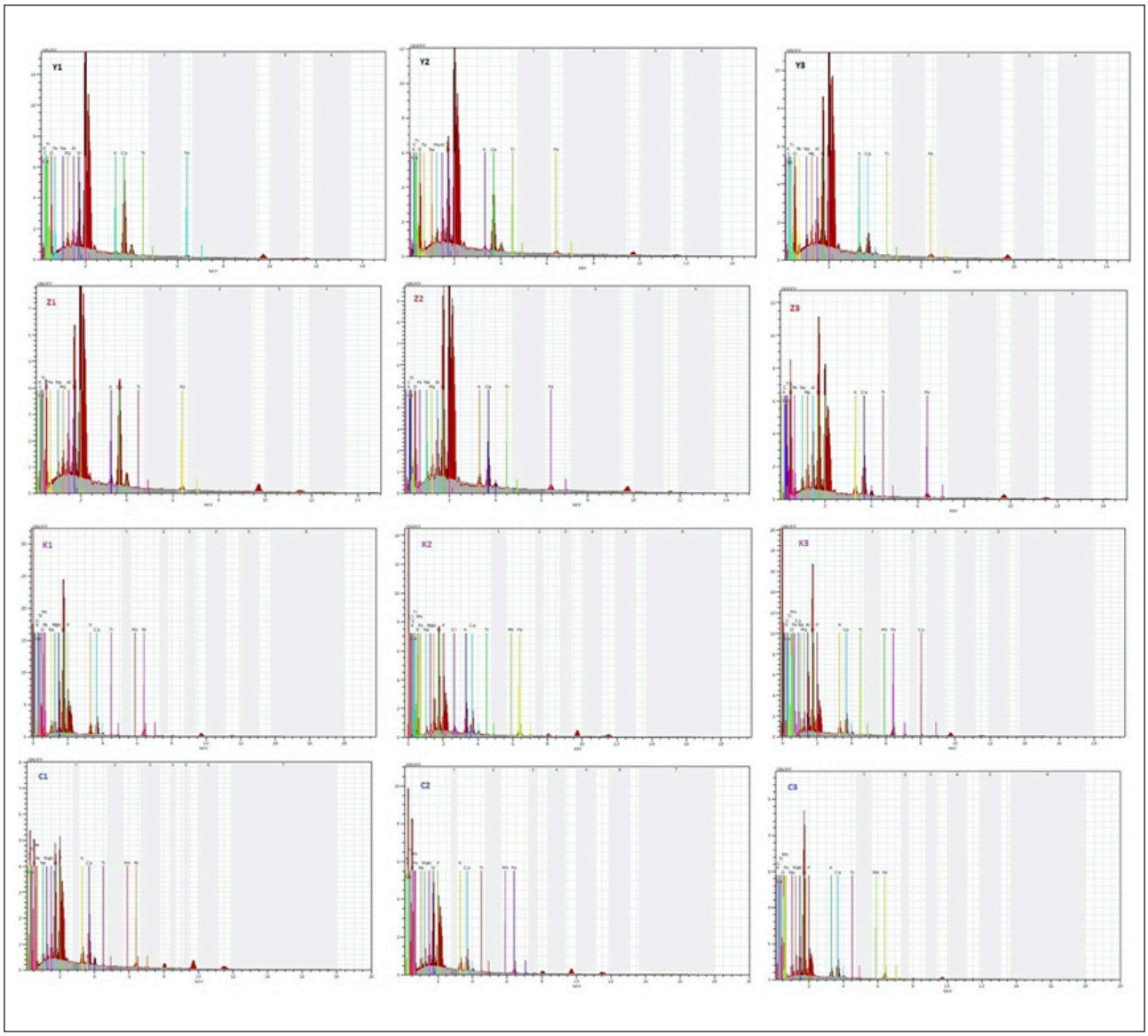


**Figure 2**. EDS results of the samples obtained by EDS.

$Z_{eff}$ is found by the help of Eqs. (7) and (8) as;

$$Z_{eff} = \frac{\sigma_a}{\sigma_e} \quad (9)$$

Build up factors can be found by the equations given below [22, 23]. The geometric progression (G-P) fitting parameters is obtained by using values [24] in Eq. 14. EBF and EABF can be obtained using Eq. (12) or (13) by obtaining K(E, x) in Eq. (14), where x is thickness in mean free path (mfp) and a, b, c, d, $X_k$ are the exposure GP fitting parameters. The ratio (R) of Compton partial MAC to total MAC should be defined for the material at specific energy. The $R_1$ and $R_2$ values indicate the $(\mu m)_{Compton}/(\mu m)_{Total}$ ratios of these two adjacent elements which have $Z_1$ and $Z_2$ atomic numbers. $F_1$ and $F_2$ are the values of G-P fitting parameters identical with the $Z_1$ and $Z_2$ atomic numbers at a certain energy, respectively. E and X demonstrate primary photon energy and penetration depth, respectively. Combination of K (E, X) with X, performs the photon dose multiplication and determines the shape of the spectrum [19].

$$Z_{eq} = \frac{Z_1(logR_2 - logR) + Z_2(logR - logR_1)}{logR_2 - logR_1} \quad (10)$$

$$F = \frac{F_1(logZ_2 - logZ_{eq}) + F_2(logZ_{eq} - logZ_1)}{logZ_2 - logZ_1} \quad (11)$$

$$B(E,x) = 1 + \frac{(b-1)(K^x - 1)}{(K-1)} \quad \text{for } K \neq 1 \quad (12)$$

$$B(E,x) = 1 + (b-1)x \quad \text{for } K = 1 \quad (13)$$

$$K(E,x) = cx^a + d\frac{\tanh\left(\frac{x}{X_k} - 2\right) - \tanh(-2)}{1 - \tanh(-2)} \quad \text{for } x \leq 40 \text{ mfp} \quad (14)$$

The FNRCS ($\Sigma R$) values of the samples are found as follows [19]:

$$\Sigma R = \Sigma_i \rho_i \left(\Sigma R/\rho\right)_i \quad (15)$$

where $\rho_i$ and $\left(\Sigma R/\rho\right)_i$ are the partial density of the compound and the mass RCS of the ith constituent element, respectively.

**Table 2.** The weight (%) ratios of the elements obtained by EDS

| Samples | O | C | Ca | K | Si | Na | Fe | Ti | Mg | P | Al | Mn | Density |
|---|---|---|---|---|---|---|---|---|---|---|---|---|---|
| Y1 | 70.02 | 12.75 | 5.59 | 0.11 | 1.81 | 0.29 | 0.49 | 0.1 | 0.39 | 7.96 | 0.51 | – | 1.563 |
| Y2 | 71.74 | 11.54 | 4.37 | 0.17 | 2.86 | 0.38 | 0.68 | 0.07 | 0.41 | 6.93 | 0.84 | – | 1.570 |
| Y3 | 68.59 | 16.82 | 1.20 | 0.36 | 3.43 | 0.42 | 0.63 | 0.09 | 0.55 | 6.87 | 1.05 | – | 1.587 |
| Z1 | 66.10 | 15.32 | 5.72 | 0.34 | 3.07 | 0.50 | 0.74 | 0.07 | 0.55 | 6.66 | 0.93 | – | 1.583 |
| Z2 | 73.32 | 10.52 | 1.77 | 0.40 | 4.14 | 0.30 | 0.97 | 0.10 | 0.55 | 6.72 | 1.21 | – | 1.586 |
| Z3 | 57.60 | 4.40 | 6.71 | 1.25 | 10.97 | 1.25 | 2.34 | 0.19 | 1.85 | 9.85 | 3.60 | – | 1.684 |
| K1 | 49.35 | 1.57 | 4.59 | 2.30 | 17.18 | 2.86 | 4.31 | 0.33 | 2.73 | 7.44 | 7.26 | 0.08 | 1.781 |
| K2 | 71.34 | 12.61 | 2.10 | 2.22 | 4.14 | 0.55 | 1.60 | 0.10 | 0.42 | 2.95 | 1.57 | 0.09 | 1.559 |
| K3 | 53.73 | 2.08 | 4.47 | 1.92 | 15.00 | 2.49 | 3.84 | 0.29 | 2.57 | 6.29 | 6.23 | 0.11 | 1.788 |
| C1 | 61.64 | 23.51 | 3.29 | 1.10 | 2.90 | 0.86 | 0.68 | 0.08 | 0.63 | 3.98 | 1.24 | 0.07 | 1.574 |
| C2 | 60.45 | 25.49 | 1.96 | 1.02 | 2.93 | 1.25 | 0.67 | 0.12 | 0.89 | 3.73 | 1.42 | 0.09 | 1.586 |
| C3 | 51.37 | 1.44 | 4.40 | 1.93 | 17.01 | 3.73 | 3.78 | 0.29 | 2.86 | 5.45 | 7.59 | 0.16 | 1.760 |

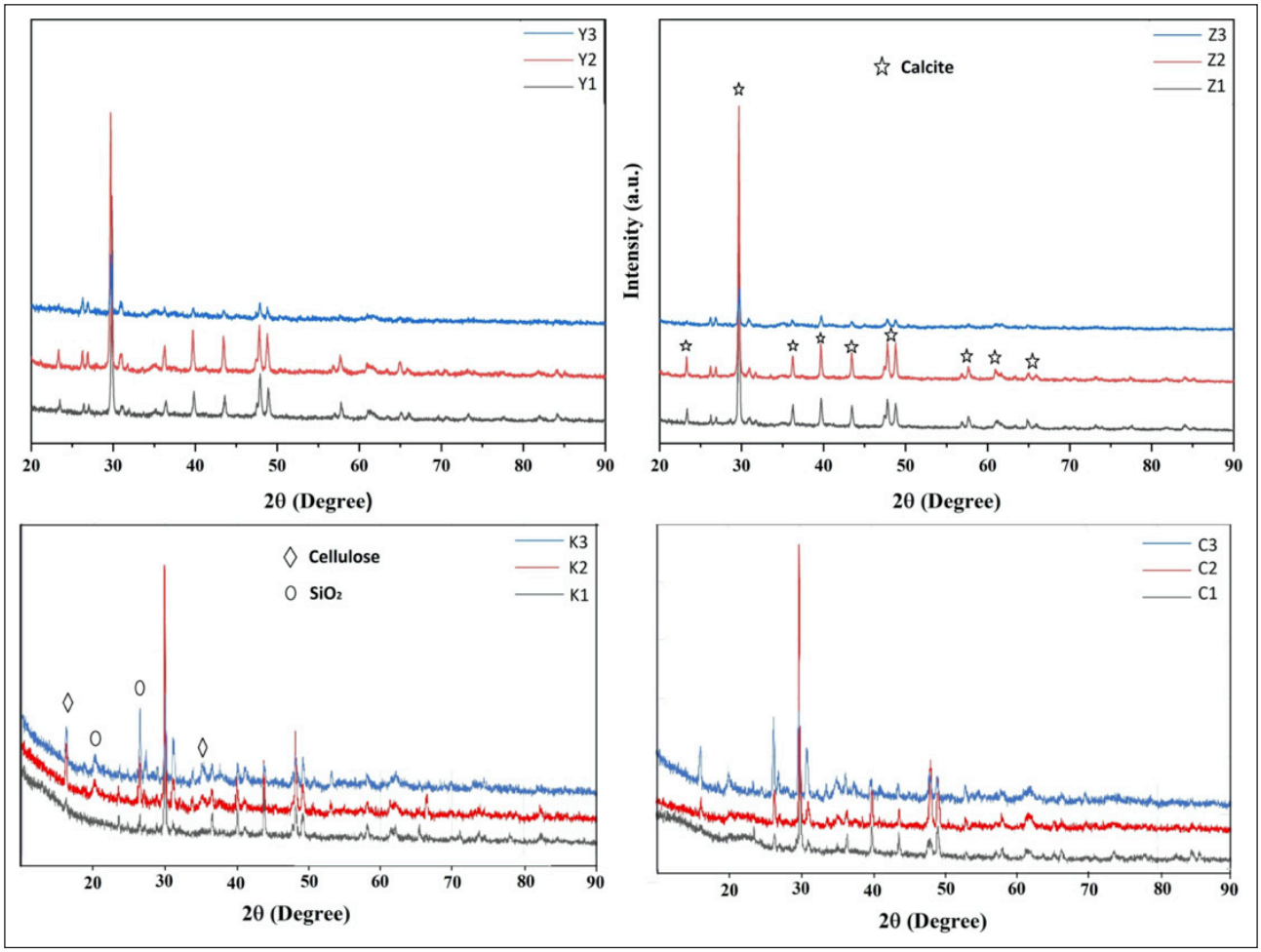


**Figure 3**. XRD patterns of the samples recorded at room temperature.

## RESULTS AND DISCUSSION

### SEM and EDS Analysis

SEM micrographs of the samples are given in Figure 1. Micro crystallites are observed for all samples in the SEM pictures. The smoothest surfaces are seen for Z1 and Y1 samples. The EDS spectra of the samples are given in Figure 2. The weight % ratios of the elements obtained from EDS are given in Table 2. It is understood from the EDS analyses that all the elements are common for all samples except from Mn. Y and Z groups do not have Mn element, while K and C groups have the element. This may be due to the device's limitations. The amount of Mn content of Y and Z groups samples may be lower than the others and so EDS cannot detect the element for the samples.

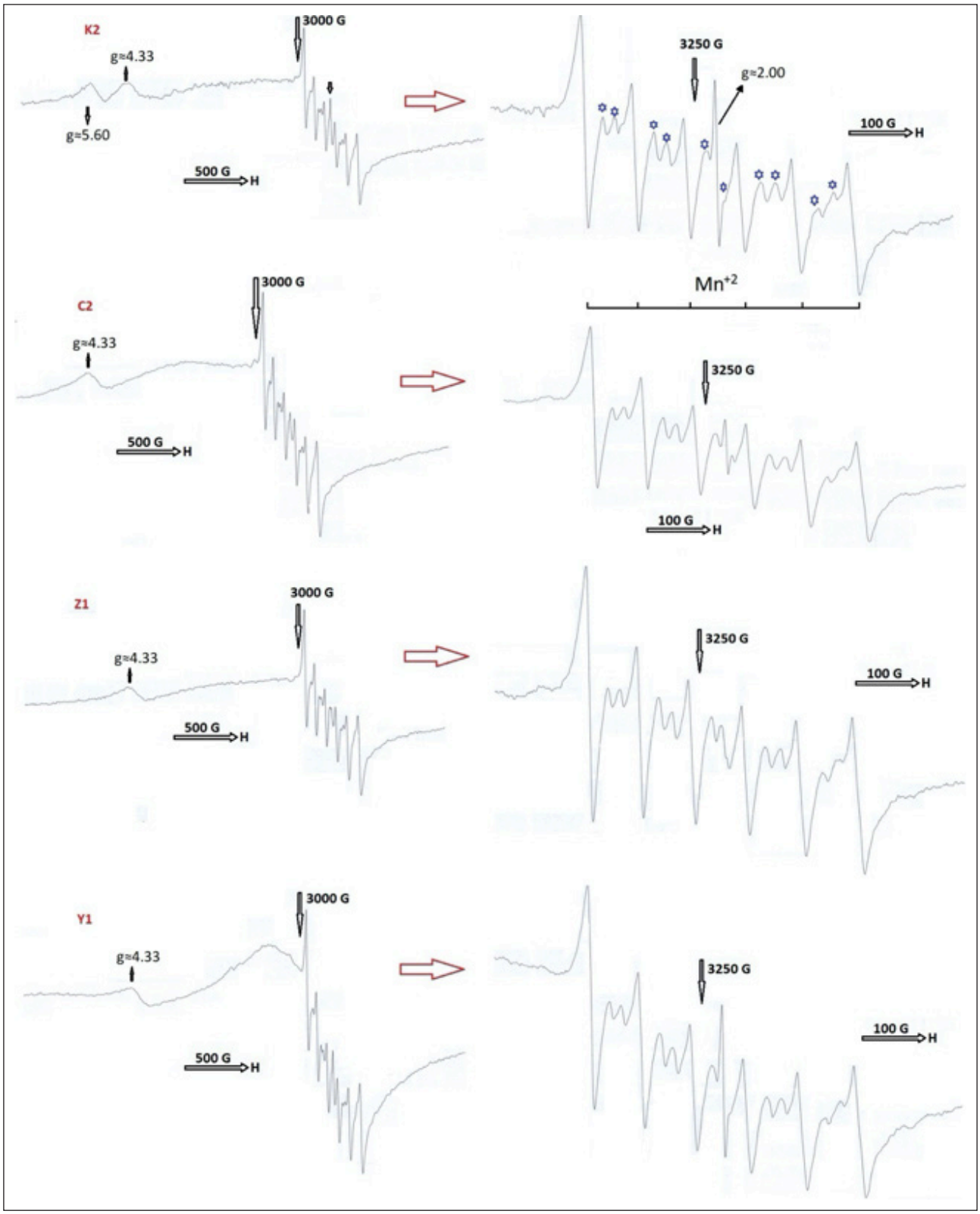


**Figure 4**. EPR spectra of the samples recorded by EPR.

**XRD Analysis**

Room temperature X-ray diffraction peaks are shown in Figure 3. The diffraction peaks were evaluated by the literature [25–28]. XRD results of the samples revealed the existence of $CaCO_3$ (calcite) main phase peak as well as $SiO_2$ and cellulose phases. The XRD peak obtained for all the samples at $2\theta \approx 29.7°$ is the characteristic crystalline structure of calcite ($CaCO_3$) [27]. The relatively broad XRD peak at the angle of ≈20° and 26° corresponds to the amorphous $SiO_2$ phase [25, 28]. The XRD peak at ≈16° and 34.7° is assigned to cellulose [25]. It is seen that diffraction peaks of the samples are generally calcite peaks, and also some peaks

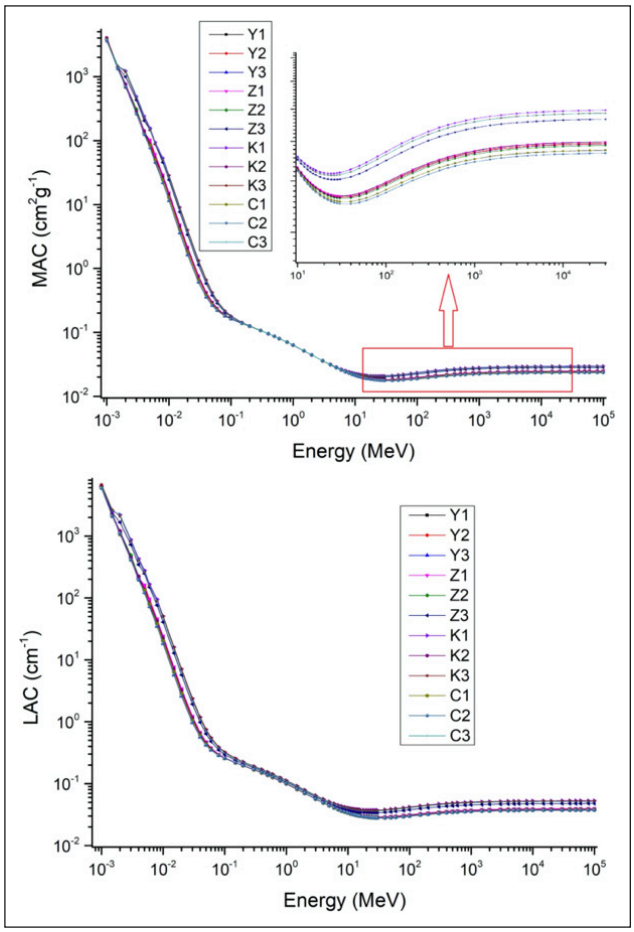


**Figure 5**. The variations of MAC and LAC versus photon energies.

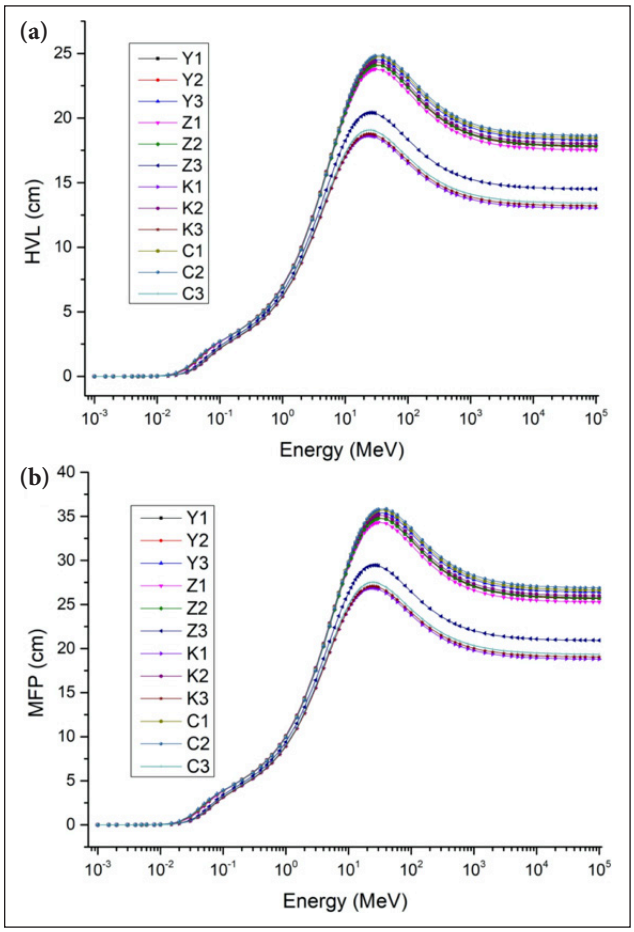


**Figure 6**. The variations of HVL **(a)** and MFP **(b)** versus photon energies.

of other phases are seen. This indicates that the samples are well crystallized.

The crystallite size for the evaluation of crystalline nature of the samples is determined by Debye-Scherer equation [29]. The full width half height (FWHM) for each diffraction can be used for this. λ is the X-ray wavelength, K is Scherer's constant and is of the order of ≅ 0.9, (β) is the FWHM in radians, d is the average size of the crystalline, and θ is the Bragg angle in degrees [30].

$$d=K\lambda/\beta\cos\theta \quad (1)$$

By using the FWHM of the most intense $CaCO_3$ peak (≈29.7°) of the samples, the crystallite sizes of $CaCO_3$ were found in the range of 33.0–63.3 nm.

**EPR Study**

Structures with paramagnetic centers can be detected by EPR technique in the existence of an external magnetic field. The EPR lines are defined by g-values by the equation of hυ = gβH. Here, β the Bohr magneton, h the Planck constant, H the magnetic field and υ the microwave frequency is used for the determination g values. Both in the crystalline nature and glassy phases, paramagnetic center affected by local magnetic fields centers can be acquired in EPR spectra. EPR spectra of the prepared samples recorded at room temperature are seen in Figure 4. For all group of samples, six hyperfine lines of $Mn^{+2}$ (I=5/2) with g value of g≈2.00 is determined. It can be also detected that there is a weak a singlet (given by arrow) with a g value of ≈2.00 and linewidth of ≈10 G was obtained and overlapping with the $Mn^{+2}$ lines. Additionally, five weak doublets which are attributed to the forbidden transition lines of $Mn^{+2}$ (ΔmI=±1) are observed and marked by asterisks [25]. The g value obtained for the samples can be a result of organic free radical or a carbon centered organic radical [31–33].

**Radiation Protection Analysis**

Chemical composition (wt. %) of the samples acquired by EDS was used to obtain radiation-material interaction parameters by Phy-X/PSD code in the energy range of 1keV-100GeV. Changes of MAC values with incident photon energies are shown in Figure 5. The variations of MAC results are affected by photoelectric effect (PE) at low energies, Compton scattering (CS) at mid energies and pair production (PP) at high energies. The MAC values were also determined by XCom [34], and convenient results are obtained. The coherent results determined by both XCom and Phy-X/PSD are given in Table 3 for some of the energies at low, mid and high regions. The values demonstrated in blue color are the highest ones for MAC. LAC is the scattered or absorbed photon beam fraction per unit thickness. LAC values change with pho-

**Table 3.** MAC values of the samples obtained by Phy-X/PSD and XCom

| Sample/code | 2.0 x10$^{-3}$ (MeV) | 2.0 x10$^{-2}$ (MeV) | 2.0 x10$^{-1}$ (MeV) | 2.0 x10$^{0}$ (MeV) | 2.0 x10$^{1}$ (MeV) | 2.0 x10$^{2}$ (MeV) | 2.0 x10$^{3}$ (MeV) |
|---|---|---|---|---|---|---|---|
| Y1 Phy-x/PSD | 677.3 | 2.087 | 0.125 | 0.045 | 0.019 | 0.021 | 0.024 |
| Y1 Xcom | 677.2 | 2.087 | 0.124 | 0.044 | 0.018 | 0.021 | 0.024 |
| Y2 Phy-x/PSD | 714.3 | 1.994 | 0.125 | 0.044 | 0.019 | 0.021 | 0.025 |
| Y2 Xcom | 714.4 | 1.994 | 0.125 | 0.045 | 0.019 | 0.021 | 0.024 |
| Y3 Phy-x/PSD | 707.4 | 1.621 | 0.124 | 0.044 | 0.018 | 0.020 | 0.023 |
| Y3 Xcom | 707.4 | 1.621 | 0.124 | 0.044 | 0.018 | 0.020 | 0.023 |
| Z1 Phy-x/PSD | 710.3 | 2.175 | 0.125 | 0.044 | 0.019 | 0.021 | 0.024 |
| Z1 Xcom | 711.1 | 2.176 | 0.125 | 0.045 | 0.019 | 0.021 | 0.024 |
| Z2 Phy-x/PSD | 752.7 | 1.828 | 0.124 | 0.044 | 0.019 | 0.021 | 0.024 |
| Z2 Xcom | 752.8 | 1.828 | 0.124 | 0.044 | 0.019 | 0.021 | 0.024 |
| Z3 Phy-x/PSD | 986.0 | 3.380 | 0.126 | 0.044 | 0.020 | 0.024 | 0.028 |
| Z3 Xcom | 986.0 | 3.379 | 0.126 | 0.044 | 0.020 | 0.024 | 0.028 |
| K1 Phy-x/PSD | 1234.1 | 4.011 | 0.126 | 0.044 | 0.021 | 0.025 | 0.029 |
| K1 Xcom | 1234.0 | 4.011 | 0.126 | 0.044 | 0.021 | 0.025 | 0.029 |
| K2 Phy-x/PSD | 770.8 | 2.079 | 0.125 | 0.044 | 0.019 | 0.021 | 0.024 |
| K2 Xcom | 771.0 | 2.080 | 0.125 | 0.044 | 0.019 | 0.021 | 0.024 |
| K3 Phy-x/PSD | 1180.0 | 3.999 | 0.126 | 0.044 | 0.021 | 0.025 | 0.029 |
| K3 Xcom | 1180.0 | 3.999 | 0.126 | 0.044 | 0.021 | 0.025 | 0.029 |
| C1 Phy-x/PSD | 691.7 | 1.811 | 0.124 | 0.044 | 0.018 | 0.020 | 0.023 |
| C1 Xcom | 691.9 | 1.811 | 0.141 | 0.044 | 0.018 | 0.020 | 0.023 |
| C2 Phy-x/PSD | 693.9 | 1.644 | 0.124 | 0.044 | 0.018 | 0.020 | 0.023 |
| C2 Xcom | 693.8 | 1.644 | 0.124 | 0.044 | 0.018 | 0.020 | 0.023 |
| C3 Phy-x/PSD | 1248.4 | 3.757 | 0.126 | 0.044 | 0.021 | 0.025 | 0.029 |
| C3 Xcom | 1248.0 | 3.757 | 0.126 | 0.044 | 0.021 | 0.025 | 0.029 |

ton energies are shown in Figure 5. The LAC parameter varies as a function of MAC values and material density. Although the MAC and LAC values of the samples seem near, clearer results can be obtained with detailed analysis. The highest MAC values are found in the order of K1>K3>C3>Z3 and the lowest ones are that of Z2>C1>C2>Y3 among the samples.

The thickness halve the amount of incident photon energy is called as HVL and the average length traveled by a photon without scattering or absorption is called as MFP. Better shielding feature can be gained by the material with lower values of HVL and MFP. HVL and MFP values change with photon energies are shown in Figure 6. The values of HVL and MFP are in the order of K1<K3<C3<Z3<Z1<Y1<Z2<Y2<K2<Y3<C1<C2. So, the highest shielding performance is seen for K1 and the lowest one is for C2.

$Z_{eff}$ is the average atomic number of material including more than one element. $Z_{eff}$ values as a function of photon energy is shown in Figure 7. The highest $Z_{eff}$ values are found at low energies based on the PE cross-section with the effect of $Z^{4-5}$. At mid-energies, a decrease is seen due to the CS cross-section changed with $E^{-3.5}$. At high energies, the PP

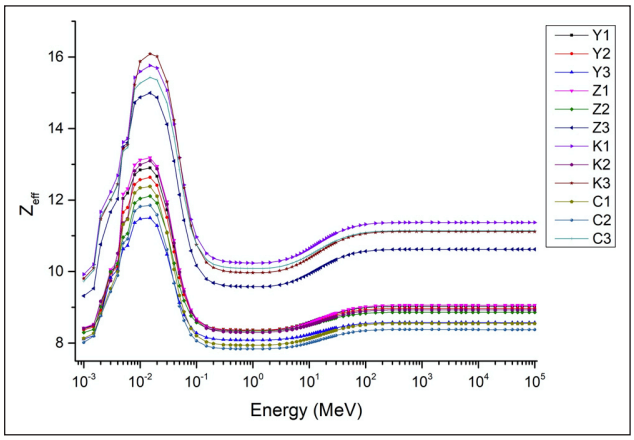


**Figure 7**. The variations of MAC and LAC versus photon energies.

cross-section variation changed with $Z^2$ causes an increase and then a stable case [30]. The presence of different atomic numbers in the material is effective on the variation of $Z_{eff}$ values. As a result of this, samples with more than one element and large atomic number differences have larger fluctuations in $Z_{eff}$ values (such as C-6; Fe-26). Among the

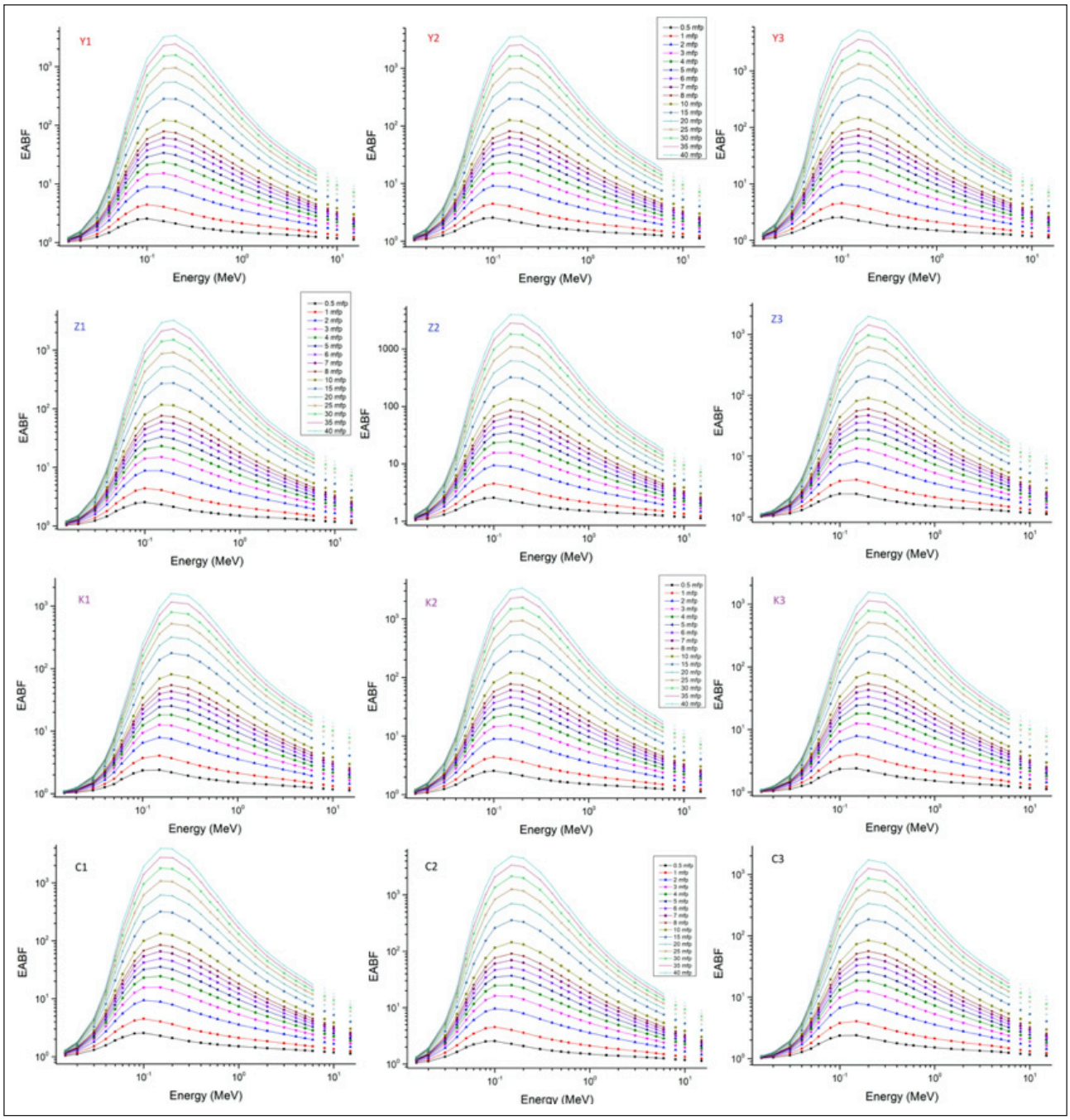


**Figure 8**. The changes of EABF of the samples versus photon energies.

samples, K1, K3, C3, Z3 and Y1 with higher Fe and Ca content have the higher $Z_{eff}$ values. It is obtained that RSP of K1, K3, C3, Z3 and Y1 are higher based on $Z_{eff}$ values.

Build up factor is expressed as the ratio of the total radiation at a given point to amount of uncollided radiation at the same point. EABF, one of the buildup factors, is related with the energy absorbed or deposited in the interacting material. EBF, the other one, is about the exposure in interacting material. Build up factors can be estimated as a function of mfp, and EBF and EABF values as a function of photon energies are given in Figures 8, 9. Buildup factor values are lower (due to the PE), the highest values (due to the large number of scattered photons by the CS) and lower again (due to the PP effect and strong photon absorption) in the low, mid and high energy regions, respectively [35]. Photon scattering and the probability of penetration depth related closely causes the buildup effect intensely at mid-energies. When the obtained buildup factors are analyzed, it is found that the photon accumulation, so the CS process is more for Y3 and C2 than the other samples, while that is less for K1 and K3.

Fast neutron attenuation capabilities of the samples were also obtainable by Phy-X/PSD and the cross sections are given in Figure 10. It is obtained that FNRCS value is the highest for C2 and that is the lowest for Z3 among the samples. It is possible to note that the samples C2 with lower photon shielding capability has higher neutron shielding capability.

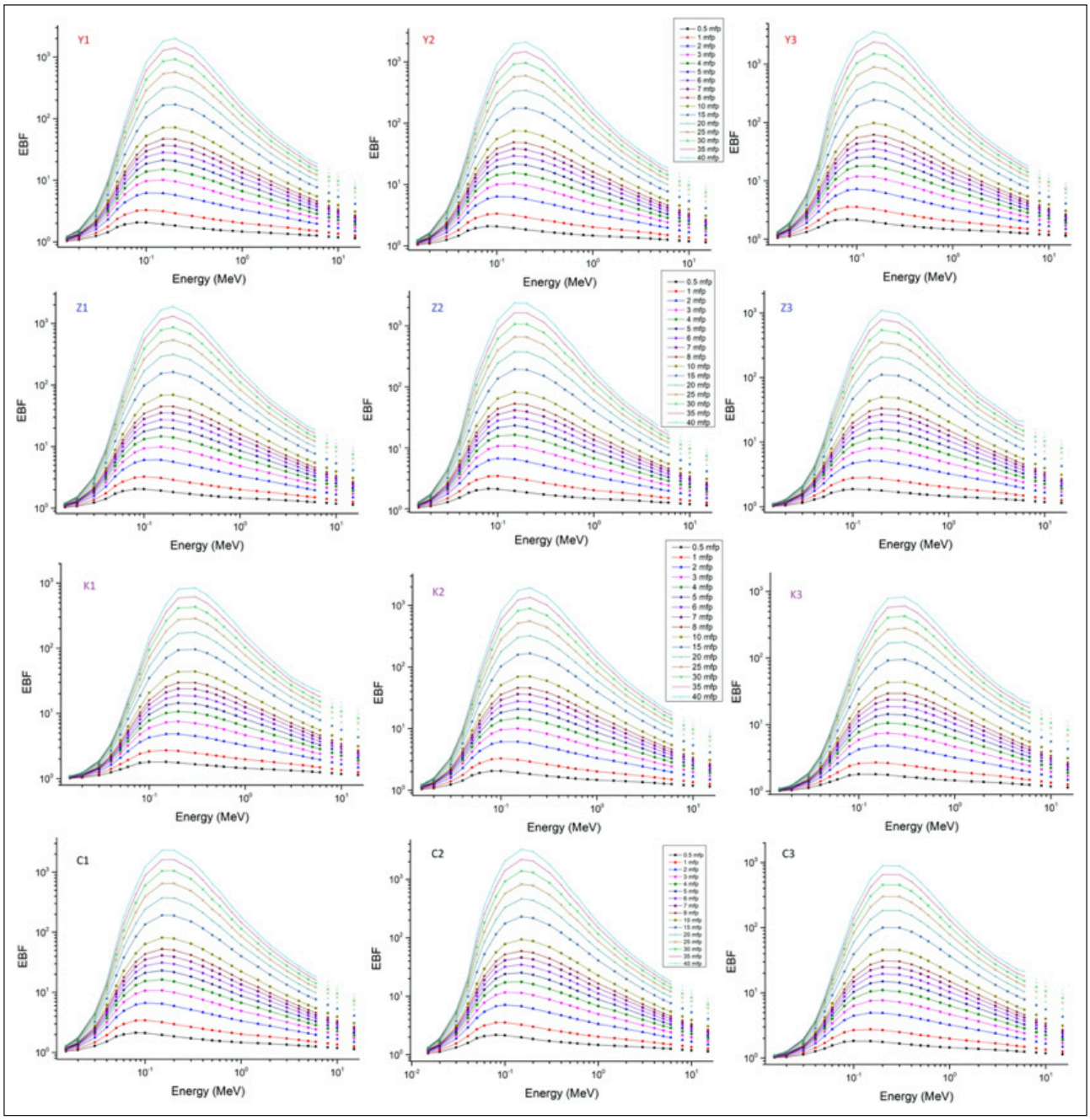


**Figure 9**. The changes of EBF of the samples versus photon energies.

## CONCLUSION

The purpose for performing the study was to produce new materials with higher RSP and good structural properties convenient for applications. In line with this aim, spectroscopic features and RSP of four groups of samples consisting of waste materials were examined by experimentally and theoretically with Phy-X/PSD code. By the help of XRD patterns, the Debye-Scherer equation was used for the crystallite size determination of the samples. Sharp peaks show the high crystallinity properties of the samples. The existence of calcite main phase peaks as well as $SiO_2$ and cellulose phases were observed by XRD. $Mn^{+2}$ sextets with five weak doublets ascribed to the forbidden transition lines of $Mn^{+2}$ and a singlet assigned to a carbon centered radical with a g value of

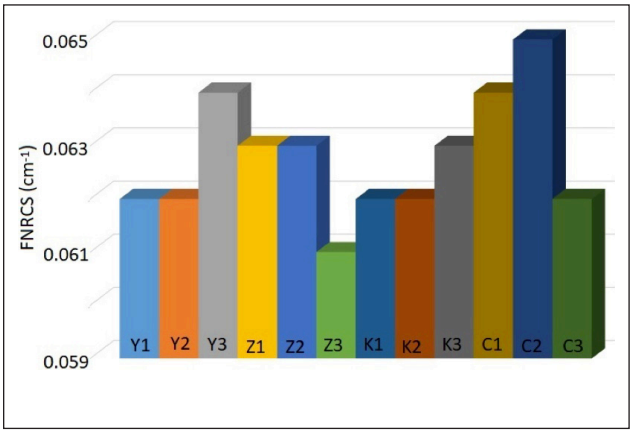


**Figure 10**. FNRCS values of the samples versus photon energies.

≈2.00 were recorded by EPR. The evaluation of the RSP of the samples were made by obtaining photon-matter interaction parameters by Phy-X/PSD and XCom codes. More shielding properties are observed for K1 (RC(20%)-ESW(60%)-BSW(20%)), K3 (RC(60%)-ESW(20%)-BSW(20%)), C3 (RC(60%)-ESW(20%)-WSW(20%)) and Z3 (GC(60%)-ESW(20%)-BSW(20%)), and lower RSP are found for Z2, C2, C1 and Y3. It is concluded that FNRCS value is the highest for C2 and that is the lowest for Z3. In order to reuse and recycle wastes, it can be recommended that all samples examined with good protection performance can be used as substitute materials instead of cement or aggregate.

## ACKNOWLEDGEMENTS

Authors acknowledge the financial support of Bitlis Eren University Scientific Research Projects Coordination Unit (BEBAP) with a project grant number 2023.14. Experimental results were obtained from Advanced Technology Research & Application Center (ILTEK) of Selcuk University.

## DATA AVAILABILITY STATEMENT

The author confirm that the data that supports the findings of this study are available within the article. Raw data that support the finding of this study are available from the corresponding author, upon reasonable request.

## CONFLICT OF INTEREST

The author declared no potential conflicts of interest with respect to the research, authorship, and/or publication of this article.

## USE OF AI FOR WRITING ASSISTANCE

Not declared.

## ETHICS

There are no ethical issues with the publication of this manuscript.

## REFERENCES

[1] M. S. Nasr, A. A. Shubbar, Z. A. R. Abed, and M. S. Ibrahim "Properties of eco-friendly cement mortar recycled materials from different sources," Journal of Building Engineering, Vol. 31, Article 101444, 2020. [CrossRef]

[2] Z. He, A. Shen, H. Wu, W. Wang, L. Wang, C. Yao, and J. Wu, "Research progress on recycled clay brick waste as an alternative to cement for sustainable construction materials," Construction Building Material, Vol. 274, Article 122113, 2021. [CrossRef]

[3] N. Sathiparan, and H. T. S. M. De Zoysa, "The effects of using agricultural waste as partial substitute for sand in cement blocks," Journal of Building Engineering, Vol. 19, pp. 216–227, 2018. [CrossRef]

[4] S. F. Olukotun, S. T. Gbenu, F. I. Ibitoye, O. F. Oladejo, H. O. Shittu, M. K. Fasasi, and F. A. Balogun, "Investigation of gamma radiation shielding capability of two clay materials," Nuclear Engineering and Technology, Vol. 50(6) pp.957–962, 2018. [CrossRef]

[5] N. F. N. Zuhairi, H. N. Mohd, A. Ripin, M. I. Idris, and N. A. Mohd Radzali, "Study on clay bentonite and kaoline as shielding material," Sains Malaysiana Vol. 49(3), pp. 683–691, 2020. [CrossRef]

[6] I. Akkurt, A. Alomari, M. Y. Imamoglu, and I. Ekmekçi, "Medical radiation shielding in terms of effective atomic numbers and electron densities of some glasses," Radiation Physics and Chemistry, Vol. 206, pp. 1–5, 2023. [CrossRef]

[7] B. Alım, A" comprehensive study on radiation shielding characteristics of Tin-Silver, Manganin-R, Hastelloy-B, Hastelloy-X and Dilver-P alloy's, Applied Physics A, Vol. 126, pp. 262, 2020. [CrossRef]

[8] O. Agar, H.O. Tekin, M. I. Sayyed, M. E. Korkmaz, O. Culfa, and C. Ertugay, "Experimental investigation of photon attenuation behaviors for concretes including natural perlite mineral," Results in Physics, Vol. 12, pp. 237–243, 2019. [CrossRef]

[9] Z. Aygun, M. Aygun, and N. Yarbasi, "A study on radiation shielding potentials of green and red clayey soils in Turkey reinforced with marble dust and waste tire," Journal of New Results in Science, Vol. 10, pp. 46–59, 2021. [CrossRef]

[10] Z. Aygun, N. Yarbasi, and M. Aygun, "Spectroscopic and radiation shielding features of Nemrut, Pasinler, Sarıkamıs and Ikizdere obsidians in Turkey: Experi-mental and theoretical stud," Ceramics Internation-al, Vol. 47(24), pp. 34207–34217, 2021. [CrossRef]

[11] Z. Aygun, and M. Aygun, "A study on usability of Ahlat ignimbrites and pumice as radiation shielding materials, by using EpiXS code," International Journal of Environmental Science and Technology, Vol. 19, pp. 5675–5688, 2022.

[12] M. Aygun, and Z. Aygun, "A comprehensive anal-ysis on radiation shielding characteristics of boro-gypsum (boron waste) by Phy-X/PSD code," Revis-ta Mexicana de Física, Vol. 69(4), Article 040401, 2023. [CrossRef]

[13] M. I. Sayyed, "The Impact of Chemical Composition, Density and Thickness on the Radiation Shielding Properties of CaO–Al2O3–SiO2 Glasses," Silicon, Vol. 15 pp. 7917–7926, 2023. [CrossRef]

[14] H. M. H. Zakaly, H. A. Saudi, H. O. Tekin, M. Rashad, A. M. Shams, Y. S. Issa, A. I. Rammah, M. M. Elazaka, and H. A. Ene, "Glass fabrication using ceramic and porcelain recycled waste and lithium niobate: physical, structural, optical and nuclear radiation attenuation properties," Journal of Material Research Technology, Vol. 15, pp. 4074–4085, 2021. [CrossRef]

[15] B. Oruncak, "Computation of neutron coefficients for B2O3 reinforced composite," International Journal of Computational and Experimental Science and Engineering, Vol. 9, pp. 50–53, 2023. [CrossRef]

[16] R. D. Malidarre, H. O. Tekin, K. Günoğlu, and H. Akyıldırım, "Assessment of gamma ray shielding properties for skin," International Journal of Computational and Experimental Science and Engineering, Vol. 9, pp. 6–10, 2023. [CrossRef]

[17] Q. A. A. D. Rwashdi, F. Q. Waheed, K. Günoğlu, and İ. Akkurt, "Experimental testing of the radiation shielding properties for steel," International Journal of Computational and Experimental Science and Engineering Vol. 8(3), pp. 74-76, 2022.

[18] Z. Aygun, and M. Aygun, "An analysis on radiation protection abilities of different colored obsidians," International Journal of Computational and Experimental Science and Engineering, Vol. 9, pp. 170–176, 2023. [CrossRef]

[19] E. Sakar, O. F Ozpolat, B. Alım, M. I. Sayyed, and M. Kurudirek, "Phy-X / PSD: Development of a user friendly online software for calculation of parameters relevant to radiation shielding and dosimetry," Radiation Physics and Chemistry, Vol. 166, Article 108496, 2020. [CrossRef]

[20] C. Xiang, E. H. Han, Z. M. Zhang, H. M. Fu, J. Q. Wang, H.F. Zhang, and G. D. Hu, "Design of single-phase high-entropy alloys composed of low thermal neutron absorption cross-section elements for nuclear power plant application," Intermetallic, Vol. 104, pp. 143–153, 2019. [CrossRef]

[21] D. F. Jackson, and D. J. Hawkes, "X-ray attenuation coefficients of elements and mixtures," Physics Re-ports, Vol. 70, pp. 169–233, 1981. [CrossRef]

[22] Y. Harima, Y. Sakamoto, S. Tanaka, and M. Kawai, "Validity of geometric progression formula in approximating gamma-ray buildup factors," Nuclear Science and Engineering, Vol. 94, pp. 24–35, 1986. [CrossRef]

[23] Y. Harima, "An historical review and current status of buildup factor calculations and applications," Radiation Physics and Chemistry, Vol. 41, pp. 631–672, 1993. [CrossRef]

[24] ANSI/ANS 6.4.3, "Gamma-ray Attenuation Coefficients and Buildup Factors for Engineering Materials," American Nucl Soc, La Grange Park, Illinois, 1991.

[25] Z. Aygun, "Application of spectroscopic techniques for antioxidant property analysis of various food supplements and ganoderma lucidum coffee," Pakistan Journal of Science Industrial Research B: Biological Scince, Vol. 60(3), pp. 145–153, 2017. [CrossRef]

[26] M. S. El-Mahllawy, A. M. Kandeel, M. L. Abdel Latif, and A. M. El Nagar, "The feasibility of using marble cutting waste in a sustainable building clay industry," Recycling Vol. 3, Article 39, 2018. [CrossRef]

[27] T. Thriveni, S.Y. Nam, J.W. Ahn, "Enhancement of arsenic removal efficiency from mining waste water by accelerated carbonation," IMPC, 2014.

[28] B. Yu, G. Fan, S. Zhao, Y. Lu, Q. He, Q, Cheng, J. Yan, B. Chai, and G. Song, "Simultaneous isolation of cellulose and lignin from wheat straw and catalytic conversion to valuable chemical products," Applied Biology and Chemistry, Vol. 64, Article 15, 2021. [CrossRef]

[29] P. Scherrer, "Bestimmung der Grösse und der inneren Struktur von Kolloidteilchen mittels Röntgenstrahlen," Nachr Ges Wiss Göttingen, Vol. 26, pp. 98–100, 1918. [Deutsch]

[30] M. Aygun, Z. Aygun, and E. Ercan, "Radiation protection efficiency of newly produced W-based alloys: Experimental and computational study," Radiation Physics and Chemistry, Vol. 212, Article 111147, 2023. [CrossRef]

[31] Y. Shimoyama, M. Ukai, H. Nakamura, "Advanced protocol for the detection of irradiated food by electron spin resonance spectroscopy," Radiation Physics and Chemistry Vol. 76, pp. 1837–1839, 2007. [CrossRef]

[32] Y. Shimoyama, M. Ukai, and H. Nakamura, "ESR detection of wheat flour before and after irradiation," Spectrochimica Acta A, Vol. 63, pp. 888–890, 2006. [CrossRef]

[33] M. Ukai, H. Kameya, H. Nakamura, Y. Shimoyam, "An electron spin resonance study of dry vegetables before and after irradiation," Spectrochimica Acta A, Vol. 69, pp. 1417–1422, 2008. [CrossRef]

[34] M. J. Berger, and J. H. Hubbell, "XCOM: Photon Cross Sections Database," Web Version 1.2. National Institute of Standards and Technology Gaithersburg, MD. 20899 USA 1987. [CrossRef]

[35] Z. Aygun, and M. Aygun, "Radiation shielding potentials of rene alloys by Phy-X/PSD code," Acta Physica Polonica A, Vol. 5(141), pp. 507–515, 2022. [CrossRef]

*Environ Res Tec, Vol. 7, Issue. 3, pp. 347–355, September 2024*

**Environmental Research and Technology**
https://ert.yildiz.edu.tr - https://dergipark.org.tr/tr/pub/ert
DOI: https://10.35208/ert.1358852

Environmental Research & Technology

**Research Article**

# Improved demineralization of the carbon black obtained from the pyrolysis of the sidewall and tread of scrap Tires: Extraction of some micro-/macro-nutrient elements of plants

**Ufuk Sancar VURAL*[1], Abdullah YINANÇ[2]**

[1]*Department of Chemistry (retired), Selçuk University Faculty of Science, Konya, Türkiye*
[2]*Vocational College of Technical Sciences, Namık Kemal University, Tekirdağ, Türkiye*

## ARTICLE INFO

*Article history*
Received: 12 September 2023
Revised: 06 March 2024
Accepted: 20 March 2024

**Key words:**
Deashing; Micro-nutrients; Macro-nutrients; Pyrolytic residue; Zinc

## ABSTRACT

In parallel with the increasing tyre production in the world, the amount of scrap tyres is also increasing. Within the scope of scrap tyre management, studies aimed at preventing the accumulation of tyres that threaten the world in terms of human health and the environment can be briefly defined as 4RL, including recycling, reuse, recovery, regeneration, landfill. Current methods have not yet completely controlled the accumulation of scrap tires. In this study, sidewall and tread parts of scrap tires with different compositions were pyrolyzed separately. Pyrolytic carbon black has been upgraded with an improved acid-base extraction method. Two different carbon blacks of high commercial value were obtained from the tire sidewall and tread. Since the mixture obtained from acidic-basic extraction, consisting of elements such as Zn, K, Na, Ca and S, are micro and macro nutrients of plants, the solution can be used directly in the fertilizer industry. With this study, the commercial value of solid residue, which is a major bottleneck in tire pyrolysis plants, has been increased. The pyrolysis method has been transformed into a more feasible project.

**Cite this article as:** Vural US, Yinanç A. Improved demineralization of the carbon black obtained from the pyrolysis of the sidewall and tread of scrap Tires: Extraction of some micro-/macro-nutrient elements of plants. Environ Res Tec 2024;7(3)347–355.

## INTRODUCTION

The amount of scrap tyres is increasing day by day with the increase in passenger vehicles, public transportation vehicles, and construction machines around the world. More than 1.5 billion tons of tyre scrap is generated every year. Tyre scraps left in the environment fall into the group of hazardous waste and remain without self-degradation due to its chemical structure consisting of strong polymeric crosslinks [1]. The rainwater accumulated in the scrap tyres thrown into the environment or stored regularly becomes the habitat of mosquitoes and parasites, which poses a great threat to living things as it causes the spread of epidemics. The flammability of tyres collected in landfills is very high and the fires cause great environmental pollution [2]. In the USA, a fire in a tyre storage area lasted about 9 months [3]. Scrap tyre management around the world has become important to minimize these threats. The methods of combating scrap tyres, which seriously threaten life, are generally grouped under five headings as reduction, reuse, recycling, recovery, and reclamation, and it would not be wrong to call these studies 4RL.

Obtaining pyrolytic fuel (energy) and pyrolytic carbon black (polymer filler and dye) from the pyrolysis of scrap tires is one of the most important methods in waste tire manage-

***Corresponding author.**
*E-mail address: usvural@gmail.com

ment [4–8]. The process of converting hydrocarbons into smaller molecules by thermal cracking in oxygen-free conditions at high temperatures is called pyrolysis [7–10]. Carbon black (CB) and polymer (rubber) are the main components of the tyre body. The pyrolytic carbon black ($CB_p$) and pyrolytic oil (liquid fuel) are the two major products of tire pyrolysis [9]. World carbon black production is around 14 million metric tons according to 2020 data [10]. The carbon black is the most important filler and dyestuff used in the tyre and polymer industry. In tire manufacturing, 20–30% CB is added to the rubber [1]. Depending on tire types and pyrolysis conditions, between 30% and 40% $CB_p$ is obtained from the pyrolysis of scrap tires [1, 6]. The two major components of ash in carbon black are $SiO_2$ and Zn (zinc oxide, zinc sulfide). Industrial use of $CB_p$ is difficult due to the high ash content. To date, some acid-base leaching methods with mineral acids (HCl, $H_2SO_4$, $HNO_3$, HF) and NaOH have been studied to reduce the ash amount of $CB_p$ [1, 11, 12]. In metal and sulfur extraction, the highest efficiency was obtained in two-stage acidic demineralization studies (mineral acid and HF) [11]. However, due to the difficulty of application and high cost of toxic HF, it has not become popular in industrial applications. Mineral acid-NaOH methods could not achieve as much success as HF because the interaction between $CB_p$ and the extraction solution was not strong. There is still a need for continued research on upgrading $CB_p$.

Seventeen elements in soil are important nutrients for plants [13]. Among these, macro-nutrient elements are N, P, K, Ca, Mg and S, and micro-nutrient are Fe, Zn, Cu, B, Mn, Mo, Cl and others [13]. It is known that Zn, which is one of the two major components of ash in $CB_p$, shows important activity in plant development [14–16]. These elements are the cornerstones of many biological reactions that are vital in plant metabolism, such as enzymes and the formation of amino acids. The ash composition in $CB_p$ consists of micro-nutrients and macro-nutrients such as Zn, Ca, K, Fe and S.

In this study, solid-liquid extraction efficiency was increased by adding dispersive, wetting and complexing agents to the know acid-base extraction method in $CB_p$ demineralization studies. It was determined that the elements in the extract constitute micro-nutrients and macro-nutrients that are vital for plants. Thus, $CB_p$ obtained from pyrolysis of tire, which has a very low market value and constitutes a serious bottleneck for the pyrolysis method, has been converted into carbon black with high commercial value, and an important raw material source for the fertilizer industry has been obtained as a by-product of extraction method. Recycling scrap tires using the pyrolysis method has become a more feasible project.

## EXPERIMENTAL

The pyrolysis processes were carried out in a mechanism consisting of heating the shredded tyres in a fixed bad reactor, gas-liquid separation by cooling in a condenser, and cleaning (desulfurization) of non-condensed gases. In the heating process, a fixed bad reactor made of 2 mm stainless steel, 100 mm in diameter, 200 mm in height, heated with a 4 kW electrical resistance was used. The reactor was isolated by wrapping it with silica wool. Temperature and pressure in the reactor were controlled by PID. A straight tube bundle condenser with a length of 700 mm and a diameter of 100 mm was used to separate the pyrolytic gases. The non-condensed gases were desulfurized by passing through a container with a basic solution and burned with a burner flame. The pyrolysis processes were carried out at atmospheric pressure. Leco, CHNS-932 elemental analyzer was used for C, H, N, S analysis in carbon black. Carbon black surface area was measured with the Gemini VII 2390 series from Micromeritics. The metal composition of the ash was determined with a 50 kV, 500 μA, Malvern Pananalytical Epsilon 1 X-ray fluorescence spectrometer (XRF). In the carbon black refining process, a blanket-wrapped Dissolver Dispermat® LC55 dispersive mixing device heated with a 2 kW resistance was used. Binder FP 720 model oven was used for drying operations, Microtest MKF-7 model muffle furnace was used for high-temperature heating. Scrap tyres were obtained from tyre changing services. The sidewall and back parts of the tyres were separated with chisel blades and sliced in 1–2 cm sizes. It was then washed with water and acetone and dried at room temperature. Elemental analyzes of the selected tyres are given in Table 1.

**Table 1.** Sidewall and tread compositions of tyres used in research

| Component | Sidewall | Tread |
|---|---|---|
| Ultimate analysis, % | | |
| C | 81.67 | 74.93 |
| H | 7.74 | 6.59 |
| N | 0.41 | 0.26 |
| O | 2.68 | 1.89 |
| S | 1.22 | 0.76 |
| Proximate analysis, % | | |
| Moisture (M) | 1.46 | 3.25 |
| Volatile matter (VM) | 66.23 | 61.88 |
| Ash (A) | 6.28 | 15.57 |
| Fixed carbon (FC) | 26.03 | 19.30 |
| Zn | 2.68 | 2.36 |

### Pyrolysis

The tyre sidewall and tread pieces, which were previously sliced in 1–2 cm sizes, were weighed separately 800 g and filled into the pyrolysis reactor, heated at 5 °C/min, and the pyrolysis process was carried out at 450, 500, 550, 600 °C temperatures for 4 hours. Pyrolytic gases were condensed and accumulated in the liquid collection container, and non-condensed gases were passed through a 4 M NaOH solution and burned in the burner. The reactor cover, which was cooled to room temperature, was opened and all carbon black was discharged. Metallic impurities in carbon black were separated by a water trap and magnet.

**Demineralization of $CB_P$**

Metal extraction from pyrolytic carbon black consists of acidic and basic ash removal steps. In acidic ash removal (deashing) process, zinc metal is extracted by treating pyrolytic carbon black with acid solution, dispersing agent and complexing agent, and acidic washing precipitate is obtained by washing the solid phase. In the basic ash removal process, the acidic precipitate is treated with a basic solution and an oxidizing agent to extract the silicon component, the solid phase is filtered, washed and dried.

**The Acidic Deashing**

A mixture of 10 g of carbon black, 100 ml of HCl, 10 ml of ethyl alcohol (EA) as a dispersing agent and 0,5 g of citric acid (CA) as a complexing agent is mechanically mixed at 50 °C until it becomes a homogeneous solution. Then it is mixed for another 2 hours with a 40 kHz ultrasonic mixer. The solution is filtered and the precipitate is washed until pH=7. The zinc rich aqueous phase is zinc extraction solution.

**The Basic Deashing**

A solution of 5 g of $CB_P$, $4.10^{-3}$ wt.% of potassium ferrate, 5 M NaOH in 50 mL of water is heated up to 85 °C with mechanical mixing until a homogeneous solution is obtained. Next, the mixture was stirred for 1 hour with a 40 kHz ultrasonic stirrer at 85 °C, 300 rpm. 25 mL of 30% sodium hypochlorite was added to the mixture twice with one hour intervals and mixed for 2 more hours. Then it was cooled to room temperature, centrifuged at 5000 rpm, washed until pH=7 and filtered. The precipitate dried in an oven at 120 °C is refined carbon black.

## RESULTS AND DISCUSSION

In the thermochemical cracking reaction of scrap tires, volatile compounds and carbonaceous residue are formed. Most of the volatile components are condensed to obtain pyrolytic oil. Non-condensed gases consisting of C1–C4 hydrocarbons are considered gas-fuel since they have high calorific value. At the end of pyrolysis, carbon black, silica, zinc, other minerals and sulfur compounds added in the manufacture of the tire are obtained as solid residue and are also called pyrolytic carbon black ($CB_p$) [6].

Carbon black, used as one of the main components in tire manufacturing, is classified by ASTM with various codes between N100-N900, depending on parameters such as size, surface area, pore diameter and surface activity [17]. N refers to the normal carbonation rate, and numbers refer to grain size. Carbon blacks with small particle sizes have a microporous structure and are highly structured. The dispersion of high-structure CB in the polymer is more difficult than low-structure CB, but the dyeing intensity is stronger [17]. Although low-structure carbon blacks are better dispersed in the polymer, they reduce the mechanical strength of the polymer. In the interactions between the polymer and carbon black, alcoholic, carboxylic acid, carboxylic anhydride, lactone, lactols, phenol, and hydroxyl groups on the surface of carbon black play an important role in surface activity [18, 19].

Some changes occur in the surface morphology of carbon black due to the volacanization reactions of rubber and thermochemical reactions during high temperature pyrolysis [18, 19]. Substances formed during the vulcanization reactions that occur between CB and rubber molecules, S and inorganic substances fill the pores of carbon black. Additionally, some functional groups may be deactivated due to reactions between the functional groups on the $CB_P$ surface with rubber molecules and sulfur. Carbonaceous residues formed by repolymerization and dealkylation reactions occurring in the gas phase during pyrolysis refill the $CB_P$ pores in the form of coked deposits [18, 19]. The physicochemical properties of $CB_P$ differ from commercial carbon blacks due to changes in the pore diameter and surface activity of $CB_P$, as well as the masking of the surface activity by carbonaceous residues. Another reason why $CB_P$ does not have a specific standard is that different types of carbon black and silica combinations are used in the sidewall and tread during tire manufacturing [20, 21]. High-structure carbon blacks with a large surface area, which provide high wear and friction resistance even at low temperatures, are preferred in the tire tread. Carbon blacks, which provide high strength and flex resistance and are easily dispersed in polymer, are preferred on the sidewall. Since carbon blacks such as N110, which have high structure and large surface area, are difficult to disperse in the polymer, they are not preferred to be used in tire manufacturing. Recently, carbon blacks and inorganic additives such as $SiO_2$ and $CaCO_3$ have begun to be used in tire manufacturing as hybrid fillers [20, 21]. For example, in Toyoya Car Corp.'s patented work, the use of a hybrid filler consisting of Seast 3 coded carbon black (equivalent to N330) and silica in the manufacture of the tire sidewall is described. In the patented work of Sumitomo Rubber Industries Ltd, N359 carbon black and silica hybrid filler was used in the tire tread [20, 21]. As a general approach, it can be said that high-structure carbon blacks with mesopore diameter are used instead of low-structure carbon blacks, which have high porosity and weaken the wear resistance of the polymer, in the tire tread and sidewall. Additionally, it seems impossible to define a specific standard quality for revovered carbon black, as different types of carbon black are used in different tire types and tire parts, depending on tire manufacturers' formulations.

In this study, the tire tread and sidewall parts were pyrolyzed separately to separate the two different types of carbon black used in the tire tread and sidewall parts. Since the main subject of the study was the removal of inorganic components in carbon black, no catalyst was used to change the mineral composition of the ash, and parameters that would affect the pyrolysis efficiency such as heating rate and tire size were not examined. Regardless of the brand of tyre types, sidewall and tread tyres were separated and cut into 1–2 cm sizes with the help of chisels. Sidewall and tread tyres have been pyrolyzed separately between 450 °C and 600 °C. Product yields depending on the temperature in the pyrolysis process are given in Table 2. Maximum pyrolytic oil was obtained as 49.76 wt.% from the tire tread and 51.26 wt.% from the tire sidewall at 550 °C. The highest

**Table 2.** The proportions of tread and sidewall pyrolysis products at different temperatures

| T, °C | Tread/% | | | Side wall/% | | |
|---|---|---|---|---|---|---|
| | $CB_p$ | Oil | Gas | $CB_p$ | Oil | Gas |
| 450 | 41.5 | 44.74 | 13.76 | 39.12 | 47.21 | 13.67 |
| 500 | 39.42 | 45.62 | 14.96 | 37.43 | 47.62 | 14.95 |
| 550 | 38.53 | 49.76 | 11.71 | 36.22 | 51.26 | 12.52 |
| 600 | 36.34 | 48.51 | 15.15 | 34.16 | 49.74 | 16.1 |

**Table 3.** The pyrolytic carbon black composition obtained from sidewall and tread tyres depending on the pyrolysis temperature

| | Ultimate analysis (wt.%) | | | | | Proximate analysis (wt.%) | | | |
|---|---|---|---|---|---|---|---|---|---|
| T, °C | C | H | N | O | S | A | M | VM | FC |
| Side wall | | | | | | | | | |
| 450 | 80.86 | 1.58 | 0.59 | 3.95 | 1.63 | 12.28 | 1.66 | 7.45 | 78.61 |
| 500 | 84.92 | 1.65 | 0.43 | 3.79 | 1.69 | 10.52 | 0.86 | 4.77 | 83.85 |
| 550 | 86.41 | 1.73 | 0.52 | 3.21 | 1.2 | 9.82 | 0.82 | 4.57 | 84.79 |
| 600 | 87.16 | 1.78 | 0.56 | 3.39 | 1.66 | 9.12 | 0.87 | 4.32 | 85.69 |
| Tread | | | | | | | | | |
| 450 | 49.12 | 1.63 | 0.55 | 2.68 | 2.48 | 49.41 | 2.97 | 8.67 | 38.95 |
| 500 | 54.23 | 1.54 | 0.41 | 2.47 | 2.13 | 46.23 | 2.68 | 4.98 | 46.11 |
| 550 | 56.92 | 1.48 | 0.43 | 2.51 | 1.86 | 44.89 | 2.41 | 4.82 | 47.88 |
| 600 | 57.16 | 1.45 | 0.49 | 2.18 | 1.98 | 44.18 | 2.18 | 4.58 | 49.06 |

A: Ash; M: Moisture; VM: Volatile matter; FC: Fixed carbon.

amount of carbon black was obtained at 450 °C, 41.5 wt.% and 39.12 wt.% for the tire tread and sidewall, respectively. There was no significant increase in the amount of $CB_p$ and oil after 550 °C. The high amount of $CB_p$ at 450 °C show that the hydrocarbons in the carbon black matrix are not completely cracked, the carbon-like deposit formed by secondary reactions between gas molecules covers the carbon black surface, and pyrolysis is not completed. Moulin et al. [22], as seen in Figure 1, stated that in the dTG and TG diagram obtained from termogravimetric analyzes of the tire up to 800 °C, thermal degradation started at 150 °C, and mass loss began to be observed around 300 °C due to the degradation of additives such as process oils and plasticizers. They showed in dTG curves that most of the rubber decomposes between 350 °C and 500 °C, and mass loss is completed at 550 °C.

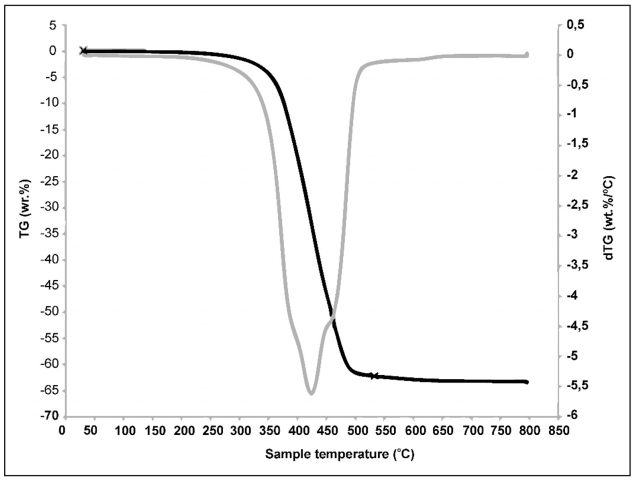


**Figure 1**. TGA-DTA analysis on the tire sample at 5 °C/min heating rate [22].

In the pyrolysis experiments carried out by Yazdani et al. [23] between 400 °C–600 °C, distinct peaks were observed in the range of 660–3000 $cm^{-1}$ from the FT-IR analyzes of the pyrolytic oil. They determined that the 3050 $cm^{-1}$ band of C-H strench indicates the aromatic structure and shows the highest value at 500 °C and 550 °C. Researchers stated that pyrolysis was completed at 550 °C [23]. In the experiments conducted with tire tread and sidewalls, the maximum pyrolytic oil yield was obtained at 550 °C, which coincides with both literature studies [22, 23]. It has been understood that in order to complete the thermal pyrolysis of scrap tires, the temperature must be exceeded 500 °C, and since there is no change in the yield of the products after 550 °C, the pyrolysis temperature must be between 500 °C and 550 °C.

Ultimate and proximate analyzes of $CB_p$ obtained at different temperatures are given in Table 3. As seen in Table 3, the amount of volatile matter (VM) of carbon blacks obtained from the tire sidewall and tread between 450 °C and 600 °C varies in the range of 7.45 wt%–4.32 wt% and 8.67 wt%–4.58 wt%, respectively. At low temperature, the VM value was found to be higher than the sidewall due to the presence of

**Table 4.** Analysis results of demineralized pyrolytic carbon black at 550 °C

| Samples | Sidewall | Tread | N234 | N330 | N339 | N550 |
|---|---|---|---|---|---|---|
| C | 94.29 | 94.33 | 95.2 | 96 | 97.79 | 98.7 |
| H | 0.50 | 0.60 | | | | |
| N | 0.34 | 0.48 | | | | |
| O | 3.66 | 3.50 | | | | |
| S | 0.80 | 0.73 | | | | |
| Ash | 0.41 | 0.36 | | | | |
| M | 0.53 | 0.60 | | | | |
| VM | 3.40 | 3.82 | | | | |
| FC | 94.38 | 94.46 | | | | |
| SA, $m^2/g$ | 76.82 | 99.76 | 126 | 83 | 96 | 42 |
| Iodine number, mg/g | 77.40 | 84.43 | 120 | 82 | 93 | 43 |
| $DB_p$, $cm^3/100$ g | 98.12 | 101.50 | 125 | 102 | 115 | 121 |

DPPA: Dibutylphtalate adsorption; M: Moisture; VM: Volatile matter; FC: Fixed carbon.

more carbonaceous deposits on the carbon black surface obtained from the tire tread. At high temperatures, the amount of VM for both $CB_p$ was found to be close to each other.

Table 3 shows that the ash values for the tire tread are almost four times higher than those for the sidewall. One of the reasons for this is that due to the larger pore diameter of the carbon black used in the tire tread, more coked carbon residues and mineral matter cover the carbon black surface and fill its pores. The other main reason is the use of high amounts of silica as a filler along with carbon black in the tire tread. As a result, the FC values of the carbon blacks obtained from the tire tread were found to be much lower than those from the tire sidewall. From these data, it is understood that the carbon black used in the tire tread has a larger pore diameter and lower structure than the tire sidewall. FC values increased due to the decrease in the amount of volatile matter with the increase in temperature. Since carbonaceous residues containing polymer molecules cross-linked with sulfur and ZnS, which is formed as a result of the reaction of S and Zn, are more in the tread part, the sulfur value is higher than in the sidewall part. In Figure 2, Mis-Fernandez et al. [24], from X-Ray Diffraction analysis of tire pyrolysis between 450–750 °C, show that characteristic peaks of ZnO are very strong at 450 °C, characteristic peaks of ZnS begin to appear after 550 °C, and ZnS peaks are very strong at 750 °C. They stated that after 750 °C, almost all Zn reacted with S to form ZnS.

The amount of iodine adsorption (iodine number) and $N_2$ adsorption provide important information about the surface area and pore structure of carbon black [1, 25]. Although the iodine number is found to be slightly different from the surface area determined according to $N_2$ adsorption due to the interaction of iodine with carbonaceous residues on the surface, the difference gives an idea about the carbonaceous residue and mineral substance covering the pore structure. An important parameter that determines

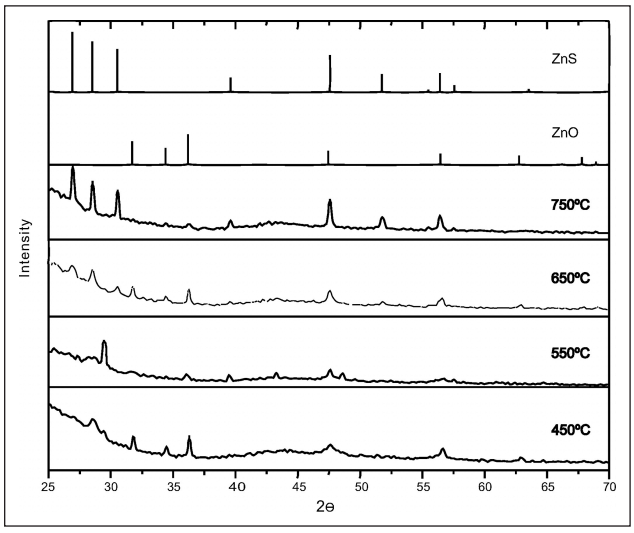


**Figure 2**. X-ray diffraction for pyrolytic process from 450 °C to 750 °C [24].

the quality of carbon black is the size of the branched chains in carbon black aggregates, which can be determined by di-butyl phthalate adsorption (DBP) [1, 25]. As seen in Table 4, in demineralized $CB_p$ obtained from the tire tread, although the analysis results were slightly different from N339 due to the carbonaceous residues and inorganic substances weakening the formation of a great, the values were found closer to N339. It is desirable to use high-structure, microporous carbon blacks in the tire tread, which improve the friction and wear resistance of the polymer. However, from the iodine number, $N_2$ adsorption and DBP adsorption data, it was understood that carbon black with a lower structure was used from the sidewall (similar to N330). The possible reason for this may be that since high-structure microporous carbon blacks are difficult to disperse in rubber, mesoporous carbon blacks, which are more easily dispersed, have been adopted to increase the wear and friction

**Table 5.** Elemental analysis results of $CB_P$ from acidic and basic deashing steps at 550 °C

| Samples | Sidewall | | | | Tread | | | |
|---|---|---|---|---|---|---|---|---|
| | $CB_P$ wt. % | HCl wt. % | HCl+CA+EA wt. % | NaOH+Oxidant wt. % | $CB_P$ wt. % | HCl wt. % | HCl+CA+EA wt. % | NaOH+Oxidant wt. % |
| Si | 17,23 | 65,22 | 74,20 | 1,18 | 40,68 | 63,63 | 70,87 | 1,96 |
| Zn | 47,36 | 6,96 | 3,76 | 0,74 | 20,66 | 5,50 | 3,73 | 0,44 |
| K | 1,07 | 1,14 | 0,90 | n.r. | 1,13 | 1,21 | 1,03 | n.r. |
| Na | 1,01 | 1,16 | 0,80 | n.r. | 1,10 | 1,18 | 0,75 | n.r. |
| Al | 3,45 | 1,79 | 0,14 | n.r. | 3,09 | 1,69 | 0,13 | n.r. |
| Fe | 3,23 | 1,07 | 0,12 | n.r. | 3,32 | 1,11 | 0,11 | n.r. |
| Mg | 1,28 | 1,06 | 0,18 | n.r. | 1,54 | 1,36 | 0,16 | n.r. |
| Ca | 5,63 | 1,86 | 0,15 | n.r. | 5,38 | 1,23 | 0,13 | n.r. |

n.r.: Note reported under 0,1 wt. %.

resistance with silica reinforcement. The negative effects of mesoporous carbon blacks producing larger aggregations were eliminated with silica. It can be said that, not being a general rule, low-structure, high-pore diameter carbon blacks such as N550 or N660 were not used on the sidewall and tread of the tire sample studied.

In Table 4, it is observed that the sulfur value also decreased significantly. It has been observed that sulfur in the form of metal sulfides is successfully reduced in the two-stage extraction method with the addition of complexing agents and oxidants.

Demineralization of $CB_P$ consists of a two-stage solid-liquid extraction (acid-base extraction) method. The method is also known as leaching. $CB_P$ was first treated with HCl, then the acid step was repeated by adding ethyl alcohol as a surface wetting and dispersing agent and citric acid as a complexing agent to the acid solution. In the continuation of the study, the acid-treated $CB_P$ was treated with NaOH solution containing oxidant substances to extract silica, sulfur and other metals. In Table 5, the extraction results of single-stage HCl extraction, HCl extraction with CA and EA addition, and NaOH extraction with oxidant addition are given.

Acidic Extraction: The following reactions occur between HCl and the major metallic components in $CB_P$,

$$ZnO + 2HCl \rightarrow ZnCl_2 + H_2O \quad (1)$$

$$Ca(OH)_2 + 2HCl = CaCl_2 + 2H_2O \quad (2)$$

$$Fe_2O_3 + 6HCl = 2FeCl_3 + 3H_2O \quad (3)$$

$$Al_2O_3 + 6HCl = 2AlCl_3 + 3H_2O \quad (4)$$

As seen from Eq (1), 2 mol of HCl is required for every 1 mol of ZnO. Since ZnO is 81.40 g/mol, theoritically 89,68 g of HCl is required stoichiometrically for every 100 grams of zinc oxide. The amount of zinc in $CB_P$ obtained from tire sidewall and tread regions at 550 °C, are 47.36% and 20.66%, respectively. Theoretically, 52.18 g HCl and 22.76 g of HCl are required for tread and sidewall $CB_P$, respectively. An acid solution 10 times the weight of $CB_P$ was used in the experiments. Considering the other elements in the carbon surface matrix, the use of 4 M HCl is also compatible with literature information [1, 15, 16].

As seen in Table 5, zinc extraction efficiency is low without the use of surface wetting EA and complexing CA. Depending on the metal extraction amount of HCl, the $SiO_2$ ratio in $CB_P$ increased. The addition of surface wetting EA increased the hydrophilicity of metals, and CA not only gave more protonium ions to the solution, but also significantly increased the extraction efficiency by complexing with metals. After the acidic stage, silica concentration increases due to the extraction of other metals.

Basic Extraction: The reaction between ZnS, $SiO_2$ with NaOH is as follows.

$$SiO_2 + 2NaOH \rightarrow Na_2SiO_3 + H_2O \quad (5)$$

$$ZnS + 2NaOH \rightarrow Na_2S + Zn(OH)_2 \quad (6)$$

Since $Zn(OH)_2$ has low solubility in water, it passes into the aqueous phase during neutralization of the solid phase with sulfuric acid, as seen in Eq. 7.

$$H_2SO_4 + Zn(OH)_2 \rightarrow ZnSO_4 + 2H_2O \quad (7)$$

After acidic metal extraction experiments in the range of 450 °C–600 °C, remaining $SiO_2$ for the tire sidewall and tread are 74.20 wt.% and 70.87 wt%, respectively. The amount of Zn is 3.76 wt.% and wt. 3.73 wt.%, respectively. Theoretically, 102.50 g and 98.03 g of NaOH are required to remove Zn and Si from every 100 g of sidewall and tread carbon black after the acidic deashing stage. 2.56 M and 2.45 M NaOH were calculated for each 100 g of sidewall and tread carbon black, respectively. It was taken into account that more base should be used due to the steric hindrance of other metals in $CB_P$ and carbonaceous residues of the $CB_P$ surface matrix, and 5 M NaOH was used in accordance with the literature [1, 5, 16]. As seen in Table 5, the amount of Si in the sidewall and tread decreased from 17.23 wt.% to 1.18 wt.% and from 40.68 wt.% to 1.96 wt.%, respectively.

As seen in Table 5, potassium ferrate and hypochlorite added in the basic extraction stage, zinc, silica and calcium, which are the major components of carbon black, were ex-

**Table 6.** Amounts of inorganic elements extracted from $CB_p$ at 550 °C

| | Sidewall | | | Tread | | |
|---|---|---|---|---|---|---|
| **Sample** | **Wt.% in ash** | **Recovery, wt. %** | **Extraction, g/L** | **Wt. % in ash** | **Recovery, wt.%** | **Extraction, g/L** |
| Si | 17.23 | 16.05 | 1.51 | 40.68 | 38.72 | 13.50 |
| Zn | 47.36 | 46.62 | 4.40 | 20.66 | 20.22 | 7.05 |
| K | 1.07 | 1.07 | 0.10 | 1.13 | 1.13 | 0.40 |
| Na | 1.01 | 1.01 | 0.10 | 1.10 | 1.10 | 0.39 |
| Al | 3.45 | 3.45 | 0.33 | 3.09 | 3.09 | 1.08 |
| Fe | 3.23 | 3.23 | 0.30 | 3.32 | 3.32 | 1.16 |
| Mg | 1.28 | 1.28 | 0.12 | 1.54 | 1.54 | 0.54 |
| Ca | 5.63 | 5.63 | 0.53 | 5.38 | 5.38 | 1.88 |

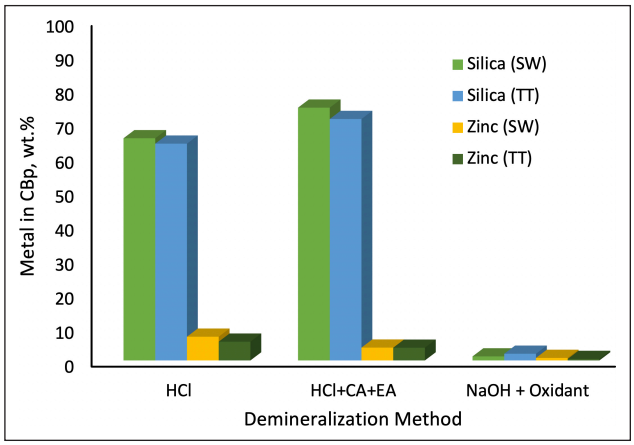


**Figure 3**. Zn and Si in CBP as a result of acidic and basic deashing steps at 550 °C.

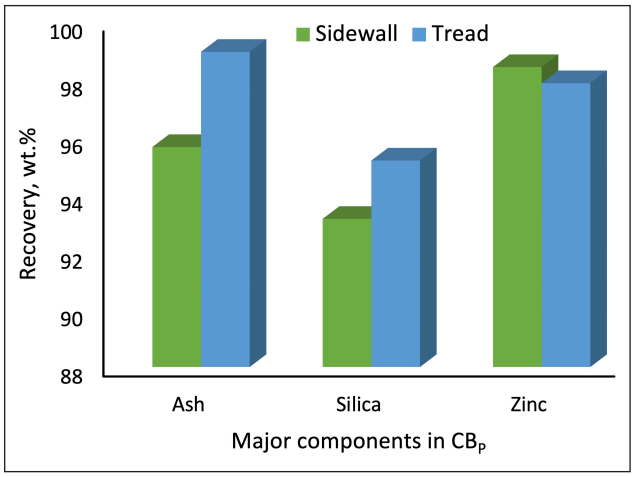


**Figure 4**. Deminerlization results of CBP at 550 °C.

tracted with great efficiency in the basic stage. Components above 1 wt.% are given in Table 5. As seen in Figure 3, silica could not be extracted alone in the acid phase, zinc was largely removed, and all minerals were extracted with great efficiency in the basic phase.

Although $SiO_2$ is the main component of the hybrid filler, it reduces the staining intensity of $CB_p$ because it changes the pore diameter and surface activity of carbon black. Additionally, $SiO_2$, which has a hydrophilic surface, reduces the dispersion of carbon black in the hydrophobic polymer matrix. $SiO_2$ decomposes as a commercially valuable by-product in the form of $Na_2SiO_3$ (water-glass) as a result of a basic reaction.

Sodium hypochlorite ionization reaction is given in Eq. 8 and Eq. 9. It is unstable at low pH values. Stable at pH>10 with addition of NaOH [26].

$$HClO \rightarrow H^+ + ClO^- \qquad K = 3.3 \times 10^{-8} \qquad (8)$$

$$HClO + Cl^- + H^+ \rightarrow Cl_2 + H_2O \qquad K = 2.3 \times 10^{3} \qquad (9)$$

Sulfonyl compounds are formed as a result of reactions between sulfur compounds in the form of sulfide or disulfide in the hydrocarbon structure and hypochlorite. The sulfonyl then oxidizes into sulfonate or sulfate.

$$R - S - R' + 2ClO^- \rightarrow RSClO^- + R'ClO^- \qquad (10)$$

$$RS - S - R' + 2ClO^- \rightarrow RSClO^- + R'SClO^- \qquad (11)$$

$$RSClO^- + 2H_2O \rightarrow RSO_3H + 3H^+ + Cl^- + 3e \qquad (12)$$

$$RSClO^- + 3H_2O \rightarrow RCl + 6H^+ + SO_4^{2-} + 5e \qquad (13)$$

The reaction between metallic compounds of sulfur, for example ZnS, and hypochlorite is given in Eq. (14).

$$ZnS + 4ClO^- + 2H_2O \rightarrow Zn(OH)_2 + 4Cl^- + SO_4^{2-} + 2H^+ \qquad (14)$$

As can be clearly seen from Table 5, after the demineralization studies of the sidewall and tread carbon blacks, the sulfur value decreased from 1.2 wt.% to 0.8 wt.% and from 1.86 wt.% to 0.73 wt.%. has decreased. CA and EA added in the acidic stage and hypochlorite added in the basic stage made a great contribution to the desulfurization of $CB_p$. As seen in Figure 4, the amount of zinc recovery is higher in the tire sidewall. Silica and ash removal is greater on the tread.

### Micro-Nutrients and Macro-Nutrients of Plants

Zinc is an important component of various enzymes that drive metabolic reactions in plants. These enzymes in the plant tissue contribute to the growth and development of the plant. Zinc deficiency causes a decrease in the formation of carbohydrates, proteins, and chlorophyll in plants.

Zinc is an important plant micronutrient that strengthens roots and leaves in fertilizers. Fertilizers containing zinc, which is a very important nutrient source for plants, especially in barren soils with high lime content, cannot be used as widely as desired due to the high cost of zinc. Efforts to reduce the cost of zinc-containing fertilizers will increase the use of such fertilizers in a wider area [14]. As seen in Table 6, K and Ca minerals, which are macro-nutrient elements of plants, are also included in carbon black ash. Micro and macro-nutrient elements in the solution obtained from pyrolytic carbon black are given in Table 6.

$CB_p$ obtained from tire sidewall and tread was treated with 10 times solution in acidic and basic levels, and the amount of mimeral substance extracted for 100 g $CB_p$ is given in g/L. Solutions can be used directly as stock material in fertilizer formulations containing micro and macro nutrients, their concentration can be increased by evaporation-crystallization, or they can be obtained as pure components by electrochemical methods. For example, as a result of the mineral recovery of 1 ton of $CB_p$, extract containing 40.40 kg and 70.50 kg of zinc is obtained from the sidewall and tread parts, respectively. 1 ton of solution prepared with a 1:1 mixture of extracts yields 57.05 kg Zn, 12.05 kg Ca, 7.05 kg Al, 7.30 kg Fe, 2.50 kg K and 2.45 Na. 1 ton, 1:1 extract mixture, 121.64 kg of sulfur component went into solution.

Thus, the solution obtained from the demineralization reactions of $CB_p$ is an important input in the manufacture of fertilizer as a plant nutrient raw material, as it contains potassium as well as rich zinc, sulfur and remarkable iron and calcium components. Zinc compound is an expensive substance with wide industrial use. Although the use of zinc element in plants as a fertilizer has proven to be extremely important for the plant and is used throughout the world, it cannot be used widely due to its high cost [27]. The use of zinc obtained from the recycling of scrap tyres in fertilizers will reduce the cost of fertilizer and increase the prevalence of zinc fertilizer.

Although the demineralization of pyrolytic carbon black will result in additional costs to the investor, it will be a sustainable and highly profitable project in terms of scrap tyre management, as demineralized carbon black with higher commercial value and also zinc that can be used for fertilizer will be obtained in the market. Thus, the bottleneck in the existing pyrolysis facilities will be overcome.

## CONCLUSION

In this study, carbon black, one of the two main products obtained from the recycling of scrap tires by the pyrolysis method, was upgraded with an improved acid-base extraction method. Pyrolytic carbon black is very difficult to use industrially and find a market due to the high ash and carbon residues it contains. Since tire manufacturers use different carbon blacks and fillers such as $SiO_2$ in different tires and components, it is not possible to obtain carbon black that exactly matches the ASTM carbon black classification standard from pyrolytic carbon black upgrade studies. However, since carbon black that has better dispersion and dyeing intensity in the polymer and has the average qualities of carbon black within a certain range in the ASTM classification can be obtained, carbon black suitable for use in the polymer industry can be obtained.

It has been understood that when the tire sidewall and tread are pyrolyzed separately, two different types of carbon black can be obtained depending on the pore diameter, surface area and activity. In the upgrade study of $CB_p$, the ash amount of $CB_p$ was reduced with a much higher efficiency than known acid-base methods.

Inorganic components obtained from carbon black are macro- and micro-nutrient elements that are vital for plants. The by-product (extraction and washing solutions) obtained from the $CB_p$ upgrade study can be evaluated in the fertilizer industry and will reduce $CB_p$ upgrade costs and provide a new perspective to the sector. Thus, pyrolysis facilities will come to the fore as a more feasible recycling method.

## ACKNOWLEDGEMENTS

I would like to thank KOSGEB Adana Provincial Directorate for supporting this study.

## DATA AVAILABILITY STATEMENT

The author confirm that the data that supports the findings of this study are available within the article. Raw data that support the finding of this study are available from the corresponding author, upon reasonable request.

## CONFLICT OF INTEREST

The author declared no potential conflicts of interest with respect to the research, authorship, and/or publication of this article.

## USE OF AI FOR WRITING ASSISTANCE

Not declared.

## ETHICS

There are no ethical issues with the publication of this manuscript.

## REFERENCES

[1] X. Zhang., H. Li, Q. Cao, J. Li, and F. Wang, "Upgrading pyrolytic residue from waste tyres to commercial carbon black," Waste Management & Research, Vol. 36(5), pp. 436–444, 2018. [CrossRef]

[2] E. R. Umeki, C. F. Oliveira, R. B. Torres, and R. G. Santos, "Physico-chemistry properties of fuel blends composed of diesel and tyre pyrolysis oil," Fuel, Vol. 185, pp. 236–242, 2016. [CrossRef]

[3] M. R. Islam, M.U.H. Joardder, S.M. Hasan, K. Takai, and H. Haniu, "Feasibility study for thermal treatment of solid tire wastes in Bangladesh by using pyrolysis technology," Waste Management, Vol. 31(9-10), pp. 2142–2149, 2011. [CrossRef]

[4] S. B. Liang, and Y. C. Hao, "A novel cryogenic grinding system for recycling scrap tyre peels," Advanced Powder Technology, Vol. 11, pp. 187–197, 2000. [CrossRef]

[5] N. Sunthonpagasit, and M. R. Duffey, "Scrap tyres to crumb rubber: Feasibility analysis for processing facilities," Resources, Conservation and Recycling, Vol. 40, pp. 281–299, 2004. [CrossRef]

[6] U. S. Vural, S. Uysal, and A. Yinanc, "The improved diesel-like fuel from upgraded tire pyrolytic oil," Journal of the Serbian Chemical Society, Vol 87(10), pp. 1219–1235, 2022. [CrossRef]

[7] P. T. Williams, and R. P. Bottrill, "Sulfur-polycyclic aromatic-hydrocarbons in tyre pyrolysis oil," Fuel, Vol. 74, pp. 736–742, 1995. [CrossRef]

[8] A. Quek, "Balasubramanian, R., Low-energy and chemical-free activation of pyrolytic tyre char and its adsorption characteristics," Journal of the Air and Waste Management Association, Vol. 59, pp. 747–756, 2009. [CrossRef]

[9] I. Hita, M. Arabiourrutia, M. Olazar, J. Bilbao, J. M. Arandes, and P. Castano, "Opportunities and barriers for producing high quality fuels from the pyrolysis of scrap tyres," Renewable and Sustainable Energy Reviews, Vol. 56, pp. 745–759, 2016. [CrossRef]

[10] EMR, "Global Carbon Black Market Size, Share, Price, Trends, Report and Forecast 2020-2025," Expert Market Research, EMR Press, UK, Available: http://www.expertmarketresearch.com Accessed on Jun 22, 2021).

[11] J. Yu, J. Xu, Z. Li, W. He, J. Huang, J. Xu, and G. Li. "Upgrading pyrolytic carbon-blacks (CBp) from end-of-life tires: Characteristics and modification methodologies," Frontiers of Environmental Science & Engineering, Vol. 14(2), Article 19, 2020. [CrossRef]

[12] A. Chaala, H. Darmstadt, and C. Roy, "Acid-base method for the demineralization of pyrolytic carbon black", Fuel Processing Technology, Vol. 46, pp. 1–15, 1996. [CrossRef]

[13] S. Kumar, S. Kumar, and T. Mohapatra, "Interaction between macro- and micro-nutrients in plants," Frontiers in Plant Science, Vol.12, Article 665583, 2021. [CrossRef]

[14] M. Rao. "Essential Plant Nutrients and their Functions," CIAT Working Document No: 209. Colombia. 36, 2009.

[15] F. Ozkutlu, B. Torun, and I. Cakmak, "Effect of Zinc humate on growth of soybean and wheat in Zinc-deficient calcareous soil," Communications in Soil Science and Plant Analysis, Vol. 37(15-20), pp. 2769–2778, 2006. [CrossRef]

[16] J. J. Mortvedt, and R. J. Gilkes, Zinc Fertilizers: In. A. D. Robson (Eds.), "Zinc in Soils and Plants, Developments in Plant and Soil Sciences," Dordrecht: Springer; Vol 55, pp. 33–34, 1993. [CrossRef]

[17] W. Balasooriya, B. Schrittesser, G. Pinter, T. Schwarz, and L. Conzatti, "The effect of the surface area of carbon black grades on HNBR in harsh environments, Polymers," Vol 11(61), pp.1–20, 2019. [CrossRef]

[18] M. Wang, L. Zhang, A. Li, M. Irfan, Y. Du, and W. Di, "Comparative pyrolysis behaviors of tire tread and side wall from waste tire and characterization of the resulting chars," Journal of Environmental Management, Vol. 232, pp. 364–371, 2019. [CrossRef]

[19] N. Cardona, F. Campuzano, M. Betancur, L. Jaramillo, and J. D. Martínez, "Possibilities of carbon black recovery from waste tyre pyrolysis to be used as additive in rubber goods -a review-." IOP Conference Series: Materials Science and Engineering Vol. 437, Article 012012, 2018. [CrossRef]

[20] Toyota Car Corp. "Rubber composition for tire sidewall," Patent No: JP2009114254A, 2009-05-28.

[21] Sumitomo Rubber Industries Ltd. "Rubber composition for a base tread, and tire," Patent No: JP5466415B2, 2014-04-09.

[22] L. Moulin, S. Silva, A. Bounaceur, M. Herblot, and Y. Soudais. "Assessment of recovered carbon black obtained by waste tires steam water thermolysis: An industrial application," Waste and Biomass Valorization, Vol. 8(8), pp. 2757–2770, 2017. [CrossRef]

[23] E. Yazdani, S. H. Hashemabadi, and A. Taghizadeh, "Study of waste tire pyrolysis in a rotary kiln reactor in a wide range of pyrolysis temperature," Waste Management, Vol. 85, pp. 195–201, 2019. [CrossRef]

[24] R. Mis-Fernandez, J. A. Azamar-Barrios, and C. R. Rios-Soberanis, "Characterization of the powder obtained from wasted tires reduced by pyrolysis and thermal shock process," Journal of Applied Research and Technology, Vol. 6(2), pp. 95–105, 2008. [CrossRef]

[25] H. Fang, Z. Hou, L. Shan, X. Cai, and Z. Xin., "Influence of pyrolytic carbon black derived from waste tires at varied temperatures within an industrial continuous rotating moving bed system," Polymers, Vol. 15, Article 3460, 2023. [CrossRef]

[26] W. Li, "Coal desulfurization with sodium hypochlorite," Graduate Theses, Dissertations, and Problem Reports. West Virginia University, Article 1498, 2004.

[27] M. Van Leeuwen, "Recent developments in the global zinc and HDG markets," ACSZ 25th Hot Dip Galvanizing Conference, České Budějovice, October 2–4, 2019.

*Environ Res Tec, Vol. 7, Issue. 3, pp. 356–377, September 2024*

**Environmental Research and Technology**
https://ert.yildiz.edu.tr - https://dergipark.org.tr/tr/pub/ert
DOI: https://10.35208/ert.1434390

Environmental Research & Technology

**Research Article**

# Bibliometric analysis of Indian research trends in air quality forecasting research using machine learning from 2007–2023 using Scopus database

**Asif ANSARI*, Abdur Rahman QUAFF**

*Department of Civil Engineering, National Institute of Technology, Patna, India*

## ARTICLE INFO

*Article history*
Received: 09 February 2024
Revised: 10 March 2024
Accepted: 20 April 2024

**Key words:**
Air quality; Air pollution; Bibliometric analysis; Prediction; Machine learning; Vosviewer; R-package

## ABSTRACT

Machine-learning air pollution prediction studies are widespread worldwide. This study examines the use of machine learning to predict air pollution, its current state, and its expected growth in India. Scopus was used to search 326 documents by 984 academics published in 231 journals between 2007 and 2023. Biblioshiny and Vosviewer were used to discover and visualise prominent authors, journals, research papers, and trends on these issues. In 2018, interest in this topic began to grow at a rate of 32.1 percent every year. Atmospheric Environment (263 citations), Procedia Computer Science (251), Atmospheric Pollution Research (233) and Air Quality, Atmosphere, and Health (93 citations) are the top four sources, according to the Total Citation Index. These journals are among those leading studies on using machine learning to forecast air pollution. Jadavpur University (12 articles) and IIT Delhi (10 articles) are the most esteemed institutions. Singh Kp's 2013 "Atmospheric Environment" article tops the list with 134 citations. The Ministry of Electronics and Information Technology and the Department of Science and Technology are top Indian funding agency receive five units apiece, demonstrating their commitment to technology. The authors' keyword co-occurrence network mappings suggest that machine learning (127 occurrences), air pollution (78 occurrences), and air quality index (41) are the most frequent keywords. This study predicts air pollution using machine learning. These terms largely mirror our Scopus database searches for "machine learning," "air pollution," and "air quality," showing that these are among the most often discussed issues in machine learning research on air pollution prediction. This study helps academics, professionals, and global policymakers understand "air pollution prediction using machine learning" research and recommend key areas for further research.

**Cite this article as:** Ansari A, Quaff AR. Bibliometric analysis of Indian research trends in air quality forecasting research using machine learning from 2007–2023 using Scopus database. Environ Res Tec 2024;7(3)356–377.

## INTRODUCTION

Annually, the deleterious effects of air pollution on the environment, human health, and the global economy render it a pervasive hazard with far-reaching implications for all individuals. According to the World Health Organisation, the annual number of preventable deaths caused by indoor and outdoor pollution exceeds seven million [1]. This phenomenon can be attributed to the elevated mortality rates associated with various health conditions, such as stroke [2], coronary heart disease [3], chronic obstructive pulmonary disease [4], lung cancer [5], and acute respiratory infections [6, 7]. Furthermore, it is worth noting that in the year 2019, a significant majority of the global population, specifically 99%, resided in geographical areas that failed to meet the air quality standards set out by the World Health Organisation

***Corresponding author.**
*E-mail address: asifa.ph21.ce@nitp.ac.in

(WHO). Furthermore, as stated by the World Health Organisation (WHO), the deleterious impacts of air pollution on the environment in Southeast Asia account for a staggering 91% of avoidable fatalities in nations with lower and moderate income levels. In a study conducted in 2013, led by the International Agency for Research on Cancer of the World Health Organisation, it was found that particulate matter components have been classified as carcinogenic to humans [8]. These components are believed to be the primary contributors to the increasing prevalence of cancer, particularly lung cancer [9]. There is a need to enhance public knowledge regarding the development and dissemination of pollution maps that provide timely alerts for hazardous air pollutants.

In recent times, numerous noteworthy occurrences of natural and anthropogenic pollution have had severe detrimental effects on both human well-being and the ecological system [10–14]. The prevalent natural air pollutants include ozone ($O_3$), sulphur dioxide ($SO_2$), carbon monoxide (CO), particle matter (PM), and nitrogen dioxide ($NO_2$). The primary sources of air pollution resulting from human activities encompass electricity generation, emissions from stationary vehicles, industrial emissions, agricultural emissions, emissions from home heating systems, including aquatic surfaces, cooking activities, and so forth. Multiple studies [9, 15, 16] have indicated that air pollution in any given place is influenced by both regional and international sources, as well as adjacent local sources. The levels of air pollution vary significantly across different locations as a result of variances in factors such as the quantity, composition, fuel type, emission control technology, and concentration of several sources. The temporal patterns of air pollutant concentrations exhibit considerable fluctuation due to weather restrictions that vary on a daily, weekly, and yearly basis, as well as the presence of several sources. Various machine learning techniques have been employed in the domain of air pollution to forecast air pollution levels [17, 18], determine the sources of pollution [19, 20], and monitor air pollution [21–23], among other diverse applications.

Scholars employ a range of qualitative and quantitative methodologies in their literature reviews to evaluate and structure their texts and discoveries. Bibliometrics is a commonly employed method for assessing the existing state of knowledge on a certain subject [24–26]. This discipline offers a methodical, replicable, statistically rigorous, and transparent approach to conducting reviews. This approach involves utilising specific elements such as titles, abstracts, author names, journal names, keywords, affiliations, references, and other relevant information sourced directly from academic databases, including but not limited to Scopus and WoS. Consequently, the analysis derives the issues that have been examined, identifies the most prominent institutions and scholars, along with enduring patterns, detects shifts in the disciplinary parameters through time, and provides a comprehensive outlook on the topic. A significant increase in bibliometric research has been observed across various academic areas, such as tourism [27], health and infection [28] and educational administration [29, 30]. In order to gain clarity and establish a clear direction for addressing the global problem of air pollution, it is necessary to do a bibliometric study, as suggested by author [31]. Numerous bibliometric studies have been conducted in the past, exploring various aspects of air pollution. In the study conducted by author [32], an analysis was performed on a comprehensive dataset of global scientific papers pertaining to pollution research spanning the years 2000 to 2016. The analysis encompassed both quantitative and qualitative aspects, allowing for a comprehensive understanding of the research landscape in this field. In their study, Kumar [33] performed an analysis encompassing all the studies on air pollution published in the Web of Science (WoS) database over the period from 2005 to 2014. In their study, M. Kumar [34] undertake a thorough examination of the existing body of research pertaining to the health consequences associated with the exposure of young individuals to air pollution. Yang [35] conducted a comprehensive analysis of the existing literature pertaining to the factors contributing to air pollution throughout the period from 2006 to 2015. The authors conducted a bibliometric analysis of scholarly works pertaining to respiratory health issues associated with outdoor air pollution [36]. Furthermore, a comprehensive analysis was conducted on several scholarly articles pertaining to the utilisation of machine learning techniques in the context of air pollution-related applications. Dogra [37] have undertaken a bibliometric examination of statistical forecasting and prediction methodologies pertaining to air pollution. The researchers employed the Markov chain and evolving trees methodologies to project forthcoming advancements in the study of significant air contaminants. Rybarczyk [38] conducted a comprehensive literature review on the utilisation of machine learning in the context of air pollution. The study revealed that researchers tend to favour regression techniques for estimation purposes, while prediction applications commonly employ neural network algorithms and support vector machines. This finding underscores the prevalent preferences within the research community regarding the selection of machine learning methods for addressing air pollution challenges. In their study, Guo [39] conducted a comprehensive search of the Web of Science database to identify all relevant scholarly articles. Subsequently, they employed CiteSpace 5.8.R1, a widely used software tool, to analyse various aspects such as countries, organisations, authors, keywords, and references. The primary objective of this analysis was to identify prominent areas of research and emerging trends pertaining to the application of artificial intelligence in the domain of air pollution. The purpose of this endeavour was to identify areas of concentrated activity and emerging trends in the field of artificial intelligence. The topic of predicting air pollution has been extensively investigated [40]. Statistical forecasting, numerical forecasting methodologies, and artificial intelligence were employed to classify the forecasting models. Most studies that employ time-series and machine learning techniques to predict air quality commonly utilise multilayer neural networks. However, it is worth noting that these networks were originally designed for tasks other

than time-series modelling [41, 42]. The utilisation of machine learning and time series analysis in the prediction of air quality has been investigated by researchers. There have been proposed methodologies utilising data-driven techniques for the purpose of predicting air pollution levels. Zong [43] propose a methodology that integrates meteorological features and air quality data to develop a predictive model for air quality with a lead time of two days. In 2019, Cabaneros [44] conducted a comprehensive assessment of 139 research articles pertaining to the prediction and estimation of ambient air pollution levels. P. Guo [45] conducted a comprehensive analysis of the research landscape pertaining to construction dust, including its distribution, emerging fields of investigation, and potential avenues for future study, utilising the CiteSpace programme. The primary objective of this study was to examine scholarly articles published in the Web of Science (WoS) database from 2010 onwards, with a specific emphasis on those that addressed the subject of "construction dust." The study presents an analysis of many properties of these publications, including their quantity trend, quality, author cluster, related institution, and journal category. Additionally, the analysis includes article co-citation and keyword co-occurrence. A bibliometric analysis was conducted using CiteSpace 5.7.R3 to examine literature related to ozone pollution in the Web of Science (WoS) database [46]. The authors have reached the conclusion that significant emphasis has been placed on elucidating the mechanism of ozone formation and source allocation, characterising ozone pollution, modelling ozone dispersion at various scales, and assessing the risks posed to humans and plants due to short- and long-term exposure. However, it is necessary to conduct a comprehensive quantitative analysis of various academic articles that cover all potential domains where machine learning methods might be employed for addressing air pollution. This study conducts a bibliometric analysis of the existing research on "Air Pollution Prediction Using Machine Learning" with the aim of providing valuable recommendations for future studies and practical applications.

To the best of the author's knowledge, a limited number of scholars have utilised the WoS database for conducting bibliometric evaluations pertaining to the domains of air pollution and machine learning for global research. Several studies have been conducted on air pollution prediction using machine learning approaches [47–49]. Nevertheless, it is important to acknowledge that the Scopus database has not been employed in any bibliometric assessments pertaining to this subject matter. Additionally, there is no documented evidence of any researcher utilising bibliometric analysis to study machine learning techniques for the specific objective of air quality prediction from an Indian perspective.

The primary aim of this research is to acquire a full comprehension of the utilisation of machine learning methodologies in the examination of air pollution. The researchers conducted an analysis of the literature available in the Scopus online database, focusing on subject categories, article volumes, and journal kinds. This analysis aimed to obtain a thorough grasp of the current status of progress in the field. The aforementioned documents were exported to the VOSviewer and Biblioshiny applications for the purpose of analysis. Through the establishment of collaborative partnerships among nations, authors, and institutions, we have successfully recognised worldwide research needs and fostered cooperative linkages. This study enables air pollution experts to realise the following different research questions: (i) Has there been an increase or reduction in research on the prediction of air pollution using machine learning? (ii) What is the annual growth rate of scholarly papers on this issue? (iii) What are the essential terms associated with the topic of "air pollution and machine learning" as identified in the existing literature? (iv) How do distinguished scientists collaborate with each other? Which academic journals and universities have the most significant impact? The remaining sections are categorised as follows: The subsequent section provides a comprehensive discussion of both the materials used and the processes employed. The findings of the bibliometric analysis conducted using VOSviewer and biblioshiny are presented and analysed in the third section of this study. The study concludes in Section 4, wherein prospective areas for further research are also highlighted.

## MATERIALS AND METHODS

In recent years, there has been a notable surge in the volume of research undertaken within technical disciplines. As a result of this phenomenon, the effort of staying abreast of the pertinent literature pertaining to a specific field is becoming more challenging. The aforementioned requirement calls for the development of quantitative bibliometric approaches that possess the capability to effectively handle extensive volumes of data, identify the most influential publications, and reveal the fundamental structure of the field [50]. These methodologies should possess the capability to effectively manage and process large volumes of data. We conducted a comprehensive review of the existing literature on the application of machine learning in air pollution forecasting, with a focus on identifying trends and key factors influencing this subject. To accomplish this, we employed the bibliometric approach proposed by Garfield [51]. The aforementioned technique was employed by our research team. Zupic [52] assert that bibliometric methods employ a quantitative approach to classify, evaluate, and monitor published research. The purpose of this endeavour is to implement a systematic, clear, and replicable process for conducting reviews, with the ultimate goal of enhancing the overall quality of the reviews. Scholars sometimes find it beneficial to derive their conclusions from a corpus of accumulated bibliographic data provided by fellow academics in the discipline who express their perspectives through written works, citations, and collaborative efforts. Scholars use this methodology to draw conclusions. In contrast to the research conducted on air pollution projections utilising machine learning techniques, bibliometrics has been extensively employed in many disciplines, including administration, biology, nutrition, engineering, and various medical

specialties. As a result of this, a search was done on August 7, 2023, in the Scopus database using a Boolean search strategy to identify pertinent literature published throughout the timeframe of 2007 to 2023. To determine the keywords for the present study, the research team utilised their own pre-existing expertise on the subject matter, as well as previously conducted research, keyword analysis of specific databases, and assessment of relevant studies conducted in other locations. The search queries include [TITLE-ABS-KEY ("air pollution" OR "air quality") AND TITLE-ABS-KEY ("prediction" OR "forecasting") AND TITLE-ABS-KEY ("machine learning" OR "artificial intelligence")] with the longest period permitted by the database to encompass all possible articles. Zupic [52] conducted a process of selecting and importing relevant texts from a database using biblioshiny, a web interface designed for the bibliometrix programme. In order to assess subtle distinctions, an examination was conducted on the most reliable Indian scholarly publications within the English-language domains of Article, Review, Conference Paper, Conference Review, and Book Chapter. The results were organised based on the number of citations, resulting in a total of 326 instances. Figure 1 shows a flow chart diagram for the collection of literature (identification, screening, and eligibility).

VOSviewer has also performed document analysis to enhance the comprehensibility of network diagrams and overlay diagrams. The methodology incorporates performance assessment and science mapping as key components [53–56]. As a component of performance analysis, scholarly publications are scrutinised with respect to the authors, countries, and institutions involved. In contrast, science mapping uses bibliometric approaches to identify and analyse patterns within the realm of scientific study. The review articles by Abafe [31] and Velasco-Muñoz [50] contribute quantitative rigour to the assessment of subjective literature judgements and provide empirical evidence for theoretically defined categories. The following indicators were specifically examined: (i) A comprehensive summary encompassing pertinent information such as important details, annual scientific output, and the annual average of citations (ii) Various sources, including those commonly referenced within a certain locality, the most relevant sources, and the impact of sources The focus of this inquiry is on the primary relationships and their evolutionary progression. (iiib) The analysis also focuses on authors, including their relevance to the topic, the frequency of citations received locally, the impact they have had on the field, and their productivity over a period of time. In this section, we will discuss the study of author keyword cooccurrence, the identification of the most commonly used terms, and the examination of trending issues. The corpus comprises various texts, including those that have garnered the highest number of citations on national scales.

In this study, S-curve analysis was utilized to show how the work changed over time. Several modeling approaches have been used to forecast the future of invention. However, researchers have used the S-curve to predict technological

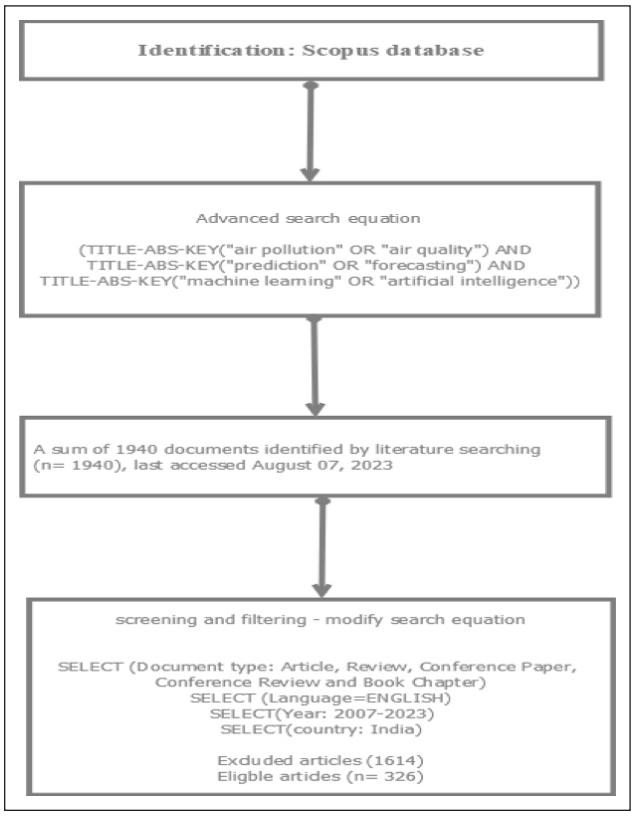


**Figure 1**. Flow chart diagram for the collection of literature (identification, screening, and eligibility).

advancements [15, 57], and inventions and technologies typically follow it. The four stages of a technical structure's transformation can be simulated using an S-curve simulation: emergence, growth, maturity, and saturation or decline [58]. Using S-curve analysis, we could conduct a quantitative study on the prediction of air quality in the future using a variety of machine learning models. We employed the logistic model, where k and an act as the determinants of the shape of the curve, and x denotes the time bucket. An analysis of variance (ANOVA) and an independent t-test were conducted in order to look into the study's potential implications further.

## RESULTS AND DISCUSSIONS

### Descriptive Analysis

The dataset, which spans the years 2007 to 2023 and is derived from 231 sources, including books and journals, is shown in Table 1 and has a total of 326 documents. The figures show a strong yearly growth rate of 32.1% over this time period. The dataset's documents are 1.74 years old on average and have 6.911 citations on average per document. The total number of references cited in all papers is 9053. The dataset includes a wide range of information in terms of content. To classify and describe the papers, 1746 keywords and 808 author-specific keywords were included. Only six of the 984 authors in the sample contributed to documents with a single author. The data also shows a trend towards author collaboration, with 3.6 co-authors on average per

**Table 1.** Main information about data

| Description | Results |
|---|---|
| Timespan | 2007:2003 |
| Sources (Journals, Books, etc) | 231 |
| Documents | 326 |
| Annual growth rate % | 32.1 |
| Document avarage age | 1.74 |
| Average citations per doc | 6.911 |
| References | 9053 |
| Keywords plus | 1746 |
| Author's keywords | 808 |
| Authors | 984 |
| Authors of single-authored docs | 6 |
| Single-authors per doc (collabration) | 6 |
| Co-authors per doc (collabration) | 3.6 |
| International co-authorships % | 14.42 |
| Article | 133 |
| Book chapter | 22 |
| Conference paper | 161 |
| Review | 10 |

document. The percentage of international co-authorships in collaborations is about 14.42%. The dataset has 133 articles (41%), 22 book chapters (7%), 161 conference papers (49%), and 10 reviews (3%), among other document types. The various document types employed in the study are shown in Figure 2a. The dataset's multidisciplinary nature and its ability to contribute to numerous fields of study are reflected in the wide variety of document formats. Overall, the dataset offers a thorough selection of academic papers that span a wide range of topics and exhibit notable development and collaboration within the academic community.

Figure 2b displays the annual number of papers published along with the publication patterns from 2007 to 2023. An intriguing pattern of intellectual activity can be seen in the distribution of articles over several years. There were few or no publications published in the years from 2007 to 2012, indicating a comparative lull in activity. However, in later years, this pattern changed. A single essay published in 2013 served as the catalyst for a revitalised scholarly production. Three articles in 2015 helped the momentum pick up, and two pieces each in 2016 and 2017 helped it continue to gain ground. The genuine uptick started in 2018 with six articles, then increased significantly in 2019 with 27 articles. With 49 articles, the year 2020 saw a notable increase in scholarly contributions; this trend continued into the next year, 2021, with 58 articles. The maximum number of articles—91—was recorded in 2022, marking the peak of this expansion. While 2023 saw a small decline with 86 publications, the overall trend highlights a tremendous uptick in research activity, indicating a vibrant and alive environment for academic inquiry and information sharing.

**S-Curve Analysis of Publications**

Figure 2c shows S-curve plot of cumulative publication over time. Using a logistic growth model, the investigation sought to simulate the growth of total articles from 2007 to 2023. The parameters of this model, which give information about publication trends, stand for the carrying capacity (K), the growth rate (a), and the inflection point (t0). Estimates of these parameters were obtained by fitting the logistic function to the data. The carrying capacity (K) was roughly estimated at 468.21, reflecting the highest publishing level at which the model converges. It was calculated that the growth rate (a), which represents the speed at which publications approach the carrying capacity, is approximately 0.7790. The transition year into a phase of more rapid growth, designated as the inflection point (t0), was determined to be about 2021.94. The coefficient of determination (R2) was calculated to assess the model's performance, yielding a value of about 0.9992. This R2 score implies that the logistic growth model fits the observed data with extraordinary strength. The logistic growth model's high R2 value suggests that it accurately represents the trends in cumulative publications throughout the selected years. The analyses' deep understanding of how publications grow over time makes it easier to understand the patterns and trends in academic work over the time period that was looked at.

**Most Influential Journals**

Table 2 provides a list of variables related to several air pollution journals and the metrics they are associated with. There is information on the starting year (PY_start), total number of citations (TC), number of articles (NP), g-index, h-index, and m-index. The top 10 most pertinent sources out of 231 sources, as determined by the total number of documents, are an indication of their significant contributions to their respective disciplines. Leading this compilation is "Lecture Notes in Networks and Systems," a noteworthy source with 12 pages, a strong h-index of 3, an excellent g-index of 5, a significant m-index of 0, and a total of 30 citations since it was first published in 2020. Similar to "Lecture Notes in Electrical Engineering," which started its significant journey in 2020, "Lecture Notes in Electrical Engineering" stands out with 7 documents, an h-index of 2, a respectable g-index of 3, and a balanced m-index of 0.5. Since its debut in 2018, "Procedia Computer Science" has maintained its position with six documents, as evidenced by astounding h-index and g-index totals of 6, a notable m-index of 1, and a noteworthy citation total of 251. Furthermore, with 6, 6, and 5 documents each, journals like "Advances in Intelligent Systems and Computing," "Environmental Monitoring and Assessment," and "Communications in Computer and Information Science" continue to be important sources that offer insightful information in their fields. Not to be disregarded, "Atmospheric Pollution Research," "Atmospheric Environment," "Air Quality, Atmosphere, and Health," and "Journal of Cleaner Production," each with 4, 3, 3, and 3 papers, strengthen their places as key sources,

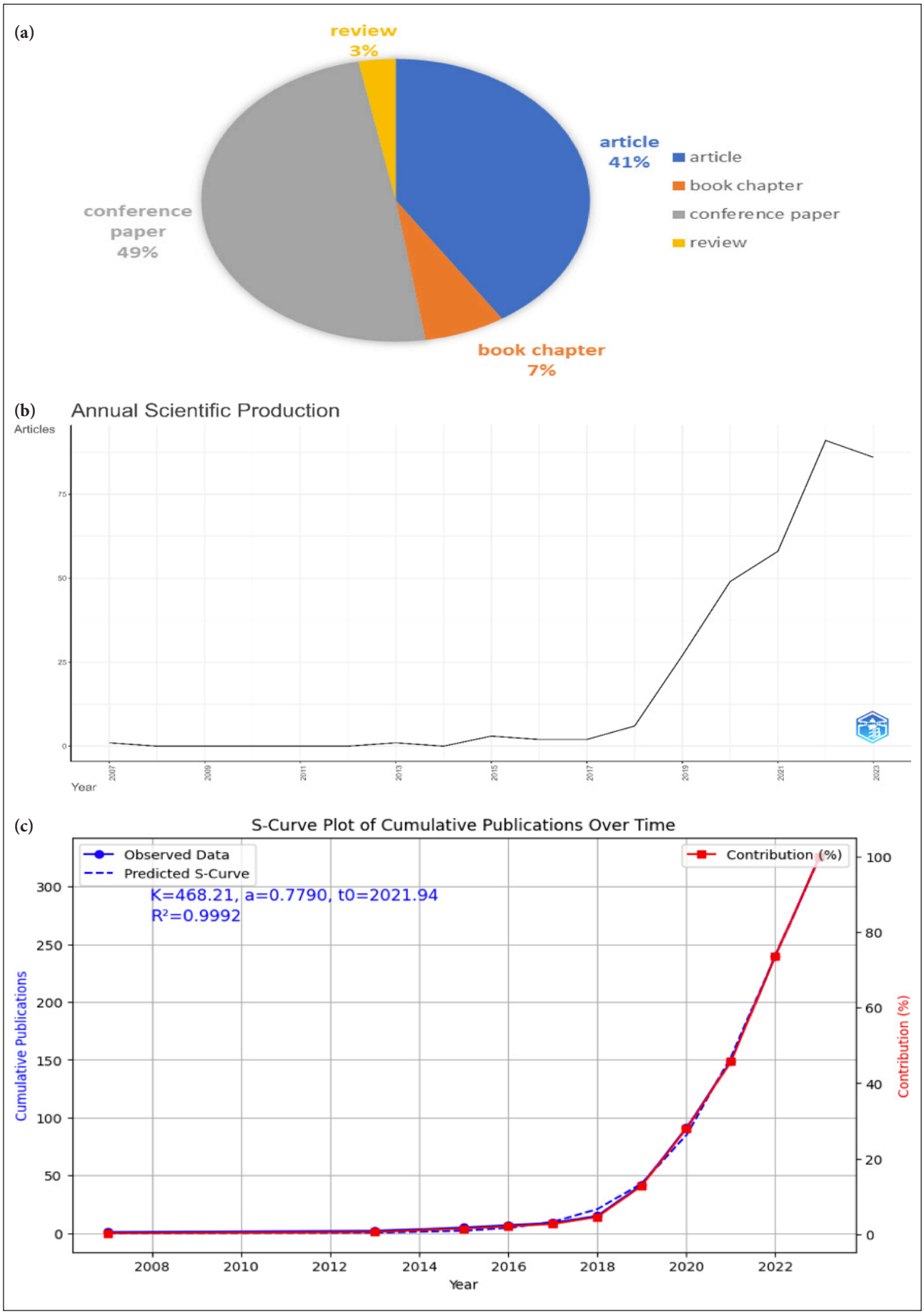


**Figure 2**. **(a)** Document type. **(b)** Annual scientific publication distribution. **(c)** S-curve plot of cumulative publication over time.

**Table 2.** Number of publications (NP), total citations (TC), publication year (PY)

| Most relevant sources | NP | h_index | g_index | m_index | TC | PY_start |
|---|---|---|---|---|---|---|
| Lecture notes in Networks and Systems | 12 | 3 | 5 | 0.75 | 30 | 2020 |
| Lecture notes in Electrical Engineering | 7 | 2 | 3 | 0.5 | 11 | 2020 |
| Procedia Computer Science | 6 | 6 | 6 | 1 | 251 | 2018 |
| Advances in Intelligent Systems and Computing | 6 | 2 | 2 | 0.4 | 7 | 2019 |
| Environmental Monitoring and Assessment | 6 | 2 | 2 | 1 | 7 | 2022 |
| Communications in Computer and Information Science | 5 | 1 | 2 | 0.25 | 6 | 2020 |
| Atmospheric Pollution Research | 4 | 4 | 4 | 0.444 | 233 | 2015 |
| Atmospheric Environment | 3 | 3 | 3 | 0.273 | 263 | 2013 |
| Air Quality, Atmosphere and Health | 3 | 2 | 3 | 0.4 | 93 | 2019 |
| Journal of Cleaner Production | 3 | 3 | 3 | 1 | 62 | 2021 |

**Table 3.** Sources local impact by total citation (TC) index

| Sources local impact by total citation (TC) index | TC | h_index | g_index | m_index | NP | PY_start |
|---|---|---|---|---|---|---|
| Atmospheric Environment | 263 | 3 | 3 | 0.273 | 3 | 2013 |
| Procedia Computer Science | 251 | 6 | 6 | 1 | 6 | 2018 |
| Atmospheric Pollution Research | 233 | 4 | 4 | 0.444 | 4 | 2015 |
| Air Quality, Atmosphere and Health | 93 | 2 | 3 | 0.4 | 3 | 2019 |
| Plos One | 83 | 1 | 1 | 0.143 | 1 | 2017 |
| Journal of Cleaner Production | 62 | 3 | 3 | 1 | 3 | 2021 |
| Sensors and Actuators, B: Chemical | 51 | 1 | 1 | 0.25 | 1 | 2020 |
| Proceedings of the International Conference on Inventive Communication and Computational Technologies, ICICCT 2018 | 48 | 1 | 1 | 0.167 | 1 | 2018 |
| Environmental Science and Pollution Research | 46 | 2 | 2 | 0.5 | 2 | 2020 |
| Journal of Ambient Intelligence and Humanized Computing | 46 | 2 | 2 | 1 | 2 | 2022 |

encouraging a comprehensive awareness of relevant topics. The top 10 sources, ranked by the quantity of documents published, are shown in Figure 3a.

Similar to Table 2, Table 3 lists a variety of elements related to several air pollution journals and their related metrics. The starting year (PY_start), overall number of citations (TC), total number of publications (NP), and g-, h-, and m-indices are all given. The summary provides a brief overview of the top 10 sources (out of 231) according to the Total Citation (TC) index, which rates them according to their local influence. "Atmospheric Environment" is in first place with a respectable TC index of 263, closely followed by "Procedia Computer Science" with 251 citations and "Atmospheric Pollution Research" with 233 citations. While "Plos One" and "Journal of Cleaner Production" show significant local impact with 83 and 62 citations, respectively, "Air Quality, Atmosphere, and Health" maintains its dominance with 93 citations. With 51 citations, "Sensors and Actuators, B: Chemical" is next, followed by "Proceedings of the International Conference on Inventive Communication and Computational Technologies, ICICCT 2018," "Environmental Science and Pollution Research," and "Sensors and Actuators, B: Chemical," which each have 48. Last but not least, the regional influence is mirrored by the "Journal of Ambient Intelligence and Humanised Computing," with 46 citations. Together, these sources demonstrate their power within their spheres of expertise and make a substantial impact on the academic scene. According to the Total Citation (TC) index, Figure 3b displays the top 10 sources that have the most influence.

**Anova Analysis**

We used an analysis of variance (ANOVA) to investigate differences in the mean total citations (TC) across various document formats (Table 4). A statistical test called ANOVA identifies significant mean differences between many groups or categories. Our goal was to determine whether there is a discernible difference between publication document categories and the mean TC. The results of our ANOVA show a significant difference in mean TC between various document categories. The calculated F-statistic, which is roughly 3.12, measures how much the TC means vary from type to type of document. If the variability within each group is compared to the F-statistic, the difference between group averages is likely to be more evident. Additionally, the accompanying p-value, which is roughly 0.0264, is crucial in

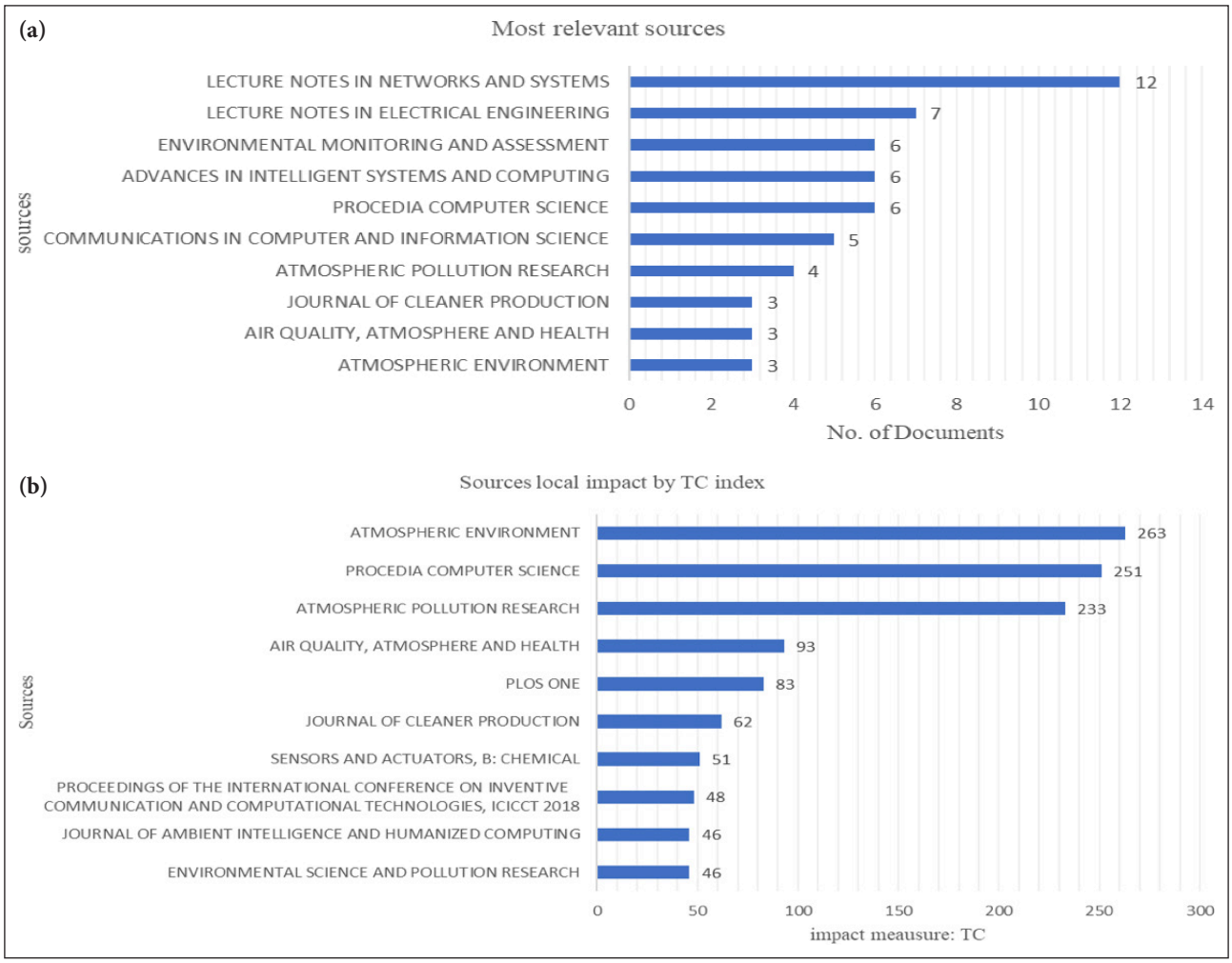


**Figure 3**. **(a)** Most relevant sources. **(b)** Sources local impact by total citations (TC).

**Table 4.** ANOVA analysis

| Source | Sum of squares | Df | Mean square | F | Sig. |
|---|---|---|---|---|---|
| Between groups | 2596.517 | 3 | 865.5056 | 3.115282 | 0.02642 |
| Within groups | 89459.9 | 322 | 277.8258 | | |
| Total | 92056.42 | 325 | | | |

proving statistical importance. It denotes how likely it is that such large mean discrepancies will arise simply by chance. The null hypothesis is strongly refuted when the p-value is appreciably small (usually below the selected significance level, frequently set at 0.05). The extremely small p-value in this case clearly suggests that random chance is extremely unlikely to account for the observed mean discrepancy. As a result, our ANOVA results clearly show that the mean number of citations (TC) for different types of documents is different. This finding has consequences for scholars and decision-makers, highlighting the need to take document type into account when evaluating and interpreting citation data. The necessity for careful examination is highlighted by the possibility that various publication types would exhibit distinctive citation behavior patterns.

**T-Test Analysis**

To determine whether there is a statistically significant difference in securing citations between open access and subscription journals, a t-test was used in this investigation. The alternative hypothesis (H1) proposed that there is a major distinction, whereas the null hypothesis (H0) asserted that there is no significant difference. The t-test produced a t-statistic of around 2.2742 and a corresponding p-value of roughly 0.0236 when using an alpha level (or threshold) of significance (0.05) as the reference point. According to the interpretation of these results, open access and subscription publications secure statistically significantly fewer citations than each other. In particular, the p-value of 0.0236 is less than the chosen level of significance. This means that it is not likely that the changes seen in the number of citations between these types of journals are just random. As a result,

we have enough statistical data to reject the null hypothesis and confirm that the availability of a journal (open access or subscription) has a significant impact on the number of citations it receives. It is important to recognize that even though statistical significance has been demonstrated, there may still be practical disparities in situations that occur in real life. We are unable to firmly declare these practical distinctions, however, in light of the conducted study and data. In conclusion, the t-test results strongly imply that there is a statistically significant difference in citation rates between open access and subscription journals.

We also performed a t-test in this analysis to assess whether there is a statistically significant difference in the number of citations received for various document types, including articles, conference papers, conference reviews, reviews, and book chapters. In contrast to the null hypothesis (H0), which claimed there is no significant variation in the number of citations received among different document categories, the alternative hypothesis (H1) stated that there is a substantial difference in citation counts. After applying the t-test to all pairwise comparisons of document categories, we found that the p-values for each pairwise comparison were all greater than the conventional significance level of 0.05. Because we were unable to reject the null hypothesis for any of the comparisons, it is clear that there is no statistically significant difference in the number of citations obtained between any of the document categories included in this research. Conclusion: Based on our data, the number of citations a publication receives is not significantly influenced by the form of document it picks, be it an article, conference paper, review, book chapter, or another kind. The number of citations for academic work appears to be unaffected by the kind of article writers and researchers choose, giving them peace of mind.

**Authors**

According to Indian Perspective, a total of 984 authors contributed 326 publications to the study on machine learning-based air quality prediction. A graph of author productivity using Lotka's law is shown in Figure 4a, which illustrates how authors contribute to the generation of documents. It demonstrates that, in line with Lotka's distribution pattern, the majority of authors (87.7%) have created just one document, while fewer authors have written more. For example, 7.7% of authors produced two documents, and lower percentages (1.5%) created three to seven documents. This pattern demonstrates a concentrated contribution from a small number of authors, which exemplifies Lotka's Law [59].

According to the number of documents, Table 5 identifies the top 10 authors, and Figure 4b also shows an analysis of their output. The summary offers information about various writers' publication histories. With 15 papers, Kumar A emerges as the most prolific author, followed by Singh S with 7. Six articles each have been submitted by Roy S, Sharma S, Dutta M, Gupta S, Kapoor NR, Kumar P, Marques G, and Middya AI. The dataset receives a significant amount of work from these writers that covers a wide range of issues and topics.

Figure 4c shows the total number of citations and the local effect of the author. The synopsis is a list of local citations for different authors. With 12 local citations apiece, Middya AI, Nath P, and Roy S have strong local recognition. Thomas B. and Babu S. come in second and third, with nine local citations each. With seven local citations, Bhosale A, Gokul PR, Matthew A, and Nair AT have had a significant local influence. Four local citations from Dilliswar Reddy P. bring up the rear of the list. Collectively, these authors demonstrate varying degrees of regional sway, which adds to the dataset's varied intellectual contributions.

Figure 4d displays the top 10 most productive authors from 2007 to 2023. The overview provides a thorough look at the production data for the top 10 authors throughout time. The size of the bubbles represents the volume of published materials. A small one stands in for one publication, and a large one for two. The number of citations every year is directly related to the colour intensity. Notably, in 2020 and 2022, writers like Dutta M. received citations with different total citation counts (TC) and TC per year ratios. Similar to this, authors like Kapoor NR received citations in 2022 and 2023, while Gupta S witnessed high citation activity in 2013. Citations for Kumar A increased significantly in 2022 and 2023, indicating an expanding effect. Between 2020 and 2022, Kumar P received citations, and in 2022, Marques G and Middya AI both received a significant number of citations. While Sharma S's work received citations over the years, Roy S's work received citations in 2022 and 2023. The number of citations for Singh S peaked in 2019, and sporadic activity persisted in the following years.

**Distribution of the Most Productive Affiliation**

The most pertinent affiliations and associated article counts of Indian research institutions are shown in Figure 5. Notably, Jadavpur University's computer science and engineering department in Kolkata takes the top spot with 12 articles, indicating its prodigious research output. With 10 articles, the Indian Institute of Technology Delhi's centre for atmospheric sciences has a commanding position and demonstrates extensive research activity. Additionally, Sri Sivasubramaniya Nadar College of Engineering and the department of computer science and engineering at the National Institute of Technology Durgapur, both of which have seven articles each, are highlighted for their important contributions to the subject. The department of computer science and engineering at Koneru Lakshmaiah Education Foundation, the University of Engineering & Management in Kolkata, the department of computer science and engineering at Sathyabama Institute of Science and Technology, the department of information science and engineering at M S Ramaiah Institute of Technology, the applied cognitive science lab at Indian Institute of Technology Mandi, and the department of inf This collection of several institutions highlights their significant contributions to India's comput-

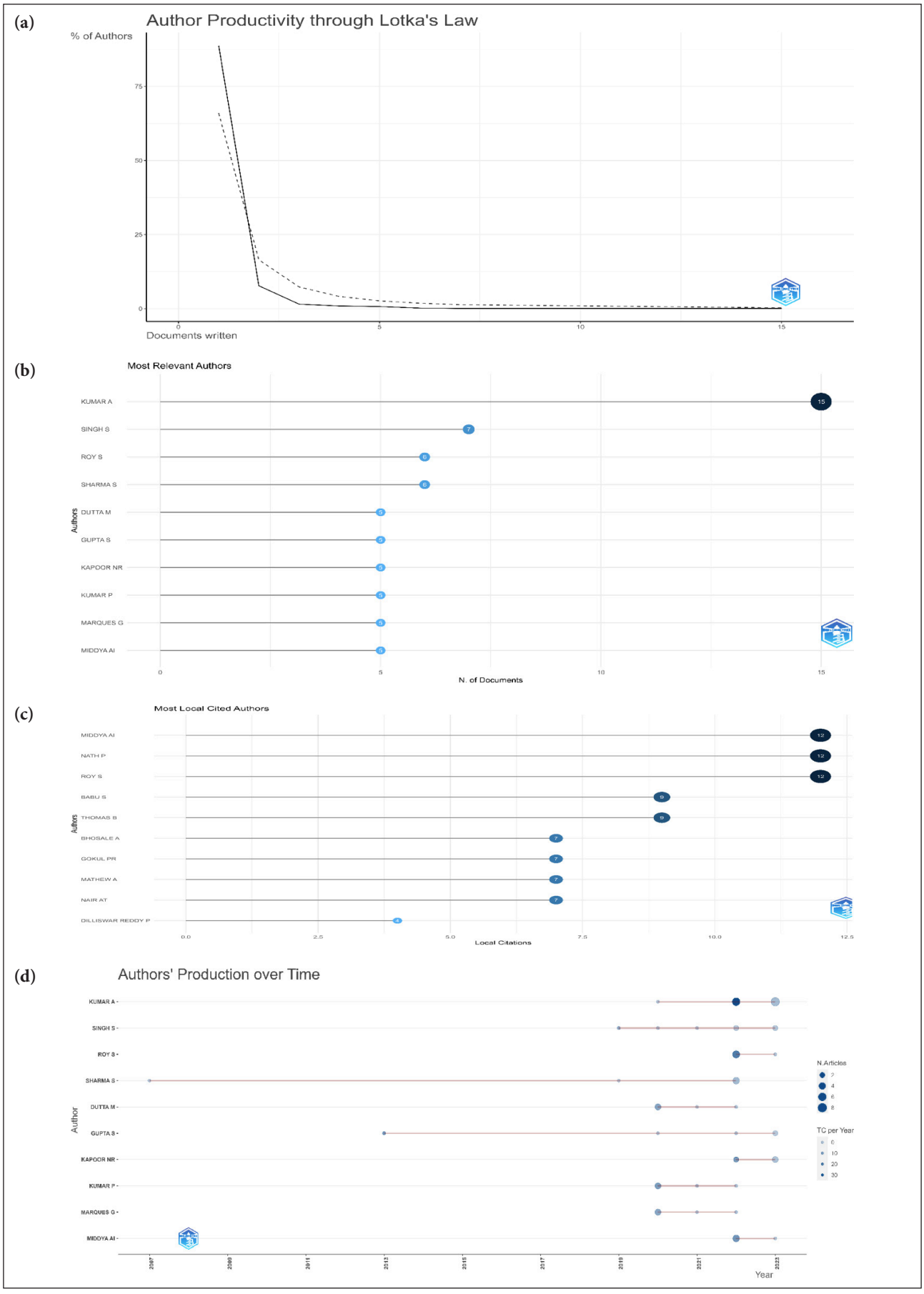


**Figure 4**. **(a)** Author productivity through Lotka's law. **(b)** The top ten most relevant authors. **(c)** Author local impact. **(d)** Top author's production from 2007–2023.

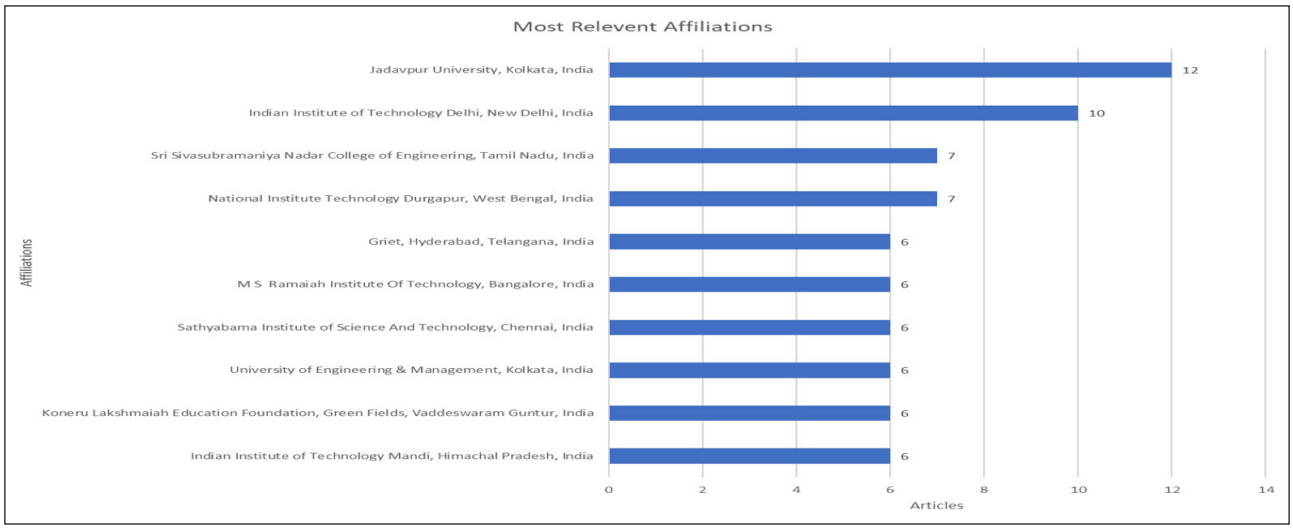


**Figure 5**. Most relevant affiliations.

**Table 5.** The top ten leading authors on machine learning-based air pollution prediction

| Authors | Articles | Articles fractionalized |
|---|---|---|
| Kumar A | 15 | 3.45 |
| Singh S | 7 | 2.17 |
| Roy S | 6 | 2.03 |
| Sharma S | 6 | 1.51 |
| Dutta M | 5 | 1.67 |
| Gupta S | 5 | 1.33 |
| Kapoor NR | 5 | 0.93 |
| Kumar P | 5 | 1.07 |
| Marques G | 5 | 1.67 |
| Middya AI | 5 | 1.53 |

er science and engineering fields.

**Most Global Cited Documents**

Understanding how this research stream has developed requires finding the articles that have contributed to the machine learning-based air quality forecast from an Indian perspective. Similar to this, using machine learning to study the patterns of citations in air pollution prediction may offer important suggestions about the direction of future research. Each of the 326 documents, with an average age of 1.74, that were part of the analysis averaged 6.91 citations. The top 10 documents, as shown in Table 6 and Figure 6a, have had a substantial impact in their respective domains and have received broad notice and recognition for their contributions. The article by Singh Kp from 2013, which was published in "Atmospheric Environment," is at the top of the list with 134 citations. Following closely after with 103 citations is the paper by Mishra D., which was also published in "Atmospheric Environment" in 2015. Krishan M.'s research on "Air Quality, Atmosphere, and Health" received 91 citations in 2019. The study by Doreswamy from 2020, which has an impressive 79 citations, is presented in "Procedia Computer Science," strengthening the list even more. The 2015 publication of Mishra D's study in "Atmospheric Pollution Research" received 63 citations and made a notable impact on the subject. It is clear that Rubal's article in "Procedia Computer Science" in 2018 had a significant impact because it was mentioned 54 times. 51 citations support the importance of Acharyya S's article from "Sensors and Actuators, B: Chemical" from 2020. With Ayele Tw's work obtaining 48 citations, "Proceedings of the International Conference on Inventive Communication and Computational Technologies (ICICCT) 2018" is added to the list. Masood A's work from 2021 was cited 46 times in "Journal of Cleaner Production," whereas Amuthadevi C's paper from 2022 has been quoted 39 times in "Journal of Ambient Intelligence and Humanised Computing." These widely cited papers serve as an example of the influence that research has on the greater scientific community and has had on the development of their respective subjects.

**Most Local Cited Documents**

The top 10 articles that are locally cited most frequently are shown in Table 7 and Figure 6b. There are 11 local citations for "Mahalingam U's" 2019 submission to the International Conference on Wireless Communications, Signal Processing, Networking, and WISPNET. Similar to this, Ayele Tw's article from the 2018 International Conference on Inventive Communication and Computational Technologies (ICICCT) has gotten nine local citations, highlighting its influence in that particular community. Pasupuleti Vr's work from the 2020 International Conference on Advanced Computing and Communication Systems (ICACCS) has also received seven local citations, demonstrating its importance in the neighbourhood. A total of four local citations have been made for "Yarragunta S's" contribution to the 2021 International Conference on Intelligent Computing and Control Systems (ICICCS). Three local citations have been awarded to Sur S's work at the IEEE International Conference on Convergence in Engineering (ICCE), and

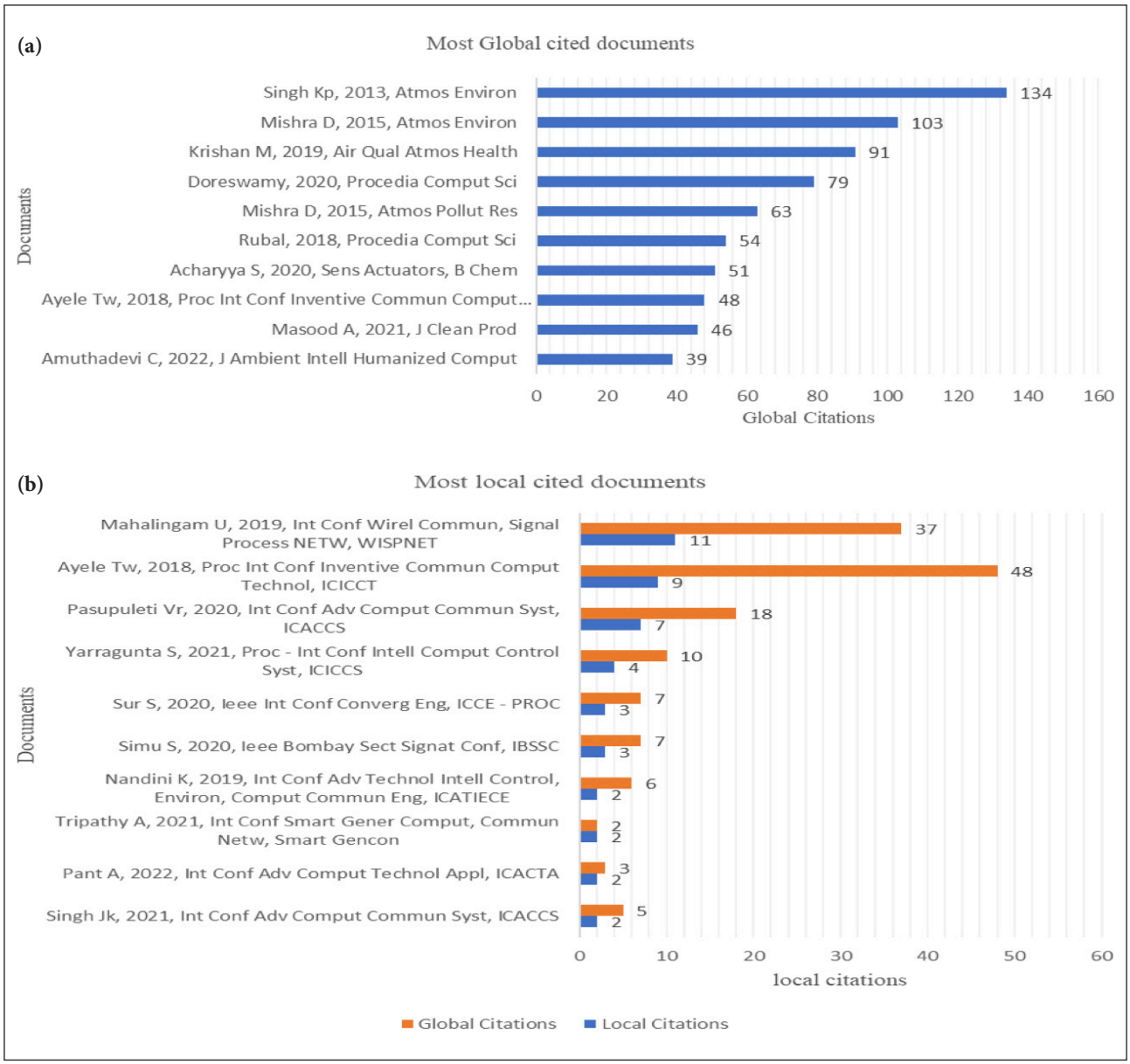


**Figure 6**. **(a)** Documents citation: Top 10 most global cited documents. **(b)** Documents citation: Top 10 Most local cited documents.

**Table 6.** Top 10 most global cited documents

| Paper | DOI | Total citations | TC per year | Normalized TC | Ref |
|---|---|---|---|---|---|
| Singh Kp, 2013, Atmos Environ | 10.1016/j.atmosenv.2013.08.023 | 134 | 12.18 | 1.00 | [60] |
| Mishra D, 2015, Atmos Environ | 10.1016/j.atmosenv.2014.11.050 | 103 | 11.44 | 1.75 | [61] |
| Krishan M, 2019, Air Qual Atmos Health | 10.1007/s11869-019-00696-7 | 91 | 18.20 | 8.87 | [62] |
| Doreswamy, 2020, Procedia Comput Sci | 10.1016/j.procs.2020.04.221 | 79 | 19.75 | 5.77 | [63] |
| Mishra D, 2015, Atmos Pollut Res | 10.5094/APR.2015.012 | 63 | 7.00 | 1.07 | [64] |
| Rubal, 2018, Procedia Comput Sci | 10.1016/j.procs.2018.05.094 | 54 | 9.00 | 1.71 | [65] |
| Acharyya S, 2020, Sens Actuators, B Chem | 10.1016/j.snb.2020.128484 | 51 | 12.75 | 3.72 | [66] |
| Ayele Tw, 2018, Proc Int Conf Inventive Commun Comput Technol, Icicct | 10.1109/ICICCT.2018.8473272 | 48 | 8.00 | 1.52 | [67] |
| Masood A, 2021, J Clean Prod | 10.1016/j.jclepro.2021.129072 | 46 | 15.33 | 8.42 | [68] |
| Amuthadevi C, 2022, J Ambient Intell Humanized Comput | 10.1007/s12652-020-02724-2 | 39 | 19.50 | 15.70 | [69] |

three local citations have been awarded to Simu S's paper that was presented at the IEEE Bombay Section Signature Conference (IBSSC) in 2020. " Two local citations for Singh Jk's work from the International Conference on Advanced Computing and Communication Systems (ICACCS) in 2021 attest to its importance in the neighbourhood. Similar to Pant A, Tripathy A's work at the International Conference on Smart Generation in Computing, Communication, and Networking (Smart Gencon) in 2021 received two local citations, as did Pant A's contribution to the International Conference on Advanced Computing Technology and Applications (ICACTA) in 2022. Last but not least, Nandini K.'s article won two local citations for its presentation at the 2019 International Conference on Advanced Technology, Intelligent Control, Environment, Computing, and Communication Engineering (ICATIECE). These locally referenced works indicate their significance within certain geographical contexts and reflect their influence on the regional academic scene.

The Local Citations to Worldwide Citations Ratio (LC/GC Ratio) is a useful indicator that illustrates how important documents are in relation to one another in local contexts versus on a worldwide scale. This ratio shows how much of a document's influence is felt locally or regionally compared to how much of an impact it has globally. A lower ratio means that the text's influence is more evenly spread across local and international audiences, whereas a greater LC/GC Ratio indicates that the work holds considerably more relevance within its local community than its global recognition. We can see that the LC/GC Ratios for each document differ when we look at the examples that have been given. For instance, "Tripathy A's" paper from the 2021 International Conference on Smart Generation in Computing, Communication, and Networking (Smart Gencon) has a remarkable LC/GC Ratio of 100.00%, indicating that this paper's impact is solely local and all of its citations are from the same local community. However, "Pasupuleti Vr's" work from the International Conference on Advanced Computing and Communication Systems (ICACCS) in 2020 has an LC/GC Ratio of 38.89%, indicating that it keeps a significant local effect while also attracting attention on a global level. The LC/GC Ratio aids in comprehending the document's reach and resonance throughout distinct academic communities and offers a nuanced view on the value of research within particular contexts.

**Analysis and Co-Occurrence Network of Keywords**

The co-occurrence of 808 author keywords was examined in order to use machine learning to highlight the research hotspots in the air pollution forecast area. The top 10 author keywords, along with the number of times each term appeared, are shown in Figure 7a. Notably, the term "machine learning" is mentioned 127 times, indicating its importance. The term "air pollution" appears 78 times, showing that it is frequently brought up. 41 times, the term "air quality index" is mentioned, most likely in connection with tracking and rating air quality. Both "air quality" and "deep learning" occur 32 times, indicating an emphasis on enhancing air quality and utilising cutting-edge machine learning methods. 29 instances of the word "prediction" are present, presumably indicating a focus on predictive modelling. There are 23 references to "LSTM," a type of neural network that may be related to time-series analysis. The terms "forecasting" and "random forest" both appear 22 times, indicating that both methods are probably used in air quality investigations. Finally, the phrase "air quality index (AQI)" is cited 18 times, referring to a particular metric usually brought up while discussing how to assess air quality.

The VOSviewer co-occurrence analysis demonstrates significant partnerships between authors' terms in the fields of air pollution, air quality, machine learning, forecasting, and related topics [54]. 50 of the 808 keywords meet the requirement of having at least five occurrences. These terms serve as hubs for study and information sharing in the field. Figure 7b depicts the author's Keywords as a co-occurrence network, and Figure 7c displays a co-occurrence overlay network. The number of times the highlighted terms appeared in the text was represented by the size of the circles. The larger the circle, the more the author's keyword has been co-selected in the literature on air pollution prediction. The distances between the elements of each pair were used to visually show the similarity and relative intensity of each topic. Different phrase clusters were given different circle colours. 78 instances and a total connection strength of 170 support the research on "air pollution," which is an important issue. This subject includes a number of different elements, including "air pollution forecasting," "monitoring," "prediction," and "particulate matter." The terms "air quality" and its different aspects, such as "air quality index (AQI)," "indoor air quality," and "PM2.5," highlight how crucial it is to comprehend and improve air quality. With a startling 127 occurrences and a total connection strength of 260, machine learning appears to be a crucial technology. It is a crucial tool for tackling the problems caused by air pollution. The use of cutting-edge algorithms in the analysis and forecasting of air quality trends is highlighted by terms like "deep learning," "LSTM," "random forest," "regression," "support vector machine (SVM)," and "XGBoost". Interdisciplinary fields are included in collaborative initiatives as well. The terms "artificial intelligence," "internet of things (IoT)," "smart city," and "COVID-19" show how technology advancement, urban growth, and public health connect. Additionally, techniques like "time series forecasting" and "ensemble learning" show that academics are focused on reliable model performance and precise forecasts. The VOSviewer co-occurrence analysis highlights a dynamic network of author keyword collaborations, highlighting the complicated interplay between air pollution research, machine learning, data analysis methods, and rising trends like IoT. These partnerships promote information transfer and development, which eventually helps people make well-informed decisions and find solutions to urgent environmental problems [79].

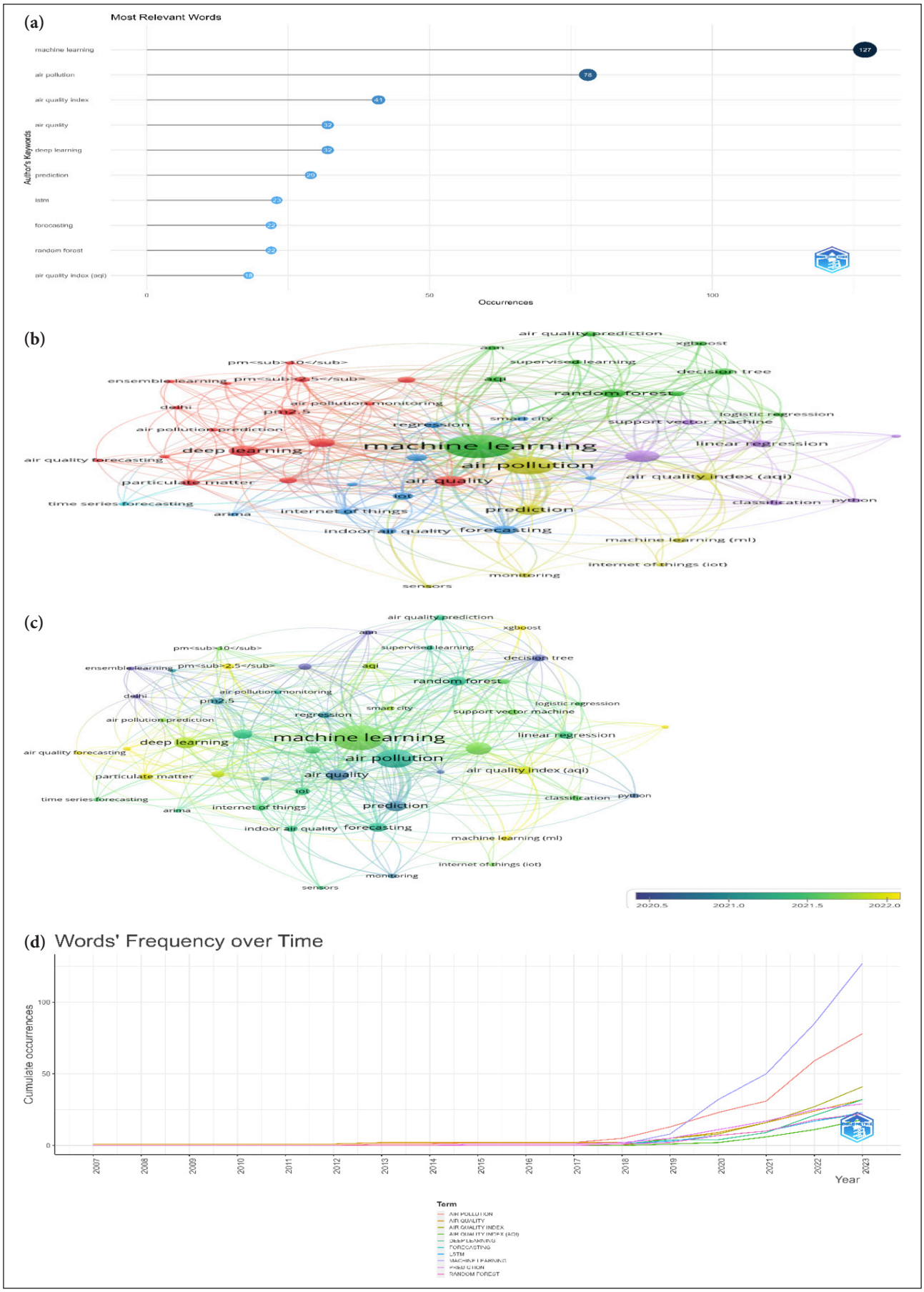


**Figure 7**. **(a)** Co-occurrence network of top 10 most relevant authors keywords. **(b)** Co-occurrence network visualization of author's keywords. **(c)** Co-occurrence overlay network of author keyword. **(d)** Words frequency over time.

**Table 7.** Top 10 most local cited documents

| Document | DOI | Year | Local citations | Global citations | LC/GC ratio (%) | Normalized local citations | Normalized global citations | Ref |
|---|---|---|---|---|---|---|---|---|
| Mahalingam U, 2019, Int Conf Wirel Commun, Signal Process NETW, WISPNET | 10.1109/WiSPNET45539.2019.9032734 | 2019 | 11 | 37 | 29.73 | 17.47 | 3.61 | [70] |
| Ayele Tw, 2018, Proc Int Conf Inventive Commun Comput Technol, ICICCT | 10.1109/ICICCT.2018.8473272 | 2018 | 9 | 48 | 18.75 | 4.91 | 1.52 | [67] |
| Pasupuleti Vr, 2020, Int Conf Adv Comput Commun Syst, ICACCS | 10.1109/ICACCS48705.2020.9074431 | 2020 | 7 | 18 | 38.89 | 18.05 | 1.31 | [71] |
| Yarragunta S, 2021, Proc - Int Conf Intell Comput Control Syst, ICICCS | 10.1109/ICICCS51141.2021.9432078 | 2021 | 4 | 10 | 40.00 | 23.20 | 1.83 | [72] |
| Simu S, 2020, Ieee Bombay Sect Signat Conf, IBSSC | 10.1109/IBSSC51096.2020.9332184 | 2020 | 3 | 7 | 42.86 | 7.74 | 0.51 | [73] |
| Sur S, 2020, Ieee Int Conf Converg Eng, ICCE - PROC | 10.1109/ICCE50343.2020.9290698 | 2020 | 3 | 7 | 42.86 | 7.74 | 0.51 | [74] |
| Singh Jk, 2021, Int Conf Adv Comput Commun Syst, ICACCS | 10.1109/ICACCS51430.2021.9441902 | 2021 | 2 | 5 | 40.00 | 11.60 | 0.91 | [75] |
| Pant A, 2022, Int Conf Adv Comput Technol Appl, ICACTA | 10.1109/ICACTA54488.2022.9753636 | 2022 | 2 | 3 | 66.67 | 60.67 | 1.21 | [76] |
| Tripathy A, 2021, Int Conf Smart Gener Comput, Commun Netw, Smart Gencon | 10.1109/SMARTGENCON51891.2021.9645787 | 2021 | 2 | 2 | 100.00 | 11.60 | 0.37 | [77] |
| Nandini K, 2019, Int Conf Adv Technol Intell Control, Environ, Comput Commun Eng, ICATIECE | 10.1109/ICATIECE45860.2019.9063845 | 2019 | 2 | 6 | 33.33 | 3.18 | 0.58 | [78] |

**Table 8.** Author keywords cumulative frequency over time

| Year | 2007 | 2008 | 2009 | 2010 | 2011 | 2012 | 2013 | 2014 | 2015 | 2016 | 2017 | 2018 | 2019 | 2020 | 2021 | 2022 | 2023 |
|---|---|---|---|---|---|---|---|---|---|---|---|---|---|---|---|---|---|
| Machine learning | 0 | 0 | 0 | 0 | 0 | 0 | 0 | 0 | 0 | 0 | 0 | 1 | 8 | 32 | 50 | 85 | 127 |
| Air pollution | 0 | 0 | 0 | 0 | 0 | 0 | 1 | 1 | 2 | 2 | 2 | 5 | 13 | 23 | 31 | 59 | 78 |
| Air Quality Index | 0 | 0 | 0 | 0 | 0 | 0 | 0 | 0 | 0 | 0 | 0 | 0 | 5 | 8 | 16 | 27 | 41 |
| Air quality | 1 | 1 | 1 | 1 | 1 | 1 | 2 | 2 | 2 | 2 | 2 | 2 | 5 | 9 | 16 | 24 | 32 |
| Deep learning | 0 | 0 | 0 | 0 | 0 | 0 | 0 | 0 | 0 | 0 | 0 | 1 | 4 | 4 | 9 | 21 | 32 |
| Prediction | 0 | 0 | 0 | 0 | 0 | 0 | 0 | 0 | 1 | 1 | 1 | 2 | 5 | 11 | 17 | 25 | 29 |
| LSTM | 0 | 0 | 0 | 0 | 0 | 0 | 0 | 0 | 0 | 0 | 0 | 1 | 3 | 7 | 10 | 17 | 23 |
| Forecasting | 0 | 0 | 0 | 0 | 0 | 0 | 0 | 0 | 0 | 0 | 0 | 1 | 3 | 7 | 10 | 17 | 22 |
| Random forest | 0 | 0 | 0 | 0 | 0 | 0 | 0 | 0 | 0 | 0 | 0 | 1 | 2 | 7 | 10 | 18 | 22 |
| Air Quality Index | 0 | 0 | 0 | 0 | 0 | 0 | 0 | 0 | 0 | 0 | 0 | 0 | 1 | 2 | 6 | 11 | 18 |

**Table 9.** Top 10 most global cited documents

| S. No. | Type of modelling/approach | Location(s) | Air pollutants examined | Study period | Ref. |
|---|---|---|---|---|---|
| 1 | A three-layer neural network model with a hidden recurrent layer | Delhi, India | $SO_2$ | 1997–1998 | [80] |
| 2 | Neural network model with backpropagation | Kolkata, India | $NO_2$ | 1997–2002 | [81] |
| 3 | ANN | New Delhi, India | $NO_2$ | Two-year data | [82] |
| 4 | Neuro-fuzzy models | Delhi City, India | CO | One-hour average CO concentration data have been obtained from CPCB for a period of 2 years, i.e., January 2004 to December 2005 | [83] |
| 5 | Neural networks (NN) and multiple-regression (MR) analysis. | New Delhi, India | $O_3$ | 1999–2004 | [84] |
| 6 | Recurrent neural network model | New Delhi, India | CO; $NO_2$; NO; $O_3$; $SO_2$; $PM_{2.5}$ | January 2009–June 2010 (1.5 years) | [85] |
| 7 | ANN-PCA | Kolkata, India | $O_3$ | 1997–2002 | [86] |
| 8 | Partial least squares regression (PLSR), multivariate polynomial regression (MPR), and artificial neural network (ANN) | Lucknow, India | $PM_{10}$; $SO_2$; $NO_2$ | Fve years (2005–2009) | [87] |
| 9 | ANN–MLP (Multi layer perceptron) Forecasting model | Agra, India | $NO_2$ | Central Pollution Control Board (CPCB) at Sanjay Place, Agra, India sampled the relevant data. The sampling period was 18 November to 27 November 2013 at Sanjay Place, Agra (10 days) | [64] |
| 10 | TSA (Time series analysis), ANN, ANFIS (Adaptive neuro-fuzzy inference system) | Kolkata, India | $NO_2$ | CPCB for the year 2010–2018 | [88] |

**Analysis and Co-Occurrence of Authors Keyword Over Time**

The dynamics of word recurrence through time provide fascinating new perspectives on the changing trends and emphases in the area. The cumulative frequency of the top 10 writers' keywords is shown in Table 8 and Figure 7d. Terms like "Machine Learning" and "Air Pollution" had a minimal presence in earlier years, such as 2007 to 2011, representing a period of relatively restrained interest in these subjects. However, as time goes on, particularly after 2012, there is a noticeable increase in debates about "Air Pollution," reflecting a growing awareness of environmental issues. The term "Air Quality Index" began to acquire popularity in 2013, and up to 2023, its total mentions grew steadily. This increased trend is consistent with the growing initiatives to thoroughly monitor and effectively inform the public about air quality conditions. In a similar vein, the word "Air Quality" first appeared in 2012 and has a steady growth pattern, underscoring the ongoing interest in analysing and resolving problems linked to air quality. Around 2018, "Deep Learning" and "Prediction" started to become noticeable in the conversation, and their combined appearances continued to rise over the following years. This problem reflects the growing use of complex methods like deep learning for predictive modelling. In particular, "LSTM," a specialised deep learning architecture, acquired popularity starting in 2018, indicating an increase in its use across numerous domains, including air quality prediction. In 2018, terms like "Forecasting" and "Random Forest" started gaining attention as well, indicating a growing interest in predictive modelling techniques. It's interesting to note that the cumulative incidence pattern of "Random Forest" closely resembles that of "Machine Learning," highlighting its importance as a prominent strategy within the larger environment. In conclusion, the cumulative dynamics of word occurrences provide a vivid account of the evolving research scene across time. This story highlights how important subjects including machine learning, deep learning, air pollution, and predictive modelling have become the preeminent areas of study and application in the field of air quality research.

**Analysis of Funding Agency**

Organisations that are essential to advancing research and innovation in India are highlighted in the top 10 Indian funding agencies list (Fig. 8). The Ministry of Electronics

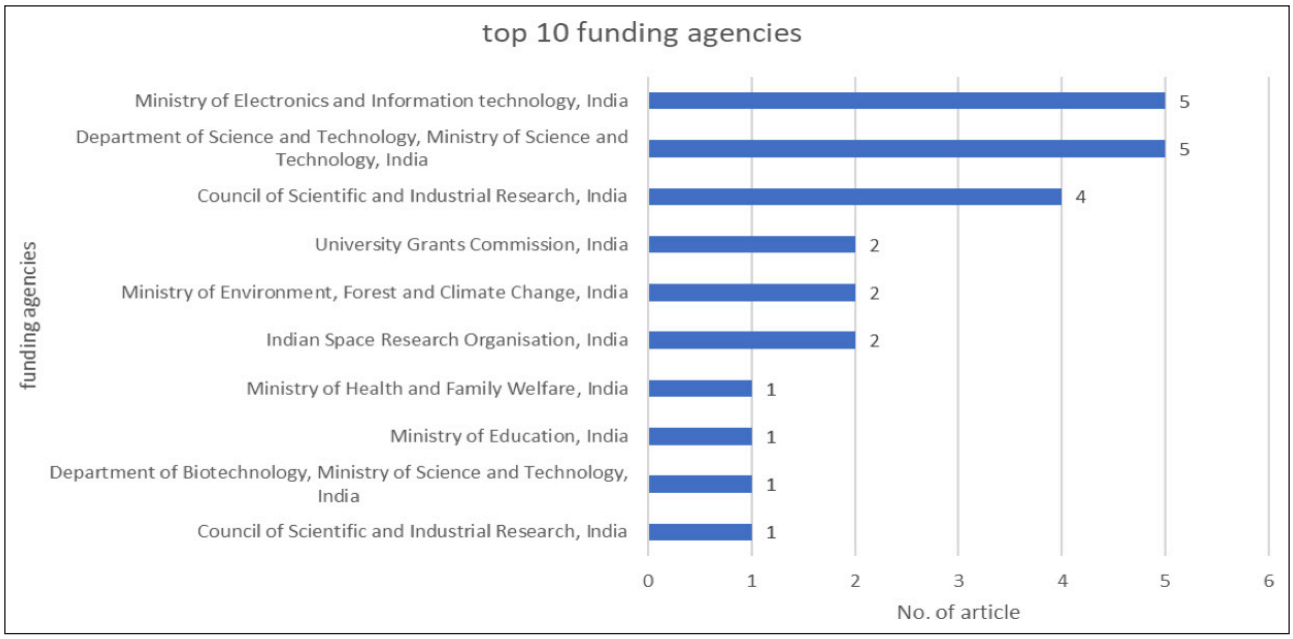


**Figure 8**. Top 10 funding agency.

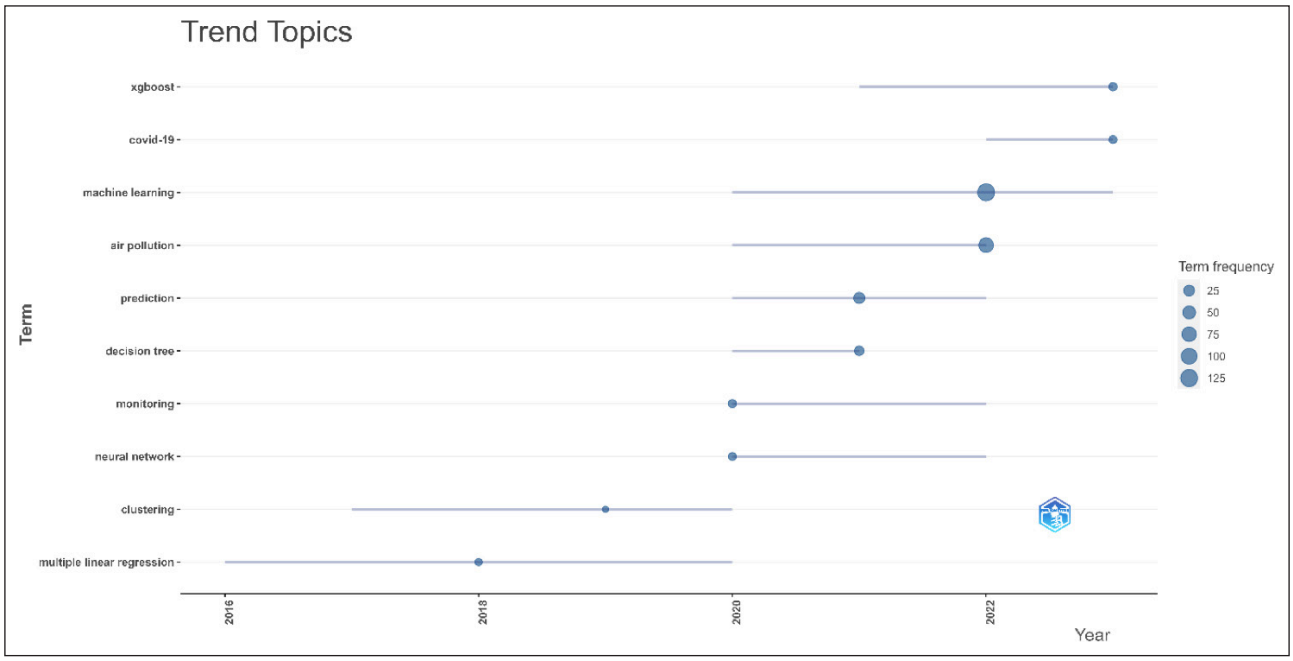


**Figure 9**. Trendy topics from 2016–2022.

and Information Technology and the Department of Science and Technology are at the top of the list, each receiving five units of funding, underscoring their dedication to advancing technology. With four financing organisations, the Council of Scientific and Industrial Research has a major presence and is clearly supporting numerous research projects. Two funding units have been given to the Indian Space Research Organisation, highlighting its contribution to space-related research. The Ministry of Education, the Ministry of Health and Family Welfare, the University Grants Commission, the Department of Biotechnology, and the Ministry of Environment, Forestry, and Climate Change all allocate one unit of funding each to show their commitment to advancing various fields of research in the nation. Together, these funding organisations create an active research ecosystem in India that encourages a variety of scientific inquiry and advancement.

**Analysis of Machine Learning Techniques on Forecasting Air Quality**

The Table 9 gives a brief summary of various air pollution modeling methodologies and techniques that have been adjusted for Indian settings. It covers study locations, air contaminants evaluated, and study times, offering light on key approaches for evaluating and forecasting air quality in the context of India.

**The Future of Research into Machine Learning in the Field of Air Pollution**

Figure 9 displays co-occurrence network mappings organised by topic area or publication date to highlight current hot topics and potential future directions in the study of air pollution. The analysis of trends in a variety of topics offers important insights into how research has changed over time. "Multiple Linear Regression" was one of the issues that received the most attention, with its frequency rising from 2016 to 2020. This indicates that the use of linear regression models for multi-dimensional analysis in air quality studies is expanding. From 2017 to 2020, "clustering" was consistently present, demonstrating a continued interest in combining related air quality data points for further study. The years 2020 to 2022 will see a clear emphasis on cutting-edge methods, particularly "Monitoring" and "Neural networks," demonstrating a heightened desire for precise and immediate data analysis. With a significant frequency of 29, the word "Prediction" appears as the prominent subject. Its prominence increases from 2020 to 2022, underscoring a spike in initiatives to forecast air quality situations using predictive models. Similar to how "Decision Tree" receives a lot of attention between 2020 and 2021, this is a reflection of its function in offering understandable insights into complicated air quality information. A critical turning point occurs in 2020, when "Machine Learning" undergoes a dramatic increase in frequency and dominates the conversation through 2023. This highlights a paradigm shift towards applying machine learning methods to problems related to air quality. In line with this, "Air Pollution" hits its peak in 2020 and continues to air often through 2022, highlighting continuous efforts to understand and reduce pollution levels. From 2021 to 2023, "XGBoost," a well-known boosting algorithm, emerges strongly, indicating its use for improving prediction accuracy. Last but not least, "COVID-19" becomes an important topic starting in 2022, showing the significance of the global context on air quality studies, maybe in response to the effects of the pandemic on environmental conditions.

## CONCLUSION

Researchers can employ bibliometric analysis to consider many criteria, including the productivity of the field, different nations, the most relevant journals, authors, institutions, and so on, when making decisions about what and where to publish. Additionally, it is beneficial to examine the trends and patterns in publications in order to gain insight into the nature and productivity of a certain academic field. This research endeavour pertaining to the prediction of air pollution through the utilisation of machine learning encompasses a corpus of around 326 scholarly articles authored by 984 scholars and disseminated throughout 231 academic journals spanning the temporal domain from 2007 to 2023. Due to the significant significance of this area of research, it is unsurprising that there has been a notable increase in the number of articles published on these subjects since 2018, exhibiting an annual growth rate of 32.1%. The findings indicate that prominent scholarly journals have assumed a prominent role in advancing the field of machine learning-based air pollution prediction. Notably, Atmospheric Environment, with 263 citations; Procedia Computer Science, with 251 citations; Atmospheric Pollution Research, with 233 citations; and Air Quality, Atmosphere, and Health, with 93 citations, have emerged as key contributors in this area of research, as evidenced by their respective Total Citation Index scores. Jadavpur University, with its 12 articles, and IIT Delhi, with its 10 articles, are widely regarded as two of the most prestigious academic institutions in India. Singh Kp's (2013) essay titled "Atmospheric Environment" holds the highest position on the list, having accumulated a total of 134 citations. The Ministry of Electronics and Information Technology, along with the Department of Science and Technology, each earn a total of five units, which serves as a clear indication of their dedication and support towards the advancement of technology. The findings of the authors' analysis indicate that machine learning, air pollution, and air quality index are the most frequently occurring keywords in the keyword co-occurrence network mappings, with 127, 78, and 41 occurrences, respectively. The inclusion of phrases such as "air pollution," "machine learning," and "air quality" in our Scopus database search queries indicates that these topics are frequently examined in scholarly investigations pertaining to machine learning-driven predictions of air pollution. One of the emerging concepts in this field that indicates potential future advancements is the integration of XGBoost, neural networks, and machine learning techniques. However, there remain certain gaps that require completion. The necessity for further comparative studies in the aforementioned nations that are now underrepresented is arguably of utmost significance. Due to the extensive body of literature on the subject of air pollution prediction research and the inherent limitations of relying on a single database to offer a comprehensive overview of a research domain that holds substantial global significance, it is worthwhile to explore alternative avenues for investigation. These may include the integration of the two primary bibliographic databases, namely Web of Science (WoS) and Scopus, or the utilisation of supplementary databases. This paper aims to provide professionals, scholars, and worldwide policymakers with an understanding of the current status of the "air pollution prediction using machine learning" field while also highlighting certain areas that necessitate further investigation. This review offers a comprehensive guide for writers, reviewers, and journal editors to consider while contemplating their future work, its value, and the various challenges that may arise in the publication process.

## DATA AVAILABILITY STATEMENT

The author confirm that the data that supports the findings of this study are available within the article. Raw data that support the finding of this study are available from the corresponding author, upon reasonable request.

## CONFLICT OF INTEREST

The author declared no potential conflicts of interest with respect to the research, authorship, and/or publication of this article.

## USE OF AI FOR WRITING ASSISTANCE

Not declared.

## ETHICS

There are no ethical issues with the publication of this manuscript.

## REFERENCES


[1] World Health Organization (WHO), "Exposure & health impacts of air pollution," Available at: https://www.who.int/teams/environment-climate-change-and-health/air-quality-energy-and-health/health-impacts/exposure-air-pollution#:~:text=The%20combined%20or%20joint%20effects,cancer%20and%20acute%20respiratory%20infections. Accessed on Jul 19, 2024.

[2] Y. C. Hong, J. T. Lee, H. Kim, and H. J. Kwon, "Air pollution: A new risk factor in ischemic stroke mortality," Stroke, Vol. 33(9), pp. 2165–2169, 2002. [CrossRef]

[3] R. Ruckerl, A. Ibald-Mulli, W. Koenig, A. Schneider, G. Woelke, J. Cyrys…, and A. Peters, "Air pollution and markers of inflammation and coagulation in patients with coronary heart disease," American Journal of Respiratory and Critical Care Medicine, Vol. 173(4), pp. 432–441, 2006. [CrossRef]

[4] Z. J. Andersen, "Chronic obstructive pulmonary disease and long-term exposure to traffic-related air pollution: A cohort study," American Journal of Respiratory and Critical Care Medicine, Vol. 183(4), pp. 455–461, 2011. [CrossRef]

[5] F. Nyberg, P. Gustavsson, L. Jarup, T. Bellander, N. Berglind, R. Jakobsson, and G. Pershagen, "Urban air pollution and lung cancer in Stockholm," Epidemiology, Vol. 11(5), pp. 487–495, 2000. [CrossRef]

[6] M. Ezzati, and D. M. Kammen, "Indoor air pollution from biomass combustion and acute respiratory infections in Kenya: An exposure-response study," Lancet, Vol. 358(9282), pp. 619–624, 2001. [CrossRef]

[7] L. A. Darrow, M. Klein, W. D. Flanders, J. A. Mulholland, P. E. Tolbert, and M. J. Strickland, "Air pollution and acute respiratory infections among children 0–4 years of age: An 18-year time-series study," The American Journal of Epidemiology, Vol. 180(10), pp. 968–977, 2014. [CrossRef]

[8] D. Loomis, W. Huang, and G. Chen, "The International Agency for Research on Cancer (IARC) evaluation of the carcinogenicity of outdoor air pollution: Focus on China," Chinese Journal of Cancer, Vol. 33(4), pp. 189–196, 2014. [CrossRef]

[9] D. Loomis, Y. Grosse, B. Lauby-Secretan, F. El Ghissassi, V. Bouvard, L. Benbrahim-Tallaa…, and K. Straif; International Agency for Research on Cancer Monograph Working Group, "The carcinogenicity of outdoor air pollution," The Lancet Oncology, Vol. 14(13), pp. 1262–1263, 2013. [CrossRef]

[10] Mokhtari, W. Bechkit, H. Rivano, and M. R. Yaici, "Uncertainty-aware deep learning architectures for highly dynamic air quality prediction," IEEE Access, Vol. 9, pp. 14765–14778, 2021. [CrossRef]

[11] M. Kampa, and E. Castanas, "Human health effects of air pollution," Environmental Pollution, Vol. 151(2), pp. 362–367, 2008. [CrossRef]

[12] E. Tagaris, K. J. Liao, A. J. DeLucia, L. Deck, P. Amar, and A. G. Russell, "Potential impact of climate change on air pollution-related human health effects," Environmental Science and Technology, Vol. 43(13), pp. 4979–4988, 2009. [CrossRef]

[13] M. I. Qureshi, A. M. Rasli, U. Awan, J. Ma, G. Ali, A. Alam…, and K. Zaman, "Environment and air pollution: Health services bequeath to grotesque menace," Environmental Science and Pollution Research, Vol. 22, pp. 3467–3476, 2015. [CrossRef]

[14] H. Orru, K. L. Ebi, and B. Forsberg, "The interplay of climate change and air pollution on health," Current Environmental Health Reports, Vol. 4, pp. 504–513, 2017. [CrossRef]

[15] H. Du, D. Liu, Z. Lu, J. Crittenden, G. Mao, S. Wang, and H. Zou, "Research development on sustainable urban infrastructure from 1991 to 2017: A bibliometric analysis to inform future innovations," Earth's Future, Vol. 7(7), pp. 718–733, 2019. [CrossRef]

[16] D. L. Crouse, N. A. Ross, and M. S. Goldberg, "Double burden of deprivation and high concentrations of ambient air pollution at the neighbourhood scale in Montreal, Canada," Social Science & Medicine, Vol. 69(6), pp. 971–981, 2009. [CrossRef]

[17] J. Kerckhoffs, G. Hoek, L. Portengen, B. Brunekreef, and R. C. H. Vermeulen, "Performance of prediction algorithms for modeling outdoor air pollution spatial surfaces," Environmental Science and Technology, Vol. 53(3), pp. 1413–1421, 2019. [CrossRef]

[18] W. Wang, C. Men, and W. Lu, "Online prediction model based on support vector machine," Neurocomputing, Vol. 71(4–6) pp. 550–558, 2008. [CrossRef]

[19] R. S. Batth, M. Gupta, K. S. Mann, S. Verma, and A. Malhotra, "Comparative study of tdma-based mac protocols in vanet: A mirror review," Proceedings of the 2019 International Conference on Innovative Computing and Communications (ICICC). Ostrava, Czech Republic, 2019.

[20] M. Kaur, and S. Verma, "Flying ad-hoc network (FANET): Challenges and routing protocols," Journal of Computational and Theoretical Nanoscience Vol. 17(6) pp. 2575–2581, 2020. [CrossRef]

[21] T. Sharma, and S. Verma, "Prediction of heart disease using cleveland dataset: A machine learning approach," International Journal of Recent Research Aspects, Vol. 4(3), pp. 17–21, 2017.

[22] X. Tian, Y. Huang, S. Verma, M. Jin, U. Ghosh, K. M. Rabie, and D. T. Do, "Power allocation scheme for maximizing spectral efficiency and energy efficiency tradeoff for uplink NOMA systems in B5G/6G," Physical Communication, Vol. 43, Article 101227, 2020. [CrossRef]

[23] G. Ghosh, M. Sood, and S. Verma, "Internet of things based video surveillance systems for security applications," Journal of Computational and The-oretical Nanoscience, Vol. 17(6), pp. 2582–2588, 2020[CrossRef]

[24] V. P. Diodato, and P. Gellatly, "Dictionary of Bibliometrics," Routledge, 2013

[25] R. N. Broadus, "Toward a definition of 'bibliometrics,'" Scientometrics, Vol. 12, pp. 373–379, 1987. [CrossRef]

[26] Pritchard, "Statistical bibliography or bibliometrics," Journal of Documentation, Vol. 25(4), pp. 348–349, 1969. [CrossRef]

[27] M. A. Koseoglu, R. Rahimi, F. Okumus, and J. Liu, "Bibliometric studies in tourism," Annals of Tourism Research Vol. 61(1) pp. 180–198, 2016. [CrossRef]

[28] Y. Yu, Y. Li, Z. Zhang, Z. Gu, H. Zhong, Q. Zha…, and E. Chen, "A bibliometric analysis using VOSviewer of publications on COVID-19," Annals of Translational Medicine, Vol. 8(13), pp. 816–816, 2020. [CrossRef]

[29] P. Hallinger, and J. Kovačević, "A bibliometric review of research on educational administration: Science mapping the literature, 1960 to 2018," Review of Educational Research, Vol. 89(3), pp. 335–369, 2019. [CrossRef]

[30] P. Hallinger, and C. Chatpinyakoop, "A bibliometric review of research on higher education for sustainable development, 1998–2018," Sustainability, Vol. 11(8), Article 2401, 2019. [CrossRef]

[31] E. A. Abafe, Y. T. Bahta, and H. Jordaan, "Exploring biblioshiny for historical assessment of global research on sustainable use of water in agriculture," Sustainability, Vol. 14(17), Article 10651, 2022. [CrossRef]

[32] H. Babbar, S. Rani, M. Masud, S. Verma, D. Anand, and N. Jhanjhi, "Load balancing algorithm for migrating switches in software-defined vehicular networks," Computers, Materials & Continua, Vol.67(1), pp. 1301–1316, 2021. [CrossRef]

[33] S. Kumar, R. Shanker, and S. Verma, "Context aware dynamic permission model: A retrospect of privacy and security in android system," Procedings of the 2018 International Conference on Intelligent Cir-cuits and Systems (ICICS). Phagwara, India, 2018.

[34] M. Kumar, K. S. Raju, D. Kumar, N. Goyal, S. Verma, and A. Singh, "An efficient framework using visual recognition for IoT based smart city surveillance," Multimedia Tools and Applications, Vol. 80, pp. 31277–31295, 2021. [CrossRef]

[35] G. Yang, M. A. Jan, A. U. Rehman, M. Babar, M. M. Aimal, and S. Verma, "Interoperability and data storage in internet of multimedia things: Investigating current trends, research challenges and future directions," IEEE Access, Vol. 8, pp. 124382–124401, 2020. [CrossRef]

[36] S. Dash, S. Verma, Kavita, S. Bevinakoppa, M. Wozniak, J. Shafi, and M. F. Ijaz, "Guidance image-based enhanced matched filter with modified thresholding for blood vessel extraction," Symmetry (Basel), Vol. 14(2), Article 194, 2022. [CrossRef]

[37] V. Dogra, A. Singh, S. Verma, Kavita, N. Z. Jhanjhi, and M. N. Talib, "Analyzing DistilBERT for sentiment classification of banking financial news," Proceedings of the 2021 Intelligent Computing and Innovation on Data Science (ICTIDS). Ahmedabad, India, 2021. [CrossRef]

[38] Y. Rybarczyk, and R. Zalakeviciute, "Machine learning approaches for outdoor air quality modelling: A systematic review," Applied Sciences, Vol. 8(12), Article 2570, 2018. [CrossRef]

[39] Q. Guo, M. Ren, S. Wu, Y. Sun, J. Wang, Wang Q…, and Y. Chen, "Applications of artificial intelligence in the field of air pollution: A bibliometric analysis," Frontiers in Public Health, Article 2972, 2022. [CrossRef]

[40] L. Bai, J. Wang, X. Ma, and H. Lu, "Air pollution forecasts: An overview," International Journal of Environmental Research and Public Health, Vol. 15(4), Article 780, 2018. [CrossRef]

[41] X. Li, Y. Choi, B. Czader, A. Roy, H. Kim, B. Lefer, and S. Pan, "The impact of observation nudging on simulated meteorology and ozone concentrations during DISCOVER-AQ 2013 Texas campaign," Atmospheric Chemistry and Physics, Vol. 16(5), pp. 3127–3144, 2016. [CrossRef]

[42] C. Vitolo, Y. Elkhatib, D. Reusser, C. J. A. Macleod, and W. Buytaert, "Web technologies for environ-mental Big Data," Environmental Modelling & Soft-ware, Vol. 63(3), pp. 185–198, 2015. [CrossRef]

[43] Z. Zong, Y. Chen, C. Tian, Y. Fang, X. Wang, G. Huang…, G. Zhang,"Radiocarbon-based impact assessment of open biomass burning on regional carbonaceous aerosols in North China," Science of the Total Environment Vol. 518–519, pp. 1–7, 2015. [CrossRef]

[44] S. M. Cabaneros, J. K. Calautit, and B. R. Hughes, "A review of artificial neural network models for ambient air pollution prediction," Environmental Modelling & Software, Vol. 119, pp. 285–304, 2019. [CrossRef]

[45] P. Guo, W. Tian, H. Li, G. Zhang, and J. Li, "Global characteristics and trends of research on construction dust: Based on bibliometric and visualized analysis," Environmental Science and Pollution Research, Vol. 27, pp. 37773–37789, 2020. [CrossRef]

[46] Y. Hou, and Z. Shen, "Research Trends, hotspots and frontiers of ozone pollution from 1996 to 2021: A review based on a bibliometric visualization analysis," Sustainability, Vol. 14(17), Article 10898, 2022. [CrossRef]
[47] S. Jain, N. Kaur, S. Verma, Kavita, A. S. M. S. Hosen, and S. S. Sehgal, "Use of machine learning in air pollution research: A bibliographic perspective," Electronics, Vol. 11(21), Article 3621, 2022. [CrossRef]
[48] Y. Li, Z. Sha, A. Tang, K. Goulding, and X. Liu, "The application of machine learning to air pollution research: A bibliometric analysis," Ecotoxicology and Environmental Safety, Vol. 257, Article 114911, 2023. [CrossRef]
[49] K. Mehmood, Y. Bao, Saifullah, W. Cheng, M. A. Khan, N. Siddique…, R. Naidu, "Predicting the quality of air with machine learning approaches: Current research priorities and future perspectives," Journal of Cleaner Production, Vol. 379(Part 2), Article 134656, 2022. [CrossRef]
[50] J. F. Velasco-Muñoz, J. A. Aznar-Sánchez, L. J. Belmonte-Ureña, and I. M. Román-Sánchez, "Sustainable water use in agriculture: A review of worldwide research," Sustainability, Vol. 10(4), Article 1084, 2018. [CrossRef]
[51] E. Garfield, and I. H. Sher, "New factors in the evaluation of scientific literature through citation indexing," American Documentation, Vol. 14(3), pp. 195–201, 1963. [CrossRef]
[52] Zupic, and T. Čater, "Bibliometric methods in management and organization," Organizational Research Methods, Vol. 18(3), pp. 429–472, 2015. [CrossRef]
[53] M. Aria, and C. Cuccurullo, "Bibliometrix: An R-tool for comprehensive science mapping analysis," Journal of Informetrics, Vol. 11(4), pp. 959–975, 2017. [CrossRef]
[54] N. J. van Eck, and L. Waltman, "Software survey: VOSviewer, a computer program for bibliometric mapping," Scientometrics, Vol. 84(2), pp. 523–538, 2010. [CrossRef]
[55] N. J. Van Eck, and L. Waltman, "Visualizing Bibliometric Networks." Edited by Ding, Y., Rousseau, R., and Wolfram D. Measuring Scholarly Impact, Springer. pp. 285–320, 2014.
[56] N. J. Van Eck, and L. Waltman, "Text mining and visualization using VOSviewer," arXiv Prepr. 2011.
[57] H. Ernst, "The use of patent data for technological forecasting: The diffusion of CNC-technology in the machine tool industry," Small Business Economics, Vol. 9, pp. 361–381, 1997. [CrossRef]
[58] G. Mao, H. Hu, X. Liu, J. Crittenden, and N. Huang, "A bibliometric analysis of industrial wastewater treatments from 1998 to 2019," Environmental Pollution Vol. 275, Article 115785, 2021. [CrossRef]
[59] J. Daniels, and P. Thistlethwaite, "Measuring Scholarly Impact," Cambridge University Press, 2022.
[60] K. P. Singh, S. Gupta, and P. Rai, "Identifying pollution sources and predicting urban air quality using ensemble learning methods," Atmospheric Environment, Vol. 80, pp. 426–437, 2013. [CrossRef]
[61] D. Mishra, P. Goyal, and A. Upadhyay, "Artificial intelligence based approach to forecast PM2. 5 during haze episodes: A case study of Delhi, India," Atmospheric Environment, Vol. 102, pp. 239–248, 2015. [CrossRef]
[62] M. Krishan, S. Jha, J. Das, A. Singh, M. K. Goyal, and C. Sekar, "Air quality modelling using long short-term memory (LSTM) over NCT-Delhi, India," Air Quality Atmosphere Health, Vol. 12(8), pp. 899–908, 2019. [CrossRef]
[63] K. S. Harishkumar, K. M. Yogesh, and I. Gad, "Forecasting air pollution particulate matter (PM2. 5) using machine learning regression models," Procedia Computer Science, Vol. 171, pp. 2057–2066, 2020. [CrossRef]
[64] D. Mishra, and P. Goyal, "Development of artificial intelligence based $NO_2$ forecasting models at Taj Mahal, Agra," Atmospheric Pollution Research, Vol. 6(1), pp. 99–106, 2015. [CrossRef]
[65] Rubal, and D. Kumar, "Evolving differential evolution method with random forest for prediction of Air Pollution," Procedia Computer Science, Vol. 132, pp. 824–833, 2018. [CrossRef]
[66] S. Acharyya, B. Jana, S. Nag, G. Saha, and P. K. Guha, "Single resistive sensor for selective detection of multiple VOCs employing $SnO_2$ hollowspheres and machine learning algorithm: A proof of concept," Sensors and Actuators B Chemical, Vol. 321, Article 128484, 2020. [CrossRef]
[67] T. W. Ayele, and R. Mehta, "Air pollution monitoring and prediction using IoT," Proceedings of the 2018 International Conference on Inventive Communication and Computational Technologies (ICICCT). New Delhi, India, 2018. [CrossRef]
[68] Masood, and K. Ahmad, "A review on emerging artificial intelligence (AI) techniques for air pollution forecasting: Fundamentals, application and performance," Journal of Cleaner Production, Vol. 322, Article 129072, 2021. [CrossRef]
[69] Amuthadevi, D. S. Vijayan, and V. Ramachandran, "Development of air quality monitoring (AQM) models using different machine learning approaches," Journal of Ambient Intelligence and Humanized Computing, Vol 13. pp. 33–34, 2021. [CrossRef]
[70] U. Mahalingam, K. Elangovan, H. Dobhal, C. Valliappa, S. Shrestha, and G. Kedam, "A machine learning model for air quality prediction for smart cities," Proceedings of the 2019 International Conference on Wireless Communications Signal Processing and Networking (WISPNET). Chennai, India, 2019. [CrossRef]
[71] V. R. Pasupuleti, P. Kalyan, and H. K. Reddy, "Air quality prediction of data log by machine learning," Proceedings of the 6th International Conference on Advanced Computing and Communication Systems (ICACCS). Coimbatore, India, 2020. [CrossRef]
[72] S. Yarragunta, and M. A. Nabi, "Prediction of air pollutants using supervised machine learning," Proceedings of the 5th International Conference on Intelligent Computing and Control Systems (ICICCS). Madurai, India, 2021. [CrossRef]

[73] S. Simu, V. Turkar, and R. Martires, "Air pollution prediction using machine learning," Proceedings of the 2020 IEEE Bombay Section Signature Conference (IBSSC). Mumbai, India, 2020. [CrossRef]

[74] S. Sur, R. Ghosal, and R. Mondal, "Air pollution hotspot identification and pollution level prediction in the City of Delhi," Proceedings of the 1st International Conference for Convergence in Engineering (ICCE), Kolkata, India, 2020. [CrossRef]

[75] J. K. Singh, and A. K. Goel, "Prediction of air pollution by using machine learning algorithm," Proceedings of the 7th International conference on advanced computing and communication Systems (ICACCS), Coimbatore, India, 2021. [CrossRef]

[76] Pant, S. Sharma, M. Bansal, and M. Narang, "Comparative analysis of supervised machine learning techniques for AQI prediction," Proceedings of the 2022 International Conference on Advanced Computing Technologies and Applications (ICACTA), Coimbatore, India, 2022. [CrossRef]

[77] Tripathy, D. Vaidya, A. Mishra, S. Bilolikar, and V. Thoday, "Analysing and predicting air quality in Delhi: Comparison of industrial and residential area," Proceedings of the 2021 International Conference on Smart Generation Computing, Communication and Networking (SMART GENCON), Pune, India, 2021. [CrossRef]

[78] K. Nandini, and G. Fathima, "Urban air quality analysis and prediction using machine learning," Proceedings of the 1st International Conference on Advanced Technologies in Intelligent Control, Environment, Computing & Communication Engineering (ICATIECE), Bangalore, India, 2019. [CrossRef]

[79] Janik, A. Ryszko, and M. Szafraniec, "Scientific landscape of smart and sustainable cities literature: A bibliometric analysis," Sustainability, vol. 12(3), Article 779, 2020. [CrossRef]

[80] B. Chelani, C. V. C. Rao, K. M. Phadke, and M. Z. Hasan, "Prediction of sulphur dioxide concentration using artificial neural networks," Environmental Modelling & Software, Vol. 17(2), pp. 159–166, 2002. [CrossRef]

[81] B. Chelani, R. N. Singh, and S. Devotta, "Nonlinear dynamical characterization and prediction of ambient nitrogen dioxide concentration," Water, Air, and Soil Pollution, Vol. 166, pp. 121–138, 2005. [CrossRef]

[82] S. M. S. Nagendra, and M. Khare, "Artificial neural network approach for modelling nitrogen dioxide dispersion from vehicular exhaust emissions," Ecological Modelling, Vol. 190(1–2) pp. 99–115, 2006. [CrossRef]

[83] S. Jain, and M. Khare, "Adaptive neuro-fuzzy modeling for prediction of ambient CO concentration at urban intersections and roadways," Air Quality, Atmosphere & Health, Vol. 3(4), pp. 203–212, 2010. [CrossRef]

[84] Mahapatra, "Prediction of daily ground-level ozone concentration maxima over New Delhi," Environmental Monitoring and Assessment, Vol. 170, pp. 159–170, 2010. [CrossRef]

[85] Prakash, U. Kumar, K. Kumar, and V. K. Jain, "A wavelet-based neural network model to predict ambient air pollutants' concentration," Environmental Modeling & Assessment, Vol. 16, pp. 503–517, 2011. [CrossRef]

[86] S. Chattopadhyay, and G. Chattopadhyay, "Modeling and prediction of monthly total ozone concentrations by use of an artificial neural network based on principal component analysis," Pure and Applied Geophysics, Vol. 169(10) pp. 1891–1908, 2012. [CrossRef]

[87] K. P. Singh, S. Gupta, A. Kumar, and S. P. Shukla, "Linear and nonlinear modeling approaches for urban air quality prediction," Science of the Total Environment, Vol. 426, pp. 244–255, 2012. [CrossRef]

[88] R. Bhardwaj, D. Pruthi, "Development of model for sustainable nitrogen dioxide prediction using neuronal networks," International Journal of Environmental Science and Technology, Vol. 17, pp. 2783–2792, 2020. [CrossRef]

*Environ Res Tec, Vol. 7, Issue. 3, pp. 378–394, September 2024*

**Environmental Research and Technology**
https://ert.yildiz.edu.tr - https://dergipark.org.tr/tr/pub/ert
DOI: https://10.35208/ert.1284481

Environmental Research & Technology

**Research Article**

# Sustainable waste management practices in the informal sector: Towards industrial symbiosis

**Sudipti BISWAS***

*Department of Architecture, Military Institute of Science and Technology, Dhaka, Bangladesh*

## ARTICLE INFO

*Article history*
Received: 17 April 2023
Revised: 12 March 2024
Accepted: 20 March 2024

**Key words:**
Informal industries; Industrial symbiosis; Informal waste management; Material cycle

## ABSTRACT

Industrial pollution is considered to be routed in the waste and byproducts of the production process. Traditional pollution control approaches try to eliminate and/or treat the pollutants which are often technically complicated and expensive. In this regard, industrial ecology and industrial symbiosis have emerged as effective strategy to eliminate industrial pollution. This principle requires the generated waste/by-products absorbed in the same or other industrial process cycles and thus the material cycle remains closed. Industrial pollution appears as a big problem in the global south countries, where industrialization is considered as the main thrust of economic development. Usually, in such countries formal pollution control approaches are primarily directed to the formal sectors (such as state owned and legally registered industries), informal sectors are often left behind. Although the role of informal sector is increasingly being recognized for sustainable development, their significance in pollution abatement is a less discussed topic. This article attempts to investigate the informal industrial sector in Dhaka, Bangladesh with empirical evidence. Adopting a qualitative approach with field investigation of the informal industries and detail interviews, this study identified that the informal industries are closely linked in clusters according to the manufacturing process and continue material/byproduct/waster exchange primarily from the need to minimize cost. The studied patterns of waste management practice indicate existence of industrial symbiosis without adequate academic/technical knowledge and designed efforts. This suggests that the informal sector can meaningfully contribute to sustainable development offering insights for the application of similar approaches in the formal sector.

**Cite this article as:** Biswas S. Sustainable waste management practices in the informal sector: Towards industrial symbiosis. Environ Res Tec 2024;7(3)378–394.

## INTRODUCTION

Concern about the environment is ever increasing, and so is the concern for sustainability. Sustainable practices now receive the highest priority to save resources for the present and future generations [1–4]. Since the Brundtland Report to date, environmental protection, economic efficiency, and social equity are unquestionably considered the core objectives of sustainable development [2, 5–7]. Sustainable development is a well-recognized research domain with a great volume, and this study explores the environmental enclave. Within the vast literature in this field, there exists an assumption regarding the role of the state in regulating, controlling, and coordinating activities for sustainable development, focusing on the environment, through technological and non-technological means [5]. The role of the state is obvious, however, the path to sustainability is far from straightforward, and the participants are not always the known ones.

***Corresponding author.**
*E-mail address: sudipti.biswas@arch.mist.ac.bd

Beyond the conventional formal stakeholders, the informal sector has also emerged as a significant player in this protracted journey [5, 8, 9]. Scholars consider that the informal sector often remains obscured in the mainstream sustainability discourse due to its unique characteristics such as nonstandard, illegal, hidden, shadowy, invisible, unobserved, irregular, and unofficial [10–14]. Though the question of administering the informal sector is still in the academic debate, their role is being widely accepted for inclusive sustainable development [8, 9]. Gradually the informal sector is being considered, sometimes, in the policy framework too. In some fields, such as waste management, recycling etc. the contribution of informal sector is well recognized [15–19]. While informal sector waste management and recycling is a recognized academic field, there is deficiency of scientific knowledge regarding the contribution of informal sector in pollution generation and abatement [20–24]. On the other hand, informality is often associated with many countries in the global south [25–27] where development is often prioritizes over environment and the drive is mostly towards growth at any cost being blind to the environmental burdens [28–31]. In addition, they often opt for traditional expensive ways of treating the generated waste [22, 32].

In such context, this research is focused towards the informal waste management from the perspective of industrial pollution control, which is often left outside the mainstream pollution control domain [22]. It attempts to study the informal industrial sector in relation to the concept of Industrial Symbiosis (IS) taking the examples from the city of Dhaka in Bangladesh, a country where more than 80% of the national employment is offered by informal sector and the rate varies between 60-90% in the urban areas [33]. Bangladesh shows typical pattern of development-environment dilemma where the environmental concern is recognized only since the 1990s [34] and the focus is to control environmental pollution caused by the industrial sector through treatment of the pollutants [35–37].

Informal small and scale industries contribute to a significant portion of the manufacturing sector in Bangladesh and they are often blamed for environmental pollution of varying extent [38, 39]. This study attempts to investigate the waste management practices in the informal industrial sector in Dhaka, in a qualitative manner, with the aim to look for sustainable practices that can reduce the environmental burden. This study aimed to get a clear understanding of.

- How the informal industries manage their waste.
- If the industries are consciously adopting any strategies to reduce waste.
- The state of material cycle within the industries or within the expanded boundary of the industrial unit incorporating other industries.

Due to the lack of scientific and/or national level databased on the informal manufacturing industries, this qualitative study was exercised with observation of the industries and semi structured interviews with the entrepreneurs. Data was analyzed with qualitative content analysis method to understand how these informal industries manage their waste or by-products and how the material cycles relate to the principles of Industrial Ecology (IE) and IS.

The scope of this study is restricted only the informal those industrial units that use new or used or both types of materials as raw material for their production process leaving the recycling activities out of the scope. Therefore, this study is distinguished from other studies that uncovers symbiotic activities in the formal industrial sectors that might include informal activities within the broader industrial enclave, for example the studies in Sitakunda-Bhatiary of Bangladesh [40] and Nanjagud in India [41].

The implication of the study is multifaceted. This study contributes to understanding the informal sector, particularly to the character of small-scale manufacturing industries regarding production, clustering, interconnectedness etc. This identifies that the informal industries exercise sustainable waste management practices and suggest that more of such examples await to be explored. A significant driver behind this sustainable practice is economic benefit, rather environmental concern. This suggests the policymaker about the adoption of IE/IS and CP principles for informal sector and the directives for the formal sector.

**The Material Perspective for Pollution Abatement**

Analysis of material flow in the industrial process makes it clear that industrial pollution is routed in the waste and by-products generated from the industrial process. Thus, to diminish industrial pollution, elimination of industrial waste is considered the best approach. The traditional End-of-Pipe (EOP) method of pollution control approach treats the wastes and recuses pollution, but does not necessarily eliminate the polluting wastes and increase the production cost [32, 42, 43]. Yet pollution control approaches are applied, and even sometimes enforced by regulations, for industrial waste management in most of the global south countries [22, 32]. The response to industrial pollution has been shifted from initial EOP towards the recent IE for a sustainable industrial development in terms of both resource consumption and waste management. The basic principle of IE is that output from one industrial process could be used as input for other industrial process/processes [44, 45]. Thus IE aims to optimize the material cycle from raw materials to final disposal, and ultimately striving for a zero-waste, non-polluting industrial system [43, 46–48]. With the growing concern of dealing with environmental issues, IE concept denotes a vital step and is believed to lead towards a society with sustainable production and consumption because it incorporates the technological perspective of Pollution Prevention (P2) Cleaner Production (CP) and Life Cycle Assessment (LCA) [49–51]. In this vein, IS is considered as a subset of IE enclave.

The notion of industrial symbiosis is derived from biological symbiotic relationships of species in the natural environment. It is the relationship among different industrial enterprises. This idea was initially recognized as the matrix of complex relationship among different entities to strive

for a collective benefit greater than the sum of individual benefits [52]. IS is usually developed within a specified place boundary like an (eco)industrial park [52–55]. However, studies also indicate that it is necessary to extend the geographical boundary beyond that specified formal park so that other industries in the wider area can be included in the material flow [56]. Also it is noted that outside the industrial parks, there are possibilities of meaningful benefits achieved from sharing of resources among the business in industrial districts [52, 57].

Industrial Symbiosis is usually developed either as designed or evolved from mutual understanding and benefits. IS in Kalundborg, Denmark is a classic example of mutual understanding [52, 57]. IS usually emerges as 'self-organized' business among willing firms with a common strategy to reduce the increasing cost of waste management stipulated by the legislative requirements [58]. Usually, such businesses are located in close geographical proximity, such as designated industrial areas. Such 'spontaneous co-location' of businesses in industrial districts can offer many public and private benefits including labor availability, access to capital, technological innovation, infrastructure efficiency etc. [59–61]. Such 'unplanned' development of IS may produce better result that planned developments, in new or underdeveloped eco-industrial parks [62]. It is also noted that 'anterior territorial agglomerations' is not always necessary for industrial symbiosis and entrepreneurial activities can lead to symbiotic relationship as well [40]. However, the modern literature generally overlooks environmental benefits of agglomeration through resource sharing [63] and there is a consensus that 'self-organized' symbiosis networks are insufficient and urge that delicate policy instruments, facilitatory environment and enabling framework are required to develop successful industrial ecosystem [53, 57]. The enabling framework for development of industrial symbiosis is influenced by social, informational, technological, economic and political factors [58]. Perhaps this is why IS is very often perceived as some designed and deliberate effort for the industrialized societies. Although, studies have identified examples of IS in the emerging and developing economies as well, such as Puerto Rico [64], China [54, 55, 65], Vietnam [66] etc., and there are also initiatives in some Latin American and African countries [67]. There have been also a few studies to identify spontaneous development of symbiotic activities in formalized industrial areas in the developing economies such as India [41], Bangladesh [40] etc. Studies in this field has grown sufficiently in the last decade and they suggest increasing concern about the IS principle and practice, however there are relatively few studies in the global south and extremely rare example in the informal sector, even though waste management in the informal sector is well recognized in such countries.

**Waste Management in the Informal Sector**

In the informality discourse, the core idea that the informal sector works outside the established legal/regulatory framework which restricts greater benefit is quite old fashioned [68]. Contemporary studies have identified the informal sector with organizing logic and a system of norms that governs the process of urban transformation itself [69–71]. For this study, the character of informality is perceived not on the illegality issue, but on the modality of informal activity. This signifies that informality is identified by what they lack, but by what they are [69].

Informality is a distinguished feature in the South and South-East Asian cities with a considerable share in employment generation [69, 72–75]. The significance of informal sector in the domain for material recycling and recovery is well established [41, 76–81]. The waste business operates in a 'grey market' outside the regulatory framework of concerned authorities [82]. It is quite difficult to keep track of materials in this multilayered waste business that involves several actors and run for both domestic and non-domestic waste. At the lower level, collectors gather waste door-to-door or scavenge from dumpsites. Some collectors purchase waste and old staff from households for cash or new products. Organized door-to-door waste collection and transportation to dumpsites are common [78, 83]. Collectors sort the waste and sell it to scrap dealers, who, in turn, contract collectors to obtain waste from diverse sources. These dealers often secure agreements to collect waste from non-domestic waste producers based on their capacity and social influence. Subsequently, the scrap dealers sort the waste and sell it to different clients, either directly or through intermediaries.

**Informal Waste Management in Dhaka**

Dhaka, the capital of Bangladesh is a densely populated city. The city has a waste production rate of approximately 1,950 tons/day for domestic source and 1,050 tons/day for non-domestic source including industries [84]. At best half of the waste is collected and a large portion of the waste handling is performed in the informal sector [76, 81, 84, 85].

The waste business involves various actors, including waste collectors and treaders operating at varying scale. Door-to-door waste collection is usually organized. Waste pickers, known locally as 'tokai', scavenge for waste, while 'feriwala' buy discarded items from households and businesses. These feriwalas then sell the collected items to scrap dealers, referred to as 'vangari', who play a central role in sorting, dismantling, and selling various types of waste to different user groups on demand. There is a dearth of academic research about this waste business related to informal industries, but it is perceived that the informal industries collect materials from the waste market [86].

In Dhaka the southern periphery is the house of scrap business as well as informal industries for a long time [19, 86, 87]. These industries are usually small scale and mostly termed as workshops in the local culture. Industries with similar production process are clustered together and they work on mutual understanding. Clustering of similar industries is a defining and historical characteristic of the older part of Dhaka resulting in specific areas becoming renowned for particular types of industries [39, 86, 87].

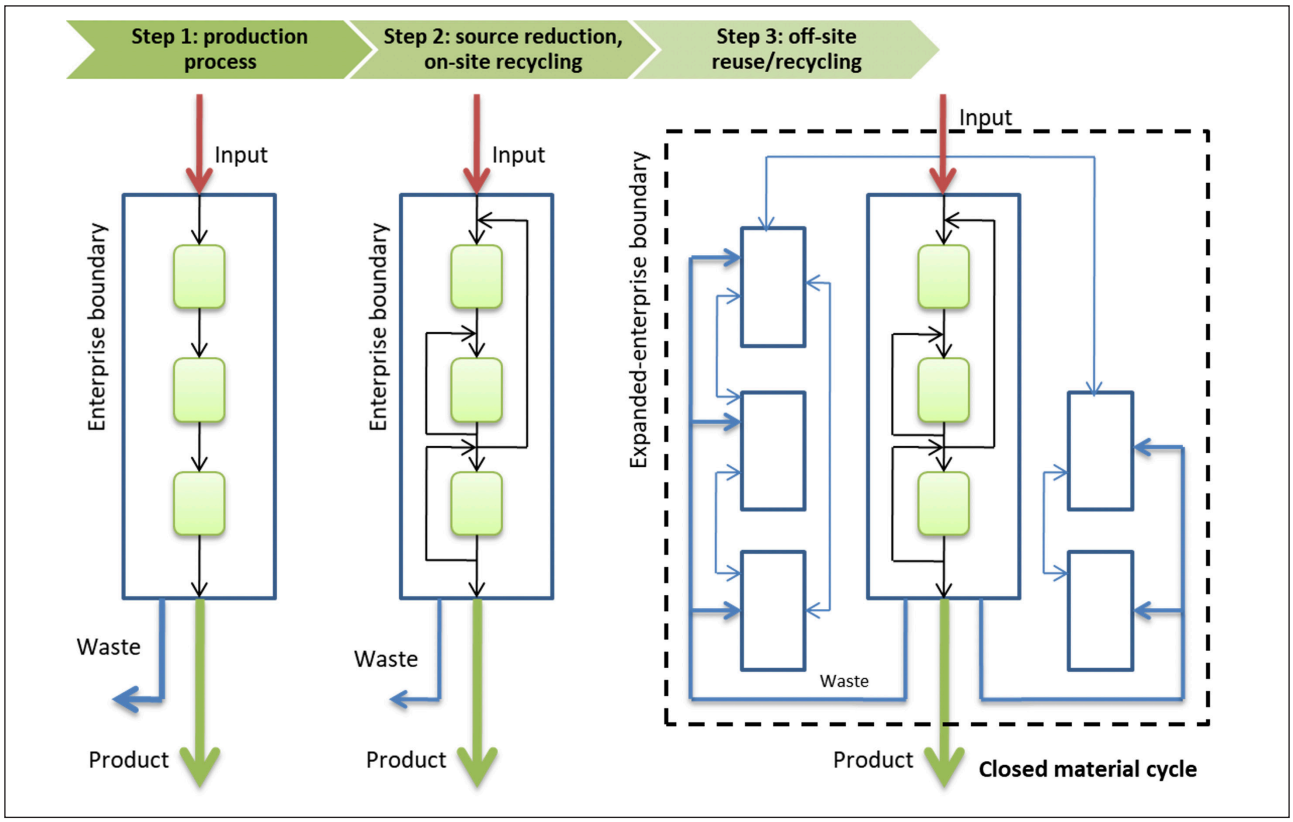


**Figure 1**. Conceptual framework to address the waste stream, based on [48].

## METHODOLOGY

### Conceptual Framework Regarding IEs

The concept of Industrial Ecology (IE) suggests that any residuals or by-products should be considered as potential inputs for other industrial units. It also requires the design of products for reuse, ensuring that the material cycle closes effectively. Following this principle, a three-step conceptual framework was developed for this study with the aim to analyze material flow and waste streams and as a guideline to close the material cycle. The framework, illustrated in the following figure, is based on a previous study [48] (Fig. 1).

### Identification of Informal Industries

Academic research in Bangladesh typically consider the characteristics of activities to define informality [39, 75, 78, 85, 86, 88]. Accordingly, for this this research, industrial units were considered informal if they had one or more of certain characteristics: non-permanence and casualness, operation in open spaces or in space that is not assigned for that use by the concerned authority, operation in residence or backyard, remaining outside the scope of company law or factory act or trade license or any other government regulations, small scale with less capital investment and mostly relying on household labor [88, 89].

### Selection of Study Area

No comprehensive database is available regarding the type of informal industrial clusters in Dhaka. The old part of Dhaka (including the southern periphery along the Buriganga river) is generally considered as the hub, nevertheless some studies have identified specific areas for industrial concentration, to name a few Dholaikhal, Lalbagh, Islambagh, Chawak Bazar, Imamganj, Postogola, Keraniganj, Kamrangir Char, etc. [19, 39, 86, 88, 90–92]. Following the available literature and field investigation, three areas of old Dhaka were selected for detail investigation, namely Dholaikhal, Imamganj and Kamalbagh (near Lalbagh and Islambagh).

Dholaikhal is well known for its concentration of metal works and iron business as well as specialized for repairing and remanufacturing services for the automobiles and light engineering works. At least one study indicated that the industries in this area have some connection regarding waste and material flow [86]. Imamganj is specialized for waste business for the entire Dhaka citys and connects with waste business outside the city. This area is dotted with industries that use recovered or recycled materials such as plastic, metal, paper etc. Kamalbagh is close to Lalbagh and Islambagh, well known for plastic manufacturing. Kamalbagh has a concentration of small industries that manufacture mainly cheap shoes/sandals and a variety of cheap trifle items.

### Data Collection and Analysis

This research is carried out in a qualitative manner. Industrial units from different industrial process clusters of Dholaikhal, Imamgonj and Kamalbagh are selected following purposive and snowball sampling [93, 94]. First, based on field observation informal industries were identified, then

**Figure 2**. Product sample, molded metal section and foundry works (left to right).

**Figure 3**. Dice making, molded metal section and finished product (left to right).

industrial units were observed, and entrepreneur were interviewed. From this round of interview other interview contacts were obtained, and this snowballing was carried until the loop in the conceptual framework was (nearly) complete and collected information reached the saturation point. Some entrepreneurs refused to cooperate, and some loops were found open and/or did not comply with the conceptual framework; such cases were not considered in the final analysis.

Observation primarily focused on the production chain covering the issues of production process, input and output materials, flow of materials, waste/byproducts generation, recycling/reuse of materials/waste/byproducts, waste disposal/management, link with other industrial units/clusters etc. Interviews were informal in nature, this means notes were taken instead of recording and conducted with semi-structured questionnaire. Interviews aimed to know more about the industrial process and get deeper understanding of their reasoning behind their actions/decisions, environmental concern, knowledge about pollution and industrial ecology, support for pollution/waste reduction or technological improvement from public/other agencies etc. Alongside, field notes from observation were also considered for analyzing the total matrix. There were a few assistants for field data collection, for consistency assistants were assigned to the same group of industries.

All the collected information was analyzed, following qualitative content analysis though constant comparison with the conceptual framework and relevant literature [95–97]. The analysis aimed identify the flow of material in the production process and relate the industrial unit/cluster with relevant stage identified in the conceptual framework. It also attempted to identify if any relation existed among the clusters in the area or within a wider area.

A total of 44 industrial units were observed and interviewed in detail. 12 for lathe engineering works and 10 for old tire business making a total of 22 in Dholaikhal, 16 for metal works in Imamganj and 6 for plastic shoemaking in Kamalbagh. In addition, 3 more expert interviews were conducted with the concerned regulatory authorities in Bangladesh, namely the Ministry of Industries, Bangladesh Small and Cottage Industries Corporation (BSCIC) and SME Foundation, to know about the formal initiative regarding IE or any other concepts for environmental concern for the industrial sector. At least 4 examples of (nearly) closed material cycle loops were identified in the study area, counting 2 in Dholaikhal, 1 in Imamganj and 1 in Kamalbagh area.

## RESULTS AND DISCUSSION

The investigation identified at least 4 patterns of closed loops. It was quite interesting that there were efforts of resource recycling, recovery, and reuse, clustering of similar industries, and interconnectedness of similar and related production. Such efforts from the entrepreneurs were not made with any consciousness for the IE concept or with any considerations to reduce environmental burden, or with any support or knowledge from the concerned authorities, but purely driven by economic constraints. All of the entrepreneurs confirmed that the connections developed predominantly with the aim of reducing resource consumption and starting new business with minimum investment while

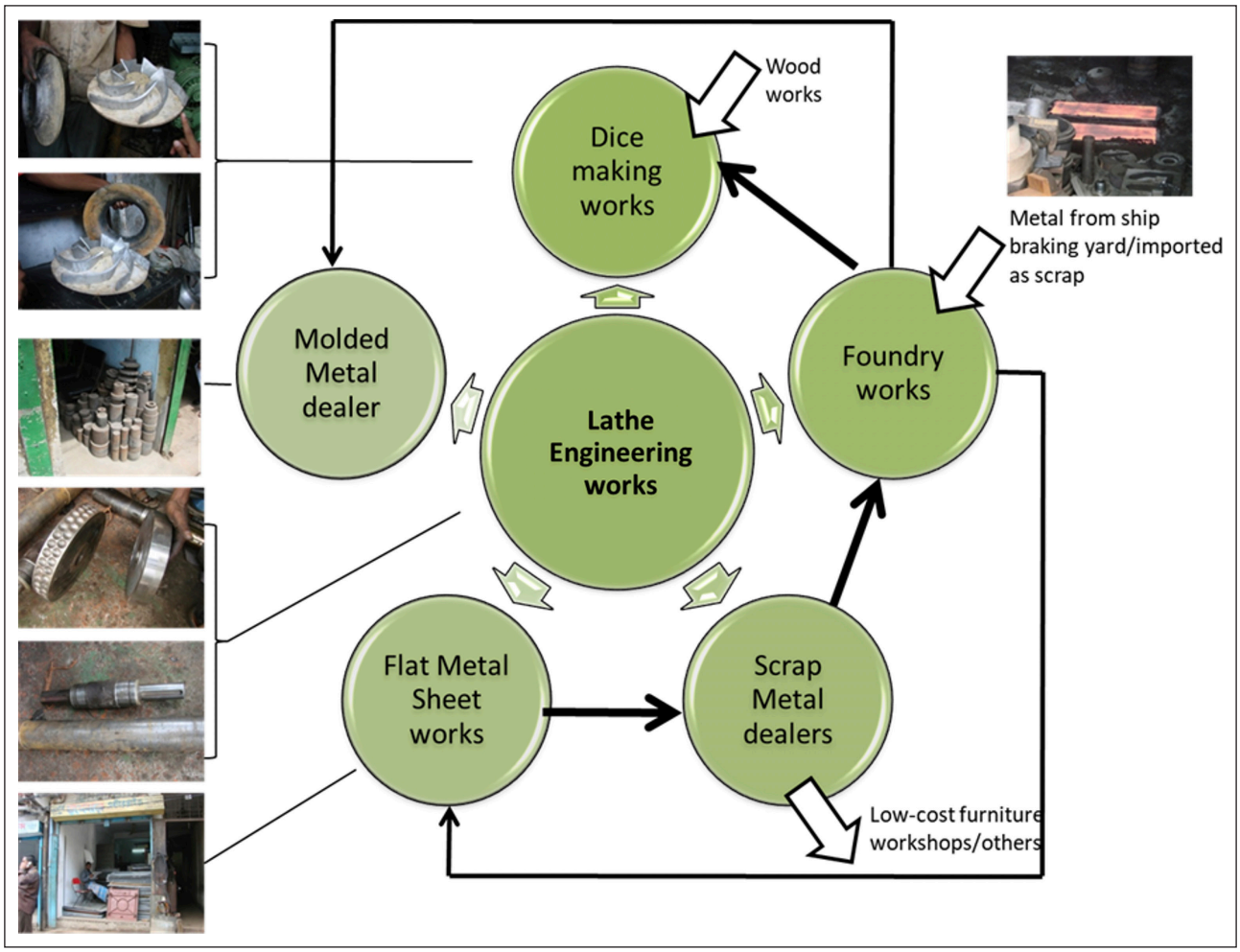


**Figure 4**. Material flow in Lathe engineering works in Dholaikhal.

they expanded by mimicking others doing the same. The identified cycles are described here.

**Pattern 1: Lathe Engineering Works**

Lathe engineering workshops in Dholaikhal typically received orders along with product samples. For simple products, the workshops collected metal sections from molded metal shops, usually found in Dholaikhal or nearby areas like Jatrabari, Demra, and Postogola. These shops sell metal sections in various forms and sizes, often casting them in small and large foundries. A significant portion of the metal used were recycled from scrap generated in Dholaikhal workshops, with some imported or collected from ship-breaking yards in Chittagong.

For more complex products, lathe works contacted dice-making workshops, mostly located in Bongram, to acquire molds for casting metal sections. Dice making often involves woodwork and cast-iron works. The sole responsibility of completing the mold fall on the dice maker. Woodwork was typically found in Badamtoli, and foundry works for cast iron sections in Dholaikhal and Bongram. Occasionally, lathe engineering works needed flat metal sheets, however flat metal sheet works normally function as separate business. Additional accessories are usually sourced from Nawabpur (Fig. 2).

Scrap dealers collected scrap metals from various workshops, sorted and sold them on demand. Shredded metals were recycled in foundries, while larger portions of flat metal sheet were sold to furniture-making workshops, commonly located in Jatrabari and Sayedabad. This network formed a closed flow of metal, connecting dispersed industries in different locations without significantly increasing production costs due to additional transport. The flow is presented graphically here (Fig. 3).

**Pattern 2: Old Tire Retreading**

This cluster of workshops were found to deal with old tires. All the parts of an old tire were either reused or used to manufacture variety of different products. This tire cluster comprised five main groups of workshops. The first group purchased old and rejected tires, sorted them, and sold to other workshops based on types and demand. The second group repaired less damaged tires for rural vehicles. The third group collected irreparable damaged tires, cut them into sections, and separated bead wires, which were sold to the fourth group producing springs and shock absorbers, located in Jinjira and Keraniganj on the other side of the river Buriganga. Cut tire sections were sold to different workshops (Fig. 4).

**Figure 5**. Tire retreading cluster, manual cutting, separated bead wires (left to right).

**Figure 6**. Different products made from old tires (left to right).

The fifth group produced diverse products from cut sections, including belts for various machines, hinge protectors, shock absorbers for engines and vehicle bodies, and components for machinery used in textiles, river digging, low-cost furniture, shoemaking, boat building, and bolt joining. Workers were observed to have a high level of manual cutting skill (Fig. 5).

Scrap dealers collected shredded tires from cutting workshops year-round for sale. Shredded tires served two purposes, oil production and fuel for brick kilns. In the oil production process, scrapped tires were burned to yield oil and carbon black. The oil was usually used as industrial fuel or further refined to diesel, while carbon black served as fuel or occasionally refined. Brick kilns used scrapped tires as fuel. In this, a closed material flow was observed with every part of an old tire as recovered or reused to manufacture new products. The bead wire workshops were the only cluster located away from Dholaikhal in this cycle. The cycle is represented graphically as follows (Fig. 6).

**Pattern 3: Metal Products Manufacturing**

At least 16 mall-scale industrial units, popularly referred to as workshops, that manufactured various trifle metal products in Imamganj were studied in detail. These workshops utilized both new and old/used input materials in their production processes. Typically, thin flat metal sheets were imported and stored in warehouses, locally called godown. Imamganj hosting the majority of such warehouses, served the entire city for bulk and retail. Some of the godowns were equipped with cutting machines for efficient business (Fig. 7).

Household items like mugs, measuring cups, cooking pans, buckets, and box trunks were generally manufactured in the Imamganj area. Metal handles for box trunks and buckets were not produced on-site; instead, old metal handles were purchased from vangari shops (scrap dealers) and reused. Containers for various purposes, like baking molds, oil cans, biscuit tins, kerosene containers, tar cans etc. were also crafted here. Container labeling was carried out in a different area across the Buriganga River. Leftover metal sections were sold to workshops producing very small containers, such as those for tobacco, betel nut, and spices (Fig. 8).

Additionally, some workshops in the area manufactured kerosene lamps with used metal cans, such as different types of aluminum beverage cans, spray cans etc. These slender, cylindrical cans were cut into two or three sections, depending on length, with the lamp's handle and bottom section made from the same can or leftover metal sections. Nozzles were crafted separately and affixed to the lamps. Cotton filaments, produced in unrelated industrial processes, were retailed to end-users in separate shops. Discarded lamps and other metal products were reintegrated into the waste recycling cycle (Fig. 9).

Lastly, scrap dealers collected scrap metals from the manufacturers multiple times a year, sorting and selling them to different users. Larger discarded metal sections were used for manufacturing rivet fasteners, low-cost furniture, kitchen tools, and for binding deformed bars in construction sites and steel mills. Shredded metals too small for reuse were recycled in foundry workshops. The remaining metal sections reached end-users through scrap dealers (Fig. 10).

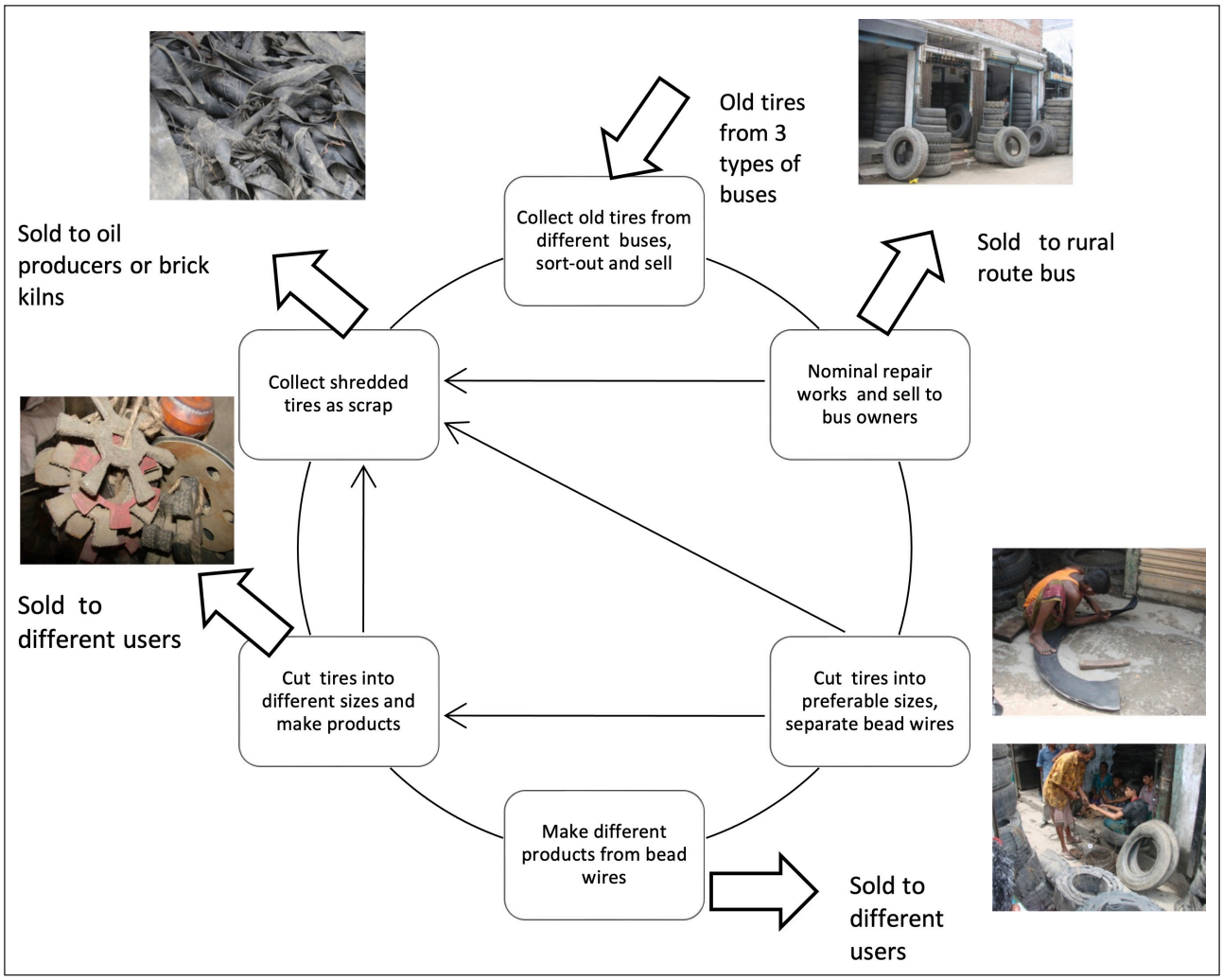


**Figure 7**. Material flow in the old tire retreading business in Dholaikhal.

**Figure 8**. New metal sheets, old and cut sections of metal sheets, metal handles of rejected buckets (left to right).

**Figure 9**. Manufacturing of box trunk, bucket, mug and cooking pan (left to right).

**Figure 10**. Manufacturing of metal containers and kerosene lamp (left to right).

**Figure 11**. Left over metal sections, rivet fasteners and washers, kitchen tools (grater) and shredded metals for recycling (left to right).

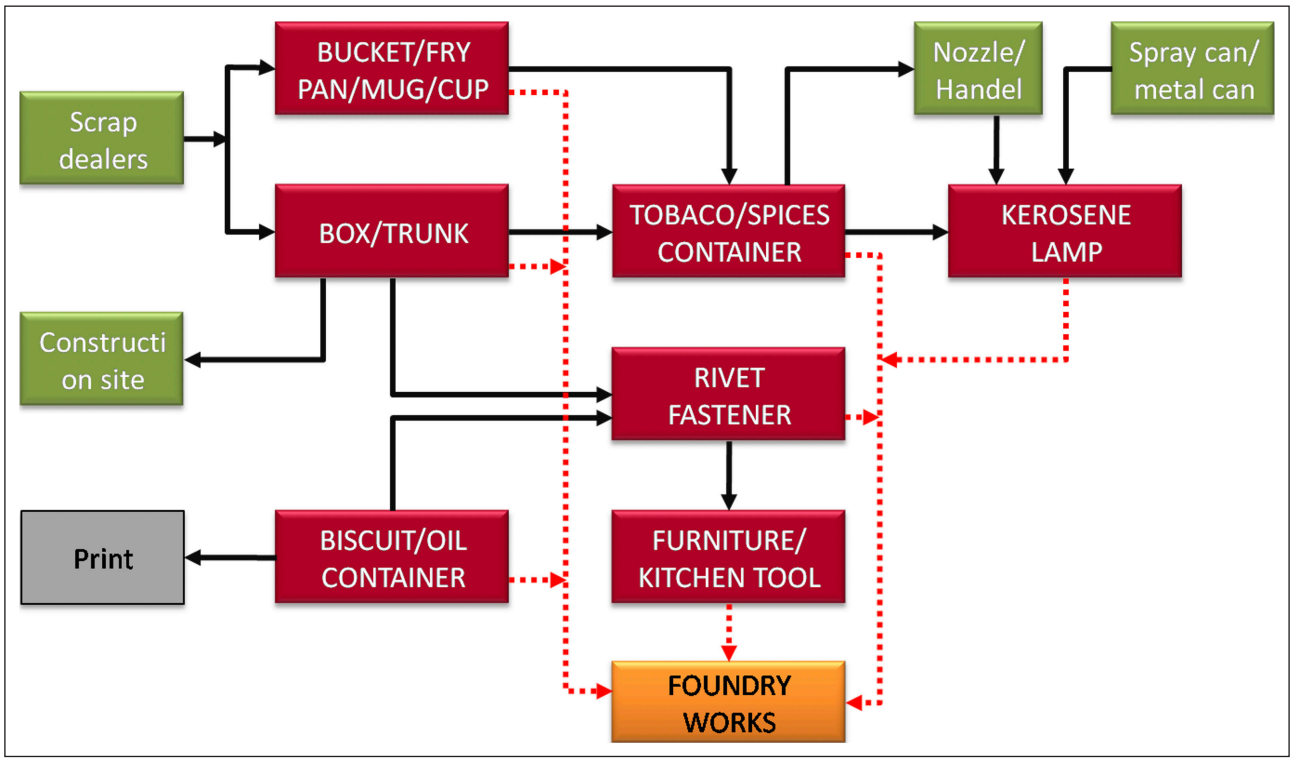


**Figure 12**. Flow of material in the metal products manufacturing clusters in Imamganj.

In this example, flow of metal was closed with nearly all industrial units located in Imamganj. The material cycle is graphically represented as follows (Fig. 11).

**Pattern 4: Shoe Manufacturing**

This was a cluster of industries in the Kamalbagh area that manufactured affordable plastic shoes, sandals, small toys and trifle items. The industries were popularly termed as factories. This study focused on shoemaking.

The factories primarily used Chlorinated Paraffin Wax (CPW) and Ethylene Vinyl Acetate (EVA) as raw materials, obtained locally or imported. CPW and EVA were used in the production of rubber and Polymerized Vinyl Chloride (PVC) in the shoe factories. Rubber formed the sole and lower part of the shoe, while PVC was used for the upper part. Rubber sheets were cut for soles, with leftover sheets recycled for reuse. PVC was molded into desired shapes for the upper parts, and any leftover PVC was recycled within the production cycle. Occasionally, minimal amount of waste PVC was sold to the nearby plastic factories that manufacture small toys and trifle items like tiffin box, container box, mug, watering can, soap case, pen stand etc (Fig. 12).

**Figure 13**. EVA raw material for producing rubber sheets, newly produced rubber sheets, dice for preparing shoe sole and newly produced PVC sandal straps (left to right).

**Figure 14**. First grade (newly produced) shoes, left over cuts of soles to be reused in the production (left to right).

Shoes produced from new raw materials were termed as first grade shoes. In addition to the standard production chain, waste and used plastic shoes were utilized as raw materials. Such items were collected from scrap dealers and various sources cleaned and different parts were crushed and incorporated into the production line. Recycling occurred at least twice resulting in second and third-grade shoes with diminishing quality. The color in recycled shoes had non uniform color and the blend had back or close to black hue. Recycled shoes were often painted black or another dark hue to mask their messy colors (Fig. 13, 14).

The quality of shoes decreased with each recycle, with third-grade shoes being the lowest in quality, but cheapest. Newly produced and recycled parts were sometimes mixed in the same shoe to reduce costs but at the expense of quality. Shredded plastic and rubber items that couldn't be reused were sold to scrap dealers and brick kilns, serving as fuel (Fig. 15).

This shoe cluster maintained a closed material cycle, with all residuals reused within the production line. Old and scrapped shoes underwent recycling up to three times in the same production line. Any remaining waste, if produced, was utilized in nearby plastic factories. This cycle closely resembled the conceptual framework of a closed material cycle, with onsite and offsite recycling, resulting in various types of new, recycled, and mixed-grade shoes. The material cycle is graphically presented below (Fig. 16).

The IE and IS concepts are often seen as designed approaches, hence, leading to a perception that their application are primarily confined to eco industrial parks [52–55]. Although there are examples of such relation that have evolved gradually, but again such examples are usually found within a specified place boundary like the Kalundborg [52, 57]. The studied examples in Dhaka are outside the scope of eco-industrial park or any other kind of formal approach of industrial area. Hence, the designed territorial approaches cannot be applied as verbatim, instead relevance with the core idea of IS is meaningful (Fig. 17).

In the industrial enclave, it is not uncommon to observe many types of exchanges among the industrial units, but this does not necessarily mean IS [98]. The development of symbiotic relation can be identified in different stages such as Sprouting, Uncovering and Embeddedness and Institutionalization [98]. Sprouting is the early stage where firms begin to exchange resources randomly. This initial exchange is considered as the kernels of IS which many or may not lead to further exchange activities [57]. Uncovering refers to the disclosure of exchange networks with environmental bene-

**Figure 15**. Old shoes for recycling, crushed chips of old shoes and recycled sheets (left to right).

**Figure 16**. Second grade shoes in black hue, third grade shoes in black hue, painted third grade shoes and mixed grade shoe soles where the pink part is new and the black part is recycled (left to right).

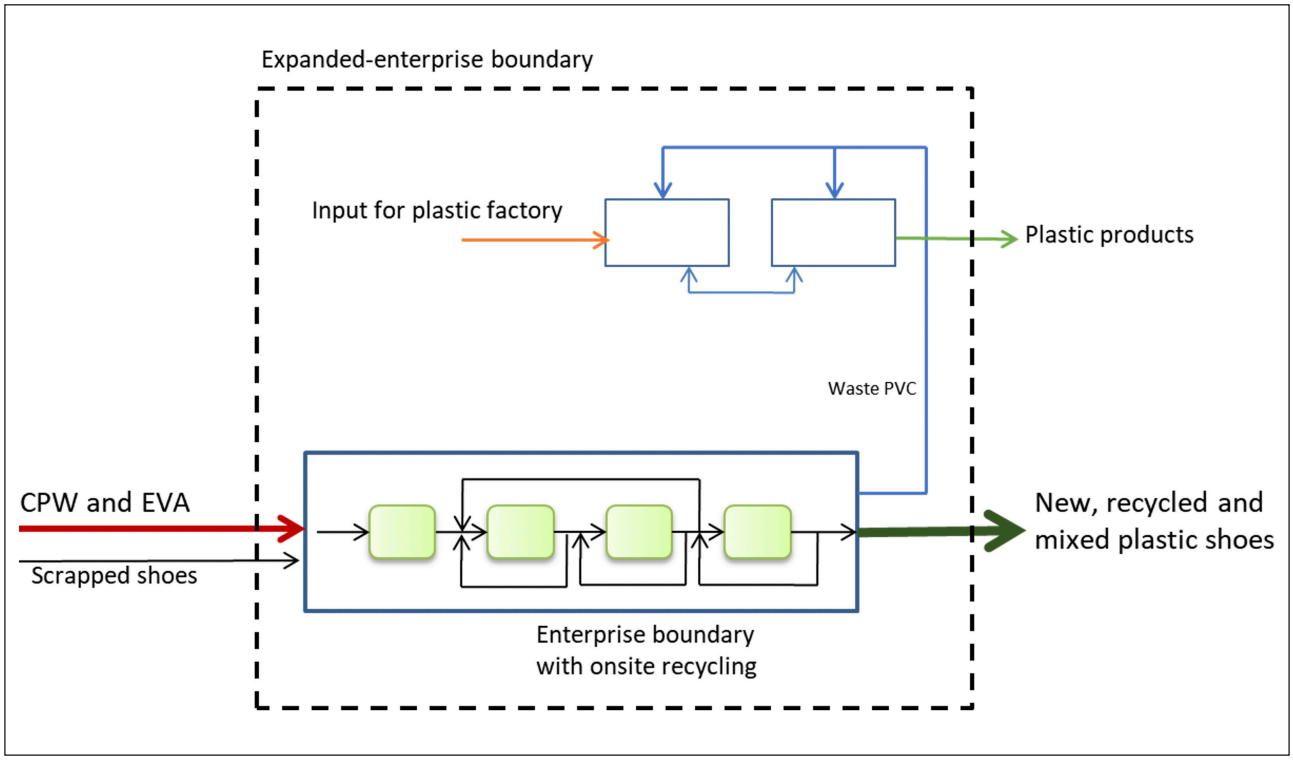


**Figure 17**. Flow of material in the plastic shoe manufacturing cluster in Kamalbagh area.

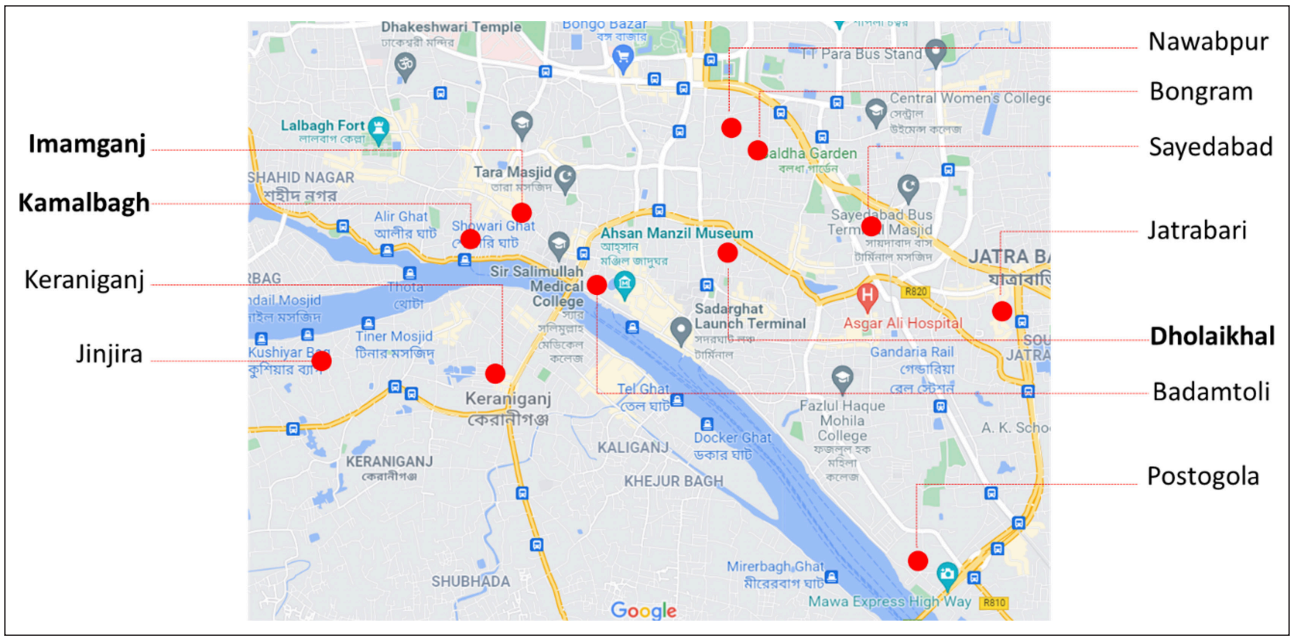


**Figure 18**. Geographical location of the industrial clusters, modified from Google Map view.

fits through observation, usually by an actor whose focus is beyond the private transactional network [57]. Usually in this stage, horizon and members of the networks increase. Further nourishment of such self-organizing developments leads to institutionalization of the entire system to support maneuvering and growth. 5 types of exchange networks are considered for eco-industrial parks [52]. They are

- Type 1: through waste exchanges
- Type 2: within a facility, firm, or organization
- Type 3: among firms co-located in a defined eco-industrial park
- Type 4: among local firms that are not co-located
- Type 5: among firms organized "virtually" across a broader region

In this typology, type 1 is the simplest category and the type 2 to type 5 are considered as true industrial symbiosis in the eco-industrial park model. Type 5 model depends more on the virtual linkage than the physical co-location although such virtual eco-industrial parks are of course place based. This model simply takes the advantage of increasing the number of participating firms by increasing the boundary.

The studied examples contain several types of industrial units or clusters of similar industrial units. Clustering, a common feature of old Dhaka, was observed in close proximity, if not in the same area, and occasionally sparsely scattered, such as on the other side of the river. Typically, the distance was always to be covered either by foot or with informal transport like handcart or pushcart, without contributing to the production cost substantially. Geographical location of the clusters is shown in Figure 18. Such arrangements of clusters were not designed or guided, rather evolved out of need. Thus, clusters were found place based and virtually linked, aligned with the argument for extending the boundary of industrial park for considering IS [56] and reveal that geographical proximity is not an absolute necessity for IS [99]. There was no mention of any support program related to IS or similar principles by any public or private agencies. Therefore, the studied examples clearly demonstrate a 'self-organizing' system. The examples also goes in line with the observation in the study of ship braking industries in Sitakunda-Bhatiary that entrepreneurial activities foster more than the territorial agglomeration for IS, at least in Bangladesh [40].

Considering the analysis of material flow, inside the enterprise boundary, outside the enterprise boundary, within the extended enterprise boundary, within the enterprise cluster boundary and inside/outside of related clusters of enterprises, this study identified sustainable waste management practices. These practices and the links among different industrial units/clusters clearly show the application of Industrial Symbiosis principles.

The studied loops identified more developed stages than the sprouting level and uncovered the existence of different exchange networks and sustainable practices of resource consumption, but not much beyond this. The clusters were geographically scattered and virtually linked, which resembles with the Type 5 exchange network. Metal industries and metal scrap dealing business are usually considered as Type 5 exchange [100]. The tire retreading cluster and shoe manufacturing clusters demonstrated the level of decent practice with almost all the residual waste reused in the production line within the cluster or with a little extended boundary of the cluster, particularly the shoe cluster additionally incorporated recycling of old and scrapped products in the production line. Thus, these clusters resemble the Type 2 exchange, which contains the true nature of IS.

During this study, the entrepreneurs were asked about the rationale for recycle, recover and reuse of material and

questioned about IE principles, CP technologies and environmental concerns. Their responses provide a simple and logical answer, to minimize the cost; there was no evidence of knowledge of IE or CP, nor any concern for environmental responsibility. This is a sharp contrast from the academic literature that put much emphasis in the environmental benefit. Theoretical conceptualization portrays environmental concern as a prominent driving force for IS [52, 57, 63, 98, 101–104], and literature about real-life examples, mostly in the Euro-American region and Eastern Asia, indeed demonstrate environmental benefit [54, 55, 65, 101, 103, 105–107]. However, it appears that the academic discourse has not dig deeper into the question if environmental benefit is the prime drive for IS, and significance of other drivers. This study clearly revealed that environmental benefit was not the prime consideration for waste exchange, suggesting sustainable resource consumption not necessarily stem solely from environmental concerns; economic benefit can dominate the drive. This realization can be helpful in pollution reduction strategies for developing economies. Beside formal legislative controls, emphasis on economic benefit and example form the informal sector may have positive impact for the organized industrial sector as well.

This study, covering only a few areas with concentration of informal industries in old Dhaka, identifies various economic activities driven by resource sharing and consumption minimization. The informal businesses, spanning manufacturing, recycling, and services, are observed to be closely interconnected and operated within the same or extended household oriented small enterprise. Such chains are difficult to separate and attempts to disrupt these interconnected chains may impact business flow. Beyond the 4 closed loops that were studied in detail, the initial exchange, which is the kernel of IS, were observed in many areas. This study suggests potential unexplored exchange networks that demand further research for comprehensive understanding.

## CONCLUSION

This study recognizes sustainable waste management practices in some selected small scale informal industries in Dholaikhal, Imamganj and Kamalbagh areas of Dhaka. Considering material flow analysis, this study identifies industrial symbiosis in the study areas. It also suggests that more examples are likely to be recognized in other industrial clusters there. There is a clear indication that the entire informal manufacturing business sector practices waste recovery and recycling at various levels and there exist complicated and intricate symbiotic relations amongst the different types of industrial clusters. However, in identifying this, the study had some limitations, it only looked at the flow of material and the flow of energy or other components were out of the scope in this research. Moreover, the flow of material was studied qualitatively, it was not inclusive nor quantified.

Though the study does not provide quantifiable data, but it provides a generalized qualitative overview of the waste management practice in the informal sector manufacturing industries. This suggests that application of IE and CP principles has a great potential to be exercised in other industrial sectors, provided that a strong knowledge and human resource base is created, and necessary technologies are made available and supported. It may sound simple, but the task is not easy. Further investigations and in-depth studies are required to identify examples and the modality for transferring the concept. Formalization of the informal sector may not be the target, rather identification and promotion of best practices as well as incentives may be more helpful in the informal sector. Proper policy support, regulatory mechanism and an enabling framework can extend such practice in the formal industrial sector which can contribute considerably to pollution abatement.

## ACKNOWLEDGEMENTS

Hereby the author expresses gratitude to Devashis Biswas, Emon Choudhury, Fayaz Lazim and Maisha Samiha for their contribution in collecting field data. The author is also thankful to the unknown reviewers for their valuable suggestion that enhanced this article.

## DATA AVAILABILITY STATEMENT

The author confirm that the data that supports the findings of this study are available within the article. Raw data that support the finding of this study are available from the corresponding author, upon reasonable request.

## CONFLICT OF INTEREST

The author declared no potential conflicts of interest with respect to the research, authorship, and/or publication of this article.

## USE OF AI FOR WRITING ASSISTANCE

Not used.

## ETHICS

There are no ethical issues with the publication of this manuscript.

## REFERENCES

[1] A. D. Basiago, "Methods of defining 'sustainability'," Sustainable Development, Vol. 3(3), pp. 109–119, 1995. [CrossRef]

[2] J. M. Harris, "Sustainability and sustainable development," International Society for Ecological Economics, Vol. 1(1), pp. 1–12, 2003.

[3] S. Vanderheiden, "Conservation, foresight, and the future generations problem," Inquiry, Vol. 49(4), pp. 337–352, 2006. [CrossRef]

[4] T. Kuhlman, and J. Farrington, "What is sustainability?," Sustainability, Vol. 2(11), pp. 3436–3448, 2010. [CrossRef]

[5] H. Briassoulis, "Sustainable development and the informal sector: An uneasy relationship?," The Jour-

nal of Environment & Development, Vol. 8(3), pp. 213–237, 1999. [CrossRef]
[6] J. C. Dernbach, and F. Cheever, "Sustainable development and its discontents," Transnational Environmental Law, Vol. 4(2), pp. 247–287, 2015. [CrossRef]
[7] E. Holden, K. Linnerud, and D. Banister, "Sustainable development: Our common future revisited," Global Environmental Change, Vol. 26, pp. 130–139, 2014. [CrossRef]
[8] H. Briassoulis, "Sustainable development — The formal or informal way?," in Environmental Politics in Southern Europe, Vol. 29, K. Eder and M. Kousis, Eds., Dordrecht: Springer Netherlands, pp. 73–99, 2001. [CrossRef]
[9] N. Sultana, M. M. Rahman, and R. Khanam, "The effect of the informal sector on sustainable development: Evidence from developing countries," Business Strategy and Development, Vol. 5(4), pp. 437–451, 2022. [CrossRef]
[10] J. H. Jati, S. R. Giyarsih, and L. Muta'ali, "The influence of characteristics of worker and business on the income of informal sector workers in Yogyakarta," Populasi, Vol. 29(1), pp. 77–92, 2021. [CrossRef]
[11] E. Rodríguez-Oreggia, "The informal sector in Mexico: Characteristics and dynamics," Perspectivas Sociales= Social Perspectives, Vol. 9(1), pp. 89–156, 2007.
[12] C. Olaya, and S. Caicedo, "Towards a system dynamics model of De Soto's theory on informal economy," Accessed on Oct 16, 2023. https://papers.ssrn.com/sol3/papers.cfm?abstract_id=2764107
[13] J. Charmes, "The informal economy worldwide: Trends and characteristics," Margin: The Journal of Applied Economic Research, Vol. 6(2), pp. 103–132, 2012. [CrossRef]
[14] C. C. Williams, "Out of the shadows: a classification of economies by the size and character of their informal sector," Work, Employment and Society, Vol. 28(5), pp. 735–753, 2014. [CrossRef]
[15] D. C. Wilson, C. Velis, and C. Cheeseman, "Role of informal sector recycling in waste management in developing countries," Habitat International, Vol. 30(4), pp. 797–808, 2006. [CrossRef]
[16] A. O. Afon, "Informal sector initiative in the primary sub-system of urban solid waste management in Lagos, Nigeria," Habitat International, Vol. 31(2), pp. 193–204, 2007. [CrossRef]
[17] P. J. M. Nas, and R. Jaffe, "Informal waste management," Environment, Development and Sustainability, Vol. 6(3), pp. 337–353, 2004. [CrossRef]
[18] M. Vaccari, and A. Perteghella, "Resource recovery from waste by Roma in the Balkans: A case study from Zavidovici (BiH)," Waste Management & Research, Vol. 34(9), pp. 866–874, 2016. [CrossRef]
[19] M. Zahur, and S. Otoma, "Informal waste recycling activities: A case study of Dhaka City, Bangladesh," in Proceedings of the Annual Conference of Japan Society of Material Cycles and Waste Management The 24th Annual Conference of Japan Society of Material Cycles and Waste Management, Japan Society of Material Cycles and Waste Management, 2013, Article 671, 2023.
[20] H. Yang, M. Ma, J. R. Thompson, and R. J. Flower, "Waste management, informal recycling, environmental pollution and public health," Journal of Epidemiology and Community Health, Vol. 72(3), pp. 237–243, 2018. [CrossRef]
[21] S. Chaudhuri and U. Mukhopadhyay, "Informal sector, pollution and waste management," in Revisiting the Informal Sector, pp. 183–212, Springer, 2010. [CrossRef]
[22] A. Blackman, "Informal sector pollution control: What policy options do we have?," World Development, Vol. 28(12), pp. 2067–2082, 2000. [CrossRef]
[23] A. Blackman, and G. J. Bannister, "Pollution control in the informal sector: The Ciudad Juárez brickmakers' project," Natural Resources Journal, Vol. 37, Article 829, 1997.
[24] L. O. Mbeng, "Informal waste recovery and recycling: Alleviating poverty, environmental pollution and unemployment in Douala, Cameroon," Journal of Scientific Research & Reports, Vol. 2(1), pp. 474-490, 2013.
[25] S. Pratap, and E. Quintin, The Informal Sector in Developing Countries: Output, Assets and Employment. WIDER Research Paper, 2006. Accessed on Nov 07, 2023. https://www.econstor.eu/handle/10419/63326
[26] S. Pratap, and E. Quintin, "The informal sector in developing countries," United Nations University, 2006, Accessed on Nov 07, 2023. https://citeseerx.ist.psu.edu/document?repid=rep1&type=pdf&doi=3ed4931c6b036b3c8e77811d772d0867be-c63a1f
[27] H. Arvin-Rad, A. K. Basu, and M. Willumsen, "Economic reform, informal–formal sector linkages and intervention in the informal sector in developing countries: A paradox," International Review of Economics & Finance, Vol. 19(4), pp. 662–670, 2010. [CrossRef]
[28] F. Urban, and J. Nordensvard, "Low Carbon Development: Key Issues," Routledge, 2013.
[29] E. B. Barbier, "Poverty, development, and environment," Environment and Development Economics, Vol. 15(6,), pp. 635–660, 2010. [CrossRef]
[30] S. Roy, "Development, environment and poverty: Some issues for discussion," Economic and Political Weekly, pp. PE29–PE41, 1996.
[31] A. Markandya, "Poverty, environment and development," Frontiers of Environmental Economics, pp. 192–213, 2001. [CrossRef]
[32] R. G. Bell and C. Russell, "Environmental policy for developing countries," Issues in Science and Technology, Vol. 18(3), pp. 63–70, 2002.
[33] H. U. Chowdhury, "Informal economy, governance, and corruption," Philippine Journal of Development, Vol. 32(2), pp. 103–134, 2005.

[34] M. M. Hossan, "Evolution of environmental policies in Bangladesh (1972-2010)," Journal of the Asiatic Society of Bangladesh, Vol. 59(1), pp. 39–63, 2014.
[35] G. J. Alam, "Environmental pollution of Bangladesh—it's effect and control," Pulp and Paper, Vol. 51(13), Article 17, 2009.
[36] M. G. Rasul, I. Faisal, and M. M. K. Khan, "Environmental pollution generated from process industries in Bangladesh," International Journal of Environment and Pollution, Vol. 28(1/2), Article 144, 2006. [CrossRef]
[37] A. Karmaker, M. Hasan, and S. Ahmed, "A modified approach to Industrial Pollution Projection System for the assessment of sectoral pollution loads in Bangladesh," Environmental Monitoring and Assessment, Vol. 194(6), Article 406, 2022. [CrossRef]
[38] C. Lelia, and S. Maria, "Benefits and costs of the informal sector: The case of brick kilns in Bangladesh," Journal of Environmental Protection, Vol. 3(6), Article 20050, 2012.
[39] N. Sultana, M. M. Rahman, R. Khanam, K. Z. Islam, and M. R. I. Rayhan, "Investigating the prospect of cleaner production in informal enterprises: A scientific assessment of environmental burdens and economic efficiency," Heliyon, Vol. 9(3), 2023. [CrossRef]
[40] N. Gregson, M. Crang, F. U. Ahamed, N. Akter, R. Ferdous, S. Foisal, R. Hudson, "Territorial agglomeration and industrial symbiosis: Sitakunda-Bhatiary, Bangladesh, as a secondary processing complex," Economic Geography, Vol. 88(1), pp. 37–58, 2012. [CrossRef]
[41] A. Bain, M. Shenoy, W. Ashton, and M. Chertow, "Industrial symbiosis and waste recovery in an Indian industrial area," Resources, Conservation and Recycling, Vol. 54(12), pp. 1278–1287, 2010. [CrossRef]
[42] N. Dutt, and A. A. King, "The judgment of garbage: End-of-pipe treatment and waste reduction," Management Science, Vol. 60(7), pp. 1812–1828, 2014. [CrossRef]
[43] C.-Y. Young, S.-P. Ni, and K.-S. Fan, "Working towards a zero waste environment in Taiwan," Waste Management & Research, Vol. 28(3), pp. 236–244, 2010. [CrossRef]
[44] N. E. Gallopoulos, "Industrial ecology: An overview," Progress in Industrial Ecology, Vol. 3(1/2), Article 10, 2006. [CrossRef]
[45] F. den Hond, "Industrial ecology: A review," Regional Environmental Change, Vol. 1, pp. 60–69, 2000. [CrossRef]
[46] T. Curran, and I. D. Williams, "A zero waste vision for industrial networks in Europe," Journal of Hazardous Materials, Vol. 207, pp. 3–7, 2012. [CrossRef]
[47] F. S. Lyakurwa, "Industrial ecology a new path to sustainability: An empirical review," Independent Journal of Management & Production, Vol. 5(3), pp. 623–635, 2014. [CrossRef]
[48] Q. A. Mowla, and S. Biswas, "Concepts of sustainable development: An analytical review," Journal of Administrative Studies, Vol. 2(1), pp. 5–16, 2009.
[49] L. Baas, and O. Hjelm, "Support your future today: Enhancing sustainable transitions by experimenting at academic conferences," Journal of Cleaner Production, Vol. 98, pp. 1–7, 2015. [CrossRef]
[50] M. Despeisse, P. D. Ball, S. Evans, and A. Levers, "Industrial ecology at factory level–a conceptual model," Journal of Cleaner Production, Vol. 31, pp. 30–39, 2012. [CrossRef]
[51] L. W. Baas, and L. Baas, "Cleaner Production and Industrial Ecology: Dynamic Aspects of the Introduction and Dissemination of New Concepts in Industrial Practice," Eburon Uitgeverij BV, 2005. Accessed on Nov 07, 2023. https://books.google.com/books?hl=en&lr=&id=QAVFuUi-uXUC&oi=fnd&pg=PA1&dq=industrial+ecology+++baas++2005+thesis+&ots=2blSOc6v6P&sig=F444L6QOHH1VUhawD73qv6mCZIA
[52] M. R. Chertow, "Industrial symbiosis: Literature and taxonomy," Annual Review of Energy and the Environment, Vol. 25(1), pp. 313–337, 2000. [CrossRef]
[53] S. K. Behera, J.-H. Kim, S.-Y. Lee, S. Suh, and H.-S. Park, "Evolution of 'designed' industrial symbiosis networks in the Ulsan Eco-industrial Park: 'Research and development into business' as the enabling framework," Journal of Cleaner Production, Vol. 29, pp. 103–112, 2012. [CrossRef]
[54] Y. Geng, P. Zhang, R. P. Côté, and T. Fujita, "Assessment of the national eco-industrial park standard for promoting industrial symbiosis in China," Journal of Industrial Ecology, Vol. 13(1), pp. 15–26, 2009. [CrossRef]
[55] F. Yu, F. Han, and Z. Cui, "Evolution of industrial symbiosis in an eco-industrial park in China," Journal of Cleaner Production, Vol. 87, pp. 339–347, 2015. [CrossRef]
[56] T. Sterr, and T. Ott, "The industrial region as a promising unit for eco-industrial development—Reflections, practical experience and establishment of innovative instruments to support industrial ecology," Journal of Cleaner Production, Vol. 12(8–10), pp. 947–965, 2004. [CrossRef]
[57] M. R. Chertow, "'Uncovering' industrial symbiosis," Journal of Industrial Ecology, Vol. 11(1), pp. 11–30, 2008. [CrossRef]
[58] I. Costa, G. Massard, and A. Agarwal, "Waste management policies for industrial symbiosis development: Case studies in European countries," Journal of Cleaner Production, Vol. 18(8), pp. 815–822, 2010. [CrossRef]
[59] P. Desrochers, "Cities and industrial symbiosis: Some historical perspectives and policy implications," Journal of Industrial Ecology, Vol. 5(4), pp. 29–44, 2001. [CrossRef]
[60] G. Duranton, and D. Puga, "Micro-foundations of urban agglomeration economies," in Handbook of Regional and Urban Economics, Vol. 4, pp. 2063–2117, Elsevier, 2004. [CrossRef]
[61] P. Krugman, "Increasing returns and economic ge-

ography," Journal of Political Economy, Vol. 99(3), pp. 483–499, 1991. [CrossRef]
[62] L. Baas, "Planning and uncovering industrial symbiosis: Comparing the Rotterdam and Östergötland regions: Strategies for manufacturing," Business Strategy and the Environment, Vol. 20(7), pp. 428–440, 2011. [CrossRef]
[63] M. R. Chertow, and D. R. Lombardi, "Quantifying economic and environmental benefits of co-located firms," Environmental Science & Technology, Vol. 39(17), pp. 6535–6541, 2005. [CrossRef]
[64] M. R. Chertow, W. S. Ashton, and J. C. Espinosa, "Industrial symbiosis in Puerto Rico: Environmentally related agglomeration economies," Regional Studies, Vol. 42(10), pp. 1299–1312, 2008. [CrossRef]
[65] Q. Zhu, E. A. Lowe, Y. Wei, and D. Barnes, "Industrial symbiosis in China: A case study of the Guitang Group," Journal of Industrial Ecology, Vol. 11(1), pp. 31–42, 2008. [CrossRef]
[66] P. H. Nhat, "Eco-Modernizing Small and Medium-Sized Agro-Industries in Vietnam," Wageningen University and Research, 2007. Accessed on Nov 07, 2023. https://search.proquest.com/openview/b811532ca3acd4d0df980d4186820871/1?pq-origsite=gscholar&cbl=2026366&diss=y
[67] M. Chertow, W. Ashton, and R. Kuppalli, "The industrial symbiosis research symposium at Yale: Advancing the study of industry and environment," 2004. Accessed on Nov 07, 2023. https://elischolar.library.yale.edu/fes-pubs/23/
[68] H. De Soto, "Informality in the process of development and growth," The Other Path. Harper & Row, New York, 1989. Accessed: Nov. 07, 2023. [Online]. Available: https://pdfs.semanticscholar.org/ed48/ad31ae1779a3dce330c1afdfe152e1f7fc55.pdf
[69] A. Roy, "Why India cannot plan its cities: Informality, insurgence and the idiom of urbanization," Planning Theory, vol. 8(1), pp. 76–87, 2009. [CrossRef]
[70] A. Roy, "Urban informality: Toward an epistemology of planning," Journal of the American Planning Association, Vol. 71(2), pp. 147–158, 2005. [CrossRef]
[71] R. B. Recio, I. Mateo-Babiano, and S. Roitman, "Revisiting policy epistemologies on urban informality: Towards a post-dualist view," Cities, Vol. 61, pp. 136–143, 2017. [CrossRef]
[72] A. Hasan, "The changing nature of the informal sector in Karachi as a result of global restructuring and liberalization," Environment and Urbanization, Vol. 14(1), pp. 69–78, 2002. [CrossRef]
[73] D. Tunas, "The spatial economy in the urban informal settlement," International Forum on Urbanism, 2008.
[74] A. I. Moreno-Monroy, J. Pieters, and A. A. Erumban, "Formal sector subcontracting and informal sector employment in Indian manufacturing," IZA Journal of Labor & Development, Vol. 3(1), Article 22, 2014. [CrossRef]
[75] A. T. M. Amin, and A. Singh, "The Informal Sector in Asia from the Decent Work Perspective. International Labour Organization," 2002. Accessed on Nov 07, 2023. https://econpapers.repec.org/paper/iloilowps/993551963402676.htm
[76] S. A. Ahmed, and M. Ali, "Partnerships for solid waste management in developing countries: Linking theories to realities," Habitat International, Vol. 28(3), pp. 467–479, 2004. [CrossRef]
[77] U. Glawe, C. Visvanathan, and M. Alamgir, "Solid waste management in least developed Asian countries–a comparative analysis," in International Conference on Integrated Solid Waste Management in Southeast Asian Cities, 2005, pp. 5–7, 2023.
[78] A. Matter, M. Dietschi, and C. Zurbrügg, "Improving the informal recycling sector through segregation of waste in the household–The case of Dhaka, Bangladesh," Habitat International, Vol. 38, pp. 150–156, 2013. [CrossRef]
[79] A. Matter, M. Ahsan, M. Marbach, and C. Zurbrügg, "Impacts of policy and market incentives for solid waste recycling in Dhaka, Bangladesh," Waste Management, Vol. 39, pp. 321–328, 2015. [CrossRef]
[80] A. S. M. Riyad, "Scenario of paper waste recycling and reuse practices in Khulna city of Bangladesh," International Journal of Scientific & Engineering Research, Vol. 5(3), pp. 705–711, 2014.
[81] T. B. Yousuf, and M. Rahman, "Monitoring quantity and characteristics of municipal solid waste in Dhaka City," Environmental Monitoring and Assessment, Vol. 135, pp. 3–11, 2007. [CrossRef]
[82] P. van Beukering, "An economic analysis of different types of formal and informal entrepreneurs, recovering urban solid waste in Bangalore (India)," Resources, Conservation and Recycling, Vol. 12(3–4), pp. 229–252, 1994. [CrossRef]
[83] A. Luthra, "Efficiency in waste collection markets: Changing relationships between firms, informal workers, and the state in urban India," Environment and Planning A, Vol. 52(7), pp. 1375–1394, 2020. [CrossRef]
[84] JICA, "The Study on the Solid Waste Management in Dhaka City," Dhaka City Corporation, Dhaka, 2005. https://openjicareport.jica.go.jp/pdf/11785243.pdf Accessed on Jun 18, 2024.
[85] M. Zahur, "Solid waste management of Dhaka city: public private community partnership," 2007, Accessed on Nov 08, 2023. http://dspace.bracu.ac.bd/xmlui/handle/10361/399
[86] S. Biswas, "Exploring the Closed Material Cycle Investigating the case of Small Scale Informal Industries in Dholaikhal, Dhaka," Erasmus University Rotterdam, Rotterdam, 2008.
[87] K. Z. H. Taufique, D. Saha, and S. Biswas, "In Search for a New Urban Design Research Methodology Suitable For Dhaka, a Peripheral Megacity," in Urban Design Research: Method and Application, Birmingham: Birmingham City University, 2009, pp. 73–89. Accessed on Nov 08, 2023. https://www.

academia.edu/download/55183475/Published_Proceedings.pdf#page=77
[88] A. N. Amin, "The Informal Sector and Urban Poor," Dhaka: Bangladesh Rural Advancement Committee (BRAC), Dhaka, 2016, Accessed on Nov 08, 2023. https://www.researchgate.net/profile/Atm-Amin/publication/311649418_The_Informal_Sector_and_the_Urban_Poor/links/58523f6908ae0c0f322145af/The-Informal-Sector-and-the-Urban-Poor.pdf
[89] K. Salahauddin, and I. Shamim, "Women in Urban Informal Sector: Employment Pattern Activity Types and Problems," Women for Women, 1992.
[90] F. Siddique, "A planning study of the Dolaikhal area for its improvement as an informal enterprise industrial district in Dhaka," PhD Thesis, Masters Thesis, Asian Institute of Technology, Bangkok, 1996.
[91] M. Arif Robbani, "Factors influencing the location and distribution of small scale informal industries in Dhaka city," 2011, Accessed on Nov 08, 2023. http://lib.buet.ac.bd:8080/xmlui/handle/123456789/653
[92] S. M. Rahman, and A. L. Mayer, "How social ties influence metal resource flows in the Bangladesh ship recycling industry," Resources, Conservation and Recycling, Vol. 104, pp. 254–264, 2015. [CrossRef]
[93] R. Kumar, "Research Methodology: A Step-by-Step Guide for Beginners," Sage, 2018.
[94] A. Burger, and T. Silima, "Sampling and sampling design," Journal of Public Administration, Vol. 41(3), pp. 656–668, 2006.
[95] J. W. Drisko, and T. Maschi, "Content Analysis,"Pocket Guide to Social Work Research Methods, 2016. [CrossRef]
[96] K. A. Neuendorf, "The Content Analysis Guidebook," Sage, 2017. [CrossRef]
[97] S. M. Fram, "The constant comparative analysis method outside of grounded theory," The Qualitative Report, Vol. 18, pp. 1, 2013.
[98] M. Chertow, and J. Ehrenfeld, "Organizing self-organizing systems: Toward a theory of industrial symbiosis," Journal of Industrial Ecology, Vol. 16(1), pp. 13–27, 2012. [CrossRef]
[99] D. R. Lombardi, and P. Laybourn, "Redefining industrial symbiosis: Crossing academic–practitioner boundaries," Journal of Industrial Ecology, Vol. 16(1), pp. 28–37, 2012. [CrossRef]
[100] A. D. Sagar and R. A. Frosch, "A perspective on industrial ecology and its application to a metals-industry ecosystem," Journal of Cleaner Production, Vol. 5(1–2), pp. 39–45, 1997. [CrossRef]
[101] L. Sokka, S. Lehtoranta, A. Nissinen, and M. Melanen, "Analyzing the environmental benefits of industrial symbiosis: Life cycle assessment applied to a Finnish forest industry complex," Journal of Industrial Ecology, Vol. 15(1), pp. 137–155, 2011. [CrossRef]
[102] M. Martin, N. Svensson, and M. Eklund, "Who gets the benefits? An approach for assessing the environmental performance of industrial symbiosis," Journal of Cleaner Production, Vol. 98, pp. 263–271, 2015. [CrossRef]
[103] T. Daddi, B. Nucci, and F. Iraldo, "Using life cycle assessment (LCA) to measure the environmental benefits of industrial symbiosis in an industrial cluster of SMEs," Journal of Cleaner Production, Vol. 147, pp. 157–164, 2017. [CrossRef]
[104] A. Neves, R. Godina, S. G. Azevedo, and J. C. Matias, "A comprehensive review of industrial symbiosis," Journal of Cleaner Production, Vol. 247, Article 119113, 2020. [CrossRef]
[105] N. B. Jacobsen, "Industrial symbiosis in Kalundborg, Denmark: A quantitative assessment of economic and environmental aspects," Journal of Industrial Ecology, Vol. 10(1–2), pp. 239–255, 2006. [CrossRef]
[106] A. Neves, R. Godina, H. Carvalho, S. G. Azevedo, and J. C. Matias, "Industrial symbiosis initiatives in United States of America and Canada: Current status and challenges," in 2019 8th International Conference on Industrial Technology and Management (ICITM), IEEE, 2019, pp. 247–251, 2019. [CrossRef]
[107] M. J. Eckelman, and M. R. Chertow, "Life cycle energy and environmental benefits of a US industrial symbiosis," International Journal of Life Cycle Assessment, Vol. 18(8), pp. 1524–1532, 2013. [CrossRef]

*Environ Res Tec, Vol. 7, Issue. 3, pp. 395–405, September 2024*

**Environmental Research and Technology**
https://ert.yildiz.edu.tr - https://dergipark.org.tr/tr/pub/ert
DOI: https://10.35208/ert.1385026

Environmental Research & Technology

**Research Article**

# Thermal analysis of St. John's Wort wastes and biochars: A study of combustion characteristics and kinetics

**Anıl Tevfik KOÇER***

*Health Biotechnology Joint Research and Application Center of Excellence, Yıldız Technical University, İstanbul, Türkiye*

## ARTICLE INFO

*Article history*
Received: 02 November 2023
Revised: 19 March 2024
Accepted: 22 April 2024

**Key words:**
Biochar; Biomass; Combustion kinetic; Thermogravimetric analysis

## ABSTRACT

St. John's wort, extensively utilized in industries such as food, medicine, and cosmetics, generates substantial biomass waste. Utilizing these wastes is crucial to reducing environmental harm and making an economic contribution. This study aimed to determine the potential of St. John's wort wastes and biochar forms produced from these wastes to be used as solid fuel. In this context, the combustion behavior of the biomass and biochar were determined by thermogravimetric analysis method. Additionally, the Kissenger-Akahira-Sunosa and Flynn-Wall-Ozawa techniques were used to compute the combustion activation energies of these samples. According to the analysis, biomass combustion commenced at approximately 250°C and occurred in two stages, whereas biochar combustion initiated at around 400°C and proceeded in a single stage. Furthermore, over 90% of the mass from both samples was observed to decompose during combustion, with average combustion activation energies ranging between 70.08 and 203.86 kJ/mol for biomass and biochar, respectively. These findings suggest that biomass exhibits more readily combustible characteristics compared to biochar but is less energy efficient. In conclusion, optimizing the biochar production process could enhance its energy efficiency and potentially narrow the performance gap between biomass and biochar. Additionally, further research into alternative methods or additives to improve the energy efficiency of biomass combustion is warranted.

**Cite this article as:** Koçer AT. Thermal analysis of St. John's Wort wastes and biochars: A study of combustion characteristics and kinetics. Environ Res Tec 2024;7(3)395–405.

## INTRODUCTION

Waste solid biomass, which includes various organic materials such as agricultural residues, wood waste, and food waste, is becoming one of the most important environmental and economic problems due to the ever-increasing human population and consumption [1]. When stored in landfills or open dumping sites, these wastes can pose risks to human health and ecosystems by releasing some greenhouse gases that intensify climate change, as well as creating leaks that contaminate groundwater and drinking water [2]. Disposal of these wastes by methods such as incineration is not only economically costly but can also result in the release of gases and ashes that can pollute the air, water and soil [3]. For these reasons, people have researched and developed alternative methods to utilize these wastes. One common technique is composting, which involves the controlled decomposition of organic waste to produce nutrient-rich compost [4]. When waste solid biomass is composted, it reduces its volume, prevents methane emissions, and produces a valuable soil amendment. Compost can enhance soil fertility, improve water retention, and reduce the need for chemical fertilizers, hence providing economic benefits for agriculture [5]. Additionally, waste solid bio-

***Corresponding author.**
*E-mail address: anilkocer66@gmail.com

mass can be used as feedstock for the production of bio-based products. Technologies such as anaerobic digestion, pyrolysis and bio-refineries can convert biomass waste into biogas, biochar, bio-based polymers, and biochemical [6]. This facilitates the shift towards a circular economy, where waste is converted into valuable resources, minimizing waste disposal and reducing reliance on non-renewable resources. These techniques not only mitigate environmental impacts but also provide economic benefits, including renewable energy generation, improved soil fertility, and the creation of job opportunities. It is crucial for governments, industries, and individuals to embrace these techniques and promote sustainable waste management practices to safeguard the environment and sustain economic growth [7].

One of the most widely used methods for the utilization of waste solid biomass is biochar production via pyrolysis. Pyrolysis is a thermal decomposition process that involves the breakdown of organic materials at high temperatures in the absence of oxygen. This process is commonly used to convert biomass into valuable by-products such as bio-oil or bio-crude, syngas and biochar [8]. Biochar, a solid carbon-rich residue, is one of the primary outputs of pyrolysis. It is characterized by its high surface area and porosity, attributes that contribute to its remarkable water-holding capacity and nutrient retention capabilities in soils. These properties make biochar an invaluable tool for soil improvement and sustainable agriculture practices [9]. Moreover, biochar exhibits exceptional thermal stability, enabling it to persist in soils for extended periods, effectively sequestering carbon and mitigating climate change as a long-term carbon sink [10]. Its presence in the soil not only enhances soil fertility but also promotes microbial activity, fostering a healthier and more resilient ecosystem [11]. Another area where biochar is widely used is in environmental applications. Biochar, either directly or in the form of activated carbon, is effectively used to remove various pollutants from wastewater [10]. In addition, biochar can also be used in combustion and gasification applications and is recommended as a sustainable alternative to traditional fossil fuels as it contributes to a significant reduction in greenhouse gas emissions [11]. Furthermore, biochar's structural integrity make it an attractive option for construction materials, providing a sustainable solution for building materials and contributing to the development of eco-friendly infrastructure [5]. A wide range of biomass feedstocks can be used for production of biochar by pyrolysis, including but not limited to agricultural residues, forest biomass, energy crops, and industrial waste [9].

One of the most intensive uses of biochar is its use as a source in combustion systems. In this context, in order to increase the combustion efficiency of biochar and to use them more effectively in combustion systems, it is very important to determine their combustion behavior, to examine their combustion mechanisms and to determine their combustion kinetics [11]. Thermogravimetric method is an effective method used extensively for this purpose. This method allows for the investigation of solid fuel combustion behavior and processes as well as the calculation of kinetic parameters utilizing various mathematical models and methodologies [12]. Numerous investigations on the combustion processes of biomasses and the biochar generated from these biomasses have been conducted recently. For instance, in the prior work, the thermogravimetric method was used to examine the combustion of waste biomass (*Aloe vera*) and biochar. The activation energy values of the two materials were determined to be 285 kJ/mol and 150 kJ/mol, respectively [11]. In another study, *Ulva lactuca* seaweed's and its charcoal form's combustion activation energies were found to be around 261 kJ/mol and 146 kJ/mol, respectively [13]. Apart from these, studies on the combustion of biochar produced from different materials such as orange peel [14], bamboo [15] and woody [16] are available in the literature.

This study aims to figure out the combustion characteristics of St. John's wort (*Hypericum perforatum*) plant wastes remaining after extraction and the biochars produced from them, to calculate the combustion kinetics parameters and to compare biomass with biochar in this context. St. John's wort is a medicinal plant known for its intriguing properties and numerous potential uses. In the pharmaceutical sector, it is utilized for the production of herbal remedies, including capsules, tablets, and tinctures, which are commonly used to treat depression and associated symptoms [17]. The plant is also used in the cosmetic industry, where it is incorporated into skincare products such as creams, oils, and lotions due to its potential skin-soothing and healing properties [18]. The demand for St. John's wort products has increased in recent years, driven by a growing interest in natural remedies and alternative medicine. Therefore, it can be said that the waste potential of this plant is quite high. When the literature is examined, although there is a study on the pyrolysis of St. John's wort plant and the characterization of the products released by the pyrolysis reaction [19], there is no study on the combustion of these plant wastes and char produced from them. When considered in this context, the novelty of the present paper lies in its focus on exploring the combustion characteristics of St. John's wort plant wastes and the biochars derived from them, filling a gap in the literature regarding the combustion behavior of this particular biomass waste.

## MATERIALS AND METHODS

### Sample Preparation

St. John's wort plant samples were purchased from a local vendor in İstanbul, Türkiye. 100 grams of dry plant samples were ground into small pieces and then added to 1 L of distilled water and extracted by boiling for about 30 minutes. The suspension obtained after extraction was separated with filter paper and the remained solid pulp was dried in a furnace at the temperature of 70 °C for 1 night. The dried samples were ground again and stored in a desiccator for use in experiments of characterization, production of biochar and combustion.

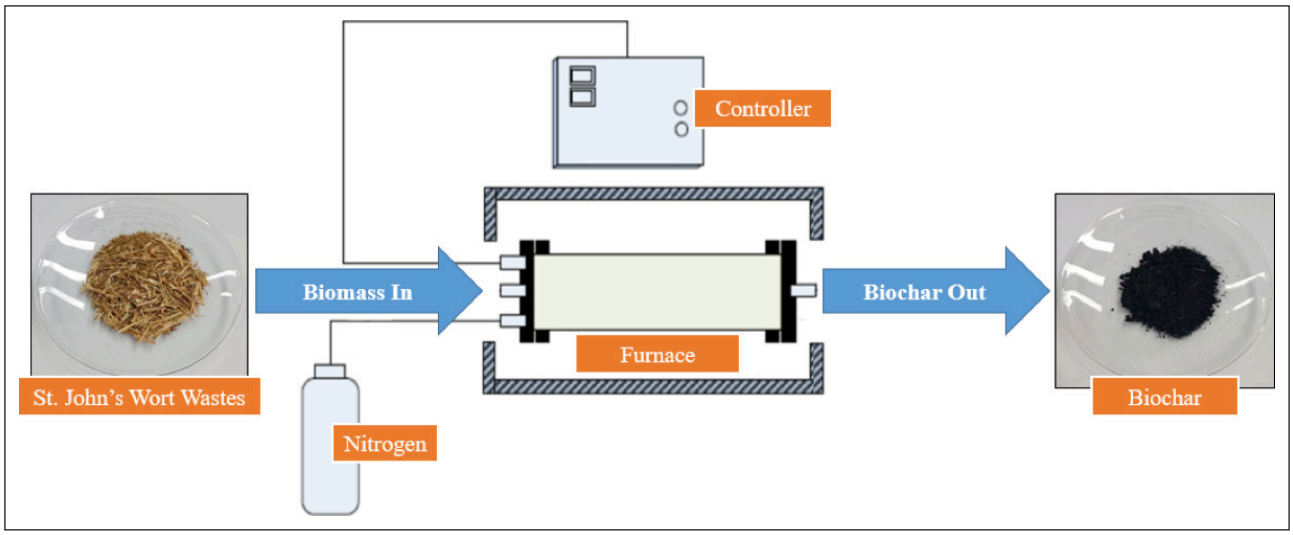


**Figure 1**. Scheme of biochar samples preparation.

The manufacture of biochar from waste biomass was done in a split furnace (Protherm ASP 11/100/500) with a diameter of 0.10 m and dimensions of 0.51 m × 0.40 m × 0.50 m, according to the process outlined by Koçer and Özçimen [13]. The parameters for the biochar synthesis process were determined to be 400 ˚C, 20 ˚C/min of heating, 30 minutes of retention, and 200 mL/min of nitrogen flow. The split furnace was filled with around 20 g of dried and ground biomass samples, and nitrogen gas was introduced for 15 minutes to remove oxygen. The produced biochar samples were removed from the split furnace and stored for characterization and combustion following the thermal reaction and cooling. The diagram showing the biochar production stages is shown in Figure 1.

### Characterization Analyses

Thermal, structural, and proximate analyzes were used to characterize the extracted biomass samples and their biochars. The thermogravimetric analysis (TGA) instrument TA Instruments SDT Q600 was utilized for the thermal analyses of the raw biomass and biochar samples. In this article, five milligrams (mg) of dried samples were placed in an alumina crucible and heated in a dry air environment to a temperature of 800 ˚C, with three different heating speeds (10, 20 and 40 ˚C/min). At 40 mL/min, the dry air flow rate was kept constant. The procedures outlined in Lu and Chen [20] were used to calculate the values of ignition (Ti) and burnout temperature (Tb).

The proximate examination of the biomass and biochar revealed the samples' ash, moisture, volatile matter, and fixed carbon contents. The moisture, volatile matter (VMC), and ash content (AC) of the biomass were determined using a thermogravimetric analyzer in accordance with ASTM standards E 871, E872, and E 1755, in that order. Fixed carbon (FCC) content of biomass was determined by difference [21]. The following Eqs. (1) provided in Parikh et al. [22] were used to compute the higher heating values (HHV) of these samples:

$$HHV=0.3536FCC+0.1559VMC-0.0078AC \quad (1)$$

The elemental compositions of raw biomass and its biochar form were determined using the following equations based on proximate analysis results [23, 24]:

$$C\ (\%)=-35.9972+0.7698VMC+1.3269FCC+0.3250AC \quad (2)$$

$$H\ (\%)=55.3678-0.4830VMC-0.5319FCC-0.5600AC \quad (3)$$

$$O\ (\%)=223.6805-1.7226VMC-2.2296FCC-2.2463AC \quad (4)$$

$$N\ (\%) = 100 - (C + H + O + AC) \quad (5)$$

### Kinetic Theory

Model-free kinetic approaches are most frequently used to pyrolysis and combustion kinetics, as they offer an approximate activation energy estimate based on isothermal and non-isothermal observations [25]. Two of these techniques, the Flynn-Wall-Ozawa (FWO) method and the Kissenger-Akahira-Sunosa (KAS) method, are expressed as follows:

• KAS method [26] expressed as follows:

$$\ln\left[\frac{\beta}{T^2}\right] = \ln\left[\frac{A.E}{R.g(\alpha)}\right] - \frac{E}{R.T} \quad (6)$$

where the activation energy (E) value is determined from the slope of a plot of $\ln(\beta/T^2)$ against 1/T.

• FWO method [27, 28] expressed as follows:

$$\ln\beta = \ln\left[\frac{A.E}{R.g(\alpha)}\right] - 5.331 - 1.052\frac{E}{R.T} \quad (7)$$

where the activation energy (E) value is determined from the slope of a plot of $\ln(\beta)$ against 1/T.

In these equations, β represents the heating rate (K/min), T denotes the temperature (K), A denotes for the frequency factor (1/s), R represents the universal gas constant (8.314 J/mol·K), and α expresses the conversion ratio.

## RESULTS AND DISCUSSION

### Properties of St. John's Wort Wastes

Table 1 presents the characterization results of both the biomass and biochar samples obtained in this study, along

**Table 1.** Characterization of St. John's wort plant waste and biochar samples

| | Units | Biomass | Biochar | Biomass* | Biochar* |
|---|---|---|---|---|---|
| Volatile matter | % | 74.04 | 12.59 | 69.7 | – |
| Fixed carbon | % | 22.81 | 81.28 | 17.6 | – |
| Ash | % | 3.15 | 6.13 | 3.8 | – |
| C | % | 52.29 | 83.58 | 45.6 | 79.6 |
| H | % | 5.71 | 2.62 | 6.4 | 2.48 |
| O | % | 38.21 | 7.00 | 45.5 | 15.12 |
| N | % | 0.64 | 0.71 | 1.8 | 2.06 |
| HHV | MJ/kg | 19.58 | 30.66 | 16.52 | 27.84 |

*: Ateş et al. [19].

with a comparative analysis against findings from existing literature. In this table, the effect of the carbonization process on the biomass content is quite clear. Volatile matter content decreased from 74.04% to 12.59% with the carbonization process, while fixed carbon content increased from 22.81% to 78.41%. The ash content in the biomass did not change during the carbonization process, but the percentage of ash content mathematically increased as the total mass decreased. When the change in elemental composition was examined, it was seen that C and N content increased with the carbonization process, but H and O content decreased. As expected, the increase in C content was due to the transformation of the biomass into a carbon-rich char-like structure. The decrease in H and O content can be attributed to the progressive dehydration reactions and the release of oxygen and hydrogen containing volatiles [29]. The increase in N content can also be attributed to the N content found in non-volatilized structures resistant to thermal degradation and this is supported by studies in the literature [30, 31]. When the higher heating values are compared, it has seen that this value of biochar is higher. This is because the increase in higher heating value is due to the increase in the carbon content of the biochar formed as a result of the pyrolysis reaction, thus leading to an intensification of the mass-energy density [29].

Comparison of the data from the study conducted by Ateş et al. [19] reveals that the biomass samples exhibit similar proximate and elemental compositions, albeit with minor discrepancies.

Despite the utilization of the same plant species in both studies, the reason for these small differences can be attributed to the fact that the biomass used in this study was extracted. Upon comparing the biochar samples, it can be seen that other components are similar to each other, except for O and N contents. The higher O and N contents reported by Ateş et al. [19] could potentially be attributed to the extraction process employed in this study, which may have led to the removal or decomposition of certain N- and O-containing components under the influence of extraction temperatures.

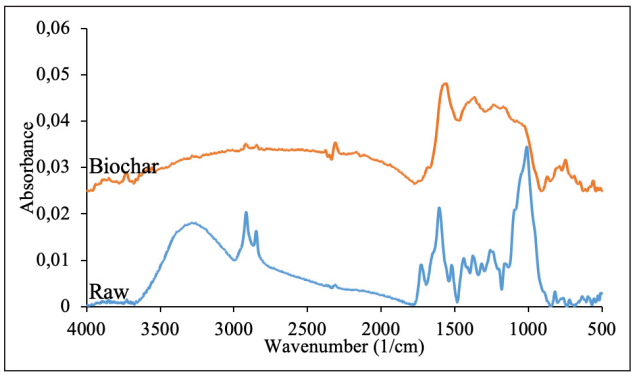


**Figure 2**. FTIR spectrum of samples.

The FTIR spectra of raw biomass waste and their biochar forms are shown in Figure 2. The broad absorption band at 3300 $cm^{-1}$ seen in the spectrum of raw biomass indicates OH stretches due to moisture and alcohol content of the materials [32]. Peaks at 2920 and 2852 $cm^{-1}$ are also due to CH and $CH_2$ stretching [33], while peaks at 1730 and 1600 $cm^{-1}$ indicate C=O stretch and $NH_2$ deformation, respectively. Peaks at 1250 and 1025 $cm^{-1}$ represent the pyranose and furanose rings [34–36]. Peaks at 1570, 1400 and 850 $cm^{-1}$ seen in the FTIR spectra of biochar are due to C=C stretching of hemicelluloses, C-H deformation in cellulose and hemicelluloses and C=C stretching alkene vinylidene, respectively [37]. The effects of the carbonization process on biomass can be seen quite clearly in this figure. Especially the OH, CH and $CH_2$ stresses in the biomass were destroyed during biochar formation. In addition, with this process, the peaks between 1800–1600 $cm^{-1}$ merged and shifted to the 1550 $cm^{-1}$ region. Furthermore, the peak at 1000 $cm^{-1}$ due to the carbohydrate content of the biomass was also reduced as expected.

The SEM images of St. John's wort waste and its biochar form at the magnification of 1000x are shown in Figure 3. In the SEM images of raw biomass waste (Fig. 3a), there are small non-porous pieces and long thin rod-shaped pieces. Due to the degredation of the structure and the movement of mass away from it as a result of the temperature increase during the carbonization reaction, pores and cracks have formed in the structure of the biochar, as depicted in Figure 3b. Con-

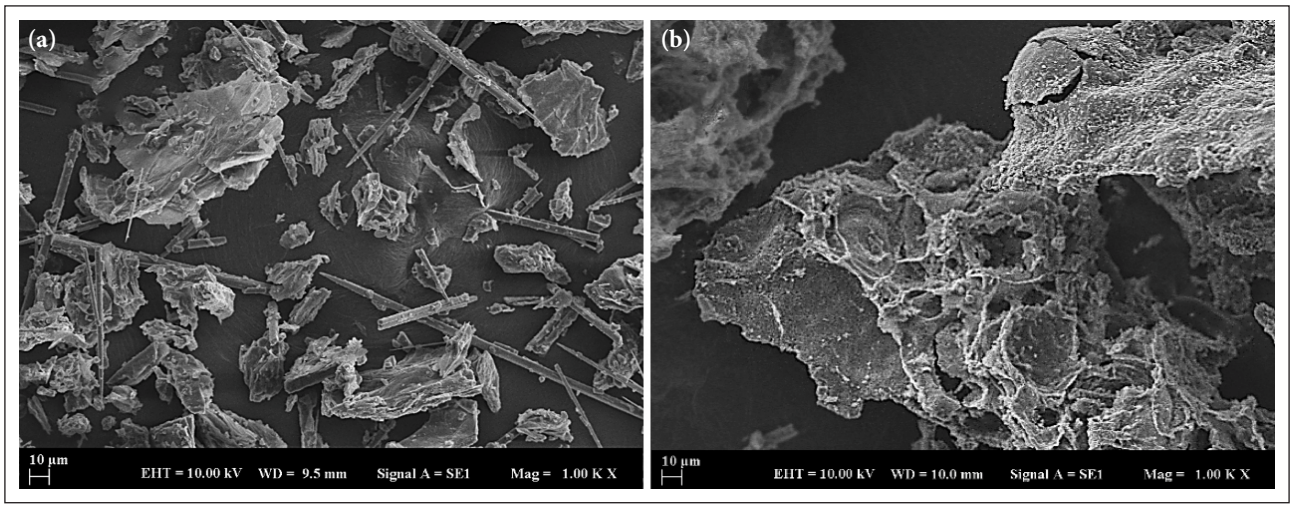


**Figure 3**. SEM images at 1000 x magnifications **(a)** St. John's wort waste, **(b)** biochar.

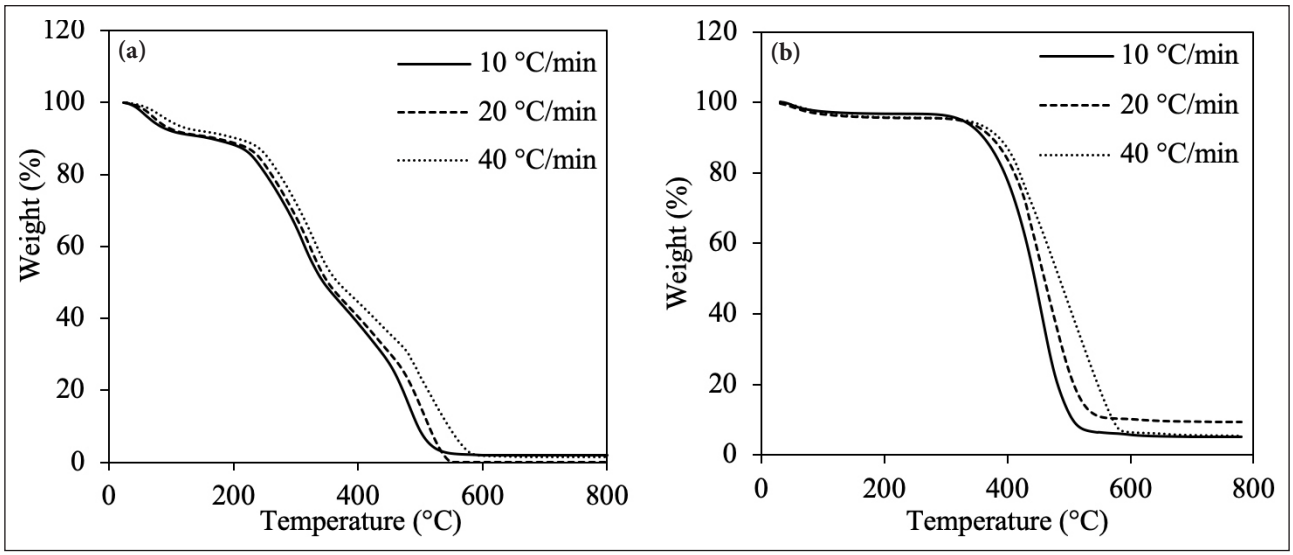


**Figure 4**. TG curves of combustion of **(a)** Raw biomass, **(b)** Biochar.

sequently, it can be concluded that the porosity and surface area of biochar are higher than those of biomass [38]. When compared to the SEM image of biochar derived from St. John's wort biomass at a temperature of 500 °C as provided in the study by Ateş et al. [19], it can be said that the pores and cracks in the structure are similar to those in this study.

**Thermal Behaviours of Samples**

The combustion thermograms of St. John's wort wastes and their biochars are shown in Figure 4 and the data in this figure are shown in Table 2. According to this figure, it can be seen that all samples burned at a rate of approximately 90% to 99% and that this process occurred in 2 temperature zones. In the first zone, it can be said that the relative humidity or the moisture adsorbed from the air is removed as the temperature increases up to about 175 °C for each material [39]. The mass losses in this region are around 10% for raw biomass and around 5% for biochar. The second region was realized differently for raw biomass and biochar. For raw biomass, this zone was realized in two stages. The first one took place between about 200 and 400 °C and in this zone the proteinic, cellulosic and hemicellulosic contents of the materials were burned [13]. The second stage took place between 400 and 550 °C, where char remaining after devolatilization of the samples was burned [40].

When the combustion thermograms of biochar samples are examined, it has seen that the main mass loss is in the second region and this loss occurs in a single stage. The reason for this situation is that structures such as protein and carbohydrate in the biomass are degraded during biochar production and removed from the char [13]. The mass loss in this region was measured to be approximately 85–90%. The main reason for such high values can be attributed to the low ash content of the biomass and consequently of the biochar. Another conclusion that can be drawn about the combustion reactions of raw biomass and biochar is that the second zone of biomass combustion starts earlier than that of biochar. The reason for this is that the easily ignitable volatiles in the biomass are removed from the char structure during biochar production [11].

**Table 2.** Thermal degredation characteristics

| Heating rate (°C/min) | Parameters | Biomass | | Biochar |
|---|---|---|---|---|
| | | 200–400 °C | 400–550 °C | 200–650 °C |
| 10 | $T_i$ | 249 | – | 387 |
| | $T_{max}$ | 311 | 478 | 447 |
| | $T_b$ | – | 512 | 492 |
| | WL | 44.37 | 42.76 | 90.17 |
| 20 | $T_i$ | 254 | – | 391 |
| | $T_{max}$ | 322 | 490 | 453 |
| | $T_b$ | – | 540 | 524 |
| | WL | 44.15 | 47.10 | 85.33 |
| 40 | $T_i$ | 261 | – | 396 |
| | $T_{max}$ | 328 | 494 | 462 |
| | $T_b$ | – | 568 | 570 |
| | WL | 43.63 | 45.32 | 89.17 |

$T_i$: Ignition temperature; $T_{max}$: Temperature at maximum loss rate; $T_b$: Burnout temperature; WL: Weight loss.

**Table 3.** The combustion activation energy values of raw biomasses

| α | Raw | | | | Biochar | | | |
|---|---|---|---|---|---|---|---|---|
| | KAS | | FWO | | KAS | | FWO | |
| | $E_a$ (kJ/mol) | $R^2$ | $E_a$ (kJ/mol) | $R^2$ | $E_a$ (kJ/mol) | $R^2$ | $E_a$ (kJ/mol) | $R^2$ |
| 0.1 | 97.33 | 0.990 | 100.86 | 0.991 | 183.73 | 0.997 | 185.14 | 0.997 |
| 0.2 | 98.31 | 0.957 | 102.24 | 0.963 | 203.03 | 0.983 | 203.86 | 0.984 |
| 0.3 | 97.89 | 0.929 | 102.21 | 0.940 | 201.23 | 0.999 | 202.44 | 0.999 |
| 0.4 | 88.65 | 0.930 | 93.77 | 0.943 | 166.44 | 0.976 | 169.64 | 0.979 |
| 0.5 | 57.35 | 0.897 | 64.50 | 0.923 | 139.17 | 0.960 | 143.97 | 0.966 |
| 0.6 | 42.68 | 0.880 | 51.14 | 0.920 | 117.89 | 0.953 | 123.96 | 0.961 |
| 0.7 | 43.44 | 0.862 | 52.48 | 0.909 | 102.82 | 0.947 | 109.86 | 0.958 |
| 0.8 | 48.55 | 0.847 | 57.79 | 0.896 | 93.87 | 0.946 | 101.59 | 0.958 |
| 0.9 | 56.53 | 0.918 | 65.86 | 0.943 | 92.88 | 0.937 | 100.95 | 0.952 |
| Ave. | 70.08 | | 76.76 | | 144.56 | | 149.05 | |

**Combustion Kinetics**

In order to determine the combustion kinetic parameters of raw St. John's wort waste and biochar, the non-isothermal curves of KAS and FWO methods were shown in Figure 5. Based on the findings from Figure 5, the values of the combustion activation energy and the regression coefficients of the samples were computed and are shown in Table 3. When the combustion activation energy values of St. John's wort calculated by the KAS method were examined, it was seen that these values varied between 42.68 kJ/mol and 98.31 kJ/mol. When the regression coefficients are examined, it can be said that the coefficients except for the conversions of 0.7 and 0.8 are within the acceptable range and the regression coefficients of the conversions 70% and 80% are slightly below the limit. All of the regression coefficients calculated with FWO were found to be within the acceptable range, and accordingly, it can be concluded that this method is more suitable for determining the combustion kinetics of St. John's wort waste. Using the FWO method, activation energy values were calculated between 51.14 kJ/mol and 102.24 kJ/mol. When studies on combustion kinetics in the literature are examined, it is noted that a large number of biomass types are used as raw materials. For example, Lopez et al. [41] used the Vyazovkin and Ozawa-Flynn-Wall techniques to assess the microalgae and corn blends' combustion kinetics and computed the activation energy value, which came out to be around 171.5 kJ/mol. According to Koçer and Özçimen [13] *Ulva lactuca* macroalgae burned in two phases, with activation energy levels of around 295 kJ/mol and 225 kJ/mol in each. Yorulmaz and Atimtay [42] calculated the combustion kinetics of waste wood samples between 123–136 kJ/mol using the Coats-Redfern method, while Gao et al. [43] determined the combustion activation energy of waste wood as 184.2 kJ/mol using the Broido method.

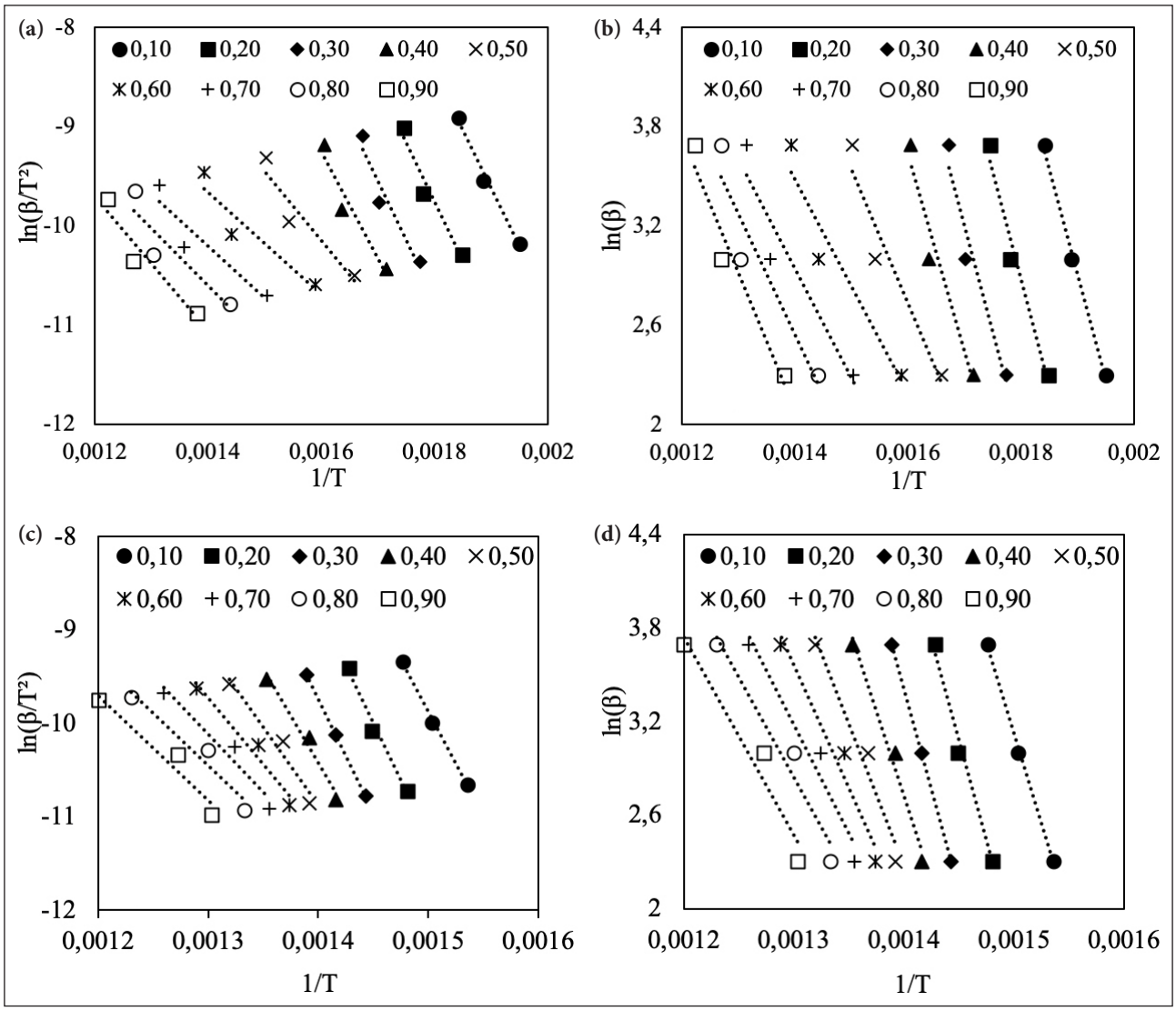


**Figure 5**. **(a)** Raw biomass KAS, **(b)** Raw biomass FWO, **(c)** Biochar KAS and **(d)** Biochar FWO.

The activation energy values determined by both techniques exhibit a rising trend up to 20% conversion and a decreasing trend between 20% and 60% when the combustion activation energies of St. John's wort are studied. After the conversion of 60%, activation energy values tended to rise once again. When the rates of change in activation energies were analyzed, it was observed that there was no significant change up to 30% conversion, but there was a decrease of approximately 30 kJ/mol especially between 40% and 50% conversion rates. These findings indicate that the biomass's proteinic, cellulosic, and hemicellulosic components were burnt to a 60% conversion rate, after which point the char-like structure that resulted from devolatilization was burned. The activation energy estimates tended to rise after 60% conversion because the char structure is considerably harder to burn.

The average combustion activation energy values of biochar samples were calculated to be approximately 150 kJ/mol, respectively. Regression coefficients higher than 0.9, like those of biomass, indicate that these methods can be used to determine the combustion kinetic parameters of these biochar samples. When the studies in the literature in which the combustion kinetics of biochar are calculated, it is seen that there are different results according to the biomass used and the methods applied. Koçer and Özçimen [13] reported that the average combustion activation energy values of biochar produced from *Ulva lactuca* macroalgae were 146.61 kJ/mol and 140.81 kJ/mol using KAS and FWO methods. Islam et al. [44] calculated the average combustion activation energy of Karanj fruit hulls biochar as 62.13 kJ/mol and 68.53 kJ/mol using KAS and FWO methods. Wang et al. [45] used Random Pore Model and Volume Model approaches for combustion kinetics of Palm Kernel Shell Biochar and calculated the activation energy values as 113.3 kJ/mol and 116.6 kJ/mol. Yu et al. [46] determined the average combustion kinetic energy of pine sawdust biochar as approximately 200 kJ/mol by Friedman Friedman differential isoconversional method.

When the behavior of the activation energy values according to the conversion rate is examined, it can be said

**Table 4.** Activation energy values and regression coefficients in some studies

| Sample | Methods | Results | References |
|---|---|---|---|
| Pine | DAEM | $E_a$: 111.41–208.62 kJ/mol | [40] |
| | | $R^2$: 0.906–0.995 | |
| Corn straw | | $E_a$: 97.58–189.13 kJ/mol | |
| | | $R^2$: 0.906–0.999 | |
| Seaweed (*U. lactuca*) | KAS | $E_a$: 296.97–225.17 kJ/mol | [13] |
| | | $R^2$: 0.980–0.996 | |
| | FWO | $E_a$: 292.39–216.73 kJ/mol | |
| | | $R^2$: 0.979–0.996 | |
| Seaweed (*U. lactuca*) biochar | KAS | $E_a$: 146.61 kJ/mol | |
| | | $R^2$: 0.938–0.990 | |
| | FWO | $E_a$: 140.81 kJ/mol | |
| | | $R^2$: 0.943–0.992 | |
| Sugarcane bagasse | Friedman | $E_a$: 8.17–275.48 kJ/mol | [50] |
| | | $R^2$: - | |
| | FWO | $E_a$: 11.04–88.56 kJ/mol | |
| | | $R^2$: - | |
| | KAS | $E_a$: 3.39–78.28 kJ/mol | |
| | | $R^2$: - | |
| Microalgae (*C. pyrenoidosa*) | Vyazovkin | $E_a$: 65.15 kJ/mol | [51] |
| | | $R^2$: - | |
| Palm kernel shell biochar | Random pore model | $E_a$: 113.3 kJ/mol | [45] |
| | | $R^2$: 0.999 | |
| | Volume model | $E_a$: 116.6 kJ/mol | |
| | | $R^2$: 0.999 | |
| Pine sawdust | KAS | $E_a$: 212.39 kJ/mol | [52] |
| | | $R^2$: 0.996–0.999 | |
| | FWO | $E_a$: 212.66 kJ/mol | |
| | | $R^2$: 0.996–0.999 | |
| St. John's wort | KAS | $E_a$: 70.08 kJ/mol | This study |
| | | $R^2$: 0.847–0.990 | |
| | FWO | $E_a$: 76.76 kJ/mol | |
| | | $R^2$: 0.896–0.991 | |
| St. John's wort biochar | KAS | $E_a$: 144.56 kJ/mol | |
| | | $R^2$: 0.937–0.999 | |
| | FWO | $E_a$: 149.05 kJ/mol | |
| | | $R^2$: 0.952–0.999 | |

that the activation energy values decrease continuously after 20% conversion for St. John's wort biochar. At these conversion levels, the activation energy values are maximum, which indicate the highest barrier to the combustion compared to that of other conversion degrees [47]. After these conversion levels, the combustion of the fixed carbon in the structure of biochars started and continued until 90% conversion. The porous structure of biochar also facilitated combustion as it increased the contact surface with oxygen [48]. Due to the decrease in fixed carbons in the structure of biochar over time and ash content, activation energy changes at high conversion levels decreased [49]. When the studies on the combustion of biochar or similar materials in the literature are examined, it has seen that similar results are obtained. For example Islam et al. [47] and Islam et al. [44] reported that activation energy values decreased continuously with increasing conversion rate in their studies

investigating the combustion of hydrochar and biochar produced from Karanj fruit hulls, respectively. Gao and Li [49] stated that the combustion activation energy values of Coal gangue continuously decreased until about 80% conversion; after 80% conversion, the activation energy increased due to the combustion of fixed carbon content and ash content. Studies on the combustion kinetics of some biomasses and biochar in the literature are summarized in Table 4.

## CONCLUSION

The thermal behavior of St. John's wort wastes and their biochars in dry air was investigated by thermogravimetric analysis and the combustion activation energies were determined using KAS and FWO methods. The combustion behavior of raw biomass and biochars after moisture content removal was different. While the combustion of raw biomass occurred in two stages (combustion of biomolecules and char remaining after devolatilization) between approximately 150 °C and 550 °C, the combustion of biochar in this temperature range occurred in one stage (combustion of char structure). The average activation energy values of St. John's wort wastes in this temperature range were calculated as 70.08 kJ/mol and 76.76 kJ/mol by KAS and FWO methods, respectively, while the average combustion activation energy values of biochar wastes in this temperature range were calculated as 144.56 kJ/mol and 149.05 kJ/mol, respectively. Based on an evaluation of the study's results, it can be concluded that these biomasses and their biochar forms can be added to fuels like coal or utilized directly in combustion processes because of their low ash content. This approach will optimize the utilization of these very promising wastes and improve the efficiency of fuels such as low quality coal.

## ACKNOWLEDGEMENTS

The author would like to thank Emre Karaduman who provided the samples.

## DATA AVAILABILITY STATEMENT

The author confirm that the data that supports the findings of this study are available within the article. Raw data that support the finding of this study are available from the corresponding author, upon reasonable request.

## CONFLICT OF INTEREST

The author declared no potential conflicts of interest with respect to the research, authorship, and/or publication of this article.

## USE OF AI FOR WRITING ASSISTANCE

Not declared.

## ETHICS

There are no ethical issues with the publication of this manuscript.

## REFERENCES

[1] S. Babu, S. S. Rathore, R. Singh, S. Kumar, V. K. Singh, S. K. Yadav, ... and O. A. Wani, "Exploring agricultural waste biomass for energy, food and feed production and pollution mitigation: A review," Bioresource Technology, Vol. 360, Article 127566, 2022. [CrossRef]

[2] A. Siddiqua, J. N. Hahladakis, and W. A. K. A. Al-Attiya, "An overview of the environmental pollution and health effects associated with waste landfilling and open dumping," Environmental Science and Pollution Research, Vol. 29(39), pp. 58514–58536, 2022. [CrossRef]

[3] L. Reijnders, "Hazardous waste incineration ashes and their utilization," Encyclopedia of Sustainability Science and Technology, pp. 1–17, 2018. [CrossRef]

[4] Y. A. Hajam, R. Kumar, and A. Kumar, "Environmental waste management strategies and vermi transformation for sustainable development," Environmental Challenges, Vol. 13, Article 100747, 2023. [CrossRef]

[5] X. Peng, Y. Jiang, Z. Chen, A. I. Osman, M. Farghali, D. W. Rooney, and P.-S. Yap, "Recycling municipal, agricultural and industrial waste into energy, fertilizers, food and construction materials, and economic feasibility: a review," Environmental Chemistry Letters, Vol. 21(2), pp. 765–801, 2023. [CrossRef]

[6] K. Wang, and J. W. Tester, "Sustainable management of unavoidable biomass wastes," Green Energy and Resources, Vol. 1(1), Article 100005, 2023. [CrossRef]

[7] M. Kumar, "Social, Economic, and Environmental Impacts of Renewable Energy Resources," in Wind Solar Hybrid Renewable Energy System, IntechOpen, 2020. [CrossRef]

[8] H. Durak, "Comprehensive assessment of thermochemical processes for sustainable waste management and resource recovery," Processes, Vol. 11(7), Article 2092, 2023. [CrossRef]

[9] D. Özçimen, B. İnan, S. Akış, and A. T. Koçer, "Utilization alternatives of algal wastes for solid algal products" in Algal biorefineries volume products and refinery design, Springer, 2015. [CrossRef]

[10] X. Pan, Z. Gu, W. Chen, and Q. Li, "Preparation of biochar and biochar composites and their application in a Fenton-like process for wastewater decontamination: A review," Science of Total Environment, Vol. 754, Article 142104, 2021. [CrossRef]

[11] A. T. Koçer, "A thermokinetic characterization study on combustion of solid biofuels from Aloe vera residue," Rendiconti Lincei – Scienze Fisiche e Naturali, Vol. 34(2), pp. 1031–1043, 2023. [CrossRef]

[12] D. I. Aslan, B. Özoğul, S. Ceylan, and F. Geyikçi, "Thermokinetic analysis and product characterization of Medium Density Fiberboard pyrolysis," Bioresource Technology, Vol. 258, pp. 105–110, 2018. [CrossRef]

[13] A. T. Koçer and D. Özçimen, "Determination of

combustion characteristics and kinetic parameters of Ulva lactuca and its biochar," Biomass Convers Biorefinery, Vol. 14, pp. 5913–5922, 2021 [CrossRef]

[14] A. T. Koçer, D. Özçimen, and İ. Gökalp, "An experimental study on the combustion behaviours of orange peel-based solid biofuels," Biomass Conversion and Biorefinery, 2023. doi: 10.1007/s13399-020-01245-4 [CrossRef]

[15] W. Tong, Z. Cai, Q. Liu, S. Ren, and M. Kong, "Effect of pyrolysis temperature on bamboo char combustion: Reactivity, kinetics and thermodynamics," Energy, Vol. 211, Article 118736, 2020. [CrossRef]

[16] C. A. Peterson and R. C. Brown, "Oxidation kinetics of biochar from woody and herbaceous biomass," Chemical Engineering Journal, Vol. 401, Article 126043, 2020. [CrossRef]

[17] K. M. Klemow, A. Bartlow, J. Crawford, N. Kocher, J. Shah, and M. Ritsick, "Medical attributes of St. John's wort (hypericum perforatum)," in Herbal Medicine: Biomolecular and Clinical Aspects: Second Edition, pp. 211–237, 2011. [CrossRef]

[18] I. Arsić, A. Zugić, V. Tadić, M. Tasić-Kostov, D. Mišić, M. Primorac, D. Runjaić-Antić, "Estimation of Dermatological Application of Creams with St. John's Wort Oil Extracts," Molecules, Vol. 17(1), pp. 275–294, 2011. [CrossRef]

[19] F. Ateş, G. Akan, and N. Erginel, "Estimating the levels of process parameters for tar and char production via fast pyrolysis of Hypericum perforatum and characterization of the products," Chemical Data Collections, Vol. 33, Article 100720, 2021. [CrossRef]

[20] J. J. Lu, and W. H. Chen, "Investigation on the ignition and burnout temperatures of bamboo and sugarcane bagasse by thermogravimetric analysis," Applied Energy, Vol. 160, pp. 49–57, 2015. [CrossRef]

[21] R. García, C. Pizarro, A. G. Lavín, and J. L. Bueno, "Characterization of Spanish biomass wastes for energy use," Bioresource Technology, Vol. 103(1), pp. 249–258, 2012. [CrossRef]

[22] J. Parikh, S. A. Channiwala, and G. K. Ghosal, "A correlation for calculating HHV from proximate analysis of solid fuels," Fuel, Vol. 84(5), pp. 487–494, 2005. [CrossRef]

[23] S. Poomsawat, and W. Poomsawat, "Analysis of hydrochar fuel characterization and combustion behavior derived from aquatic biomass via hydrothermal carbonization process," Case Studies in Thermal Engineering, Vol. 27, Article 101255, 2021. [CrossRef]

[24] D. R. Nhuchhen, "Prediction of carbon, hydrogen, and oxygen compositions of raw and torrefied biomass using proximate analysis," Fuel, Vol. 180, pp. 348–356, 2016. [CrossRef]

[25] I. Ali, and A. Bahadar, "Thermogravimetric characteristics and non-isothermal kinetics of macro-algae with an emphasis on the possible partial gasification at higher temperatures," Frontiers in Energy Research, Vol. 7, pp. 1–14, 2019. [CrossRef]

[26] H. E. Kissinger, "Reaction kinetics in differential thermal analysis," Analytical Chemistry, Vol. 29(11), pp. 1702–1706, 1957. [CrossRef]

[27] J. H. Flynn, and L. A. Wall, "A quick, direct method for the determination of activation energy from thermogravimetric data," Journal of Polymer Science. Part B: Polymer Letters, Vol. 4(5), pp. 323–328, 1966. [CrossRef]

[28] T. Ozawa, "A new method of analyzing thermogravimetric data," Bulletin of the Chemical Society of Japan, Vol. 38(11), pp. 1881–1886, 1965. [CrossRef]

[29] A. Selvarajoo, Y. L. Wong, K. S. Khoo, W. H. Chen, and P. L. Show, "Biochar production via pyrolysis of citrus peel fruit waste as a potential usage as solid biofuel," Chemosphere, Vol. 294, Article 133671, 2022.

[30] M. I. Al-Wabel, A. Al-Omran, A. H. El-Naggar, M. Nadeem, and A. R. A. Usman, "Pyrolysis temperature induced changes in characteristics and chemical composition of biochar produced from conocarpus wastes," Bioresource Technology, Vol. 131, pp. 374–379, 2013. [CrossRef]

[31] R. Calvelo Pereira, J. Kaal, M. Camps Arbestain, R. Pardo Lorenzo, W. Aitkenhead, M. Hedley, … J. A. Maciá-Agulló, "Contribution to characterisation of biochar to estimate the labile fraction of carbon," Organic Geochemistry, Vol. 42(11), pp. 1331–1342, 2011. [CrossRef]

[32] A. T. Koçer, B. Mutlu, and D. Özçimen, "Investigation of biochar production potential and pyrolysis kinetics characteristics of microalgal biomass," Biomass Convers. Biorefinery, Vol. 10(1), pp. 85–94, 2020. [CrossRef]

[33] S. Z. Tarhan, A. T. Koçer, D. Özçimen, and İ. Gökalp, "Cultivation of green microalgae by recovering aqueous nutrients in hydrothermal carbonization process water of biomass wastes," Journal of Water Process Engineering, Vol. 40, Article 101783, 2021. [CrossRef]

[34] Y. W. Mak, L. O. Chuah, R. Ahmad, and R. Bhat, "Antioxidant and antibacterial activities of hibiscus (Hibiscus rosa-sinensis L.) and Cassia (Senna bicapsularis L.) flower extracts," Journal of King Saud University, Vol. 25(4), pp. 275–282, 2013. [CrossRef]

[35] M. Sekkal, J.-P. Huvenne, P. Legrand, B. Sombret, J.-C. Mollet, A. Mouradi-Givernaud, and M.-C. Verdus, "Direct structural identification of polysaccharides from red algae by FTIR microspectrometry I: Localization of agar in Gracilaria verrucosa sections," Mikrochim. Acta, vol. 112, no. 1–4, pp. 1–10, 1993. [CrossRef]

[36] A. T. Koçer, B. İnan, S. Kaptan Usul, D. Özçimen, M. T. Yılmaz, and İ. Işıldak, "Exopolysaccharides from microalgae: production, characterization, optimization and techno-economic assessment," Brazilian Journal of Microbiology, Vol. 52(4), pp. 1779–1790, 2021. [CrossRef]

[37] M. S. Reza, S. Afroze, M. S. A. Bakar, R. Saidur, N. Aslfattahi, J. Taweekun, and A. K. Azad, "Biochar characterization of invasive Pennisetum purpureum

grass: effect of pyrolysis temperature," Biochar, Vol. 2(2), pp. 239–251, 2020. [CrossRef]

[38] A. T. Koçer, A. Erarslan, and D. Özçimen, "Pyrolysis of Aloe vera leaf wastes for biochar production: Kinetics and thermodynamics analysis," Industrial Crops and Products, Vol. 204, Article 117354, 2023. [CrossRef]

[39] A. Agrawal, and S. Chakraborty, "A kinetic study of pyrolysis and combustion of microalgae Chlorella vulgaris using thermo-gravimetric analysis," Bioresource Technology, Vol. 128, pp. 72–80, 2013. [CrossRef]

[40] I. Mian, X. Li, O. D. Dacres, J. Wang, B. Wei, Y. Jian, ... and N. Rahman, "Combustion kinetics and mechanism of biomass pellet," Energy, Vol. 205, Article 117909, 2020. [CrossRef]

[41] R. López, C. Fernández, X. Gómez, O. Martínez, and M. E. Sánchez, "Thermogravimetric analysis of lignocellulosic and microalgae biomasses and their blends during combustion," Journal of Thermal Analysis and Calorimetry, Vol. 114(1), pp. 295–305, 2013. [CrossRef]

[42] S. Y. Yorulmaz, and A. T. Atimtay, "Investigation of combustion kinetics of treated and untreated waste wood samples with thermogravimetric analysis," Fuel Processing Technology, Vol. 90(7–8), pp. 939–946, 2009. [CrossRef]

[43] M. Gao, D. X. Pan, and C. Y. Sun, "Study on the thermal degradation of wood treated with amino resin and amino resin modified with phosphoric acid," Journal of Fire Sciences, Vol. 21(3), pp. 189–201, 2003. [CrossRef]

[44] M. A. Islam, M. Auta, G. Kabir, and B. H. Hameed, "A thermogravimetric analysis of the combustion kinetics of karanja (Pongamia pinnata) fruit hulls char," Bioresource Technology, Vol. 200, pp. 335–341, 2016. [CrossRef]

[45] P. Wang, G. Wang, J. Zhang, J. Y. Lee, Y. Li, and C. Wang, "Co-combustion characteristics and kinetic study of anthracite coal and palm kernel shell char," Applied Thermal Engineering, Vol. 143, pp. 736–745, 2018. [CrossRef]

[46] Y. Yu, X. Fu, L. Yu, R. Liu, and J. Cai, "Combustion kinetics of pine sawdust biochar," Journal of Thermal Analysis and Calorimetry, Vol. 124(3), pp. 1641–1649, 2016. [CrossRef]

[47] M. A. Islam, G. Kabir, M. Asif, and B. H. Hameed, "Combustion kinetics of hydrochar produced from hydrothermal carbonisation of Karanj (Pongamia pinnata) fruit hulls via thermogravimetric analysis," Bioresource Technology, Vol. 194, pp. 14–20, 2015. [CrossRef]

[48] H. Wang, and C. You, "Experimental investigation into the spontaneous ignition behavior of upgraded coal products," Energy and Fuels, Vol. 28(3), pp. 2267–2271, 2014. [CrossRef]

[49] H. Gao and J. Li, "Thermogravimetric analysis of the co-combustion of coal and polyvinyl chloride," PLoS One, Vol. 14(10), Article e0224401, 2019. [CrossRef]

[50] L. C. Morais, A. A. D. Maia, M. E. G. Guandique, and A. H. Rosa, "Pyrolysis and combustion of sugarcane bagasse," Journal of Thermal Analysis and Calorimetry, Vol. 129(3), pp. 1813–1822, 2017. [CrossRef]

[51] C. Gai, Z. Liu, G. Han, N. Peng, and A. Fan, "Combustion behavior and kinetics of low-lipid microalgae via thermogravimetric analysis," Bioresource Technology, Vol. 181, pp. 148–154, 2015. [CrossRef]

[52] T. Chen, J. Cai, and R. Liu, "Combustion kinetics of biochar from fast pyrolysis of pine sawdust: isoconversional analysis," Energy Sources, Part A Recover. Util. Environ. Eff., vol. 37, no. 20, pp. 2208–2217, 2015. [CrossRef]

*Environ Res Tec, Vol. 7, Issue. 3, pp. 406–421, September 2024*

**Environmental Research and Technology**
https://ert.yildiz.edu.tr - https://dergipark.org.tr/tr/pub/ert
DOI: https://10.35208/ert.1443393

**Research Article**

# Investigating the emissions and performance of ethanol and biodiesel blends on $Al_2O_3$ thermal barrier coated piston engine using response surface methodology design - multiparametric optimization

**P.KUMARAN[*,1], Natarajan SENGODAN[2], Sudesh KUMAR MP.[3], A. ANDERSON[4], S. PRAKASH[5]**

[1]*Department of Mechanical Engineering, Aarupadai Veedu Institute of Technology, Vinayaka Mission's Research Foundation, Deemed to be University, Tamil Nadu, India*

[2]*Vinayaka Missions Kirupananda Variyar Engineering College, Vinayaka Mission's Research Foundation, Salem, Tamil Nadu, India*

[3]*Department of Mechanical Engineering, Global Institute of Engineering and Technology, Tamil Nadu, India*

[4]*School of Mechanical Engineering, Sathyabama Institute of Science and Technology, Chennai, India*

[5]*Department of Mechanical Engineering, Aarupadai Veedu Institute of Technology, Vinayaka Mission's Research Foundation, Deemed to be University, Tamil Nadu, India*

## ARTICLE INFO

*Article history*
Received: 27 February 2024
Revised: 22 March 2024
Accepted: 01 April 2024

**Key words:**
Emission; Ethanol; Optimization; Performance; Thermal barrier coating; Tomato methyl ester

## ABSTRACT

The Response Surface Methodology (RSM) optimization technique was used to examine the effect of load, Tomato Methyl Ester (TOME), and Ethanol injection enhanced diesel on engine performance and exhaust gas emissions with a normal piston and an $Al_2O_3$ coated piston. TOME biodiesel (10, 20, and 30%) and ethanol (10, 20, and 30%) were chosen to increase BTE while minimizing BSFC, NOx, CO, smoke, and HC. The RSM technique was used to operate the engine by load (0–100%). The results revealed that engine load, TOME, and ethanol concentration all exhibited a considerable effect on the response variables. The ANOVA results for the established quadratic models specified that for each model, an ideal was discovered by optimizing an experiment's user-defined historical design. The present research efforts to improve the performance of a diesel engine by using a thermal barrier-coated piston that runs on biodiesel blends. $Al_2O_3$ is the chosen material for TBC due to its excellent thermal insulation properties. B20E30 has a 4% higher brake thermal efficiency than diesel, but B10E20 and B30E20 mixes have a 3.6% and 12% reduction in BSFC. The B20 blends lowered CO and HC emissions by 6% and 8% respectively. In terms of performance and emissions, biodiesel blends performed similarly to pure diesel, and the combination was optimized through the design of an experiment tool.

**Cite this article as:** Kumaran P, Natarajan Sengodan S, Kumar SMP, Anderson A, Prakash S. Investigating the emissions and performance of ethanol and biodiesel blends on $Al_2O_3$ thermal barrier coated piston engine using response surface methodology design - multiparametric optimization. Environ Res Tec 2024;7(3)406–421.

***Corresponding author.**
*E-mail address: kumaranp@avit.ac.in

## INTRODUCTION

The application of piston TBC is highly beneficial in mini-mizing heat dissipation during the operation of an internal combustion engine's process. Total combustion is hindered throughout the process of combustion due to multiple factors. The loss of warmth in the combustion cylinder is a contributing factor to incomplete combustion. The primary objective of piston TBC is not alone to prevent heat loss, but also to pro-vide fatigue protection and reduce emissions. This research aims to mitigate engine heat loss by applying a TBC material on the piston, specifically using copper-chromium-zirconium (CuCr1Zr) [1]. The application of CuCr1Zr as a TBC material on pistons is an innovative method that has been evaluated using Tamanu mixed diesel fuel [2]. An examination was con-ducted on an IC engine that had a coating applied to it, the piston was coated using the plasma spray technique with a layer of Ni-Cr measuring 0.2 mm in thickness [3]. Mamey sapote oil was utilized as a source of biodiesel. Consequently, there was a 1% improvement in thermal efficiency, accompanied by a decrease in (CO) emissions [4]. A study was di-rected to evaluate the act of a single cylinder IC engine with copper coating [5]. The findings shown that the implementation of a Cu-coated piston and combustion chamber in the engine effectively decreases the levels of (HC) and (CO) emissions [6]. Conducted research on the impact of plasma sprayed zirconium coatings on the piston. One effective method for enhancing the performance of internal combustion engines and decreasing the emission of (CO) and hydrocarbons (HC) is the use of thermal barrier coatings on the piston and combustion chamber [7]. Declared that a diesel engine with a coating exhibits superior performance [8]. It has been asserted that cotton seed biodiesel can serve as a substitute fuel to regulate the pollutants, such as carbon monoxide (CO) and hydrocarbons (HC), produced by a diesel engine [9]. It was asserted that cotton seed biodiesel was employed as a substitute fuel to regulate the emissions of carbon monoxide (CO) and hydrocarbons (HC) from a diesel engine [10]. The combustion parameters have an impact on power generation, emission of pollutants from the exhaust, fuel consumption, engine vibrations, and noise levels [11]. Coating cylinders and adding nanoparticles to biodiesel reduce fuel consumption [12] Compressed air's pressure and temperature affect how long it takes to ignite. During compression, the cooling system effectively absorbs a significant quantity of heat. Engines equipped with thermal barrier coatings can reduce heat dissipation and improve the effective output by employing materials with low thermal conductivity and high resilience to high temperatures to cover the combustion chambers [13, 14]. A zirconia coating is applied to engine components, which results in a reduction in the heat conduction of such components [15]. Furthermore, the utilization of a glow plug in conjunction with the utilization of ethanol as a fuel consequences in a discount in the emission of pollutants emitted by exhaust [16, 17]. On the other hand, as compared to the utilization of diesel fuel, it results in a decrease in efficiency. SVM and Bagging methods perform second-best for Cp max and smoke output variables, respectively [18]. On the other hand, there is a certain degree of improvement in the thermal efficiency of the engine when the timing of injection is delayed [19]. This results in a reduction in emissions of $CO_2$ and hydrocarbons that have not been burned, as well as an improvement in thermal efficiency [20]. In spite of this, it outcomes in an increase in the amount of nitrogen oxide emissions since it causes the combustion temperatures to rise [21]. As a result of their improved thermal and mechanical efficiency, fewer pollutant emissions, and decreased fuel consumption, thermal barrier coatings have become increasingly prevalent in engine components. The waste heat created by the engine's insulation can be harnessed to oxidize the soot precursors generated during hydrocarbon combustion, leading to a reduction in emissions [22]. Exhaust emissions decreased with the addition of Di Ethylene Butyl Glycol Ether [23]. Table 1 show the literature based on various biodiesel.

**Table 1.** Literature on different biodiesel and methods

| Author | Oil used | Methods | Result |
|---|---|---|---|
| A. P. Venkatesh [1] | Rubber seed biodiesel | Ethanol additive, nanocoated pistons, optimization | A biodiesel-compatible thermal barrier-coated piston improves diesel engine performance in the study. Thermal insulation makes yttria-stabilized zirconia appropriate for thermal barrier coatings. |
| Saxena [5] | Acacia Concinna | Response surface methodology, nanofluid | $TiO_2$ nanoparticle-enhanced Acacia Concinna biodiesel-diesel blends improve engine performance; BTE, BSFC, ID, HC, and smoke emissions decrease; NOx emissions increase. |
| Salih Ozer [12] | Coalbed methane | Nanoparticle (molybdenum) additive, coated pistons | $Al_2O_3$ + 13% $TiO_2$ coating tractor engine cylinders and adding molybdenum nanoparticles to biodiesel reduced fuel consumption, HC, CO, PM, exhaust gas temperature, and NOx emission. |
| Viswanathan [20] | Pine oil | Thermal barrier coating and antioxidants | Pine oil biofuel was utilized to test diesel engine with thermal barrier and antioxidants. PO+TBHQ combination gave the best performance, combustion, and emissions, suggesting engine efficiency and pollution reduction. |
| Mejia et al. [15] | Castor oil biodiesel, palm oil bio diesel | Dual Biodiesel, Compression ratio | It was not a viable alternative to use blends of palm oil biodiesel and castor oil biodiesel (POB COB) in order to generate a sort of pure biodiesel that had a low cloud point and a low viscosity. |

The objective of this research is to describe the use of the (RSM) optimization technique in examining the impact of load, Tomato Methyl Ester (TOME), and Ethanol injection on engine performance and exhaust gas emissions. The main aims to highlight the experimental design, factors considered (TOME and Ethanol concentrations), and the use of RSM for optimization. The goal of the paragraph is to present research efforts focused on improving the performance of a diesel engine using biodiesel blends. It introduces the application of a TBC piston running on biodiesel blends, specifically B20E30, B10E20, and B30E20, and compares their performance and emissions with pure diesel. The use of $Al_2O_3$ as the material for thermal barrier coatings is mentioned, and the overall aim is to maximize (BTE), minimize (BSFC), and reduce NOx, CO, smoke, and HC emissions.

## MATERIALS AND METHODS

### Tomato Methyl Ester Formation

Tomato seeds are not commonly used for biodiesel production due to their relatively low oil content in comparison to other oilseed crops like soybeans or canola. Nevertheless, the wastage of seed extracted from sauce factory within the scope of investigating the creation of biodiesel from non-traditional sources, below is a comprehensive outline of the biodiesel manufacturing procedure, commonly referred to as transesterification. Figure 1 shows the Tomato seed oil extraction: Obtain oil from tomato seeds. Typically, this procedure involves either mechanical pressing or solvent extraction. The oil concentration in tomato seeds is quite modest in comparison to specialized oilseed crops, thus potentially limiting the production. Oil Refining: Purify the produced oil if necessary. The enhancement of oil quality can be achieved through several refining techniques such as degumming, neutralization, bleaching, and deodorization. Transesterification: Convert the purified oil into biodiesel using the process of transesterification. The process of chemically interacting vegetable oil or animal fat with an spirits, characteristically methanol or ethanol, in the occurrence of a catalyst, typically sodium or potassium hydroxide [23]. This process transforms the triglycerides present in the oil into esters, which are commonly known as biodiesel, as well as glycerol. Separation and Washing: Following the transesterification process, the biodiesel should be separated from the glycerol and subjected to a washing procedure in order to eliminate any contaminants. Dehydration: from the biodiesel by the process of drying. Table 2 shows the chemical properties.

### TBC – Before & After Piston Crown

Following the application of the TBC, the piston crown is depicted in Figure 2: According to the findings of the research analysis, the materials that are utilized for thermal barrier coating include NicrAl, $Al_2O_3$, molybdenum, titanium oxide, Yttrium stabilized zirconium, magnesium stabilized zirconia, and other similar substances.

**Table 2.** Properties of fuels

| Properties | TME | Diesel | Ethanol |
|---|---|---|---|
| Viscosity (cSt) | 28 | 2.62 | 1.52 |
| Flashpoint (°C) | 189 | 68 | 13 |
| Calorific value (MJ/kg) | 35.9 | 42.7 | 27.3 |
| Density (kg/m$^3$) | 915.1 | 855 | 720 |

TME: Tomato methyl ester.

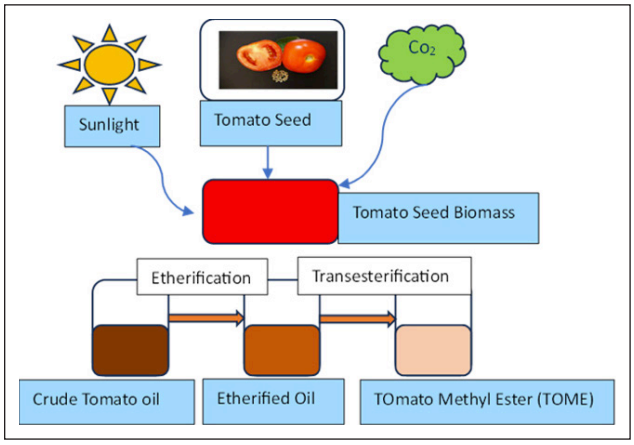


**Figure 1**. Preparation of tomato methyl ester.

The simplified chemical reaction is as follows: Triglyceride + Alcohol → Biodiesel + Glycerol


**Figure 2**. Piston before/after coating.

The barrier coating that was used for this work was a piston-based coating with NiCr – 80 (Micron), Top Piston Crown $Al_2O_3$-100, and Total TBC – 180 (Microns). As a covering material, the ceramic material known as "Aluminum oxide" was utilized for the piston crown associated with the diesel engine. There are a number of vital features that the artistic material must possess, including strong thermal conduction, good mixing, wear fence, and from top to bottom heat shock resistance. There was a shielding thermal barrier that was placed above the piston crown. With the use of the plasma splash technique, the substance Al203 that had been fired was coated over the substratum to a thickness of 200 µm [24]. All of the experimental work on the piston crown has been finished, as shown in Figure 3.

**Figure 3**. Experimental work on piston crown.

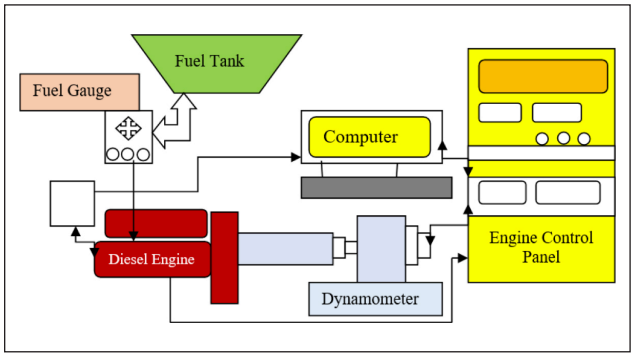


**Figure 4**. Experimental setup.

**Figure 5**. Experimental setup of VCR diesel engine (photographic view).

### Uncertainty Analysis

Visualization, range, devices, atmosphere, and calibration were used to estimate error as well as uncertainty evaluation, which was then split down into assigned and fixed errors by process time. For accurate results, undertake an uncertainty analysis. The transfer of uncertainty technique, or root mean square, was used to assess engine systems uncertainty. The equation (1) was used to analyze engine efficiency parameter uncertainty.

$$\varphi_R = \left[\left(\frac{\partial R}{\partial x_1}\varphi_1\right)^2 + \left(\frac{\partial R}{\partial x_2}\varphi_2\right)^2 + \cdots + \left(\frac{\partial R}{\partial x_n}\varphi_n\right)^2\right]^{\frac{1}{2}} \quad (1)$$

### Experimental Setup

A kirloskar engine single chamber, four strokes, and an engine which links are connected to the control panel make up the design illustrated in Figure 4. Figure 5 illustrated the photographic view of experimental engine; The load can range from 0 to 5.2 KW according to the arrangement. In instruction to facilitate reading, the power output of the engine is 5.2 kilowatts when it is operating at 0 percent load, 50% load, and 100% full load. In the fuel container, the air mixture with fuel that is used with diesel and biodiesel is permitted, and the amount of the combination of fuels is controlled by the fuel calculator that is located on the control panel. The smoke meter and inlet manifold are some of the other configurations that may be programmed due to the open digital control panel. Sensors such as the fuel sensor, level sensor and load sensor, are monitored on (ECUs) and data analytics devices [25]. The engine specifications for the test engine are listed in Table 3.

### Experimental Design

The trial design, optimization, and validation processes have all been carried with the support of the Design-Expert® application, version 13. In the Table 4, the data input factors and

**Table 3.** Specifications of test engine

| Make | Kirloskar, 4S |
|---|---|
| No. of cylinder | One |
| Bore | 87.5 millimeter |
| Stroke | 110 millimeter |
| Power | 5.2 kilo watt |
| Compression ratio | 17.5:1 |
| Speed | 1500 rpm |
| Fuel injection timing | 23o b TDC |
| Injection pressure | 200 bars |

their respective levels are presented. A numerical calculation is performed on each and every variable that is entered. In order to maximize BTE while simultaneously improving BSFC, and diminishing NOx, CO, smoke, and HC, the load was selected to be between 0 and 100%, the TOME mix biodiesel (10, 20 and 30%), and the ethanol (10, 20 and 30%).

In the process of developing quadrat-ic and Box-Behnken models of estimation for inputs and response variables, RSM is a method of analysis that is generally utilized. RSM is helpful in assessing the influence that input parameters have on response variables, reducing the number of trials that are conducted, and maximizing the effectiveness of response variables. The experimental setup

**Table 4.** Factors and levels for TOME Blends with ethanol and load

| Process parameters | Levels | | |
|---|---|---|---|
| | 1 | 2 | 3 |
| A- Load (KG) | 0 | 50 | 100 |
| B- TOME blend (%) | 10 | 20 | 30 |
| C- Ethanol (%) | 10 | 20 | 30 |

TME: Tomato methyl ester.

matrix for tomato methyl ester blends mixed with ethanol and load (in kilograms) is presented in Table 5. The result is obtained for the Normal Piston and Thermal Barrier ($Al_2O_3$) Coated Piston.

## RESULT AND DISCUSSION

Exhibited values of R2, Adj. R2, Pred. R2, and a suitable precise appropriate within the required constraints for precision and adequate of the model for aimed responses are presented here, along with a summary of the analysis of variance (Table 6 for Normal piston and Table 7 for coated piston) and a review of the models for the performance of the normal piston and the $Al_2O_3$ coating piston in BTE and BSFC. Additionally, the presented data includes the emission characteristics of CO, HC, NoX, and smoke.

**Table 5.** Experimental design matrix for load/TOME/ethanol – normal & Al2O3 piston

| Sl. No | Load (kg) | TOME (%) | Ethanol (%) | Normal piston | | | | | | Thermal barrier ($Al_2O_3$) coated piston | | | | | |
|---|---|---|---|---|---|---|---|---|---|---|---|---|---|---|---|
| | | | | BTE | BSFC | CO | HC | NoX | Smoke | BTE | BSFC | CO | HC | NoX | Smoke |
| 1 | 50 | 30 | 30 | 29 | 0.27 | 0.02 | 55 | 540 | 3.8 | 30.5 | 0.66 | 0.038 | 52.7 | 385.4 | 18.9 |
| 2 | 0 | 20 | 30 | 19 | 0.67 | 0.02 | 45 | 797 | 6 | 31.5 | 0.39 | 0.108 | 50.6 | 568.1 | 38.2 |
| 3 | 50 | 20 | 20 | 28 | 0.4 | 0.01 | 48 | 398 | 11 | 30 | 0.28 | 0.036 | 50.2 | 529.4 | 23.8 |
| 4 | 50 | 20 | 20 | 31 | 0.29 | 0.09 | 45 | 573 | 23 | 27 | 0.23 | 0.039 | 39.8 | 762.9 | 18.6 |
| 5 | 100 | 20 | 30 | 32 | 0.24 | 0.01 | 48 | 560 | 17 | 25 | 0.65 | 0.046 | 56.5 | 395.8 | 10.7 |
| 6 | 50 | 10 | 10 | 30 | 0.66 | 0.02 | 35 | 755 | 4.5 | 19 | 0.39 | 0.117 | 54.4 | 578.5 | 30 |
| 7 | 50 | 20 | 20 | 31.6 | 0.4 | 0.01 | 45 | 367 | 5.6 | 15 | 0.3 | 0.045 | 53.9 | 539.8 | 15.6 |
| 8 | 0 | 30 | 20 | 30 | 0.31 | 0.08 | 49 | 528 | 10 | 14 | 0.25 | 0.047 | 43.6 | 773.3 | 10.42 |
| 9 | 50 | 30 | 10 | 27.5 | 0.26 | 0.02 | 41 | 494 | 28 | 21 | 0.2 | 0.031 | 50.8 | 400.4 | 7.76 |
| 10 | 100 | 30 | 20 | 25 | 0.21 | 0.02 | 37 | 752 | 14.2 | 23 | 0.66 | 0.102 | 48.7 | 583.1 | 27 |
| 11 | 0 | 20 | 10 | 19 | 0.67 | 0.04 | 44 | 638 | 5.5 | 28.5 | 0.67 | 0.03 | 48.3 | 544.4 | 12.67 |
| 12 | 100 | 20 | 10 | 15.4 | 0.68 | 0.01 | 47 | 662 | 28.5 | 15 | 0.7 | 0.032 | 37.9 | 777.9 | 7.48 |
| 13 | 100 | 10 | 20 | 14 | 0.71 | 0.005 | 40 | 686 | 19 | 25 | 0.3 | 0.04 | 54.6 | 364 | 8.33 |
| 14 | 0 | 10 | 20 | 21 | 0.46 | 0.03 | 52 | 659 | 4.15 | 29 | 0.67 | 0.11 | 52.5 | 546.7 | 27.6 |
| 15 | 50 | 20 | 20 | 23 | 0.34 | 0.11 | 58 | 258 | 18.5 | 19 | 0.42 | 0.038 | 52 | 508 | 13.25 |
| 16 | 50 | 20 | 20 | 28.5 | 0.31 | 0.025 | 45 | 536 | 19 | 28 | 0.32 | 0.041 | 41.7 | 741.5 | 8.05 |
| 17 | 50 | 10 | 30 | 15 | 0.68 | 0.08 | 63 | 343 | 12.5 | 31 | 0.45 | 0.054 | 46.6 | 658.4 | 21 |

BTE: Brake thermal efficiency; BSFC: Brake-specific fuel consumption.

**Table 6.** Test of hypotheses for BSFC, BTE, CO, HC, NoX, and smoke as predictor variables for normal piston

| | Normal piston | | | | | |
|---|---|---|---|---|---|---|
| | **BTE (%)** | **BSFC (kg/kW-h)** | **CO (% vol)** | **HC (ppm)** | **NoX (ppm)** | **Smoke (BSU)** |
| Standard deviation | 6.69 | 0.2091 | 0.0330 | 6.91 | 138.47 | 8.61 |
| Mean | 24.65 | 0.4447 | 0.0353 | 46.88 | 561.53 | 13.54 |
| C.V. % | 27.14 | 47.02 | 93.50 | 14.74 | 24.66 | 63.59 |
| $R^2$ | 0.4989 | 0.4593 | 0.5612 | 0.5952 | 0.6482 | 0.5229 |
| Adjusted $R^2$ | -0.1453 | -0.2359 | -0.0030 | 0.0748 | 0.1958 | -0.0906 |
| Predicted $R^2$ | -4.6141 | -4.8640 | -2.5474 | -4.0777 | -1.0519 | -2.4841 |
| Adeq precision | 3.4768 | 3.2113 | 3.4076 | 3.9860 | 3.9806 | 3.4070 |

BTE: Brake thermal efficiency; BSFC: Brake-specific fuel consumption.

**Table 7.** Test of hypotheses for BSFC, BTE, CO, HC, NoX, and smoke as predictor variablesfor $Al_2O_3$ coated piston

| | Thermal barrier ($Al_2O_3$) coated piston | | | | | |
|---|---|---|---|---|---|---|
| | **BTE (%)** | **BSFC (kg/kW-h)** | **CO (% vol)** | **HC (ppm)** | **NoX (ppm)** | **Smoke (BSU)** |
| Standard deviation | 5.55 | 0.1927 | 0.0326 | 4.71 | 138.65 | 10.24 |
| Mean | 24.21 | 0.4435 | 0.0561 | 49.11 | 568.09 | 17.61 |
| C.V. % | 22.94 | 43.45 | 58.14 | 9.59 | 24.41 | 58.14 |
| $R^2$ | 0.6259 | 0.5154 | 0.5179 | 0.6762 | 0.5550 | 0.4531 |
| Adjusted $R^2$ | 0.1449 | -0.1075 | -0.1020 | 0.2600 | -0.0171 | -0.2500 |
| Predicted $R^2$ | -0.4493 | -3.1506 | -1.5571 | -1.2407 | -3.0634 | -1.9570 |
| Adeq precision | 4.1089 | 3.4164 | 3.4715 | 5.0048 | 4.1483 | 2.9339 |

BTE: Brake thermal efficiency; BSFC: Brake-specific fuel consumption.

The outcomes of the experiment were subjected to (ANOVA), and a number of models were created in the design expert. The projected values were then calculated using the equations. Therefore, in order to determine the most desirable parameter configurations, acceptability analysis was applied using the direct equation for getting better results.

**Performance Result**

Equation 2 for a Normal Piston and Equation 3 for an $Al_2O_3$ Coated Piston were derived from the RSM quadratic model of BTE based on the measured parameters.

[BTE=27.82+-1.075*A+-2.3125*B+-0.3875*C+-4.25*AB+-0.9AC+4.625*BC+-3.0475*A^2+-3.5225*B^2+-0.1725*C^2] (2)

[BTE=26.8+-2.75*A+-1.5625*B+1.4375*C+-0.5*AB+-6AC+0.375*BC+-5.0875*A^2+-1.2125*B^2+0.7875*C^2] (3)

Figure 6 (a) 2D and (b) 3D surface plot shows the BTE performance of normal piston, the impact of the quadratic factors Initialize, TOME Mix with the addition of ethanol infusion When subjected to the highest possible load circumstances, the (BTE) of B20E30 was determined to be around 4% more than that of pure diesel. Increased the amount of oxygen in ethanol enhances its combustion efficiency, leading to heightened thermal performance [26, 27]. Due to the increased viscosity and subsequent decrease in combustion rate coming from the elevated ethanol concentration in the mixture, the (BTE) is lower compared to B10E20, as shown in Table 6. As the ethanol concentration in the fuel blend improves, the TE of the brakes enhances. The outside temperature of the combination of air and fuel drops as the ethanol energy share increases because of the heat that ethanol absorbs and its high volatility. This is because they create an increase in the blend density, which in turn causes the temperature to decrease. In comparison to previous engines, the low heat rejection engine, which was fitted with a fully stabilised $Al_2O_3$ coating, demonstrated a higher level of thermal efficiency.

This can be ascribed to the ceramics coating's ability to act as a heat barrier, which effectively separates the engine from the environment around it. The B20E30 blend exhibited an approximately 3.5% increase in comparison to pure diesel, however its (BTE) was lower than that of the B30E20 blend [12]. Minimizing heat dissipation enables a boost in engine output and thermal effectiveness which shown in Figure 7 (a & b) The ANOVA Table 8 provides information on the variability between groups and within groups, helping to determine the significance of the factors and their interactions of BTE.

Equation 4 for a Normal Piston and Equation 5 for an $Al_2O_3$ Coated Piston were derived from the RSM quadratic model of BSFC based on the measured parameters

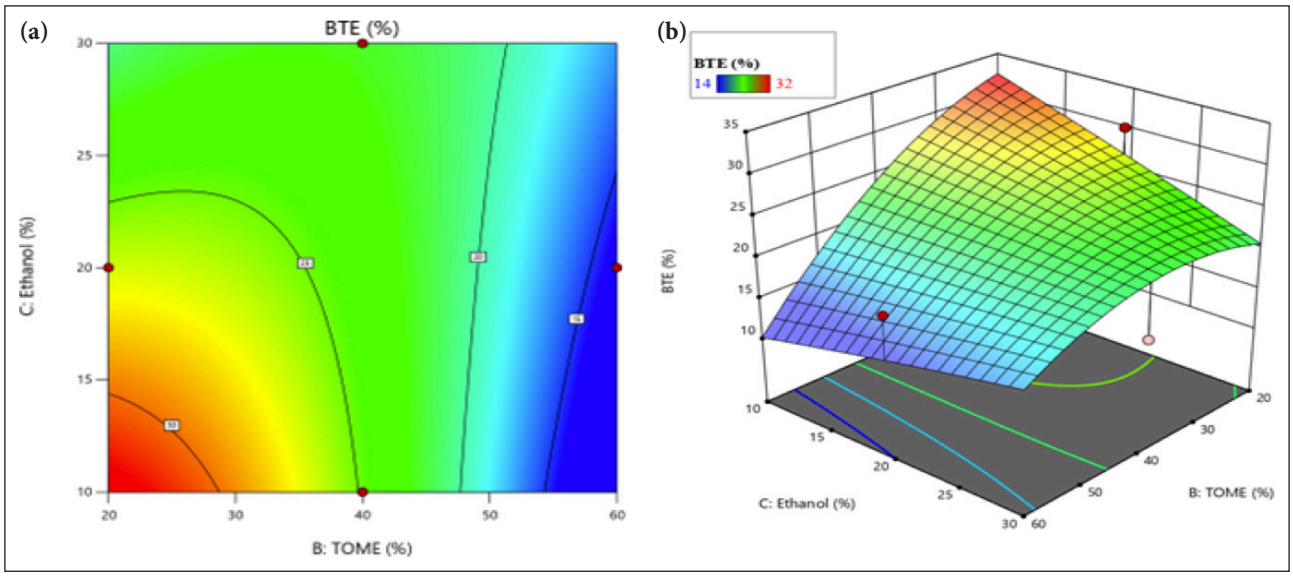


**Figure 6**. **(a)** 2D and **(b)** 3D Surface plot with load/TOME/ethanol with normal piston – BTE performance.

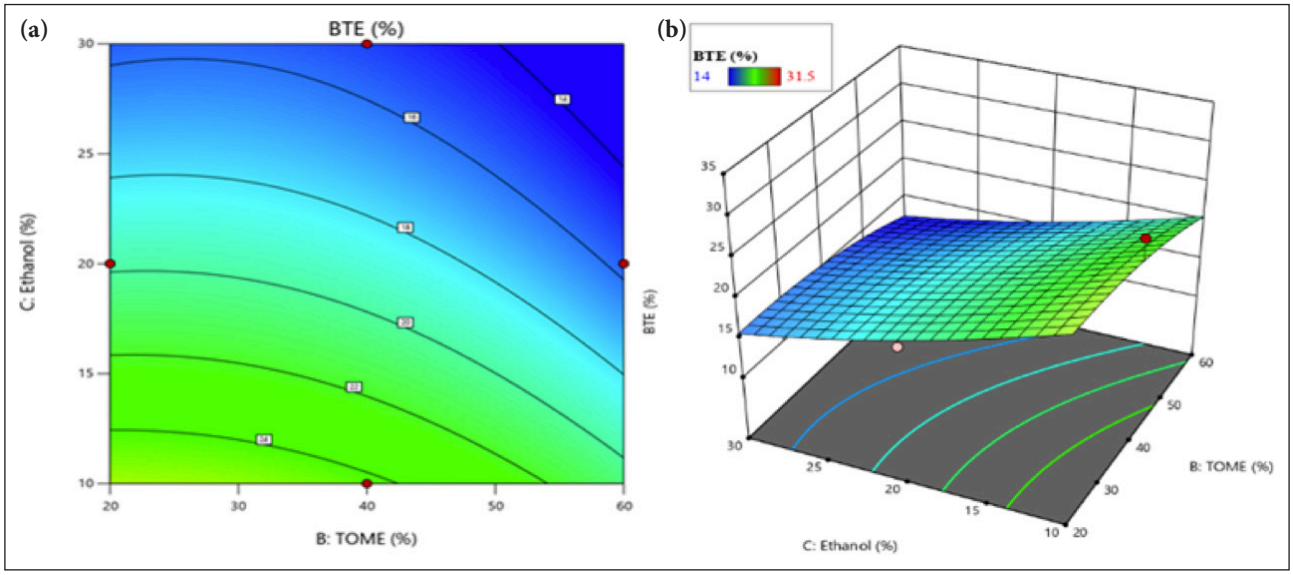


**Figure 7**. **(a)** 2D and **(b)** 3D Surface plot with Load/TOME/Ethanol with Al2O3 Coated piston – BTE.

[BSFC=0.388+0.07125*A+0.03*B+-0.00625*C+0.0575*AB+0.045*AC+-0.0875*BC+0.136*A^2+0.0935*B^2+-0.109*C^2] (4)

[BSFC=0.468+-0.00375*A+0.05125*B+0.0225*C+-0.02*AB+0.0325*AC+0.1675*BC+-0.0765*A^2+0.1285*B^2+-0.104*C^2] (5)

Figure 8 (a) 2D and (b) 3D surface plot shows the BSFC performance of normal piston, the increase in (BSFC) was qualified to the simultaneous rise in injected fuel and ethanol. Demonstrates that the (BSFC) reduces as the engine load rises when using ethanol ratios. When compared to diesel, B10E20 and B30E20 blends obtained a reduction of 3.6% and 12% in (BSFC), with values of 0.71 kg/kW-h and 0.21 kg/kW-h, respectively. However, B30E20 blends showed an increase of 8% in fuel consumption compared to diesel. Engines running on blends of biodiesel consume a greater amount of fuel than traditional diesel engines do because biodiesel blends have a higher volume and a lower energy content than traditional diesel [28]. The ANOVA Table 9 provides information on the variability between groups and within groups, helping to determine the significance of the factors and their interactions of BSFC. As the biodiesel blend ratio increases, the fuel consumption increases due to the decrease in the amount of energy and the density of the combination of fuels [26]. Due to the excellent heat retention properties of the $Al_2O_3$ coating, shown in Figure 9 (a & b) it allows for higher temperatures inside the cylinder, leading to improved oxidation of the biodiesel mixture. This, in turn, enhances atomization and vaporization. The B20E10 mix demonstrated a roughly 3.5% improvement compared to pure diesel, but its (BSFC) was higher in comparison to that of the B30E10 blend, resulting in reduced consumption of fuel while maintaining a constant engine speed.

**Table 8.** Anova parametric results – BTE

| | Normal piston | | | Thermal barrier ($Al_2O_3$) coated piston | | |
|---|---|---|---|---|---|---|
| **Source** | **Sum of squares** | **F-value** | **p** | **Sum of squares** | **F-value** | **p** |
| Model | 311.88 | 0.7744 | 0.6477 | 361.17 | 1.30 | 0.3724 |
| A-load | 9.24 | 0.2066 | 0.6632 | 60.50 | 1.96 | 0.2040 |
| B-TOME | 42.78 | 0.9561 | 0.3608 | 19.53 | 0.6334 | 0.4523 |
| C-ethanol | 1.20 | 0.0268 | 0.8745 | 16.53 | 0.5361 | 0.4878 |
| AB | 72.25 | 1.61 | 0.2444 | 1.0000 | 0.0324 | 0.8622 |
| AC | 3.24 | 0.0724 | 0.7956 | 144.00 | 4.67 | 0.0675 |
| BC | 85.56 | 1.91 | 0.2092 | 0.5625 | 0.0182 | 0.8964 |
| $A^2$ | 39.10 | 0.8739 | 0.3810 | 108.98 | 3.53 | 0.1022 |
| $B^2$ | 52.24 | 1.17 | 0.3157 | 6.19 | 0.2007 | 0.6677 |
| $C^2$ | 0.1253 | 0.0028 | 0.9593 | 2.61 | 0.0847 | 0.7795 |
| Residual | 313.23 | | | 215.86 | | |
| Lack of fit | 209.18 | 2.68 | 0.1823 | 34.56 | 0.2542 | 0.8552 |
| Pure error | 104.05 | | | 181.30 | 1.30 | 0.3724 |

TOME: Tomato methyl ester.

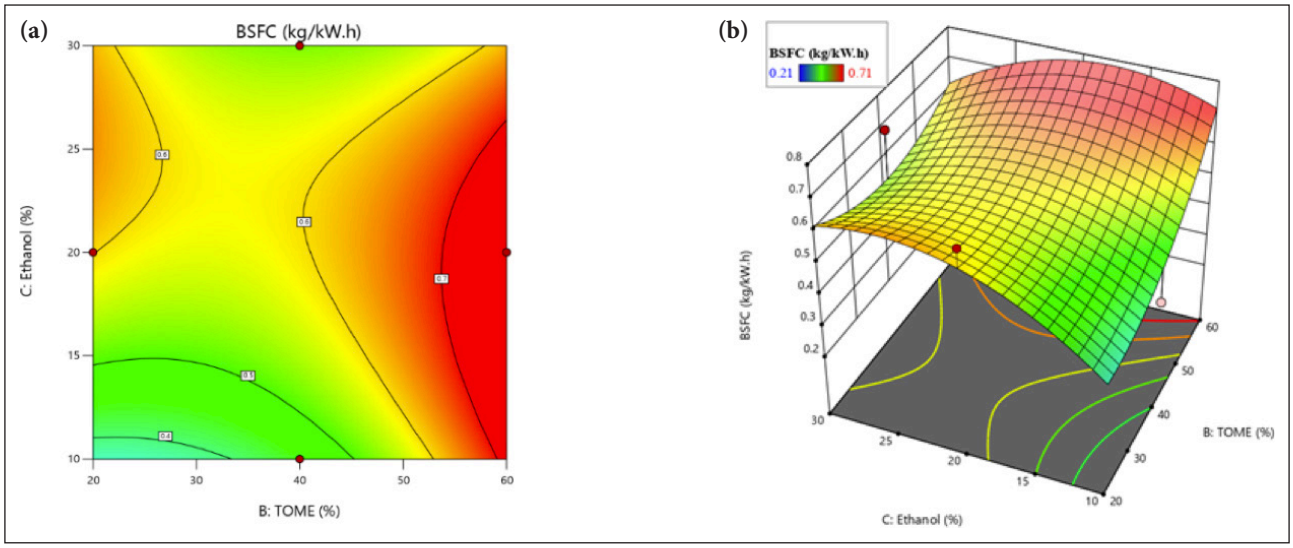


**Figure 8**. **(a)** 2D and **(b)** 3D surface plot with load/TOME/Ethanol with normal piston – BSFC performance.

**Emission Result**

Equation 6 for a Normal Piston and Equation 7 for an $Al_2O_3$ Coated Piston were derived from the RSM quadratic model of CO emission based on the measured parameters.

[CO=0.033+0.00625*A+-0.013125*B+-0.018125*C+0.0175*AB+-0.025*AC+0.01875*BC+0.006625*A^2+0.002875*B^2+-0.004625*C^2] (6)

[CO=0.0684+-0.017375*A+0.002125*B+-0.00825*C+-0.017*AB+0.02225*AC+-0.00225*BC+0.00205*A^2+-0.01745*B^2+-0.0107*C^] (7)

Equation 8 for a Normal Piston and Equation 9 for an $Al_2O_3$ Coated Piston were derived from the RSM quadratic model of CO emission based on the measured parameters.

[CO=0.033+0.00625*A+-0.013125*B+-0.018125*C+0.0175*AB+-0.025*AC+0.01875*BC+0.006625*A^2+0.002875*B^2+-0.004625*C^2] (8)

[CO=0.0684+-0.017375*A+0.002125*B+-0.00825*C+-0.017*AB+0.02225*AC+-0.00225*BC+0.00205*A^2+-0.01745*B^2+-0.0107*C^] (9)

Figure 10 (a) 2D and (b) 3D surface plot shows the CO emission of normal piston, the emission of (CO) from diesel is reduced when full combustion takes place under low loads. More biodiesel blends are available than diesel, and it has fewer carbon monoxide emissions. As a result of the incorporation of biodiesel into gasoline blends, the researchers discovered that CO and $CO_2$ emissions were influenced. It is because biodiesel has a greater amount of oxygen. Therefore, carbon monoxide (CO) is decreased, and carbon dioxide ($CO_2$) is the bigger load mass. This is connected to chemical

**Table 9.** ANOVA Parametric results – BSFC

| | Normal piston | | | Thermal barrier ($Al_2O_3$) coated piston | | |
|---|---|---|---|---|---|---|
| **Source** | **Sum of squares** | **F-value** | **Source** | **Sum of squares** | **F-value** | **Source** |
| Model | 0.2600 | 0.6607 | Model | 0.2600 | 0.6607 | Model |
| A-load | 0.0406 | 0.9289 | A-load | 0.0406 | 0.9289 | A-load |
| -B-TOME | 0.0072 | 0.1647 | -B-TOME | 0.0072 | 0.1647 | -B-TOME |
| C-ethanol | 0.0003 | 0.0071 | C-ethanol | 0.0003 | 0.0071 | C-ethanol |
| AB | 0.0132 | 0.3025 | AB | 0.0132 | 0.3025 | AB |
| AC | 0.0081 | 0.1853 | AC | 0.0081 | 0.1853 | AC |
| BC | 0.0306 | 0.7004 | BC | 0.0306 | 0.7004 | BC |
| $A^2$ | 0.0779 | 1.78 | $A^2$ | 0.0779 | 1.78 | $A^2$ |
| $B^2$ | 0.0368 | 0.8419 | $B^2$ | 0.0368 | 0.8419 | $B^2$ |
| $C^2$ | 0.0500 | 1.14 | $C^2$ | 0.0500 | 1.14 | $C^2$ |
| Residual | 0.3061 | | Residual | 0.3061 | | Residual |
| Lack of fit | 0.1968 | 2.40 | Lack of fit | 0.1968 | 2.40 | Lack of fit |
| Pure error | 0.1093 | | Pure error | 0.1093 | | Pure error |

BSFC: Brake-specific fuel consumption; TOME: Tomato methyl ester.

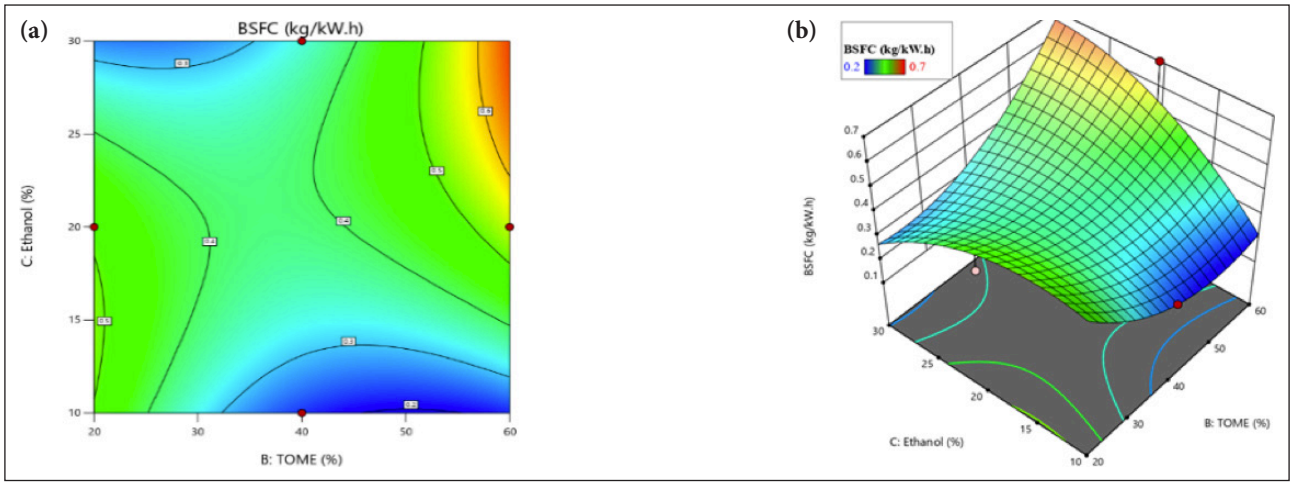


**Figure 9**. **(a)** 2D and **(b)** 3D surface plot with load/TOME/ethanol with $Al_2O_3$ coated piston – BSFC performance.

reactions that increase the generation of carbon monoxide [6]. Based on the data presented in Figure 9, it can be observed that B20E20 blends, which have a greater CO emission, and B10E20 blends, which have lower CO emissions by 5.6% and 10.2%, respectively, in comparison to pure diesel, whereas B30 blends produce higher CO emissions than diesel shown in Figure 11 (a & b). In addition, the thermal barrier $Al_2O_3$ coatings had an effect on carbon monoxide emissions, with coated engines producing a lower level of emissions compared to engines that were not treated. It is through late-phase burning and the subsequent oxidation of carbon monoxide that nanocoated thermal resistance is triggered. The ANOVA Table 10 provides information on the variability between groups and within groups, helping to determine the significance of the factors and their interactions of CO emission. There was a decrease in the amount of carbon monoxide emissions as the speed of the engine increased, and when it was working at its optimal speed, the amount of CO emissions was decreased.

Equation 10 for a Normal Piston and Equation 11 for an $Al_2O_3$ Coated Piston were derived from the RSM quadratic model of HC emission based on the measured parameters.

[HC=47+-3.375*A+-0.875*B+-2.75*C+5*AB+-2.75*AC+3.25*BC+5*A^2+-3.5*B^2+-1.75*C^2] (10)

[HC=50.28+-4.325*A+-3*B+-1.6*C+-2.05*AB+2*AC+1.85*BC+-2.765*A^2+0.785*B^2+-0.515*C^2] (11)

Figure 12 (a) 2D and (b) 3D surface plot shows the HC emission of normal piston, as a result of the presence of oxygen in ethanol, the oxidation of air hydrocarbons is accelerated, which leads to an improvement in fuel economy. Hydrocarbon (HC) emissions are lowered, which also contributes to the improvement. When opposed to the burning of hydrogen mix, the burning of ethanol results in a lower

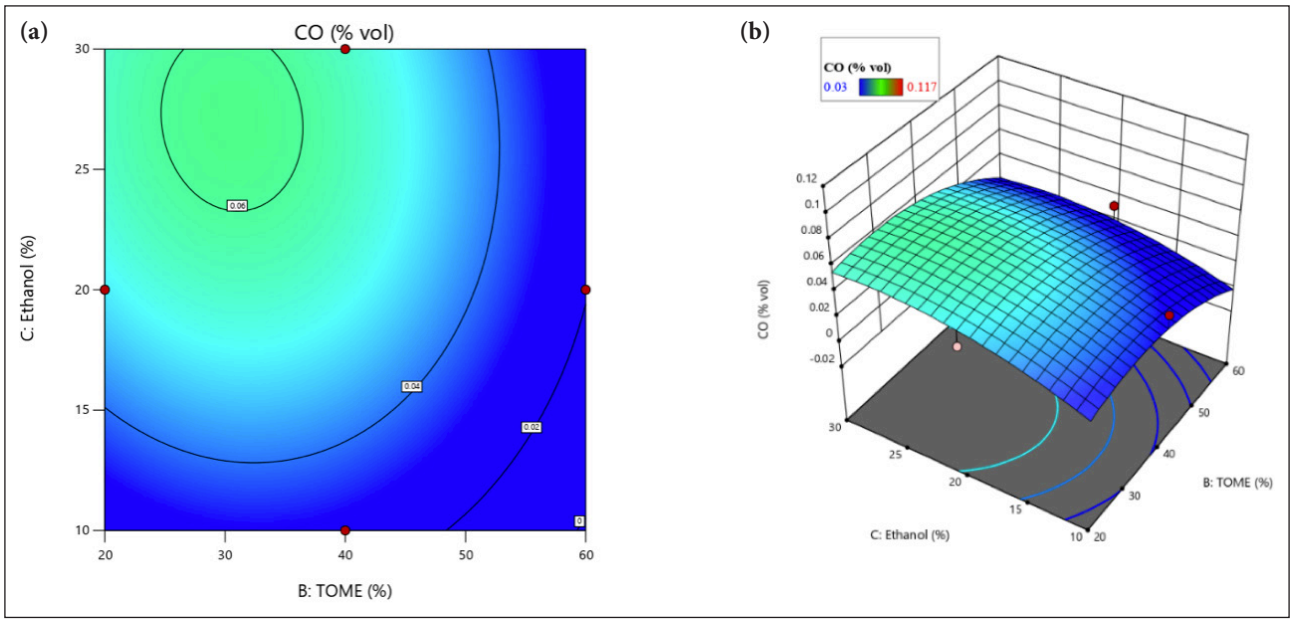


**Figure 10**. **(a)** 2D and **(b)** 3D Surface plot with load/TOME/ethanol with normal piston – CO emission.

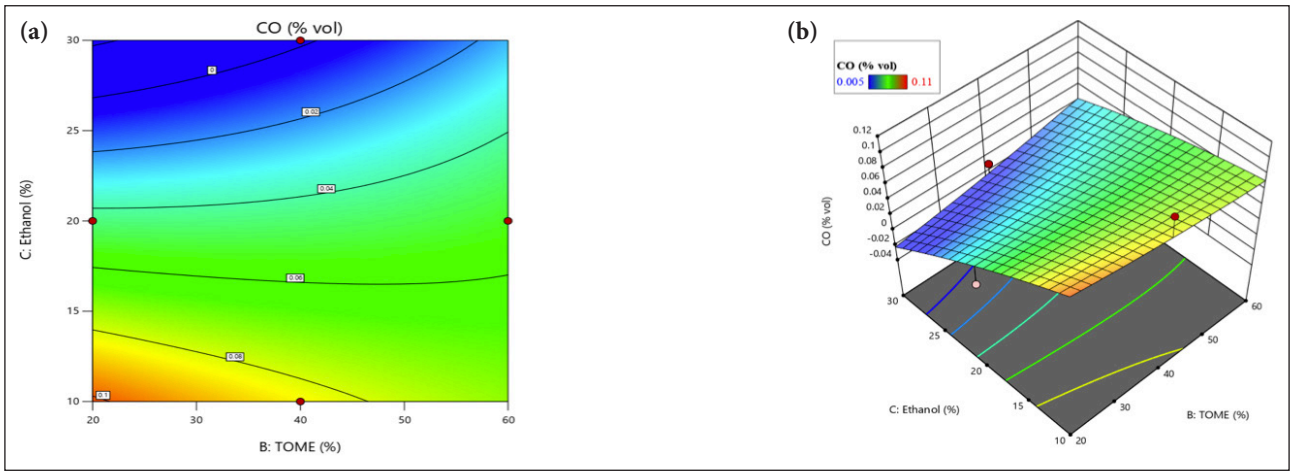


**Figure 11**. **(a)** 2D and (b) 3D surface plot with load/TOME/ethanol with Al2O3 coated piston – CO emission.

burning temperature and pressure, which leads to a lesser oxidation of hydrocarbons [7]. This is responsible for of the larger HC emissions that are produced. As can be seen in Figure 13, B10E30, which produces higher emissions, and B10E10 blends produce lower hydrocarbon emissions by 3.5% and 10.6%, accordingly, relative to unadulterated diesel. If B10E10 blends are contrasted to diesel, they result in 10.6% more HC. A coated piston and higher temperatures in the engine's combustion area head both contributed to an increase in the pace at which gasoline evaporated. Because of the higher combustion temperature provided by the thermal barrier $Al_2O_3$ layer, fuel combustion is made easier and more efficient. Because of the enhanced pace at which the thermal barrier coating breaks down hydrocarbons into hydrogen as well as oxygen in the combustion process, coated pistons were found to have lower levels of hydrocarbon emissions as shown in Figure 13(a &b). The ANOVA Table 11 provides information on the variability between groups and within groups, helping to determine the significance of the factors and their interactions of HC emission. It is necessary to take into consideration other parameters, such as quenching range and combustibility threshold, in order to reduce the amount of hydrocarbon emissions that are produced by heat barrier coatings [25].

Equation 12 for a Normal Piston and Equation 13 for an $Al_2O_3$ Coated Piston were derived from the RSM quadratic model of NoX emission based on the measured parameters.

[NoX=562.6+44.125*A+12.375*B+34.25*C+-108.25*AB+141.5*AC+-104*BC+-54.675*A^2+90.825*B^2+-38.425*C^2] (12)

[NoX=556.3+95.8875*A+47.45*B+45.9875*C+12.7*AB+14.875*AC+-29.65*BC+81.6125*A^2+-79.6625*B^2+23.1125*C^2] (13)

Figure 14 (a) 2D and (b) 3D surface plot shows the NoX emission of normal piston, Lowering the rate at which the premixed fuel is burned reduces the emissions of nitrogen oxide (NoX) while minimizing the release of heat. There is

**Table 10.** ANOVA parametric results – CO emission

| | Normal piston | | | Thermal barrier ($Al_2O_3$) coated piston | | |
|---|---|---|---|---|---|---|
| **Source** | **Sum of squares** | **F-value** | **p** | **Sum of squares** | **F-value** | **p** |
| Model | 0.0097 | 0.9947 | 0.5149 | 0.0080 | 0.8355 | 0.6085 |
| A-load | 0.0003 | 0.2869 | 0.6088 | 0.0024 | 2.27 | 0.1758 |
| B-TOME | 0.0014 | 1.27 | 0.2977 | 0.0000 | 0.0339 | 0.8591 |
| C-ethanol | 0.0026 | 2.41 | 0.1643 | 0.0005 | 0.5114 | 0.4977 |
| AB | 0.0012 | 1.12 | 0.3241 | 0.0012 | 1.09 | 0.3320 |
| AC | 0.0025 | 2.30 | 0.1735 | 0.0020 | 1.86 | 0.2149 |
| BC | 0.0014 | 1.29 | 0.2932 | 0.0000 | 0.0190 | 0.8942 |
| $A^2$ | 0.0002 | 0.1697 | 0.6927 | 0.0000 | 0.0166 | 0.9010 |
| $B^2$ | 0.0000 | 0.0320 | 0.8632 | 0.0013 | 1.20 | 0.3088 |
| $C^2$ | 0.0001 | 0.0827 | 0.7820 | 0.0005 | 0.4528 | 0.5226 |
| Residual | 0.0076 | | | 0.0075 | | |
| Lack of fit | 0.0034 | 1.10 | 0.4467 | 0.0019 | 0.4664 | 0.7215 |
| Pure error | 0.0042 | | | 0.0055 | 0.8355 | 0.6085 |

BSFC: Brake-specific fuel consumption; TOME: Tomato methyl ester.

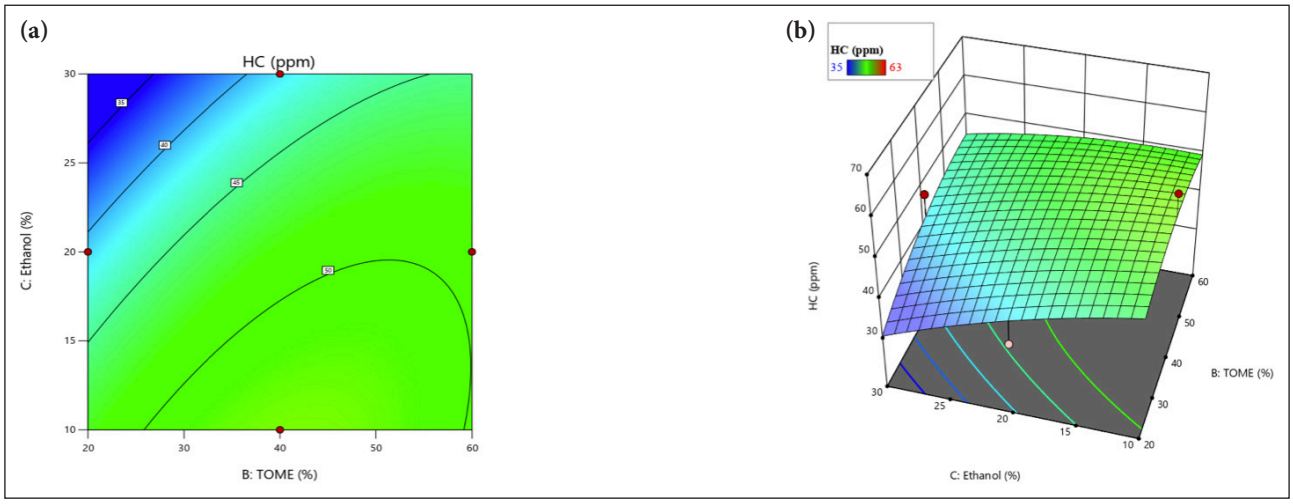


**Figure 12**. **(a)** 2D and **(b)** 3D surface plot with load/TOME/ethanol with normal piston – HC emission.

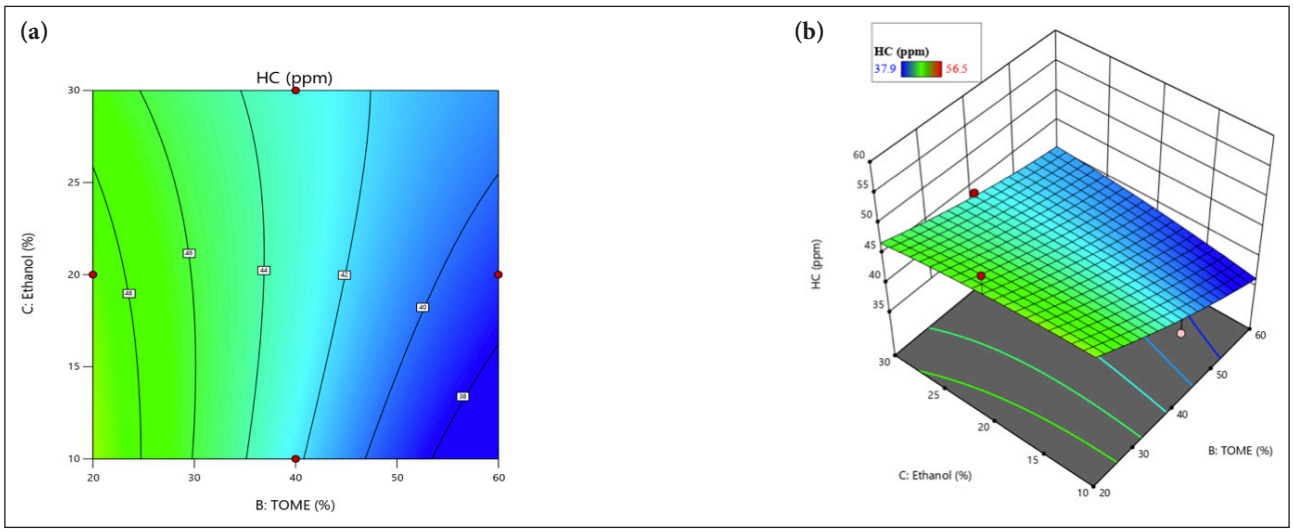


**Figure 13**. **(a)** 2D and **(b)** 3D surface plot with load/TOME/ethanol with Al2O3 coated piston – HC emission.

**Table 11.** ANOVA şarametric results – HC emission

| | Normal piston | | | Thermal barrier ($Al_2O_3$) coated piston | | |
|---|---|---|---|---|---|---|
| **Source** | **Sum of squares** | **F-value** | **p** | **Sum of squares** | **F-value** | **p** |
| Model | 491.51 | 1.14 | 0.4396 | 324.20 | 1.62 | 0.2676 |
| A-load | 91.13 | 1.91 | 0.2096 | 149.64 | 6.75 | 0.0355 |
| B-TOME | 6.13 | 0.1283 | 0.7308 | 72.00 | 3.25 | 0.1146 |
| C-ethanol | 60.50 | 1.27 | 0.2974 | 20.48 | 0.9236 | 0.3685 |
| AB | 100.00 | 2.09 | 0.1911 | 16.81 | 0.7581 | 0.4128 |
| AC | 30.25 | 0.6335 | 0.4522 | 16.00 | 0.7216 | 0.4237 |
| BC | 42.25 | 0.8848 | 0.3782 | 13.69 | 0.6174 | 0.4578 |
| $A^2$ | 105.26 | 2.20 | 0.1812 | 32.19 | 1.45 | 0.2674 |
| $B^2$ | 51.58 | 1.08 | 0.3332 | 2.59 | 0.1170 | 0.7423 |
| $C^2$ | 12.89 | 0.2700 | 0.6193 | 1.12 | 0.0504 | 0.8288 |
| Residual | 334.25 | | | 155.21 | | |
| Lack of fit | 254.25 | 4.24 | 0.0984 | 57.61 | 0.7869 | 0.5606 |
| Pure error | 80.00 | | | 97.61 | | |

HC: Hydrocarbon; TOME: Tomato methyl ester.

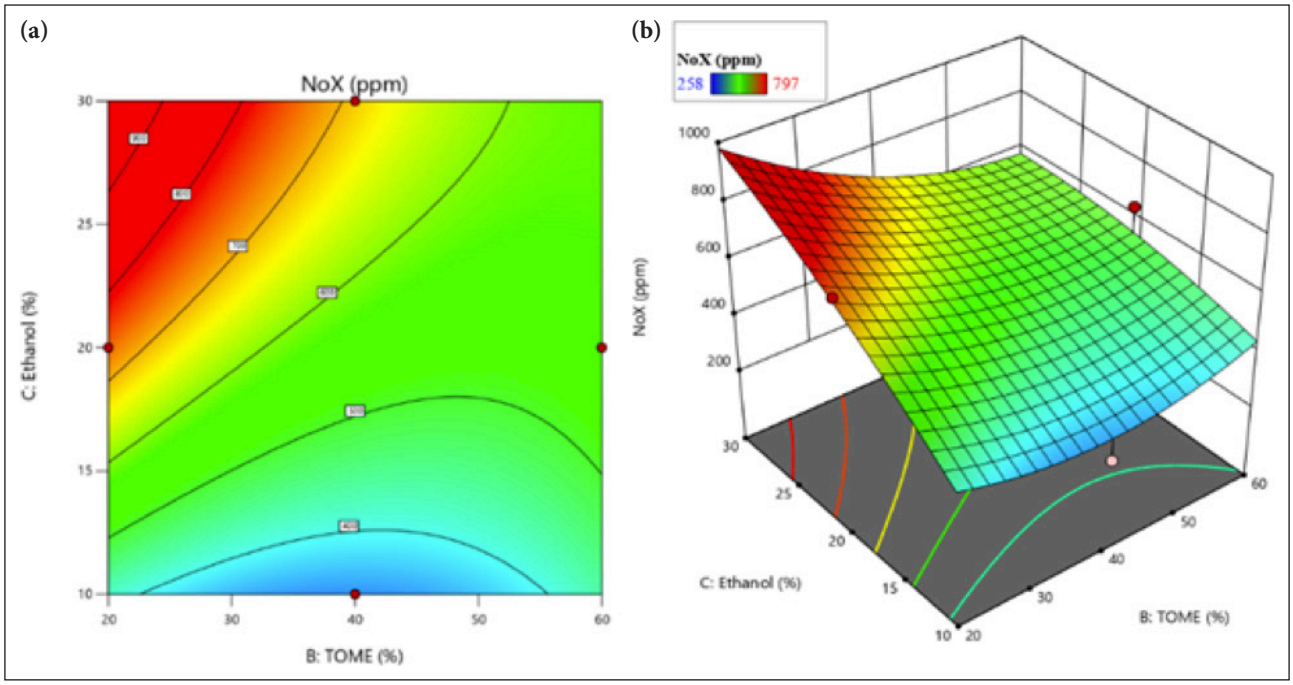


**Figure 14**. **(a)** 2D and **(b)** 3D surface plot with load/TOME/ethanol with Normal piston – NoX emission.

a correlation between the increase in ethanol's energy contribution and the increase in NOX emissions throughout all states. In ethanol biodiesel dual-fuel engines, the formation of NOX is influenced by a wide variety of parameters. As the temperature of the fire and the rate at which it burns drop, the amount of NOX that is produced increases [1]. Because of a greater use of gasoline, the rise in the strain on the engine was attributed to the increase in the amount of NOX emissions. Blends produce NoX at a rate that is higher than diesel at the highest load conditions, as shown in Figure 13. The rates of production for B20E30, B10E10, and B30E20 blends are 5.5%, 6.5%, and 7.5% respectively. However, there is just one problem that needs to be fixed with the engine that has been coated with $Al_2O_3$, and that is the emission of NoX. The ANOVA Table 12 provides information on the variability between groups and within groups, helping to determine the significance of the factors and their interactions of NoX. The NO emission of a coated piston engine is greater compared to that of a noncoated piston engine shown in Figure 15 (a & b) and the operating temperature of the coated piston engine may be higher. This combination of factors leads to an earlier start of com-

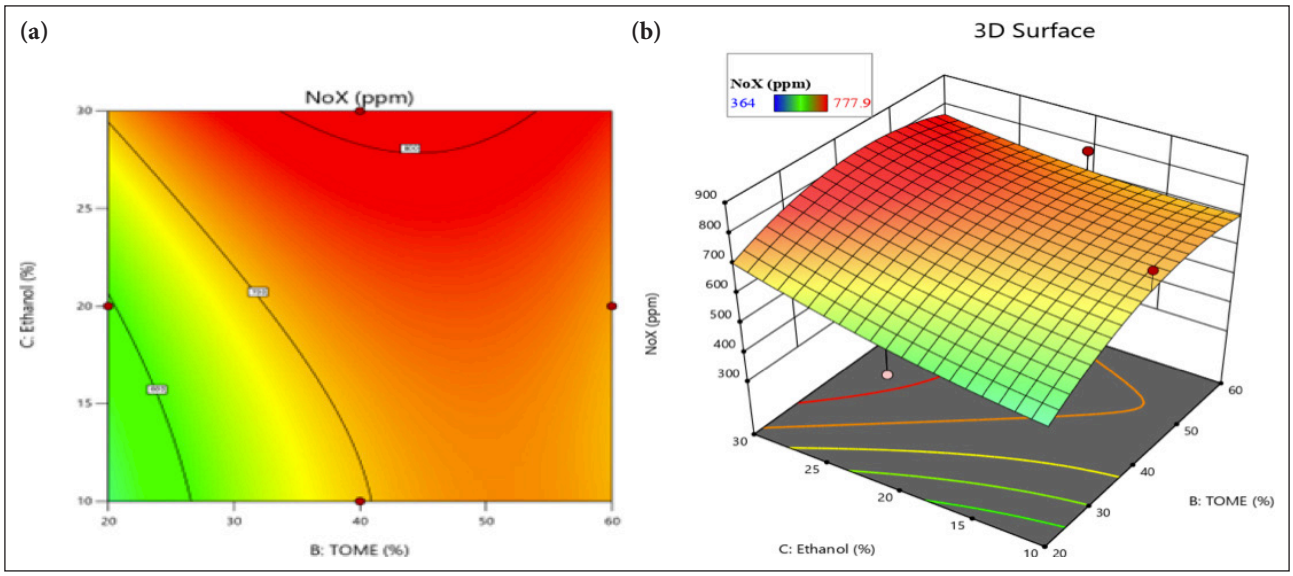


**Figure 15**. **(a)** 2D and (b) 3D surface plot with load/TOME/ethanol with Al2O3 coated piston – NoX Emission.

**Table 12.** ANOVA parametric results – NoX emission

| | Normal piston | | | Thermal barrier ($Al_2O_3$) coated piston | | |
|---|---|---|---|---|---|---|
| **Source** | **Sum of squares** | **F-value** | **p** | **Sum of squares** | **F-value** | **p** |
| Model | 2.473E+05 | 1.43 | 0.3249 | 1.678E+05 | 0.9702 | 0.5284 |
| A-load | 15576.13 | 0.8123 | 0.3974 | 73555.30 | 3.83 | 0.0913 |
| B-TOME | 1225.12 | 0.0639 | 0.8077 | 18012.02 | 0.9370 | 0.3653 |
| C-ethanol | 9384.50 | 0.4894 | 0.5068 | 16918.80 | 0.8802 | 0.3794 |
| AB | 46872.25 | 2.44 | 0.1619 | 645.16 | 0.0336 | 0.8598 |
| AC | 80089.00 | 4.18 | 0.0803 | 885.06 | 0.0460 | 0.8362 |
| BC | 43264.00 | 2.26 | 0.1768 | 3516.49 | 0.1829 | 0.6817 |
| $A^2$ | 12586.76 | 0.6564 | 0.4445 | 28044.63 | 1.46 | 0.2663 |
| $B^2$ | 34733.39 | 1.81 | 0.2203 | 26720.48 | 1.39 | 0.2769 |
| $C^2$ | 6216.76 | 0.3242 | 0.5869 | 2249.21 | 0.1170 | 0.7423 |
| Residual | 1.342E+05 | | | 1.346E+05 | | |
| Lack of fit | 39692.75 | 0.5599 | 0.6693 | 70548.11 | 1.47 | 0.3495 |
| Pure error | 94529.20 | | | 64009.50 | | |

TOME: Tomato methyl ester.

bustion, which in turn transfers pressure and temperature. During the premixing phase, the majority of premixed biofuels are burned, which results in a reduction in the amount of NOX emissions [10].

Equation 14 for a Normal Piston and Equation 15 for an $Al_2O_3$ Coated Piston were derived from the RSM quadratic model of Smoke opacity emission based on the measured parameters.

Smoke=[11.48+1.54375*A+1.93125*B+2.15*C+2.3375*AB+4*AC+1.2*BC+-1.93375*A^2+-2.88375*B^2+9.20375*C^2] (14)

Smoke= [21.67+-4.9225*A+0.20375*B+0.10375*C+-6.11*AB+-0.495*AC+-1.3475*BC+0.00875*A^2+-7.66375*B^2+-0.97375*C^2] (15)

Figure 16 (a) 2D and (b) 3D surface plot shows the smoke emission of normal piston, inefficient combustion of the fuel results in the production of smoke. This is because smoke is produced when the fuel is burned. Additionally, as the engine's load grows, the unused energy of evaporation decreases and the ensuing delay in igniting occurs, both of which have an impact on reducing the amount of smoke emissions. By comparing pure diesel to B20E10, which creates greater emissions, and B30E30 blends, which produce reduced smoke emissions by 4.5% and 8.6%, respectively, as shown in Figure 15, it is clear that the former produces higher emissions. The application of an $Al_2O_3$ coating to engine components results in the production of high burning temperatures shown in Figure

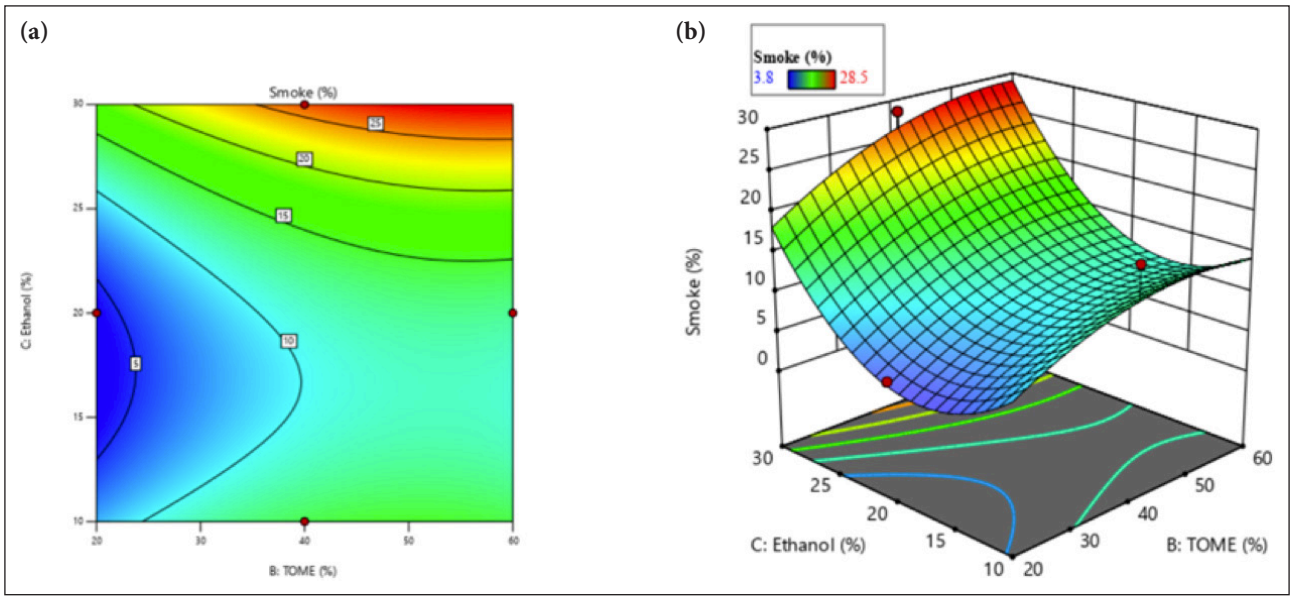


**Figure 16**. **(a)** 2D and **(b)** 3D surface plot with load/TOME/ethanol with normal piston – smoke opacity.

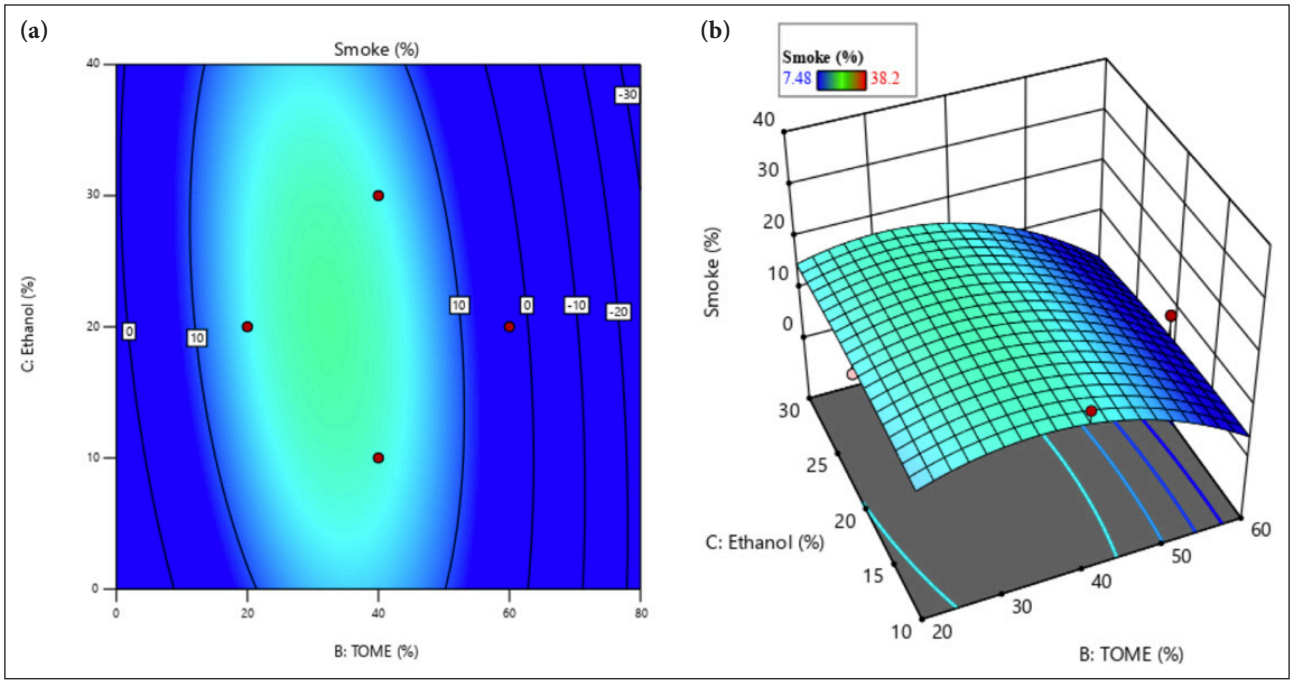


**Figure 17**. **(a)** 2D and **(b)** 3D surface plot with Load/TOME/ethanol with $Al_2O_3$ coated piston – Smoke opacity.

17 (a & b) which has the effect of completely consuming the fuel. Because of this, the amount of smoke emissions produced by coated pistons at high ratios of compression is reduced, as evidenced by the fact that [16]. can be recorded. The ANOVA Table 13 provides information on the variability between groups and within groups, helping to determine the significance of the factors and their interactions of Smoke opacity.

## CONCLUSION

The (RSM) optimization technique proved to be effective in investigating the influence of load, Tomato Methyl Ester (TOME), and Ethanol injection on engine performance and exhaust gas pollutants.

- The use of thermal barrier coatings, particularly $Al_2O_3$, on the piston operating with biodiesel blends exhibited potential in enhancing engine performance and minimizing emissions.
- Blends of biodiesel, such as B20E30, B10E20, and B30E20, exhibited comparable performance and emission levels to those of pure diesel. The B20E30 mix displayed a marginal 3.5% reduction in brake thermal efficiency (BTE) in comparison to pure diesel. However, its BTE was inferior to that of the B30E20 blend.

**Table 13.** ANOVA parametric results – smoke opacity

| | Normal piston | | | Thermal barrier ($Al_2O_3$) coated piston | | |
|---|---|---|---|---|---|---|
| **Source** | **Sum of squares** | **F-value** | **p** | **Sum of squares** | **F-value** | **p** |
| Model | 569.08 | 0.8523 | 0.5979 | 608.08 | 0.6445 | 0.7359 |
| A-Load | 19.07 | 0.2570 | 0.6278 | 193.85 | 1.85 | 0.2161 |
| B-TOME | 29.84 | 0.4022 | 0.5461 | 0.3321 | 0.0032 | 0.9567 |
| C-Ethanol | 36.98 | 0.4985 | 0.5030 | 0.0861 | 0.0008 | 0.9779 |
| AB | 21.86 | 0.2946 | 0.6041 | 149.33 | 1.42 | 0.2716 |
| AC | 64.00 | 0.8627 | 0.3839 | 0.9801 | 0.0093 | 0.9257 |
| BC | 5.76 | 0.0776 | 0.7886 | 7.26 | 0.0693 | 0.8000 |
| $A^2$ | 15.74 | 0.2122 | 0.6590 | 0.0003 | 3.075E-06 | 0.9986 |
| $B^2$ | 35.01 | 0.4720 | 0.5142 | 247.30 | 2.36 | 0.1684 |
| $C^2$ | 356.67 | 4.81 | 0.0644 | 3.99 | 0.0381 | 0.8508 |
| Residual | 519.30 | | | 733.85 | | |
| Lack of Fit | 206.45 | 0.8799 | 0.5228 | 195.42 | 0.4839 | 0.7113 |
| Pure Error | 312.85 | | | 538.43 | 0.6445 | 0.7359 |

TOME: Tomato methyl ester.

- Ethanol, when used as a fuel along with a glow plug, decreased polluting emissions from the exhaust. However, it also resulted in lower efficiency compared to diesel fuel.
- Delaying the ethanol injection enhanced the thermal efficiency of the engine and decreased carbon monoxide and unburned hydrocarbon emissions. However, it resulted in higher nitrogen oxide emissions as a result of increased combustion temperatures. The low heat rejection engine, which was fitted with a partially stabilized $Al_2O_3$ coating, demonstrated a higher thermal efficiency in comparison to alternative engines.
- Ethanol, when used as a fuel with a glow plug, decreases the emission of pollutants from the exhaust. However, it also results in a decrease in efficiency compared to the usage of diesel fuel. Delaying the injection timing of the engine enhances its thermal efficiency to a certain extent, resulting in a reduction in carbon monoxide and unburned hydrocarbon emissions.

## ACKNOWLEDGEMENTS

The authors are obliged to Aarupadai Veedu Institute of Technology, Vinayaka Mission's Research Foundation for providing laboratory facilities.

## DATA AVAILABILITY STATEMENT

The author confirm that the data that supports the findings of this study are available within the article. Raw data that support the finding of this study are available from the corresponding author, upon reasonable request.

## CONFLICT OF INTEREST

The author declared no potential conflicts of interest with respect to the research, authorship, and/or publication of this article.

## USE OF AI FOR WRITING ASSISTANCE

Not declared.

## ETHICS

There are no ethical issues with the publication of this manuscript.

## REFERENCES

[1] A. P. Venkatesh, T. P. Latchoumi, S. Chezhian Babu, K. Balamurugan, S. Ganesan, M. Ruban, and L. Mulugeta, "Multiparametric optimization on influence of ethanol and biodiesel blends on nanocoated engine by full factorial design," Journal of Nanomaterials, Vol. 2022, Article 5350122, 2022. [CrossRef]

[2] A. Bernardo, D. Boeris, A. I. Evins, G. Anichini, and P. E. Stieg, "A combined dual-port endoscope-assisted pre-and retrosigmoid approach to the cerebellopontine angle: An extensive anatomo-surgical study," Neurosurgical Review, Vol. 37, pp. 597–608, 2014. [CrossRef]

[3] H. Solmaz, "A comparative study on the usage of fusel oil and reference fuels in an HCCI engine at different compression ratios," Fuel, Vol. 273, Article 117775, 2020. [CrossRef]

[4] S. Prakash, M. Prabhahar, O. P. Niyas, S. Faris, and C. Vyshnav, "Thermal barrier coating on IC engine piston to improve efficiency using dual fuel," Materials Today: Proceedings, Vol. 33, pp. 919–924, 2020. [CrossRef]

[5] V. Saxena, N. Kumar, and V. K. Saxena, "Multi-objective optimization of modified nanofluid fuel blends at different TiO2 nanoparticle concentration in diesel engine: Experimental assessment and modeling," Applied Energy, Vol. 248, pp. 330–353, 2019. [CrossRef]

[6] B. J. Kalita, and N. Sit, "Optimization of the culture conditions for cellulase production from suitable food waste using fungal strain isolated from different soils," Biomass Conversion and Biorefinery, pp. 1–14, 2023. [CrossRef]

[7] S. Kumar, A. Kumar, A. R. Sharma, and A. Kumar, "Heat transfer correlations on combustion chamber surface of diesel engine experimental work," International Journal of Automotive Science and Technology, Vol. 2(3), pp. 28–35, 2019. [CrossRef]

[8] G. Najafi, B. Ghobadian, T. Yusaf, S. M. S. Ardebili, and R. Mamat, "Optimization of performance and exhaust emission parameters of a SI (spark ignition) engine with gasoline–ethanol blended fuels using response surface methodology," Energy, Vol. 90, pp. 1815–1829, 2015. [CrossRef]

[9] S. Kundu, S. K. Das, and P. Sahoo, "Friction and wear behavior of electroless Ni-PW coating exposed to elevated temperature," Surfaces and Interfaces, Vol. 14, pp. 192–207, 2019. [CrossRef]

[10] S. Yessian, and P. A. Varthanan, "Optimization of performance and emission characteristics of catalytic coated IC engine with biodiesel using grey-taguchi method," Scientific Reports, Vol. 10(1), Article 2129, 2020. [CrossRef]

[11] M. Prabhahar, and K. Rajan, "Performance and combustion characteristics of a diesel engine with titanium oxide coated piston using Pongamia methyl ester," Journal of Mechanical Science and Technology, Vol. 27(5), pp. 1519–1526, 2013. [CrossRef]

[12] S. Ozer, F. Haciyusufoglu, and E. Vural, "Experimental investigation of the effect of the use of nanoparticle additional biodiesel on fuel consumption and exhaust emissions in tractor using a coated engine," Thermal Science, Vol. 27(4) Part B, pp. 3189–3197, 2023. [CrossRef]

[13] I. Uogintė, G. Lujanienė, and K. Mažeika, "Study of Cu (II), Co (II), Ni (II) and Pb (II) removal from aqueous solutions using magnetic Prussian blue nano-sorbent," Journal of Hazardous Materials, Vol. 369, pp. 226–235, 2019. [CrossRef]

[14] B. Vinay, A. K. Singh, and A. K. Yadav, "Optimisation of performance and emission characteristics of CI engine fuelled with Mahua oil methyl ester–diesel blend using response surface methodology," International Journal of Ambient Energy, Vol. 41(6), pp. 674–685, 2020. [CrossRef]

[15] J. D. Mejía, N. Salgado, and C. E. Orrego, "Effect of blends of Diesel and Palm-Castor biodiesels on viscosity, cloud point and flash point," Industrial Crops and Products, Vol. 43, pp. 791–797, 2013. [CrossRef]

[16] H. Venu, and P. Appavu, "Analysis on a thermal barrier coated (TBC) piston in a single cylinder diesel engine powered by Jatropha biodiesel–diesel blends," SN Applied Sciences, Vol. 1(12), p. 1669, 2019. [CrossRef]

[17] Y. J. Yang, S. Aziz, S. M. Mehdi, M. Sajid, S. Jagadeesan, and K. H. Choi, "Highly sensitive flexible human motion sensor based on ZnSnO3/PVDF composite," Journal of Electronic Materials, Vol. 46, pp. 4172–4179, 2017. [CrossRef]

[18] M. Akcay, S. Ozer, and G. Satilmis, "Analytical formulation for diesel engine fueled with fusel oil/diesel blends," Journal of Scientific & Industrial Research, Vol. 81, pp. 712–719, 2022. [CrossRef]

[19] R. Bhagavatha, S. Subrahmaniana, and G. Narendrakumar, "Enhanced removal of Ni (II) from electroplating effluents using herbal biomass as alum substituents," Desalination and Water Treatment, Vol. 244, pp. 241–252, 2021. [CrossRef]

[20] K. Viswanathan, D. Balasubramanian, T. Subramanian, and E. G. Varuvel, "Investigating the combined effect of thermal barrier coating and antioxidants on pine oil in DI diesel engine," Environmental Science and Pollution Research, Vol. 26, pp. 15573–15599, 2019. [CrossRef]

[21] G. A. Miraculas, N. Bose, and R. E. Raj, "Optimization of biofuel blends and compression ratio of a diesel engine fueled with Calophyllum inophyllum oil methyl ester," Arabian Journal for Science and Engineering, Vol. 41, pp. 1723–1733, 2016. [CrossRef]

[22] K. Nanthagopal, R. S. Kishna, A. E. Atabani, A. Ala'a, G. Kumar, and B. Ashok, "A compressive review on the effects of alcohols and nanoparticles as an oxygenated enhancer in compression ignition engine," Energy Conversion and Management, Vol. 203, Article 112244, 2020. [CrossRef]

[23] O. Z. E. Salih, and C. Cenab, "Effects of adding waste oil ethylene glycol butyl ether to diesel fuel," International Journal of Automotive Science and Technology, Vol. 7(4), pp. 279–284, 2023. [CrossRef]

[24] S. Prakash, M. Prabhahar, and M. Saravana Kumar, "Experimental analysis of diesel engine behaviours using biodiesel with different exhaust gas recirculation rates," International Journal of Ambient Energy, Vol. 43(1), pp. 1508–1517, 2022. [CrossRef]

[25] M. R. Saxena and R. K. Maurya, "Optimization of engine operating conditions and investigation of nano-particle emissions from a non-road engine fuelled with butanol/diesel blends," Biofuels, 2017. [CrossRef]

[26] S. Koçyiğit, S. Ozer, S. Çelebi, and U. Demir, "Bio-based solutions for diesel engines: Investigating the effects of propolis additive and ethanol on performance and emissions," Thermal Science and Engineering Progress, Vol. 48, Article 102421, 2024. [CrossRef]

[27] M. Tomar, and N. Kumar, "Influence of nanoadditives on the performance and emission characteristics of a CI engine fuelled with diesel, biodiesel, and blends–a review," Energy Sources, Part A: Recovery, Utilization, and Environmental Effects, Vol. 42(23), pp. 2944–2961, 2020. [CrossRef]

[28] M. K. Parida, H. Joardar, A. K. Rout, I. Routaray, and B. P. Mishra, "Multiple response optimizations to improve performance and reduce emissions of Argemone Mexicana biodiesel-diesel blends in a VCR engine," Applied Thermal Engineering, Vol. 148, pp. 1454–1466, 2019. [CrossRef]

*Environ Res Tec, Vol. 7, Issue. 3, pp. 422–434, September 2024*

**Environmental Research and Technology**
https://ert.yildiz.edu.tr - https://dergipark.org.tr/tr/pub/ert
DOI: https://10.35208/ert.1446909

Environmental Research & Technology

**Research Article**

# Crop cover identification based on different vegetation indices by using machine learning algorithms

**Saurabh PARGAIEN[1], Rishi PRAKASH[*,1], Ved Prakash DUBEY[2], Devendra SINGH[2]**

*[1]Department of Electronics and Communication Engineering, Graphic Era (Deemed to be University), Dehradun, Uttarakhand, India*
*[2]Department of Computer Sciences and Engineering, Graphic Era Hill University, Dehradun, Uttarakhand, India*

## ARTICLE INFO

*Article history*
Received: 05 March 2024
Revised: 04 April 2024
Accepted: 20 April 2024

**Key words:**
ARIMA; BNDVI; GNDVI; LSTM; MSE; NDVI

## ABSTRACT

In this article, three different indices NDVI, BNDVI and GNDVI are used for the identification of wheat, mustard and sugarcane crop of Saharanpur district's region of Uttar Pradesh. Sentinel 2B satellite images are collected from October 02, 2018 to April 15, 2019. These images are processed using Google Earth Engine. These sentinel images are used to generate NDVI, BNDVI and GNDVI images using GEE. These three different indices images are further processed using SNAP software and particular indices values for 210 different locations are calculated. The same process is used for calculating BNDVI and GNDVI values. ARIMA, LSTM and Prophet models are used to train the time series indices values (NDVI, BNDVI and GNDVI) of wheat, mustard and sugarcane crop. these models are used to analyse MSE (mean absolute percentage error) and RMSE values by considering various parameters. Using ARIMA Model, for wheat crop GNDVI indices shows minimum RMSE 0.020, For Sugarcane crop NDVI indices shows minimum RMSE 0.053, For Mustard crop GNDVI indices shows minimum RMSE 0.024. Using LSTM model, for wheat crop NDVI indices shows minimum RMSE 0.036, For Sugarcane crop BNDVI indices shows minimum RMSE 0.054, For Mustard crop GNDVI indices shows minimum RMSE 0.026. Using Prophet model, for wheat crop GNDVI indices shows minimum RMSE 0.055, For Sugarcane crop NDVI indices shows minimum RMSE 0.088, For Mustard crop GNDVI indices using Prophet model shows minimum RMSE 0.101.

**Cite this article as:** Pargaien S, Prakash R, Dubey VP, Singh D. Crop cover identification based on different vegetation indices by using machine learning algorithms. Environ Res Tec 2024;7(3)422–434.

## INTRODUCTION

The frequent availability of satellite images opens up a multitude of opportunities for scientists engaged in phenological investigation and crop classification. Understanding various land use classes, such as built-up areas, rivers, bare soil, forests, and farmland, requires the selection of an appropriate technique [1]. Satellite images can be used to forecast Earth's surface analyses at various sizes and resolutions. Satellite images can be used to access and analyse all the necessary spectral and spatial feature data for the various land surfaces on Earth [2, 3]. The use of machine learning along with remote sensing images makes it more acceptable for the land use land cover classification. Multi-temporal images are used to extract crop features based on time [4]. Using spectral curves, the earthly objects are categorised. The radiant energy emitted by the items in the ground is the foundation of these spectral curves. Numerous indices are employed to categorise data to differentiate crops on the basis of dif-

***Corresponding author.**
*E-mail address: rishi.prakas@gmail.com

ferent characteristics [5]. Data mining and ML techniques have been used in many real-world applications. Traditional ML techniques make the assumption that training and testing statistics came from the same domain and have a similar input feature space and set of data distribution properties [6]. In other situations, collecting training data is impractically expensive, time-consuming, and difficult in rural areas [7]. Therefore, it is necessary to develop high-performance learners using information that may be more easily obtained from many sources. Many CNN based techniques (such ResNet, VGG, and Inception) have been built in the domains of artificial intelligence, language processing, medical domain, and remote sensing application [8, 9]. Deep learning helps in target identification and classification. DL methods typically depend on enormous volumes of tagged training data. Big, potent deep learning models have been known for being data-hungry. They must be trained with thousands of data points before they can produce an accurate forecast. Resources and time are both quite expensive when it comes to training [10]. Whereas, ML algorithms typically operate independently. Over a huge dataset, it gains knowledge about how to perform a certain task. It is impossible to use previous knowledge when analysing a new task. For the algorithm to start learning again, it usually needs a second dataset. To improve performance, a pre-trained CNN can be tuned on a particular dataset. Moreover, it reduced the target labelled data in comparison to starting from scratch [11, 12].

Transfer learning is the process of using previously learned tasks to learn new ones. The necessary data can be recorded and accessed by the algorithm. The model is loaded with features. Transfer learning is a ML technique that builds a model for one job on top of a model generated for another task. This transfer learning strategy has two major benefits: First and foremost, transfer learning accelerates learning. Since the algorithm does not have to learn as many new things, it can generate high-quality results more rapidly. Transfer learning, on the other hand, requires less data. In conventional learning, a sufficient amount of training data-which may number in the millions-must be fed to an algorithm before it can learn new knowledge. It is possible that the cost to generate and prepare this data for the model will be too high or that it won't be available at all. The issue of inadequate training information for the target task is frequently addressed through the use of transfer learning [13, 14]. The BA-based clustering technique has been suggested as a solution to crop type classification issues using multispectral satellite images [15]. This study created a new plant feature band set (FBS), optimised it, and combined it with an object-oriented classification (OOC) technique to create a new crop classification method. To distinguish different types of vegetation, 20 spectral indices sensitive to the biological factors of the vegetation are added to the FBS in addition to the spectral and textural aspects of the original image. Additionally, a class-pair separability (CPS) based spectral dimension optimization approach of FBS is suggested to enhance class pair separability while minimising data redundancy [16]. Several spectral indices have been generated using the time sequences of Landsat ETM+ and Rapid Eye data, and a framework for classification based on HMMs was developed for modelling crop vegetation patterns over a rural Mediterranean area with significant spatiotemporal crop variability [17]. A total of 12 commonly used spectral vegetation indicators were computed using 14 Sentinel-2 images. Principal component analysis (PCA) was also employed to evaluate the impact of decreased dimensionality on crop type mapping accuracy. The four original PCA components were processed in order to examine classifications for each index alone as well as for groups of various indices, all under the supervision of RF [18]. This article examined the use of optical imagery data in a multi-temporal crop type identification based on very high-resolution spatial imaging. Utilizing the red, green, and near-infrared spectral bands, three vegetation indices (VIs), including the NDVI, GNDVI and SAVI were created using the images of WorldView-3 and Sentinel-2 between April and July 2016 over Coalville (UK). The combination of DT and RF classification algorithms was predicted to have an OA of 91% [19]. The significance of 82 calculated indices for categorising crop types was assessed. Cropland categorization using MSI data was carried out using RF and SVM. Overall accuracy of 90.2–92.2% was achieved using Super learning [20]. The MSI data were used to produce 91 spectral indices [21]. A method for compositing the multi-temporal NDVI to map the locations for planting winter crops using optical data from Landsat-7, -8, and Sentinel-2 was suggested in this article [22]. For crop mapping, the RF classifier-PSO ensemble method was employed [23]. SVM, RF and XG Boost using known vegetative indicators (VIs) were also used [24]. SDA and RF, two feature selection and evaluation techniques, were used to determine the red edge vegetation index of the NDRE based on PCA [25]. The three most important reflectance bands for crop classification, in our opinion, are SWIR1, Green, and Red Edge2. The LSWI, NDWI, and EVI were the top three vegetation indicators for crop classification [26]. SVM, RF, CNN, RNN with LSTM, and RNN with GRU models were analysed to perform crop classification [27]. Phenological cycles of crops are explored utilising temporal NDVI patterns. By compiling spectral data from various phenological stages, most crops with comparable spectral properties may be recognised [28]. Land surface temperature (LST) and the NDVI was used to improve crop categorization accuracy [29]. The Double Exponential Smoothing and Autoregressive Integrated Moving Average with Explanatory Variables ensemble was created to improve prediction performance using forecasting models based on time series analysis [30]. Using four different approaches—KELM, multilayer feedforward NNs, RF, and SVM—six crop kinds— beetroot, beans, winter wheat, grass, potato and maize were recognized from one MSI image and five C-SAR images collected during the year 2016 [31]. Landsat 8 OLI multi-temporal data of year 2013 was employed to find 7 crops varieties in Northern Italy. The study investigated the relationship between crop map delivery time and accuracy using four supervised algorithms that were fed multi-temporal spectral indices (EVI, NDFI, and RGRI) during the course of the season [32, 33]. Nineteen

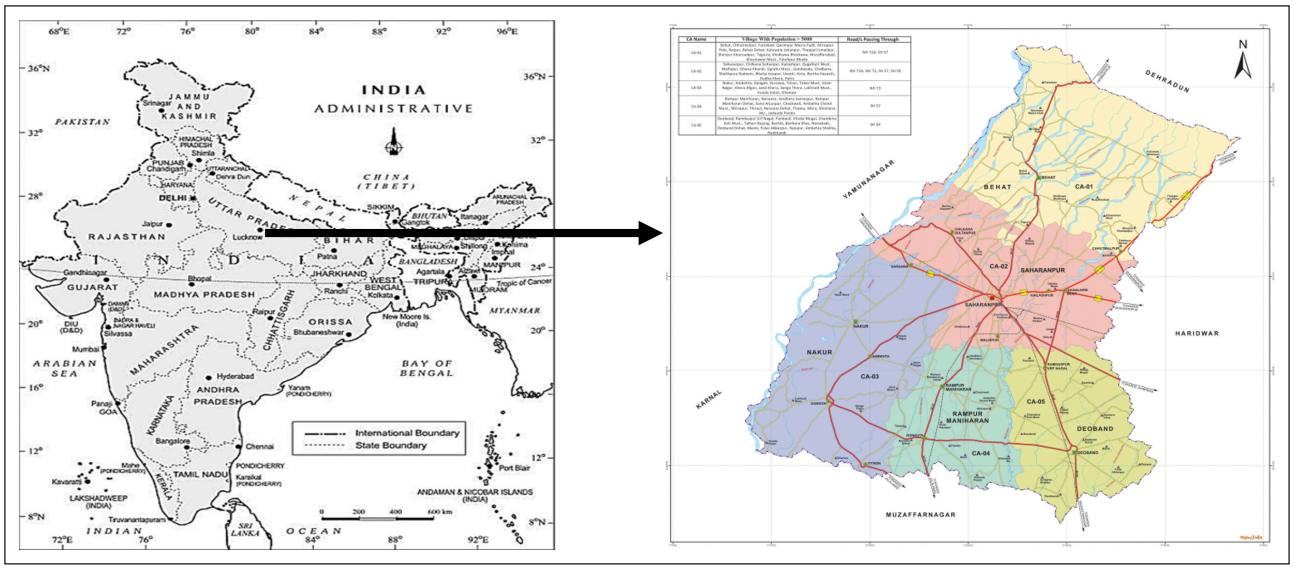


**Figure 1**. Saharanpur District map, Uttar Pradesh, India.

multitemporal images captured by the Landsat-8 and Sentinel-1A RS satellites are used in experiments for the joint experiment of agricultural assessment and monitoring test site in Ukraine to classify crops in a heterogeneous environment using ML methods [34]. A supervised classification is carried out using a group of MLP classifiers for broad area crop mapping at the JECAM test site in Ukraine. The MLP committee achieves an overall classification accuracy of 85% (OA=85.32% and Kappa 0.8235). Accuracy for Winter wheat, winter rapeseed, maize, and sugar beet were 85%. Sunflower, soybeans, and spring crops show poor performance [35]. This study compares two methods for classifying crops using multitemporal optical (Landsat-8) and synthetic-aperture radar (SAR) Sentinel-1 imagery: pixel-based and parcel-based methods for the Joint Experiment of Crop Assessment and Monitoring test site in Ukraine, which will encompass the Odessa and Kyiv oblasts in 2014 and 2015, respectively [36]. According to this study, phenology-based algorithms can be recognised for classifying crops across a wide area. Annual maps of winter crops with UA 96.61%, PA 94.13%, OA 94.56%, and Kappa coefficient of 0.89 were produced using rule-based algorithms and decision trees [37].

## MATERIALS AND METHODS

### Study Area and Data Set Used

The study area lies in Saharanpur district of Uttar Pradesh in India which is located 29° 57' 34.8984" N latitudes and 77° 32' 56.6052" E as shown in Figure 1. Saharanpur district is located in the north part of the India near the foothills of Shivalik ranges and lies in the Doab region. The area of Saharanpur district is 3689 sq. km. It is one of the most agriculturally developed districts of Uttar Pradesh. The important crops of the region are wheat, rice, maize, jawar, bajara, sugarcane and mustard. Wheat, sugarcane, and mustard were chosen for this study because they are the main crops grown in the study area during the winter. The climate in Saharanpur district is warm where the temperate ranges from 5 °C to 45 °C with an annual average temperature of 23 °C. The range of humidity of Saharanpur region varies from 34% to 84%. In winter season its ranges from 62% to 74%, in summer season its ranges from 34% to 54% and in rainy season its ranges from 80% to 84%. The annual rainfall ranges from 498 to 1566 mm with an average rainfall value of 1027 mm. The district's soil composition consists primarily of coarse sandy loam, with some pockets of clay loam. There is a 6.8 to 8.2 PH range. In general, the subsurface water quality is good.

This study utilizes Sentinel – 2B level 1 C data. Level-1C product provides orthorectified Top-of-Atmosphere (TOA) reflectance, with sub-pixel multispectral registration. The Level-2A processing includes a Scene Classification and an Atmospheric Correction applied to Top-of-Atmosphere (TOA). With a revisit time of two to three days at mid-latitudes and five days at the equator, Sentinel-2B offers a high level of temporal resolution, increasing the likelihood of finding images free of clouds or scenes that have less cloud cover. Sentinel-2's high spatial resolution (10, 20, and 60 m pixels for different spectral bands) makes it possible to identify and eliminate clouds and cloud shadows with greater accuracy. With 13 bands spanning from the visible to the shortwave infrared, the broad spectral range makes it possible to distinguish between clouds and surface characteristics using a variety of indices and algorithms. This study identifies wheat, sugarcane and mustard crops of Saharanpur region using NDVI, BNDVI and GNDVI indices. Sentinel – 2B data between October 2018 to April 2019 was observed for this study whose details are provide in Table 1.

This paper focuses on the identification of different crops using three ML models. A flow chart of modelling approach is shown in Figure 2. Wheat, sugarcane and mustard crop has been used to identify from the study area by utilizing ARIMA, LSTM and Prophet models. RMSE and MSE values were computed for all models to determine the most suitable ML model and vegetation indices to identify the

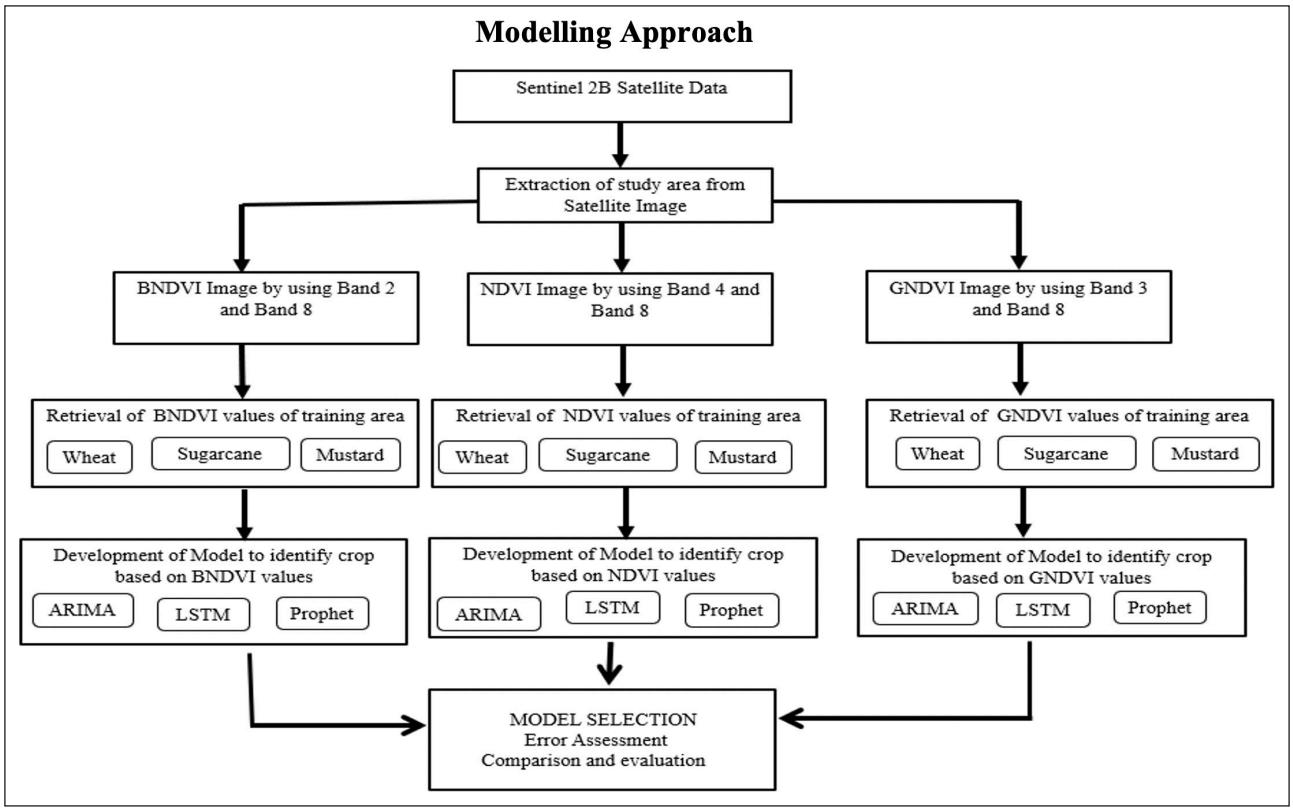


**Figure 2**. The methodology used for crop identification.

specific crop. Following steps were performed to identify different crops based on ML approach:

Step 1: Sentinel – 2B satellite images of study area was processed using GEE. As a first step, the images of study area were extracted and vegetation indices images were formed with the help of GEE. NDVI, BNDVI and GNDVI images were formed to identify different crop.

Step 2: Machine learning models require training data set to train the selected model. Therefore, for each crop, i.e., wheat, sugarcane and mustard the training data set of vegetation indices, i.e., NDVI, BNDVI and GNDVI were extracted with the help of SNAP software. 15 different areas within the study area were selected to determine the indices values. A dataset of 210 points was created for three different crops using three different vegetation indices.

Step 3: Univariate time series models based on ARIMA, LSTM and Prophet were developed with vegetation indices, i.e., NDVI, BNDVI and GNDVI for each crop, i.e., wheat, sugarcane and mustard. These developed models were further used to predict the different crop based on vegetation indices.

Step 4: RMSE and MSE were evaluated for different models for the prediction of crop based on the vegetation indices. A comparison of ML models and vegetation indices were carried out to access the suitability of predication of specific crop.

Total 210 ground points of wheat, mustard and sugarcane were collected during this duration of the study area. 180 sample points are used to train the ARIMA, LSTM and Prophet model and 30 sample points are used for validation.

**Table 1.** Details of Sentinel 2B data used in the study

| S. No. | Acquisition date | Sensor | Spatial resolution | Cloud cover |
|---|---|---|---|---|
| 1 | 02-Oct-18 | | | |
| 2 | 18-Oct-18 | | | |
| 3 | 05-Nov-18 | | | |
| 4 | 21-Nov-18 | | | |
| 5 | 08-Dec-18 | | | |
| 6 | 21-Dec-18 | | | |
| 7 | 15-Jan-19 | Sentinel | 10 | Less than |
| 8 | 28-Jan-19 | 2B | meters | 10% |
| 9 | 09-Feb-19 | | | |
| 10 | 26-Feb-19 | | | |
| 11 | 06-Mar-19 | | | |
| 12 | 26-Mar-19 | | | |
| 13 | 02-Apr-19 | | | |
| 14 | 15-Apr-19 | | | |

**Machine Learning Models to Train the Vegetation Indices**

Three ML models ARIMA, LSTM and Prophet has been utilised in this study. Following paragraphs provide a brief description of these ML models.

***a) ARIMA Model***

The ARIMA model, also known as the Autoregressive Integrated Moving Average Model, is a prominent stochastic time series model that was established in the literature. The time series is shown to be regressed on its own historical data by the AR component of ARIMA. The prediction error is a linear combination of the corresponding previous errors, according to the MA component of ARIMA. As required by the ARIMA model technique, the I part of ARIMA illustrates how the data values have been substituted with differenced values of d in order to obtain data that is stationary. The time series under consideration is linear and has a normal distribution, which is the essential premise upon which this model is built. This model is employed in time-series analysis. It entails looking for patterns in the data and then forecast events based on those patterns. To capture various facets of a time series, the model integrates three elements: moving averages, differencing, and autoregression. In order to create an ARIMA model, the proper parameters must be chosen using strategies like grid search and cross-validation. An ARIMA model has three order parameters: p, d, and q. The number of lag observations, or lag order, in the model is represented by the symbol p. The symbol d denotes the degree of differencing, which is used to represent the number of differences between raw observations. The moving average window's size, or the moving average's order, is represented by the symbol q. $\beta_i$ is the auto regressive parameter of order p, $\emptyset_i$ is moving average parameter of order q, α and μ are constant, $y_t'$ prediction estimate at time t, ϵ error term, t is integer index. Auto ARIMA (p, d, and q) automatically generates the most suitable parameter values. The best values that were created will be used by the model to produce accurate forecast results. Only past values (lags) are used by the AR model to predict future values. The AR model in its generalized form is expressed in equation 1.

$$AR(p): x_t = \alpha + \sum_{i=1}^{p} \beta_i x_{t-i} + \epsilon \quad (1)$$

The amount of prior values "p" will be considered for deciding the forecast value. More historical values will be considered as the model's order increases. To difference the data, the difference between consecutive observations is computed. Mathematically, it can be shown in equation 2.

$$y_t' = y_t - y_{t-1} \quad (2)$$

Differencing removes the changes in the level of a time series, eliminating trend and seasonality and consequently stabilizing the mean of the time series. On the other hand, the moving-average, MA, model relies on previous forecasting failures to produce predictions. The MA model in its generalized form is expressed in equation 3.

$$MA(q): x_t = \mu + \sum_{i=1}^{q} \emptyset_i \epsilon_{t-1} \quad (3)$$

The linear combination of q historical forecast errors can be thought of as the MA model. For predicting time series, ARIMA models have a number of benefits, such as the ability to capture a variety of patterns and behaviours in the data, such as seasonality, cycles, or trends. As they only need three parameters and some fundamental statistical assumptions, they are also fairly simple and easy to implement. For the forecasts, these models can include confidence ranges and error metrics like standard errors or root mean squared errors. When predicting time series, ARIMA models can be constrained and difficult. Due to the fact that they are linear models, they are unable to manage complicated dynamics or nonlinear relationships, such as rapid shocks or regime transitions. Before using ARIMA models, the data may need to be pre-processed to remove outliers and missing values, which can have an impact on the model estimation and forecasting performance. They are not appropriate for extremely brief or extremely long time series because they might not have enough data or get unstable with time.

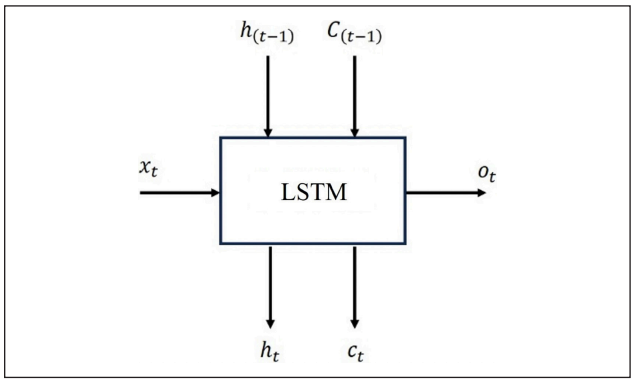


**Figure 3**. LSTM Model.

***b) LSTM Model***

Exploding/vanishing gradient issues are common while learning long-term interdependence. Strong recurrent neural networks like the LSTM model were created expressly to address these issues, even in cases where the minimal time lags are quite large. The LSTM architecture is composed of a group of sub-networks that are linked recurrently. The memory block's functions include data flow control with non-linear gating units and state maintenance over time. Three gates and a cell state give an LSTM module the capacity to learn, unlearn, or retain information from each of the units in a selected manner. In LSTM, the cell state facilitates continuous information transfer between units by permitting a limited number of linear interactions.

$$f_{(t)} = \sigma_g\ (W_f \times x_t + U_f \times h_{t-1} + b_f \quad (4)$$

$$i_{(t)} = \sigma_g\ (W_i \times x_t + U_i \times h_{t-1} + b_i \quad (5)$$

$$o_{(t)} = \sigma_g\ (W_o \times x_t + U_o \times h_{t-1} + b_o \quad (6)$$

$$c'_{(t)} = \sigma_c\ (W_c \times x_t + U_c \times h_{t-1} + b_c \quad (7)$$

$$c_{(t)} = f_{(t)} * c_{(t-1)} + i_{(t)} * c'_{(t)} \quad (8)$$

$$h_{(t)} = o_{(t)} * \sigma_c\ (c_t) \quad (9)$$

The Figure 3 shows the input and outputs of an LSTM for a single time step. This is one time step input; output and the equations are used for a time unrolled representation. Equation 4 represents $f_{(t)}$ (forget gate), equation 5 represents $i_{(t)}$ (input gate), equation 6 represents $o_{(t)}$ (output gate),

equation 7 and 8 represents $c'_{(t)}$ and $c_{(t)}$ (cell gate) respectively, equation 9 represents $h_{(t)}$ (hidden gate), $\sigma_g$ is sigmoid, $\sigma_c$ is tanh and * is element wise multiplication. The input sequence directly or the output of a CNN can be used as the input for the LSTM x(t). These are the inputs from the previous timestep LSTM: $h_{(t-1)}$ and $c_{(t-1)}$. The LSTM's output for this timestep is $o_{(t)}$. In addition, the LSTM produces the $c_{(t)}$ and $h_{(t)}$ that can be utilised by the subsequent time step LSTM. Observe that $f_{(t)}$, $i_{(t)}$, $c'_{(t)}$ are also produced by the LSTM equations. These are utilised to generate $c_{(t)}$ and $h_{(t)}$ for the LSTM's internal consumption. There is no time dependence in the weight matrices $W_f$, $W_i$, $W_o$, $W_c$, $U_f$, $U_i$, $U_o$, $U_c$ and biases $b_f$, $b_i$, $b_o$, $b_c$. This indicates that these weight matrices remain constant throughout time steps.

The LSTM network is used in a variety of problem domains, both alone and in combination with other deep learning designs. LSTM is capable of addressing any problem requiring periodic memory, such as time series forecasts. They are more complicated and require more training data in order to learn efficiently than regular RNNs. Secondly, they are unsuitable for online learning assignments like forecasting or classification tasks where the provided data is not a sequence.

***c) Prophet Model***

Prophet is a time series prediction technique that fits the appropriate seasonality to the non-linear trends in the series using an additive model. It works well with highly seasonal time series and numerous seasons of previous information. The Prophet models' primary inputs are growth and changepoint range. For growth, the trend's "linear" or "logistic" forms are used. In changepoint range, how close the changepoints can be to the time series' end depends on the range. The trend is more malleable as the value increases. It consists of two seasonal components: a weekly-based model using dummy variables, and an annual-based model using Fourier series. In Prophet model, there is no need of much prior experience in forecasting time series data. With a set of data, it is capable of recognizing seasonal patterns and offers easily understood characteristics. Prophet has a number of advantages over other models, one of which being its interpretability. For seasonality, there are smoothing parameters that let you control how closely to fit historical cycles. When compared to the forecasting model with no change, Prophet did not offer any overall improvement.

Prophet can be considered a nonlinear regression model, of the form as shown in equation 10.

$$y_t = g(t) + s(t) + h(t) + \epsilon_t \quad (10)$$

where s(t) reflects the different seasonal patterns, h(t) records the effects of the holidays, and εt is a white noise error term. g(t) represents a piecewise-linear trend (or "growth term").

**Accuracy Assessment**

Accuracy assessment is important to determine the strength of model in predicting the unknown. The assessment of accuracy can be performed based on evaluating the error between the actual and prediction. Therefore, in this paper Root mean square error and mean square error are calculated and analysed. RMSE and MSE are explained below

***a) RMSE***

One of the most popular metrics for assessing the accuracy of forecasts is the root mean square error, often known as the root mean square deviation. It uses the Euclidean distance to illustrate the deviation between predicted and measured true values. Mean Squared Error (MSE) and Root Mean Squared Error (RMSE) are regression measures that are actually connected because RMSE's computation is based on MSE.

$$\text{RMSE}=\sqrt{\frac{\sum_{i=1}^{N}\left\|y(i)-\widehat{y(i)}\right\|^2}{N}} \quad (11)$$

RMSE is explained by equation 11, where N is the number of data points, y(i) are the observed values, and y'(i) are the predicted values.

***b) MSE***

The average squared difference between the actual and expected numbers is known as the mean squared error. Squared error is a row-level error calculation that squares the difference between the real and the predicted. It is also frequently referred to as L2 loss. By looking at the MSE, or mean of these errors, we may assess the model's performance more accurately throughout the whole dataset. One of the most used measures when working with regression models is RMSE, which is usually chosen more than MSE. This is mainly because the resulting number has a much easier to understand interpretation due to its substantially bigger value.

$$\text{MSE}=\frac{\sum_{i=1}^{N}\left\|y(i)-\widehat{y(i)}\right\|^2}{N} \quad (12)$$

MSE is explained by equation 12, where y(i) represents the observed values, N is the number of data points, and y'(i) represents the predicted values.

We utilise the RMSE more frequently when evaluating a model's fit to a dataset since its units of measurement match those of the response variable. The MSE, on the other hand, is expressed in response variable squared units.

## RESULT AND DISCUSSION

**Determination of Vegetation Indices and Preparation of Training Data**

The NDVI, GNDVI, and BNDVI images can be calculated using the red, near-infrared, green, and blue bands available in Sentinel satellite images. The GEE Code Editor can be accessed by going to code.earthengine.google.com using GEE. The "COPERNICUS/S2" image collection contains Sentinel 2 data, which needs to be imported. We must first supply the region of interest (ROI) in order to compute the vegetation indices. We can construct a geometry object for our ROI. It is necessary to decide on the analysis's time frame. We need to filter the Sentinel-2 data based on our time range and ROI. The image from each day with the fewest clouds must be se-

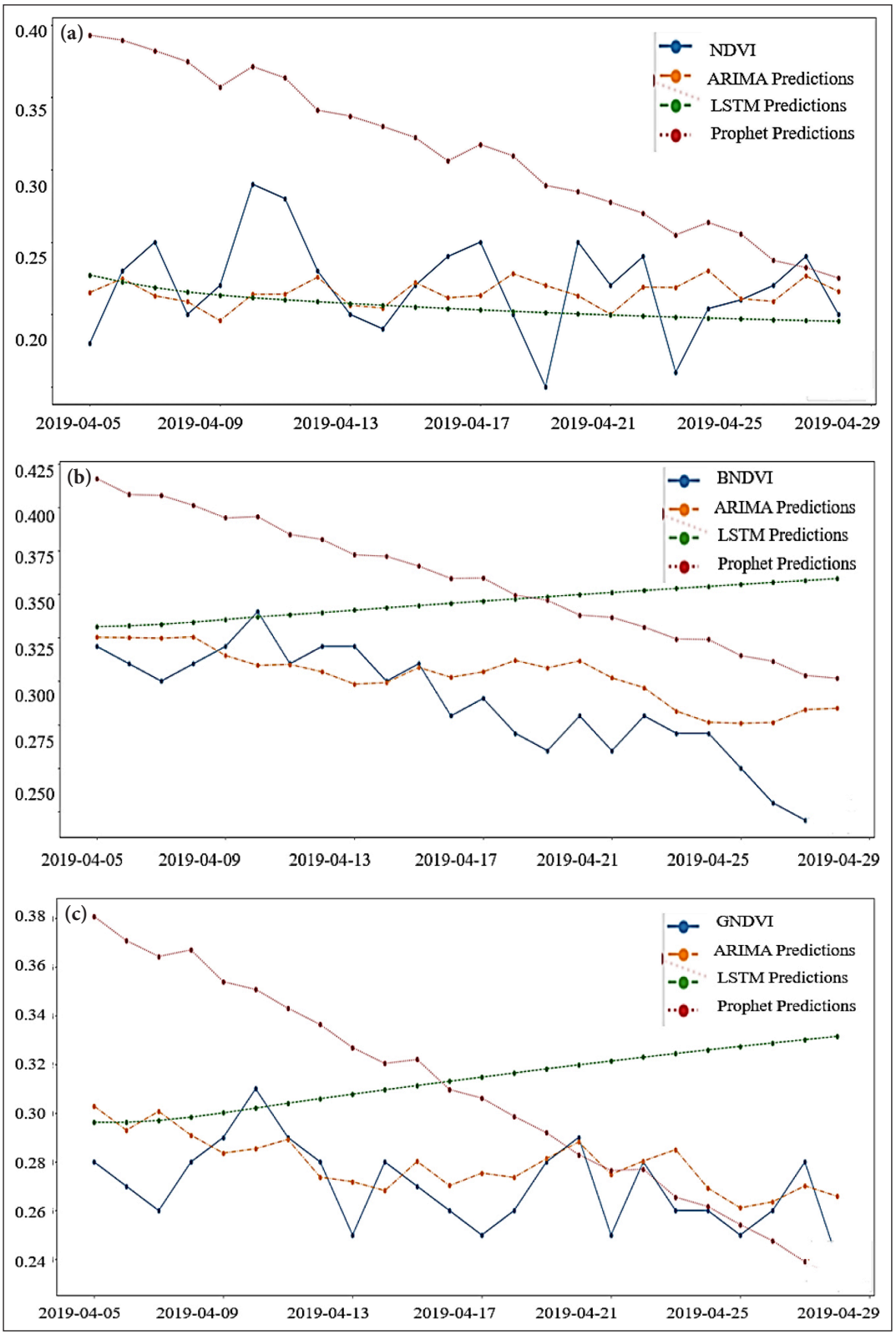


**Figure 4**. **(a)** NDVI indices predicted graph for ARIMA, LSTM and Prophet model. **(b)** BNDVI indices predicted graph for ARIMA, LSTM and Prophet model. **(c)** GNDVI indices predicted graph for ARIMA, LSTM and Prophet model.

lected after the collection has been sorted by cloud cover. We can compute these vegetation indices by creating a function to do so and mapping it across the collection of images. We will then see the NDVI, GNDVI, and BNDVI images on the map. We can adjust the visualisation settings (min, max, and palette) to suit our tastes. Following the processing of the study area's NDVI, BNDVI, and GNDVI images with GEE, the SNAP software is used to further process the images and determine the region of interest's indices values. The specific index values for 210 distinct points are determined.

**Table 2a.** NDVI indices RMSE and MSE Errors for ARIMA, LSTM and Prophet model

| | Wheat NDVI | | |
|---|---|---|---|
| S. No. | Models | RMSE errors | MSE errors |
| 0 | ARIMA | 0.0345 | 0.0012 |
| 1 | LSTM | 0.0367 | 0.0013 |
| 2 | Prophet | 0.1072 | 0.0115 |

**Table 2b.** BNDVI indices RMSE and MSE Errors for ARIMA, LSTM and Prophet model

| | Wheat BNDVI | | |
|---|---|---|---|
| S. No. | Models | RMSE errors | MSE errors |
| 0 | ARIMA | 0.0300 | 0.0009 |
| 1 | LSTM | 0.0548 | 0.0030 |
| 2 | Prophet | 0.0748 | 0.0056 |

**Table 2c.** GNDVI indices RMSE and MSE Errors for ARIMA, LSTM and Prophet model

| | Wheat GNDVI | | |
|---|---|---|---|
| S. No. | Models | RMSE errors | MSE errors |
| 0 | ARIMA | 0.0200 | 0.0004 |
| 1 | LSTM | 0.0509 | 0.0026 |
| 2 | Prophet | 0.0556 | 0.0031 |

**Table 3a.** NDVI indices RMSE and MSE Errors for ARIMA, LSTM and Prophet model

| | Sugarcane NDVI | | |
|---|---|---|---|
| S. No. | Models | RMSE errors | MSE errors |
| 0 | ARIMA | 0.0538 | 0.0029 |
| 1 | LSTM | 0.0806 | 0.0065 |
| 2 | Prophet | 0.0883 | 0.0078 |

**Table 3b.** BNDVI indices RMSE and MSE Errors for ARIMA, LSTM and Prophet model

| | Sugarcane BNDVI | | |
|---|---|---|---|
| S. No. | Models | RMSE errors | MSE errors |
| 0 | ARIMA | 0.0616 | 0.0038 |
| 1 | LSTM | 0.0547 | 0.0030 |
| 2 | Prophet | 0.0889 | 0.0079 |

**Table 3c.** GNDVI indices RMSE and MSE Errors for ARIMA, LSTM and Prophet model

| | Sugarcane GNDVI | | |
|---|---|---|---|
| S. No. | Models | RMSE errors | MSE errors |
| 0 | ARIMA | 0.0670 | 0.0045 |
| 1 | LSTM | 0.0741 | 0.0055 |
| 2 | Prophet | 0.0883 | 0.0078 |

**Development of Machine Learning Models**

The ARIMA (Auto Regressive Integrated Moving Average) model is a time series forecasting method that combines autoregressive (AR) and moving average (MA) components. It was developed to capture and model different aspects of time series data, making it a versatile tool for analyzing and predicting time-dependent phenomena. For ARIMA model, the start value of p, d, and q is considered as 0. The maximum value of p and q is 5 and maximum value of d is considered as 8. The maximum value of P, D and Q is considered as 5. The starting value of P, Q is 0 and D is considered as 1. The value of m is 12 and random state is 20. The value of n fits is 5. The Boolean value of seasonal and trace is true. The best ARIMA model of order = (4,0,1), and seasonal order = (2,1,1,12) is considered in this time series analysis.

The LSTM model using "relu" activation functions and a single LSTM layer with 200 neurons. Since there is just one time-step and one feature in this data, the input shape is (1,1). Adam optimization method is used in this analysis. loss function, which can be used to calculate the model's loss and adjust the weights in order to lower the loss on the subsequent evaluation. The loss function in this case is mean square error. The model is trained for 1000 epochs.

The parameter with the greatest impact on the Prophet model is the changepoint prior scale parameter. It establishes the trend's degree of flexibility, namely how much the trend fluctuates at trend changepoints. In this analysis the value of this parameter is 0.5. The seasonality mode parameter is multiplicative.

**Selection of ML Model and Vegetation Indices For Prediction of Crop**

***Wheat Crop***

Figure 4a, 4b and 4c showed NDVI BNDVI, and GNDVI indices predicted graph for ARIMA, LSTM, and Prophet model for wheat crop. Table 2a show RMSE error and MSE error for ARIMA, LSTM, and Prophet model using wheat NDVI indices values. NDVI indices for wheat crop show RMSE errors of 0.0345, 0.0367 and 0.1072 for ARIMA, LSTM, and Prophet model respectively. It can be clearly observed from the Table 2a that RMSE for wheat NDVI using ARIMA model is minimum. Table 2b show RMSE error and MSE error for ARIMA, LSTM, and Prophet model using wheat BNDVI indices values. BNDVI indices for wheat crop show RMSE errors of 0.03, 0.0548 and 0.0748 for ARIMA, LSTM, and Prophet model respectively. It can be clearly observed from the Table 2b that RMSE for wheat BNDVI using ARIMA model is minimum. Table 2c show RMSE error and MSE error for ARIMA, LSTM, and Prophet model using wheat GNDVI indices values. GNDVI indices for wheat crop show RMSE errors of 0.02, 0.0509 and 0.0556 for ARIMA, LSTM, and Prophet model respectively. It can be clearly observed from the Table 2c that RMSE for wheat GNDVI using ARIMA model is minimum. Therefore, based on RMSE values,

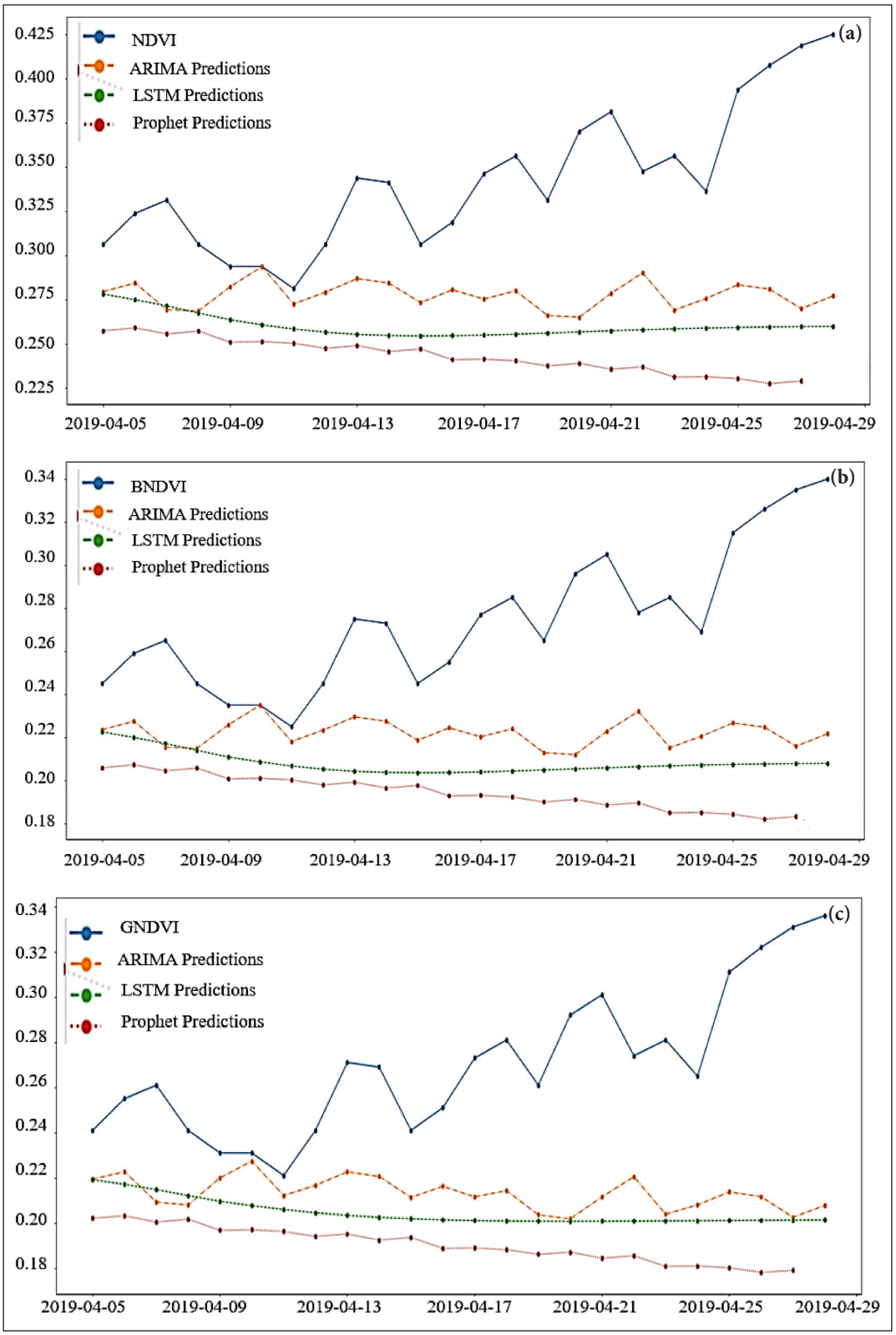


**Figure 5**. **(a)** NDVI indices predicted graph for ARIMA, LSTM and Prophet model. **(b)** BNDVI indices predicted graph for ARIMA, LSTM and Prophet model. **(c)** GNDVI indices predicted graph for ARIMA, LSTM and Prophet model.

ARIMA model may be selected to classify wheat crop using NDVI, BNDVI, GNDVI indices. For wheat crop, if we compare the RMSE values of NDVI, BNDVI and GNDVI. GNDVI indices shows minimum RMSE 0.02 using ARIMA model. NDVI indices shows minimum RMSE 0.0367 using LSTM model. GNDVI indices shows minimum RMSE 0.0556 using Prophet model. On the basis of these results, it may be analysed that to predict wheat crop, GNDVI indices are better for ARIMA and Prophet model and NDVI indices are better for LSTM model.

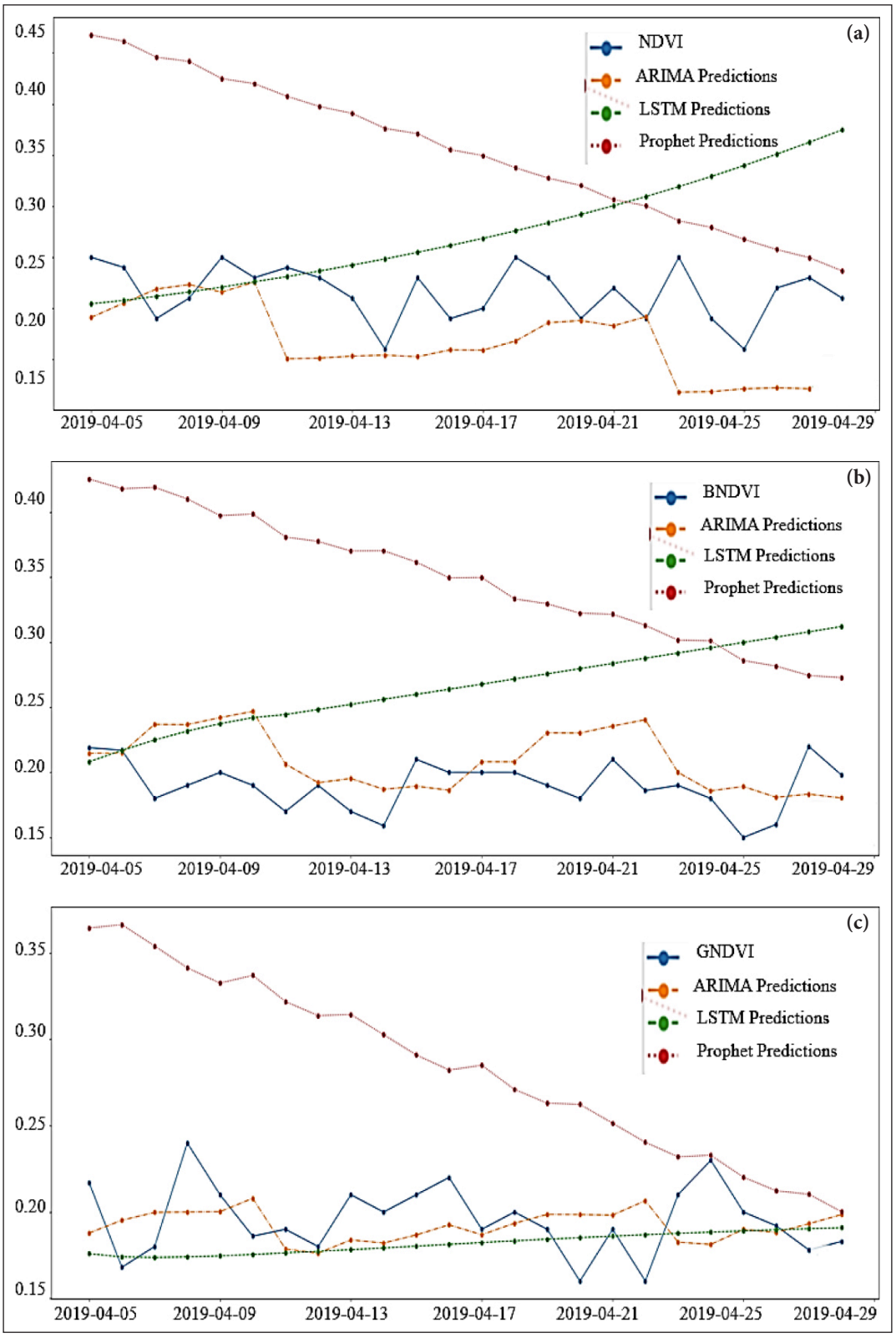


**Figure 6**. **(a)** NDVI indices predicted graph for ARIMA, LSTM and Prophet model. **(b)** BNDVI indices predicted graph for ARIMA, LSTM and Prophet model. **(c)** GNDVI indices predicted graph for ARIMA, LSTM and Prophet model.

***Sugarcane Crop***

Figure 5a, 5b and 5c showed NDVI, BNDVI, and GNDVI indices predicted graph for ARIMA, LSTM, and Prophet model for sugarcane crop. Table 3a show RMSE error and MSE error for ARIMA, LSTM, and Prophet model using sugarcane NDVI indices values. NDVI indices for sugarcane crop show RMSE errors of 0.0538, 0.0806 and 0.0883 for ARIMA, LSTM, and Prophet model respectively. It can be analysed from the Table 3a that RMSE for sugarcane NDVI using ARIMA model is minimum. Table 3b

show RMSE error and MSE error for ARIMA, LSTM, and Prophet model using sugarcane BNDVI indices values. BNDVI indices for sugarcane crop show RMSE errors of 0.0616, 0.0547 and 0.0889 for ARIMA, LSTM, and Prophet model respectively. It can be analysed from the Table 3b that RMSE for sugarcane BNDVI using LSTM model is minimum. Table 3c shows RMSE error for ARIMA, LSTM, and Prophet model using sugarcane GNDVI indices values. GNDVI indices for sugarcane crop show RMSE errors of 0.0670, 0.0741 and 0.0883 for ARIMA, LSTM, and Prophet model respectively. It can be analysed from the Table 3c that RMSE for sugarcane GNDVI using ARIMA model is minimum. Therefore, based on RMSE values, ARIMA model may be selected to classify sugarcane crop using NDVI and GNDVI indices. LSTM model may be selected to classify sugarcane crop using BNDVI indices. For sugarcane crop, if we compare the RMSE values of NDVI, BNDVI and GNDVI. NDVI indices shows minimum RMSE 0.0538 using ARIMA Model. BNDVI indices shows minimum RMSE 0.0547 using LSTM model. GNDVI indices shows minimum RMSE 0.067 using ARIMA model. On the basis of these results, it may be analysed that to predict sugarcane crop, NDVI and GNDVI indices are better for ARIMA model and BNDVI indices are better for LSTM model.

**Mustard Crop**

Figure 6a, 6b and 6c showed NDVI, BNDVI, and GNDVI indices predicted graph for ARIMA, LSTM, and Prophet model for mustard crop. Table 4a show RMSE error and MSE error for ARIMA, LSTM, and Prophet model using mustard NDVI indices values. NDVI indices for mustard crop show RMSE errors of 0.0632, 0.0860 and 0.1533 for ARIMA, LSTM, and Prophet model respectively. It can be analysed from the Table 4a that RMSE for mustard NDVI using ARIMA model is minimum. Table 4b show RMSE error and MSE error for ARIMA, LSTM, and Prophet model using mustard BNDVI indices values. BNDVI indices for mustard crop show RMSE errors of 0.0331, 0.0842 and 0.1655 for ARIMA, LSTM, and Prophet model respectively. It can be analysed from the Table 4b that RMSE for mustard BNDVI using ARIMA model is minimum. Table 4c show RMSE error and MSE error for ARIMA, LSTM, and Prophet model using mustard GNDVI indices values. GNDVI indices for mustard crop show RMSE errors of 0.0244, 0.0264 and 0.1019 for ARIMA, LSTM, and Prophet model respectively. It can be analysed from the Table 4c that RMSE for mustard GNDVI using ARIMA model is minimum. Therefore, based on RMSE values, ARIMA model may be selected to classify mustard crop using NDVI, BNDVI and GNDVI indices. For mustard crop, if we compare the RMSE values of NDVI, BNDVI and GNDVI. GNDVI indices shows minimum RMSE 0.0244 using ARIMA Model. GNDVI indices shows minimum MSE 0.0264 using LSTM model. GNDVI indices shows minimum MSE 0.1019 using Prophet model. On the basis of these results, it may be analysed that to predict mustard crop, GNDVI indices are best for ARIMA, Prophet, and LSTM model.

**Table 4a.** NDVI indices RMSE and MSE Errors for ARIMA, LSTM and Prophet model

| | Mustard NDVI | | |
|---|---|---|---|
| S. No. | Models | RMSE errors | MSE errors |
| 0 | ARIMA | 0.0632 | 0.0040 |
| 1 | LSTM | 0.0860 | 0.0074 |
| 2 | Prophet | 0.1533 | 0.0235 |

**Table 4b.** BNDVI indices RMSE and MSE Errors for ARIMA, LSTM and Prophet model

| | Mustard BNDVI | | |
|---|---|---|---|
| S. No. | Models | RMSE errors | MSE errors |
| 0 | ARIMA | 0.0331 | 0.0011 |
| 1 | LSTM | 0.0842 | 0.0071 |
| 2 | Prophet | 0.1655 | 0.0274 |

**Table 4c.** GNDVI indices RMSE and MSE Errors for ARIMA, LSTM and Prophet model

| | Mustard GNDVI | | |
|---|---|---|---|
| S. No. | Models | RMSE errors | MSE errors |
| 0 | ARIMA | 0.0244 | 0.0006 |
| 1 | LSTM | 0.0264 | 0.0007 |
| 2 | Prophet | 0.1019 | 0.0104 |

## CONCLUSION

In this Study ARIMA, LSTM and Prophet models are used to train the time series indices values (NDVI, BNDVI and GNDVI) of wheat, mustard and sugarcane crops of the study area. These models are used to analyse MSE and RMSE values by considering various parameters. For wheat crop, on the basis of individual vegetation indices, ARIMA model show least RMSE error of 0.0345 for NDVI indices, least RMSE error of 0.03 for BNDVI indices, and least RMSE error of 0.02 for GNDVI indices. So ARIMA model may be selected to classify wheat crop using NDVI, BNDVI, GNDVI indices. To predict wheat crop on the basis of model, GNDVI indices show least RMSE error of 0.02 for ARIMA model and least RMSE error of 0.0556 for Prophet model. NDVI indices show least RMSE error of 0.0367 for LSTM model. So GNDVI indices are better for ARIMA and Prophet model and NDVI indices are better for LSTM model. For sugarcane crop, on the basis of individual vegetation indices, ARIMA model show least RMSE error of 0.0538 for NDVI indices, LSTM model show least RMSE error of 0.0547 for BNDVI indices, and least RMSE error of 0.0741 for GNDVI indices. So ARIMA model may be selected to classify sugarcane crop using NDVI, LSTM model may be selected using BNDVI and GNDVI indices. To predict sugarcane crop on the basis of model, NDVI indices show least RMSE error of 0.0538 for ARIMA model, NDVI and GNDVI shows least RMSE error of 0.0883 for Proph-

et model. BNDVI indices show least RMSE error of 0.0547 for LSTM model. So NDVI indices are better for ARIMA model, NDVI and GNDVI indices are better for Prophet model and BNDVI indices are better for LSTM model. For mustard crop, on the basis of individual vegetation indices, ARIMA model show least RMSE error of 0.0632 for NDVI indices and least RMSE error of 0.0331 for BNDVI indices. LSTM model show least RMSE error of 0.0264 for GNDVI indices. So ARIMA model may be selected to classify mustard crop using NDVI, BNDVI indices and LSTM model may be selected using GNDVI indices. To predict mustard crop on the basis of model, GNDVI indices show least RMSE error of 0.0244 for ARIMA model, least RMSE error of 0.0264 for LSTM model, and least RMSE error of 0.1019 for Prophet model. So GNDVI indices are better for ARIMA, Prophet, and LSTM model. In order to analyse the crops of those localities that have similar environmental circumstances to the trained locale, the optimal model and vegetation indices may be chosen based on this training.

## DATA AVAILABILITY STATEMENT

The author confirm that the data that supports the findings of this study are available within the article. Raw data that support the finding of this study are available from the corresponding author, upon reasonable request.

## CONFLICT OF INTEREST

The author declared no potential conflicts of interest with respect to the research, authorship, and/or publication of this article.

## USE OF AI FOR WRITING ASSISTANCE

Not declared.

## ETHICS

There are no ethical issues with the publication of this manuscript.

## REFERENCES


[1] V. Avashia, S. Parihar, and A. Garg, "Evaluation of classification techniques for land use change mapping of Indian Cities," Journal of the Indian Society of Remote Sensing, Vol. 48(6), pp. 877–908, 2020. [CrossRef]

[2] P. Patil, V. Panpatil, and S. Kokate, "Crop prediction system using machine learning algorithms," International Research Journal of Engineering and Technology, Vol. 7(2), pp. 748–753, 2020.

[3] B. E. Bunker, "Classification of satellite time series-derived land surface phenology focused on the northern fertile crescent," [Dissertation thesis], University of Arkansas, 2013.

[4] X. X. Zhou, Y.-Y. Li, Y.-K. Luo, Y.-W. Sun, Y.-J. Su, C.-W. Tan, and Y.-J. Liu, "Research on remote sensing classification of fruit trees based on Sentinel-2 multi-temporal imageries," Scientific Reports, Vol. 12(1), 2022. [CrossRef]

[5] L. Wang, Q. Dong, L. Yang, J. Gao, and J. Liu, "Crop classification based on a novel feature filtering and enhancement method," Remote Sensing (Basel), Vol. 11(4), 2019. [CrossRef]

[6] E. Omia et al, H. Bae, E. Park, M. S. Kim, I. Baek, I. Kabenge, and B.-K. Cho, "Remote sensing in field crop Monitoring: A comprehensive review of sensor systems, data analyses and recent advances," Remote Sensing (Basel), Vol. 15(2), Article 354, 2023. [CrossRef]

[7] R. Filgueiras, E. C. Mantovani, D. Althoff, E. I. Fernandes Filho, and F. F. da Cunha, "Crop NDVI monitoring based on sentinel 1," Remote Sensing (Basel), Vol. 11(12), 2019. [CrossRef]

[8] A. Orynbaikyzy, U. Gessner, B. Mack, and C. Conrad, "Crop type classification using fusion of sentinel-1 and sentinel-2 data: Assessing the impact of feature selection, optical data availability, and parcel sizes on the accuracies," Remote Sensing (Basel), Vol. 12(17), 2020. [CrossRef]

[9] P. Hao, L. Wang, and Z. Niu, "Comparison of hybrid classifiers for crop classification using normalized difference vegetation index time series: A case study for major crops in North Xinjiang, China," PLoS One, Vol. 10(9), Article 0137748, 2015. [CrossRef]

[10] Q. Li, J. Tian, and Q. Tian, "Deep Learning application for crop classification via multi-temporal remote sensing images," Agriculture (Switzerland), Vol. 13(4), Article 906, 2023. [CrossRef]

[11] J. Dyson, A. Mancini, E. Frontoni, and P. Zingaretti, "Deep learning for soil and crop segmentation from remotely sensed data," Remote Sensing (Basel), Vol. 11(16), Article 1859, 2019. [CrossRef]

[12] N. Yang, D. Liu, Q. Feng, Q. Xiong, L. Zhang, T. Ren, … and J. Huang, "Large-scale crop mapping based on machine learning and parallel computation with grids," Remote Sensing (Basel), Vol. 11(12), Article 1500, 2019. [CrossRef]

[13] G. A. Abubakar, K. Wang, A. R. Shahtahamssebi, X. Xue, M. Belete, A. J. Abdallah Gudo, … and M. Gan, "Mapping maize fields by using multi-temporal sentinel-1a and sentinel-2a images in Makarfi, Northern Nigeria, Africa," Sustainability (Switzerland), Vol. 12(6), Article 2539, 2020. [CrossRef]

[14] X. Guan, C. Huang, G. Liu, X. Meng, and Q. Liu, "Mapping rice cropping systems in Vietnam using an NDVI-based time-series similarity measurement based on DTW distance," Remote Sens (Basel), Vol. 8(1), Article 19, 2016. [CrossRef]

[15] J. Senthilnath, S. Kulkarni, J. A. Benediktsson, and X. S. Yang, "A novel approach for multispectral satellite image classification based on the bat algorithm," IEEE Geoscience and Remote Sensing Letters, Vol. 13(4), pp. 599–603, 2016. [CrossRef]

[16] X. Zhang, Y. Sun, K. Shang, L. Zhang, and S. Wang, "Crop classification based on feature band set construction and object-oriented approach using hyperspectral images," IEEE Journal of Selected Topics in Applied Earth Observations and Remote Sensing, Vol. 9(9), pp. 4117–4128, 2016. [CrossRef]

[17] S. Siachalou, G. Mallinis, and M. Tsakiri-Strati, "Analysis of time-series spectral index data to enhance crop identification over a mediterranean rural landscape," IEEE Geoscience and Remote Sensing Letters, Vol. 14(9), pp. 1508–1512, 2017. [CrossRef]

[18] M. Pasternak, and K. Pawluszek-Filipiak, "The evaluation of spectral vegetation indexes and redundancy reduction on the accuracy of crop type detection," Applied Sciences (Switzerland), Vol. 12(10), Aricle 5067, 2022. [CrossRef]

[19] Y. Palchowdhuri, R. Valcarce-Diñeiro, P. King, and M. Sanabria-Soto, "Classification of multi-temporal spectral indices for crop type mapping: A case study in Coalville, UK," Journal of Agricultural Science, Vol. 156(1), pp. 24–36, 2018. [CrossRef]

[20] R. Sonobe, Y. Yamaya, H. Tani, X. Wang, N. Kobayashi, and K. Mochizuki, "Crop classification from Sentinel-2-derived vegetation indices using ensemble learning," Journal of Applied Remote Sensing, Vol. 12(02), pp. 1, 2018. [CrossRef]

[21] N. Kobayashi, H. Tani, X. Wang, and R. Sonobe, "Crop classification using spectral indices derived from sentinel-2a imagery," Journal of Information and Telecommunication, Vol. 4(1), pp. 67–90, 2020. [CrossRef]

[22] H. Tian, N. Huang, Z. Niu, Y. Qin, J. Pei, and J. Wang, "Mapping winter crops in China with multi-source satellite imagery and phenology-based algorithm," Remote Sensing (Basel), Vol. 11(7), 2019. [CrossRef]

[23] E. Akbari, A. D. Boloorani, N. N. Samany, S. Hamzeh, S. Soufizadeh, and S. Pignatti, "Crop mapping using random forest and particle swarm optimization based on multi-temporal sentinel-2," Remote Sensing (Basel), Vol. 12(9), 2020. [CrossRef]

[24] K. Goldberg, I. Herrmann, U. Hochberg, and O. Rozenstein, "Generating up-to-date crop maps optimized for sentinel-2 imagery in Israel," Remote Sensing (Basel), Vol. 13(17), 2021. [CrossRef]

[25] Y. Kang, X. Hu, Q. Meng, Y. Zou, L. Zhang, M. Liu, and M. Zhao, "Land cover and crop classification based on red edge indices features of gf-6 wfv time series data," Remote Sensing (Basel), Vol. 13(22), Article 4522, 2021. [CrossRef]

[26] Y. Hu, H. Zeng, F. Tian, M. Zhang, B. Wu, S. Gilliams, … and H. Yang, et al., "An interannual transfer learning approach for crop classification in the Hetao Irrigation District, China," Remote Sensing (Basel), Vol. 14(5), Article 1208, 2022. [CrossRef]

[27] K. Ravali, and M. Teng-Sheng, Machine Learning in Indian Crop Classification of Temporal Multi-Spectral Satellite Image, 14th IMCOM 2020. Taichung, Taiwan, 2020.

[28] K. Aleem, P. Leonardo, and C. Marcello, "Land cover and crop classification using multitemporal sentinel-2 images based on crops phenological Cycle," IEEE Workshop EESMS. Salerno, Italy, 2018.

[29] X. Chen, Y. Zhan, Y. Liu, X. Gu, T. Yu, … and Y. Zhang, "Improving the classification accuracy of annual crops using time series of temperature and vegetation indices," Remote Sensing (Basel), Vol. 12(19), Article 3202, 2020. [CrossRef]

[30] F. Carreño-Conde, A. E. Sipols, C. Simón, and D. Mostaza-Colado, "A forecast model applied to monitor crops dynamics using vegetation indices (Ndvi)," Applied Sciences (Switzerland), Vol. 11(4), pp. 1–25, 2021. [CrossRef]

[31] R. Sonobe, Y. Yamaya, H. Tani, X. Wang, N. Kobayashi, and K. ichiro Mochizuki, "Assessing the suitability of data from Sentinel-1A and 2A for crop classification," GIsci Remote Sensing, Vol. 54(6), pp. 918–938, 2017. [CrossRef]

[32] R. Azar, P. Villa, D. Stroppiana, A. Crema, M. Boschetti, and P. A. Brivio, "Assessing in-season crop classification performance using satellite data: A test case in Northern Italy," European Journal of Remote Sensing, Vol. 49, pp. 361–380, 2016. [CrossRef]

[33] A. Bouguettaya, H. Zarzour, A. Kechida, and A. M. Taberkit, "Deep learning techniques to classify agricultural crops through UAV imagery: a review," Neural Computing and Applications, Vol. 34(12), pp. 9511–9536, 2022. [CrossRef]

[34] N. Kussul, M. Lavreniuk, S. Skakun, and A. Shelestov, "Deep learning classification of land cover and crop types using remote sensing data," IEEE Geoscience and Remote Sensing Letters, Vol. 14(5), pp. 778–782, 2017. [CrossRef]

[35] N. Kussul, S. Skakun, A. Shelestov, M. Lavreniuk, B. Yailymov, and O. Kussul, "Regional scale crop mapping using multi-temporal satellite imagery," in International Archives of the Photogrammetry, Remote Sensing and Spatial Information Sciences - ISPRS Archives, International Society for Photogrammetry and Remote Sensing, 2015, pp. 45–52, 2015. [CrossRef]

[36] N. Kussul, G. Lemoine, F. J. Gallego, S. V. Skakun, M. Lavreniuk, and A. Y. Shelestov, "Parcel-Based Crop Classification in Ukraine Using Landsat-8 Data and Sentinel-1A Data," IEEE Journal of Selected Topics in Applied Earth Observations and Remote Sensing, Vol. 9(6), pp. 2500–2508, 2016. [CrossRef]

[37] L. Pan, H. Xia, X. Zhao, Y. Guo, and Y. Qin, "Mapping winter crops using a phenology algorithm, time-series sentinel-2 and landsat-7/8 images, and google earth engine," Remote Sens (Basel), Vol. 13(13), Article 2510, 2021. [CrossRef]

*Environ Res Tec, Vol. 7, Issue. 3, pp. 435–447, September 2024*

**Environmental Research and Technology**
https://ert.yildiz.edu.tr - https://dergipark.org.tr/tr/pub/ert
DOI: https://10.35208/ert.1441001

Environmental Research & Technology

**Research Article**

# Does the material recycling rate matter in the effect of the generated waste on environmental pollution? Panel smooth transition regression approach

**Fahriye MERDİVENCİ[1], Celil AYDIN[2], Hayrullah ALTINOK[*,2]**

*[1]Department of International Trade and Logistics, Akdeniz University Faculty of Applied Sciences, Antalya, Türkiye*
*[2]Department of Transportation Services, Maritime Vocational School, Bandırma Onyedi Eylül University, Balıkesir, Türkiye*

## ARTICLE INFO

*Article history*
Received: 08 February 2024
Revised: 05 April 2024
Accepted: 14 April 2024

**Key words:**
Environmental pollution; Panel smooth transition regression; Recycling rate; Waste; White paper

## ABSTRACT

This study examined the effect of material recycling on the relationship between the waste amount and environmental pollution in EU-15 countries for the 1995–2019 period through panel smooth regression analysis by using the material recycling rate as the threshold variable. Based on the analysis results, the material recycling rate threshold level was estimated as 11.79. In these countries, if the material recycling rate is below the threshold level, the rise in the waste amount will increase environmental pollution. If the material recycling rate is above the threshold value, the rise in the waste amount will still increase environmental pollution, but the pollution increase rate will decrease. With the increase in the waste amount in the long term, environmental pollution can only be reduced by raising the material recycling rate. For the reduction of environmental pollution, which is one of the most prioritized issues in Europe in recent years, policy makers should take measures to increase the material recycling rate by taking the results of this study into consideration and pay attention to the implementation of these measures.

**Cite this article as:** Merdivenci F, Aydın C, Altınok H. Does the material recycling rate matter in the effect of the generated waste on environmental pollution? Panel smooth transition regression approach. Environ Res Tec 2024;7(3)435–447.

## INTRODUCTION

Urbanization and industrial advances accompanying the rapid increase in the world population directly increase the amount of solid, liquid, and gaseous waste [1–3]. In recent years, this has managed to focus the attention of environmental scientists and policy makers on the waste generated as a result of consumer goods [4, 5]. Waste is considered as any discarded or unwanted material [6–8]. Concerns about the disposal of the generated waste are increasing to include "upstream" environmental problems [6, 9]. This is because these wastes create hazards when released into the environment without recycling, proper treatment, and disposal procedures [2, 10, 11]. These hazards cause environmental problems such as greenhouse gas emissions (GHG), global warming, climate change, groundwater pollution, air pollution, and land degradation [12, 13]. It is said that the production amount of these wastes, which affect the environment in many ways, is increasing (across the world). This will cause a pile of garbage to occur and means that the damage done will increase gradually. Storage, composting, reuse, recycling, recovery and incineration are shown as ways to get rid of these piles [8, 14, 15].

Recycling waste is one of the primary methods of minimizing the damage of produced waste to the environment and the economy [8, 16, 17]. In the recycling process of the wastes produced, waste materials are primarily collected from land-

***Corresponding author.**
*E-mail address: haltinok@bandirma.edu.tr

fills. Afterward, they are separated according to their types (paper, plastic, glass, metal, etc.), compressed in volume, and transported to the facilities where they will be included in the production chain again [18]. As a result of recycling, less damage is done to the environment, both by recycling waste and by reducing the use of raw materials and energy. When products cannot be recycled or reused, new products must be produced in order to meet people's needs [19, 20]. And this will cause the raw material to be extracted and used. The damage to the environment, both when extracting raw materials and when producing a new product, will be much greater than when recycling products. In addition, while producing a new product, more energy is used than energy spent in the recycling phase [21–23]. Therefore, waste recycling plays a critical role in minimizing environmental damage.

Municipal solid waste (MSW) is the type of waste that has attracted the most attention recently regarding the recycling of solid waste. The production of MSW is said to be 1.2 kg per person per day worldwide, and this will increase to 1.42 kg by 2035. A large part of these wastes comprises "plastics-including rubber, paper and cardboard, glass, textiles, organic-animal and vegetal origin, wood, metals, minerals" which are called material wastes [24]. Therefore, policies should be produced and implemented to increase the material recycling rate.

By creating environmental policies by countries, it is aimed at recycling waste through taxes, incentives, and subsidies and reducing the damage to the environment [25, 26]. In this context, EU countries especially show the importance they attach to recycling with their decisions. The main goal of the decisions is to reduce the amount of waste, as well as to recycle or recover the majority of waste and reduce waste storage. Since the implementation of these decisions started, the amount of recycling has increased. Despite these increases, it is seen that the decrease in both the amount of waste produced, and the amount of waste stored is not at the desired level and even increases in some countries [27, 28]. As a result, it can be said that the damage to the environment cannot be reduced to the desired level. While this is the case in EU, where developed and developing countries take part in the developments to reduce the damage to the environment, it cannot be said that it will be different in the rest of the world. Based on all these, it is of great importance to investigate after which level the recycling rate in the amount of waste produced will reduce the damage to the environment.

Considering the study's contribution to the literature, three different contributions come to the fore. First contribution; The non-linear panel data analysis technique, which is not a frequently used method in this field, is the use of PSTR (Panel Smooth Regression Model) analysis. This model reveals the role of material recycling rate in the non-linear relationship between the amount of waste produced and environmental pollution (EP). Although there are similarities between them, the PSTR analysis developed by González et al. [29], differs from the PTR (Panel Threshold Regression) analysis developed by Hansen [30] in that the regression parameters change gradually, not sharply and abruptly.

Using quadratic models to model the non-linear relationship between the waste amount and ecosystem pollution is the second contribution. There is an important limitation to using this method. Using the square of the waste amount in the relationship between the amount of waste and EP; imposes a limitation that the effect of the amount of waste on EP increases and decreases in a monotonous or symmetrical way depending on the level of the amount of waste. In addition, the negative intervals found in the relationship may differ in absolute effect from the positive ones. Based on this, a regression model that calculates the threshold value is used to reveal how the increase in the amount of waste affects EP.

The third contribution is the inclusion of the EU-15 countries into the analysis. The EU-15 countries are the countries that signed the White Paper titled "An Energy Policy for the EU", which was adopted in 1995 and sets out the general principles and targets for the EU's internal energy market. The EU's energy policy objectives are based on striking a balance between competitiveness, energy supply security, and environmental protection. In this context, one of the main objectives is to reduce EP by reducing carbon dioxide ($CO_2$) emission levels. As the waste amount increases, EP increases as well. On the other hand, if the wastes are recycled instead of being randomly released to nature, stored, or incinerated, the damage to the environment can be minimized. In this regard, it is important to analyze the role of the material recycling rate in the non-linear relationship between the waste amount and EP in the countries of the White Paper titled "An Energy Policy for the EU."

This study aims to clarify whether the material recycling rate plays a decisive role in the relationship between the waste amount and EP in the EU-15 country group of the White Paper. To this end, in the first section of the study, the possible effects of the material recycling rate on the waste amount-environmental pollution relationship have been addressed. In the following sections, the interaction between the waste amount and EP covering the 1995–2019 period and whether there is a threshold for the material recycling rate in this relationship will be examined. In the last stage, the consistence of the empirical analysis findings with the existing literature will be evaluated.

## LITERATURE REVIEW

With the developments such as industrialization, technological developments, urbanization and population growth in the world, the damage to the environment is increasing [26]. One of the most basic ways that increase the damage to the environment is the production of waste. The wastes produced are managed in different ways, such as being released to nature, storage, incineration and recycling. With this, waste management is becoming an increasingly important issue when considering the damage to the environment. It is stated that one of the ways to minimize the damage to the environment through waste management is recycling [31]. Many studies have been carried out in the literature to define, scope, increase and make recycling more efficient.

When the literature is examined, studies dealing with the relationship between waste reduction, recycling and EP from different aspects have been encountered. Classifying these studies by associating them with the environment in economic, socio-political, and technical terms is possible.

In a pioneering study, Leontief [32] mentioned the benefits of cross-industry applications for the analysis of environmental problems such as the release of pollutants into the atmosphere. Duchin [33] extended Leontief's study by considering the disposal and recycling of non-treatable waste the environment is exposed to. Nakamura [34], on the other hand, claims that while increasing recycling efforts contribute to the protection of unprocessed materials, total $CO_2$ emissions will go up due to the increased need for transportation to waste recycling centers. Along with increasing waste, the inability to manage waste in cities due to information, public participation rate, regulatory, financial, technical and institutional deficiencies creates more environmental problems [35]. In accordance with the principles of solid waste management (SWM), energy, economy, aesthetics and protection, it is the management of activities related to the collection, and proper transportation of solid wastes in an environmentally friendly environment, the separation of harmful wastes from harmless wastes and the disposal of harmful wastes [36]. The main objectives of SWM are to increase economic development by improving the environmental quality in densely populated urban areas and to raise awareness about the hygiene and health problems arising from harmful waste [37]. With the development of logistics operations and production technologies related to waste collection, transportation and recycling, the concern of protecting the environment and resources led many countries to specific applications [38].

In line with global trends, systems focus on sustainable issues with technologies based on 3R[2] [39]. Transitioning from a linear economy to a circular economy is an essential strategy to minimize waste in line with environmental sustainability [40]. While the first definitions of circular economy focused on 3R[1], Potting et al. [41] offered a more comprehensive circular design based on the 9R[2] principles. Recycling for the recovery of pure materials, which saves resources while minimizing EP, is one of the most fundamental approaches of SWM [42]. Recycling and composting minimize the use of resources and waste, ensuring that the value of products is preserved for a long time [43]. Therefore, the literature contains various studies on the advantages of recycling solid waste [18, 44–46]. The recycling system provides advantages such as improving the economy by creating new employment areas and gaining income from trade, as well as having positive effects on human and living health by reducing the EP [38, 42]. The importance attributed to recycling as a sustainable waste management strategy has revealed that the traditional collection and disposal methods have changed and should be improved. This is because recycling has the potential to extend the life of landfills and reduce waste transportation and disposal costs. There is increasing interest in turning waste into valuable resources that provide sustainable benefits, as it offers one of the most helpful solutions for waste management to protect waste both economically and ecologically [47, 48].

Studies dealing with the issue in economic terms show that recycling costs are generally higher than disposal costs. However, when negative and positive externalities are taken into account, it is seen that recycling has become more economically significant and efficient [49]. Brisson [50] proposed a model that equates the marginal costs of landfill disposal with those of recycling to find the optimal amount of recycling. Acuff and Kaffine [51] examined cost-reducing policies to reduce greenhouse gas-generating waste related to product manufacturing from diverse materials. The authors, who suggest that carbon pricing should be made for emission reduction, state that alternative approaches should be determined when these policies are unavailable. In this context, they compared waste reduction and recycling costs to show the benefits of greenhouse gas reduction. Franchetti and Kilaru [12] developed a model to estimate the impact of solid waste disposal and recycling on GHG. The model estimates the potential economic benefits and GHG of increased recycling. Friedrich and Trois [52] focus on the problem of the lack of a consistent framework in reporting and calculations of waste management in developing country cities. They state that the highest emissions are caused by methane gas, which is formed from garbage and landfills and mixed into the air. Jamasb and Nepal [53] stated that generating energy from waste is a renewable resource and investigated the effects of focusing on this on sustainability. They presented socio-economic benefit analyses of the selected waste management scenarios, discussing how recycling and waste-to-energy production are compatible.

As to studies addressing the subject in technical terms, Chen and Lo [54] evaluated MSW treatment scenarios, including landfill, waste-to-energy, and material recycling, to reduce GHG. The authors state that recycling will have a more significant impact on reducing GHG than converting waste into electricity. Batool and Chuadhry [55] summarize, as a result of their study, how the best available technologies (biogas recovery from landfills and use system and energy recovery from waste system in power plants) significantly reduce GHG and how smart urban SWM is. Chen [56] used data normalization to evaluate the environmental performance of waste-to-energy production technology and addressed urban waste and general industrial solid waste in terms of energy recovery and GHG.

When it comes to studies handling the issue in socio-political terms, King and Gutberlet [57] touch upon the socio-economic benefits of reducing GHG through recycling and resource recovery. The authors created a "GHG accounting calculator" that estimates the reduction to see

[1] 3R: reduce, reuse, and recycle.

[2] 9R: refuse, rethink, reduce, reuse, repair, refurbish, remanufacture, repurpose, recycle, and recover.

**Table 1.** Basic information about the variables

| Variable | Variable description | Sources | Measure | Measure (used in this study) |
|---|---|---|---|---|
| Growth oil | GHG emissions from fuel Combustion-oil | International Energy Agency | Million tons of $CO_2$ | Growth |
| Growth gen | Waste generated | Eurostat | Thousand tons | Growth |
| MatGen | Recycling-material | Eurostat | Thousand tons | % of waste generated |
| GDP | Gross domestic product | World Bank | Constant 2015 (billion Us Dollars) | |
| FDI | Foreign direct investment | World Bank | Net inflows (% of GDP) | |
| OP | Oil prices | U.S. Energy Information Administration | RBRTE- Europe brent spot price FOB (Dollars per barrel) | |

if emissions reductions have occurred. Lee et al. [58] stated that recycling will reduce environmental damage in two ways. The first is reducing the amount of waste, as in other studies. Secondly, they emphasize that carbon emissions in the waste sector will also decrease. They say the government should develop alternative strategies, such as promoting waste-to-energy production. Razzaq et al. [44] examined the impact of recycling on economic growth and environmental quality in the context of the USA. They emphasized that recycling both creates economic value and reduces $CO_2$ emissions. Corsten et al. [59] argue that recycling in the EU is still effective in reducing $CO_2$ emissions but differs in quality. They indicate to decision-makers that they should consider the issue of high-quality and low-quality recycling when making policy. Nakamura and Kondo [60] developed a mathematical waste input-output model. They used that model to evaluate the effects of waste disposal and recycling options on garbage consumption, $CO_2$ emission, and industrial production level. That analysis is concerned with the supply (emission) and demand (recycling) of waste at the macro level, not taking into account regional aspects. It is reported that the existence of regional imbalances is one of the most important problems affecting waste recycling. Aydınbaş and Erdinç [61] revealed that there is a positive and significant relationship between the circular economy and GDP per capita, human capital index, renewable energy consumption and trade openness. In addition, as a result of the study, they stated that recycling, which is the most important part of the circular economy, is of great importance in ensuring economic growth.

This study, on the other hand, reveals the importance of material recycling rate in the relationship between the amount of waste summarized in the literature and EP from a different perspective. As the amount of waste increases, EP also increases. One way to prevent this situation is to ensure the recycling of waste. However, the fact that recycling efforts are not easy and progress slowly reveals the difficulty of the issue. This difficulty has been examined from the literature in terms of technical, economic and socio-political dimensions. Therefore, the answer to the question of "what proportion of recycling should be provided in order to reduce EP" is extremely important.

## MODEL AND DATASET

This study examines the nonlinear relationship between EP ($Co_2$Oil) and the amount of waste generation (WasteGen) in the EU-15 country using the PSTR method in the period 1995–2019[3]. After comprehensive literature review, this study; Utilizing the theoretical framework established by Giovanis [62] and nonlinear panel data analysis, it examines the impact of material recycling rate on the relationship between waste and EP. Equation (1) contains the model;

$$ENV_{i,t}=\beta_0+\beta_1\ Waste_{i,t}+\varepsilon_{i,t} \quad (1)$$

*ENV* is the EP; *Waste* represents the amount of waste generated; ε represents the error term; $t = 1, 2, \ldots, T$ represents time periods; $i = 1, 2, 3\ldots, N$ represents countries.

The basic information about the variables is given in Table 1. $CO_2$ emission representing EP was used as the dependent variable, and the total amount of waste generated was the independent variable. The waste recycling rate (MatGen) in the total amount of waste generated was included in the analysis as the threshold variable in this relationship. Additionally, GDP (gross domestic product), FDI (Foreign direct investment), and OP (Oil Prices) was used as control variables. Data on the amount of $CO_2$ emissions, which represent EP and originate from the combustion of fossil fuels, have been taken from the IEA (International Energy Agency) database. The data on the other two variables, the amount of waste generated and the recycling rate, were obtained from the EU Commission (ec-europa. eu).

Descriptive statistics for these variables are given in Table 2. Accordingly, the average of the variables in 15 countries, respectively; The $CO_2$ emission is 91.18, the total amount of waste produced is 14,552.07, recycling rate (3576.47) in the amount of waste produced is %24.57, GDP is 952.13, FDI is 6.70 and OP is 57.24.

[3] Data from the 1995–2019 period were included in the evaluation. This is mainly because there are great deficiencies in the data of the years before or after that period (at the time the data for the variables were obtained). While these deficiencies were seen in the years after the determined period in the dependent variable, they were seen before and after in the independent and threshold variables.

**Table 2.** Descriptive statistics

| | $CO_2$Oil | WasteGen | MatGen | GDP | FDI | OP |
|---|---|---|---|---|---|---|
| Mean | 91.18 | 14,552.07 | 3576.47 | 952.13 | 6.70 | 57.24 |
| Std. Dev. | 86.86 | 15,194.80 | 5485.77 | 983.78 | 4.78 | 31.31 |
| Max. | 339.12 | 53,966.00 | 25435.00 | 3597.32 | 234.25 | 111.63 |
| Min. | 6.53 | 291.00 | 54.00 | 42.95 | -117.37 | 12.76 |
| Obs. | 348 | 348 | 348 | 348 | 348 | 348 |

Min., Max. and Std. Dev. respectively; minimum value, maximum value and standard deviation.

**Table 3.** Cross-section dependence

| | $CO_2$Oil | WasteGen | MatGen | GDP | FDI | OP | Model |
|---|---|---|---|---|---|---|---|
| $CD_{BP}$ | 1,381.58*** | 935.49*** | 1501.42*** | 1852.08*** | 235.66*** | 2520.0*** | 998.52*** |
| $CD_{LM}$ | 88.09*** | 57.31*** | 96.36*** | 120.56*** | 9.02*** | 166.65*** | 61.66*** |
| CD | 87.77*** | 56.98*** | 96.03*** | 120.23*** | 8.69*** | 166.32*** | – |
| $LM_{adj}$ | 31.80*** | 17.34*** | 37.70*** | 41.00*** | 6.38*** | 50.20*** | 19.99*** |

$CD_{LM}$: Pesaran 2004 $CD_{Lm}$ test, $CD_{BP}$: Breusch and Pagan 1980 test, $LM_{adj}$: Bias-adjusted CD test and, CD: Pesaran 2004 CD test. *, **, and *** denote statistical significance at the 10%, 5%, and 1% levels, respectively.

## METHODOLOGY

PSTR analysis was used in the study. Panel threshold regression (PTR), developed by Hansen [30], is known as the first panel data analysis method that analyzes the nonlinear relationship between variables. PTR analysis assumes that the parameter change is abrupt when switching from one regime to another. Here, the regimes are separated according to the determined threshold value. From an economic point of view, changes are not always sudden [63]. This approach divides the countries in the panel into groups according to their material recycling rates in the relationship between the amount of waste and EP. It also estimates different parameters for groups. Therefore, it assumes apparent differences between countries with a low rate of material recycling and those with a high rate. Thus, it is accepted that a country with a low material recycling rate suddenly can turns into a country with a high material recycling rate. However, the change in the material recycling rate of a country takes place over time. In summary, the estimated parameters do not change abruptly but smoothly. Based on this result, it was deemed more appropriate to use the PSTR model, which allows the regression parameters to change gradually, not sharply and abruptly, from one regime to another [29].

In order to examine the role of material recycling rate in the relationship between the amount of waste and EP, the model in the first Equation (1) was taken as a basis. Based on this basis, in Equation (2), a constant PSTR model with two regimes has been constructed.:

$$ENV_{i,t}=\mu_i+\beta_0\ Waste_{i,t}+\beta_1\ Waste_{i,t} * g(q_{i,t};\gamma,\theta)+\varepsilon_{i,t} \quad (2)$$

The $ENV_{i,t}$ specified in the model represents EP (dependent variable), and $Waste_{i,t}$ represents the total amount of waste generated (independent variable). In addition, $\varepsilon$ represents standard error, $i$ countries, $t$ time period, $q_{i,t}$ represents the threshold variable (recycling rate), and $\mu_i$ represents constant unit effects. The time period t in the equation is from 1 to T, the term $i$ representing the countries is from 1 to N, and the $g(q_{i,t};\gamma,\theta)$ used as the transition function and takes values between 0 and 1.

While performing the PSTR analysis, three stages are followed: testing the linearity, determining the number of regimes, and estimating [29, 64].

**Table 4.** Pesaran and Yamagata (2008) Slope homogeneity test

| Slope Homogenity Tests | Δ | p-value |
|---|---|---|
| Δ Test | 19.733*** | 0.000 |
| $\Delta_{adj}$ Test | 21.530*** | 0.000 |

*, **, and *** denote statistical significance at the 10%, 5%, and 1% levels, respectively.

## EMPIRICAL RESULTS

In this study, in which the nonlinear relationship between EP and the amount of waste for 15 EU countries is evaluated, cross-sectional dependence and unit root tests were performed; the results are presented in Tables 3 and 4, respectively.

As shown in Table 3, it has been determined that there is a cross-sectional dependence between EP and the amount of waste. This result requires applying one of the second-generation unit root tests, which considers the cross-sectional dependency.

As shown in Table 4, the presence of heterogeneity seen in the model. This result, which was realized at the 1% significance level in the Delta and Delta adjusted slope test developed by Pesaran and Yamagata [65], rejects the null hypothesis and takes heterogeneity into account.

**Table 5.** Pesaran (2007) CADF unit root test results

| | Level values intercept-trend | | Difference values intercept-trend | |
|---|---|---|---|---|
| | Statistics | p-values | Statistics | p-values |
| $CO_2$Oil | -2.327 | 0.488 | -4.249*** | 0.000 |
| WasteGen | -2.462 | 0.277 | -3.113*** | 0.000 |
| MatGen | -1.906 | 0.958 | -3.073*** | 0.000 |
| GDP | -2.398 | 0.373 | -2.805** | 0.022 |
| FDI | -1.913 | 0.955 | -3.896*** | 0.000 |
| OP | 2.610 | 1.000 | 1.700*** | 0.000 |

*, **, and *** denote statistical significance at the 10%, 5%, and 1% levels, respectively.

**Table 6.** Panel cointegration test results (Structural breaks & cross-section dependence)

| Model | Zφ(N) | Zτ(N) |
|---|---|---|
| Mean shift | -2.182** | -2.711*** |
| Regime shift | -5.806*** | -5.491*** |

The distributions of the LM-based test statistics $Z\varphi(N$ and $Z\tau(N)$ are normal. Information criteria suggested by Bai and Ng (2004) is used to determine the number of common factors (max is 5). *, **, and *** denote statistical significance at the 10%, 5%, and 1% levels, respectively.

In Table 5, one of the second-generation unit root tests, the Pesaran CADF [66] test, was performed. According to the test results, it was determined that the series did not contain unit roots and were stationary at the first difference. Then, the LM-based cointegration test developed by Westerlund and Edgerton [67] was conducted to determine whether there is a long-term relationship between the series. The test results are given in Table 5.

As seen in Table 6, it was concluded that there is a cointegration relationship between the series. From this point of view, it has been determined that there are structural breaks in the cointegration equations of the series, and the results are given in Table 6.

According to the results in Table 7, it is seen that structural breaks generally occurred in 1997, 1998 and 2007. When these years are considered, the ruptures are associated with the Asian financial, Russian economic and global economic crises experienced in these years, respectively. With the determination of the structural break dates, the next step was the PSTR analysis. In the first step of the PTSR analysis, the linearity of the model is tested, and in the second step, it is decided how many threshold variables are in the model. The results of the tests performed are given in Tables 8 and 9, respectively.

The results in Table 8 show that the model is nonlinear and that the PSTR model with at least one nonlinear threshold variable is valid in the model.

According to the results in Table 9, it was determined that there was only one threshold variable in the model. In the last step, the relationship between EP and the amount of waste was estimated with the two-regime PSTR model.

As can be seen in Table 10, the smoothing value was 324.6962. This means that there is no sharp transition in

**Table 7.** Estimated breaks

| Country | Mean shift | Regime shift |
|---|---|---|
| Austria | 2009 | 1998 |
| Belgium | 2001 | 2001 |
| Denmark | 2013 | 1999 |
| Finland | 2013 | 2013 |
| France | 2000 | 2000 |
| Germany | 2006 | 2006 |
| Greece | 2012 | 2012 |
| Ireland | 2007 | 2007 |
| Italy | 2012 | 2012 |
| Luxembourg | 2008 | 2008 |
| Netherlands | 2008 | 2008 |
| Portugal | 2004 | 2004 |
| Spain | 2006 | 2006 |
| Sweden | 1998 | 1998 |
| United Kingdom | 2008 | 1998 |

The break dates are selected by means of the test approach suggested in Westerlund and Edgerton (2008) which follows the strategy of Bai and Perron (1998) to determine the location of structural breaks.

**Table 8.** Linearity test results

| Threshold variables (MatGen) | |
|---|---|
| $H_0$ Linear Model $H_1$ PSTR Model at least one Threshold Variable | |
| *LM* | 11.137 ** |
| | (0.011) |
| $LM_F$ | 3.638 ** |
| | (0.013) |
| $LR_T$ | 11.317*** |
| | (0.000) |

*, **, and *** denote statistical significance at the 10%, 5%, and 1% levels, respectively.

**Table 9.** Non-linearity test results (PSTR model)

| Threshold variables (MatGen) | |
|---|---|
| $H_0$ r=1 *vs* $H_1$:*r*=2 | |
| LM | 0.997 |
| | (0.802) |
| LMF | 0.310 |
| | (0.818) |
| LRT | 0.998 |
| | (0.802) |

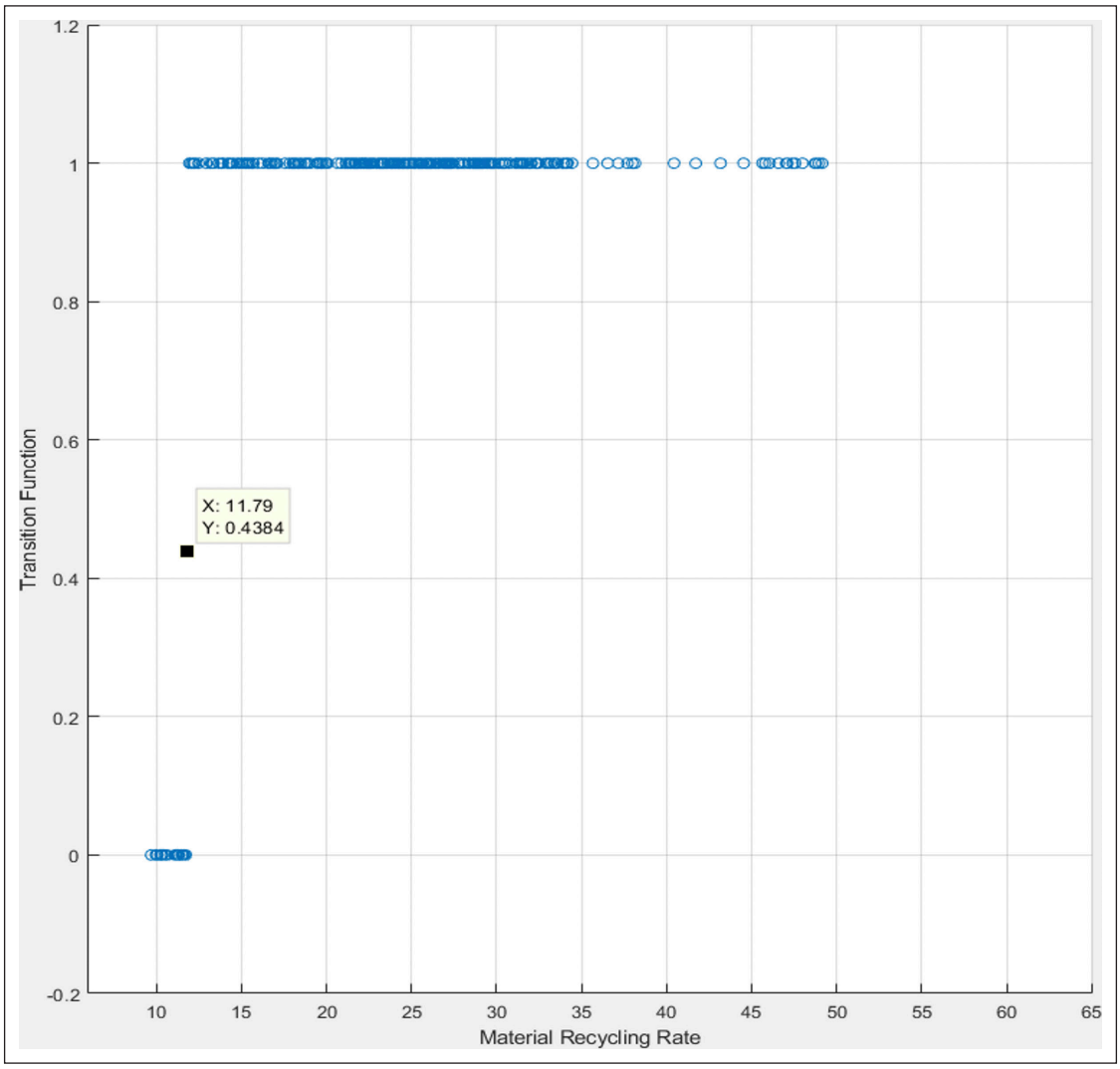


**Figure 1**. Estimated transition function of the PSTR model.

**Table 10.** Estimated PSTR model results

| Threshold variables (MatGen) | Model |
|---|---|
| $Waste_1$ | 0.4941*** |
| | (0.1069) |
| $Waste_2$ | -0.3959** |
| | (0.1423) |
| $Mean\_Dummy_1$ | -3.6338 |
| | (4.2830) |
| $Mean\_Dummy_2$ | 1.9226 |
| | (4.3020) |
| $Regime\_Dummy_1$ | -0.4857 |
| | (0.5622) |
| $Regime\_Dummy_2$ | -0.5512 |
| | (0.5541) |
| Location parameters, $\theta$ | 11.7912 |
| Slope parameters, $\gamma$ | 324.6962 |

The values in parentheses are standard deviation values. *, **, and *** denote statistical significance at the 10%, 5%, and 1% levels, respectively.

the relationship between the $CO_2$ emission change rate and the generated waste amount change rate, and the transition from one regime to the other is smooth. This is shown in Figure 1.

As indicated in Table 10, the threshold value for the material recycling rate was found to be 11.79%. The coefficient ($\beta_0$) estimated for the generated waste amount change rate in the first regime where the material recycling rate is below the threshold value was found to be statistically significant and positive (0.4941) at the 1% significance level. In the second regime where the material recycling rate is above the threshold value, the coefficient estimated for the generated waste amount change rate formed by the sum of ($\beta_0$+$\beta_1$) is statistically significant and still positive at the 5% significance level (0.0982). In other words, if the material recycling rate is below 11.79%, the $CO_2$ emissions amount increases as the generated waste amount increases. On the contrary, when the material recycling rate exceeds the threshold value, the increase in the generated waste amount does not reduce the $CO_2$ emissions amount but decreases its increase rate. In addition, considering the regime coefficients, it can be said that the effect is stronger in

**Table 11.** Results of PSTR with additional explanatory variable(s)

| Threshold variables (MatGen) | Model A | Model B | Model C | Model D |
|---|---|---|---|---|
| $Waste_1$ | 0.4798*** | 0.4194*** | 0.2679*** | 0.2681** |
| | (0.1210) | (0.1148) | (0.0974) | (0.1038) |
| $Waste_2$ | -0.3820** | -0.3217** | -0.2574** | -0.2622* |
| | (0.1524) | (0.1501) | (0.1285) | (0.1336) |
| $Mean\_Dummy_1$ | -3.0871 | -3.2344 | -1.8945 | -2.4721 |
| | (4.4983) | (4.4260) | (4.2121) | (5.0590) |
| $Mean\_Dummy_2$ | 1.4147 | 1.6522 | 1.4778 | 2.1369 |
| | (4.4888) | (4.4370) | (4.2529) | (5.1172) |
| $Regime\_Dummy_1$ | -0.7685 | -0.6925 | -0.6359 | -0.6100 |
| | (0.6276) | (0.6293) | (0.5401) | (0.6089) |
| $Regime\_Dummy_2$ | 0.8238 | 0.7528 | 0.7809 | 0.7116 |
| | (0.6208) | (0.6237) | (0.5313) | (0.6032) |
| $GDP_1$ | 0.0015 | | | 0.0018 |
| | (0.0021) | | | (0.0021) |
| $GDP_2$ | -0.0005 | | | 0.0004 |
| | (0.0006) | | | (0.0006) |
| $FDI_1$ | | 0.1490 | | 0.0951 |
| | | (0.1634) | | (0.1627) |
| $FDI_2$ | | -0.1660 | | -0.1100 |
| | | (0.1633) | | (0.1629) |
| $OP_1$ | | | -0.0308 | -0.0315 |
| | | | (0.0232) | (0.0284) |
| $OP_2$ | | | -0.0245 | -0.0254 |
| | | | (0.0219) | (0.0281) |
| Location parameters, $\theta$ | 11.6819 | 11.7907 | 11.7920 | 11.7915 |
| Slope parameters, $\gamma$ | 8.9027 | 30.5722 | 333.1064 | 336.3252 |

The values in parentheses are standard deviation values. *, **, and *** denote statistical significance at the 10%, 5%, and 1% levels, respectively. $Waste_1$: Coefficient below the threshold level; $Waste_2$: Coefficient above the threshold level.

the first regime, where the material recycling rate is below the threshold, than in the second regime, where it is above the threshold.

As the amount of recycled material in the generated waste decreases, the wastes are stored instead of being recycled, or they are incinerated to provide heat and energy. The use of waste in heat and energy production causes more GHG than waste recycling [54]. The storage of waste, on the other hand, causes visual pollution as well as increasing GHG [68]. For this reason, as the waste amount increases, EP also increases. On the other hand, as the share of the recycled material amount in the total waste increases, waste landfill and incineration and therefore the GHG resulting from these processes decrease [69]. In addition, not much greenhouse gas emission occurs during reuse or reuse by shredding (just combining different parts without any technical process) in the recycling of wastes. However, in some cases, it may be necessary to subject the materials to various processes. During these processes, harmful gases are released to the environment [70]. However, considering the resources used and the energy consumed during the first production of these materials, this causes less EP [54, 68, 69, 71, 72]. Therefore, although the increase in the waste amount still causes EP if the material recycling rate is above the threshold level, it can be said that it causes less EP than if the material recycling rate is below the threshold level.

In order to check the robustness of the model, control variables were added to the model both one by one and collectively. The results in Table 11 show that the material recycling rate threshold value at each stage is similar and the direction of the coefficient signs remains the same. This shows the robustness of the model. Additionally, when the control variables are examined, it is seen that they are insignificant below the threshold and above the threshold. This means that no comments can be made for the control variables within the scope of this relationship.

The results of the model obtained from the study can be summarized as follows;

**a)** A non-linear relationship was found between the total amount of $CO_2$ emissions and the total waste amount generated in 15 EU countries taken as EU-15 in the 1995–2019 period.

**b)** In this relationship, the threshold level for the material recycling rate was found to be 11.79%. Moreover, a significant and positive relationship was detected between the amount of $CO_2$ emissions and the waste amount generated when the material recycling rate was below the threshold. On the other hand, a significant and positive relationship was also detected when the material recycling rate was above the threshold, but the effect was lower than the case where the material recycling rate was below the threshold.

## CONCLUSION

In the globalizing world, with industrialization and urbanization, resources are consumed unconsciously, and wastes are formed as a result of increased consumption. The problem of waste, which is increasing day by day, negatively affects the environment, like almost every part of the society, and increases EP. Recycling, which is defined as the reprocessing, reproduction, and reuse of previously collected materials, has an important place in today's world. From this point of view, the study examined the role of the material recycling rate in the relationship between EP and the waste amount in 15 EU countries that signed the White Paper titled "An Energy Policy for the EU" in the 1995–2019 period.

The material recycling rate threshold value for the analysis period covered by the study was found to be 11.79%. The effect of the material recycling rate on the environmental pollution-waste amount relationship differed depending on whether it was above or below the calculated threshold value. While the environmental pollution-waste amount relationship was positive and statistically significant in the case that the material recycling rate was below the determined threshold value, it was still positive and statistically significant when the material recycling rate exceeded the determined threshold value. However, although a positive relationship was also detected when the material recycling rate was above the threshold, the effect was lower than the case where the material recycling rate was below the threshold. The findings of the present study on the relationship between the waste amount and EP seem to be consistent with those of Giovanis [62], Lave et al. [71], and Mohareb et al. [69].

The results of this study emphasize that approaches indicating an asymmetrical relationship between the waste amount and EP can only be true when the material recycling rate is above the threshold value. In this context, the findings will be useful for policy makers on the necessity of keeping the material recycling rate above the threshold level in order to ensure low EP with the increasing waste amount. Thus, in the context of economic and environmental targets, it is thought that the target of low EP will not conflict with the target of reducing the waste amount, and the waste recycling rate will contribute to the reduction of EP by creating a suitable environment for the waste amount and the environment in the long term.

When the findings are considered in general, policy makers may implement the following policies for the effect of the waste amount on environmental sustainability in their countries:

- First of all, policy makers should ensure that waste management is established for the waste generated. The waste amount generated is important in reducing EP. However, it is not possible to reduce waste to zero. Therefore, waste management is of vital importance. Within the scope of waste management, the focus should be first on the collection of waste. Collecting waste will only contribute to the environment and sustainability through recycling. Otherwise, it will not be possible to go beyond creating a waste pile.
- Recycling activities may provide a cost disadvantage. The way to reduce this is to achieve efficiency in collection, separation, and recycling. In this way, it will be possible to save energy and resources used compared to the first production.
- After the solid wastes are collected, the majority of them are converted into energy by incineration. Considering that incinerated wastes cause more EP than recycling, policies should be established to reduce the rate of incineration of wastes and increase the recycling rate.
- Not much gas emission occurs during reuse or reuse by shredding (just combining different parts without any technical process) in recycling. However, in some cases, it may be necessary to subject the materials to various processes. During these processes, harmful gases are released to the environment. However, considering the resources used and the energy consumed during the first production of these materials, this may be more advantageous. For these reasons, policy makers paying attention to directing the collected waste to recycling can reduce both the damage to the environment resulting from the storage or incineration of wastes and the damage to the environment and consumption of resources for obtaining raw materials during the first production.

To conclude, in order to reduce EP in EU-15 countries, it should be aimed to increase the rate of material recycling in the waste amount, in addition to the above-mentioned policies.

In addition to all these results, there are various limitations in this study. The first limitation of this study is that it only examines the role of the material recycling rate in the relationship between carbon emissions and the amount of waste produced. Although material recycling includes many wastes, there are also missing some. Second, this relationship is limited only to the available country, year and data. Increasing data availability and quality in the future and choosing different country groups will better test the accuracy of the results. The third limitation is that the material recycling

rate is considered as a whole for all sectors. However, in some sectors, a high recycling rate may be more important for the environment than in other sectors. Fourth, a limited number of control variables were used in the study. Increasing number of these variables may help to obtain more robust results. Future researchers can better support the results of our study by taking these limitations into consideration.

## ACKNOWLEDGEMENTS

The authors would like to thank the editor and anonymous reviewers for their helpful comments on an earlier draft of this paper.

## DATA AVAILABILITY STATEMENT

The author confirm that the data that supports the findings of this study are available within the article. Raw data that support the finding of this study are available from the corresponding author, upon reasonable request.

## CONFLICT OF INTEREST

The author declared no potential conflicts of interest with respect to the research, authorship, and/or publication of this article.

## USE OF AI FOR WRITING ASSISTANCE

Not declared.

## ETHICS

There are no ethical issues with the publication of this manuscript.

## REFERENCES

[1] K. D. Sharma, and S. Jain, "Overview of municipal solid waste generation, composition, and management in India," Journal of Environmental Engineering, Vol. 145(3), Article 04018143. 2019. [CrossRef]

[2] A. G. Mukherjee, U. R. Wanjari, R. Chakraborty, K. Renu, B. Vellingiri, A. George…, and A. V. Gopalakrishnan, "A review on modern and smart technologies for efficient waste disposal and management," Journal of Environmental Management, Vol. 297, Article 113347. 2021. [CrossRef]

[3] S. Guoyan, A. Khaskheli, S. A. R. Syed Ali, and M. Ahmed, "Nonlinear impact of municipal solid waste recycling and energy efficiency on environmental performance and economic growth: Evidence from non-parametric causality-in-quantiles," Environmental Science and Pollution Research, Vol. 29, pp. 16066–16081. 2022. [CrossRef]

[4] S. Khan, R. Anjum, S. T. Raza, N. A. Bazai, and M. Ihtisham, "Technologies for municipal solid waste management: Current status, challenges, and future perspectives," Chemosphere, Vol. 288, Article 132403. 2022. [CrossRef]

[5] C. Zhang, M. Hu, F. Di Maio, B. Sprecher, X. Yang, and A. Tukker, "An overview of the waste hierarchy framework for analyzing the circularity in construction and demolition waste management in Europe," Science of the Total Environment, Vol. 803, Article 149892, 2022. [CrossRef]

[6] M. Margallo, K. Ziegler-Rodriguez, I. Vázquez-Rowe, R. Aldaco, A. Irabien, and R. Kahhat, "Enhancing waste management strategies in Latin America under a holistic environmental assessment perspective: A review for policy support," Science of the Total Environment, Vol. 689, pp. 1255–1275, 2019. [CrossRef]

[7] T. D. Bui, J. W. Tseng, M. L. Tseng, and M. K. Lim, "Opportunities and challenges for solid waste reuse and recycling in emerging economies: A hybrid analysis," Resources, Conservation and Recycling, Vol. 177, Article 105968, 2022. [CrossRef]

[8] N. M. Zikali, R. M. Chingoto, B. Utete, and F. Kunedzimwe, "Household solid waste handling practices and recycling value for integrated solid waste management in a developing city in Zimbabwe," Scientific African, Vol. 16, Article e01150, 2022. [CrossRef]

[9] M. Walls, and K. Palmer, "Upstream pollution, downstream waste disposal, and the design of comprehensive environmental policies," Journal of Environmental Economics and Management, Vol. 41, pp. 94–108, 2001. [CrossRef]

[10] J. Yang, P. Jiang, M. Zheng, J. Zhou, and X. Liu, "Investigating the influencing factors of incentive-based household waste recycling using structural equation modelling," Waste Management, Vol. 142, pp. 120–131, 2022. [CrossRef]

[11] T. A. Kurniawan, C. Meidiana, M. H. D. Othman, H. H. Goh, and K. W. Chew, "Strengthening waste recycling industry in Malang (Indonesia): Lessons from waste management in the era of Industry 4.0," Journal of Cleaner Production, Vol. 382, Article 135296, 2023. [CrossRef]

[12] M. Franchetti, and P. Kilaru, "Modeling the impact of municipal solid waste recycling on greenhouse gas emissions in Ohio, US," Resources, Conservation and Recycling, Vol. 58, pp. 107–113, 2012. [CrossRef]

[13] N. Kundariya, S. S. Mohanty, S. Varjani, H. H. Ngo, J. W. C. Wong, M. J. Taherzadeh…, and X. T. Bui, "A review on integrated approaches for municipal solid waste for environmental and economical relevance: Monitoring tools, technologies, and strategic innovations," Bioresource Technology, Vol. 342, Article 125982, 2021. [CrossRef]

[14] A. Yılmaz, and Y. Bozkurt, "Türkiye'de Kentsel Katı Atık Yönetimi Uygulamaları ve Kütahya Katı Atık Birliği (KÜKAB) Örneği," Journal of Süleyman Demirel Üniversitesi İktisadi ve İdari Bilimler Fakültesi, Vol. 15(1), pp. 11–28, 2010. [CrossRef]

[15] H. Jouhara, D. Czajczyńska, H. Ghazal, R. Krzyżyńska, L. Anguilano, A. J. Reynolds, and N. Spencer, "Municipal waste management systems for domestic use," Energy, Vol. 139, pp. 485–506, 2017. [CrossRef]

[16] C. F. Chien, K. Aviso, M. L. Tseng, M. Fujii, and M. K. Lim, "Solid waste management in emerging

economies: Opportunities and challenges for reuse and recycling," Resources, Conservation and Recycling, Vol. 188, Article 106635, 2023. [CrossRef]

[17] T. A. Kurniawan, M. H. D. Othman, X. Liang, H. H. Goh, P. Gikas, T. D. Kusworo..., and K. W. Chew, "Decarbonization in waste recycling industry using digitalization to promote net-zero emissions and its implications on sustainability," Journal of Environmental Management, Vol. 338, Article 117765, 2023. [CrossRef]

[18] T. R. Ayodele, M. A. Alao, and A. S. O. Ogunjuyigbe, "Recyclable resources from municipal solid waste: Assessment of its energy, economic and environmental benefits in Nigeria," Resources, Conservation and Recycling, Vol. 134, pp.165–173, 2018. [CrossRef]

[19] M. Barma, and U. M. Modibbo, "Multiobjective mathematical optimization model for municipal solid waste management with economic analysis of reuse/recycling recovered waste materials," Journal of Computational and Cognitive Engineering, Vol. 1(3), pp. 122–137, 2022. [CrossRef]

[20] G. Haseli, A. E. Torkayesh, M. Hajiaghaei-Keshteli, and S. Venghaus, "Sustainable resilient recycling partner selection for urban waste management: Consolidating perspectives of decision-makers and experts," Applied Soft Computing, Vol. 137, Article 110120, 2023. [CrossRef]

[21] C. Aydin, H. Aydin, and H. Altinok, "Does the level of energy intensity matter in the effect of logistic performance on the environmental pollution of OBOR countries? Evidence from PSTR analysis," Journal of Environmental Planning and Management, Vol. 66(7), pp. 1494–1512, 2023. [CrossRef]

[22] T. C. Kinnaman, "Policy watch: Examining the justification for residential recycling," Journal of Economic Perspectives, Vol. 20(4), pp. 219–232, 2006. [CrossRef]

[23] M. Martin, I. D. Williams, and M. Clark, "Social, cultural and structural influences on household waste recycling: A case study," Resources, Conservation and Recycling, Vol. 48(4), pp. 357–395, 2006. [CrossRef]

[24] D. Hoornweg, and P. Bhada-Tata, "What a waste: A global review of solid waste management,"Available at: https://documents1.worldbank.org/curated/en/302341468126264791/pdf/68135-REVISED-What-a-Waste-2012-Final-updated.pdf Accessed on Jul 17, 2024.

[25] C. Aydin, and Ö. Esen, "Reducing CO2 emissions in the EU member states: Do environmental taxes work?" Journal of Environmental Planning and Management, Vol. 61(13), pp. 2396–2420, 2018. [CrossRef]

[26] C. Aydin, and Y. Cetintas, "Does the level of renewable energy matter in the effect of economic growth on environmental pollution? New evidence from PSTR analysis," Environmental Science and Pollution Research, 1-12, 2022. [CrossRef]

[27] C. Aydin, and R. D. Onay, "Does energy intensity affect the relationship between financial development and environmental pollution?" BRAIN. Broad Research in Artificial Intelligence and Neuroscience, Vol. 11(1), pp. 144–156, 2020. [CrossRef]

[28] D. Fiorillo, "Household waste recycling: National survey evidence from Italy," Journal of Environmental Planning and Management, Vol. 56(8), pp. 1125–1151, 2013. [CrossRef]

[29] A. González, T. Teräsvirta, and D. van Dijk, "Panel Smooth Transition Regression Models," SSE/EFI Working Paper Series in Economics and Finance, WP No. 604, Stockholm, 2005. [CrossRef]

[30] B. E. Hansen, "Threshold effects in non-dynamic panels: Estimation, testing and inference," Journal of Econometrics, Vol. 93(2), pp. 345–368, 1999. [CrossRef]

[31] A. Periathamby, "Chapter 8- Municipal Waste Management." Edited by T. M. Letcher, T. M., and Vallero, D. A. Academic Press. pp. 109–125, 2011. [CrossRef]

[32] W. Leontief, "Environmental repercussions and the economic structure an input output approach," The Review of Economics and Statistics, Vol. 52, pp. 262–271, 1970. [CrossRef]

[33] F. Duchin, "The conversion of biological materials and wastes to useful products," Structural Change and Economic Dynamics, Vol. 1(2), pp. 243–261, 1990. [CrossRef]

[34] S. Nakamura, "An interindustry approach to analyzing economic and environmental effects of the recycling of waste," Ecological Economics, Vol. 28, pp. 133–145, 1999. [CrossRef]

[35] U. N. Ngoc, and H. Schnitzera, "Sustainable solutions for solid waste management in Southeast Asian countries," Waste Management, Vol. 29(6), pp. 1982–1995, 2009. [CrossRef]

[36] S. Mani, and S. Singh, "Sustainable municipal solid waste management in India: A policy agenda," Procedia Environmental Sciences, Vol. 35, pp. 150–157, 2016. [CrossRef]

[37] H. I. Abdel-Shafy, and M. S. M. Mansour, "Solid waste issue: Sources, composition, disposal, recycling, and valorization," Egyptian Journal of Petroleum, Vol. 27(4), pp. 1275–1290, 2018. [CrossRef]

[38] Z. Xu, A. Elomri, S. Pokharel, Q. Zhang, X. G. Ming, and W. Liu, "Global reverse supply chain design for solid waste recycling under uncertainties and carbon emission constraint," Waste Management, Vol. 64, pp. 358–370, 2017. [CrossRef]

[39] A. Shekdar, "Sustainable solid waste management: An integrated approach for Asian countries," Waste Management, Vol. 29, pp. 1438–1448, 2009. [CrossRef]

[40] J. Malinauskaite, H. Jouhara, D. Czajczyn´ska, P. Stanchev, E. Katsou, P. Rostowksi…, and N. Spencer, "Municipal solid waste management and waste-to-energy in the context of a circular economy and energy recycling in Europe," Energy, Vol. 141, pp. 2013–2044, 2017. [CrossRef]

[41] J. Potting, M. Hekkert, E. Worrell, and A. Hanemaaijer, "Circular Economy: Measuring innovation in product chains," Available at: https://www.pbl.nl/uploads/default/downloads/pbl-2016-circular-economy-measuring-innovation-in-product-chains-2544.pdf Accessed on Jul 18, 2024.

[42] D. Cudjoe, H. Wang, and B. Zhu, "Assessment of the potential energy and environmental benefits of solid waste recycling in China," Journal of Environmental Management, Vol. 295, Article 113072, 2021. [CrossRef]

[43] C. Magazzino, M. Mele, and N. Schneider, "The relationship between municipal solid waste and greenhouse gas emissions: Evidence from Switzerland," Waste Management, Vol. 113, pp. 508–520, 2020. [CrossRef]

[44] A. Razzaq, A. Sharif, A. Najmi, M. L. Tseng, and M. K. Lim, "Dynamic and causality interrelationships from municipal solid waste recycling to economic growth, carbon emissions and energy efficiency using a novel bootstrapping autoregressive distributed lag," Resources, Conservation and Recycling, Vol. 166, Article 105372, 2021. [CrossRef]

[45] Y. C. Jang, G. Lee, Y. Kwon, J. Hong Lim, and J. Hyun Jeong, "Recycling and management practices of plastic packaging waste towards a circular economy in South Korea," Resources, Conservation and Recycling, Vol. 158, Article 104798, 2020. [CrossRef]

[46] L. S. Conke, "Barriers to waste recycling development: Evidence from Brazil," Resources, Conservation and Recycling, Vol. 134, pp. 129–135, 2018. [CrossRef]

[47] Y. C. Moh, and L. A. Manaf, "Overview of household solid waste recycling policy status and challenges in Malaysia," Resources, Conservation and Recycling, Vol. 82, pp. 50–61, 2014. [CrossRef]

[48] A. Omran, A. Mahmood, H. Abdul Aziz, and G. M. Robinson, "Investigating households attitude toward recycling of solid waste in Malaysia: A case study," Journal of Environmental Research, Vol. 3(2), pp. 275–288, 2009.

[49] D. Lavee, "Is municipal solid waste recycling economically efficient?" Environmental Management, Vol. 40, pp. 926–943, 2007. [CrossRef]

[50] I. E. Brisson, "Assessing the Waste Hierarchy: A Social Cost-Benefit Analysis Of Municipal Solid Waste Management in the European Union," AKF Forlaget, 1997.

[51] K. Acuff, and D. T. Kaffine, "Greenhouse gas emissions, waste and recycling policy," Journal of Environmental Economics and Management, Vol. 65, pp. 74–86, 2013. [CrossRef]

[52] E. Friedrich, and C. Trois, "Quantification of GHG emission from waste management processes for municipalities - A comparative review focusing on Africa," Waste Management, Vol. 31(7), pp. 1585–1596, 2011. [CrossRef]

[53] T. Jamasb, and R. Nepal, "Issues and options in waste management: A social cost-benefit analysis of waste-to-energy in the UK," Resources, Conservation and Recycling, Vol. 54, pp. 1341–1352, 2010. [CrossRef]

[54] Y. C. Chen, and S. L. Lo, "Evaluation of greenhouse gas emissions for several municipal solid waste management strategies," Journal of Cleaner Production, Vol. 113, pp. 606–612, 2016. [CrossRef]

[55] S. A. Batool, and M. N. Chuadhry, "The impact of municipal solid waste treatment methods on greenhouse gas emissions in Lahore, Pakistan," Waste Management, Vol. 29, pp. 63–69, 2009. [CrossRef]

[56] Y. Chen, "Evaluating greenhouse gas emissions and energy recovery from municipal and industrial solid waste using waste-to-energy technology," Journal of Cleaner Production, Vol. 192, pp. 262–269, 2018. [CrossRef]

[57] M. F. King, and J. Gutberlet, "Contribution of cooperative sector recycling to greenhouse gas emissions reduction: A case study of Ribeirao Pires, Brazil," Waste Management, Vol. 33, pp. 2771–2780, 2013. [CrossRef]

[58] S. Lee, J. Kim, and W. K. O. Chong, "The causes of the municipal solid waste and the greenhouse gas emissions from the waste sector in the United States," Waste Management, Vol. 56, pp. 593–599, 2016. [CrossRef]

[59] M. Corsten, E. Worrell, M. Rouw, and A. van Duin, "The potential contribution of sustainable waste management to energy use and greenhouse gas emission reduction in the Netherlands," Resources, Conservation and Recycling, Vol. 77, pp. 13–21, 2013. [CrossRef]

[60] S. Nakamura, and Y. Kondo, "Recycling, landfill consumption, and CO2 emission: Analysis by waste input–output model," Journal of Material Cycles and Waste Management, Vol. 4(1), pp. 2–11, 2002.

[61] G. Aydinbaş, and Z. Erdinç, "Panel data analysis on the circular economy and its determinants," Anadolu Üniversitesi İktisadi ve İdari Bilimler Fakültesi Dergisi, Vol. 24(2), pp. 258–275, 2023. [CrossRef]

[62] E. Giovanis, "Relationship between recycling rate and air pollution: Waste management in the state of Massachusetts," Waste Management, Vol. 40, pp. 192–203, 2015. [CrossRef]

[63] B. Güloğlu, and Ş. Nazlıoğlu, "Enflasyonun tarımsal fiyatlar üzerindeki etkileri: Panel yumuşak geçiş regresyon analizi," Siyaset, Ekonomi ve Yönetim Dergisi, Vol. 1(1), pp. 1–20, 2013.

[64] J. Fouquau, C. Hurlin, and I. Rabaud, "The feldstein-horioka puzzle: A panel smooth transition regression approach," Economic Modelling, Vol. 25(2), pp. 284–299, 2008. [CrossRef]

[65] M. H. Pesaran, and T. Yamagata, "Testing slope homogeneity in large panels," Journal of Econometrics, Vol. 142(1), pp. 50–93, 2008. [CrossRef]

[66] M. H. Pesaran, A. Ullah, and T. Yamagata, "A bias-adjusted lm test of error cross-section independence," The Econometrics Journal, Vol. 11(1), pp. 105–127, 2008. [CrossRef]

[67] J. Westerlund, and D. L. Edgerton, "A simple test for cointegration in dependent panels with structural breaks," Oxford Bulletin of Economics and Statis-

tics, Vol. 70(5), pp. 665–704, 2008. [CrossRef]

[68] T. L. Tudor, C. L. Noonan, and L. E. T. Jenkin, "Healthcare waste management: A case study from the National Health Service in Cornwall, United Kingdom," Waste Management, Vol. 25(6), pp. 606–615, 2005. [CrossRef]

[69] A. K. Mohareb, M. A. Warith, and R. Diaz, "Modelling greenhouse gas emissions for municipal solid waste management strategies in Ottawa, Ontario, Canada," Resources, Conservation and Recycling, Vol. 52(11), pp. 1241–1251, 2008. [CrossRef]

[70] K. Palmer, H. Sigman, and M. Walls, "The cost of reducing municipal solid waste," Journal of Environmental Economics and Management, Vol. 33, pp. 128–150, 1997. [CrossRef]

[71] L. B. Lave, C. T. Hendrickson, N. M. Conway-Schempf, and F. C. McMichael, "Municipal solid waste recycling issues," Journal of Environmental Engineering, Vol. 125(10), pp. 944–949, 1999. [CrossRef]

[72] S. Otoma, Y. Mori, A. Terazono, T. Aso, and R. Sameshima, "Estimation of energy recovery and reduction of CO2 emissions in municipal solid waste power generation," Resources, Conservation and Recycling, Vol. 20(2), pp. 95–117, 1997. [CrossRef]

*Environ Res Tec, Vol. 7, Issue. 3, pp. 448–456, September 2024*

**Environmental Research and Technology**
https://ert.yildiz.edu.tr - https://dergipark.org.tr/tr/pub/ert
DOI: https://10.35208/ert.1419473

Environmental Research & Technology

**Research Article**

# Should we value rain harvesting more in Türkiye for mitigating precipitation extremes

**Hamdi TEKİN**[*,1], **Şenay ATABAY**[2]

[1]*Department of Civil Engineering, İstanbul Arel University Faculty of Engineering, İstanbul, Türkiye*
[2]*Department of Civil Engineering, Yıldız Technical University Faculty of Civil Engineering, İstanbul, Türkiye*

## ARTICLE INFO

*Article history*
Received: 14 January 2024
Revised: 16 April 2024
Accepted: 24 April 2024

**Key words:**
Drought; Precipitation extremes; Rainfall; Rainwater harvesting

## ABSTRACT

Mitigating precipitation extremes is a major issue due to destructive global warming and climate change. Heavy rainfall and drought have posed a threat to human life and ecology. That said, new strategies and new action plans are needed at local and global levels through needed cooperation from different stakeholders to handle the possible risks associated with precipitation extremes. Türkiye has become one of the most vulnerable countries involved in climate change due to its geographical location, rapid urbanization, and deforestation. Many forests have been destroyed to make room for agriculture, animal grazing as well as for manufacturing and construction. The impact has caused complications in landscapes. Precipitation extremes, such as heavy rainfalls and drought, are posing significant threats for many cities in Türkiye. In recent years Türkiye has faced a large number of extreme events regarding precipitation. In this line, the present study aims to explore the potential benefits of rainwater harvesting (RWH) in mitigating precipitation extremes by overviewing regulatory actions of rainwater harvesting and best practices worldwide. In addition an interview-based survey was conducted with domain experts in the water management field to better understand the current challenges of stormwater management in Türkiye and discuss the role of rainwater harvesting against precipitation extremes. The results of the study have shown that Türkiye has several problems with infrastructure to mitigate precipitation extremes, such as shortcomings in capacity and old water management systems, unseparated water collection and sewage systems, and lack of green infrastructure. In addition to urbanization, expansion in industry and tourism may cause water unavailability. The study has also indicated that many authorities around the globe try to boost RWH use by stipulating or encouraging RWH through incentives to save a large amount of water by implementing different projects. This research has argued that RWH promises several benefits thanks to its cost-effectiveness and contribution to water storage. Therefore, this study has recommended that policymakers should take immediate action against precipitation extremes by introducing new regulations, such as mandating rainwater harvesting for old buildings, industrial and touristic places. Preparing new guidelines and applying rooftop RWH systems that comply with Building Code requirements should also be considered for the widespread use of rainwater in rural and urban areas.

**Cite this article as:** Tekin H, Atabay Ş. Should we value rain harvesting more in Türkiye for mitigating precipitation extremes. Environ Res Tec 2024;7(3)448–456.

***Corresponding author.**
*E-mail address: hamditekin@arel.edu.tr

## INTRODUCTION

Environmental awareness is growing steadily worldwide due to confronting various environmental adversities [1]. Climate change and landscape utilization patterns are crucial concerns for urban water ecosystems and human life [2]. Since urbanization brings about a rapid increase in impervious land cover and deteriorates the quality of the ecosystem [3], proper use of resources is crucial for reducing environmental impacts, protecting the ecology, and sustainable development [4]. Proper management of water, which is an economic asset is also crucial [5]. Due to the depletion of natural resources and the deep impacts of climate change as well as rapid urbanization, the reuse of rainwater is of great importance for both meeting water needs and assisting with flood retention measures in urban and rural regions. Heavier rainfall events occur more frequently in the cities because of climate change [6]. Overloading of removal systems, sewage treatment plants and recipients of water flows increases the risk of floods [7]. Furthermore, contaminated stormwater (SW) runoff from urban environments carries several contaminants to water bodies, which poses a threat to the health of living beings and ecological systems [8]. Surface water is negatively affected by excess nitrogen via eutrophication and related processes [9]. Although SW is a significant hazard, it is also a promising resource [10]. Therefore, the utilization of rainwater has a growing interest around the globe.

In the literature, there are numerous studies, which mainly focus on the performance of RWH systems and improvement methods. Ünlükaplan and Tiğiz [11] aimed to design green areas by determining the necessary amount of irrigation water and the quantity of network water used in the green areas of Dikmen Valley stages in Ankara, in addition to calculating the potential amount of water to be acquired by rain harvesting from Dikmen Stream Basin. Buçak's study [12] emphasizes the importance of residential recycling systems and their benefits on water conservation and the necessity of implementation of such systems on mass housing projects by proposing an implementation example for an apartment in Kirklareli, Türkiye. Şahin and Manioğlu [13] analysed the amount of rainwater obtained using different building forms in different climatic regions comparatively. Teston et al. [14], addressed the high potential of rainwater harvesting systems for potable water savings and control of leakages and losses caused by carelessness or poor maintenance in buildings.

Due to water shortage in urban areas, high costs of developing new replacing surface water sources, inadequate groundwater supplies in arid and semiarid lands, and the unmanageable operation and maintenance costs of large piped water supplies [15], economical rainwater management systems have become more important recently. Therefore, the cost assessment of RWH systems is also one of the most important issues to be concerned. Mumtaaz Sayed and Sawant [16] conducted a financial

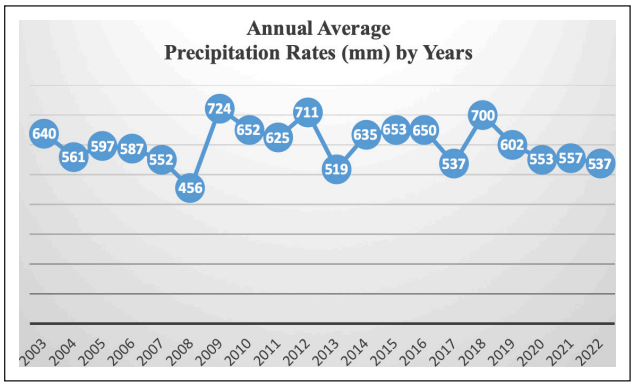


**Figure 1**. Annual precipitation rates by years (2003–2022) [20, 21].

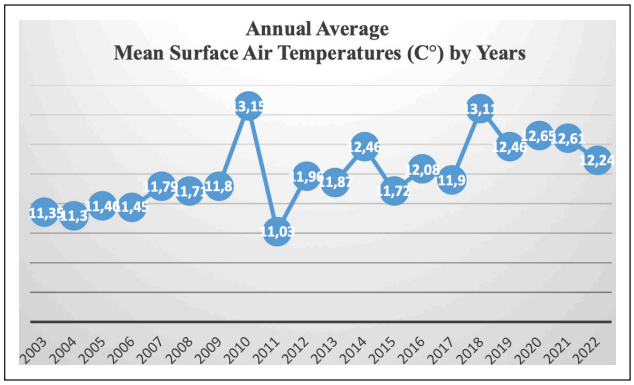


**Figure 2**. Annual average mean surface air temperatures by years (2003–2022) [22].

feasibility analysis of water conservation components considering lifecycle costs and operational savings in large mass housing projects. In their study, they presented a methodology of life cycle cost assessment of a unit RWH system for toilet flushing in an industrial site. Ghimire et al. [17], highlighted a feasible alternative design that has no pump and requires less operation and maintenance costs as well as tank refill volume.

Rainwater harvesting has a growing interest due to its potential in the world. In Türkiye, principles regarding the design and project planning of rainwater systems were regulated by the relevant legislation in 2017 [18]. It became obligatory to construct a rainwater harvesting system in any new building to be built on a parcel larger than two thousand square meters to meet building needs and garden irrigation in 2021 [19]. Although this precaution is of great importance for tackling the challenges of precipitation extremes, new actions are necessary for the reuse of water to mitigate the impacts of climate change and global warming. Figure 1 and Figure 2 show how annual average precipitation rates and surface temperatures change in Türkiye between 2003 and 2022. Figure 1 displays that there has been a drastic fall in annual average precipitation rates in the recent four years (2019–2022). On the other hand, according to Figure 2, before 2018, the annual surface temperatures were always below 12 C° except for 2010. However, the surface temperatures were measured above 12 C° in the last five years. This confirms

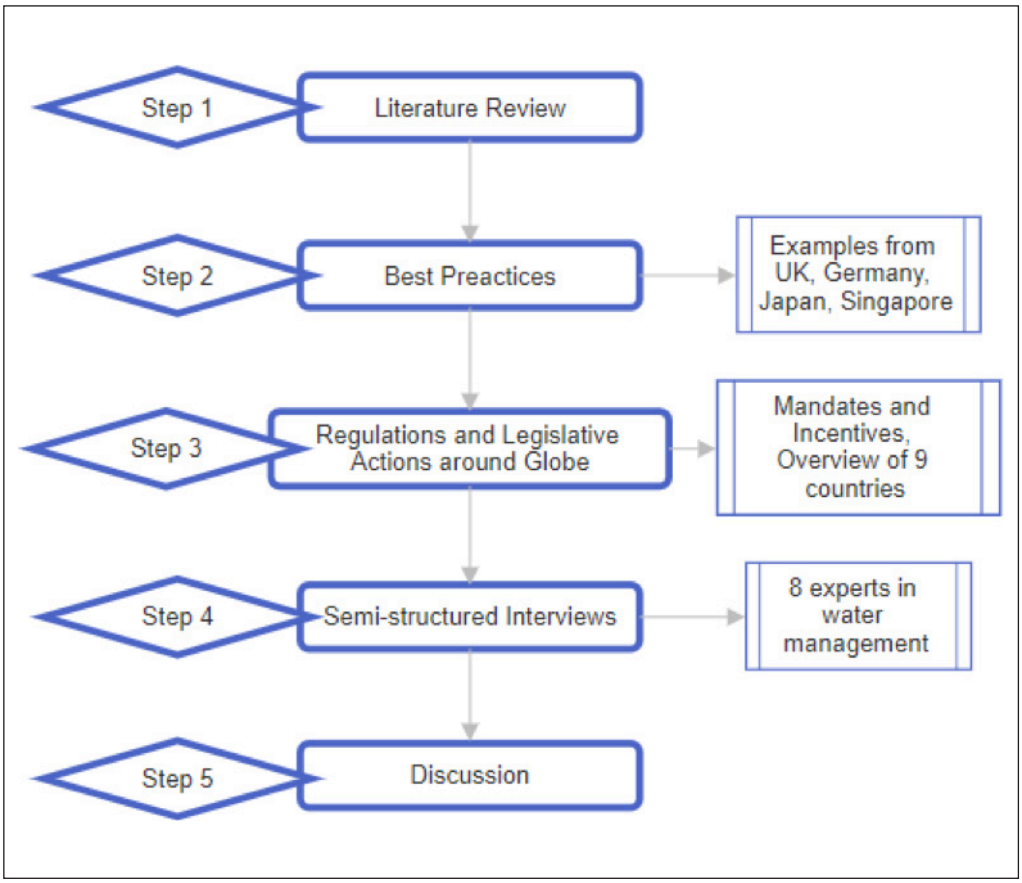


**Figure 3**. Flowchart of the study.

that while annual average precipitation rates have decreased, surface temperatures considerably have increased in recent years.

In addition to these climate impacts, precipitation extremes have occurred in the recent period. The precipitation value, which covers the period between 1 October 2023 and 31 March 2024, was above last year's precipitation, with a 41% increase compared to the same period of precipitation last year [23]. The year 2023 was recorded as the year of the most extreme weather events of all time in Türkiye, with 1,475 extreme weather events [24].

In this line, the present study aims to explore potential benefits of rain harvesting for mitigating precipitation extremes by overviewing best practices and legislative actions of rainwater harvesting worldwide as well as an interview-based survey with experts.

## MATERIALS AND METHODS

The flowchart of the study is shown in Figure 3. After the literature review, best practices were determined to understand the real benefits of RWH systems worldwide. Then, legislative actions were overviewed for different countries to explore how RW is mandated or encouraged at the international level. Afterward, semi-structured interviews were held by eight different experts.

### Best Practices

Rainwater harvesting systems offer several benefits to the built environment in different projects worldwide. Some best practices are explained by considering the scale of implementation and volume of water savings.

The 8,400 $m^2$ rooftop of a Sumo-wrestling arena in Sumida City, Japan serves as the catchment surface for the rainwater utilization system, which drains the collected rainwater into a 1,000 $m^3$ underground storage tank and uses it for toilet flushing and air conditioning [25].

In the United Kingdom, it was estimated that RWH adoption at the Velodrome project in London, a 73 percent overall reduction in potable water demand by using water-efficient fittings and rainwater topped up with recycled blackwater dirty water, one of the highest reductions in potable water demand on the Park [26].

In Germany, Frankfurt Airport has a big RWH system, which collects water from the roofs of the new terminal with an area of 26,800 square meters and helps to save approximately 1 million cubic meters of water per year [27]. Similarly, rainwater is collected and treated through rooftop water collection systems at Changi Airport, Singapore, which accounts for 28 to 33% of its total water used, resulting in savings of approximately S$390,000 per annum [28].

After the implementation of the RWH system, in HPCL Residential Colony, in Chembur Mumbai [29], site conditions drastically changed as follows: a) the recharging ca-

pacity of the bore well increased above 35000 liters per day, b) 50% of rooftop rainwater was harvested. c) yield capacity of the borewell increased from 10,000 to 20,000 liters per day, d) quality of groundwater enhanced and water level increased from 35 feet to 22 feet.

In Mexico City, RWH systems have been installed in households across the city through a notable initiative, the community-led Isla Urbana project, to mitigate water scarcity [30].

In the Caribbean, domestic RWH projects are being implemented to increase water supplies in islands lacking enough water and as a no-regret approach to adaptation to climate change [31].

These best practices are of great importance for contributing to sustainability and climate resilience. In addition, saving water reduces the cost of water supply.

**Regulations on Rainwater Harvesting Systems Worldwide**

As a global, long term and complex issue, climate change involves interactions between demographic, climatic, environmental, economic, health, political, institutional, social, and technological processes [32]. Since extreme weather conditions lead to water scarcity, drought, heat waves, and flash floods, all of which have significant impact on human life, infrastructures, and ecosystems [33], the adoption of cities to extreme weather conditions is challenging issue and handling hazards require a comprehensive and effective risk assessment [34, 35]. Therefore countries, states, and local authorities all over the world take action to manage rainwater issues. Table 1 indicates the RWH regulations in different countries around the globe.

It can be concluded that many authorities around the globe are trying to increase the use of RWH systems in different ways. While the RWH mandate is one of the most common approaches, some of the policymakers prefer to encourage RWH through different incentives and guidelines. The form of RWH systems, and their usage capacity are regulated in some regions. On the other hand, RWH is illegal in Colorado, USA, although it is encouraged in most of the countries.

**Semi-Structured Interviews**

A total of eight semi-structured interviews were held to collect further qualitative data. Professionals with invaluable water management experience participated in the survey to discuss the topics as follows: a) Threats of precipitation extremes, b) Major problems with infrastructural systems in mitigating precipitation extremes in Türkiye, c) The role of RWH against heavy rainfalls and drought. The background information of the interviewees is shown in Table 2.

Interview participants emphasized the major threats as flood due to heavier rainfalls and drought sourced by the decrease in water storage in dams in Türkiye.

I3 expressed this case as follows: '*The major threats regarding water are floods and drought in Türkiye. Although the country has moderate average annual precipitation, heavy rainfalls have occurred more frequently due to climate change recently, which cause destructive floods. On the other hand, precipitation can be lower compared to average values in some regions resulting in decreased water stored in dams*.'

Another threat was pointed out as water scarcity caused by unconscious industrialisation and touristic activities. I7 also highlighted this with the expression as follows: '*A large amount of water is utilized and released by the industry, which plays an important role in the quality and amount of water. Therefore, strict control of released water and effective use of rainwater are essential requirements for a well-established stormwater management strategy. Another key role belongs to tourism, one of the locomotives of the country. Each year, a large number of hotels are built in different regions, leading to increased water consumption of touristic cities. Existing water resources cannot even meet the needs of residents in such cities due to decreased annual precipitation*.'

After evaluating the expressions of interview participants, the major problems with the infrastructure in mitigating precipitation extremes in Türkiye were identified as follows:

- The stormwater collection and sewage systems are not separate in most of the residential areas. In the new residential regions, separate systems are being adopted, but central regions are very old and there are shortcomings in the renewal projects of infrastructure.
- The number of wastewater treatment plants does not suffice to meet the overall need.
- The capacity of infrastructural systems is inadequate. The number of RWH systems is insufficient.
- There is a lack of vegetation and green infrastructure. With increasing urbanization and the replacement of vegetation by impermeable medium, rainwater cannot infiltrate into the soil, and flow on the surface [36].
- Water is not efficiently used in agriculture. The farmers are unaware of new modern systems on how to efficiently benefit from rainwater.
- Despite the increasing population and number of houses, the number of new implementations improving stormwater management is limited.
- There are no regulations for using RWH in industrial and touristic areas, as well as existing houses and ones to be built in small parcels.

Rainwater harvesting systems were strongly recommended thanks to their promising and cost-effective solutions for surface runoff, water scarcity, and green infrastructure by all interview participants.

I6 argued: '*RWH systems are cheaper and easier to maintain. To ensure sustainable stormwater management and green infrastructure, RWH should be mandatory*.'

I8 pointed out: '*RWH systems stem from cisterns, widely used in ancient times. In applicable places, these cisterns can be renovated and also used for rainwater harvesting. The buildings with large roof space should be addressed for RWH. Unfortunately, there is a lack of awareness in such*

**Table 1.** RWH regulations in different countries around the globe

| Location | Legislation on RWH systems and rain gardens | References |
|---|---|---|
| Australia | Regulations stipulate a new rainwater collection system or alternative water source in some states such as South Australia, New South Wales, and Queensland. | Yannopoulos et al., 2019 [36]. |
| Brazil | RWH is encouraged by legislation in several cities as a policy of access to water in semi-arid cities.<br>"One Million Cisterns" program, a federal government investment to enable access to water for families in the Brazilian semi-arid region by encouraging the construction of cisterns.<br>Within the governmental program "One Land Two Waters" families of farmers get technologies and training to capture and store rainwater for agricultural use. | Teston et al., 2018 [14]; Mendonça, 2006 [37]; Gnadlinger, 2005 [38]. |
| Germany | The use of stormwater infiltration systems is stipulated by water laws and regulations in Germany.<br>There are strict regulations in drinking water standards. Household rainwater supplies are restricted to non-potable uses such as toilet flushing, clothes washing, and garden watering.<br>In many towns and cities, grants and subsidies are given to encourage householders to construct rainwater tanks and seepage wells.<br>Some form of RWH is mandated for buildings and houses in Hessen, Baden-Württemberg, Saarland, Bremen, Thuringen, and Hamburg. | Diekers et al., 2015 [39]; RWHb, 2023 [27]; Yannopoulos et al., 2019 [36]. |
| India | Some form of RWH is mandated for buildings and houses in New Delhi, Indore, Chennai, and Rajasthan.<br>The collection and storage of rainwater in earthen tanks for domestic and agricultural uses has also been very common for a long time.<br>Rooftop RWH systems are mandated for newly constructed buildings in 18 of the 28 states and 4 of the 7 federal regions. | Yannopoulos et al., 2019 [36]; Marwas, 2010 [40]. |
| Japan | Rainwater utilization is encouraged through tax breaks, subsidies, funds, policy loans, and other economic tools.<br>Tokyo Sumida set up a rainwater utilization subsidy system for underground storage cisterns, medium and small storage cisterns, to boost the implementation of technology for rainwater utilization.<br>Assistance programs have been introduced for rainwater cisterns and systems for rainwater seepage pits. | Fu, 2018 [41]. |
| Malaysia | The government proposed RWH to mitigate the water crisis.<br>Guidelines regarding planning, design, and installation of RWH, eco-efficient water infrastructure, and SW management systems were implemented by different governmental authorities. | Lee et al., 2016 [42]. |
| New Zealand | Rainwater harvesting is mandated in several urban areas of New Zealand.<br>While rainwater harvesting has long been the norm in rural areas that lack reticulated, yet it's still uncommon in New Zealand's urban areas.<br>Rainwater systems must meet Building Code requirements, such as a requirement for adequate potable (drinkable) water to be provided for consumption, oral hygiene, utensil washing and food preparation. | Gabe et al., 2012 [43]; Rose, 2014 [44]; Branz Facts, 2024 [45]. |
| Türkiye | Principles regarding the design and project planning of rainwater systems are regulated by the relevant legislation.<br>RWH is mandated in any new building to be built on a parcel larger than two thousand square meters to meet building needs and garden irrigation. | Resmi Gazete, 2017 [18]; Resmi Gazete, 2021 [19]. |
| UK | Manuals were developed about the design, construction, and management of RWH.<br>Harvested rainwater can be used without a water abstraction license. A water abstraction license, which enables permission to get water at a certain amount from the water supply, is needed to abstract or transfer harvested rainwater. | EA, 2021 [46];<br>Yannopoulos et al., 2019 [36]. |
| USA | Rainwater harvesting is not regulated by the federal government but rather it is up to individual states.<br>Some states encourage the collection and use rainwater.Size of storage capacity is regulated in some states.<br>Generally, commercial and residential applications are allowed in states with rainwater harvesting regulations.<br>In Colorado, RWH is illegal. | PNNL, 2015 [47]. |

**Table 2.** Background information of interview participants

| Interview participants | Description of expertise |
|---|---|
| 1. Expert in environmental protection and infrastructure | Experience in waste water, economics of waste and waste management, climate change and ecosystems assessment and valuation, environmental legislation. |
| | Considerable experience in international projects |
| 2. PhD researcher | Experience in urban policy planning and local governments |
| | Experience in project management |
| 3. Water, dam & energy engineer | Recent studies on sustainable urban design systems |
| | Considerable experience in water resources management |
| | Experience in water & energy projects |
| 4. Experienced senior lecturer | Head of Urban Water Management Unit |
| | Environmental awareness |
| | Experience in international project management |
| 5. Civil engineer | PhD in Water Management |
| | Water Management Advisor |
| 6. Stormwater technical director | Designing stormwater/wastewater treatment and management systems |
| | Green infrastructure for surface water |
| 7. Associate professor | Water quality |
| | Water management |
| 8. Professor in water resources | Experience more than 50 years in water resources and flood retention |
| | International experience in France and Algeria |

*systems. These systems do not require much investment and are easy to implement.*'

Nonetheless, some important issues were concerned with efficient use of RWH in Türkiye. According to the I6 and I8, rainwater harvesting is worth implementing in regions with sufficient average annual precipitation. It is also feasible in regions with lower precipitation rates, but optimal design is of great importance due to potential extra operation and maintenance costs. According to the experts, it will not be worth implementing RWH systems for single houses, but will be worth for mass housing projects. The experts also highlighted importance of specific design in implementing RWH for different types of residential buildings in different regions.

## RESULTS AND DISCUSSION

Due to its geographic location, rapid urbanization and increasing rate of deforestation, Türkiye has been deeply affected by climate change and global warming. Rapid urbanization and industrial developments considerably exploit and pollute freshwater resources [2]. In the near future, impacts may be more destructive. New strategies and new action plans are needed at local and global levels through needed cooperation from different stakeholders to handle the possible risks associated with precipitation extremes. Many forests have been destroyed to make room for agriculture and animal grazing as well as for manufacturing and construction. The impact has caused complications in landscapes. To tackle the challenges of precipitation, it became obligatory in Türkiye to construct a rainwater harvesting system in any new building to be built on a parcel larger than two thousand square meters to meet building needs and garden irrigation within the 'Regulation on Amending the Planned Areas Zoning Regulation', [19]. After this regulation was introduced, different projects were launched to promote rainwater utilisation. For example, within 'İzmir Sponge City' project, İzmir Metropolitan Municipality aims to include 5000 buildings in the incentive system with 5000 polyethylene rainwater harvest tanks [48]. However, this regulation may not be enough because of shortcomings in the current infrastructure and limited scope of buildings.

The study discussed several problems with the infrastructure, such as low quality of water due to a lack of stormwater plants and separate systems for SW collection-sewage removal, insufficient RWH, and shortcomings in green infrastructure and vegetation. It is seen that policymakers in Türkiye need to consider many precautions to mitigate precipitation extremes. The increasing number of mass housing projects, old and limited infrastructure and unavailability of separate stormwater management systems make it difficult to overcome challenges regarding heavy rainfalls. Wastewater may find its way into the receiving waters through stormwater sewers even in separate sewer systems due to cross-connections, illicit connections, overflows, and leakages through broken sewers [49]. If the systems are not separate, contamination is much higher. The local authorities and municipalities should give much more importance under the guidance of the government to replace current old systems that lack resilience against

stormwater. The Delegation of the European Union to Türkiye [50] has funded many projects on the reuse of rainwater, and wastewater, and the construction of new wastewater treatment plants. Such funding schemes could be well-informed and promoted to encourage the municipalities and relevant authorities.

Although there is a mandate for RWH use in particular new buildings in Türkiye, there is no obligation for existing buildings to be constructed for housing, industry, tourism, etc. Furthermore, residential areas are very close to the industrial regions. A large amount of water is consumed by the industry and tourism sector, leading to higher water demand and water scarcity in cities close to industry and hotels. Existing water resources do not suffice to meet the needs of residents in many cities due to higher water demand and lower annual precipitation rates sourced by climate change. Therefore, the RWH mandate should also be considered not only for new buildings but also existing ones, especially for industrial areas and touristic regions. Furthermore, introducing new guidelines, and subsidies would be good alternatives to boost rainwater utilisation. Rooftop RWH systems can be also encouraged and manuals can be developed for better use of RWH systems, which comply with the Building Code requirements.

Overview of best practices and results of interview RWH shows itself a cost-effective system for mitigating precipitation extremes. In the literature, many studies have also confirmed their feasibility. Tanik [51] argued that the investment and operation costs of such systems are usually low. Bashar et al. [52] showed that payback periods of installation and maintenance costs of RWH vary within 2–6 years depending on the topographic and climatic conditions.

Although Türkiye has a moderate annual precipitation rate, precipitation extremes pose a major threat, which can result in destructive floods and drought in Türkiye due to drastic changes in peak values. Water scarcity may be one of the major problems due to decreased dam storage, and uncontrolled water use by the industry and tourism sector. This can also lead to several problems in agriculture. Water is ineffectively used, and people are not aware of the potential benefits of RWH systems in arid regions.

## CONCLUSION

This study investigated the potential benefits of RWH for mitigating the impacts of precipitation extremes in Türkiye by overviewing regulatory actions and best practices as well as an interview-based survey. Due to the deep impacts of climate change, deforestation, and improper land use, Türkiye has been suffering from precipitation extremes. Increasing population and uncontrolled urbanization patterns have also resulted in numerous infrastructural problems, especially in metropolitan cities, such as Istanbul, Ankara, and İzmir. Therefore, water management is one of the challenging issues to be considered by authorities at the local and national levels. Rainwater harvesting has growing interest worldwide as it offers cost-effective solutions against precipitation extremes. There is a plenty of regulatory and legislative actions, which have been taken in different cities around the globe. Turkish government also implemented a new regulation which mandates RWH for particular newly constructed buildings, but further actions are needed to solve current and potential infrastructural problems in existing urban areas. Local authorities should also pioneer rainwater projects. For instance, making the practice of rain harvesting in İzmir City widespread in local governments may provide benefits throughout the country. Similar projects will boost rainwater utilisation. On the other hand, there is no RWH mandate for existing buildings and new buildings to be built in small parcels. Surface runoff will be a threatening problem in central and crowded regions since the amount and quality of water released to the infrastructural system are not well controlled. Therefore, the rule of the RWH mandate could also be applied to existing buildings. As the use of RWH may not be feasible for single houses due to investment and operation & maintenance costs, a mandate could be applied for groups of single houses. Mass housing projects are spreading all over the country. In addition, there is also a great expansion in industrial and touristic buildings, which leads to higher water demand. RWH systems with appropriate designs would be good alternatives for mitigating precipitation extremes.

In arid regions, RWH utilization is of great importance for the efficient use of rainwater and increasing harvest. Encouraging farmers to use RWH systems could decrease the need for exporting agricultural products. To obtain optimum efficiency from such systems, local authorities should find ways to separate stormwater collection and sewage systems for crowded urban regions. This is also needed to implement new water treatment systems to increase water quality. Applying for EU support with well-prepared projects would be a good option. The number of projects can be increased with the help of relevant public organizations and successful local authorities with valuable experience in such projects.

Although the research focus was only on Türkiye and further research that involves more countries may yield better results, the implications of this study are important to understand the potential problems with infrastructure against precipitation extremes and the benefits of RWH systems for handling challenges in developing countries.

## ACKNOWLEDGEMENT

This study is based upon work from COST Action CA 16209- Natural Flood Retention on Private Land, supported by COST (European Cooperation in Science and Technology).

## DATA AVAILABILITY STATEMENT

The author confirm that the data that supports the findings of this study are available within the article. Raw data that support the finding of this study are available from the corresponding author, upon reasonable request.

## CONFLICT OF INTEREST

The author declared no potential conflicts of interest with respect to the research, authorship, and/or publication of this article.

## USE OF AI FOR WRITING ASSISTANCE

Not declared.

## ETHICS

There are no ethical issues with the publication of this manuscript.

## REFERENCES


[1] A. R. M. Rashid, M. A. Bhuiyan, B. Pramanik, and N. Jayasuriya, "A comparison of environmental impacts between rainwater harvesting and rain garden scenarios," Process Safety and Environmental Protection, Vol. 159, pp. 198–212, 2022. [CrossRef]

[2] E. R. Rene, J. Ge, G. Kumar, R. P. Singh, and S. Varjani, "Resource recovery from wastewater, solid waste, and waste gas: Engineering and management aspects," Environmental Science and Pollution Research, Vol. 27(15), pp. 17435–17437, 2020. [CrossRef]

[3] O. Mehta, and K. K. Singh, "Rain garden - A solution to urban flooding: A review." Edited by Agnihotri, A., Reddy, K., Bansal, A. Sustainable Engineering. pp. 27–35, 2019. [CrossRef]

[4] I. C. Yilmaz, and D. Yilmaz, "Optimal capacity for sustainable refrigerated storage buildings," Case Studies in Thermal Engineering, Vol. 22, Article 100751, 2020. [CrossRef]

[5] J. G. Sánchez-Torija, E. L. Gómez-Rubiera, and C. B. Frutos, "The incorporation of the study into water consum ption in energy audits in schools," Revista de la Construcción, Vol. 16(3), pp. 361–373. 2017. [CrossRef]

[6] M. L. Meilvang, "From rain as risk to rain as resource: Professional and organizational changes in urban rainwater management," Current Sociology, Vol. 69(7), pp. 1034–1050, 2021. [CrossRef]

[7] G. Markovi, M. Zele, D. Káposztásová, and G. Hudáková, "Rainwater infiltration in the urban areas," WIT Transactions on Ecology and the Environment, Vol. 181, pp. 313–320, 2014. [CrossRef]

[8] C. Pla, D. Benavente, J. Valdes-Abellan, and Z. Kovacova, "Effectiveness of two lightweight aggregates for the removal of heavy metals from contaminated urban stormwater," Journal of Contaminant Hydrology, Vol. 239, Article 103778, 2021. [CrossRef]

[9] B. K. Biswal, K. Vijayaraghavan, M. G. Adam, D. Lee Tsen-Tieng, A. P. Davis, and R. Balasubramanian, "Biological nitrogen removal from stormwater in bioretention cells: A critical review," Critical Reviews in Biotechnology, Vol. 42(5), pp. 713–735, 2022. [CrossRef]

[10] S. Ahilan, J. Webber, P. Melville-Shreeve, and D. Butler, "Building urban flood resilience with rainwater management," Proceedings of the 17th International Computing and Control for the Water Industry Conference. Exeter, United Kingdom, 2019.

[11] Y. Ünlükaplan, and B. Tiğiz, "Cumhuriyetin 100. Yılında sürdürülebilir su kullanımında yeşil alan tasarım ve yönetiminin etkinliğinin araştırılması: Ankara Dikmen Vadisi örneği," Kent Akademisi, Vol. 16, pp. 115–130, 2023.

[12] Buçak, G. (2015). Kırklareli'nde evsel su kullanımı ve korunumuna yönelik bir uygulama önerisi (Master's thesis, Maltepe Üniversitesi, Fen Bilimleri Enstitüsü). Available at: https://tez.yok.gov.tr/UlusalTezMerkezi/tezDetay.jsp?id=HjLkt9rwpjTOAeBhurjveQ&no=6rFXIt_QKNiL6_h9A0DZvw. Accessed on July 25, 2024.

[13] N. İ. Şahin, and G. Manioğlu, "Water conservation through rainwater harvesting using different building forms in different climatic regions," Sustainable Cities and Society, Vol. 44, pp. 367–377, 2019. [CrossRef]

[14] A. Teston, M. S. Geraldi, B. M. Colasio, and E. Ghisi, "Rainwater harvesting in buildings in Brazil: A literature review," Water, Vol. 10(4), Article 471, 2018. [CrossRef]

[15] J. M. Wanyonyi, "Rainwater harvesting possibilities and challenges in Kenya," Kenya Rainwater Association, 2013. [CrossRef]

[16] S. S. Mumtaaz Sayed, and P. H. Sawant, "Financial feasibility analysis of water conservation components in mass housing projects: Suburban Indian Case review," Journal of Architectural Engineering, Vol. 22(2), Article 04016001, 2016. [CrossRef]

[17] S. R. Ghimire, D. W. Watkins Jr, and K. Li, "Life cycle cost assessment of a rainwater harvesting system for toilet flushing," Water Science and Technology: Water Supply, Vol. 12(3), pp. 309–320, 2012. [CrossRef]

[18] Resmi Gazete, "Yağmursuyu toplama, depolama ve deşarj sistemleri hakkında yönetmelik," Available at: https://www.resmigazete.gov.tr/eskiler/2017/06/20170623-8.htm Accessed on Apr 15, 2024.

[19] Resmi Gazete, "Planli alanlar imar yönetmeliğinde değişiklik yapilmasina dair yönetmelik," Available at: https://www.resmigazete.gov.tr/eskiler/2021/07/20210711-1.htm Accessed on Aug 15, 2023.

[20] Trading Economics, "Türkiye – Yağış," Available at: https://tr.tradingeconomics.com/turkey/precipitation Accessed on Apr 15, 2024.

[21] World Bank, "Open data," Available at: https://data.wolrdbank.org/ Accessed on Apr 15, 2024.

[22] Climate Change Knowledge Portal, "Türkiye," Available at: https://climateknowledgeportal.worldbank.org/country/turkiye Accessed on Apr 15, 2024.

[23] Turkish State Meteorological Service, "2023-2024 su yılı 6 aylık alansal kümülatif yağış raporu," Available at: https://www.mgm.gov.tr/veridegerlendirme/yagis-raporu.aspx?b=k Accessed on Apr 15, 2024.

[24] Blomberght, "Türkiye'de aşırı hava olayları 2023'te rekor kırdı," Available at: https://www.bloomberght.com/turkiye-de-asiri-hava-olaylari-2023-te-rekor-kirdi-2346873 Accessed on Apr 15, 2024

[25] RWH, "Rainwater harvesting in Tokyo," Available at: http://www.rainwaterharvesting.org/international/tokyo.htm Accessed on Jul 17, 2024.

[26] Learning Legacy, "Rainwater harvesting at the Velodrome," Available at: https://webarchive.nationalarchives.gov.uk/ukgwa/20180426101359/http://learninglegacy.independent.gov.uk//documents/pdfs/sustainability/154-rainwater-harvesting-sust.pdf Accessed on Jul 17, 2024.
[27] RWH, "Rainwater harvesting in Germany," Available at: http://www.rainwaterharvesting.org/international/germany.htm Accessed on Jul 17, 2024.
[28] RWH, "Rainwater harvesting in Singapore," Available at: http://www.rainwaterharvesting.org/international/singapore.htm Accessed on Jul 17, 2024.
[29] NS Associates, "HPCL residential colony, Chembur Mumbai," Available at: https://nsassociates.co.in/success-stories-rainwater-harvesting/ Accessed on Jul 17, 2024.
[30] Smartwateronline, "Rainwater as a solution to water scarcity: Case studies from around the world," Available at: https://smartwateronline.com/news/rainwater-as-a-solution-to-water-scarcity-case-studies-from-around-the-world Accessed on Jul 17, 2024.
[31] E. J. Peters, "Success and success factors of domestic rainwater harvesting projects in the Caribbean," Journal of Sustainable Development, Vol. 9(5), pp. 55–69. 2016. [CrossRef]
[32] H. Chander, and G. Kumar, "Rainwater harvesting structures as an alternative water resource under rain-fed conditions of district Hamirpur, Himachal Pradesh, India," CPUH-Research Journal, Vol. 3(2), pp. 226–233, 2018. [CrossRef]
[33] M. Teichmann, D. Kuta, and N. Szeligova, "Urban rainwater management tools," IOP Conference Series: Earth and Environmental Science, Vol. 444(1), Article 012052, 2020.
[34] J. A. Michel, G. Reginatto, J. Mazutti, L. L. Brandli, and R. M. L. Kalil, "Selection of Best Practices for Climate Change Adaptation with Focus on Rainwater Management. Edited by Leal Filho, W., Borges de Brito, P., Frankenberger, F. International Business, Trade and Institutional Sustainability. pp. 915–932, 2020. [CrossRef]
[35] B. Liu, J. J. Huang, E. McBean, and Y. Li, "Risk assessment of hybrid rain harvesting system and other small drinking water supply systems by game theory and fuzzy logic modeling," Science of The Total Environment, Vol. 708, Article 134436, 2020. [CrossRef]
[36] S. Yannopoulos, I. Giannopoulou, and M. Kaiafa-Saropoulou, "Investigation of the current situation and prospects for the development of rainwater harvesting as a tool to confront water scarcity worldwide," Water, Vol. 11(10), Article 2168, 2019. [CrossRef]
[37] M. C. Mendonça, "Plano nacional de recursos hídricos," Available at: https://www.gov.br/mdr/pt-br/assuntos/seguranca-hidrica/plano-nacional-de-recursos-hidricos-1/pnrh_2022_para_baixar_e_imprimir.pdf Accessed Jul 17, 2024.
[38] J. Gnadlinger, A. de Souza Silva, L. T. de Lima Brito, "O programa uma terra e duas águas para um semi-arido sustentavel," Available at: https://www.alice.cnptia.embrapa.br/alice/bitstream/doc/159651/1/OPB1516.pdf. Accessed Jul 17, 2024.
[39] C. Dierkes, T. Lucke, and B. Helmreich, "General technical approvals for decentralised sustainable urban drainage systems (SUDS)—The current situation in Germany," Sustainability, Vol. 7(3), pp. 3031–3051, 2015. [CrossRef]
[40] A. G. Marwas, "Water & Water Treatment in India," OSEC, 2010.
[41] L. Fu, "Advancing rainwater harvesting systems to help mitigate the urban flooding problems in China," Available at: https://getd.libs.uga.edu/pdfs/fu_li_201805_mla.pdf Accessed on Jul 17, 2024.
[42] K. E. Lee, M. Mokhtar, M. M. Hanafiah, A. A. Halim, and J. Badusah, "Rainwater harvesting as an alternative water resource in Malaysia: Potential, policies and development," Journal of Cleaner Production, Vol. 126, pp. 218–222, 2016. [CrossRef]
[43] J. Gabe, S. Trowsdale, and D. Mistry, "Mandatory urban rainwater harvesting: Learning from experience," Water Science and Technology, 65(7), pp. 1200–1207. 2012. [CrossRef]
[44] R. Rose, "Rainwater harvesting, building and technology," Available at: https://organicnz.org.nz/magazine-articles/rainwater-harvesting/ Accessed on Jul 17, 2024.
[45] Branz Facts, "Harnessing rainwater and greywater. rainwater harvesting systems in New Zealand houses," Available at: https://d39d3mj7qio96p.cloudfront.net/media/documents/BRANZ-Facts-HRG-1-Rainwater-harvesting-systems.pdf.Accessed on Jul 17, 2024.
[46] Environment Agency, "Rainwater harvesting: Regulatory position statement," Available at: https://www.gov.uk/government/publications/rainwater-harvesting-regulatory-position-statement/rainwater-harvesting-regulatory-position-statement Accessed Jul 17, 2024.
[47] Pacific Northwest National Laboratory, "Rainwater harvesting state regulations and technical resources," Available at: https://www.pnnl.gov/main/publications/external/technical_reports/PNNL-24347.pdf Accessed Jul 17, 2024.
[48] İzmir Belediyesi, "Izmir sponge city," Available at: https://yagmusuyu.izmir.bel.tr/ Accessed on Apr 17, 2024.
[49] O. Panasiuk, A. Hedström, J. Marsalek, R. M. Ashley, and M. Viklander, "Contamination of stormwater by wastewater: A review of detection methods," Journal of environmental management, Vol. 152, pp. 241–250, 2015. [CrossRef]
[50] Delegation of the European Union to Türkiye, (2022) https://www.avrupa.info.tr/ Accessed on Nov 22, 2022.
[51] A. Tanik, "Yağmur suyu toplama, biriktirme ve geri kullanımı" Available at: https://www.skb.gov.tr/wp-content/uploads/2017/11/Prof.-Dr.-Aysegul-TANIK.pdf Accessed Jul 17, 2024.
[52] M. Z. I. Bashar, M. R. Karim, and M. A. Imteaz, "Reliability and economic analysis of urban rainwater harvesting: A comparative study within six major cities of Bangladesh," Resources, Conservation and Recycling, Vol. 133, pp. 146–154, 2018. [CrossRef]

*Environ Res Tec, Vol. 7, Issue. 3, pp. 457–470, September 2024*

**Environmental Research and Technology**
https://ert.yildiz.edu.tr - https://dergipark.org.tr/tr/pub/ert
DOI: https://10.35208/ert.1461700

**Review Article**

# Multidisciplinary perspective: A review of the importance of communication in managing climate change challenges

**Beyza KARACAOĞLU*, Mehmet Fatih AKBABA**

*Department of Bioengineering, Yıldız Technical University, Faculty of Chemical and Metallurgical Engineering İstanbul, Türkiye*

## ARTICLE INFO

*Article history*
Received: March 30 2024
Accepted: June 03 2024

**Key words:**
Climate change; Communication; Social awareness

## ABSTRACT

Climate change is a global issue that affects the entire world, associated with greenhouse gas emissions and resulting in long-term changes in climate conditions. Scientists conduct numerous research studies focused on climate change and mitigating its effects, making it a central topic of discussion. Overall approaches are typically centered around sustainability and reducing greenhouse gas emissions through green and innovative technologies. However, these approaches and scientific expressions can appear complex and abstract to the public, governments, and civil society organizations. In this regard, the role of communication is significant in creating long-term awareness among the public and generating action-oriented solution proposals. The use of effective language and storytelling techniques, localization, visualization, and effective use of media can help contextualize climate change issues, raise awareness, and build consciousness. The role of communication is undeniable in breaking down barriers between scientists and the public, ensuring that solutions to climate change problems are sustainable and effective, and facilitating the development of appropriate policies by governments and civil society organizations. It is essential to prioritize and conduct advanced research and develop innovative strategies for coordinated efforts between scientists and communication experts in addressing climate change and developing effective solutions. The scope of this review is to examine the role of communication in addressing climate change. This article provides an overview of climate change, its impacts, and solutions, explores the relationship between climate change and communication, and highlights the explanation of communication strategies and intergenerational connectivity to increase awareness of climate change.

**Cite this article as:** Karacaoğlu B, Akbaba MF. Multidisciplinary perspective: A review of the importance of communication in managing climate change challenges. Environ Res Tec 2024;7(3)457–470.

## INTRODUCTION

Atmosphere, biosphere, seas and oceans, glaciers and terrestrial regions constitute the climate system, and solar radiation, ocean currents, precipitation patterns, surface characteristics, and human factors form and alter this climate system [1]. Climate change is triggered by existing greenhouse gas emissions, primarily carbon dioxide ($CO_2$), and increases the temperature of the Earth's atmosphere, serving as the main cause of global warming [2, 3]. Besides greenhouse gases generated by natural processes like respiration, fermentation, and volcanic activity, these gases also stem from diverse industrial operations, inadequate waste management, deforestation, and notably, the combustion of fossil fuels, responsible for approximately 65% of greenhouse gas emissions [4, 5].

***Corresponding author.**
*E-mail address: beyzak@yildiz.edu.tr

A climate crisis is the negative effects of incremental and cumulative disasters caused by climate change, from the environment and health to social life and psychology [6]. Numerous factors influence the atmospheric $CO_2$ concentration, which reached 421 ppm in 2022 in the context of climate change. Current estimates suggest that if we do not control the atmospheric $CO_2$ concentration, global warming could increase by 3–5 °C by 2100. This situation leads to a climate crisis [7, 8]. For example, researchers determined that 2023 was the hottest year in human history, observing heat waves in various regions and a general increase in deaths due to these heat waves [9]. Furthermore, experts predict that children under the age of 5 will bear nearly 90% of the disease burden due to climate change, a situation that will impact the rest of the population and future generations, leading to both mental and physical harm to society [10]. Accordingly, an increase in steric sea level of 0.34±0.16 mm/year was observed in the Pacific Ocean between 2005 and 2019, and an average increase of 3.3 mm/year in global sea level was observed between 1993 and 2018 [11]. Changes in water cycles cause changes in salinity as well as warming of the oceans, which, according to climate model predictions, causes changes in the biological functions of the ocean [12]. Outside of the oceans, when looking at tree dimensions in the forestry sector as well, it has been observed that over the last 50 years, the diameter/volume growth of tree species in Central and Northern Europe has varied from -1% to +99%, while in Southern Europe, it has decreased from -12% to -49% [13].

In recent years, climate change and the climate crisis have been affecting not only environmental and natural sciences, but also geography, sociology, psychology and political science [14]. In this context, global warming and climate change have emerged as the most pressing threat facing the world today, necessitating concerted action through integrated efforts from both the natural and social sciences. Tackling these anthropogenic sources of greenhouse gas emissions is essential to mitigating the consequences of climate change. In recent years, the notion of achieving net-zero emissions has gained prominence. However, it is crucial to underline that the success of this concept relies on ensuring the maintenance of social, economic, political, and environmental integrity [15, 16].

In today's world, the concept of sustainability is not only relevant to the natural sciences but also attracts the attention of social sciences, humanities, and arts fields to create positive global social and environmental change and achieve integrated sustainability [17]. In recent years, understanding public perception and behavior towards climate change, observing how it is understood by the public, mass media, strategic communication, and how communication influences public perception and behavior towards climate change has drawn the attention of researchers [18]. Climate change communication is a complex system that encompasses not only the content and form of this communication, but also scientists, communication professionals, political and social environments. The complexities to effective climate change communication are many, diverse and often interconnected [19]. Explaining and communicating the climate crisis and its consequences correctly, adopting sustainable practices, switching to renewable energy sources, and raising public awareness are key steps towards reducing the carbon footprint and mitigating the effects of global warming [3, 20].

This review provides a concise overview of the impacts of the climate crisis, highlights strategies for reducing greenhouse gas emissions, and emphasizes the significance of communication to increase understanding and awareness of climate change and global warming. The purpose of this article is to investigate how communication could contribute to addressing climate change, as well as to review the studies conducted in this field. The review discusses climate change, the climate crisis, and strategies to combat it, delves into the role of communication in addressing this challenge, thoroughly examines relevant communication strategies and studies in this field and explains intergenerational connectivity in climate change. This study is valuable in providing readers with a multidisciplinary perspective on the natural and social sciences in addressing climate change, as well as in recognizing the role and importance of proper communication and understanding of climate change.

**Climate Change**

With the increase in greenhouse gas emissions and the consequent rise in global atmospheric temperatures, observable effects of climate change on the earth's ecosystem include shifts in seasons, changes in the frequency and intensity of weather events, increased frequency of hot days, decreased frequency of cold days and nights, desertification, melting of polar glaciers, and rising sea levels, forest fires and acid rains [21–23]. Along with these effects, seasonal changes have an impact on industries like tourism [24], building and transport [7, 25], food, and energy [26, 27], as well as habitat loss, changes in the timing of species migration, increased extinction rates [28], threats to agriculture and food security [27], and the increased occurrence of natural disasters [29, 30]. The escalating disasters, shifts in agriculture and water resources, along with the increasing migration due to these changes, have brought about the emergence of the climate crisis [6]. Sectors affected by climate change and how they are/will be affected by climate crisis are summarized in Figure 1.

This crisis necessitates urgent action, as it has particularly adverse effects on the well-being of children worldwide. This crisis has a particularly negative impact on the well-being of children worldwide, and is generating negative public sentiments. The eco-anxiety and climate change-related concerns, especially among Generation Z, is an important issue as it triggers new directions in environmental thinking and awareness. Raising awareness among all sectors of society to prioritize action on this issue is crucial for the future of the world and generations to come [31, 32]. Also, increasing temperatures and extreme weather conditions threaten food security, leading to deteriorating food quali-

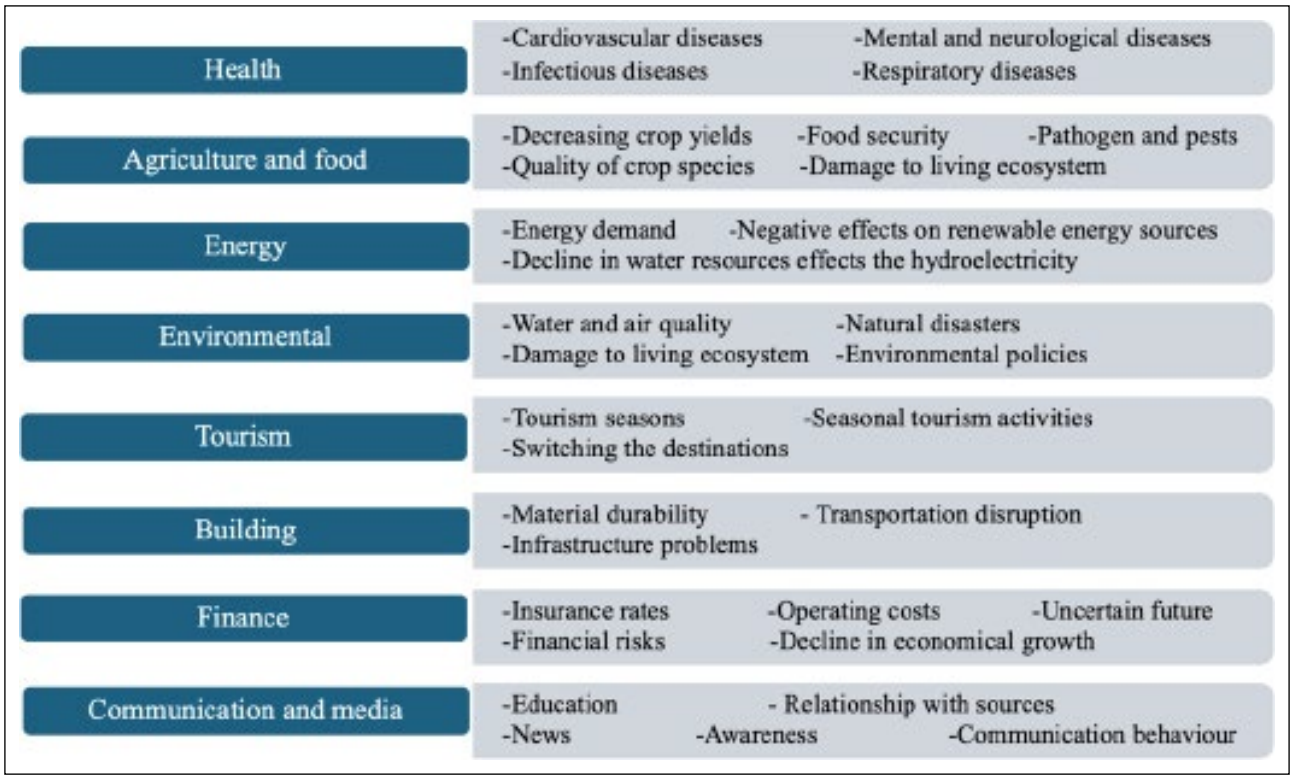


**Figure 1**. Sectors affected by climate crisis.

ty, difficulties in finding food for people, and consequently, higher food prices in the agriculture and food sector [33]. On the other hand, since climate change directly affects the ecosystem, it results in adverse effects such as harm to marine life [34], reduction in soil retention due to plant destruction by pathogens [35] and an increase in plant pathogens such as wheat crown rot (Fusarium spp.) due to drought [36], decrease in bee populations [37], and reduction in habitats for many plant and animal species. Furthermore, studies have shown that extreme weather events have negative effects on human physical and mental health, education, and employment [38]. Changes in animal migration routes have led to an increased potential for the emergence of new vector-borne (such as West Nile virus [13]), waterborne diseases (such as diarrhoeal disease [39]) and foodborne diseases (diarrhoeal and invasive infections [40]) [41], and an increase in the frequency and severity of allergies has been observed [42].

**Adressing the Challenge of Climate Change**

The impacts of climate change are deepening, transforming into a global crisis. In the collective effort to combat this crisis, the roles of governments, civil society organizations, and various entities are significant [43]. After the acknowledgment of the reality of climate crisis at the first climate conference held in Geneva in 1979, the establishment of the Intergovernmental Panel on Climate Change in 1988, the acceptance of the United Nations Framework Convention on Climate Change in 1992 and its entry into force in 1994, the adoption of the Kyoto Protocol in 1997 and its entry into force in 2005, the acceptance of the Paris Agreement in 2015 and its entry into force in 2016, and the signing of the Kigali Amendment in 2016, numerous actions have been undertaken by the international community to combat climate crisis [2]. The United Nations Framework Convention on Climate Change encourages international cooperation to reduce greenhouse gas emissions and adapt to climate change in order to prevent dangerous levels of global warming [44], while the Kyoto Protocol aims for industrialized countries to reduce their greenhouse gas emissions to specific levels [45], the Paris Agreement aims to limit global warming to below 2 °C and preferably to 1.5 °C [46], and the Kigali Amendment aims to reduce the production and use of hydrofluorocarbon greenhouse gases [47].

Many countries have recently made sustainable development a key component of their national policies, strategies, and economic growth plans. Australia and Canada, for example, are leading countries in terms of environmental sustainability because they use fewer natural resources and capital for economic growth [48]. China, on the other hand, is establishing policies to support the green transformation of the maritime economy [49] and reduce energy expenditure [50] through environmental regulations and effective mechanisms. In the UK, the Climate Change Act, which came into force in 2008, was revised in 2019, aiming to reduce greenhouse gas emissions to net zero [51]. Moreover, 193 countries gathered under the framework of the United Nations are obliged to realize the "Sustainable Development Goals" such as climate action, life below water and on land, affordable and clean energy, and responsible consumption and production by 2030. When we look at these goals in terms of climate change, it can be said that they are viewed

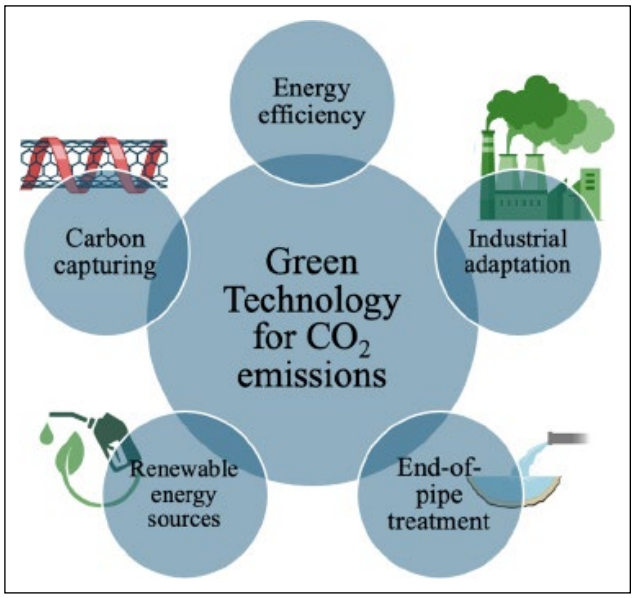


**Figure 2**. Green technology for $CO_2$ emissions.

from the perspectives of reducing carbon emissions, reducing energy consumption, and protecting biodiversity [50, 52]. In this context, controlling or reducing greenhouse gas emissions, especially $CO_2$, and monitoring the emission of greenhouse gases into the atmosphere have become the main focus of all countries [3]. While there are numerous research topics and climate crisis action plans within the realm of positive sciences aimed at reducing carbon emissions, accurately understanding and communicating the climate crisis is also crucial for the implementation and success of these action plans.

Among the efforts to reduce carbon emissions today, carbon capture, utilization, storage, and achieving net-zero carbon emissions have become prominent topics [8]. Reducing the use of fossil fuels and chemicals, which are identified as major contributors to carbon dioxide emissions, and prioritizing the adoption of green and sustainable technologies are among the crucial issues as illustrated in Figure 2.

The necessity to reduce the use of fossil fuels, due to their limited availability and significant environmental damage, is critical for both reducing greenhouse gas emissions and shaping energy security and climate change. Renewable energy sources such as solar, wind, hydroelectric, geothermal, wave, and biomass emerge as sustainable alternative energy sources. The existence of technical and economic challenges in renewable energy sources, leading to their limited adoption, represents the biggest obstacle. However, technological advancements such as the development of renewable energy harvesting devices, fuel cells, and effective carbon capture methods help overcome these limitations. Furthermore, there is a need for new regulations and policies to promote the use of renewable energy sources. Therefore, comprehensive and multidisciplinary efforts in this field have become imperative [53, 54].

For instance, research efforts have gained momentum in recent years on exploring the potential of end-of-pipe treatments [23] such as electrochemical, thermal, biochemical, chemo-enzymatic, and photocatalytic methods for capturing carbon from the atmosphere [55, 56], as well as developing porous materials as $CO_2$ adsorbents [57], advancing liquid absorption $CO_2$ techniques [58], alongside the utilization of renewable energy sources. Also many microorganisms such as plants and algae can naturally absorb $CO_2$ through photosynthesis, converting inorganic carbon in the atmosphere into organic carbon in biomass, thus contributing to the production of high-value-added products [59, 60]. The fundamental objective of every approach is to guarantee a sustainable future and bequeath a clean world as a heritage for future generations.

## The Relationship Between Communication and Climate Change

As atmospheric temperatures continue to rise, it becomes evident that the ecosystem is being affected, new diseases and viruses are emerging, and extreme weather events are becoming more frequent. In light of these developments, the need to address climate change, governments taking urgent action plans, and the necessity of societal transformation have become prominent issues that require effective communication. Although, increase in greenhouse gas emissions are not attributed to a single factor, but rather depends on various factors such as fossil fuels [61], buildings [62], transportation [63] and damage to forest ecosystem. [64] Therefore, complex models are used to understand climate change, as it involves multiple interacting elements. Consequently, predicting both its potential impacts and effectively communicating them to governments and society can be challenging [35, 65]. In this context, climate change communication has emerged as a major field of research and is becoming increasingly important in adopting and implementing a sustainable approach to combat climate change by reducing greenhouse gas emissions and the impacts of climate change [18].

Communication plays a critical role in accurately conveying climate change and its effects, using language-appropriate communication in transmission, and ensuring proper understanding by society. The term language-appropriate communication as defined here can be summarized as accepting, nonjudgmental, empathic, providing personal support, feeling adequacy and turning technical scientific concepts into understandable discussions [66, 67]. The language used in communication appears both as a barrier and a facilitator in understanding global warming and climate change. Before creating awareness in the public for societal transformation regarding the significance of climate change, it is crucial for communication tools conveying them to understand the objectives of climate change correctly and to be influenced correctly by communication tools, which is associated with the power of language used. At this point, scientists have a significant role to play because using informal language will not evoke the expected impact on the public. In this context, collective efforts and statements from scientists, official meetings and organizations, and climate change conferences will be more

effective in creating awareness among both governments and the public than individual statements [68]. Scientists should emphasize that climate change does not have a single solution and is influenced by many factors, using realistic data and engaging language. It is crucial for scientists to communicate the environmental and human consequences of climate change clearly and effectively, while also using frameworks and metaphors that effectively communicate with a wide range of expertise and stakeholders, maintaining a positive and inspiring communication approach [69]. Hence, it is important to have synchronized endeavors between scientists, journalists and social scientists [70].

The relationship between communication and climate change extends beyond language use to encompass its impact on governments, raising awareness in society, and scientific communication. Moreover, it extends to crisis management and emergency planning prompted by climate change. Crisis management in the face of climate change can be delineated into three stages: pre-crisis, crisis, and post-crisis, given the lengthy and complex nature of the process [71]. Public awareness initiatives, identification of potential emergencies, formulation of climate change policies, and enhanced communication among scientists, governments, the public, and civil society organizations all contribute to crisis preparedness. Additionally, organizing training initiatives, workshops, and outreach events to inform and empower individuals for action in their daily lives is essential [72]. Clear communication of the crisis by relevant institutions and organizations during a crisis, coupled with the prompt and effective transmission of solutions, serves to minimize its impact. The importance of an organization's communication with its external environment becomes particularly evident during times of crisis [73, 74]. Similar importance of accurate information flow, public awareness, and collective action in crisis management has been demonstrated during the COVID-19 pandemic [75].

After the first climate conference held in Geneva in 1979, climate change communication began to appear in various communication channels such as newspapers, televisions and journals [2, 76]. Due to the trust instilled by the news media and journals in the public, climate journalism has been important tools in conveying the impacts of climate change. While trust in these media outlets persists in many countries, changes in the media ecosystem, as well as economic and working conditions, have led to challenges for reporters and journalists, and their numbers are decreasing, paving the way for this change [70, 76]. In recent years, with advancements in technology, the more frequent use of visual depictions, various campaigns and the sdesire to reach more target audiences have been conducted using social media platforms such as forums, Instagram, X, and Facebook, as well as online channels, to raise awareness about climate change [77, 78]. Alongside these social media tools, climate information websites on systemic climate risks are playing an increasingly important role in climate change communication [79]. The main difference between news channels and social media lies in the fact that news sources focus on climate policy action and the consequences of climate change, while social media addresses social justice issues surrounding climate change [80]. Mavrodieva et al. [81] reported in their study that social media has an impact on changing public perceptions and can influence the public's political decision-making process. However, it is important to note that the causal relationship between the messages in social media posts and news articles and the public's awareness and intention to participate in climate strike discussions should be examined. This is because while social media can have a positive impact on promoting awareness, social debate on climate change, and raising communication between scientists, the use of bots and unrealistic sharing may also lead to backlash, making it an issue that academics need to research and focus on [76].

Another approach is related to the protest images that are circulated on social media and attract a lot of attention. While such images may have a positive effect on conscious people, they may trigger skepticism, an 'us versus them' approach, and discrimination in others [77]. In contrast, games serve as an additional means of communication for promoting social change. By engaging individuals in various interactive experiences, games can effectively enhance empathy, alleviate skepticism towards scientific knowledge, improve problem-solving abilities, particularly in scientific domains, through the cultivation of critical thinking skills, and encourage environmental protection [82, 83]. The Future Delta game, created to focus on sustainability and climate change, stands as one of the prime examples in this domain. Players assume the role of a leader of a community residing in a delta region, making decisions and developing strategies to tackle the climate crisis. Throughout the game, players are provided with visualizations of climate change effects such as rising sea levels and erosion, along with information on topics like renewable energy, thereby raising awareness among players about these issues [84]. Future Delta and others like it (e.g. Fate of the World and Anno 2070 [85]) allow children to have fun visualizing the climate crisis, learning about environmental sustainability and climate change, and developing environmental awareness and behavioral change.

One of the communication methods in combating climate change can be demonstrated through education and educational programs, and the necessity of initiating sustainability, environmental, and climate change education, especially in early childhood years, is inevitable. The importance of early climate change education, the integration of sustainability education into formal education, and preparing students for climate change were emphasized at the UNESCO Education for Sustainable Development vision [86], The Early Years Learning Framework for Australia [87], and the 28$^{th}$ annual United Nations (UN) Conference of the Parties (COP 28) held in Dubai in December 2023. [88] The growing recognition and regulations surrounding climate change in relation to children may be attributed to the understanding that the education and teachings received during childhood significantly influence their

long-term behavior and attitudes towards the environment. [89] Additionally, children are viewed as potential leaders of change in the future [90]. The importance of integrating communication strategies such as immersion in nature, providing sensory and emotional education, localization, and visualization into education programs for children and youth has been proven in studies [91–93]. Furthermore, the significance of conducting these education programs in an integrated manner with families and communities has also been demonstrated [94].

**Communication Strategies for Raising Awareness About Climate Change**

Climate change communication strategies are crucial for raising awareness of the climate crisis, mobilizing action to mitigate its effects, encouraging participation, and ensuring long-term impact. Therefore, scientists in various fields continue to work on accurately explaining, conveying, and understanding global warming and climate change. For instance, scientists have performed an experiment on the environmental risks of climate change with CLIMEX [95], an experiment on insect distribution in response to climate change based on modeling [96] and bioclimatic distribution modeling, drawing on fields such as environment, nature, and geography [14]. Scientists also draw on fields such as psychology [97] and sociology [98] to examine the impact of the climate crisis on people and societies, perceptions, and attitudes.

One of the requirements for using a multidisciplinary approach in climate change communication strategies is that it is a crisis that concerns every segment of society, from children to the elderly. Since attitudes and behaviors towards climate change, such as energy consumption, vary depending on age, individuals need to share information about sustainability and climate change with each other and learn to address issues in a discussion environment [99]. Youth and adults have the potential to create global resonance with their awareness and impact in the field of climate change. Examples such as the United Nations hosting the 'Youth Climate Summit' in 2019 [100], where young climate advocates aged 18-30 discussed ways to fulfill the Paris Agreement commitments, the Climate Smart Agriculture Youth Network in Africa educating young farmers and agricultural experts on combating climate change [101], Greta Thunberg initiating the 'school strike for climate' in front of the Swedish parliament in 2018 [102], and the school strikes and Fridays for Future movement worldwide since 2018 are prominent illustrations [103]. These examples demonstrate that adults play roles in policy-making and leadership positions, while young people engage in education, awareness-raising, activism, and innovative solutions in the fight against climate change. The elderly may face certain mental and physical health issues related to climate change, leading them to contemplate the struggles of younger generations and consider adopting certain climate crisis action plans aligned with specific political views, shaping their roles in this challenge [104]. A study conducted in the United States in 2018 [105], revealed that while the elderly population tends to be more sensitive to global challenges, the opposite is observed when it comes to issues such as climate change, renewable energy, and environmental policies. This may stem from the lack of inclusion of the elderly in climate change policies, their limited access to information about climate change, and the absence of a sense of responsibility in the fight against it.

At the core of these communication strategies lies the transmission of accurate scientific knowledge and data because the primary goal should be to build trust in the public. Subsequently, different strategies are proposed for how climate change will be presented and what impression will be created among the public, accelerating the process of adapting to climate change, and developing action-oriented plans. Fundamentally, climate change communication strategies involve using various digital and traditional sources to create mass awareness, strengthening the public's empathy, localizing and storytelling to enable individuals to relate climate change to their own lives, using various visualization techniques to provide more concrete and understandable information, and emphasizing hope and opportunity in communication and transmission. While implementing these communication strategies, coordination among scientists, civil society organizations, and governments is necessary.

**Localization**

Climate change is considered an urgent international crisis affecting the entire world; however, due to its impacts on specific communities and environments, it is also regarded as a national and local issue [84]. In the initial awareness campaigns regarding climate change, communication techniques such as emphasizing psychologically distant and continuously unseen effects like glacier melting and omitting details in explaining the effects of climate change have failed to resonate with society. When individuals do not personally witness the tangible effects of climate change, they may not perceive themselves as being threatened, thus they may not change their behavior [106]. Studies indicate that despite living in regions with higher exposure to the effects of climate change, individuals do not change their behavior without experiencing personal damage [107]. For example, Sloggy et al. [30]. reported that in order to increase the proportion of individuals supporting policies to reduce greenhouse gas emissions by one percent, more than one hurricane would have to hit the region where those individuals live. Therefore, it is crucial that communication strategies emphasize the immediate and tangible impacts of climate change that individuals can relate to their daily lives before they experience the disaster. By making the impacts of climate change more relevant and personal, assessing them from the audience's perspective, with end-users as the audience, people are more likely to take action to reduce their impact [108]. For instance, stating “Acid rain harms crops” may not prompt behavioral change, whereas stating "Following acid rain in Izmir as a consequence of climate change, cases of nutrient imbalance and aluminum poisoning were observed in individuals consuming affected crops" could evoke behavioral change. This behavioral change can

be ascribed to the adoption of appropriate, concrete, and localized language in communication. Similarly, Waters et al. [106] observed that climate crisis messages centered in Great Britain were more effective than general climate crisis messages without specific place/region names and increased the public's inclination towards behaviors to reduce energy consumption. Hence, when discussing climate change, it is imperative to emphasize the observable and immediate effects of climate change that will shape individuals' actions and to take into account the cultural and socio-economic background of the intended audience [109].

**Visualization**

Climate visualization is an effective tool for understanding and concretizing the complex models and abstract effects of climate change. The use of visual coding techniques such as color, shape, and location is crucial for making climate change-related data understandable to governments and the public [110]. Alongside visualizing data, integrating various communication methods such as linguistic text, sound, and music will further strengthen this strategy [111]. Comprehensive reviews in the literature have shown that visualizing the effects of climate change through climate visualization tools is more effective and efficient for both the public and governments, enhancing communication between scientists and stakeholders [112].

The communication strategy utilized to raise awareness about climate change is recommended to be integrated with localization, as it has been observed over time that the use of iconic figures such as polar bears, glaciers, and penguins in climate change iconography leads to the perception of climate change crisis as both temporally and spatially distant and of low risk among the Public [84, 113]. For instance, Richards et al. [109] facilitated the examination of the street-level impacts of rising waters while providing sea level rise data using an interactive sea level rise viewer, a map-based visualization tool. This aimed to raise awareness among the public by employing both visualization and localization strategies. Through various studies utilizing interactive sea level rise viewers, communication with society about social and ecological risks through localization and visualization of climate change impacts, transitioning society to a different level of understanding and communication regarding climate change, and evaluating approaches for identifying future risks and creating emergency plans are being assessed [114, 115]. Similarly, Glaas et al. [113] have demonstrated that the visualization of risk maps and the presentation of adaptation measures for local regions using the web-based VisAdapt™ visualization tool effectively emphasize the impacts of climate change and accelerate the adaptation process by influencing individual behaviors through visualizing weather risks. Besides, artistic knowledge visualizations such as news photographs, art visuals, and cartoons can also be utilized as tools for visualizing climate change alongside data, maps, and visualization techniques. However, compared to other visualization tools, the impact of this method is less significant due to artists' freedom in data focus and artistic style choices, but it can still be effective in enhancing public understanding and clarity about climate change when integrated with other methods [116]. This is because it allows the community to perceive climate change from a different perspective beyond scientific explanations in art pieces; however, the excessive emphasis on climate change in artworks may appear distant and abstract to observers, leading them to encounter exaggerated and negative expressions directly [117].

**Storytelling**

Providing accurate and reliable information about climate change through education, conferences, and seminars, while effective, is not sufficient to induce behavioral change in people [118]. In this regard, storytelling comes into play to enhance the society's empathy, raise awareness about climate change, and expedite the process of climate change adaptation, which differs from more quantitative, measurable, and generalizable data formats [119]. This strategy, by combining science and effective communication strategies, can be an effective method to break down the barriers between science and the public. Studies have shown that storytelling can assist in reaching politicians and individuals from the public and making science communication more effective. The underlying reason is that real-life stories and case studies about climate change can create an emotional connection in the public, engage our imagination, and develop sensitivity towards targeted behaviors aimed at reducing the effects of climate change [19, 120]. Additionally, storytelling aims to increase people's access to data, enhance data reading and comprehension, and reduce readers' attention deficits [121]. In an experimental study [122], the effects of a personal radio story narrating the impact of climate change on beloved places of a North Carolina athlete were investigated on moderate and conservative individuals. As a result, it was found that storytelling had positive effects on global warming beliefs and risk perceptions, indicating the usefulness of structuring climate change communications designed to motivate different audiences in the form of stories. Additionally, these effects were mediated by emotional responses such as concern and compassion [122, 123].

Since the main sources in climate change storytelling are articles, surveys, models, and various data analyses, the inevitable need for collaboration between scientists and the art of storytelling arises. This is because conveying the story accurately and effectively is as important as communicating science, selecting which information to convey, and managing uncertainty. However, making climate change data, graphics, models, and scientific language understandable to the public can prevent misinformation in both the media and institutions. In this context, leveraging folklore can be seen as a sensible approach [19, 121]. Particularly, the use of folkloric elements, creating a plot, employing motifs, and better defining actors and settings can trigger empathy and the instinct to take action among the public [119]. Using narrative style and content for climate change storytelling involves defining the target audience, conveying the prob-

lem, its causes, and context specifically and timely, adopting an action perspective, utilizing folkloric features, selecting characters with whom the reader can relate, preferring positive and inspirational communication language, ensuring that risks and human factors are relevant to the topic, and including policy solutions. Instead of providing instructions, climate storytelling should assist individuals in uncovering ways to take action [17, 124].

**Positive and Inspirational Communication**

Since emotions are intertwined with cognitive and motivational processes, the process of perceiving information, making decisions, and changing behavior is influenced by emotions. Similarly, behavior change targeted at climate change can also be guided by emotions [125]. It has been observed that even inadvertently triggering emotional states unrelated to climate change can affect policies aimed at reducing the effects of climate change [126]. The importance of positive emotions is particularly noticeable in the process of decision-making, behavior change, and the generation of action-oriented solutions related to climate change [127]. These positive emotions can also be fostered by creating hopeful messages about climate change, which enhances persuasive impact on society and encourages people to participate in climate change actions. Badullovich et al. [128] demonstrated through their experiment that certain emotions, particularly hope, serve as a fundamental tool between attitudes towards climate change policies and advocacy. Additionally, the positive emotions experienced by society as it begins to take action on climate change can promote participation in climate change actions [127]. Behavior change in climate change is not only important for adults but also for children, and it is crucial to consider that this education should begin in childhood, as it can influence behavior patterns both at this age and in later years. Baker et al. [129] have emphasized the importance of children's climate change education being inspirational, accepting of emotions, and proactive.

Nevertheless, the media language regarding climate change often emphasizes dramatic events and creates a sense of hopelessness. This can undermine interest in the issue of climate change and distance people from its problems and solutions [130]. However, some research suggests that emotions such as pride, fear, and guilt sometimes trigger climate change action, although the connections between emotions and outcomes are complex [131]. In some cases, negative emotions have been found to trigger a correct perception of climate change risks and prompt action, while in other cases, the feeling of fear may have the opposite effect. Similarly, the feeling of hope has been found to trigger action in some cases but may reduce the perception of risk in others [132, 133]. In this regard, it is important to strike a balance between generating both positive and negative emotions, avoiding the suppression of any emotion, and focusing on hopeful solutions to overcome problems while also acknowledging the importance of avoiding unrealistic or overly optimistic perspectives. Additionally, integrating neurophysiological approaches to understand how emotional climate messages influence human emotion and decision-making processes presents a new research avenue [125].

## CONCLUSION

Climate change is the long-term alteration of climate conditions on Earth, primarily associated with the increase in greenhouse gases in the atmosphere, which are mostly human-induced. Due to the acceleration and intensification of the adverse effects caused by climate change in various sectors such as health, agriculture, environment, and tourism, the entire world is facing the threat of a climate crisis. Despite the intensive efforts of scientists, including carbon capture, industrial adaptation, and the use of renewable energy sources, in the fight against climate change, the importance of a multidisciplinary approach is inevitable. In the field of social sciences, the role of communication and different communication strategies is crucial because accurately conveying climate change, which involves complex and scientific language, to diverse communities and governments can be challenging. At this point, the public should both correctly understand climate change and the climate crisis, communities should be empowered, and long-term behavioral changes towards combating climate change and attitudes towards the environment should be instilled in the public. For this, communication strategies such as localization, visualization, storytelling, and the collective use of positive and inspirational language are highly valuable. Communication strategies in climate change have the following objectives: to inform society accurately, to raise awareness about climate change, and to make behavioral change towards sustainability goals permanent in society. This would be possible through the realization and development of various strategy studies for all segments of society, including cultures, languages, genders, and age groups.

In the future, the importance of multidisciplinary studies on climate change will continue to grow. Accessing reliable and accurate information from scientists, along with the importance of reducing the effects of climate change and directing strategies correctly, will make it increasingly critical to communicate and convey these to governments, civil society organizations, and the public. As messages about climate change can reach broader audiences through technological advancements and the prevalence of social media, there will be a greater need to access more information and current news. Establishing correct communication strategies can lead to action-oriented results regarding climate change and foster social and environmental awareness. This situation will require collaboration between the media, scientists, and communication experts to develop effective communication strategies. In the future, climate change communication will not only be limited to information dissemination but will also focus on creating powerful narratives that connect people emotionally to climate change and encourage them to take action, utilizing integrated and balanced communication strategies.

## AUTHORSHIP CONTRIBUTIONS

Authors equally contributed to this work.

## DATA AVAILABILITY STATEMENT

The author confirm that the data that supports the findings of this study are available within the article. Raw data that support the finding of this study are available from the corresponding author, upon reasonable request.

## CONFLICT OF INTEREST

The author declared no potential conflicts of interest with respect to the research, authorship, and/or publication of this article.

## USE OF AI FOR WRITING ASSISTANCE

Not declared.

## ETHICS

There are no ethical issues with the publication of this manuscript.

## REFERENCES


[1] Mikhaylov, N. Moiseev, K. Aleshin, and T. Burkhardt, "Global climate change and greenhouse effect," Entrepreneurship and Sustainability, Vol. 7, pp. 2897–2913, 2020. [CrossRef]

[2] S. Fawzy, A. I. Osman, J. Doran, and D. W. Rooney, "Strategies for mitigation of climate change: a review," Environmental Chemistry Letters, Vol. 18, pp. 2069–2094, 2020. [CrossRef]

[3] Z. Ji, H. Song, L. Lei, M. Sheng, K. Guo, and S. Zhang, "A novel approach for predicting anthropogenic CO2 emissions using machine learning based on clustering of the CO2 concentration," Atmosphere, Vol. 15, Article 323, 2024. [CrossRef]

[4] T. M. Gür, "Carbon dioxide emissions, capture, storage and utilization: review of materials, processes and technologies," Progress in Energy and Combustion Science, Vol. 89, Article 100965, 2022. [CrossRef]

[5] X.-L. Yue and Q.-X. Gao, "Contributions of natural systems and human activity to greenhouse gas emissions," Advances in Climate Change Research, Vol. 9, pp. 243–252, 2018. [CrossRef]

[6] E. Klinenberg, M. Araos, and L. Koslov, "Sociology and the Climate Crisis," Annual Review of Sociology, Vol. 46, pp. 649–669, 2020. [CrossRef]

[7] L. Holappa, "A general vision for reduction of energy consumption and CO2 emissions from the steel industry," Metals, Vol. 10, Article 1117, 2020. [CrossRef]

[8] H. Wang, O. A. Carrasco-Jaim, and R. Okuno, "Aqueous nanobubble dispersion of CO2 in sodium formate solution for enhanced CO2 mineralization using basaltic rocks," CCUS, 1–18. [CrossRef]

[9] C. Barcellos, "Heat waves, climate crisis and adaptation challenges in the global south metropolises," PLOS Climate, Vol. 3, Article e0000367, 2024. [CrossRef]

[10] S. D. Chitre, C. M. Crews, M. T. Tessema, I. Plėštytė-Būtienė, M. Coffee, and E. T. Richardson, "The impact of anthropogenic climate change on pediatric viral diseases," Pediatr. Res., vol. 95, pp. 496–507, 2024. [CrossRef]

[11] J. Ran, N. Chao, L. Yue, G. Chen, Z. Wang, T. Wu, and C. Li, "Quantifying the contribution of temperature, salinity, and climate change to sea level rise in the Pacific Ocean: 2005-2019," Frontiers Marine Science, Vol. 10, Article 1200883, 2023. [CrossRef]

[12] T. Röthig, S. M. Trevathan-Tackett, C. R. Voolstra, C. Ross, S. Chaffron, P. J. Durack, L. M. Warmuth, and M. Sweet, "Human-induced salinity changes impact marine organisms and ecosystems," Global Change Biology, Vol. 29, pp. 4731–4749, 2023. [CrossRef]

[13] Z. Farooq, H. Sjödin, J. C. Semenza, Y. Tozan, M. O. Sewe, J. Wallin, and J. Rocklöv, "European projections of West Nile virus transmission under climate change scenarios," One Health, Vol. 16, Article 100509, 2023. [CrossRef]

[14] T. Walter, "'Heading for Extinction': how the climate and ecological emergency reframes mortality," Mortality, Vol. 28, pp. 661–679, 2023. [CrossRef]

[15] L. Chen, G. Msigwa, M. Yang, A. I. Osman, S. Fawzy, and D. W. Rooney, "Strategies to achieve a carbon neutral society: a review," Vol. 20, pp. 2277–2310, 2022. [CrossRef]

[16] S. Fankhauser, S. M. Smith, M. Allen, K. Axelsson, T. Hale, C. Hepburn, J. M. Kendall, R. Khosla, J. Lezaun, E. Mitchell-Larson, M. Obersteiner, L. Rajamani, R. Rickaby, N. Seddon, and T. Wetzer, "The meaning of net zero and how to get it right," Nature Climate Change, Vol. 12, pp. 15–21, 2022. [CrossRef]

[17] K. D. Meyer, E. Coren, M. McCaffrey, and C. Slean, "Transforming the stories we tell about climate change: from 'issue' to 'action'," Environmental Research Letters, Vol. 16, Article 015002, 2020. [CrossRef]

[18] A. G. Ballantyne, "Climate change communication: what can we learn from communication theory?," WIREs Climate Change, Vol. 7, pp. 329–344, 2016. [CrossRef]

[19] S. Martinez-Conde, and S. L. Macknik, "Finding the plot in science storytelling in hopes of enhancing science communication," Proceedings of the National Academy of Sciences of the United States of America, Vol. 114, pp. 8127–8129, 2017. [CrossRef]

[20] K. Zhang, X. Ma, Y. Li, and S. Shuai, "Exploring NH3 combustion in environments with CO2 and H2O via reactive molecular dynamics," Journal of the Energy Institute, Vol. 114, Article 101606, 2024. [CrossRef]

[21] R. Anderson, P. E. Bayer, and D. Edwards, "Climate change and the need for agricultural adaptation," Current Opinion in Plant Biology, Vol. 56, pp. 197–202, 2020. [CrossRef]

[22] P. Grennfelt, A. Engleryd, M. Forsius, Ø. Hov, H. Rodhe, and E. Cowling, "Acid rain and air pollution: 50 years of progress in environmental science and policy," Ambio, Vol. 49, pp. 849–864, 2020. [CrossRef]

[23] B. Lin, and R. Ma, "Green technology innovations, urban innovation environment and CO2 emission reduction in China: Fresh evidence from a partially linear functional-coefficient panel model," Technological Forecasting and Social Change, Vol. 176, Article 121434, 2022. [CrossRef]

[24] F. Zhou, T. Endendijk, and W. J. W. Botzen, "A review of the financial sector impacts of risks associated with climate change," Annual Review of Resource Economics, Vol. 15, pp. 233–256, 2023. [CrossRef]

[25] K. Ahmed Ali, M. I. Ahmad, and Y. Yusup, "Issues, impacts, and mitigations of carbon dioxide emissions in the building sector," Sustainability, Vol. 12, Article 7427, 2020. [CrossRef]

[26] T.N.-D. Cao, H. Mukhtar, L.-T. Le, D.P.-H. Tran, M.T.T. Ngo, M.-D.-T. Pham, T.-B. Nguyen, T.-K.-Q. Vo, and X.-T. Bui, "Roles of microalgae-based biofertilizer in sustainability of green agriculture and food-water-energy security nexus," Science of The Total Environment, Vol. 870, Article 161927, 2023. [CrossRef]

[27] P. Marcinkowski, and M. Piniewski, "Future changes in crop yield over Poland driven by climate change, increasing atmospheric CO2 and nitrogen stress," Agricultural Systems, Vol. 213, Article 103813, 2024. [CrossRef]

[28] K. M. Gregory, C. Darst, S. M. Lantz, K. Powelson, and C. P. McGowan, "Effects of drought, invasive species, and habitat loss on future extinction risk of two species of imperiled freshwater turtle," Climate Change Ecology, Vol. 7, Article 100078, 2024. [CrossRef]

[29] J. Deng, L. Qiu, M. Xin, W. He, W. Zhao, J. Dong, and G. Xu, "Boosting electrochemical CO2 reduction on copper-based metal-organic frameworks via valence and coordination environment modulation," Small, doi: 10.1002/smll.202311060. [Epub ahead of print] [CrossRef]

[30] M.R. Sloggy, J.F. Suter, M.R. Rad, D.T. Manning, and C. Goemans, "Changing opinions on a changing climate: the effects of natural disasters on public perceptions of climate change," Climatic Change, Vol. 168, Article 25, 2021. [CrossRef]

[31] N. Rees, The Climate Crisis Is a Child Rights Crisis: Introducing the Children's Climate Risk Index, UNICEF, 2021. [Online]. Available: https://eric.ed.gov/?id=ED614506. [Accessed: May 13, 2024].

[32] I. Tsevreni, N. Proutsos, M. Tsevreni, and D. Tigkas, "Generation Z worries, suffers and acts against climate crisis—the potential of sensing children's and young people's eco-anxiety: a critical analysis based on an integrative review," Climate, Vol. 11, Article 171, 2023. [CrossRef]

[33] K. Abbass, M. Z. Qasim, H. Song, M. Murshed, H. Mahmood, I. Younis, "A review of the global climate change impacts, adaptation, and sustainable mitigation measures," Environmental Science and Pollution Research, Vol. 29, pp. 42539–42559, 2022. [CrossRef]

[34] D. P. Tittensor, C. Novaglio, C. S. Harrison, R.F. Heneghan, N. Barrier, D. Bianchi, L. Bopp, A. Bryndum-Buchholz, G.L. Britten, M. Büchner, W.W.L. Cheung, V. Christensen, M. Coll, J. P. Dunne, T. D. Eddy, J. D. Everett, J. A. Fernandes-Salvador, E. A. Fulton, E. D. Galbraith, D. Gascuel, J. Guiet, J. G. John, J. S. Link, H. K. Lotze, O. Maury, K. Ortega-Cisneros, J. Palacios-Abrantes, C. M. Petrik, H. du Pontavice, J. Rault, A. J. Richardson, L. Shannon, Y.-J. Shin, J. Steenbeek, C. A. Stock, and J. L. Blanchard, "Next-generation ensemble projections reveal higher climate risks for marine ecosystems," Nature Climate Change, Vol. 11, pp. 973–981, 2021. [CrossRef]

[35] K. A. Garrett, G. A. Forbes, S. Savary, P. Skelsey, A. H. Sparks, C. Valdivia, A. H. C. van Bruggen, L. Willocquet, A. Djurle, E. Duveiller, H. Eckersten, S. Pande, C. Vera Cruz, and J. Yuen, "Complexity in climate-change impacts: an analytical framework for effects mediated by plant disease," Plant Pathology, Vol. 60, pp. 15–30, 2011. [CrossRef]

[36] B.K. Singh, M. Delgado-Baquerizo, E. Egidi, E. Guirado, J.E. Leach, H. Liu, and P. Trivedi, "Climate change impacts on plant pathogens, food security and paths forward," Nature Reviews Microbiology, Vol. 21, pp. 640–656, 2023. [CrossRef]

[37] P. Soroye, T. Newbold, and J. Kerr, "Climate change contributes to widespread declines among bumble bees across continents," Science, Vol. 367, pp. 685–688, 2020. [CrossRef]

[38] S. Lindsay, S. Hsu, S. Ragunathan, and J. Lindsay, "The impact of climate change related extreme weather events on people with pre-existing disabilities and chronic conditions: a scoping review," Disability and Rehabilitation, Vol. 45, pp. 4338–4358, 2023. [CrossRef]

[39] G. I. Davies, L. McIver, Y. Kim, M. Hashizume, S. Iddings, and V. Chan, "Water-Borne diseases and extreme weather events in cambodia: review of impacts and implications of climate change," International Journal of Environmental Research and Public Health, Vol. 12, pp. 191–213, 2015. [CrossRef]

[40] G. Cissé, "Food-borne and water-borne diseases under climate change in low- and middle-income countries: Further efforts needed for reducing environmental health exposure risks," Acta Tropica, Vol. 194, pp. 181–188, 2019. [CrossRef]

[41] P. J. Edelson, R. Harold, J. Ackelsberg, J. S. Duchin, S. J. Lawrence, Y. C. Manabe, M. Zahn, and R. C. LaRocque, "Climate change and the epidemiology of infectious diseases in the United States," Clinical Infectious Diseases, Vol. 76, pp. 950–956, 2023. [CrossRef]

[42] K.- C. Bergmann, R. Brehler, C. Endler, C. Höflich, S. Kespohl, M. Plaza, M. Raulf, M. Standl, R. Thamm, C. Traidl-Hoffmann, and B. Werchan, "Impact of climate change on allergic diseases in Germany," Journal of Health Monitoring, Vol. 8, pp. 76–102, 2023.

[43] S. Atvur, A.G. Güneş Gülal, and C. Uysal Oğuz, "İklim krizi ve ekolojik bağlamda devletin rolünü yeniden düşünmek," Politik Ekonomik Kuram, Vol. 7, pp. 44–57, 2023. [Turkish] [CrossRef]

[44] J. Ford, M. Maillet, V. Pouliot, T. Meredith, A. Cavanaugh, S. Lwasa, A. Llanos, L. Berrang-Ford, C. Carcamo, D. B. Namanya, S. Harper, and IHACC Research Team, "Adaptation and indigenous peoples in the United Nations framework convention on climate change," Climatic Change, Vol. 139, pp. 429–443, 2016. [CrossRef]

[45] C. Breidenich, D. Magraw, A. Rowley, J. W. Rubin, "The Kyoto protocol to the United Nations framework convention on climate change," American Journal of International Law, Vol. 92, pp. 315–331, 1998. [CrossRef]

[46] A. Savaresi, "The Paris agreement: a new beginning?" Journal of Energy & Natural Resources Law, Vol. 34, pp. 16–26, 2016. [CrossRef]

[47] P. Purohit, N. Borgford-Parnell, Z. Klimont, and L. Höglund-Isaksson, "Achieving Paris climate goals calls for increasing ambition of the Kigali Amendment," Nature Climate Change, Vol. 12, pp. 339–342, 2022.

[48] V. Tawiah, A. Zakari, and R. Alvarado, "Effect of corruption on green growth," Environment, Development and Sustainability, Vol. 26, pp. 10429–10459, 2024. [CrossRef]

[49] J. Sun, N. Zhai, J. Miao, H. Mu, and W. Li, "How do heterogeneous environmental regulations affect the sustainable development of marine green economy? Empirical evidence from China's coastal areas," Ocean & Coastal Management, Vol. 232, Article 106448, 2023. [CrossRef]

[50] L. Xing, E.N. Udemba, M. Tosun, I. Abdallah, and I. Boukhris, "Sustainable development policies of renewable energy and technological innovation toward climate and sustainable development goals," Sustainable Development, Vol. 31, pp. 1178–1192, 2023. [CrossRef]

[51] D. Banister, "The climate crisis and transport," Transport Reviews, Vol. 39, pp. 565–568, 2019. [CrossRef]

[52] THE 17 GOALS | Sustainable Development," United nations, department of economic and social affairs. https://sdgs.un.org/goals. [Accessed: May 13, 2024].

[53] A.G. Olabi, M.A. Abdelkareem, "Renewable energy and climate change," Renewable and Sustainable Energy Reviews, vol. 158, 2022, p. 112111. [CrossRef]

[54] P.A. Owusu, and S. Asumadu-Sarkodie, "A review of renewable energy sources, sustainability issues and climate change mitigation," Cogent Engineering, Vol. 3, Article 1167990, 2016. [CrossRef]

[55] T. Fatima, U. Shahzad, L. Cui, "Renewable and nonrenewable energy consumption, trade and CO2 emissions in high emitter countries: does the income level matter?" Journal of Environmental Planning and Management, Vol. 64, pp. 1227–1251, 2021. [CrossRef]

[56] A. Saravanan, P. Senthil Kumar, D.-V.N. Vo, S. Jeevanantham, V. Bhuvaneswari, V. Anantha Narayanan, P.R. Yaashikaa, S. Swetha, B. Reshma, "A comprehensive review on different approaches for CO2 utilization and conversion pathways," Chemical Engineering Science, Vol. 236, Article 116515, 2021. [CrossRef]

[57] S. Kumar, R. Srivastava, J. Koh, "Utilization of zeolites as CO2 capturing agents: Advances and future perspectives," Journal of CO2 Utilization, Vol. 41, Article 101251, 2020. [CrossRef]

[58] F. O. Ochedi, J. Yu, H. Yu, Y. Liu, and A. Hussain, "Carbon dioxide capture using liquid absorption methods: a review," Environmental Chemistry Letters, Vol. 19, pp. 77–109, 2021. [CrossRef]

[59] M. G. de Morais, E. G. de Morais, J. H. Duarte, K. M. Deamici, B. G. Mitchell, and J. A. V. Costa, "Biological CO2 mitigation by microalgae: technological trends, future prospects and challenges," World Journal of Microbiology and Biotechnology, Vol. 35, Article 78, 2019. [CrossRef]

[60] H. Salehizadeh, N. Yan, and R. Farnood, "Recent advances in microbial CO2 fixation and conversion to value-added products," Chemical Engineering Journal, Vol. 390, Article 124584, 2020. [CrossRef]

[61] M. D. Staples, R. Malina, and S. R. H. Barrett, "The limits of bioenergy for mitigating global life-cycle greenhouse gas emissions from fossil fuels," Nature Energy, Vol. 2, pp. 1–8, 2017. [CrossRef]

[62] R. Hingorani, N. Dittrich, J. Köhler, and D. B. Müller, "Embodied greenhouse gas emissions in structural materials for the German residential building stock — Quantification and mitigation scenarios," Building and Environment, Vol. 245, Article 110830, 2023. [CrossRef]

[63] D. L. Bleviss, "Transportation is critical to reducing greenhouse gas emissions in the United States," WIREs Energy and Environment, Vol. 10, Article e390, 2021. [CrossRef]

[64] R. K. Shrestha, B. D. Strahm, and E. B. Sucre, "Greenhouse gas emissions in response to nitrogen fertilization in managed forest ecosystems," New Forests, Vol. 46, pp. 167–193, 2015. [CrossRef]

[65] T. Balint, F. Lamperti, A. Mandel, M. Napoletano, A. Roventini, A. Sapio, "Complexity and the economics of climate change: A survey and a look forward," Ecological Economics, Vol. 138, pp. 252–265, 2017. [CrossRef]

[66] G. L. Forward, K. Czech, C. M. Lee, "Assessing Gibb's supportive and defensive communication climate: An examination of measurement and construct validity," Communication Research Reports, Vol. 28, pp. 1–15, 2011. [CrossRef]

[67] A. Kluczkovski, R. Lait, C. A. Martins, C. Reynolds, P. Smith, Z. Woffenden, J. Lynch, A. Frankowska, F. Harris, D. Johnson, J. C. G. Halford, J. Cook, J. Tereza da Silva, X. Schmidt Rivera, J. L. Huppert, M. Lord, J. Mclaughlin, and S. Bridle, "Learning in lockdown: Using the COVID-19 crisis to teach children about food and climate change," Nutrition Bulletin, Vol. 46, pp. 206–215, 2021. [CrossRef]

[68] R. Marschan-Piekkari, D. Welch, and L. Welch, "In the shadow: the impact of language on structure, power and communication in the multinational," International Business Review, Vol. 8, pp. 421–440, 1999. [CrossRef]

[69] C. Kueffer, and B. M. H. Larson, "Responsible use of language in scientific writing and science communication," BioScience, Vol. 64, pp. 719–724, 2014. [CrossRef]

[70] B. Nerlich, N. Koteyko, and B. Brown, "Theory and language of climate change communication," WIREs Climate Change, Vol. 1, pp. 97–110, 2010. [CrossRef]

[71] M.L. Ruiu, M. Ragnedda, and G. Ruiu, "Similarities and differences in managing the Covid-19 crisis and climate change risk," Journal of Knowledge Management, Vol. 24, pp. 2597–2614, 2020. [CrossRef]

[72] K. Günay, and Y. Güçdemir, "Topic modeling analysis of NGO's twitter postings between 2020- 2021 in Turkey within the context of climate change communication," TOJDAC, Vol. 12, pp. 1026–1045, 2022. [CrossRef]

[73] M.E. Civelek, M. Çemberci, and N.E. Eralp, "The Role of Social Media in Crisis Communication and Crisis Management," (2016). https://papers.ssrn.com/abstract=3338292. [Accessed: Mar. 17, 2024].

[74] Y. Cheng, "How social media ıs changing crisis communication strategies: Evidence from the updated literature," Journal of Contingencies and Crisis Management, Vol. 26, pp. 58–68, 2018. [CrossRef]

[75] M. C. J. Stoddart, H. Ramos, K. Foster, and T. Ylä-Anttila, "Competing crises? Media coverage and framing of climate change during the COVID-19 pandemic," Environmental Communication, Vol. 17, pp. 276–292, 2013. [CrossRef]

[76] M. S. Schäfer, and J. Painter, "Climate journalism in a changing media ecosystem: Assessing the production of climate change-related news around the world," WIREs Climate Change, Vol. 12, Article e675, 2021. [CrossRef]

[77] A. Mooseder, C. Brantner, R. Zamith, and J. Pfeffer, "(Social) Media Logics and Visualizing Climate Change: 10 Years of #climatechange Images on Twitter," Social Media + Society, Vol. 9, Article 20563051231164310, 2023. [CrossRef]

[78] W. Pearce, S. Niederer, S. M. Özkula, and N. Sánchez Querubín, "The social media life of climate change: Platforms, publics, and future imaginaries," WIREs Climate Change, Vol. 10, Article e569, 2019. [CrossRef]

[79] B. Hewitson, K. Waagsaether, J. Wohland, K. Kloppers, and T. Kara, "Climate information websites: an evolving landscape," WIREs Climate Change, Vol. 8, Article e470, 2017. [CrossRef]

[80] K. Chen, A. L. Molder, Z. Duan, S. Boulianne, C. Eckart, P. Mallari, and D. Yang, "How climate movement actors and news media frame climate change and strike: Evidence from analyzing twitter and news media discourse from 2018 to 2021," The International Journal of Press/Politics, Vol. 28, pp. 384–413, 2023. [CrossRef]

[81] A. V. Mavrodieva, O. K. Rachman, V. B. Harahap, and R. Shaw, "Role of social media as a soft power tool in raising public awareness and engagement in addressing climate change," Climate, Vol. 7, Article 122, 2019. [CrossRef]

[82] D. B. Dhiman, "Games as tools for social change communication: A critical review," (2023). [Online]. https://papers.ssrn.com/abstract=4401202. [Accessed: Mar. 17, 2024].

[83] J. S. Wu, and J. J. Lee, "Climate change games as tools for education and engagement," Nature Climate Change, Vol. 5, pp. 413–418, 2015. [CrossRef]

[84] O. Schroth, J. Angel, S. Sheppard, and A. Dulic, "Visual climate change communication: From ıconography to locally framed 3D visualization," Environmental Communication, Vol. 8, pp. 413–432, 2014. [CrossRef]

[85] B. J. Abraham, and D. Jayemanne, "Where are all the climate change games? Locating digital games' response to climate change," (2017). https://opus.lib.uts.edu.au/handle/10453/121664. [Accessed: Apr. 22, 2024].

[86] M. M. Catana, and J. B. Brilha, "The role of UNESCO global geoparks in promoting geosciences education for sustainability," Geoheritage, Vol. 12, Article 1, 2020. [CrossRef]

[87] S. Cheeseman, J. Sumsion, and F. Press, "Infants of the knowledge economy: the ambition of the Australian Government's early years learning framework," Pedagogy, Culture & Society, Vol. 22, pp. 405–424, 2014. [CrossRef]

[88] G. Kidman, and C.-H. Chang, "Sustainability education: meeting the demands of climate change aspirations," International Research in Geographical and Environmental Education, Vol. 33, pp. 1–5, 2024. [CrossRef]

[89] E. R. Hahn, and M. K. Garrett, "Preschoolers' moral judgments of environmental harm and the influence of perspective taking," Journal of Environmental Psychology, Vol. 53, pp. 11–19, 2017. [CrossRef]

[90] R. Raby, and L. C. Sheppard, "Constructs of childhood, generation and heroism in editorials on young people's climate change activism: Their mobilisation and effects," Children & Society, Vol. 35, pp. 380–394, 2021. [CrossRef]

[91] B. C. Beaver, and L. A. Borgerding, "Climate change education in early childhood classrooms: A nature-based approach," International Journal of Early Childhood Environmental Education, Vol. 11, pp. 3–19, 2023.

[92] A. C. Rule, and K. S. Zhbanova, "Guardians of the earth: Teaching children to care for all living things," in: M. Renck Jalongo, Ed., Teaching Compassion: Humane Education in Early Childhood, Springer Netherlands, Dordrecht, pp. 197–211, 2014. [CrossRef]

[93] T. Rooney, "Weather worlding: learning with the elements in early childhood," Environmental Education Research, Vol. 24, pp. 1–12, 2018. [CrossRef]

[94] Z. Mintoff, P. Andersen, J. Warren, S. Elliott, C. Nicholson, H. Byfield-Fleming, and F. Barber, "The effectiveness of a community-based playgroup in ınspiring positive changes in the environmental attitudes and behaviours of children and their parents: A qualitative case study," Australian Journal of Environmental Education, Vol. 40, pp. 22–34, 2024. [CrossRef]

[95] J. Poutsma, A. J. M. Loomans, B. Aukema, and T. Heijerman, "Predicting the potential geographical distribution of the harlequin ladybird, Harmonia axyridis, using the CLIMEX model," in: H.E. Roy, E. Wajnberg, Eds., From Biological Control to Invasion: The Ladybird Harmonia Axyridis as a Model Species, Springer Netherlands, Dordrecht, pp. 103–125, 2008. [CrossRef]

[96] J.-M. Jung, W.-H. Lee, and S. Jung, "Insect distribution in response to climate change based on a model: Review of function and use of CLIMEX," Entomological Research, Vol. 46, pp. 223–235, 2016. [CrossRef]

[97] G.N. Somero, "The physiology of climate change: how potentials for acclimatization and genetic adaptation will determine 'winners' and 'losers,'" Journal of Experimental Biology, vol. 213, 2010, pp. 912–920. [CrossRef]

[98] T. Dietz, R. L. Shwom, and C. T. Whitley, "Climate change and society," Annual Review of Sociology, Vol. 46, pp. 135–158, 2020. [CrossRef]

[99] L. Ayalon, S. Roy, O. Aloni, and N. Keating, "A scoping review of research on older people and intergenerational relations in the context of climate change," The Gerontologist, Vol. 63, pp. 945–958, 2023. [CrossRef]

[100] H. Han, and S. W. Ahn, "Youth mobilization to stop global climate change: narratives and impact," Sustainability, Vol. 12, Article 4127, 2020. [CrossRef]

[101] C. Mungai, T. Muchaba, L. Szilagyi, M. A. O. Radeny, V. Atakos, and D. Ntiokam, "Youth engagement in climate-smart agriculture in Africa: Opportunities and challenges," 2018. https://hdl.handle.net/10568/92979. [Accessed: Apr. 21, 2024].

[102] A. Sabherwal, M. T. Ballew, S. van der Linden, A. Gustafson, M. H. Goldberg, E. W. Maibach, J. E. Kotcher, J. K. Swim, S. A. Rosenthal, and A. Leiserowitz, "The Greta Thunberg Effect: Familiarity with Greta Thunberg predicts intentions to engage in climate activism in the United States," Journal of Applied Social Psychology, Vol. 51, pp. 321–333, 2021. [CrossRef]

[103] K. Sporre, "Young people – citizens in times of climate change? A childist approach to human responsibility," HTS Teologiese Studies / Theological Studies, Vol. 77, pp. 1–8, 2021. [CrossRef]

[104] H. Frumkin, L. Fried, and R. Moody, "Aging, climate change, and legacy thinking," The American Journal of Public Health, Vol. 102, pp. 1434–1438, 2012. [CrossRef]

[105] M. A. Andor, C. M. Schmidt, and S. Sommer, "Climate change, population ageing and public spending: Evidence on ındividual preferences," Ecological Economics, Vol. 151, pp. 173–183, 2018. [CrossRef]

[106] Y. L. Waters, K. A. Wilson, and A. J. Dean, "The role of iconic places, collective efficacy, and negative emotions in climate change communication," Environmental Science & Policy, Vol. 151, Article 103635, 2024. [CrossRef]

[107] P. Lujala, H. Lein, and J. K. Rød, "Climate change, natural hazards, and risk perception: the role of proximity and personal experience," Local Environment, Vol. 20, pp. 489–509, 2015. [CrossRef]

[108] J. Kiwanuka-Tondo, and K. M. Pettiway, "Localizing complex scientific communication: a SWOT analysis and multi-sectoral approach of communicating climate change," Communication Design Quarterly Review, Vol. 4, pp. 74–85, 2017. [CrossRef]

[109] D. P. Richards, "Not a cape, but a life preserver: the importance of designer localization in interactive sea level rise viewers," Communication Design Quarterly Review, Vol. 6, pp. 57–69, 2018. [CrossRef]

[110] J. D. Walker, B. H. Letcher, K. D. Rodgers, C. C. Muhlfeld, and V. S. D'Angelo, "An ınteractive data visualization framework for exploring geospatial environmental datasets and model predictions," Water, Vol. 12, Article 2928, 2020. [CrossRef]

[111] A. G. Ballantyne, E. Glaas, T.- S. Neset, and V. Wibeck, "Localizing climate change: Nordic homeowners' ınterpretations of visual representations for climate adaptation," Environmental Communication, Vol. 12, pp. 638–652, 2018. [CrossRef]

[112] S. Lumley, R. Sieber, and R. Roth, "A framework and comparative analysis of web-based climate change visualization tools," Computers & Graphics, Vol. 103, pp. 19–30, 2022. [CrossRef]

[113] E. Glaas, A. Gammelgaard Ballantyne, T.-S. Neset, B.-O. Linnér, C. Navarra, J. Johansson, T. Opach, J. K. Rød, and M. E. Goodsite, "Facilitating climate change adaptation through communication: Insights from the development of a visualization tool," Energy Research & Social Science, Vol. 10, 2015, pp. 57–61. [CrossRef]

[114] S. H. Stephens, D. E. DeLorme, and S. C. Hagen, "Evaluation of the design features of interactive sea-level rise viewers for risk communication," Environmental Communication, Vol. 11, pp. 248–262, 2017. [CrossRef]

[115] R. E. Roth, C. Quinn, and D. Hart, "The competitive analysis method for evaluating water level visualization Tools," in: J. Brus, A. Vondrakova, V. Vozenilek, Eds., Modern Trends in Cartography: Selected Papers of CARTOCON 2014, Springer International Publishing, Cham, pp. 241–256, 2015. [CrossRef]

[116] U. Hahn, and P. Berkers, "Visualizing climate change: an exploratory study of the effectiveness of artistic information visualizations," World Art, Vol. 11, pp. 95–119, 2021. [CrossRef]

[117] R. Aydın, and M. Demirbaş, "21. yüzyılın en büyük tehdidi: Küresel iklim değişikliği," NWSA, Vol. 15, pp. 163–179, 2020. [Turkish] [CrossRef]
[118] S. C. Moser, "More bad news: The risk of neglecting emotional responses to climate change information," in: Creating a Climate for Change: Communicating Climate Change and Facilitating Social Change, Cambridge University Press, New York, NY, US, pp. 64–80, 2007. [CrossRef]
[119] M. Moezzi, K. B. Janda, and S. Rotmann, "Using stories, narratives, and storytelling in energy and climate change research," Energy Research & Social Science, Vol. 31, pp. 1–10, 2017. [CrossRef]
[120] E. F. Bloomfield, and C. Manktelow, "Climate communication and storytelling," Climatic Change, Vol. 167, Article 34, 2021. [CrossRef]
[121] C. Fish, "Storytelling for making cartographic design decisions for climate change communication in the United States," Cartographica, Vol. 55, pp. 69–84, 2020. [CrossRef]
[122] A. Gustafson, M. T. Ballew, M. H. Goldberg, M. J. Cutler, S. A. Rosenthal, and A. Leiserowitz, "Personal stories can shift climate change beliefs and risk perceptions: The mediating role of emotion," Communication Reports, Vol. 33, pp. 121–135, 2020. [CrossRef]
[123] B. S. Morris, P. Chrysochou, J. D. Christensen, J. L. Orquin, J. Barraza, P. J. Zak, and P. Mitkidis, "Stories vs. facts: triggering emotion and action-taking on climate change," Climatic Change, Vol. 154, pp. 19–36, 2019. [CrossRef]
[124] M. D. Jones, and H. Peterson, "Narrative persuasion and storytelling as climate communication strategies," in: Oxford Research Encyclopedia of Climate Science, 2017. [CrossRef]
[125] T. Brosch, "Affect and emotions as drivers of climate change perception and action: a review," Current Opinion in Behavioral Sciences, Vol. 42, pp. 15–21, 2021. [CrossRef]
[126] H. Lu, and J. P. Schuldt, "Exploring the role of incidental emotions in support for climate change policy," Climatic Change, Vol. 131, pp. 719–726, 2015.
[127] C. R. Schneider, L. Zaval, and E. M. Markowitz, "Positive emotions and climate change," Current Opinion in Behavioral Sciences, Vol. 42, pp. 114–120, 2021. [CrossRef]
[128] N. Badullovich, W. J. Grant, and R. M. Colvin, "Framing climate change for effective communication: a systematic map," Environmental Research Letters, Vol. 15, 2020, Article 123002, 2020. [CrossRef]
[129] C. Baker, S. Clayton, and E. Bragg, "Educating for resilience: parent and teacher perceptions of children's emotional needs in response to climate change," Environmental Education Research, Vol. 27, pp. 687–705, 2021. [CrossRef]
[130] L. Feldman, and P. S. Hart, "Is there any hope? How climate change news ımagery and text ınfluence audience emotions and support for climate mitigation policies," Risk Analysis, Vol. 38, pp. 585–602, 2018. [CrossRef]
[131] M. J. Bissing-Olson, K. S. Fielding, and A. Iyer, "Experiences of pride, not guilt, predict pro-environmental behavior when pro-environmental descriptive norms are more positive," Journal of Environmental Psychology, Vol. 45, pp. 145–153, 2016. [CrossRef]
[132] S. Wang, Z. Leviston, M. Hurlstone, C. Lawrence, and I. Walker, "Emotions predict policy support: Why it matters how people feel about climate change," Global Environmental Change, Vol. 50, pp. 25–40, 2018. [CrossRef]
[133] H. Bilandzic, A. Kalch, and J. Soentgen, "Effects of goal framing and emotions on perceived threat and willingness to sacrifice for climate change," Science Communication, Vol. 39, pp. 466–491, 2017. [CrossRef]

*Environ Res Tec, Vol. 7, Issue. 3, pp. 471–488, September 2024*

**Environmental Research and Technology**
https://ert.yildiz.edu.tr - https://dergipark.org.tr/tr/pub/ert
DOI: https://10.35208/ert.1433696

Environmental Research & Technology

**Review Article**

# Assessment of heavy metal contamination in the groundwater of Gujarat, India using the Heavy Metal Pollution Index

**Mukesh CHAUDHARI, Ritu CHOTALIYA, GH ALI, Ajay PANDYA, Pranav SHRIVASTAV***

*Department of Chemistry, Gujarat University School of Sciences, Navrangpura, Gujarat, India*

## ARTICLE INFO

*Article history*
Received: 08 February 2024
Revised: 03 April 2024
Accepted: 16 April 2024

**Key words:**
Groundwater; Gujarat; Heavy metal ion contamination; Heavy metal pollution index; Removal technologies

## ABSTRACT

Groundwater serves as a vital water source for a significant population in the Gujarat region of India. However, substantial contamination from heavy metals, pose a serious threat to human health through various pathways, including drinking water. The rapid industrial and agricultural growth in recent years has exacerbated heavy metal pollution in the state. This study focuses on assessing the heavy metal contamination in the groundwater of Gujarat using the Heavy Metal Pollution Index (HPI). The research covers the entire state, considering its diverse physical, climatic, topographical, and geographical conditions. The HPI scores obtained from individual studies highlight the extent of pollution caused by heavy metals. The overall findings underscore the severe problem of heavy metal contamination in Gujarat's groundwater and the associated health risks. Various other pollution indicators, including the Heavy Metal Evaluation Index, Degree of Contamination, Metal Index, and Water Pollution Index are discussed as tools to assess contamination levels. These indices compare concentrations of different heavy metals with established limits to determine the pollution level. The goal is to provide valuable insights for investors and policymakers in formulating strategies to manage and reduce heavy metal contamination across the state. Additionally, the paper explores effective, environmentally friendly, and economically viable treatment techniques to remove heavy metals from aquatic systems, safeguarding the environment. By employing pollution indicators and remedial actions, this study aims to guide efforts in mitigating the impact of heavy metal contamination in the groundwater of Gujarat.

**Cite this article as:** Chaudhari M, Chotaliya R, Ali GH, Pandya A, Shrivastav P. Assessment of heavy metal contamination in the groundwater of Gujarat, India using the Heavy Metal Pollution Index. Environ Res Tec 2024;7(3)471–488.

## INTRODUCTION

The quality and accessibility of water sources are crucial for the survival of all living organisms, including humans, and the well-being of the environment. However, these invaluable resources are susceptible to contamination by both organic and inorganic pollutants, compromising water purity and its suitability for sustaining life [1, 2]. In India, a significant portion of the population relies on groundwater for daily needs, with approximately one-third of the country's groundwater being unsuitable for human consumption [3]. Groundwater pollution, particularly from heavy metals, stands as a critical environmental challenge due to the highly toxic nature of these contaminants, even at low concentrations. The word "heavy metal" refers to a broad category of metals and metalloids having an atomic density of more than 4,000 kg/m$^3$, or five times that of water [4]. These elements exist in water in various forms, including colloidal, particulate, and dispersed segments, with their presence being either natural or anthropogenic [5]. Cu, Cd, Zn, Pb, Hg, As, Ag, Cr, Fe and Pt are some examples of heavy metals. The human body can be exposed to these toxic elements through

***Corresponding author.**
*E-mail address: pranav_shrivastav@yahoo.com

multiple pathways, such as direct ingestion, dermal contact, inhalation, and oral ingestion, with drinking water serving as a primary source for the entry of heavy metals into the human body [3, 6]. The introduction of these toxic elements into water sources occurs regularly from both natural and human-induced sources. In numerous locations globally, the levels of Cr, Mn, Fe, Co, Ni, As, and Cd in surface water exceed permissible values for drinking water, raising widespread concerns. Heavy metals do not break down easily, leading to bioaccumulation in organisms over time. Their persistent nature, coupled with biomagnification, can have detrimental effects on various organisms. Many heavy metal ions are known carcinogens and pose risks to organs such as the respiratory system, urinary tract, liver, prostate, stomach, digestive system, skin, as well as contributing to neurodegenerative conditions like Alzheimer and Parkinson [7].

Gujarat exhibits distinctive geographical features and considerable variability in annual rainfall. The rocky terrain and coastal areas render three-fourths of the state unsuitable for groundwater extraction. Additionally, historical instances of droughts have been prevalent due to limited surface water availability. The state encounters unpredictable and uneven rainfall patterns, leading to disparities in water distribution across regions. Despite having only 5% of the nation's population, Gujarat possesses merely 2% of the country's water resources [8]. Notably, both the industrial and agricultural sectors in Gujarat have undergone rapid expansion. However, the surge in heavy metal pollution poses significant risks to public health, with policymakers yet to address this pressing environmental concern. Although there is a lack of comprehensive scientific investigations into heavy metal contamination in the groundwater of Gujarat, several studies have assessed the groundwater quality for heavy metals across multiple regions in the state [9–12].

This study aimed to assess the groundwater quality in Gujarat, focusing on the presence of heavy metal contamination. The research outlines the primary sources of heavy metals in water and discusses their potential impacts on human health. Additionally, the study explores various methods for eliminating heavy metals from water. Consequently, the review provides evidence regarding the prevalence of heavy metals in the groundwater of Gujarat and its implications for safeguarding human health.

## MATERIALS AND METHODS

### Data Collection

We identified 14 research articles, conference papers, and scientific studies focusing on surface and groundwater bodies in Gujarat, India, spanning from 2007 to 2024. These publications are accessible through Web of Science, Science Direct, Google Scholar, ResearchGate, and PubMed. Our search targeted terms like "heavy metals pollution," "surface water," "groundwater," "pollution index," and "Gujarat," as these platforms primarily utilize English for broader international dissemination. We did not include some local databases or publications that solely report heavy metal concentration levels without additional applications.

### Study Area

The Indian state of Gujarat (1,96,024 $km^2$) is situated between the longitudes of 68° 10' 00" and 74° 28' 00" in the east and the latitudes of 20° 06' 00" to 24° 42' 00" in the north. Gujarat has the longest coastline in the country, spanning approximately 1600 km from Daman in the south to Lakhpat in the north, surpassing all other states in India. The state of Gujarat opens international borders in the northwest with Pakistan as well as shared borders with the states of Rajasthan, Madhya Pradesh, and Maharashtra. The Union territory of Daman & Diu covers 106 $km^2$ area which is included in Gujarat. Different regions of the state exhibit distinct groundwater conditions because of diverse physiography, climate, topography, and geology. Groundwater presence and movement are influenced by a range of rock formations with varying compositions and structures, spanning from the Archean to Recent eras. Similarly, the landforms vary, encompassing hilly tracts, uplands in Kachchh and Saurashtra, alluvial plains from Banaskantha in the north to Valsad in the south, low-lying coastal areas surrounding the uplands of Kachchh and Saurashtra, and marshy to saline areas like the Rann of Kachchh and Little Rann of Kachchh. The climate across the state also exhibits diversity, transitioning from a humid climate in the south to sub-humid in the centre and further to semi-arid and arid conditions in the north and west. Due to insufficient and unpredictable rainfall, droughts are a frequent occurrence in the northern Gujarat, Saurashtra, and Kachchh regions [13, 14]. Figure 1 shows the regions studied up till now for heavy metal ion pollution in the state of Gujarat.

### Hydro-Geological Setup of Study Area

According to geological formation, Gujarat offers a diverse range of rock types with varying ages, ranging from unconsolidated alluvial and sandy gravel that is only a few thousand years old in the central and western parts of the state to 2500 million years old in the north-eastern region. The state contains metamorphic rocks, igneous rocks, and sedimentary rocks of every type. Gujarat's geology is made up of younger rocks from the Mesozoic (Jurassic and Cretaceous), Tertiary, and Quaternary deposited over a Precambrian basement. However, there are no rocks from the Palaeozoic era. Deccan basalt covers the majority of Saurashtra, a small portion of Kachchh, and the majority of South Gujarat, with numerous locations having stepping in Cretaceous and Tertiary rocks [13]. Different groundwater conditions have emerged in the state because of the state's varied topography. Gneisses, schists, phyllites, intrusive, medium- to coarse-grained sandstones, basalts, and recent alluvium are among the rock formations with ages ranging from the Archaean to the recent. There is not much groundwater potential in the high relief area in the eastern and north-eastern part occupied by the Archaean and Deccan Trap due to the steep gradient that allows for high runoff. The yield of wells in these formations ranges from 5 to 10 $m^3/h$, while that of wells tapping quaternary alluvium in the Cambay basin ranges from 75 to 150 $m^3/h$ and that of sandstones from 50 to 170 $m^3/h$. Due to excessive withdrawal, the top aquifer among the five main ones in alluvial sediments has begun to dry up. Almost the

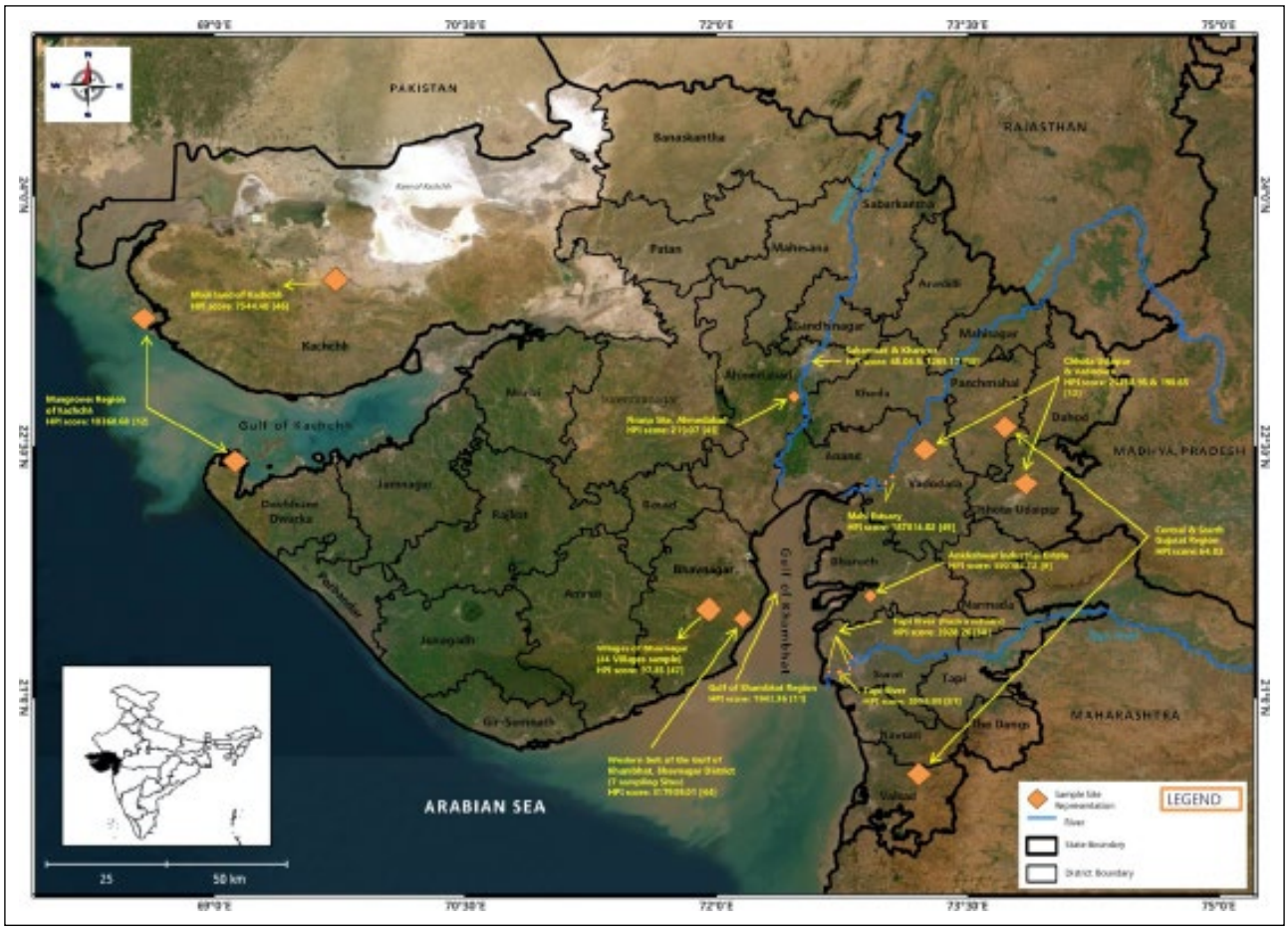


**Figure 1**. Map showing the regions studied for heavy metal ion pollution in the state of Gujarat.

entire Saurashtra and Kachchh areas are covered in a variety of hard and fissured formations that include basalt and consolidated sedimentary formations in addition to semi consolidated sediments, improving the low-lying coastal zones. Both the irregular aquifers created by the compact and fissured rocks and the aquifer created by the friable semi-consolidated sandstone have a moderate yield potential [14].

**Sources of Heavy Metals in Groundwater**

Contamination with heavy metals in water sources is now recognised as a major worldwide threat to the environment, endangering aquatic ecosystems as well as human wellness. Due to industrialization, climate change, and urbanisation, pollution from heavy metals in water bodies is on the rise. Mining waste, landfill leachates, municipal and industrial wastewater, urban runoff, and natural occurrences such as eruptions of volcanoes, weathering, and rock abrasion are all pollution sources [15]. Heavy metals can be identified in organic matrices in different forms, including hydroxides, oxides, sulphides, sulphates, phosphates, silicates, and carbonates. They come from both anthropogenic and natural sources [16].

**Natural Sources**

The concentration of ions in groundwater and its quality are influenced by natural factors such as local geology, weathering rates, rock-water interactions during recharge, and groundwater flow characteristics [17, 18]. Volcanic eruptions, a natural occurrence, release particles and ash into the atmosphere, often containing heavy metals. These metals can be washed into the environment during rain and transported over distances. Volcanic ash, a byproduct of eruptions, contains impurities like Pb, Zn, Cu, Cd, Cr, Fe, and Al [16]. While geogenic sources typically have lower heavy metal concentrations within the acceptable ranges set by local or international protecting environment agencies, the collision of volcanic rocks with water is a geogenic source of metals like As, B, Fe, Pb, Zn, and Cu [18]. Heavy metals can manifest in various forms like sulphates, hydroxides, oxides, sulphides, phosphates, and silicates [19].

Dissolved ions in groundwater and surface water primarily come from the weathering and dissolution of silicate, carbonate, sulphide minerals, and evaporates [18, 20]. The speed of mineral weathering is influenced by factors such as climate and chemical composition, with silicates and carbonates generally reacting more slowly than sulphides [18, 21]. Soils with significant heavy metal content may have natural sources from the weathering of the bedrock beneath them. Heavy metals can be obtained from rocks as minerals, appearing as ores in different chemical states, including sulphides and oxides [6]. Mining and ore processing contribute to heavy metal presence in surface water through water-intensive ore processing and potential contamination from mine effluent discharges and waste rock reservoirs [22].

The connection between surface water and groundwater poses a risk of groundwater pollution, as chemicals from sewage and ores can travel through soil fragments via gravitational processes and end up in groundwater [23].

**Anthropogenic Sources**

Numerous human activities contribute to the introduction of heavy metals into the environment. The main anthropogenic activities include the production and transportation of energy sources, manufacturing of microelectronic devices, waste disposal, and metallurgical processes such as mining, smelting, and metal finishing. Additionally, heavy metals from fertilizers, livestock waste, and pesticides are commonly utilized in agricultural practices. The details of these anthropogenic sources are elaborated below.

### Mining and Mineral Exploration

Mining stands out as one of the most perilous human endeavours globally, despite its numerous societal benefits. The various stages of mineral extraction, such as grinding, concentrating ores, and disposing of residues, along with mine and mill water runoff, contribute significantly to soil pollution [24]. Ore deposits often contain metals in low concentrations, leading to the generation of substantial amounts of waste rock during extraction. These waste rocks retain heavy metal residues from the ore-bearing rock and are typically deposited in mine tailings or rock spoils. In cases involving pyrite, exposure to oxidizing environmental conditions in the tailings can result in the formation of acid mine drainage, mobilizing heavy metals due to the acidic conditions. The disposal of waste rock in tailings or rock spoils can lead to the leaching of heavy metals, posing environmental and health risks through water consumption, respiration, and the consumption of crops grown in soils influenced by irrigation with contaminated water [25]. Additionally, mineral processing activities, including leaching from ore and tailings stockpiles, as well as extraction methods that involve size reduction, can intensify heavy metal contamination by increasing the contact area for mass conversion [26].

### Agricultural Route

Agricultural activities have been identified as a significant contributor to groundwater pollution, primarily due to the use of pesticides and fertilizers that release substantial amounts of chemicals into water bodies. Farmers rely on fertilizers and manures to enhance productivity and meet the growing demand for food caused by the increasing global population [22, 27]. Chemical elements like nitrate, phosphate, and potassium from fertilizers can persist in the Earth's crust for extended periods, posing a risk of water contamination through runoff and soil erosion. This nutrient influx into water bodies not only jeopardizes water quality for drinking but also has ecological consequences, impacting both groundwater and surface water ecosystems [22, 28]. Modern crop varieties heavily depend on agrochemicals, contributing to the frequent use of these substances by farmers. Agrochemicals, including fertilizers and pesticides, often contain various heavy metals and metalloids such as Cu, Co, Cr, Mo, Sr, Ti, V, Mn, Fe, Ni, Zn, Cd, Pb, Hg, Ba, Sc, and As [29]. Despite the significant role pesticides play in global agricultural production, their adverse effects have gained more attention. The use of pesticides has been steadily increasing, with an annual usage of 2.3 million metric tonnes. Some widely used pesticides contain high concentrations of heavy metals, including Cu, Hg, Mn, Pb, and Zn, along with hazardous organophosphate and organochlorine compounds like DDT, lindane, endosulfan, and chlordane [29, 30]. Furthermore, animal manure has been identified as another source of heavy metals (Cu, Zn, and Cd) and metalloids (As) in varying concentrations. These contaminants can accumulate in surface soils over time due to the prolonged use of animal manure, leading to runoff and leaching that contaminate water sources [29].

### Industrial Activities

Gujarat boasts one of the fastest-growing economies in India and holds the fourth-highest GDP in the country. However, it has emerged as a source of environmental concern due to the proliferation of industries in recent decades [12]. Several industrial processes, such as petro-coal combustion, waste disposal, effluent streams, and wastewater irrigation, contribute to the release of heavy metals into the environment. This has led to an increase in heavy metal levels in waterways, causing soil and sediment contamination with detrimental effects on the ecosystem and irreversible damage to nature [31]. The combustion of fossil fuels, especially in coal-burning power plants for electricity generation, significantly influences heavy metal emissions in the environment. Only a third of fly ash, a by-product of coal combustion, is recycled, while the rest is used in various industrial applications. The composition of parent coal, combustion conditions, efficiency of emission control devices, by-product storage, handling, and climate all impact heavy metal emissions [25]. Notably, heavy metals like As, Cd, Mo, Se, and Zn exhibit significant mobility due to natural weathering of coal residues. Coal fly ash has garnered attention for its high levels of heavy metals and metalloids, such as Cd, Cr, Cu, Ni, Mo, Pb, Se, Zn, and As, making it a concern for soil and water contamination [29, 32]. Urban, peri-urban, and rural areas contribute to heavy metal emissions through manufacturing processes, domestic septic tanks, vehicle leaks, and exhaust emissions. Specifically, urban areas face heavy metal emissions from moving vehicles, petrol spills, and light industries [33].

Improper wastewater management in sewage treatment plants leads to the release of organic contaminants, thus contaminating groundwater. Sewage sludge, rich in organic pollutants like triclosan and aromatics, poses a threat to groundwater when improperly managed. Industries, such as wood and pharmaceuticals, release chlorophenols into the environment without adequate treatment, adding to pollution concerns. These chlorophenols, characterized by high chlorination levels, join alkylphenols (APs), volatile organic compounds (VOCs), and polycyclic aromatic hydrocarbons (PAHs) in industrial wastewater [34]. Roads and automobiles, among other sectors, contribute signifi-

cantly to heavy metal pollution. Particulate matter in traffic emissions contains heavy metals like Pb, Cd and As, amplifying the adverse effects on the environment [35].

### Circulation and Distribution of Heavy Metals in Groundwater

Contaminants introduced into the groundwater system can spread through various mechanisms, namely advection, dispersion, and retardation, influenced by environmental factors and the characteristics of the contaminants. Advection refers to the movement of contaminants at the average groundwater flow rate, determined by effective flow velocities calculated using aquifer properties and hydraulic gradients [22, 36]. Effective flow velocities are calculated using the bulk characteristics of aquifer structures and the mean hydraulic gradient that induces the flow. This method overlooks pollutant behaviour, such as solubility, impacting the flow rate measured by advection. Dispersion involves the movement and distribution of dissolved pollutants due to groundwater flow, resulting from mechanical mixing and molecular diffusion. Molecular diffusion is the process of components moving from lower to higher solute concentrations, while mechanical mixing occurs when factors like pore geometry or friction alter groundwater velocity. Retardation is the process wherein the velocity of the contaminant decreases compared to advective groundwater velocity due to interaction with porous media. Retardation methods, like adsorption and biodegradation, can significantly slow down contaminant transport, with retardation rates varying up to ten times slower than advective velocity. The slower the transport, the more the contaminant is absorbed in a small area [22, 36].

## POLLUTION INDICES FOR EVALUATION OF HEAVY METAL CONTAMINATION

In recent decades, considerable attention has been dedicated to assessing heavy metal pollution in both ground and surface waters [37]. Various pollution indices have been employed to comprehensively analyze the extent of heavy metal contamination in water bodies, utilizing multiple reproducible assessments to streamline the evaluation process. The subsequent sections provide a detailed explanation of these indices.

### Heavy Metal Pollution Index (HPI)

In recent years, there has been significant focus on evaluating heavy metal pollution in surface and groundwater. One notable approach is the development of a Heavy Metal Pollution Index (HPI), which aims to assess the combined impact of various metals on water quality. While traditional assessments often focus on individual metals, the HPI provides a comprehensive measure of overall pollution by considering the collective influence of all monitored heavy metals. HPI is used to evaluate the overall impact of heavy metals in water and determine the extent of water contamination. The HPI involves a two-phase process and employs a weighted numerical quality mean approach. Initially, a rating scale with assigned weights for selected parameters is established. Subsequently, a pollution level parameter is chosen to serve as the foundation for the index. The rating scale is arbitrary, ranging from 0 to 1, and the selection of values depends on the relative importance of each quality factor in comparison to other considerations. Alternatively, values can be determined by their inverse proportionality to the standard applicable to the respective parameter [37, 38]. HPI can be calculated using equations (1), (2) and (3):

$$HPI = \frac{\sum_{i=0}^{n} Wi\, Qi}{\sum_{i=0}^{n} Wi} \quad \text{Eq. 1}$$

Where, $W_i$ represents the unit weightage of the $i^{th}$ parameter, $Q_i$ represents its sub-index, and n represents the number of parameters to be considered.

The unit weight (Wi) is calculated through the following equation:

$$Wi = \frac{K}{Si} \quad \text{Eq. 2}$$

Here, K is the proportionality constant, and $S_i$ represents the $i^{th}$ parameter's standard permissible limit.

The sub-index ($Q_i$) for the parameter is calculated from the following expression.

$$Q_i = \sum_{i=0}^{n} \frac{Mi\,(-)\,Ii}{Si - Ii} \times 100 \quad \text{Eq. 3}$$

Where, $M_i$ represents the measured heavy metal value of the ith parameter, $I_i$ is the ideal value, and Si is the standard value. A negative sign (–) indicates a numerical difference between two values. The standard and ideal values used for calculating HPI for different heavy metals are given in Table 1. A HPI

**Table 1.** Standard permissible values and ideal values for heavy metals

| Sr. No. | Heavy metal | Standard permissible value ($S_i$) µg/L | Ideal value ($I_i$) µg/L | Reference |
|---|---|---|---|---|
| 1 | Fe | 300 | 0 | [55] |
| 2 | Cr | 50 | 0 | [55] |
| 3 | Zn | 15000 | 5000 | [55] |
| 4 | Mn | 300 | 100 | [55] |
| 5 | Cd | 3 | 0 | [55] |
| 6 | Pb | 10 | 0 | [55] |
| 7 | Ni | 20 | 0 | [55] |
| 8 | Cu | 1500 | 50 | [55] |
| 9 | Co | 0.05 | 0 | [55] |
| 10 | Mo | 70 | 0 | [55] |
| 11 | As | 50 | 10 | [55] |
| 12 | Cs | 1 | 0 | [58] |
| 13 | Sr | 4000 | 0 | [56] |
| 14 | Al | 200 | 30 | [55] |
| 15 | Hg | 1 | 0 | [55] |
| 16 | Tl | 2 | 0.5 | [57] |
| 17 | Ti | 1 | 0 | [12] |

value below 100 indicates a minimal presence of heavy metal pollution, while a score of 100 signifies a potential risk at the threshold of heavy metal pollution. If the HPI surpasses 100, the water is deemed unsafe for consumption [38].

**Heavy Metal Evaluation Index (HEI)**

The equation used to calculate the HEI represents the total surface water quality in terms of heavy metal content [39].

$$HEI = \sum_{i=0}^{n} \frac{Hc}{Hmac} \quad \text{Eq. 4}$$

Where, $H_c$ and $H_{mac}$ represent the measured value and highest permissible concentration of the $i^{th}$ parameter, respectively. A HPI below 100 indicates a minimal presence of heavy metal pollution, while a score of 100 signifies a potential risk at the threshold of heavy metal pollution. If the HPI surpasses 100, the water is deemed unsafe for consumption [40].

**Degree of Contamination ($C_d$)**

The degree of contamination ($C_d$) can be determined through the combination of the effects of various quality of water parameters.

$$C_d = \sum_{i=0}^{n} C_{fi} \quad \text{Eq. 5}$$

Here, $C_{fi}=[C_{Ai}/C_{Ni}] - 1$

Where, $C_{fi}$ is the contamination factor, $C_{Ai}$ is the measured value of the ith parameter and $C_{Ni}$ is the $i^{th}$ component's maximum allowable concentration (N stands for the "normative" value). Based on $C_d$ values, the levels of heavy metal pollution in a surface water body are categorized as follows: A score of less than one [<1] indicates low pollution, a score between one to three [1–3] signifies moderate pollution, and a score exceeding three [>3] indicates high pollution [40, 41].

**Metal Index (MI)**

The metal index is a tool used for rapidly assessing the overall water quality, considering the potential combined effects of metal elements on human health. The mathematical expression is used to calculate the metal index [42].

$$MI = \sum_{i=0}^{n} \frac{Ci}{MACi} \quad \text{Eq. 6}$$

Here, $C_i$ represents the average concentration of each component, and $MAC_i$ is the maximum permissible concentration. Different contamination levels are categorized based on the metal index value: highly pure if MI <0.3, pure if 0.3< MI <1, mildly affected if 1< MI <2, moderately affluent if 2< MI <4, strongly affluent if 4< MI <6, and seriously affluent if MI >6. A metal index value greater than 1 is considered a warning sign, indicating a decline in water quality, with higher metal levels compared to the corresponding maximum permissible concentrations [43].

**Water Pollution Index (WPI)**

The utilization of water, encompassing the control and supervision of water pollution, is governed by the Water Purity Index (WPI). This index offers a numerical value relative to the minimum allowable threshold for a specific heavy metal as shown below [40].

$$WPI=(M_i - Min_i)/R_i \quad \text{Eq. 7}$$

Here, Mi represents the monitoring value, Mini is the minimum permissible limit, and Ri denotes the acceptable limit range for a specific heavy metal as extracted from relevant sources.

## CURRENT SCENARIO ON THE PRESENCE OF HEAVY METALS IN GUJARAT

Access to clean water is crucial for both humans and the environment, as water is a vital resource for life on Earth. Water quality has been negatively impacted by population growth, accelerating urbanisation, and unsustainable resource use in recent years. Heavy metal ions are one of the most commonly released contaminants, making them a cause for concern [7].

In a study conducted at Bhavnagar, which is located on the western coast of the Gulf of Khambhat in Gujarat. The Gulf of Khambhat is a distinct tropical coastal marine habitat with strong continental effect. The region has diverse habitats and is a susceptible ecological area. The industrial zone releases treated or untreated wastewater into the Gulf of Khambhat. In this study, approximately 63 samples were collected from the Bhavnagar coastal line over three seasons and at seven different locations. Together with the physicochemical parameters, seasonal dissolved heavy metal levels were also examined. The mean amount of dissolved heavy metals in all sites decreased in the following order: Pb > Cr > Ni > Co > Fe > Cd > Mn > Cu > Zn. Compared to the monsoon period, the dry season (pre- and post-monsoon) had higher levels of dissolved heavy metals in coastal waters. During the dry season, anthropogenic activities lead to higher levels of heavy metals in the water. The amount of Pb exceeded the acceptable limit. Except for Pb and Ni, all metals are within permissible limits. The high concentration of Pb in coastal water was ascribed to ship paint and repair activities, as well as the discharge of waste from industries. Ni levels were above the BIS standards. Ni was found in sewage sludge, paint and dyes, old batteries, fertilisers, and industrial wastewater. The study revealed significant spatial and temporal variation in the physical and chemical characteristics of water and dissolved heavy metals, which may pose a threat to marine ecosystems [44].

In a study conducted in Ankleshwar Industrial Estate (AIE), South Gujarat, 38 water samples collected to analyse heavy metal contamination. The sampling wells were selected using a method of random sampling, considering industrial, urbanised and oil field regions, as well as road networks and polluted streams. The hydrogeology of AIE is dominated by quaternary alluvium. The alluvial (shallow alluvial aquifer) sediments have been classified according to their depositional surroundings. The AIE, characterized by urban and industrial areas comprising of chemical, fertiliser, paint, dye, glass, pharmaceutical, and other allied in-

dustries, has undergone significant environmental impact. The work aimed to characterize spatial variations in toxic metals, identify potential sources, and assess their impact on surface water using GIS-based methods. Geochemical maps were created to estimate concentrations of ten trace elements, revealing high levels of heavy metals, especially Mo, Zn, Pb, Ni, Co, Fe, and Cd. Groundwater in the oil field area exhibited alarming concentrations, implicating oil field development as a major contributor to subsurface environmental damage, affecting over 20 $km^2$ area. Heavy metal concentrations were found to be higher in Panoli region compared to Ankleshwar and surrounding areas due to industrial sources located in recharge zones. The study also assessed metal concentrations in the Amla Khadi stream, distinguishing between geological (U) and anthropogenic (P) sources. The "extremely" high P/U ratio for Mo and "high" ratios for Cr indicated significant contaminant growth in the polluted stream area, raising concerns about potential migration into cultivated food crops due to elevated technological elements in groundwater [9].

Singh et al. [45] conducted a study at the Pirana landfill site in Ahmedabad, focusing on assessing the quality and toxicity of waste, particularly in terms of heavy metals, and its impact on groundwater quality. They collected a total of 11 groundwater samples, 5 municipal solid waste (MSW) samples, and 1 leachate sample. The hydrogeology of the study area is characterized by extensive Quaternary alluvial deposits, which are notably thick. These deposits consist of a mixture of sand, silt, clay, and gravel beds, forming the lithology of Ahmedabad. Within these deposits, there is a recurring pattern of alternating layers of sand, silt, clay, and gravel. Typically, multiple layers of sand are found within the first 50 m of the ground. Separating the upper unconfined aquifers from the deeper aquifers, which lie beyond 100 m in depth, is a layer of silt or clay, typically measuring 20 to 25 m thick. The study aimed to monitor levels of heavy metals such as Cd, Cr, Cu, Fe, Ni, Mn, Pb, and Zn to evaluate the landfill's influence on groundwater quality. The chemical analysis of MSW indicated a general trend of metal abundance as Fe>Mn>Zn>Cu>Pb>Cr>Ni>Cd. In leachate and groundwater, the observed trend was Fe>Zn>Mn>Cu>Pb>Cr>Ni>Cd. The results suggested that Fe and tin-based wastes at the landfill site might contribute to high iron values, and the Mn concentration was generally elevated except for some samples from coal and municipal waste burning. Cu levels were within acceptable limits, while Zn concentration was high, potentially due to the presence of Zn-based waste like zinc-plated material, fertilizer, and cement. The majority of Ni and Cr values were within acceptable ranges, and Pb and Cd levels were also found to be within acceptable limits. Factor analysis results indicated that pollution sources were more prevalent than natural processes near the landfill site. Positive loading of heavy metal factors demonstrated the landfill's impact on groundwater quality, particularly in the pattern of groundwater movement. Cluster analysis identified two major groups of samples: those with and without landfill impact, along with contaminated leachates.

Another study was aimed to investigate the seasonal variations in water and sediment quality in the Sabarmati River and its tributary, the Kharicut canal, at Ahmedabad, Gujarat [10]. These locations receive industrial waste from various sectors such as plastics, engineering, machinery, chemicals, paints, pharmaceuticals, foundries, and textiles. The concentrations of heavy metals in sediments were notably higher than those in water samples, with Cr being the most prevalent metal. The hierarchy of heavy metal concentrations observed in water samples was Cr > Zn > Cu > Ni > Pb. The study revealed seasonal variations in heavy metal concentrations, with the highest levels during the pre-monsoon season, followed by the monsoon and post-monsoon seasons. The Pollution Load Index (PLI) indicated that surface sediments were more contaminated with heavy metals than river waters. The contamination degree (Cd) values demonstrated a very high level of contamination in the Kharicut canal and a significant level of contamination at three sites along the Sabarmati River.

Keesari and co-workers [46] conducted a study where they collected and analyzed 25 groundwater samples from the Mainland Kachchh. Their study focused on examining the general geochemistry and levels of trace metals present. The study area encompasses hydrogeological formations dating back to the Mesozoic (up to 250 million years) and Cenozoic (up to 65 million years) eras. The drainage patterns in this region are shaped by lithological characteristics, tectonic activities, and fluctuations in sea levels during the Quaternary period. The results revealed that the levels of all trace elements fell within the permissible drinking water limits set by the World Health Organization (WHO) in 2008, except for manganese (Mn2+) in two samples [10]. This suggests that there is no significant influence from industrial waste or essential geological contributions affecting the groundwater system.

Upadhyaya et al. [11] conducted a study on the presence and distribution of specific heavy metals (As, Co, Cr, Cu, Fe, Mn, Ni, Pb, and Zn) in the Gulf of Khambhat (GoK), Gujarat, during different seasons (post-monsoon, winter, and pre-monsoon). They collected and analyzed groundwater samples from 11 stations. The hydrogeology of the GoK region consists of a typical alluvial landscape characterized by shallow water tables and moderate to high salinity levels. Due to the composition of the alluvium, which is primarily fine clay with a layer of silty sand on top in the unconfined aquifers, groundwater flow is notably sluggish in these regions. Through different seasons, Zn exhibited the highest average concentrations, followed by Cu, Cr, and B in the pre-monsoon, post-monsoon, and winter periods. Post-monsoon seasons had relatively high concentrations of Cd, Co, Ni, and Pb, while pre-monsoon seasons showed elevated levels of As, Cr, and Mn. The decreasing trend in average metal levels was observed as follows: Zn > Cu > Pb > Ni > Cr > Cd > B > Co > Mn > As for pre-monsoon, Zn > Cu > Pb > Ni > Mn > Cd > As > Co for post-monsoon, and Zn > B > Cr > Cu > Mn > As > Ni > Pb > Cd > As > Co for winter seasons. Principal Component Analysis (PCA) was employed to understand the un-

derlying data structure. PC1 revealed that Co, Cu, Cd, and Zn accounted for 31.72% of total variances, originating from sources like municipal sewage, metallurgical industries, and landfill leachate infiltrating aquifers. PC2 contributed 20.6% of total variance, characterized by high Mn, Ni, and B loadings. PC3 with 11.26% total variance had moderate As loading and minor B loading, while PC4, accounting for 9.17%, comprised Cr and Pb. According to the PCA, groundwater chemistry in the study area was primarily influenced by mineral weathering, anthropogenic pollutants, and atmospheric deposition. The detection of toxic metals like Cd and Pb in some samples raises concerns about the health implications for those consuming the water.

An evaluation of the hydrochemical characteristics of groundwater in Bhavnagar District, Gujarat, revealed that heavy metal analysis indicated elevated values in most samples, surpassing permissible limits [47]. Building on this, Patel et al. [48] provided substantial insights into the groundwater quality evolution in the southern and central regions of Gujarat. Most of the studied region is enveloped by Quaternary deposits, with older Proterozoic rocks predominantly found in the north and Deccan basalt covering the southern part of the area. The study specifically investigated heavy metal concentrations, including Cr, Zn, and Pb. Zn emerged as the most prevalent metal in the groundwater samples, followed by Cr and Pb. Importantly, none of the metal concentrations exceeded the limits set by the Bureau of Indian Standards (BIS). The study suggested that the adequate concentrations of these metals during both post-monsoon and pre-monsoon seasons could be attributed to an abundance of $HCO_3^-$ ions in water. This excess of ions may play a regulatory role by precipitating toxic metals, such as Pb, out of solution.

A two-year study spanning from June 2015 to May 2017 was conducted, focusing on the levels of heavy metals such as Cd, Pb, Ni, Cr, Hg, Cu, Zn, Fe, and Mn in water, sediment, and fish tissues within the aquatic region of the River Mahi in Gujarat [49]. Sampling was carried out at two designated stations, E1 (upstream) and E2 (downstream). The water samples from E1 exhibited elevated concentrations of all examined heavy metals compared to those from E2. This disparity was attributed to the discharge of industrial waste into area E1 through a canal connected to the Nandesari industrial zone. Additionally, the industries in and around Vadodara were identified as sources of substantial amounts of hazardous chemicals dumped into the Mahi River, contributing to the heightened heavy metal concentrations at station E1. Analysis revealed that heavy metal concentrations in water peaked during the monsoon period (June to August) and decreased during the summer months (March to May) at both E1 and E2 stations. Notably, both stations displayed positive correlations between the levels of heavy metals in the water. The sequence of heavy metal concentrations in the water at stations E1 and E2 was found to be Fe>Mn>Zn>Pb>Ni>Cu>Cd>Hg>Cr. Except for Zn, the concentrations of other heavy metals exceeded permissible limits in the surrounding environment.

Siddha and Sahu [50] conducted a study utilizing Principal Component Analysis (PCA) to gain insights into the significant hydrogeochemical processes influencing groundwater changes in the Vishwamitri River Basin (VRB) in Gujarat, India. PCA, a statistical technique, was employed to identify and reduce data outliers. The normal distribution of the dataset was assessed using the Shapiro-Wilk statistic. The analysis included the examination of trace heavy metals such as Fe, Zn, Mn, Mo, Li, Sr, As, Se, Tl and V, which were integrated into the PCA framework. The overall PCA results indicated that the groundwater chemistry was influenced by both mineral dissolution and human activities.

Dubey and Ujjania [51] studied the water quality in the estuarine vicinity of the Tapi River in Gujarat, focusing on heavy metal pollution and concentrations. Water samples were collected monthly from the Hazira estuary of the Tapi River between January and September 2014, analysing Cd, Cr (VI), Pb and Co levels. To assess pollution levels, they utilized statistical techniques for metal concentration, specifically the contamination factor (CF) and pollution load index (PLI), which are interrelated. The results revealed a consistent order of increasing metal concentrations as Pb < Co < Cd < Cr(VI), with both CF and PLI indicating a state of extreme pollution, attributed to the direct discharge of industrial wastewater.

A study was performed to assess the hydrochemical processes influencing spatial and seasonal variations in nutrient and heavy metal concentrations in the water of mangroves located in the Gulf of Kutch (GoK), India [12]. GoK is a semi-closed basin surrounded by Kachchh mainland to the north, Saurashtra peninsula to the south, and the Arabian Sea to the west. Kachchh's major lithological features include sandstone, shale, limestone, and basalt. The Saurashtra peninsula is made up of tertiary shale and limestone, as well as late-cretaceous basalt and laterite rocks that form the shoreline. Surface water samples were collected during the pre-monsoon and monsoon seasons, specifically during low tide in May 2018 (pre-monsoon) and December 2018 (post-monsoon). A total of 36 mangrove locations in the northern and southern Gulf of Kachchh were sampled. The analysis focused on heavy metals, including As, Cu, Fe, Li, Mn, Mo, Pb, Si, Sr, Ti, Tl, and Zn. GIS software was employed to create spatial distribution maps, and statistical techniques such as agglomerative hierarchical clustering (AHC), PCA, and correlation analysis were applied to the hydrochemical data to identify spatial patterns, relationships between variables, and the sources of chemical components. During the pre-monsoon period, the mean concentrations of heavy metals were ranked as follows: Sr> Fe> Zn> Cu> Li> Mn> As> Ni> Pb> Ti> Tl> Mo. In the post-monsoon season, the mean concentrations were as follows: Fe> Sr> Zn> Mn> Cu= Li> Ti> As = Pb> Ni> Tl= Mo. Overall, heavy metal concentrations increased during the pre-monsoon season, with Fe, Sr, Zn, and Mn being the most abundant. Elevated levels of Fe and Mn suggested a prevalence of related biological productivity and redox processes at the sediment-water interface. The study identified

metal contaminations (Zn, Cu, Li, As, Ni, Pb, Ti, Tl, and Mo) as originating from non-point sources due to human activities in the investigated area.

A two-year study was conducted to investigate the presence of heavy metals, including Hg, Cd, Pb, and Zn in the Tapi river estuary in Surat [52]. The average concentrations of these heavy metals in water over the two sampling years were found to follow the order Pb>Zn>Cd>Hg. Statistical analyses indicated significant differences in the levels of mercury, cadmium, lead, and zinc in water among the three sampling sites. Patel et al. [53] conducted a study to assess the status of groundwater quality in Vadodara and Chhota Udaipur districts. Groundwater in both areas exists in unconfined and confined conditions. Unconfined aquifers consist of saturated zones of unconsolidated shallow alluvium, weathered zones, and shallow depth jointed and fractured rocks. Multilayered aquifers are present beneath impervious clay horizons in alluvium formation and interflow zones of basalts, intertrappean beds, deep-seated fracture zones, and shear zones in basalts, granites, and gneisses, leading to semi-confined to confined conditions. The study included an examination of both physicochemical parameters and the presence of various heavy metals. To identify potential heavy metal pollution in groundwater, they analysed Pb, Cd, Fe, Ni, Cr, Zn and As. The findings indicated that, except for Fe and Pb, the levels of heavy metals fell within permissible limits as per Indian standards, set at 0.3 mg/L for Fe and 0.01 mg/L for Pb. The analysis revealed a maximum Fe concentration of 9.9 mg/L and a maximum Pb concentration of 0.057 mg/L. It was noted that Fe concentrations generally exceeded the recommended range of 0.3 mg/L to 0.8 mg/L. Prolonged exposure to heavy metals beyond the established limits could pose severe health risks, potentially leading to fatal outcomes. The details of the study area, methodology followed, and significant observations are summarized in Table 2.

## ASSESSMENT OF CONTAMINATION USING THE HEAVY METAL POLLUTION INDEX

Quality indices play a crucial role in consolidating the impact of all pollution factors to provide a comprehensive evaluation. Numerous methods have been proposed for estimating surface water features using water quality parameters [54]. Monitoring heavy metals in drinking water is especially vital for human health, and assessing heavy metal pollution in the groundwater of Gujarat is imperative. This study aims to demonstrate the extent of heavy metal contamination in the region by applying the HPI to existing work on heavy metals in the groundwater of Gujarat.

The HPI is a tool that gauges the collective influence of individual heavy metals on water quality, offering insights into the overall impact on environmental health. The weighted factors in HPI correspond to the inverse of the suggested standard for each metal. Notably, the sum of these weighted factors does not equal 1. In contrast to other Water Quality Indices (WQI) where higher values indicate better quality, higher HPI values signify deteriorated water quality concerning metals. Unlike other WQIs that calculate sub-indices using only standard values, HPI incorporates both ideal (Ii) and standard (Si) values, making it a more comprehensive metric [37]. In the HPI calculations performed in the present study, the values for Si and Ii were adapted from BIS (2012) [55], representing the standard permissible limit and ideal acceptable limit values of heavy metals in drinking water. If there is no ideal acceptable limit, the Ii value is considered 0. For certain heavy metals such as As, Cd, Co, Cu, Cr, Mn, Ni, Pb, and Zn, recommended values were used [55]. The standard limit for strontium (Sr) is 4 mg/L, according to ATSDR (2004) [56]. Thallium (Tl) values were obtained from USEPA (2009) [57], with Si and Ii values set at 0.5 ppb and 2 ppb, respectively. Cesium (Cs) value of 1 µg/L was adopted from ATSDR (2004) [58].

The HPI was employed to assess groundwater accessibility in pollution studies conducted in Gujarat. The tabulated results display the index, which holds applicability across various water usage scenarios (Table 2). The critical threshold for this pollution index was set at 100. Heavy metal values contributing to the HPI are expressed in µg/L. The calculation of HPI involved utilizing the mean concentrations of heavy metals measured at distinct sampling sites during the conducted studies. In instances where values for different seasons were available, the overall mean value was selected for HPI computation. If the study provided a direct mean value, the calculation was performed accordingly.

Cobalt (Co): With Co making a major contribution of 317882.34, the total composite HPI score at the Bhavnagar Costal line was 317939.01. This result indicates the impact of human-induced disturbances and the proliferation of diverse activities in the area [44]. The AIE recorded a comprehensive HPI score of 550182.72, with Co contributing significantly at 550052.27, indicating substantial groundwater contamination. This contamination is attributed to the dispersal pattern of elevated Co concentrations, primarily observed in industrial areas where coal combustion serves as a major energy source [9]. However, in the mainland of the Kachchh region, there was negligible contributions from industrial wastes and geological factors to the groundwater system [46]. Nevertheless, the HPI calculation revealed that the score of Co exceeded the established threshold in the Gulf of Khambhat. In this region, the HPI score for Co also surpassed the critical limit of 1941.99, indicating a notably high level of Co contamination within the broader context of heavy metal pollution [11].

Lead (Pb): According to a study conducted by Kumar et al. [10] at the Sabarmati River and Kharicut canal in Ahmedabad, the HPI score for Pb at the Sabarmati River was below the permissible limit, indicating that this site was free from heavy metal contamination. However, at the Kharicut canal, the HPI score for Pb was notably high at 632.44, classifying it as a major contaminant, alongside Cr with an HPI score of 565.67. This indicates significant heavy metal pollution at this site, with industries like dyeing, chrome plating,

**Table 2.** Groundwater studies of different regions of Gujarat for heavy metal ion pollution

| Sr. No. | Ref. | Study area | Water type | No of samples analysed; heavy metals studied | Methods/parameters evaluated | Heavy Metal Pollution Index (HPI) score | Remarks |
|---|---|---|---|---|---|---|---|
| 1 | [44] | Western belt of the Gulf of Khambhat, Bhavnagar | Surface water | 7; Cd, Co, Cr, Cu, Fe, Mn, Ni, Pb, Zn | Correlation Coefficient, Principal Component Analysis, Cluster Analysis | 317939.01 | The HPI score was significantly higher than the threshold limit, with Co (317882.3445) being the major contributor. |
| 2 | [9] | Ankleshwar Industrial Estate, Bharuch | Groundwater | 38; Cd, Co, Cr, Cu, Fe, Mn, Mo, Ni, Pb, Zn | Clutching geochemical analysis, GIS-based colour composites methods | 550182.72 | Overall, the HPI score was much higher than the threshold limit; The major contributor for high HPI score was Co (550052.27) and to a lesser extent Cd (106.45). |
| 3 | [45] | Pirana Site, Ahmedabad | Groundwater | 17#; Cd, Cr, Cu, Fe, Ni, Mn, Pb, Zn | Correlation analysis, Cluster analysis, Factor analysis | 219.07 | Overall, the HPI score was above the threshold limit; Major contributor for high HPI was Fe (113.13). |
| 4 | [10] | Sabarmati River, Ahmedabad | Surface water | 15; Cr, Cu, Ni, Pb, Zn | Contamination factor, Contamination degree and Pollution load index | 48.06 | Overall, the HPI score was much below the threshold limit. Free from heavy metal ion contamination |
| | | Kharicut canal, Ahmedabad | Surface water | | | 1269.17 | Overall, the HPI score was above the threshold limit; The major contributor for high HPI score were Cr (565.67) and Pb (632.45). |
| 5 | [46] | Mainland of Kachchh, Kachchh | Groundwater | 25; Al, As, B, Ba, Cu, Co, Cs, Fe, Mn, Ni, Sr, Pb, Zn | Isotope analysis, Graphical methods | 7544.40 | Overall, the HPI score was above the threshold limit; The major contributor for high HPI score was Co (7521.47). |
| 6 | [11] | Gulf of Khambhat, Khambhat | Groundwater | 11; As, Cd, Co, Cr, Cu, Mn, Ni, Pb, Zn, B | In-situ parameters analysis; Correlation matrix analysis, Principal component analysis | 1943.36 | Overall, the HPI score was above the threshold limit; The major contributor for high HPI score was Co (1941.99). |
| 7 | [47] | Villages of Bhavnagar | Groundwater | 174; Fe, Pb | In-situ parameters analysis | 97.85 | Overall, the HPI score was below the threshold limit. Free from heavy metal ion contamination |
| 8 | [48] | Bharuch, Dang, Anand, Tapi, Narmada, Surat, Navsari, Chhota Udaipur, Mahisagar, Dahod, Valsad, Vadodara, Panchmahal | Groundwater | 45; Cr, Zn, Pb | Irrigation Indies, Correlation analysis | 64.82 | Overall, the HPI score was below the threshold limit. Free from heavy metal ion contamination |
| 9 | [49] | Mahi Estuary, Vadodara | Surface water | 50; Cr, Cd, Cu, Fe, Hg, Mn, Ni, Zn | Correlation analysis | 187814.02 | Overall, the HPI score was much higher than the threshold limit; The major contributor for high HPI score was Hg (187624.07) and to a lesser extent Cd (132.39). |

**Table 2 (cont).** Groundwater studies of different regions of Gujarat for heavy metal ion pollution

| Sr. No. | Ref. | Study area | Water type | No of samples analysed; heavy metals studied | Methods/parameters evaluated | Heavy Metal Pollution Index (HPI) score | Remarks |
|---|---|---|---|---|---|---|---|
| 10 | [50] | Vishwamitri River Basin, Vadodara, Panchmahal | Groundwater | 60; As, Fe, Li, Mg, Mo, Se, Sr, Th, V, Zn | Principal component analysis | – | – |
| 11 | [51] | Tapi River (Hazira estuary), Surat | Surface water | 3; Cd, Cr(VI), Pb, Co | Contamination factor, Pollution Load Index | 3928.26 | Overall, the HPI score was above the threshold limit; The major contributor for high HPI score were Cd (2349.48) and Pb (1570.48). |
| 12 | [12] | Mangroves Region of Kachchh | Surface water | 36; As, Cu, Fe, Li, Mn, Mo, Pb, Si, Sr, Ti, Tl, Zn | Correlation Analysis, Cluster analysis, Principal component analysis | 10360.68 | Overall, the HPI score was above the threshold limit; The major contributor for high HPI score were Ti (9456.62) and Tl (778.20). |
| 13 | [52] | Tapi River, Surat | Surface water | --; Cd, Hg, Pb, Zn | Statistical analysis | 2099.09 | Overall, the HPI score was above the threshold limit; The major contributor for high HPI score were Hg (1772.01) and Pb (296.85). |
| 14 | [53] | Chhota Udaipur | Groundwater | 162; As, Cd, Cr, Fe, Ni, Zn | Water quality index, Correlation, and regression analysis | 25238.96 | Overall, the HPI score was above the threshold limit; Major contributor for high HPI was Pb (25215.83). |
| | | Vadodara | Groundwater | | | 190.65 | Overall, the HPI score was above the threshold limit; Major contributor for high HPI was Pb (155.12). |

textiles, tanning, leather, and paints being particularly susceptible to elevated metal levels. In the estuary of the Tapi River, the calculated HPI score was 3928.26 [51]. Pb emerged as the predominant pollutant with a score of 1570.48, attributed to direct discharges of industrial effluents into the river. Cadmium (Cd) also affected the Tapi River, as indicated by its HPI score of 2349.48. Another study on the Tapi River estuary highlighted Pb as a dominant metal pollutant, with an HPI score of 296.84 [52]. In the villages of Vadodara and Chhota Udaipur districts of Gujarat, a study revealed significant dominance of metal pollutants in both the districts [48]. The overall HPI scores were 190.64 and 25238.96, and the Pb scores were 155.11 and 25215.83, respectively. This underscores the substantial impact of Pb pollution in these regions.

Mercury (Hg) is a non-essential metal devoid of recognized physiological functions and exhibits toxicity even at low concentrations. According to a study [49], the Mahi River estuary recorded an overall HPI score of 187814.01, with Hg contributing significantly through an individual HPI score of 187624.07. This indicates a pronounced contamination attributed to human activities. Similarly, in the Tapi River ecosystem [52], an increased level of metal ions was evident due to anthropogenic influences. Specifically, the HPI score for Hg at the Tapi estuary reached 1772.01, underscoring a substantial pollution impact.

Cadmium (Cd): A study conducted by Kumar et al. [9] revealed elevated levels of Cd contamination in AIE, South Gujarat, India. The HPI score for Cd in this region surpassed the critical limit of 106.49, indicating significant pollution in the analyzed water sample. Additionally, Pandey et al. [49] highlighted heavy metal pollution in the Mahi River, with a Cd HPI score of 132.38, rendering the water unsafe for drinking and other purposes. Notably, the Tapi river exhibited the highest Cd contamination, with an HPI score of 2349.48, underscoring Cd as the predominant contaminant at this site [52].

Research conducted at the Pirana site in Ahmedabad focused on assessing the quality and toxicity of waste in relation to heavy metals [45]. The application of the HPI revealed high score for Fe, exceeding the threshold limit, registering at 113.12, indicating the presence of heavy metals. In a separate study conducted by Maurya and Kumari [12], the investigation aimed to analyze the spatial and seasonal variations of nutrients and heavy metals in the water of mangroves located in the Gulf of Kachchh. The primary heavy metals contributing to overall pollution were Ti and Tl, with corresponding HPI scores of 9456.62 and 778.20, respectively.

## TECHNOLOGIES FOR REMOVAL OF HEAVY METALS IN GROUNDWATER

The degradation of heavy metals in water poses a challenge due to their complex bioaccumulation characteristics. Excessive exposure to these metals beyond permissible limits can lead to health issues in humans, as heavy metals are highly toxic and often carcinogenic, accumulating in various bodily systems [59]. Given the potential health risks associated with even slight excesses of metal ions, the removal process is as crucial as detection. To ensure the complete elimination of specific metal ions from water systems, it is essential to employ an appropriate removal technique. Care must be taken to choose a method that is not only effective but also safe, environmentally friendly, and cost-effective [60]. Various methods are employed for removing heavy metals from contaminated water, including membrane filtration, ion exchange, coagulation, adsorption, reduction or oxidation, and chemical precipitation [61]. The selection of a suitable method is critical to achieving comprehensive removal while meeting safety and cost considerations.

### Chemical Precipitation

Chemical precipitation is a widely used and effective industrial process due to its simplicity and cost-effectiveness. This method involves the reaction of chemicals with heavy metal ions, forming insoluble precipitates. The precipitates can then be separated from water through sedimentation or filtration. After treatment, the water can be released or recycled. Hydroxide precipitation and sulphide precipitation are two common chemical precipitation processes, with hydroxide precipitation being particularly popular due to its simplicity, low cost, and easy pH control [59]. In hydroxide precipitation, chemicals like lime are often used to react with heavy metal ions in the pH range of 8.0 to 11.0, minimizing the solubility of metal hydroxides. Flocculation and sedimentation processes are employed to remove the metal hydroxides. While hydroxide precipitation is cost-effective, the method produces large amounts of low-density sludge, presenting challenges in dewatering and disposal [62]. The addition of coagulants, such as alum and iron salts, can enhance heavy metal removal. Sulphide precipitation is another successful technique for removing toxic metallic ions. Unlike hydroxide precipitation, sulphide precipitates have lower solubilities and are not amphoteric, allowing for high metal removal over a broad pH range. The resulting metal sulphide sludges also have better dewatering and dehydration properties. However, there are risks associated with the sulphide precipitation process, as heavy metal ions and sulphide precipitants in acidic environments can lead to the formation of toxic H2S emissions. Therefore, the process must be conducted in a neutral or basic medium [62]. Alternatively, chelating precipitants like trimercapto triazine, potassium-sodium thiocarbonate, and sodium dimethyl dithiocarbamate can be used as another option for removing heavy metals from aquatic environments [63]. The data highlights the presence of heavy metals such as Pb, Cr, Ni, Cd, and Zn in various water bodies across Gujarat. Chemical precipitation, particularly hydroxide precipitation and sulphide precipitation, can be effective in treating water contaminated with these heavy metals. For instance, hydroxide precipitation using lime can help reduce the solubility of metal hydroxides like Pb and Cd, while sulphide precipitation can target metals like Ni and Zn.

### Adsorption Method

Adsorption has been identified as a highly effective method for purifying contaminated water due to its economic and technical viability. The design and functionality of this technique are practical, and the treated water meets high-quality standards. Furthermore, the adsorbents can be reused after regeneration through appropriate desorption procedures [64]. Various adsorbents, such as carbon-based compounds, polymers, resins, clays, minerals, nanoparticles, and nanocomposites, have been utilized for removing heavy metals from wastewater [65]. The process of removing heavy metal ions through adsorption is known for its cost-effectiveness, high removal capacity, ease of implementation, and straightforward treatment [66].

#### Activated Carbon

The effective removal of metal pollutants from aquatic environments has been demonstrated through the utilization of activated carbon as a potent adsorbent. This method is frequently employed in wastewater treatment owing to the substantial surface area offered by activated carbon. The effectiveness of activated carbon stems from its diverse surface functional groups and well-established pore structure, making it a proficient purifier of contaminated water [60]. Carbon-based nanoporous adsorbents, including activated carbons (ACs), carbon nanotubes (CNTs), and graphene (GN), are widely applied in the removal of heavy metals due to their significant surface areas ranging from 500 to 1500 $m^2/g$. Common modification methods such as nitrogenation, oxidation, and sulfuration are employed to enhance specific surface area, pore structure, adsorption capacity, thermal stability, and mechanical strength [66].

#### Biosorption

The utilization of dry biomass to extract harmful metallic elements from industrial effluents, known as biosorption, represents an alternative approach in commercial wastewater treatment. In the process of adsorbing heavy metal ions, both physisorption and chemisorption play crucial roles [59, 66]. The notable advantages of biosorption include its remarkable efficiency in reducing heavy metal ions and the use of cost-effective biosorbents. Biosorption processes are particularly well-suited for treating diluted heavy metal wastewater. These biosorbents can be derived from three main sources: (1) non-living biomass such as bark, lignin, prawns, krill, squid, crab shell, etc., (2) algal biomass and (3) microbial biomass, including bacteria, fungi, and yeast [61, 67]. Biosorbents offer extensive source coverage, cost-effectiveness, and rapid adsorption. However, it is important to note that these investigations are still in the experimental and theoretical stages, and the separation of biosorbents after absorption poses a potential challenge [62].

### Mineral Adsorbents

Mineral adsorbents like zeolite, silica, and clay are considered cost-effective options for water purification. Clay possesses favourable characteristics such as high cation exchange capacity (CEC), selectivity for cation exchange, hydrophilic surface, swelling capability, and surface electronegativity. Various enhancement techniques like acid washing, thermal treatment, and the addition of pillars can increase pore size, volume, and specific surface area, significantly improving adsorption efficiency [65, 68, 69]. Clay components inherently contain exchangeable cations like $Na^+$, $Ca^{2+}$, and $K^+$, enhancing their adsorption capabilities. Most clay minerals carry a negative charge due to the substitution of $Si^{4+}$ and $Al^{3+}$ with other cations, making them effective in removing heavy metal cations from water. The process of heavy metal adsorption by clay and clay composites involves ion exchange, surface complexation, and direct bonding of heavy metal cations to the clay surface. Furthermore, clay materials can become more organophilic and hydrophobic through treatment or modification, expanding their ability to absorb non-ionic organic substances [70].

### Carbon Nanotubes

Carbon nanotubes (CNTs) have received a great deal of attention due to their excellent properties and applications. CNTs, as relatively new adsorbents, have demonstrated great potential for removing heavy metal ions such as Pb, Cd, Cr, Cu and Ni from wastewater. They are classified as either single-walled CNTs (SWCNTs) or multi-walled CNTs (MWCNTs). The processes by which metal ions are absorbed onto CNTs are complex but they involve electromagnetic attraction, sorption-precipitation, and chemical interaction among metal ions and CNT surface functional groups [61, 70, 71].

Adsorption techniques using activated carbon, biosorbents, and mineral adsorbents can be applied to remove heavy metals like Pb, Cd, Cr, Cu, Ni, Zn, and Fe from contaminated water. Activated carbon, with its high surface area, can effectively adsorb various heavy metal ions present in water samples from different locations in Gujarat.

**Membrane Filtration**

Membrane filtration has become increasingly popular for the treatment of inorganic wastewater due to its ability to eliminate suspended solids, organic matter, and heavy metals. Various membrane filtration techniques, including ultrafiltration (UF), nanofiltration (NF), and reverse osmosis (RO), are employed depending on the particle size. Ultrafiltration, with a membrane pore size of 5–20 nm, selectively separates heavy metals, macromolecules, and suspended solids from water, permitting the passage of water and low-molecular-weight solutes while retaining larger macromolecules [72]. RO relies on osmosis, reversing the natural flow by applying pressure to a semipermeable membrane separating solutions of different concentrations. RO membranes, which are essentially nonporous, allow water to pass through while retaining most solutes, achieving ion removal rates of 95–99.9%. This process, characterized by high operational pressures (2,000–10,000 kPa), is commonly used to produce pure water for industrial purposes but may not be optimal for highly concentrated solutions. Nanofiltration membranes, featuring pores of 2 to 5 nm, partially retain ions, allowing small monovalent ions and low-molecular-weight organics to pass through. NF membranes exhibit higher water permeability than RO membranes, operating at lower pressures (700–3,000 kPa) [73]. Microfiltration (MF) employs microporous membranes with a separation limit of 0.02 to 10 m to separate particles, microorganisms, and large molecules through a sieving effect. Inorganic (ceramic) membranes, with lower porosity than polymer membranes, offer thermal stability for use at high temperatures. MF is effective in wastewater and water treatment, removing dissolved materials and colloidal particles that are too large for other separation methods [73]. In Gujarat, UF, NF and RO can be employed to remove suspended solids and heavy metals like Pb, Cd, Ni, and Zn from water. This is particularly relevant in areas where water samples showed elevated concentrations of heavy metals during certain seasons.

**Ion Exchange**

The ion exchange technique is a reversible chemical process employed to replace harmful metal ions in wastewater with beneficial ones. In this method, a heavy metal ion is extracted from a wastewater solution by binding it to an immobile solid particle, serving as a substitute for the cation of the solid particle. The composition of these solid ion-exchange particles can be either natural, such as inorganic zeolites, or synthetic, like organic resins. Heavy metal ions such as $Pb^{2+}$, $Hg^{2+}$, $Cd^{2+}$, $Ni^{2+}$, $V^{4+}$, $V^{5+}$, $Cr^{3+}$, $Cr^{4+}$, $Cu^{2+}$, and $Zn^{2+}$ can be effectively removed from wastewater through ion exchange [74]. Different types of ion exchange materials, including Diaion CR11 and Amberlite, have been investigated for cation removal. Zeolites, due to the negative charge generated by $Si^{4+}$ at the center of the tetrahedron, with isomorphous replacement by $Al^{3+}$ cations, exhibit a high capacity for ion exchange. The ion exchange mechanism for metal removal is explained by the reaction that occurs when an ion exchange particle, with an ion exchanger of $M{-}EC^+$ (where $M^-$ is the fixed anion and $EC^+$ is the exchange cation, commonly $Na^+$ and $H^+$), exchanges its cation ($EC^+$) with the wastewater cation ($WC^+$) [66].

$$M\text{-}EC^+ + WC^+ \leftrightarrow M\text{-}WC^+ + EC^+ \quad \text{Eq. 8}$$

Ion exchange techniques using materials like zeolites can help in removing heavy metal ions such as Pb, Cd, Ni, and Zn from wastewater. This method can be applied in regions of Gujarat where groundwater quality is affected by industrial activities and urbanization.

**Electrodialysis**

Electrodialysis (ED) is a versatile technology that can be used to treat acidic effluents which include metallic species. Its perpetual operation capability, scalability, and ease of operation can overcome most of the shortcomings of

current technologies, and the direct reuse of concentrated metal streams eliminates the need for chemical addition and precipitation. The application of an electric field causes anions and cations to migrate across anion exchange membranes (AEM) and cation exchange membranes (CEM). The CEM attracts metallic cations because it is negatively charged, whereas the AEM attracts anions as it is positively charged. The electric field acts as a driving force for species migration, promoting or preventing migration, removal, and recovery [75]. Electrodialysis, although less commonly used, can be effective in treating acidic effluents containing metallic species like Cr, Cu, and Zn. This method can be suitable for targeted removal of specific heavy metals based on their ionic properties.

**Phytoremediation**

Phytoremediation represents a sustainable approach for cleansing polluted soils, sewage, sediments, and water containing various organic and inorganic pollutants. This eco-friendly and cost-effective strategy harnesses the unique capabilities of plant root systems, enabling the absorption and uptake of metals, as well as the translocation, bioaccumulation, and breakdown of contaminants throughout the plant body. Diverse techniques within phytoremediation, such as phytoextraction, phytofiltration, phytostabilization, phytovolatilization, phytodegradation, and rhizodegradation, are employed to address different types of pollution [65]. While phytoremediation is effective for shallow contamination, remediating metal-contaminated groundwater can be achieved through rhizofiltration, where plant biomass adsorbs pollutants. Phytoextraction involves the absorption of metals by crops, grasses, trees, and herbs from the soil. Phytostabilization, on the other hand, entails plants releasing elements to lower soil pH and form metal complexes. It is crucial to isolate these plants from agricultural and wildlife areas, considering factors like climate and metal bioavailability. Proper disposal methods, including drying, incineration, gasification, pyrolysis, acid extractions, anaerobic digestion, oil extraction, and plant chlorophyll fibre extraction, are necessary when plants become contaminated. For phytoremediation to be effective, it is recommended for polishing shallow soils with low contamination levels (2.5–100 mg/kg). Despite its advantages, the main drawback of phytoremediation is its time-intensive nature. Certain plants, such as Thlarpi, Urtica, Chenopodium, Polygonum rachalare, and Alyrrim, known for accumulating cadmium, copper, lead, nickel, and zinc, can serve as indirect agents for treating contaminated soils and aquifers [76]. Phytoremediation techniques, can be explored in Gujarat's main agricultural areas or near water bodies where plants can naturally uptake heavy metals from the soil and water, contributing to environmental sustainability. Especially rhizofiltration and phytoextraction, can be beneficial in areas where heavy metals like Cd, Cu, Pb, Ni, and Zn have contaminated soils and groundwater. Specific plant species known for their metal-accumulating properties can be utilized for remediation purposes.

## CONCLUSION

Groundwater serves as a crucial resource for drinking, agriculture, and industrial purposes in Gujarat. However, the escalating heavy metal pollution poses a significant threat to its quality and, consequently, public health. Both human activities such as mining, agriculture, and industry, as well as natural processes like weathering and volcanic eruptions, contribute to this contamination. Assessing heavy metal pollution through indices like HPI, HEI, $C_d$, MI, and WPI is essential for evaluating water quality. In Gujarat, common heavy metal contaminants include cobalt, lead, mercury, and copper. Research indicates that dry seasons in the Bhavnagar region exhibit higher levels of heavy metals due to human activities. Seasonal variations are observed in the Kachchh mangrove region, with elevated concentrations before the monsoon. The AIE, Mahi River, and Tapi River are heavily contaminated with mercury, rendering the water unsuitable for consumption. Direct industrial effluent discharge contributes to lead pollution, particularly in the Sabarmati River, Kharicut Canal, Tapi River, Vadodara, and Chhota Udaipur districts. The ecosystem of the Tapi River and Mahi River estuary bears evident signs of mercury contamination, indicating severe pollution from human activities. Various methods for reducing heavy metal pollution have been discussed, emphasizing the importance of tailored approaches to specific contaminants and environmental conditions. Implementing environmentally friendly and cost-effective remediation methods is crucial to mitigate health risks and safeguard groundwater quality in Gujarat. Long-term solutions must be prioritized to address this pressing issue effectively.

## ACKNOWLEDGEMENTS

The authors gratefully acknowledge Department of Chemistry, Gujarat University for supporting this work.

## DATA AVAILABILITY STATEMENT

The author confirm that the data that supports the findings of this study are available within the article. Raw data that support the finding of this study are available from the corresponding author, upon reasonable request.

## CONFLICT OF INTEREST

The author declared no potential conflicts of interest with respect to the research, authorship, and/or publication of this article.

## USE OF AI FOR WRITING ASSISTANCE

Not declared.

## ETHICS

There are no ethical issues with the publication of this manuscript.

## REFERENCES

[1] Cipriani-Avila, J. Molinero, E. Jara-Negrete, M. Barrado, C. Arcos, S. Mafla, F. Custode, G, Vilaña, N. Carpintero, and V. Ochoa-Herrera, "Heavy metal

assessment in drinking waters of Ecuador: Quito, Ibarra and Guayaquil," Journal of Water and Health, Vol. 18(6), pp. 1050–1064, 2020. [CrossRef]

[2] S. Jiménez-Oyola, P.E. Valverde-Armas, P. Romero-Crespo, D. Capa, A. Valdivieso, J. Coronel-León, F. Guzmán-Martínez, and E. Chavez, "Heavy metal(loid)s contamination in water and sediments in a mining area in Ecuador: a comprehensive assessment for drinking water quality and human health risk," Environmental Geochemistry and Health, Vol. 45(7), pp. 4929–4949, 2023. [CrossRef]

[3] N. Vig, K. Ravindra, and S. Mor, "Heavy metal pollution assessment of groundwater and associated health risks around coal thermal power plant, Punjab, India," International Journal of Environmental Science and Technology, Vol. 20(6), pp. 6259–6274, 2023. [CrossRef]

[4] G. Singh and R. K. Kamal, "Heavy metal contamination and its indexing approach for groundwater of Goa mining region, India," Applied Water Science, Vol. 7(3), pp. 1479–1485, 2017. [CrossRef]

[5] H. Kada, A. Demdoum, F. Baali, H. Aouati, and H. D. Eddine, "Heavy metal contamination and exposure risk assessment via drinking groundwater in Ain Azel territory, north-eastern Algeria," Sustainable Water Resources Management, Vol. 8(5), Article 163, 2022. [CrossRef]

[6] A. S. Mohammed, A. Kapri, and R. Goel, "Heavy metal pollution: Source, impact, and remedies," in Biomanagement of Metal-Contaminated Soils, Vol. 20, M. S. Khan, A. Zaidi, R. Goel, and J. Musarrat, Eds. Dordrecht: Springer Netherlands, pp. 1–28, 2011. [CrossRef]

[7] C. Zamora-Ledezma, D. Negrete-Bolagay, F. Figueroa, E. Zamora-Ledezma, M. Ni, F. Alexis, and V.H. Guerrero, "Heavy metal water pollution: A fresh look about hazards, novel and conventional remediation methods," Environmental Technology & Innovation, Vol. 22, p. 101504, 2021. [CrossRef]

[8] "Water Profile of Gujarat." https://www.gidb.org/water-supply-scenario-in-gujarat (Accessed on Jan 05, 2024).

[9] S. Kumar, K. D. Shirke, and N. J. Pawar, "GIS-based colour composites and overlays to delineate heavy metal contamination zones in the shallow alluvial aquifers, Ankaleshwar industrial estate, south Guja-rat, India," Environmental Geology, Vol. 54(1), pp. 117–129, 2008. [CrossRef]

[10] R. N. Kumar, R. Solanki, and J. I. N. Kumar, "Sea-sonal variation in heavy metal contamination in wa-ter and sediments of river Sabarmati and Kharicut canal at Ahmedabad, Gujarat," Environmental Mon-itoring and Assessment, Vol. 185(1), pp. 359–368, 2013. [CrossRef]

[11] D. Upadhyaya, M.D. Survaiya, S. Basha, S.K. Mandal, R.B. Thorat, S. Haldar, S. Goel, H. Dave, K. Baxi, R.H. Trivedi, and K.H. Mody, "Occurrence and distribution of selected heavy metals and boron in groundwater of the Gulf of Khambhat region, Gujarat, India," Environmental Science and Pollution Research, Vol. 21(5), pp. 3880–3890, 2014. [CrossRef]

[12] P. Maurya and R. Kumari, "Spatiotemporal variation of the nutrients and heavy metals in mangroves using multivariate statistical analysis, Gulf of Kachchh (India)," Environmental Research, Vol. 195, Article 110803, 2021. [CrossRef]

[13] S. Chopra and P. Choudhury, "A study of response spectra for different geological conditions in Gujarat, India," Soil Dynamics and Earthquake Engineering, Vol. 31(11), pp. 1551–1564, 2011. [CrossRef]

[14] S. Siddha and P. Sahu, "Status of seawater intrusion in coastal aquifer of Gujarat, India: A review," SN Applied Sciences, Vol. 2(10), p. 1726, 2020. [CrossRef]

[15] K. H. Hama Aziz, F. S. Mustafa, K. M. Omer, S. Hama, R. F. Hamarawf, and K. O. Rahman, "Heavy metal pollution in the aquatic environment: efficient and low-cost removal approaches to eliminate their toxicity: a review," RSC Advances, Vol. 13(26), pp. 17595–17610, 2023. [CrossRef]

[16] V. Masindi, P. Mkhonza, and M. Tekere, "Sources of Heavy Metals Pollution," in Remediation of Heavy Metals, Vol. 70, Inamuddin, M. I. Ahamed, E. Lichtfouse, and T. Altalhi, Eds. Cham: Springer International Publishing, 2021, pp. 419–454. [CrossRef]

[17] L. André, M. Franceschi, P. Pouchan, and O. Atteia, "Using geochemical data and modelling to enhance the understanding of groundwater flow in a regional deep aquifer, Aquitaine Basin, south-west of France," Journal of Hydrology, Vol. 305(1–4), pp. 40–62, 2005. [CrossRef]

[18] A. Punia, S. K. Singh, and R. Bharti, "Source, Assessment, and Remediation of Metals in Groundwater," in Groundwater Geochemistry, 1st ed., S. Madhav and P. Singh, Eds. Wiley, 2021, pp. 79–104. [CrossRef]

[19] A. Singh, A. Sharma, R.K. Verma, R.L. Chopade, P.P. Pandit, V. Nagar, V. Aseri, S.K. Choudhary, G. Awasthi, K.K. Awasthi, and M.S. Sankhla, "Heavy Metal Contamination of Water and Their Toxic Effect on Living Organisms," in The Toxicity of Environmental Pollutants, D. Junqueira Dorta and D. Palma De Oliveira, Eds. IntechOpen, 2022. [CrossRef]

[20] A. K. Singh, B. Raj, A. K. Tiwari, and M. K. Mahato, "Evaluation of hydrogeochemical processes and groundwater quality in the Jhansi district of Bundelkhand region, India," Environmental Earth Sciences, Vol. 70(3), pp. 1225–1247, 2013. [CrossRef]

[21] E. J. Sherlock, R. W. Lawrence, and R. Poulin, "On the neutralization of acid rock drainage by carbonate and silicate minerals". Environmental Geology Vol. 25, pp. 43–54, 1995. [CrossRef]

[22] A. Ismanto, T. Hadibarata, S. Widada, E. Indrayanti, D.H.Ismunarti, N. Safinatunnajah, W. Kusumastuti, Y. Dwiningsih, and J. Alkahtani, "Groundwater contamination status in Malaysia: level of heavy metal, source, health impact, and remediation technologies," Bioprocess and Biosystems Engineering, Vol. 46(3), pp. 467–482, 2023. [CrossRef]

[23] N. Sasakova, G. Gregova, D. Takacova, J. Mojzisova, I. Papajova, J. Venglovsky, T. Szaboova and S. Kovacova, "Pollution of surface and ground water by sources related to agricultural activities," Frontiers in Sustainable Food Systems, Vol. 2, Article 42, 2018. [CrossRef]

[24] A. K. Krishna, K.R. Mohan, N.N. Murthy, V. Periasamy, G. Bipinkumar, K. Manohar, and S.S. Rao, "Assessment of heavy metal contamination in soils around chromite mining areas, Nuggihalli, Karnataka, India," Environmental Earth Sciences, Vol. 70(2), pp. 699–708, 2013. [CrossRef]

[25] H. B. Bradl, "Chapter 1 Sources and origins of heavy metals," in Interface Science and Technology, Vol. 6, Elsevier, pp. 1–27, 2005, [CrossRef]

[26] M. S. Sankhla, M. Kumari, M. Nandan, R. Kumar, and P. Agrawal, "Heavy metals contamination in water and their hazardous effect on human health-A review," International Journal of Current Microbiology and Applied Sciences, Vol. 5(10), pp.759–766, 2016. [CrossRef]

[27] K. Sardar, S. Ali, S. Hameed, S. Afzal, S. Fatima, M. B. Shakoor, S. A. Bharwana, H. M. Tauqeer, "Heavy metals contamination and what are the impacts on living organisms," Greener Journal of Environmental Management and Public Safety, Vol. 2(4), pp. 172–179, 2013. [CrossRef]

[28] J.-K. Böhlke, "Groundwater recharge and agricultural contamination," Hydrogeology Journal, Vol. 10(1), pp. 153–179, 2002. [CrossRef]

[29] K. K. I. U. Arunakumara, B. C. Walpola, and M.-H. Yoon, "Current status of heavy metal contamination in Asia's rice lands," Reviews in Environmental Science and Bio/Technology, Vol. 12(4), pp. 355–377, 2013. [CrossRef]

[30] A. P. Pinto, A. De Varennes, R. Fonseca, and D. M. Teixeira, "Phytoremediation of Soils Contaminated with Heavy Metals: Techniques and Strategies," in Phytoremediation, A. A. Ansari, S. S. Gill, R. Gill, G. R. Lanza, and L. Newman, Eds. Cham: Springer International Publishing, 2015, pp. 133–155. [CrossRef]

[31] M. A. T. M. T. Rahman, M. Paul, N. Bhoumik, M. Hassan, Md. K. Alam, and Z. Aktar, "Heavy metal pollution assessment in the groundwater of the Meghna Ghat industrial area, Bangladesh, by using water pollution indices approach," Applied Water Science, Vol. 10(8), Article 186, 2020. [CrossRef]

[32] A. Ugurlu, "Leaching characteristics of fly ash," Environmental Geology, Vol. 46(6–7), pp. 890–895, 2004. [CrossRef]

[33] X. Zhang, Q. Guo, X. Shen, S. Yu, and G. Qiu, "Water quality, agriculture and food safety in China: Current situation, trends, interdependencies, and management," Journal of Integrative Agriculture, Vol. 14(11), pp. 2365–2379, 2015. [CrossRef]

[34] R. A. Kristanti, W.J. Ngu, A. Yuniarto, and T. Hadibarata, "Rhizofiltration for removal of inorganic and organic pollutants in groundwater: A review," Biointerface Research in Applied Chemistry, Vol. 11(4), pp. 12326–12347, 2021. [CrossRef]

[35] B. Sun, F. J. Zhao, E. Lombi, and S. P. McGrath, "Leaching of heavy metals from contaminated soils using EDTA," Environmental Pollution, Vol. 113(2), pp. 111–120, 2001. [CrossRef]

[36] P. K. Sharma, M. Mayank, C. S. P. Ojha, and S. K. Shukla, "A review on groundwater contaminant transport and remediation," ISH Journal of Hydraulic Engineering, Vol 26(1), pp. 112-121, 2020. [CrossRef]

[37] S. Giri and A. K. Singh, "Assessment of Surface Water Quality Using Heavy Metal Pollution Index in Subarnarekha River, India," Water Quality, Exposure and Health, Vol. 5(4), pp. 173–182, 2014. [CrossRef]

[38] S. V. Mohan, P. Nithila, and S. J. Reddy, "Estimation of heavy metals in drinking water and development of heavy metal pollution index," Journal of Environmental Science and Health. Part A: Environmental Science and Engineering and Toxicology, Vol. 31(2), pp. 283–289, 1996. [CrossRef]

[39] H. Arslan, N. Ayyildiz Turan, K. Ersin Temizel, A Kuleyin, M. Sait Kiremit, A. Güngör, and H. Yildiz Özgül, "Evaluation of heavy metal contamination and pollution indices through geostatistical methods in groundwater in Bafra Plain, Turkey," International Journal of Environmental Science and Technology, Vol. 19(9), pp. 8385–8396, 2022. [CrossRef]

[40] V. Kumar, R.D. Parihar, A. Sharma, P. Bakshi, G.P.S. Sidhu, A.S. Bali, I. Karaouzas, R. Bhardwaj, A.K. Thukral, Y. Gyasi-Agyei, and J. Rodrigo-Comino, "Global evaluation of heavy metal content in surface water bodies: A meta-analysis using heavy metal pollution indices and multivariate statistical analyses," Chemosphere, Vol. 236, p. 124364, 2019. [CrossRef]

[41] B. Backman, D. Bodiš, P. Lahermo, S. Rapant, and T. Tarvainen, "Application of a groundwater contamination index in Finland and Slovakia," Environmental Geology, Vol. 36(1–2), pp. 55–64, 1998. [CrossRef]

[42] S. Caeiro, M.H. Costa, T.B. Ramos, F. Fernandes, N. Silveira, A. Coimbra, G. Medeiros, and M. Painho, "Assessing heavy metal contamination in Sado Estuary sediment: An index analysis approach," Ecological Indicators, Vol. 5(2), pp. 151–169, 2005. [CrossRef]

[43] V. Mukanyandwi, A. Kurban, E. Hakorimana, L. Nahayo, G. Habiyaremye, A. Gasirabo, and T. Sindikubwabo, "Seasonal assessment of drinking water sources in Rwanda using GIS, contamination degree (Cd), and metal index (MI)," Environmental Monitoring and Assessment, Vol. 191(12), Article 734, 2019. [CrossRef]

[44] H. G. Gosai, P. Mankodi Evaluation of surface water from the western coast Bhavnagar, Gulf of Khambhat, Gujarat, India. Thalassas: An International Journal of Marine Sciences, Vol. 40, pp. 669–684, 2024. [CrossRef]

[45] U. K. Singh, M. Kumar, R. Chauhan, P. K. Jha, Al. Ramanathan, and V. Subramanian, "Assessment of the impact of landfill on groundwater quality: A case study of the Pirana site in western India," Environmental Monitoring and Assessment, Vol. 141(1–3), pp. 309–321, 2008. [CrossRef]

[46] T. Keesari, U. P. Kulkarni, A. Deodhar, P. S. Ramanjaneyulu, A. K. Sanjukta, and U. Saravana Kumar, "Geochemical characterization of groundwater from an arid region in India," Environmental Earth Sciences, Vol. 71(11), pp. 4869–4888, 2014. [CrossRef]

[47] S. V. Patel, P. Chavda, and S. Tyagi, "Carrying out assessment of groundwater quality of villages of Bhavnagar district of Gujarat, India," Environmental Claims Journal, Vol. 31(1), pp. 79–92, 2019. [CrossRef]

[48] M. P. Patel, B. Gami, A. Patel, P. Patel, and B. Patel, "Climatic and anthropogenic impact on groundwater quality of agriculture dominated areas of southern and central Gujarat, India," Groundwater for Sustainable Development, Vol. 10, p. 100306, 2020. [CrossRef]

[49] H. Pandey, S. Senthilnathan, and G. A. Thivakaran, "Heavy metal contamination in water, sediment and fish of Mahi estuary, Gujarat, India", Pollution Research, Vol. 39 (2), pp. 327–334, 2020.

[50] S. Siddha and P. Sahu, "A statistical approach to study the evolution of groundwater of Vishwamitri River Basin (VRB), Gujarat," Journal of the Geological Society of India, Vol. 95(5), pp. 503–506, 2020. [CrossRef]

[51] M. Dubey and N. Ujjania, "Heavy metal contamination and pollution load index in estuarine environment of Tapi river, India," Asian Journal of Microbiology, Biotechnology and Environmental Sciences, Vol. 23, pp. 456–459, 2021.

[52] R. Bengani and M. Gadhia, "Environmental assessment of Tapi Estuary, Surat, Gujarat with reference to heavy metals," International Journal of Computational Research and Development, Vol. 6(2), pp. 1–5, 2021.

[53] S. V. Patel, N. Khatri, P. Chavda, and A. K. Jha, "Potential health concerns due to elevated nitrate concentrations in groundwater of villages of Vadodara and Chhota Udaipur districts of Gujarat, India," Journal of Water and Health, Vol. 20(1), pp. 227–245, 2022. [CrossRef]

[54] B. Prasad and J. Bose, "Evaluation of the heavy metal pollution index for surface and spring water near a limestone mining area of the lower Himalayas," Environmental Geology, Vol. 41(1–2), pp. 183–188, 2001. [CrossRef]

[55] "IS 10500 (2012): Drinking water" [Online]. Available: https://cpcb.nic.in/wqm/BIS_ Drinking_Water_Specification.pdf

[56] "Public Health Statement Strontium CAS#7440-24-6." ATSDR, Apr. 2004. [Online]. Available: https://www.atsdr.cdc.gov/ToxProfiles/tp159-c1-b.pdf

[57] "National Primary Drinking Water Regulations." USEPA, May 2009. [Online]. Available: https://www.epa.gov/sites/default/files/2016-06/documents/npwdr_complete_table.pdf

[58] "Public Health Statement Cesium CAS37440-46-2." ATSDR, Apr. 2004. [Online]. Available: https://www.atsdr.cdc.gov/ToxProfiles/tp157-c1-b.pdf

[59] S. C. Izah, N. Chakrabarty, and A. L. Srivastav, "A review on heavy metal concentration in potable water sources in Nigeria: Human health effects and mitigating measures," Exposure and Health, Vol. 8(2), pp. 285–304, 2016. [CrossRef]

[60] L. A. Malik, A. Bashir, A. Qureashi, and A. H. Pandith, "Detection and removal of heavy metal ions: a review," Environmental Chemistry Letters, Vol. 17(4), pp. 1495–1521, 2019. [CrossRef]

[61] P. Rajasulochana and V. Preethy, "Comparison on efficiency of various techniques in treatment of waste and sewage water – A comprehensive review," Resource-Efficient Technologies, Vol. 2(4), pp. 175–184, 2016. [CrossRef]

[62] F. Fu and Q. Wang, "Removal of heavy metal ions from wastewaters: A review," Journal of Environmental Management, Vol. 92(3), pp. 407–418, 2011. [CrossRef]

[63] M. M. Matlock, K. R. Henke, and D. A. Atwood, "Effectiveness of commercial reagents for heavy metal removal from water with new insights for future chelate designs," Journal of Hazardous Materials, Vol. 92(2), pp. 129–142, 2002. [CrossRef]

[64] S. Sarkar and S. Adhikari, "Adsorption Technique for Removal of Heavy Metals from Water and Possible Application in Wastewater-Fed Aquaculture," in Wastewater Management Through Aquaculture, B. B. Jana, R. N. Mandal, and P. Jayasankar, Eds. Singapore: Springer Singapore, 2018, pp. 235–251. [CrossRef]

[65] E. C. Emenike, K. O. Iwuozor, and S. U. Anidiobi, "Heavy metal pollution in aquaculture: Sources, impacts and mitigation techniques," Biological Trace Element Research, Vol. 200(10), pp. 4476–4492, 2022. [CrossRef]

[66] N. A. A. Qasem, R. H. Mohammed, and D. U. Lawal, "Removal of heavy metal ions from wastewater: a comprehensive and critical review," Clean Water, Vol. 4(1), p. 36, 2021. [CrossRef]

[67] M. N. Sahmoune, "Evaluation of thermodynamic parameters for adsorption of heavy metals by green adsorbents," Environmental Chemistry Letters, Vol. 17(2), pp. 697–704, 2019. [CrossRef]

[68] R. Apiratikul and P. Pavasant, "Batch and column studies of biosorption of heavy metals by Caulerpa lentillifera," Bioresource Technology, Vol. 99 (8), 2766-2777, 2008. [CrossRef]

[69] T. Zhang, W. Wang, Y. Zhao, H. Bai, T. Wen, S. Kang, G. Song, S. Song, and S. Komarneni, "Removal of heavy metals and dyes by clay-based adsorbents: From natural clays to 1D and 2D nano-composites," Chemical Engineering Journal, Vol. 420, p. 127574, 2021. [CrossRef]

[70] S. Gu, X. Kang, L. Wang, E. Lichtfouse, and C. Wang, "Clay mineral adsorbents for heavy metal removal from wastewater: A review," Environmental Chemistry Letters, Vol. 17(2), pp. 629–654, 2019. [CrossRef]

[71] G. Rao, C. Lu, and F. Su, "Sorption of divalent metal ions from aqueous solution by carbon nanotubes:

A review," Separation and Purification Technology, Vol. 58(1), pp. 224–231, 2007. [CrossRef]

[72] M. A. Barakat, "New trends in removing heavy metals from industrial wastewater," Arabian Journal of Chemistry, Vol. 4(4), pp. 361–377, 2011. [CrossRef]

[73] S. Vigneswaran, H. H. Ngo, D. S. Chaudhary, and Y.-T. Hung, "Physicochemical Treatment Processes for Water Reuse," in Physicochemical Treatment Processes, L. K. Wang, Y.-T. Hung, and N. K. Shammas, Eds. Totowa, NJ: Humana Press, 2005, pp. 635–676. [CrossRef]

[74] A. Dabrowski, Z. Hubicki, P. Podkościelny, and E. Robens, "Selective removal of the heavy metal ions from waters and industrial wastewaters by ion-exchange method," Chemosphere, Vol. 56(2), pp. 91–106, 2004. [CrossRef]

[75] J.-M. Arana Juve, F. M. S. Christensen, Y. Wang, and Z. Wei, "Electrodialysis for metal removal and recovery: A review," Chemical Engineering Journal, Vol. 435, Article 134857, 2022. [CrossRef]

[76] C. N. Mulligan, R. N. Yong, and B. F. Gibbs, "Remediation technologies for metal-contaminated soils and groundwater: An evaluation," Engineering Geology, Vol. 60(1–4), pp. 193–207, 2001. [CrossRef]